



DEVELOPMENT OF A CRASHWORTHY PEDESTRIAN RAIL

Submitted by

Karla A. Lechtenberg, M.S.M.E., E.I.T.
Research Associate Engineer

Jennifer D. Schmidt, Ph.D., P.E.
Research Assistant Professor

Ronald K. Faller, Ph.D., P.E.
Research Associate Professor
MwRSF Director

Ana L. Guajardo, B.S.M.E.
Graduate Research Assistant

Robert W. Bielenberg, M.S.M.E., E.I.T.
Research Associate Engineer

John D. Reid, Ph.D.
Professor

MIDWEST ROADSIDE SAFETY FACILITY

Nebraska Transportation Center
University of Nebraska-Lincoln
130 Whittier Research Center
2200 Vine Street
Lincoln, Nebraska 68583-0853
(402) 472-0965

Submitted to

WISCONSIN DEPARTMENT OF TRANSPORTATION

4802 Sheboygan Avenue
Madison, Wisconsin 53707

MwRSF Research Report No. TRP-03-321-15

January 18, 2016

TECHNICAL REPORT DOCUMENTATION PAGE

1. Report No. TRP-03-321-15	2.	3. Recipient's Accession No.	
4. Title and Subtitle Development of a Crashworthy Pedestrian Rail		5. Report Date January 18, 2016	
		6.	
7. Author(s) Lechtenberg, K.A., Schmidt, J.D., Faller, R.K., Guajardo, A.L., Bielenberg, R.W., Reid, J.D.		8. Performing Organization Report No. TRP-03-321-15	
9. Performing Organization Name and Address Midwest Roadside Safety Facility (MwRSF) Nebraska Transportation Center University of Nebraska-Lincoln 130 Whittier Research Center 2200 Vine Street Lincoln, Nebraska 68583-0853		10. Project/Task/Work Unit No.	
		11. Contract © or Grant (G) No. TPF-5(193) Supplement 41	
12. Sponsoring Organization Name and Address Wisconsin Department of Transportation 4802 Sheboygan Avenue Madison, Wisconsin 53707		13. Type of Report and Period Covered Final Report: 2011-2016	
		14. Sponsoring Agency Code	
15. Supplementary Notes Prepared in cooperation with U.S. Department of Transportation, Federal Highway Administration.			
16. Abstract <p>The National Highway Traffic Safety Administration (NHTSA) estimated that approximately 4,300 pedestrian fatalities occurred in the United States in 2010. Risk of pedestrian injury is highest when crossing the street. In locations where pedestrians choose a more direct path and cross the street at non-designated crossing areas, driver expectations are violated and perception-reaction times are delayed, thus increasing risk to the pedestrian. Pedestrian rails may be placed adjacent to roadways to protect pedestrians from dangerous excursions into the roadway as well as from hazardous drop offs. Although numerous pedestrian rails have been designed, their performance has never been evaluated during vehicular impact events. Therefore, the Wisconsin Department of Transportation funded a study to develop a crashworthy pedestrian rail system which satisfies the Manual for Assessing Safety Hardware (MASH) TL-2 channelizer evaluation criteria.</p> <p>A total of twenty-five initial pedestrian rail concepts were designed, and four were advanced for final consideration and dynamic bogie testing. An aluminum rail with welded posts, rails, and spindles was selected for full-scale crash testing. The system consisted of 2-in. x 4-in. x ¼-in. x 43-in. tall (51-mm x 102-mm x 6-mm x 1,029-mm tall) posts with three 2-in. x 2-in. x ⅛-in. (51-mm x 51-mm x 3-mm) rail components at heights of 42 in. (1,067 mm), 24¹⁵/₁₆ in. (633 mm) and 7⅞ in. (200 mm). Two full-scale crash tests were conducted according to MASH TL-2 test designation no. 2-90, but at impact angles of 25 and 0 degrees for test nos. APR-1 and APR-2, respectively. Both tests successfully satisfied the MASH channelizer evaluation criteria. However, the 0-degree impact showed that the pedestrian rail system was near the maximum ridedown acceleration limit. Thus, further modifications are recommended to improve the crashworthiness of the welded aluminum pedestrian rail design and to lower the occupant risk values.</p>			
17. Document Analysis/Descriptors Highway Safety, Crash Test, Bogie Test, Roadside Appurtenances, Roadside Safety, MASH, AASHTO, ADA, LRFD, Longitudinal Channelizer, Pedestrian Rail, and TL-2		18. Availability Statement No restrictions. Document available from: National Technical Information Services, Springfield, Virginia 22161	
19. Security Class (this report) Unclassified	20. Security Class (this page) Unclassified	21. No. of Pages 464	22. Price

DISCLAIMER STATEMENT

This report was completed with funding from the Wisconsin Department of Transportation and the Federal Highway Administration, U.S. Department of Transportation. The contents of this report reflect the views and opinions of the authors who are responsible for the facts and the accuracy of the data presented herein. The contents do not necessarily reflect the official views or policies of the Wisconsin Department of Transportation nor the Federal Highway Administration, U.S. Department of Transportation. This report does not constitute a standard, specification, regulation, product endorsement, or an endorsement of manufacturers.

UNCERTAINTY OF MEASUREMENT STATEMENT

The Midwest Roadside Safety Facility (MwRSF) has determined the uncertainty of measurements for several parameters involved in standard full-scale crash testing and non-standard testing of roadside safety features. Information regarding the uncertainty of measurements for critical parameters is available upon request by the sponsor and the Federal Highway Administration. Bogie test nos. WIPR-1 through WIPR-4 were non-certified, dynamic component tests that were conducted for research and development purposes only.

INDEPENDENT APPROVING AUTHORITY

The Independent Approving Authority (IAA) for the data contained herein was Mr. Scott Rosenbaugh, Research Associate Engineer.

ACKNOWLEDGEMENTS

The authors wish to acknowledge several sources that made a contribution to this project:

(1) the Wisconsin Department of Transportation for sponsoring this project and (2) MwRSF personnel for constructing the barriers and conducting the crash tests.

Acknowledgement is also given to the following individuals who made a contribution to the completion of this research project.

Midwest Roadside Safety Facility

J.C. Holloway, M.S.C.E., E.I.T., Test Site Manager
S.K. Rosenbaugh, M.S.C.E., E.I.T., Research Associate Engineer
C.S. Stolle, Ph.D., E.I.T., Research Assistant Professor
A.T. Russell, B.S.B.A., Shop Manager
K.L. Krenk, B.S.M.A., Maintenance Mechanic (retired)
S.M. Tighe, Laboratory Mechanic
D.S. Charroin, Laboratory Mechanic
M.A. Rasmussen, Laboratory Mechanic
E.W. Krier, Laboratory Mechanic
L.R. Kampschneider, M.S.C.E., E.I.T., Graduate Research Assistant
M.C. Holton, B.S.C.E., E.I.T., Undergraduate Research Assistant
M.J. Wiebelhaus, M.S.C.E., E.I.T., Graduate Research Assistant
M.R. Pacheco, B.S.C.E., Undergraduate Research Assistant

Wisconsin Department of Transportation

Jerry Zogg, P.E., Chief Roadway Standards Engineer
Erik Emerson, P.E., Standards Development Engineer
Rodney Taylor, P.E., Roadway Design Standards Unit Supervisor

TABLE OF CONTENTS

TECHNICAL REPORT DOCUMENTATION PAGE	i
DISCLAIMER STATEMENT	ii
UNCERTAINTY OF MEASUREMENT STATEMENT	ii
INDEPENDENT APPROVING AUTHORITY.....	ii
ACKNOWLEDGEMENTS	iii
1 INTRODUCTION	1
1.1 Background	1
1.2 Objective	2
1.3 Scope.....	2
2 LITERATURE REVIEW	6
2.1 Standards.....	6
2.1.1 Americans with Disabilities Act Design Criteria.....	6
2.1.2 AASHTO LRFD Bridge Design Specifications	7
2.1.3 International Building Code.....	8
2.1.4 Occupational Safety & Health Administration (OSHA)	9
2.1.5 AASHTO MASH Longitudinal Channelizers	9
2.2 Existing Pedestrian Rail Designs	10
2.2.1 Concrete Combination Traffic and Pedestrian Rail Designs	10
2.2.2 Plastic Fence Designs	12
2.2.3 Existing Wood Fence Designs	16
2.2.4 Metal Barrier Designs	16
3 EVALUATION OF PEDESTRIAN RAIL NEEDS.....	39
4 PRELIMINARY PEDESTRIAN RAIL DESIGN.....	41
4.1 Design Load Calculations	41
4.1.1 Longitudinal Rail Element.....	41
4.1.2 Vertical Post Element	43
4.1.3 Infill, Mesh, and Spindle Element	44
4.2 Material Selection	44
4.2.1 Material Consideration.....	44
4.2.2 Aluminum	46
4.2.3 Steel.....	46
4.2.4 Polyvinyl Chloride (PVC).....	46
4.2.5 Fiber-Reinforced Polymer (FRP).....	47
4.2.6 High Density Polyethylene (HDPE)	47
4.2.7 Wood (Douglas Fir)	47
5 INITIAL CONCEPT DEVELOPMENT	48
5.1 Preliminary Concept	48

5.2 Refined Concepts	48
5.2.1 Design Concept AM-1	49
5.2.2 Design Concept AM-2	49
5.2.3 Design Concept AW2	49
5.2.4 Design Concept PVC1	50
5.2.5 Design Concept PVC2	50
5.2.5.1 Design Concept PVC2-a	50
5.2.5.2 Design Concept PVC2-b	51
5.2.5.3 Design Concept PVC2-c	51
5.2.6 Design Concept WOOD1	51
5.2.7 Design Concept WOOD2	52
5.3 Discussion	52
6 PEDESTRIAN RAIL DESIGNS	111
6.1 Rail Component	111
6.1.1 Concentrated Load	111
6.1.2 Uniform Load	113
6.1.3 Combined Concentrated and Uniform Loads	115
6.2 Post Component	118
6.3 Infill	120
6.4 Connections	122
6.4.1 Post-to-Rail Connection	122
6.4.1.1 Maximum Shear Force	124
6.4.1.2 Maximum Bending Moment	124
6.4.2 Post-to-Base Assembly Connection	126
6.4.3 Infill-to-Rail Connection	128
6.4.4 Concrete Anchorage	129
7 DESIGN OF PROTOTYPE PEDESTRIAN RAILS	131
7.1 Introduction	131
7.2 Section Capacities	132
7.2.1 Shear	132
7.2.1.1 Rectangular tubes	132
7.2.1.2 Round and Oval Tubes	134
7.2.1.3 Solid Sections	135
7.2.2 Flexure	135
7.2.2.1 Rectangular Tubes	135
7.2.2.2 Pipe and Round Tubes	137
7.3 Connection Capacity	140
7.3.1 Welds	140
7.3.2 Baseplate	141
7.3.3 Anchors	143
7.3.3.1 Tension	144
7.3.3.2 Shear	147
7.3.4 Modular Cast Aluminum	151
7.4 Final Designs	151
7.4.1 Introduction	151

7.4.2 AW2-A Welded Aluminum	152
7.4.3 AW2-C Welded Aluminum	153
7.4.4 AM-1 Modular Aluminum	154
7.4.5 AW2-D Welded Aluminum	155
8 COMPONENT TESTING CONDITIONS	178
8.1 Purpose	178
8.2 Scope	178
8.3 Test Facility	181
8.4 Equipment and Instrumentation	181
8.4.1 Bogie Vehicle	181
8.4.2 Accelerometers	182
8.4.3 Retroreflective Optic Speed Trap	183
8.4.4 Digital Photography	183
8.5 Data Processing	184
9 DYNAMIC BOGIE TESTING RESULTS AND DISCUSSION	185
9.1 Run No. WIPR-1 (Test Nos. WIPR-1-1 and WIPR-1-2)	185
9.2 Run No. WIPR-2 (Test Nos. WIPR-2-1 and WIPR-2-2)	193
9.3 Run No. WIPR-3 (Test Nos. WIPR-3-1 and WIPR-3-2)	203
9.4 Run No. WIPR-4 (Test No. WIPR-4)	214
9.5 Discussion	221
10 FULL-SCALE TEST REQUIREMENTS AND EVALUATION CRITERIA	223
10.1 Test Requirements	223
10.2 Evaluation Criteria	225
11 TEST CONDITIONS	227
11.1 Test Facility	227
11.2 Vehicle Tow and Guidance System	227
11.3 Test Vehicles	227
11.4 Simulated Occupant	235
11.5 Data Acquisition Systems	235
11.5.1 Accelerometers	235
11.5.2 Rate Transducers	236
11.5.3 Retroreflective Optic Speed Trap	237
11.5.4 Digital Photography	237
12 DESIGN DETAILS	240
13 FULL-SCALE CRASH TEST NO. APR-1	250
13.1 Test No. APR-1	250
13.2 Weather Conditions	250
13.3 Test Description	250
13.4 System Damage	251
13.5 Vehicle Damage	253
13.6 Occupant Risk	254
13.7 Discussion	255

14 FULL-SCALE CRASH TEST NO. APR-2.....	272
14.1 Test No. APR-2.....	272
14.2 Weather Conditions	272
14.3 Test Description	272
14.4 System Damage	274
14.5 Vehicle Damage.....	275
14.6 Occupant Risk.....	276
14.7 Discussion	277
15 SUMMARY, CONCLUSIONS, AND RECOMMENDATIONS	301
16 REFERENCES	308
17 APPENDICES	312
Appendix A. Pooled Fund Survey for Pedestrian Rail Highest Priority Need	313
Appendix B. Original Design Concepts	317
Appendix C. Design Calculations	344
Appendix D. Material Specifications	370
Appendix E. Vehicle Center of Gravity Determination	399
Appendix F. Fabrication Drawings for Test Nos. APR-1 and APR-2	402
Appendix G. Vehicle Deformation Record.....	413
Appendix H. Accelerometer and Rate Transducer Data Plots, Test No. APR-1	426
Appendix I. Accelerometer and Rate Transducer Data Plots, Test No. APR-2.....	443
Appendix J. Test No. APR-2 Accelerometer Discussion.....	460

LIST OF FIGURES

Figure 1. Examples of Pedestrian Rails	3
Figure 2. Pedestrian Rail Limiting Pedestrian Maneuver Options	4
Figure 3. Vehicle Impacts with Pedestrian Rails	5
Figure 4. ADA Non-Circular Cross Section Dimensions	7
Figure 5. AASHTO Loading Criteria (Vertical 200-lb Point Load Shown).....	8
Figure 6. Minnesota Combination Traffic and Pedestrian Barrier [10].....	11
Figure 7. Examples of Existing HDPE Fences [12-14]	13
Figure 8. Examples of Existing FRP Handrail Systems [15-17]	14
Figure 9. Examples of Existing PVC Fences [18-20].....	15
Figure 10. Examples of Existing Wood Fences [21-24].....	19
Figure 11. RTA Designed Pedestrian Barrier [25]	20
Figure 12. RTA Modified Steel Mesh [25].....	21
Figure 13. VISIFLEX Pedestrian Guardrail [27].....	22
Figure 14. Iowa DOT Steel Pipe Rail [28]	23
Figure 15. Washington DOT Standard Railing (Sheet 1 of 2) [29]	24
Figure 16. Washington DOT Standard Railing (Sheet 2 of 2) [29]	25
Figure 17. Texas DOT Handrail [30].....	27
Figure 18. Horizontal Cable Frame [31].....	27
Figure 19. Vertical Cable Frame [31]	28
Figure 20. FDOT Aluminum, Pedestrian-Only Rail (Sheet 1 of 8) [32-33].....	29
Figure 21. FDOT Aluminum, Pedestrian-Only Rail (Sheet 2 of 8) [32-33].....	30
Figure 22. FDOT Aluminum, Pedestrian-Only Rail (Sheet 3 of 8) [32-33].....	31
Figure 23. FDOT Aluminum, Pedestrian-Only Rail (Sheet 4 of 8) [32-33].....	32
Figure 24. FDOT Aluminum, Pedestrian-Only Rail (Sheet 5 of 8) [32-33].....	33
Figure 25. FDOT Aluminum, Pedestrian-Only Rail (Sheet 6 of 8) [32-33].....	34
Figure 26. FDOT Aluminum, Pedestrian-Only Rail (Sheet 7 of 8) [32-33].....	35
Figure 27. FDOT Aluminum, Pedestrian-Only Rail (Sheet 8 of 8) [32-33].....	36
Figure 28. Examples of Hollaender Rail Systems [34-35]	38
Figure 29. Example of Pedestrian Rail with Vertical Concentrated Load.....	42
Figure 30. Aluminum Modular Rail with Spindles, Design Concept AM-1 (Sheet 1 of 5)	53
Figure 31. Aluminum Modular Rail with Spindles, Design Concept AM-1 (Sheet 2 of 5)	54
Figure 32. Aluminum Modular Rail with Spindles, Design Concept AM-1 (Sheet 3 of 5)	55
Figure 33. Aluminum Modular Rail with Spindles, Design Concept AM-1 (Sheet 4 of 5)	56
Figure 34. Aluminum Modular Rail with Spindles, Design Concept AM-1 (Sheet 5 of 5)	57
Figure 35. Aluminum Modular Rail with Spindles, Design Concept AM-1	58
Figure 36. Aluminum Modular Rail with Spindles, Design Concept AM-1	59
Figure 37. Aluminum Modular Rail with Wire Mesh, Design Concept AM-2 (Sheet 1 of 5)	60
Figure 38. Aluminum Modular Rail with Wire Mesh, Design Concept AM-2 (Sheet 2 of 5)	61
Figure 39. Aluminum Modular Rail with Wire Mesh, Design Concept AM-2 (Sheet 3 of 5)	62
Figure 40. Aluminum Modular Rail with Wire Mesh, Design Concept AM-2 (Sheet 4 of 5)	63
Figure 41. Aluminum Modular Rail with Wire Mesh, Design Concept AM-2 (Sheet 5 of 5)	64
Figure 42. Welded Aluminum Rail, Design Concept AW2 (Sheet 1 of 5)	65
Figure 43. Welded Aluminum Rail, Design Concept AW2 (Sheet 2 of 5)	66
Figure 44. Welded Aluminum Rail, Design Concept AW2 (Sheet 3 of 5)	67
Figure 45. Welded Aluminum Rail, Design Concept AW2 (Sheet 4 of 5)	68

Figure 46. Welded Aluminum Rail, Design Concept AW2 (Sheet 5 of 5)	69
Figure 47. Welded Aluminum Rail, Design Concept AW2	70
Figure 48. Welded Aluminum Rail, Design Concept AW2	71
Figure 49. Modular PVC Rail, Design Concept PVC1 (Sheet 1 of 5).....	72
Figure 50. Modular PVC Rail, Design Concept PVC1 (Sheet 2 of 5).....	73
Figure 51. Modular PVC Rail, Design Concept PVC1 (Sheet 3 of 5).....	74
Figure 52. Modular PVC Rail, Design Concept PVC1 (Sheet 4 of 5).....	75
Figure 53. Modular PVC Rail, Design Concept PVC1 (Sheet 5 of 5).....	76
Figure 54. Modular PVC Rail, Design Concept PVC1	77
Figure 55. Modular PVC Rail, Design Concept PVC1	78
Figure 56. Modular PVC Rail, Design Concept PVC2-a (Sheet 1 of 4)	79
Figure 57. Modular PVC Rail, Design Concept PVC2-a (Sheet 2 of 4)	80
Figure 58. Modular PVC Rail, Design Concept PVC2-a (Sheet 3 of 4)	81
Figure 59. Modular PVC Rail, Design Concept PVC2-a (Sheet 4 of 4)	82
Figure 60. Modular PVC Rail, Design Concept PVC2-a	83
Figure 61. Modular PVC Rail, Design Concept PVC2-a	84
Figure 62. Modular PVC Rail, Design Concept PVC2-b (Sheet 1 of 5)	85
Figure 63. Modular PVC Rail, Design Concept PVC2-b (Sheet 2 of 5)	86
Figure 64. Modular PVC Rail, Design Concept PVC2-b (Sheet 3 of 5)	87
Figure 65. Modular PVC Rail, Design Concept PVC2-b (Sheet 4 of 5)	88
Figure 66. Modular PVC Rail, Design Concept PVC2-b (Sheet 5 of 5)	89
Figure 67. Modular PVC Rail, Design Concept PVC2-c (Sheet 1 of 5)	90
Figure 68. Modular PVC Rail, Design Concept PVC2-c (Sheet 2 of 5)	91
Figure 69. Modular PVC Rail, Design Concept PVC2-c (Sheet 3 of 5)	92
Figure 70. Modular PVC Rail, Design Concept PVC2-c (Sheet 4 of 5)	93
Figure 71. Modular PVC Rail, Design Concept PVC2-c (Sheet 5 of 5)	94
Figure 72. Modular PVC Rail, Design Concept PVC2-c	95
Figure 73. Modular PVC Rail, Design Concept PVC2-c	96
Figure 74. Modular Wood Rail, Design Concept WOOD1 (Sheet 1 of 5).....	97
Figure 75. Modular Wood Rail, Design Concept WOOD1 (Sheet 2 of 5).....	98
Figure 76. Modular Wood Rail, Design Concept WOOD1 (Sheet 3 of 5).....	99
Figure 77. Modular Wood Rail, Design Concept WOOD1 (Sheet 4 of 5).....	100
Figure 78. Modular Wood Rail, Design Concept WOOD1 (Sheet 5 of 5).....	101
Figure 79. Fabricated Refined Design Concept WOOD1	102
Figure 80. Fabricated Refined Design Concept WOOD1	103
Figure 81. Cutout Wood Rail, Design Concept WOOD2 (Sheet 1 of 5).....	104
Figure 82. Cutout Wood Rail, Design Concept WOOD2 (Sheet 2 of 5).....	105
Figure 83. Cutout Wood Rail, Design Concept WOOD2 (Sheet 3 of 5).....	106
Figure 84. Cutout Wood Rail, Design Concept WOOD2 (Sheet 4 of 5).....	107
Figure 85. Cutout Wood Rail, Design Concept WOOD2 (Sheet 5 of 5).....	108
Figure 86. Fabricated Refined Design Concept WOOD2	109
Figure 87. Fabricated Refined Design Concept WOOD2	110
Figure 88. Rail Shear Diagram – Concentrated Load Virtually at Support.....	112
Figure 89. Rail Moment Diagram – Concentrated Load, Simply Supported Ends	113
Figure 90. Rail Shear Diagram – Uniformly Distributed Load, Simply Supported Ends	114
Figure 91. Rail Moment Diagram – Uniformly Distributed Load, Simply Supported Ends.....	115
Figure 92. Rail Moment Diagram – Combined Loads, Simply Supported Ends	117

Figure 93. Post Shear Diagram	119
Figure 94. Post Moment Diagram.....	120
Figure 95. Spindle Shear Diagram – Uniform Load, Simply Supported Ends	121
Figure 96. Spindle Moment Diagram – Uniform Load, Simply Supported Ends	122
Figure 97. Rail Moment Diagram – Concentrated Load, Fixed-Fixed Ends.....	123
Figure 98. Rail Moment Diagram – Uniformly Distributed Load, Fixed-Fixed Ends	123
Figure 99. Rail Moment Diagram – Combined Loads, Fixed-Fixed Ends.....	125
Figure 100. Baseplate Loads with Combined Axial Force and Bending Moment with Large Eccentricity	127
Figure 101. Spindle Moment Diagram – Uniformly Distributed Load, Fixed-Fixed Ends.....	129
Figure 102. Pedestrian Rail Test Setup, Designs AW2-A, AW2-C and AM-1	156
Figure 103. Pedestrian Rail Test Setup, Designs AW2-A, AW2-C and AM-1	157
Figure 104. Pedestrian Rail Design AW2-A.....	158
Figure 105. Pedestrian Rail Design AW2-A.....	159
Figure 106. Pedestrian Rail Design AW2-C.....	160
Figure 107. Pedestrian Rail Design AW2-C.....	161
Figure 108. Pedestrian Rail Design AW2-C.....	162
Figure 109. General Components, Pedestrian Rail Designs AW2-A and AW2-C.....	163
Figure 110. Pedestrian Rail Design AM-1.....	164
Figure 111. Pedestrian Rail Design AM-1.....	165
Figure 112. Pedestrian Rail Design AM-1.....	166
Figure 113. Pedestrian Rail Design AM-1.....	167
Figure 114. Bill of Materials, Pedestrian Rail Designs AW2-A and AW2-C	168
Figure 115. Bill of Materials, Continued, Pedestrian Rail Design AM-1.....	169
Figure 116. Pedestrian Rail Test Setup, Design AW2-D.....	170
Figure 117. Pedestrian Rail Design AW2-D.....	171
Figure 118. Pedestrian Rail Design AW2-D.....	172
Figure 119. Pedestrian Rail Design AW2-D.....	173
Figure 120. Pedestrian Rail Design AW2-D.....	174
Figure 121. Bill of Materials, Pedestrian Rail Design AW2-D	175
Figure 122. Pedestrian Rail AW2-A.....	176
Figure 123. Pedestrian Rail AW2-C	176
Figure 124. Pedestrian Rail AM-1	177
Figure 125. Pedestrian Rail AW2-D.....	177
Figure 126. Typical Bogie Testing Setup	180
Figure 127. Rigid-Frame Bogie Vehicle on Guidance Track	182
Figure 128. System Panels and Anchor, Run No. WIPR-1	187
Figure 129. System Installation, Run No. WIPR-1	188
Figure 130. First Panel Damage, Run No. WIPR-1, Test No. WIPR-1-1	189
Figure 131. Second Panel Damage, Run No. WIPR-1, Test No. WIPR-1-1	190
Figure 132. First Panel Damage, Run No. WIPR-1, Test No. WIPR-1-2	191
Figure 133. Second Panel Damage, Run No. WIPR-1, Test No. WIPR-1-2.....	192
Figure 134. System Panels and Anchors, Run No. WIPR-2.....	195
Figure 135. System Installation, Run No. WIPR-2	196
Figure 136. Time-Sequential Photographs, Run No. WIPR-2, Test No. WIPR-2-1	197
Figure 137. Time-Sequential Photographs, Run No. WIPR-2, Test No. WIPR-2-2	198
Figure 138. First Panel Damage, Run No. WIPR-2, Test No. WIPR-2-1	199

Figure 139. Second Panel Damage, Run No. WIPR-2, Test No. WIPR-2-1	200
Figure 140. First Panel Damage, Run No. WIPR-2, Test No. WIPR-2-2	201
Figure 141. Second Panel Damage, Run No. WIPR-2, Test No. WIPR-2-2	202
Figure 142. System Panels and Anchor, Run No. WIPR-3	204
Figure 143. System Installation, Run No. WIPR-3	205
Figure 144. Time-Sequential Photographs, Run No. WIPR-3, Test No. WIPR-3-1	206
Figure 145. Time-Sequential Photographs, Run No. WIPR-3, Test No. WIPR-3-2	207
Figure 146. System Damage, Run No. WIPR-3, Test No. WIPR-3-1	208
Figure 147. System Damage, Run No. WIPR-3, Test No. WIPR-3-1	209
Figure 148. System Damage, Run No. WIPR-3, Test No. WIPR-3-2	210
Figure 149. System Damage, Run No. WIPR-3, Test No. WIPR-3-2	211
Figure 150. Force vs. Displacement and Energy vs. Displacement, Run No. WIPR-3, Test No. WIPR-3-1	212
Figure 151. Force vs. Displacement and Energy vs. Displacement, Run No. WIPR-3, Test No. WIPR-3-2	213
Figure 152. System Panels and Anchor, Run No. WIPR-4	215
Figure 153. System Installation, Run No. WIPR-4	216
Figure 154. Time-Sequential Photographs, Run No. WIPR-4, Test No. WIPR-4	217
Figure 155. First Panel Damage, Run No. WIPR-4, Test No. WIPR-4	218
Figure 156. Second Panel Damage, Run No. WIPR-4, Test No. WIPR-4	219
Figure 157. Force vs. Displacement and Energy vs. Displacement, Run No. WIPR-4, Test No. WIPR-4	220
Figure 158. Test Vehicle, Test No. APR-1	228
Figure 159. Vehicle Dimensions, Test No. APR-1	229
Figure 160. Test Vehicle, Test No. APR-2	231
Figure 161. Vehicle Dimensions, Test No. APR-2	232
Figure 162. Target Geometry, Test No. APR-1	233
Figure 163. Target Geometry, Test No. APR-2	234
Figure 164. Camera Locations, Speeds, and Lens Settings, Test No. APR-1	238
Figure 165. Camera Locations, Speeds, and Lens Settings, Test No. APR-2	239
Figure 166. Test Installation Layout, Test No. APR-1	241
Figure 167. Test Installation Layout, Test No. APR-2	242
Figure 168. Component Details, Test Nos. APR-1 and APR-2	243
Figure 169. Component Details, Test Nos. APR-1 and APR-2	244
Figure 170. Pedestrian Rail Panel Details, Test Nos. APR-1 and APR-2	245
Figure 171. Bill of Materials, Test Nos. APR-1 and APR-2	246
Figure 172. Pedestrian Rail Test Installation	247
Figure 173. System Panels and Anchors, Test No. APR-1	248
Figure 174 Slots Cut in Baseplates to Aid in Rail Fabrication	249
Figure 175. Summary of Test Results and Sequential Photographs, Test No. APR-1	257
Figure 176. Additional Sequential Photographs, Test No. APR-1	258
Figure 177. Additional Sequential Photographs, Test No. APR-1	259
Figure 178. Documentary Photographs, Test No. APR-1	260
Figure 179. Impact Location, Test No. APR-1	261
Figure 180. Vehicle Final Position and Trajectory Marks, Test No. APR-1	262
Figure 181. System Damage, Test No. APR-1	263
Figure 182. Panel No. 11 Damage, Test No. APR-1	264

Figure 183. Panel No. 12 Damage, Test No. APR-1	265
Figure 184. Panel No. 13 Damage, Test No. APR-1	266
Figure 185. Panel No. 14 Damage, Test No. APR-1	267
Figure 186. Panel No. 15 Damage, Test No. APR-1	268
Figure 187. Vehicle Damage, Test No. APR-1	269
Figure 188. Vehicle Damage, Test No. APR-1	270
Figure 189. Occupant Compartment Damage, Test No. APR-1.....	271
Figure 190. Summary of Test Results and Sequential Photographs, Test No. APR-2.....	280
Figure 191. Additional Sequential Photographs, Test No. APR-2	281
Figure 192. Additional Sequential Photographs, Test No. APR-2	282
Figure 193. Documentary Photographs, Test No. APR-2	283
Figure 194. Impact Location, Test No. APR-2.....	284
Figure 195. Vehicle Final Position and Trajectory Marks, Test No. APR-2.....	285
Figure 196. System Damage, Test No. APR-2	286
Figure 197. Panel No. 1 Damage, Test No. APR-2	287
Figure 198. Panel No. 2 Damage, Test No. APR-2	288
Figure 199. Panel No. 3 Damage, Test No. APR-2	289
Figure 200. Panel No. 4 Damage, Test No. APR-2	290
Figure 201. Panel No. 5 Damage, Test No. APR-2	291
Figure 202. Panel No. 6 Damage, Test No. APR-2	292
Figure 203. Panel No. 7 Damage, Test No. APR-2	293
Figure 204. Panel No. 8 Damage, Test No. APR-2	294
Figure 205. Panel No. 9 Damage, Test No. APR-2	295
Figure 206. Panel No. 10 Damage, Test No. APR-2	296
Figure 207. Vehicle Damage, Test No. APR-2	297
Figure 208. Vehicle Damage, Test No. APR-2	298
Figure 209. Occupant Compartment Damage, Test No. APR-2.....	299
Figure 210. Vehicle Undercarriage Damage, Test No. APR-2.....	300
Figure B-1. Concept 1: PVC Posts, Rails, and Spindles.....	319
Figure B-2. Concept 2: PVC Posts, Rails, and Spindles.....	320
Figure B-3. Concept 3: PVC Posts, Rails, and Spindles.....	321
Figure B-4. Concept 4: PVC Posts and Rails with Mesh	322
Figure B-5. Concept 5: PVC Posts and Rails with Mesh	323
Figure B-6. Concept 6: PVC Posts and Rails	324
Figure B-7. Concept 7: PVC Posts and Rails	325
Figure B-8. Concept 8: Steel Posts and Rails	326
Figure B-9. Concept 9: Steel Posts and Rails with Mesh	327
Figure B-10. Concept 10: Steel Posts and Rails with Mesh	328
Figure B-11. Concept 11: Steel Posts, Rails, and Spindles	329
Figure B-12. Concept 12: Steel Posts and Rails	330
Figure B-13. Concept 13: Steel Posts and Rails	331
Figure B-14. Concept 14: Steel Posts, Rails, and Spindles	332
Figure B-15. Concept 15: Wood Posts and PVC Rails.....	333
Figure B-16. Concept 16: Wood Posts and PVC Rails.....	334
Figure B-17. Concept 17: Wood Posts and Steel Rails	335
Figure B-18. Concept 18: Wood Posts and Steel Rails	336
Figure B-19. Concept 19: Wood Posts and Steel Rails	337

Figure B-20. Design 1: PVC Posts, Rails, and Spindles.....	338
Figure B-21. Design 2: PVC Posts, Rails, and Spindles.....	339
Figure B-22. Design 3: HDPE Posts and Rails.....	340
Figure B-23. Design 4: Wood Posts and Rails	341
Figure B-24. Design 5: HDPE Posts, Wood Rails, FRP Spindles.....	342
Figure B-25. Design 6: FRP Posts, HDPE Rails, PVC Spindles.....	343
Figure C-1. Example Calculation of Weld, Concept AW2-A	348
Figure C-2. Post-to-Base Weld, Concepts AW2-A and AW2-D.....	348
Figure C-3. Post-to-Base Weld, Concept AW2-C.....	349
Figure C-4. Rail-to-Post Weld, Concepts AW2-A, AW2-C, and AW2-D.....	350
Figure C-5. Spindle-to-Rail Weld, Concepts AW2-A, AW2-C, and AW2-D.....	351
Figure C-6. Example Calculation of Baseplate – Method No. 1, Concept AW2-A.....	352
Figure C-7. Example Calculation of Baseplate – Method No. 2, Concept AW2-A.....	353
Figure C-8. Capacity of Baseplate – Method No. 1, Concept AW2-A	354
Figure C-9. Capacity of Baseplate – Method #No. 1, Concept AW2-C.....	354
Figure C-10. Capacity of Baseplate – Method No. 1, Concept AM-1.....	355
Figure C-11. Capacity of Baseplate – Method No. 1, Concept AW2-D	355
Figure C-12. Capacity of Baseplate – Method No. 2, Concept AW2-A	356
Figure C-13. Capacity of Baseplate – Method No. 2, Concept AW2-C.....	357
Figure C-14. Capacity of Baseplate – Method No. 2, Concept AM-1.....	358
Figure C-15. Capacity of Baseplate – Method No. 2, Concept AW2-D	359
Figure C-16. Capacity of Anchors-Tension, Concepts AW2-A and AW2-C.....	360
Figure C-17. Capacity of Anchors-Shear, Concepts AW2-A and AW2-C	361
Figure C-18. Capacity of Anchors-Tension, Concept AW2-D.....	362
Figure C-19. Capacity of Anchors-Shear, Concept AW2-D	363
Figure C-20. Capacity of Anchors-Tension, Concept AM-1.....	364
Figure C-21. Capacity of Anchors-Shear, Concept AM-1	365
Figure C-22. Final Design Calculations, Concept AW2-A	366
Figure C-23. Final Design Calculations, Concept AW2-C.....	367
Figure C-24. Final Design Calculations, Concept AW2-D	368
Figure C-25. Final Design Calculations, Concept AM-1	369
Figure D-1. Bill of Materials and Material Reference, Test Nos. WIPR-1, WIPR-2, and WIPR-4	371
Figure D-2. Bill of Materials and Material Reference, Test Nos. WIPR-3, APR-1, and APR-2	372
Figure D-3. 2"x4"x1/4" Aluminum Post Material Certificate, Test Nos. WIPR-1 and WIPR- 4.....	373
Figure D-4. 1/8" thick Aluminum Post Cap Material Certificate (Sheet 1 of 2), Test Nos. WIPR-1, WIPR-2, and WIPR-4.....	374
Figure D-5. 1/8" thick Aluminum Post Cap Material Certificate (Sheet 2 of 2), Test Nos. WIPR-1, WIPR-2, and WIPR-4.....	375
Figure D-6. Aluminum Post Base Material Certificate (Sheet 1 of 2), Test Nos. WIPR-1, WIPR-2, and WIPR-4	376
Figure D-7. Aluminum Post Base Material Certificate (Sheet 2 of 2), Test Nos. WIPR-1, WIPR-2, and WIPR-4	377
Figure D-8. 2"x2"x1/8" Aluminum Rail Material Certificate, Test Nos. WIPR-1, WIPR-2, and WIPR-4	378

Figure D-9. ½"x½" Aluminum Spindle Material Certificate, Test Nos. WIPR-1, WIPR-2, and WIPR-4	379
Figure D-10. Certificate of Conformance – ⅜" and ½" Threaded Rods, ⅜" Nut, ⅜" Washer, Test Nos. WIPR-1 through WIPR-4.....	380
Figure D-11. 2"x3"x⅛" Aluminum Post Material Certificate, Test No. WIPR-2.....	381
Figure D-12. Certificate of Conformance – ¼" Dia. x 3" Bolt and ¼" Nut, Test No. WIPR- 2.....	382
Figure D-13. 2" Dia. Schedule 80 Aluminum Post Material Certificate (Sheet 1 of 2), Test No. WIPR-3	383
Figure D-14. 2" Dia. Schedule 80 Aluminum Post Material Certificate (Sheet 2 of 2), Test No. WIPR-3	384
Figure D-15. 2" Dia. Schedule 40 Aluminum Post Material Certificate (Sheet 1 of 2), Test No. WIPR-3	385
Figure D-16. 2" Dia. Schedule 40 Aluminum Post Material Certificate (Sheet 2 of 2), Test No. WIPR-3	386
Figure D-17. ¾" Dia. Schedule 10 Aluminum Picket Material Certificate, Test No. WIPR-3...	387
Figure D-18. 2"x4"x¼" Aluminum Post Material Certificate, Test Nos. APR-1 and APR-2.....	388
Figure D-19. 1/8" thick Aluminum Post Cap Material Certificate (Sheet 1 of 2), Test Nos. APR-1 and APR-2.....	389
Figure D-20. 1/8" thick Aluminum Post Cap Material Certificate (Sheet 2 of 2), Test Nos. APR-1 and APR-2.....	390
Figure D-21. Aluminum Post Base Material Certificate, Test Nos. APR-1 and APR-2	391
Figure D-22. 2"x2"x1/8" Aluminum Rail Material Certificate, Test Nos. APR-1 and APR-2...	392
Figure D-23. ½"x½" Aluminum Spindle Material Certificate (Sheet 1 of 2), Test Nos. APR-1 and APR-2.....	393
Figure D-24. ½"x½" Aluminum Spindle Material Certificate (Sheet 2 of 2), Test Nos. APR-1 and APR-2.....	394
Figure D-25. ½" Threaded Rod Material Certificate, Test Nos. APR-1 and APR-2.....	395
Figure D-26. ½" Nut Material Certificate (Sheet 1 of 2), Test Nos. APR-1 and APR-2	396
Figure D-27. ½" Nut Material Certificate (Sheet 2 of 2), Test Nos. APR-1 and APR-2	397
Figure D-28. ½" Washer Material Certificate, Test Nos. APR-1 and APR-2	398
Figure E-1. Vehicle Mass Distribution, Test No. APR-1	400
Figure E-2. Vehicle Mass Distribution, Test No. APR-2	401
Figure F-1. Fabrication Drawings, Test Nos. APR-1 and APR-2	403
Figure F-2. Fabrication Drawings, Test Nos. APR-1 and APR-2	404
Figure F-3. Fabrication Drawings, Test Nos. APR-1 and APR-2	405
Figure F-4. Fabrication Drawings, Test Nos. APR-1 and APR-2	406
Figure F-5. Fabrication Drawings, Test Nos. APR-1 and APR-2	407
Figure F-6. Fabrication Drawings, Test Nos. APR-1 and APR-2	408
Figure F-7. Fabrication Drawings, Test Nos. APR-1 and APR-2	409
Figure F-8. Fabrication Drawings, Test Nos. APR-1 and APR-2	410
Figure F-9. Fabrication Drawings, Test Nos. APR-1 and APR-2	411
Figure F-10. Fabrication Drawings, Test Nos. APR-1 and APR-2	412
Figure G-1. Floorpan Deformation Data – Set 1, Test No. APR-1	414
Figure G-2. Floorpan Deformation Data – Set 2, Test No. APR-1	415
Figure G-3. Occupant Compartment Deformation Data – Set 1, Test No. APR-1.....	416
Figure G-4. Occupant Compartment Deformation Data – Set 2, Test No. APR-1.....	417

Figure G-5. Exterior Vehicle Crush (NASS) - Front, Test No. APR-1	418
Figure G-6. Exterior Vehicle Crush (NASS) - Side, Test No. APR-1.....	419
Figure G-7. Floorpan Deformation Data – Set 1, Test No. APR-2	420
Figure G-8. Floorpan Deformation Data – Set 2, Test No. APR-2	421
Figure G-9. Occupant Compartment Deformation Data – Set 1, Test No. APR-2.....	422
Figure G-10. Occupant Compartment Deformation Data – Set 2, Test No. APR-2.....	423
Figure G-11. Exterior Vehicle Crush (NASS) - Front, Test No. APR-2.....	424
Figure G-12. Exterior Vehicle Crush (NASS) - Side, Test No. APR-2.....	425
Figure H-1. 10-ms Average Longitudinal Deceleration (DTS), Test No. APR-1	427
Figure H-2. Longitudinal Occupant Impact Velocity (DTS), Test No. APR-1	428
Figure H-3. Longitudinal Occupant Displacement (DTS), Test No. APR-1	429
Figure H-4. 10-ms Average Lateral Deceleration (DTS), Test No. APR-1	430
Figure H-5. Lateral Occupant Impact Velocity (DTS), Test No. APR-1	431
Figure H-6. Lateral Occupant Displacement (DTS), Test No. APR-1	432
Figure H-7. Vehicle Angular Displacements (DTS), Test No. APR-1.....	433
Figure H-8. Acceleration Severity Index (DTS), Test No. APR-1	434
Figure H-9. Longitudinal Occupant Impact Velocity (SLICE-2), Test No. APR-1	436
Figure H-10. Longitudinal Occupant Displacement (SLICE-2), Test No. APR-1	437
Figure H-11. 10-ms Average Lateral Deceleration (SLICE-2), Test No. APR-1.....	438
Figure H-12. Lateral Occupant Impact Velocity (SLICE-2), Test No. APR-1	439
Figure H-13. Lateral Occupant Displacement (SLICE-2), Test No. APR-1	440
Figure H-14. Vehicle Angular Displacements (SLICE-2), Test No. APR-1	441
Figure H-15. Acceleration Severity Index (SLICE-2), Test No. APR-1	442
Figure I-1. 10-ms Average Longitudinal Deceleration (DTS), Test No. APR-2.....	444
Figure I-2. Longitudinal Occupant Impact Velocity (DTS), Test No. APR-2	445
Figure I-3. Longitudinal Occupant Displacement (DTS), Test No. APR-2	446
Figure I-4. 10-ms Average Lateral Deceleration (DTS), Test No. APR-2	447
Figure I-5. Lateral Occupant Impact Velocity (DTS), Test No. APR-2.....	448
Figure I-6. Lateral Occupant Displacement (DTS), Test No. APR-2.....	449
Figure I-7. Vehicle Angular Displacements (DTS), Test No. APR-2	450
Figure I-8. Acceleration Severity Index (DTS), Test No. APR-2	451
Figure I-9. 10-ms Average Longitudinal Deceleration (SLICE-2), Test No. APR-2.....	452
Figure I-10. Longitudinal Occupant Impact Velocity (SLICE-2), Test No. APR-2.....	453
Figure I-11. Longitudinal Occupant Displacement (SLICE-2), Test No. APR-2	454
Figure I-12. 10-ms Average Lateral Deceleration (SLICE-2), Test No. APR-2	455
Figure I-13. Lateral Occupant Impact Velocity (SLICE-2), Test No. APR-2.....	456
Figure I-14. Lateral Occupant Displacement (SLICE-2), Test No. APR-2.....	457
Figure I-15. Vehicle Angular Displacements (SLICE-2), Test No. APR-2	458
Figure I-16. Acceleration Severity Index (SLICE-2), Test No. APR-2.....	459

LIST OF TABLES

Table 1. Pooled Fund Member Responses to Highest Need–Pedestrian Rail Survey	40
Table 2. Wisconsin DOT Response to Highest Need–Pedestrian Rail Survey	40
Table 3. General Material Comparisons	45
Table 4. Relevant Material Properties [37]	45
Table 5. Aluminum Alloy 6061-T6 Material Strengths [38]	131
Table 6. Rectangular Tubes Shear Strength [38]	133
Table 7. Round or Oval Tubes Shear Strength [38]	135
Table 8. Pipe Flexural Local Buckling Strength [38]	138
Table 10. Bogie Testing Matrix	181
Table 11. MASH TL-2 Crash Test Conditions	224
Table 12. MASH Evaluation Criteria for Longitudinal Channelizers	226
Table 13. Weather Conditions, Test No. APR-1	250
Table 14. Sequential Description of Impact Events, Test No. APR-1	251
Table 15. Final Locations of Disengaged Panels, Test No. APR-1	253
Table 16. Maximum Occupant Compartment Deformations by Location	254
Table 17. Summary of OIV, ORA, THIV, PHD, and ASI Values, Test No. APR-1	255
Table 18. Weather Conditions, Test No. APR-2	272
Table 19. Sequential Description of Impact Events, Test No. APR-2	273
Table 20. Final Location of Disengaged Panels, Test No. APR-2	275
Table 21. Maximum Occupant Compartment Deformations by Location	276
Table 23. Summary of Safety Performance Evaluation Results	307
Table B-1. Material Properties, Concepts 1 through 19	318
Table B-2. Material Properties, Designs 1 through 6	318
Table C-1. Material Strengths for 6061-T6 Aluminum from Tables A.3.4, A.3.5, and A3.1 in ADM [38]	345
Table C-2. Material Strengths for 5356 Aluminum Weld Filler from Table J.2.1 in ADM [38]	345
Table C-3. Material Strengths for 535 Aluminum Alloy Castings from Table A.3.6 in ADM [38]	345

1 INTRODUCTION

1.1 Background

The National Highway Traffic Safety Administration (NHTSA) estimated that approximately 4,300 pedestrian fatalities occurred in the United States in 2010 [1]. Leaf and Preusser estimated that only 5 percent of pedestrians would die when struck by a vehicle traveling at 20 miles per hour or less, while fatality rates of 40, 80, and nearly 100 percent would occur for vehicles striking pedestrians at 30, 40 and 50 mph or more, respectively [2]. Pedestrian fatalities may be related to transportation designs as well as human behaviors [3]. Many pedestrian-vehicle events are caused by motorists and pedestrians not understanding and/or obeying laws and safe behaviors pertaining to driving and walking [4].

Risk of pedestrian injury is highest when crossing the street. Many intersections have designated crosswalk areas for pedestrians to safely cross the street, and these marked areas inform drivers to be mindful of pedestrian traffic. However, pedestrians may choose a more direct path or be distracted and enter the roadway in non-marked areas. Pedestrian rails are often placed adjacent to roadways to protect pedestrians from hazardous drop offs or dangerous excursions into the roadway. Examples of such areas, as shown in Figure 1, include (1) sidewalks over culverts where a pedestrian rail may be necessary to separate pedestrians from hazardous drop offs or (2) busy streets where median fences may be used to deter pedestrians from crossing in non-designated crossing locations. In some cases where pedestrian rails are installed to prevent pedestrians from entering areas adjacent to right of way, as shown in Figure 2, the pedestrian rail may also prevent pedestrian maneuver options like escaping an errant vehicle. Thus, pedestrian rail design and placement should be carefully considered.

Although numerous pedestrian rails have been designed, their performance has never been evaluated during vehicular impact events. The Wisconsin Department of Transportation provided some examples of vehicle impacts on pedestrian rails are shown in Figure 3. Pedestrian rails that have not been evaluated to vehicle impact safety performance standards may be hazardous to the passengers of errant vehicles due to disengaged components penetrating the windshield or occupant compartment, excessive vehicle decelerations, or vehicle instability and rollover.

1.2 Objective

The objective of this research project was to design a crashworthy pedestrian rail that will protect pedestrians from hazards while not posing an undue safety risk to motorists and pedestrians. The new pedestrian rail must meet the design standards associated with the Americans with Disabilities Act (ADA) [5] and the pedestrian rail standards contained in the American Association of State Highway and Transportation Officials (AASHTO) *Load and Resistance Factor Design (LRFD) Bridge Design Specifications* [6]. In addition, the pedestrian rail was evaluated according to the Test Level 2 (TL-2) safety performance criteria for longitudinal channelizers published in the AASHTO *Manual for Assessing Safety Hardware* (MASH) [7].

1.3 Scope

The research objective was achieved through the completion of several tasks. First, a survey was conducted of the Midwest States Pooled Fund Program members to identify the most common locations and circumstances in which a crashworthy pedestrian rail would be warranted. Next, a review was conducted of existing pedestrian rail and fence designs from State Departments of Transportation (DOT) and product manufacturers. Potential fabrication

materials, such as aluminum, steel, wood, and polymers, were investigated. Design concepts were configured, and the preferred concepts were selected for further evaluation. Bogie tests were conducted on the selected design concepts to evaluate their performance behavior. Two full-scale vehicle crash tests were performed in accordance with the MASH TL-2 impact conditions for longitudinal channelizers. The test results were analyzed, evaluated, and documented. Finally, conclusions and recommendations were made that pertain to the safety performance of the new pedestrian rail system.



Figure 1. Examples of Pedestrian Rails



Figure 2. Pedestrian Rail Limiting Pedestrian Maneuver Options



Figure 3. Vehicle Impacts with Pedestrian Rails

2 LITERATURE REVIEW

2.1 Standards

The prototype design concepts considered within this research project must meet three standards and guidelines to satisfy the objectives stated earlier. The pedestrian rail must be ADA compliant and meet AASHTO *LRFD Bridge Design Specifications*, which ensures that the rail will be accessible for use by all people as well as safely function as a longitudinal channelizer. Additional pedestrian rail design criteria included the International Building Code (IBC) [8] and Occupational Safety and Health Administration (OSHA), Part 1910 [9]. The AASHTO *LRFD Bridge Design Specifications* were used for the rail loading requirements, as they varied between the standards. The final design concept would be evaluated according to the MASH Test Level 2 safety performance criteria for longitudinal channelizers [7].

2.1.1 Americans with Disabilities Act Design Criteria

A pedestrian rail must be accessible to all people, including those with disabilities. The *2010 ADA Standards for Accessible Design* sets forth handrail criteria [5]. The handrail needs to be continuous along the full length of the walkway and not be obstructed on the top or sides. The handrail top gripping surface should be a minimum of 34 in. (864 mm) and a maximum of 38 in. (965 mm) vertically above the walking surface. There should be a minimum of 1½ in. (38 mm) separation between the back surface of the handrail and any adjacent surface. The handrail gripping surface for a circular cross section shall have minimum and maximum outside diameters of 1¼ in. (32 mm) and 2 in. (51 mm), respectively. Non-circular cross sections shall have minimum and maximum perimeters of 4 in. (102 mm) and 6¼ in. (159 mm), respectively, with the diagonal cross section length no greater than 2¼ in. (57 mm). Maximum diagonal dimensions for a non-circular cross section are shown in Figure 4. If fittings are used, the handrail shall not rotate within them. When a vertical or horizontal force of 250 lb (1,112 N) is

applied on any point on the handrail, fasteners, mounting devices, or supporting structures, the allowable stresses shall not be exceeded.

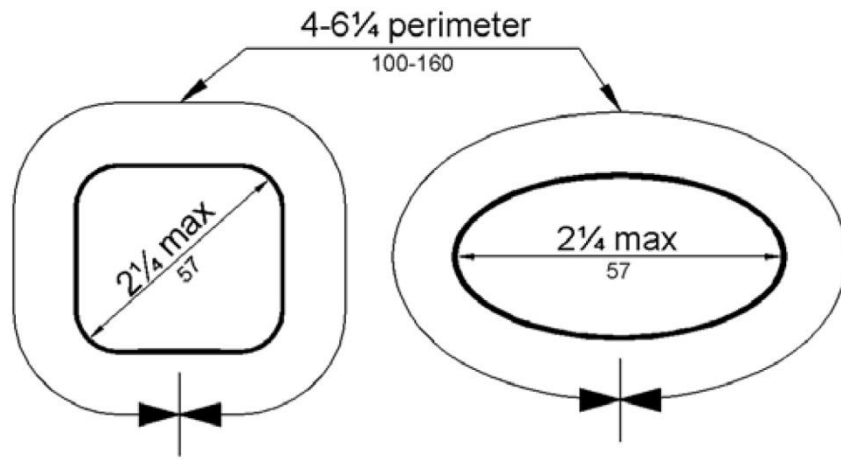


Figure 4. ADA Non-Circular Cross Section Dimensions

2.1.2 AASHTO LRFD Bridge Design Specifications

The AASHTO *LRFD Bridge Design Specifications* also provided requirements for the design of a pedestrian rail [6]. Pedestrian rail height should be a minimum of 42 in. (1,067 mm) above the walkway. A clear spacing shall apply to the lower 27 in. (686 mm) of the railing where a 6-in. (152-mm) diameter sphere cannot pass through the rail elements. The clear spacing in the upper section of the railing above 27 in. (686 mm) shall not allow an 8-in. (203-mm) diameter sphere to pass through the rail elements. Chain link or metal fabric fence should not have openings larger than 2 in. (51 mm).

Longitudinal railing elements must withstand a uniform live load of 50 lb/ft (730 N/m) simultaneously applied both transversely and vertically, along with a concentrated live load of 200 lb (890 N) applied at any point and in any direction on the longitudinal element, as shown in Figure 5. The posts are subjected to a concentrated live load, P_{LL} , defined in Equation 1. The concentrated live load P_{LL} shall be applied transversely at the center of gravity of the upper horizontal element. For a railing mounted taller than 5 ft (1.5 m), P_{LL} shall be applied at a point 5

ft (1.5 m) above the walkway. Chain link or metal fabric fence shall be designed for a distributed live wind load of 15 lb/ft² (718 N/m²) applied perpendicular to the entire mesh surface.

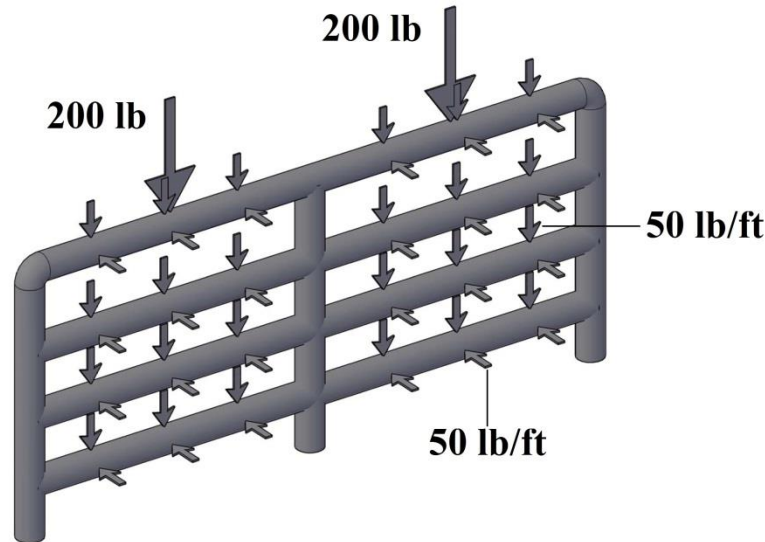


Figure 5. AASHTO Loading Criteria (Vertical 200-lb Point Load Shown)

$$P_{LL} = 200 + 50L \quad (1)$$

Where: P_{LL} = Post Point Live Load (lb)
 L = Post Spacing (ft)

2.1.3 International Building Code

The 2012 IBC [8] also contains handrail design criteria similar to the ADA code. The handrail shall be continuous along the full length of the walkway and not be obstructed on the top or side. The handrail top gripping surface should be a minimum of 34 in. (864 mm) and a maximum of 38 in. (965 mm) vertically above the walking surface. There should be a minimum separation of 1½ in. (38 mm) between the back surface of the handrail and any adjacent surface. Handrail gripping surfaces with circular cross sections shall have minimum and maximum outside diameter of 1¼ in. and 2 in. (32 mm and 51 mm), respectively. Non-circular cross sections shall have minimum and maximum surface perimeters of 4 in. and 6¼ in. (102 mm and 159 mm), respectively, with the cross section dimension of at least 1 in. (25 mm) but no greater

than 2¼ in. (57 mm). Edges shall have a minimum radius of 0.01 in. (0.25 mm). If fittings are used, the handrail shall not rotate within them. Handrails should be designed to resist a linear load of 50 lb/ft (730 N/m). Handrails should also be designed to resist a concentrated load of 200 lb (890 N) applied in any direction at any point along the top. Intermediate rails, balusters, and panel fillers should be designed to resist a concentrated load of 50 lb (222 N).

2.1.4 Occupational Safety & Health Administration (OSHA)

Handrail design criteria is also contained in *Part 1910 – Occupational Safety & Health Administration Regulations (Standards – 29 CFR)* [9]. A standard railing shall consist of a top rail, intermediate rail, and posts and shall have a vertical height of 42 in. (1,067 mm), as measured between the upper surface of top rail to the ground. The top rail shall be smooth throughout the length of the railing. Pipe railings, posts, and top and intermediate railings shall be at least 1½ in. (38 mm) nominal diameter with posts spaced not more than 8 ft (2.4 m) on center. The complete structure shall be capable of withstanding 200 lb (890 N) load applied in any direction at any point on the top rail.

2.1.5 AASHTO MASH Longitudinal Channelizers

Longitudinal channelizers are intended to provide clear visual indication of the intended vehicle path through a construction zone. They are not intended to contain and redirect impacting vehicles. The vehicle is allowed to traverse through and behind the system. Thus, the impact performance criterion for longitudinal channelizers is different from those used for longitudinal barriers. For MASH TL-2 longitudinal channelizers, two full-scale crash tests are recommended, test designation no. 2-90 with an 1100C vehicle and test designation no. 2-91 with a 2270P vehicle [7]. The impact conditions for each test vehicle are a speed of 44 mph (70 km/h) and a critical impact angle between 0 and 25 degrees that maximize the risk of vehicle rollover and excessive vehicle decelerations.

2.2 Existing Pedestrian Rail Designs

Four categories of pedestrian rails were considered: (1) concrete combination barriers, (2) plastic fences, (3) wood fences, and (4) metal rails. Concrete barriers are the most costly and are often used in combination with a metal rail or chain link fence to accommodate pedestrian safety in high-speed facilities. Metal rails are typically fabricated with aluminum or steel for strength and ease of construction. Wood fences are used for economic reasons. Current polymer fences are fabricated with polyvinyl chloride (PVC), high density polyethylene (HDPE), and fiber-reinforced polymers (FRP) for aesthetics and corrosion resistance. Most combination concrete barriers and pedestrian rail designs have been crash tested according to safety performance criteria. However, plastic, wood, and metal fences and rails historically have not been crash tested. The most prominent designs are categorized in the following sections. However, this is not an all-inclusive list of pedestrian rail designs.

2.2.1 Concrete Combination Traffic and Pedestrian Rail Designs

The Minnesota combination bridge rail is an example of a traffic and bicycle combination bridge rail that has been developed and successfully crash-tested [10]. This system successfully met all Test Level 3 (TL-3) safety performance criteria of National Cooperative Highway Research Program (NCHRP) Report No. 350, *Recommended Procedures for the Safety Performance Evaluation of Highway Features* [11]. This bridge rail utilized a 31 $\frac{7}{8}$ -in. (810-mm) high New Jersey safety shape barrier with steel panels formed from tubular steel and posts, and square vertical spindle bolted to the back-side vertical face of the concrete barrier. The steel rail extended 22 $\frac{1}{2}$ in. (572 mm) above the Jersey barrier, giving a total barrier height of 54 $\frac{3}{8}$ in. (1,381 mm). This bridge rail is a longitudinal barrier that contains and redirects impacting vehicles as well as prevents pedestrians from crossing at non-designated crossing locations, but

is more expensive and requires more installation time than a pedestrian-only rail channelizer. The Minnesota combination bridge rail is shown in Figure 6.



Figure 6. Minnesota Combination Traffic and Pedestrian Barrier [10]

2.2.2 Plastic Fence Designs

Plastic fence designs create separation between two areas and are typically fabricated using HDPE, FRP, or PVC. Many HDPE designs were observed for use in large animal containment. FRP designs were commonly used as safety handrails. PVC fences commonly serve as boundaries on personal properties.

HDPE fences are durable and virtually maintenance-free and stain resistant. HDPE is more resistant to shattering and splitting at low temperatures than common polymers. HDPE has very low material strength. The base of HDPE posts are commonly supported with a wood or metal insert. Examples of existing HDPE fences are shown in Figure 7 [12-14].

FRP is a composite material made of a polymer reinforced with fibers, usually glass. FRPs also have a low weight-to-strength ratio. FRP handrail systems are corrosion-resistant, giving them a long lifespan with little maintenance. UV inhibitors are added to the resin during fabrication, along with a synthetic surfacing veil, providing protections from UV weathering. For these reasons, FRP handrails are often used in extreme climate locations or facilities with highly corrosive chemicals. Most FRP rail systems are yellow for safety reasons but also can be fabricated in any color. Dynarail and SAFRAIL, as shown in Figure 8, are two of many FRP handrails [15-17].

PVC fencing is commonly found as decorative barriers to divide personal property. A PVC fence design offers virtually no maintenance with ultraviolet inhibitors in the vinyl to prevent it from changing color and material properties. PVC material may become brittle under low temperatures. PVC can come in a wide range of colors, but when heated, material strength properties decline. For this reason, PVC fences are usually white to reflect the sun. The PVC posts are commonly supported with a wood or metal insert. Examples of PVC fencing are shown in Figure 9 [18-20].



Figure 7. Examples of Existing HDPE Fences [12-14]



Figure 8. Examples of Existing FRP Handrail Systems [15-17]



Figure 9. Examples of Existing PVC Fences [18-20]

2.2.3 Existing Wood Fence Designs

Wood fences are generally used to separate personal property by acting as boundary lines and to contain large animals. Non-treated wood can be highly susceptible to decay, rotting, and bug deterioration. For this reason, most wood fences require preservative treatment as well as continuous maintenance and repair. Wood material properties can vary significantly, so the strength of each fence system may vary. Wood fences historically have not been crash tested, and the post and rail components may be penetrate the windshield or occupant compartment when impacted by errant vehicles in some cases, as shown in Figure 3. Examples of wood fencing are shown in Figure 10 [21-24].

2.2.4 Metal Barrier Designs

The New Southern Wales Roads and Traffic Authority (RTA) developed two steel pedestrian rail concepts, the RTA Designed Pedestrian Fence and the Modified Welded Steel Mesh Fencing [25]. The RTA Designed Pedestrian Fence, as shown in Figure 11, was composed of customized steel posts and two rails connected with steel balusters. The balusters gave the barrier an anti-climb design. Although the fence was designed to collapse during impact to minimize damage on individual elements, evidence of crash testing was not provided. The staggered layout of the balusters permits visibility on both sides. This pedestrian fence design is preferred by the RTA.

The Modified Welded Steel Mesh, as shown in Figure 12, was designed to deform safely upon vehicle impact, although no evidence of crash testing was provided. It differed from the Pedestrian Fence in that it was more difficult to see through at acute angles. Near the bottom of the fence was a longitudinal 0.4-in. (10-mm) diameter galvanized steel cable that ran through each panel and post. The cable was tied and clamped at the end posts. To prevent the bottom

from opening significantly when impacted, the bottom of the panels was secured with two heavy-gauge split links.

Based on a 1988 study in the United Kingdom, pedestrian rails placed near the roadway diminish the ability for pedestrians and vehicles to see one another [26]. This fact is most prominent when the pedestrian is a child who cannot see over the rail. Although the use of pedestrian rails has shown to effectively improve road safety, the lack of visibility has been shown to be detrimental to road safety, especially for children. For this reason, Pell & Baldwin LTD created a steel, pedestrian-only rail called the VISIFLEX pedestrian guardrail, which was a more visible rail for pedestrians and motorists [27]. The VISIFLEX pedestrian guardrail, as shown in Figure 13, was composed with only three components – standard panels with balusters, stub posts, and an end bar. All components were fabricated with galvanized steel. The balusters were placed at an angle and spaced appropriately for optimum visibility. The simple design allows for easy installation and repair of the VISIFLEX system.

The Iowa DOT designed a welded handrail as a pedestrian rail, as shown in Figure 14 [28]. The design consisted of two 2½-in. (64-mm) diameter steel pipe rails. The top rail was 45 in. (1,143 mm) above the walkway, and the second rail was 24 in. (610 mm) above the walkway. The 2½-in. (64-mm) diameter steel pipe posts were welded to the rail elements and an 8½-in. x ¾-in. x 8½-in. (216-mm x 19-mm x 216-mm) steel plate at the base of the post. The steel plate was attached with four ⅝-in. (16-mm) diameter steel stud concrete anchors, which fixed the pedestrian rail system to the ground.

The Washington State DOT designed a 42-in. (1,067-mm) tall aluminum handrail, as shown in Figures 15 and 16 [29]. Two horizontal 2½-in. (64-mm) diameter horizontal rails were spliced at the posts and were 4 in. (102 mm) and 42 in. (1,067 mm) above the walkway. Posts were 2½ in. (64 mm) in diameter and spaced at 7 ft (2.1 m). The lower pipe surface was 4 in.

(102 mm) above the walkway surface. Eleven 1-in. (25-mm) diameter baluster pipes spanned vertically between the rails in each panel section.



Figure 10. Examples of Existing Wood Fences [21-24]



Figure 11. RTA Designed Pedestrian Barrier [25]



Figure 12. RTA Modified Steel Mesh [25]

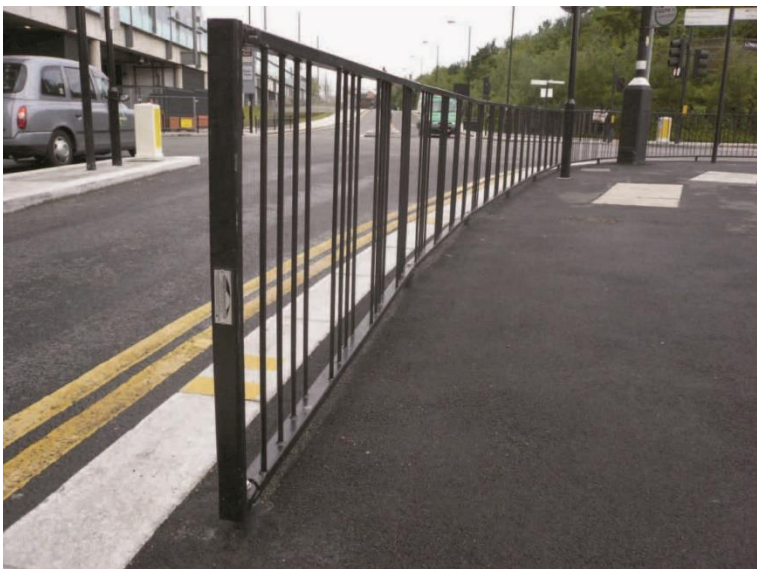


Figure 13. VISIFLEX Pedestrian Guardrail [27]

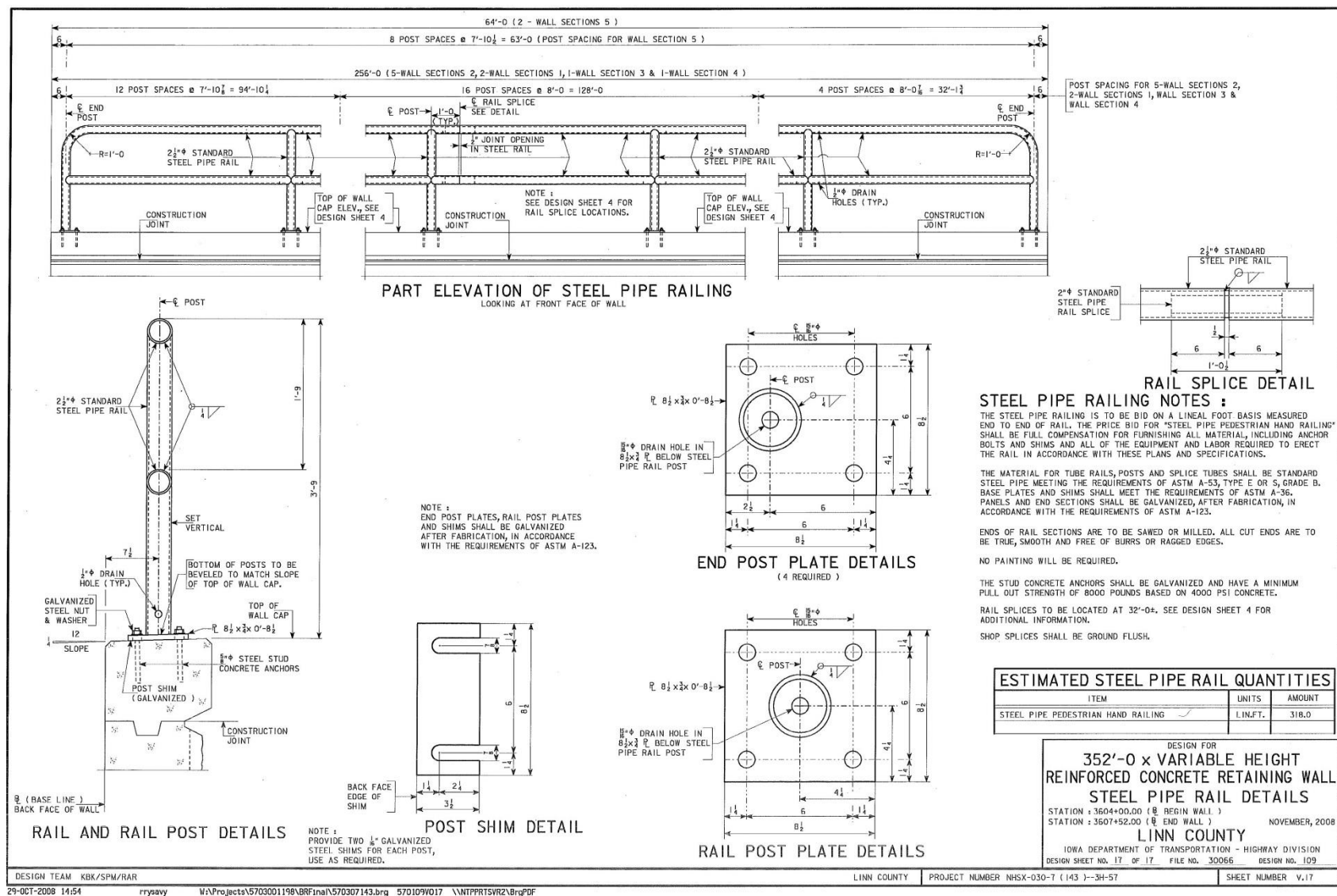
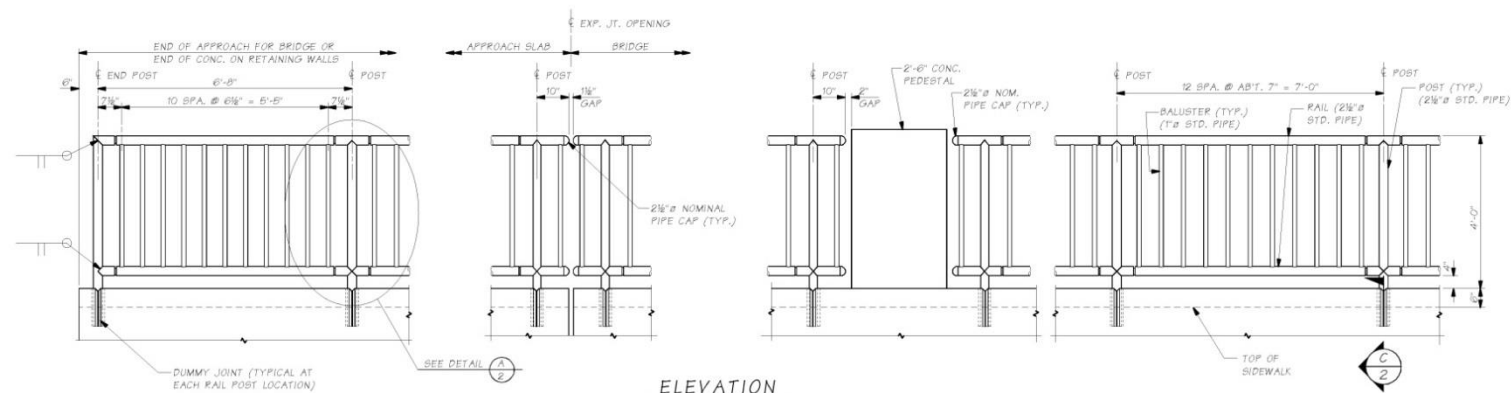


Figure 14. Iowa DOT Steel Pipe Rail [28]



ELEVATION
BALUSTERS NORMAL TO GRADE.
TOP & BOTTOM RAILS PARALLEL TO GRADE.

NOTES

1. PIPE RAILING, AND PIPE RAILING SPLICES, SHALL BE BENT TO THE HORIZONTAL CURVE WHERE THE RADIUS OF CURVATURE IS LESS THAN 200 FEET.
2. SHOP DRAWINGS OF RAILING SHALL BE SUBMITTED FOR APPROVAL SHOWING COMPLETE DIMENSIONS AND DETAILS OF FABRICATION AND INCLUDING AN ERECTION DIAGRAM. MATERIAL BEING USED SHALL BE SPECIFIED IN THE SHOP DRAWINGS.
3. PIPE RAILING, AND PIPE RAILING SPLICES, MAY BE HEATED TO NOT MORE THAN 400°F FOR A PERIOD NOT TO EXCEED 30 MINUTES TO FACILITATE FORMING OR BENDING HORIZONTAL CURVATURE.
4. CUTTING SHALL BE DONE BY SAWING OR MILLING AND ALL CUTS SHALL BE TRUE AND SMOOTH. FLAME CUTTING WILL NOT BE PERMITTED.
5. WELDING OF ALUMINUM SHALL CONFORM TO STD. SPEC. SECTION 9-20.14(3).
6. AFTER FABRICATION, POSTS SHALL BE HEAT TREATED IN ACCORDANCE WITH SECTION 6.5 OF THE AASHTO STANDARD SPECIFICATIONS FOR STRUCTURAL SUPPORTS FOR HIGHWAY SIGNS, LUMINAIRES, AND TRAFFIC SIGNALS DATED 2001 AND INTERIMS THROUGH 2003.
7. ALL ALUMINUM PARTS SHALL BE GIVEN A (CLEAR OR BRONZE)* ANODIC COATING OF AT LEAST 0.0006 INCHES THICK AND SEALED TO MEET THE REQUIREMENTS OF ASTM B 580 WITH A UNIFORM FINISH.
8. PIPE RAILING, PIPE BALUSTERS, PIPE RAILING SPLICES, SHALL BE ADEQUATELY WRAPPED TO INSURE SURFACE PROTECTION DURING HANDLING AND TRANSPORTATION TO THE JOB SITE.

* NOTE TO DESIGNER:
Designer to choose color for their project in consultation with the Bridge Architect.

PART	MATERIAL SPECIFICATION
PIPES	ASTM B 221-6005-T5 SCHEDULE 40 (STD. PIPE) ASTM B 241 OR B 429 6061-T6
BAR	ASTM B 221-6005-T5
DRIVE PINS	ASTM A 276 TYPE 302 STAINLESS STEEL

SHEET 10.5-A-1

Bridge Design Engr.	MISTANDRISBF Ralls4fsPaRail_Alumin_LMAN	DESIGN NO.	STATE	FED. AID PROJ. NO.	SHEET NO.	TOTAL SHEETS	<div align="center"> BRIDGE AND STRUCTURES OFFICE Washington State Department of Transportation </div>	<div align="center"> STANDARD RAILINGS PEDESTRIAN RAILING DETAILS 1 OF 2 </div>	DATE	REVISION	BY	APPD
Supervisor		10	WASH.									
Designed By		JOB NUMBER										
Checked By												
Bridge Projects Engr.												
Platm. Plan By												
Architect/Specifier												

Tue Feb 01 11:44:57 2011

Figure 15. Washington DOT Standard Railing (Sheet 1 of 2) [29]

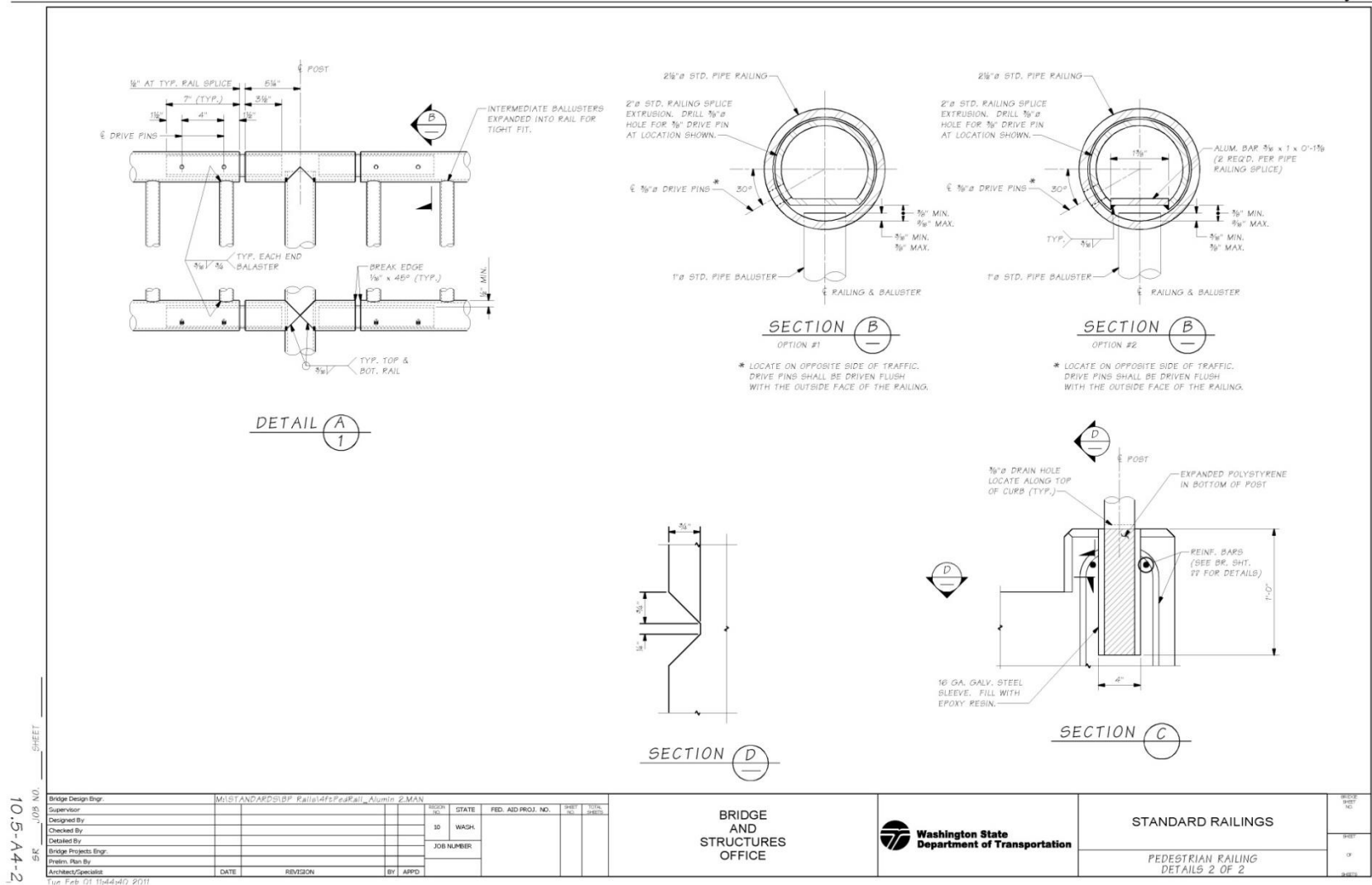


Figure 16. Washington DOT Standard Railing (Sheet 2 of 2) [29]

The Texas DOT pedestrian rail consisted of six horizontal rails, as shown in Figure 17 [30]. The top rail was a 3-in. (76 mm) standard steel pipe and the lower five rails were 2-in. (51 mm) standard steel pipe. Posts were 5 in. (127 mm) wide and spaced at a maximum of 10 ft (3.1 m) apart. The minimum rail height was 42 in. (1,067 mm) above the walkway.

The Ultra-tec Cable Railing Systems used varying cable diameters and frame constructions to accommodate for various uses, one of which was pedestrian rail [31]. Cables could be aligned horizontally or vertically across the frame, as shown in Figure 18 and Figure 19. The cables were spaced 3 in. (76 mm) from each other and had to each support a 400-lb (1,779-N) tension minimum. Support rail braces should be placed at a minimum spacing of 42 in. (1,067 mm). If the cables are not tensioned properly, the end posts may bend due to high cable tension.

An aluminum, pedestrian-only rail was designed by the Florida Department of Transportation (FDOT), to meet the AASHTO and ADA load and dimension requirements, as shown in Figure 20 through Figure 27 [32-33]. The rail consisted of structural tubes, pipes, and bars made of aluminum alloy 6061-T6. The end hoop sections of the rail were fabricated with alloy 6063-T5 for better formability. Two 2-in. x 2-in. x 1/4-in. (51-mm x 51-mm x 6-mm) square tubes were used at each post location, separated by 5 3/4 in. (146 mm). Total post spacing was specified as 5 ft – 8 in. (1.7 m). The top horizontal member was a Schedule 10 2 1/2-in. nominal pipe size (73-mm x 3-mm) round tube. The bottom and intermediate horizontal members were 2-in. x 2-in. x 1/4-in. (51-mm x 51-mm x 6-mm) square tubes. Five infill panel options were specified including 3/4-in. (19-mm) diameter round bar pickets. The pickets spanned between the intermediate and bottom longitudinal rails. This rail also specified an ADA-compliant handrail attachment.



Figure 17. Texas DOT Handrail [30]

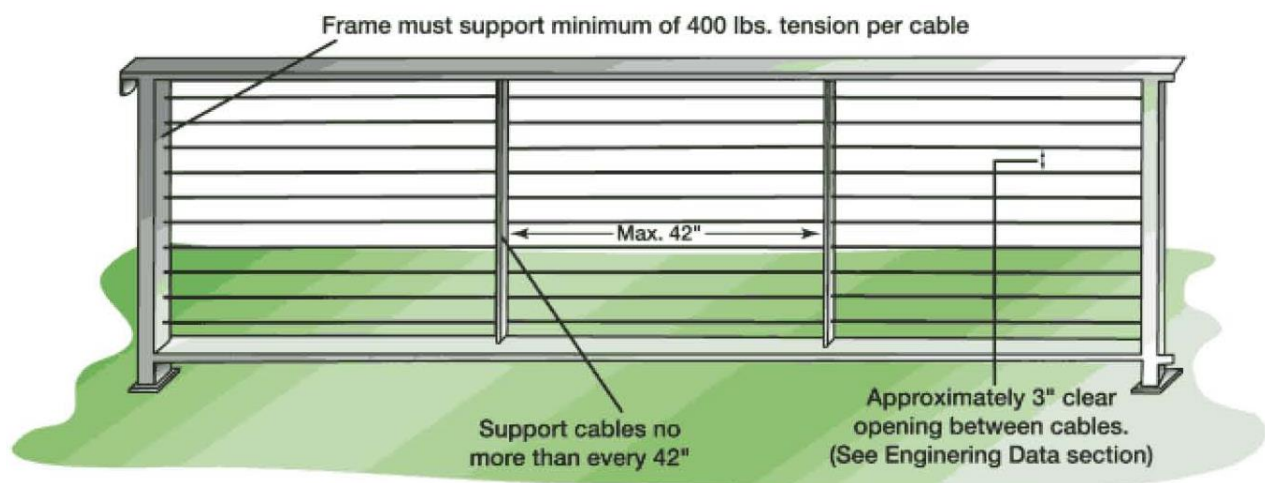


Figure 18. Horizontal Cable Frame [31]



Figure 19. Vertical Cable Frame [31]

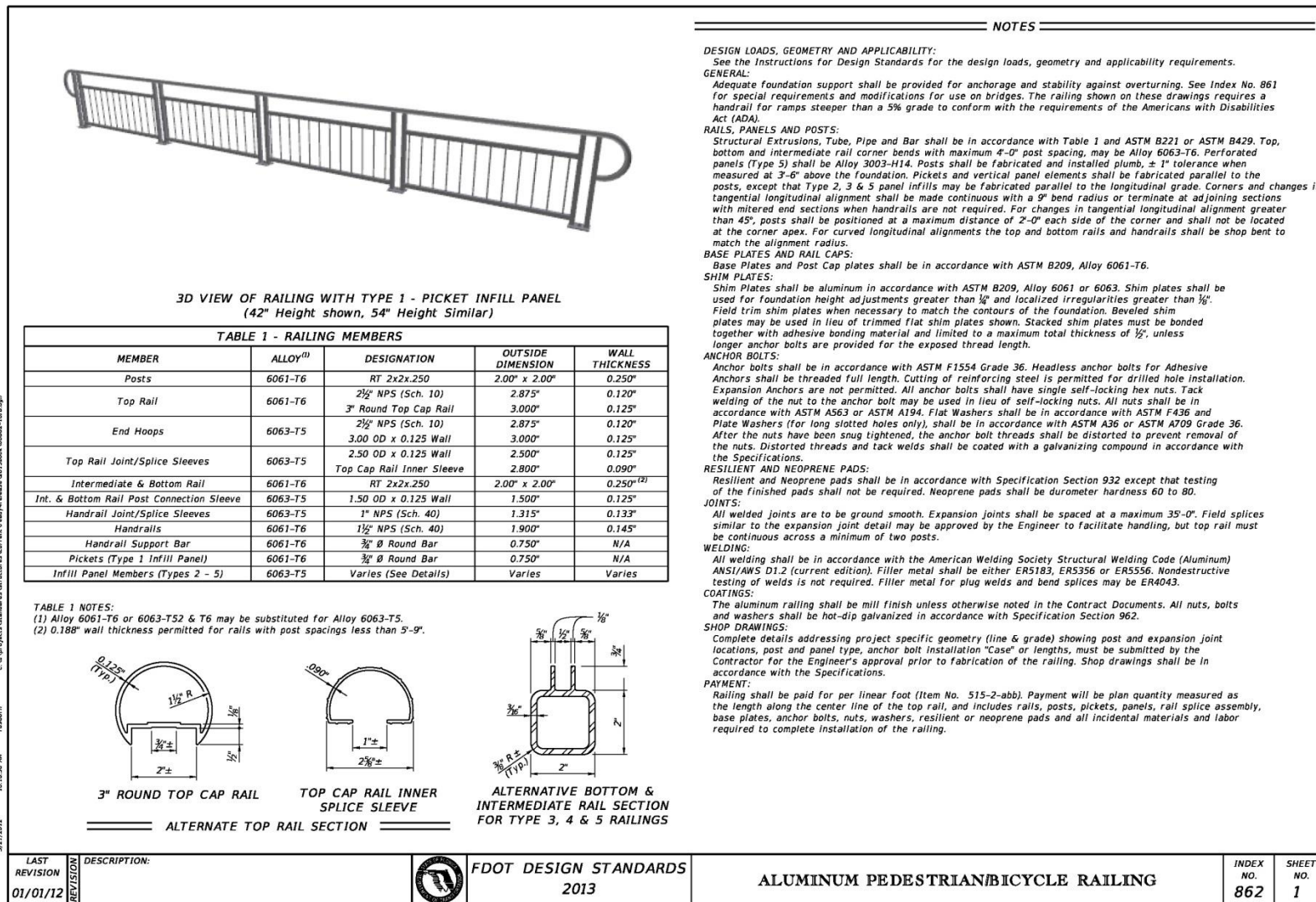


Figure 20. FDOT Aluminum, Pedestrian-Only Rail (Sheet 1 of 8) [32-33]

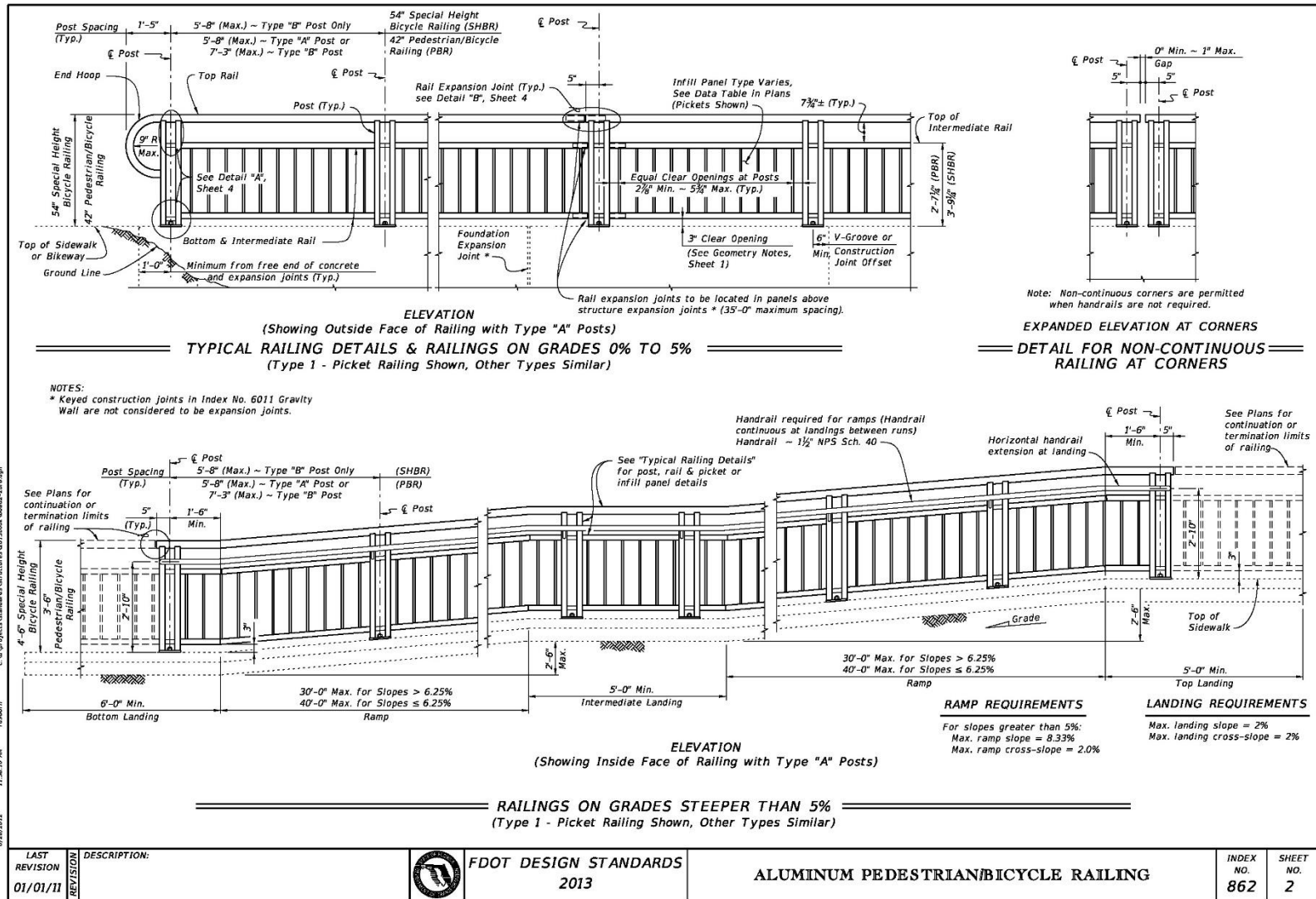


Figure 21. FDOT Aluminum, Pedestrian-Only Rail (Sheet 2 of 8) [32-33]

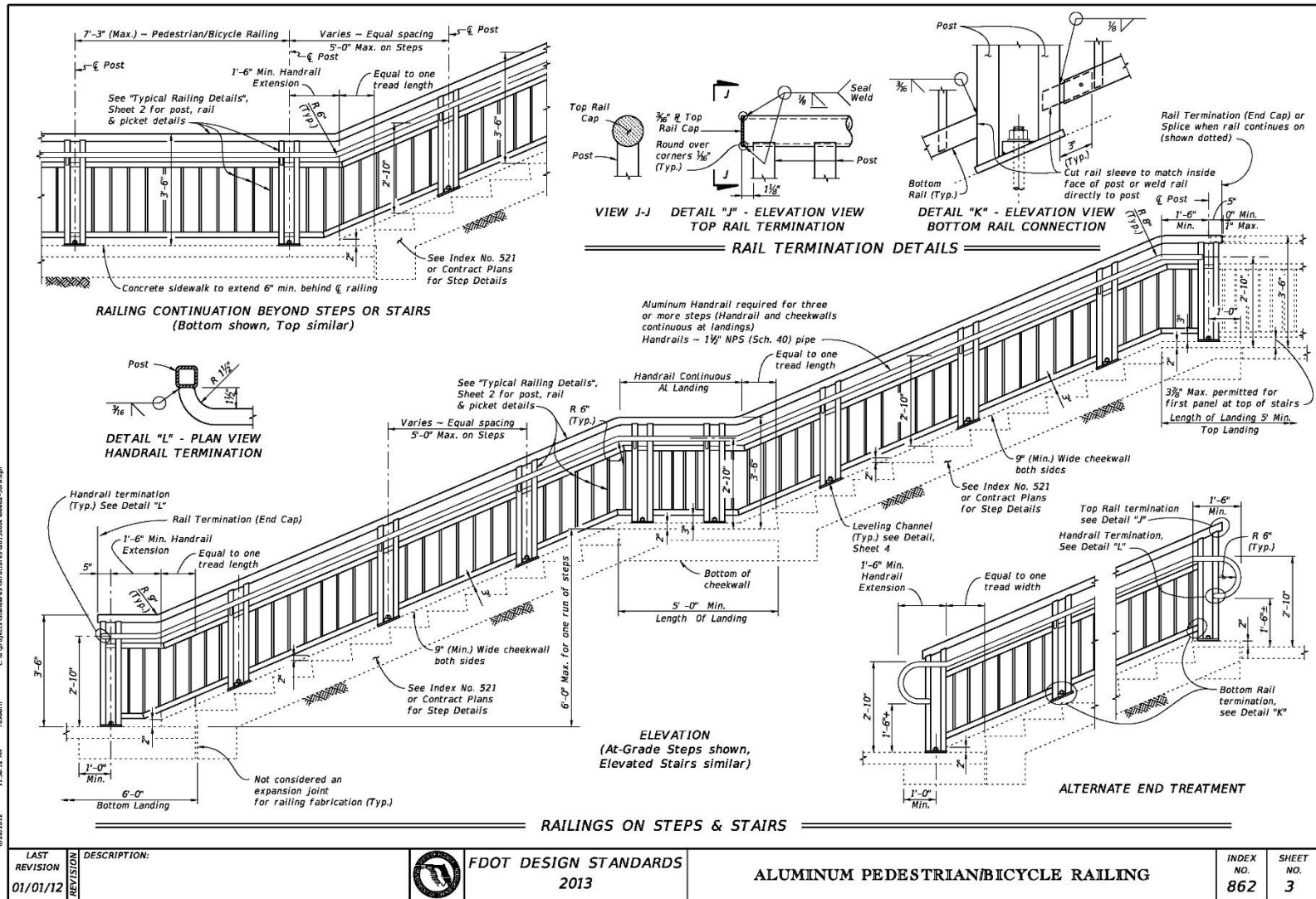


Figure 22. FDOT Aluminum, Pedestrian-Only Rail (Sheet 3 of 8) [32-33]

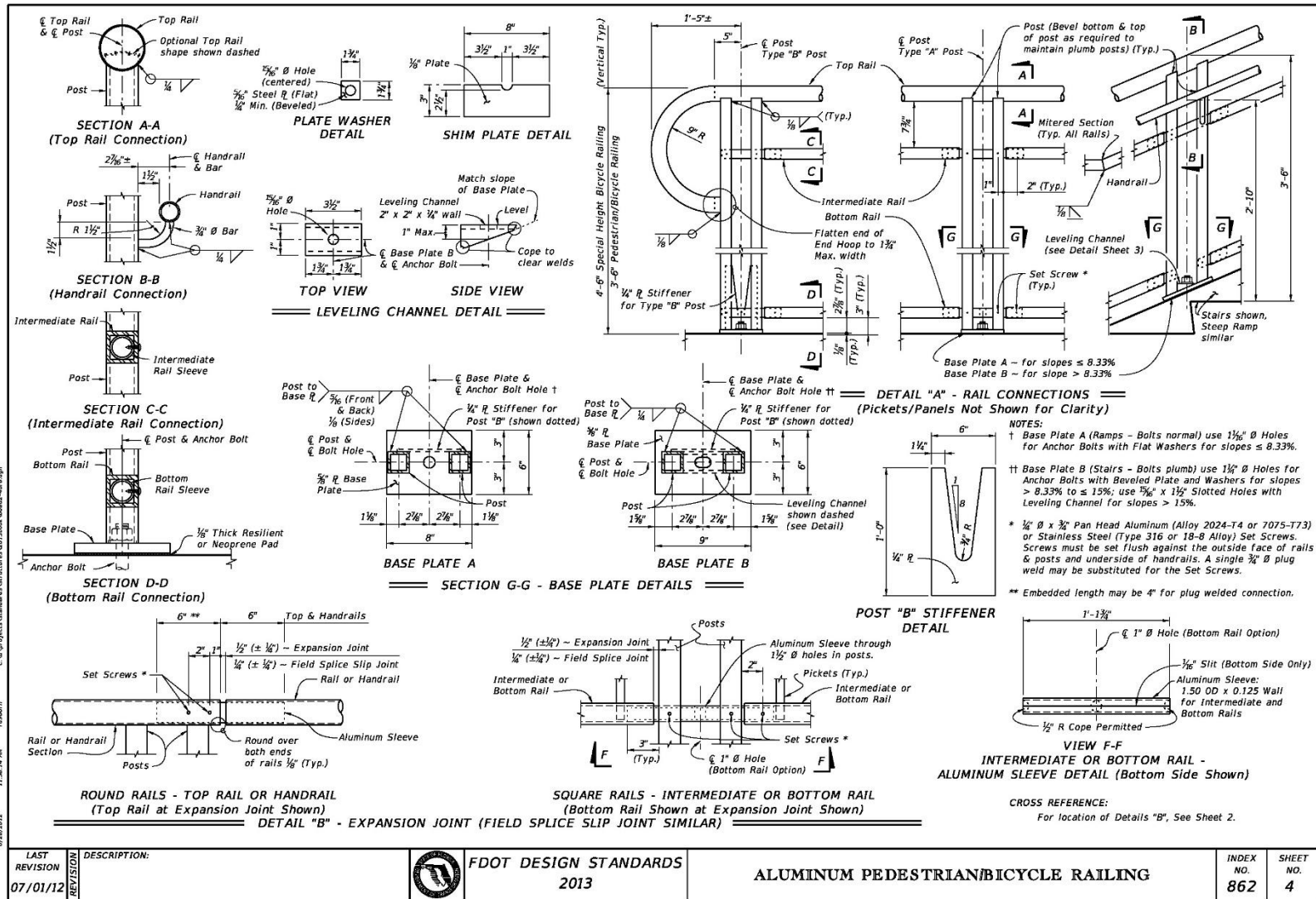


Figure 23. FDOT Aluminum, Pedestrian-Only Rail (Sheet 4 of 8) [32-33]

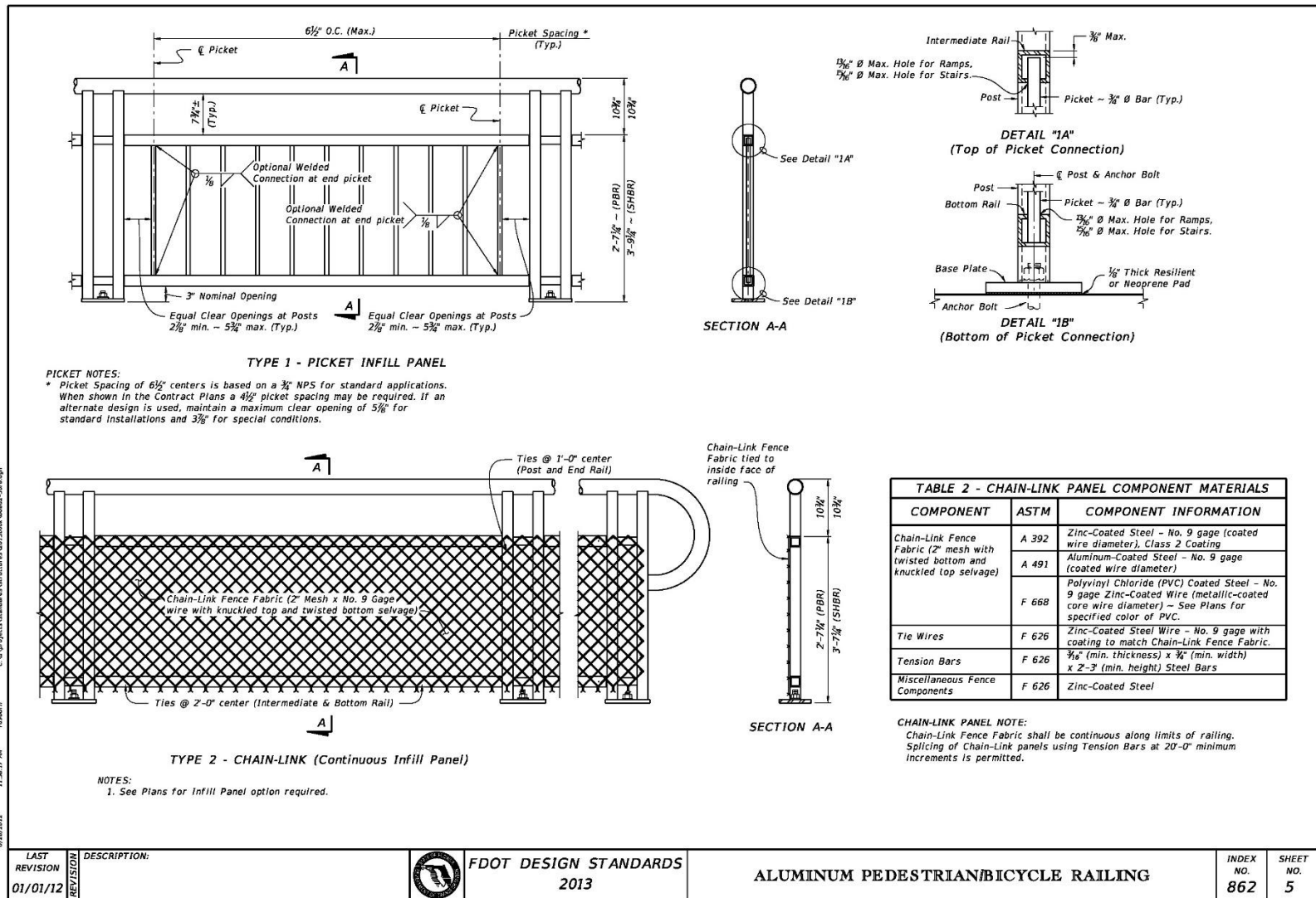


Figure 24. FDOT Aluminum, Pedestrian-Only Rail (Sheet 5 of 8) [32-33]

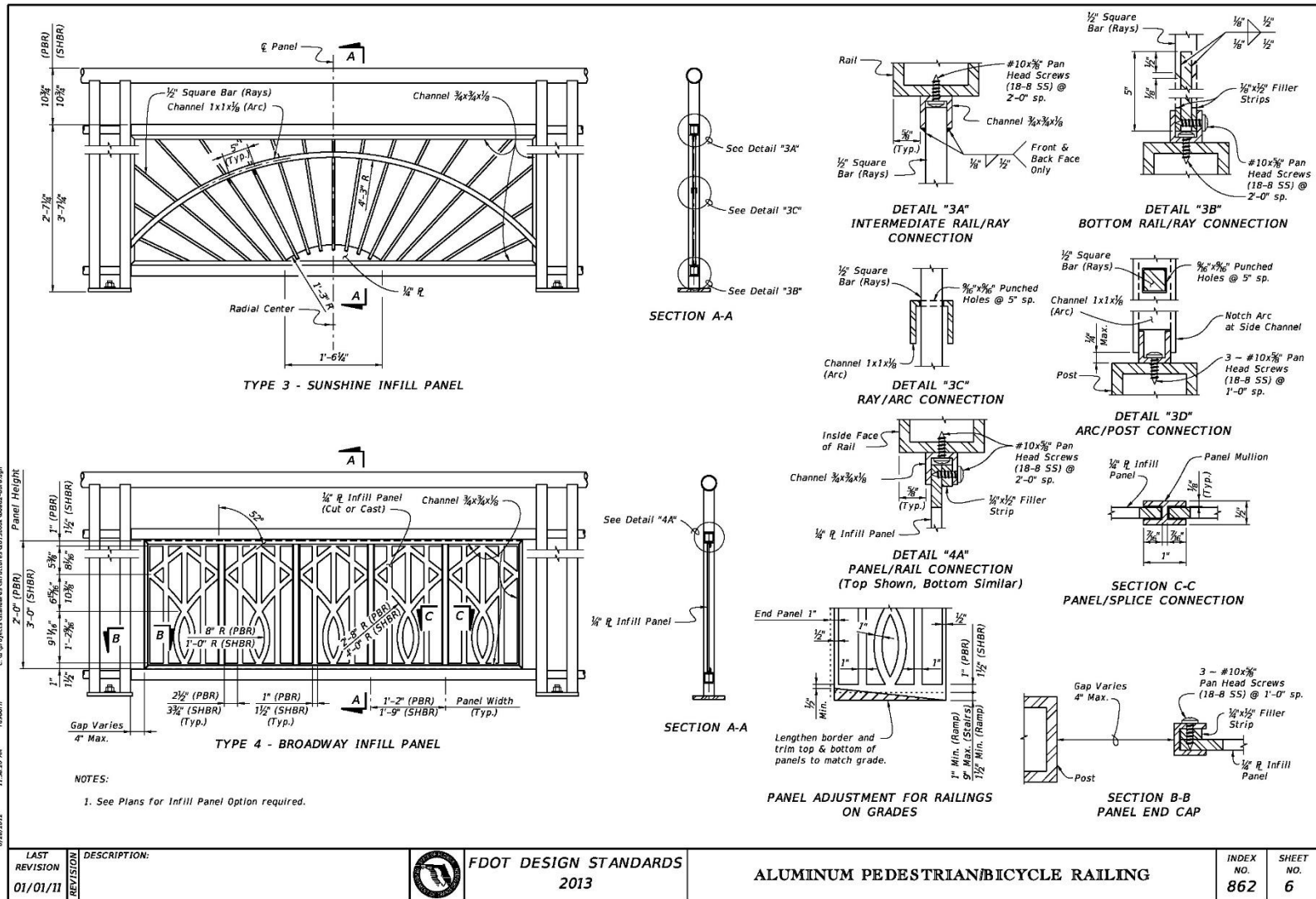


Figure 25. FDOT Aluminum, Pedestrian-Only Rail (Sheet 6 of 8) [32-33]

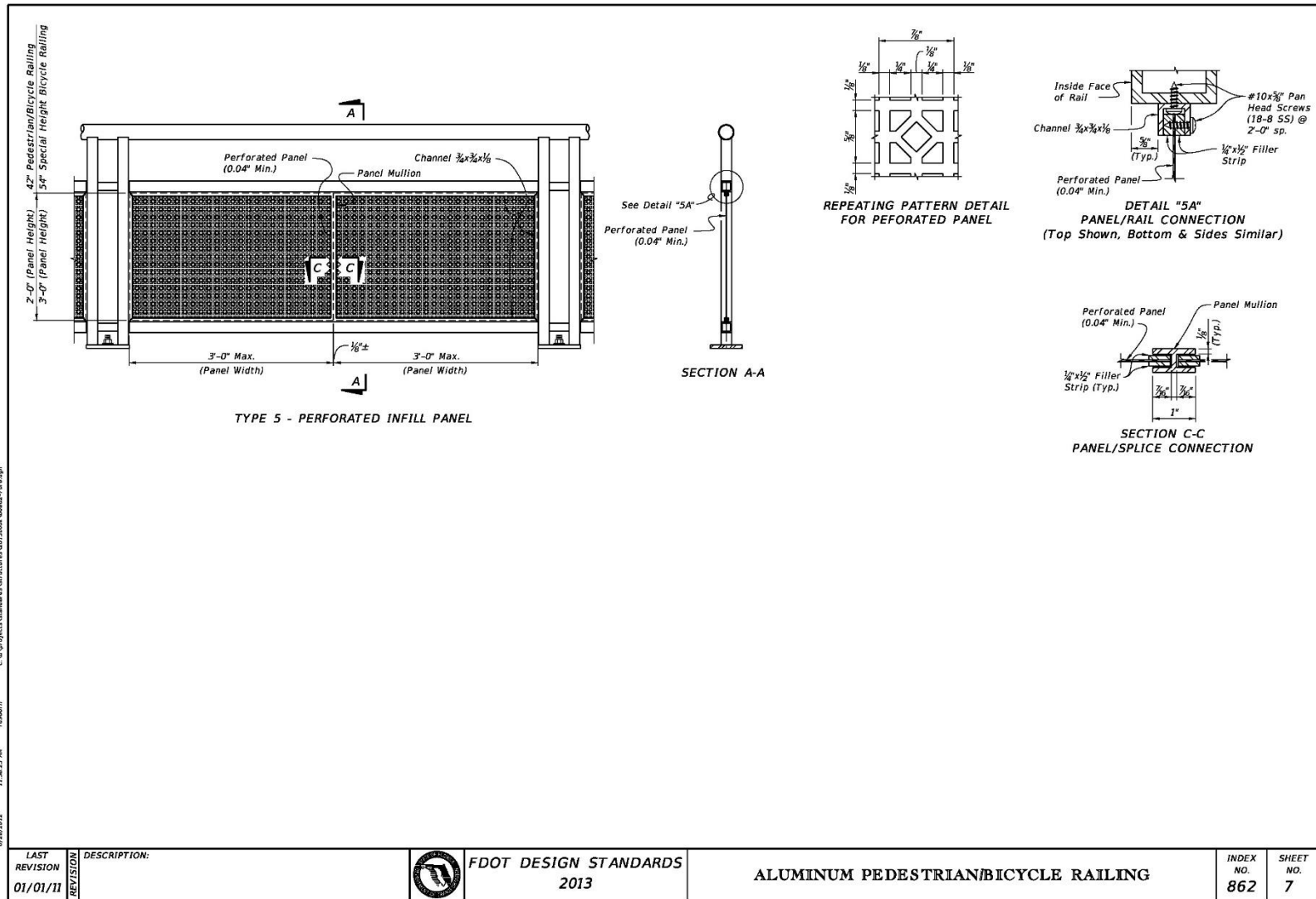


Figure 26. FDOT Aluminum, Pedestrian-Only Rail (Sheet 7 of 8) [32-33]

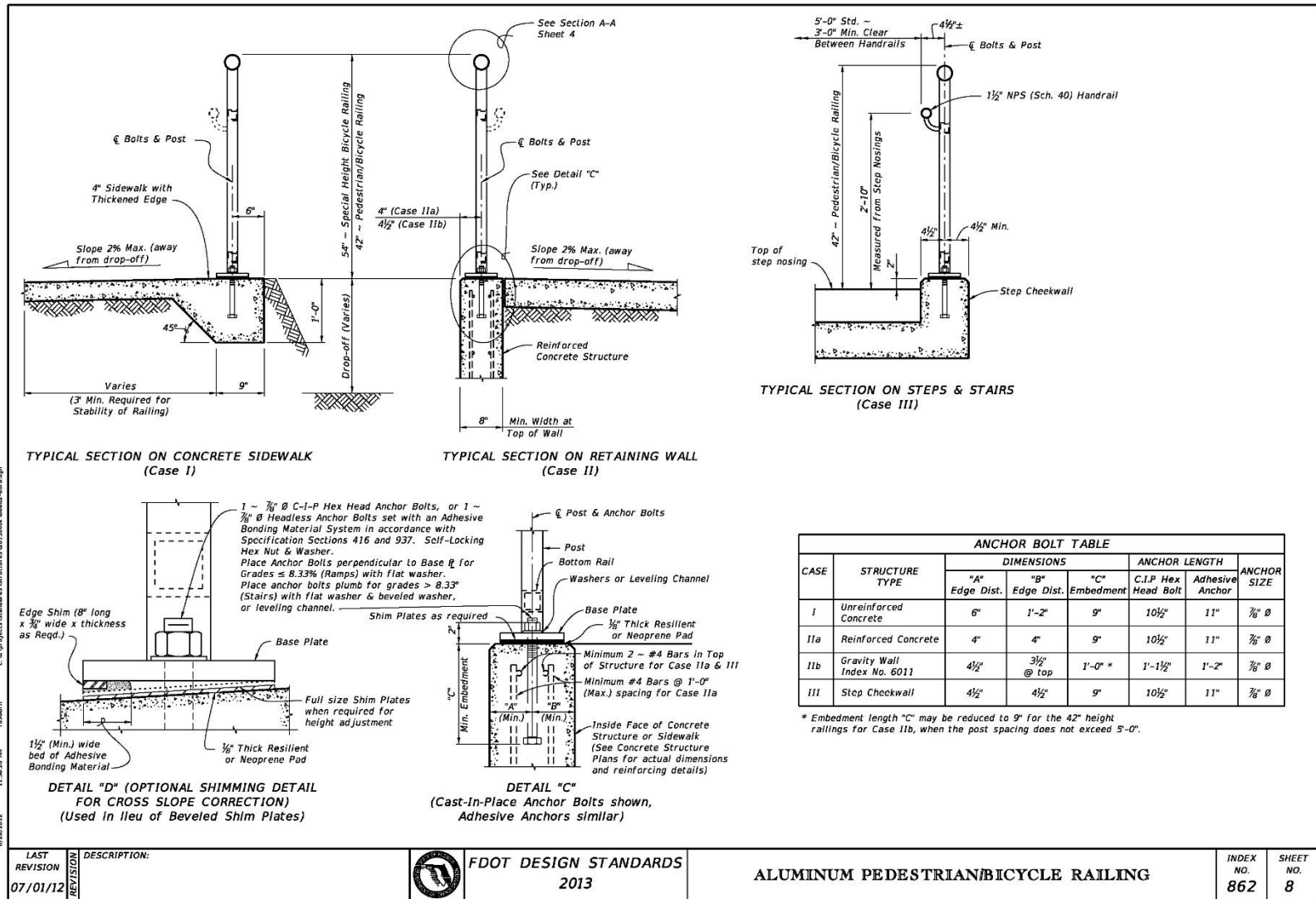


Figure 27. FDOT Aluminum, Pedestrian-Only Rail (Sheet 8 of 8) [32-33]

Prefabricated steel and aluminum rail fittings are available from many manufacturers. For example, Hollaender Manufacturing Company has many steel and aluminum systems, as shown in Figure 28 [34-35]. The Speed Rail system is an aluminum modular handrail system which is created from individual fittings and pipe sections [35]. This modular design allows for fast and simple fabrication. Repair of a modular system is less difficult, because the damaged section and fittings are the only components that need to be replaced. When impacted by a vehicle, the railing system may break into its individual elements, which may put the impacting vehicle's occupant, surrounding vehicles, and nearby pedestrians at risk of flying elements. Hollaender fabricated the railing systems to meet OSHA and IBC testing standards. A vast set of fitting sizes and shapes provide multiple design options.

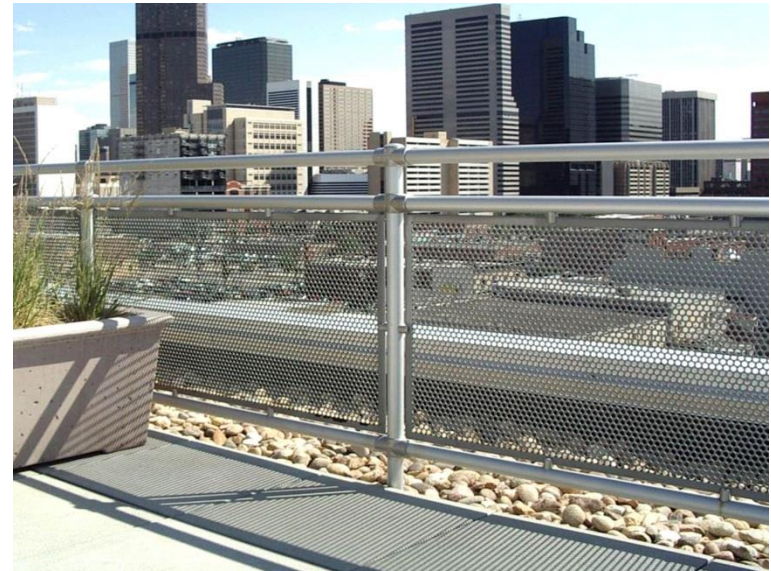


Figure 28. Examples of Hollaender Rail Systems [34-35]

3 EVALUATION OF PEDESTRIAN RAIL NEEDS

A survey was conducted to identify the most common locations and circumstances in which a crashworthy pedestrian rail would be warranted. This survey was important to find where and how these barriers would be installed. A copy of the survey that was sent to the Midwest States Pooled Fund members is shown in Appendix A. The survey results, as determined from nine member state DOTs, are shown in Table 1, while the Wisconsin DOT survey results are shown in Table 2. As stated previously, this project was funded by the Wisconsin DOT and their input was primarily used.

According to the 2011 Edition of the National Safety Council's (NSC) Injury Facts report, motor vehicle collisions with pedestrians are a significant concern and result in a fatality about one-third of the time [36]. According to NSC data from 2009, sixty percent of the pedestrian-to-motor-vehicle fatalities occur when the pedestrian tried to improperly cross a roadway or intersection. The desire to use the pedestrian rail to prevent pedestrians from crossing the street and non-designated crossing locations addresses the dangers associated with crossing the roadway at an unintended location, and may aid in reducing fatality and injury accidents between motor vehicles and pedestrians.

For the Pooled Fund, the highest-priority, crashworthy pedestrian rail need was identified for use on top of culverts. For the Wisconsin DOT, the most common, highest-priority, crashworthy pedestrian rail need was to prevent urban/suburban pedestrian crossings at non-designated locations. Based on the two findings, the highest priority was to focus on preventing pedestrian crossings at non-designated locations, since the project was funded by the Wisconsin Department of Transportation.

Table 1. Pooled Fund Member Responses to Highest Need–Pedestrian Rail Survey

Pedestrian Rail Locations/Circumstances	Usefulness Summary:					Rank
	Not Useful	Somewhat Useful		Very Useful		
On top of culverts			3	5	1	1
On top of retaining walls	1	1	4		3	2
Prevent Jaywalking	2	3	3		1	3
Rail around private/public property	2	3	3	1		4
Other:						
Bike/pedestrian path separation from roadway					1	
Bike path hazard protection					1	
Sidewalk higher than surroundings			1			
On bridges				1		

40 Table 2. Wisconsin DOT Response to Highest Need–Pedestrian Rail Survey

Pedestrian Rail Locations/Circumstances	Usefulness Summary:					Rank
	Not Useful	Somewhat Useful		Very Useful		
Prevent Jaywalking					X	1
On top of culverts			X			2
Rail around private/public property				X		3
On top of retaining walls		X				4

4 PRELIMINARY PEDESTRIAN RAIL DESIGN

The pedestrian rail must: (1) meet AASHTO standards, (2) be ADA compliant, and (3) meet AASHTO MASH TL-2 criteria for longitudinal channelizers. Two additional design goals include a desire for the rail to be aesthetically pleasing and to allow pedestrians and motorists to be visible to one another. The pedestrian rail was also to be designed to eventually accommodate an ADA-compliant handrail.

4.1 Design Load Calculations

The calculations described herein were used to design an anchored, straight, pedestrian rail with uniform post spacing. The applied loads were defined by the requirements published in the AASHTO *LRFD Bridge Design Specifications* for a pedestrian rail [6]. These loads corresponded to the critical loading that was applied to the pedestrian rail structure, which generated the critical forces/stresses. The minimum available cross sections were determined to meet all load requirements. In addition to the loading requirements, a maximum allowable deflection was set to 4 in. (102 mm) for all longitudinal and vertical elements.

4.1.1 Longitudinal Rail Element

The longitudinal rail elements were designed to withstand two types of live loads: (a) a uniformly distributed load of 50 lb/ft (730 N/m) applied both transversely (z-axis) and vertically (y-axis) and (b) a concentrated load of 200 lb (890 N) applied at any point and in any direction. In general, stresses are maximized when the concentrated load can be superposed with the uniform loads in the transverse, vertical, or resultant direction. An example of the design loading conditions with a concentrated load acting vertically downward in the center of the top longitudinal beam is shown in Figure 29.

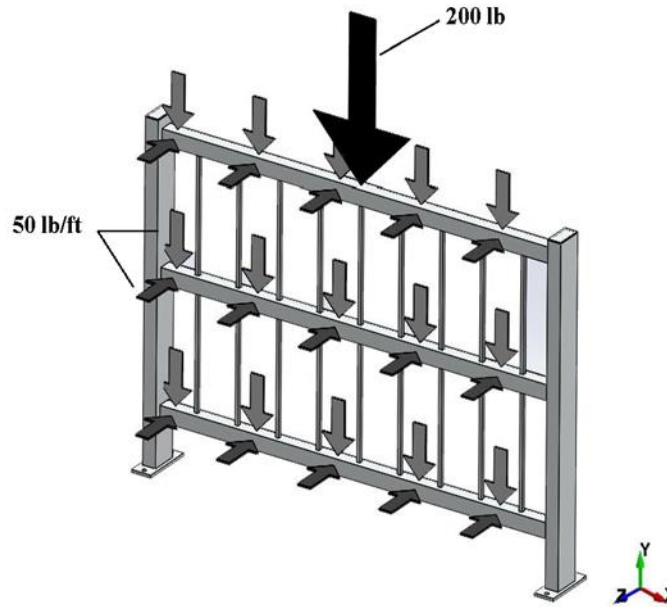


Figure 29. Example of Pedestrian Rail with Vertical Concentrated Load

The longitudinal rail element was assumed to act as a simply supported beam for the preliminary strength analysis. Total direct shear loads were calculated by summing uniform and concentrated loads together. For small-deflection, linear-elastic bending displacements, superposition can be used to estimate bending moments and stresses in beams subjected to diverse loading conditions. Thus, bending moments were calculated by superposing moments created by loads in the transverse (M_{uy}) and vertical (M_{uz}) directions, as shown in Equation 2. Note that because the uniform loads do not spatially vary in direction or magnitude, only the moment created by the concentrated load can vary.

In general, beam bending analysis must consider loads, stresses, and deflections in principal (i.e., I_{yy} and I_{zz}) and off-principal (i.e., I_{yz}) axis directions. However, the rail element was designed as a doubly-symmetric member, such that the product of inertia value (I_{yz}) was equal to zero. Several cross sections were investigated and included a circular tube, a solid circular bar, square tube, and solid square bar. As a result, the longitudinal tensile or compressive bending stresses (f_b) resulting from loads in vertical and transverse directions could be summed

together. Similarly, the maximum deflection was calculated by using the vector addition to superpose vertical and transverse deflections, as shown in Equation 3.

$$M_u = M_{uy} + M_{uz} \quad (2)$$

$$M_{uz} = \frac{wL^2}{8}$$

$$M_{uy} = \frac{(w+w_{ow})L^2}{8} + \frac{PL}{4}$$

$$\delta = \sqrt{\delta_y^2 + \delta_z^2} \quad (3)$$

$$\delta_y = \frac{1}{EI} \int M_z dx = \left(\frac{5(w+w_{ow})/12 \times (L \times 12)^4}{384EI} + \frac{P(L \times 12)^3}{48EI} \right)$$

$$\delta_z = \frac{1}{EI} \int M_y dx = \left(\frac{5w/12 \times (L \times 12)^4}{384EI} \right)$$

$$\therefore \delta = \sqrt{\left(\frac{5(w+w_{ow})/12 \times (L \times 12)^4}{384EI} + \frac{P(L \times 12)^3}{48EI} \right)^2 + \left(\frac{5w/12 \times (L \times 12)^4}{384EI} \right)^2}$$

Where:

- M_u = Applied Bending Moment (lb-in.)
- M_{uy} = Applied Bending Moment Acting in the Y-Axis (lb-in.)
- M_{uz} = Applied Bending Moment Acting in the Z-Axis (lb-in.)
- w = 50 lb/ft Distributed Load (lb/in.)
- L = Post Spacing (in.)
- w_{ow} = Rail Weight (lb/in.)
- P = 200 lb Concentrated Load
- δ = Deflection (in.)
- δ_y = Deflection in Vertical (i.e., Y-Axis) due to w , w_{ow} , and P
- δ_z = Deflection in Transverse (i.e., Z-Axis) due to w
- I = Moment of Inertia (in.⁴)
- E = Young's Modulus (psi)

4.1.2 Vertical Post Element

The posts were subjected to a concentrated live load, P_{LL} , as defined in Equation 1. The concentrated live load shall be applied transversely at the center of gravity of the upper horizontal element. The post was assumed to act as a single cantilever beam. The bending moment and deflection of the post were calculated, as shown in Equations 4 and 5, respectively.

Several cross sections were investigated for the post, including a circular tube, circular bar, square tube, square bar, rectangular tube, and rectangular bar.

$$M_p = P_{LL}(h) \quad (4)$$

$$\delta = \frac{P_{LL}h^3}{3EI} \quad (5)$$

Where:

M_p	=	Bending Moment in Post (lb-in.)
P_{LL}	=	Post Point Live Load (lb)
h	=	Distance from Ground to Center of Gravity of Upper Horizontal Element (in.)
δ	=	Deflection (in.)
E	=	Young's Modulus (psi)
I	=	Moment of Inertia (in. ⁴)

4.1.3 Infill, Mesh, and Spindle Element

Mesh elements were designed to withstand the 15-lb/ft² (718-N/m²) load defined in the AASHTO *LRFD Bridge Design Specifications*. Where spindles or other infill spanned between rail elements, 15 lb/ft² (718 N/m²) was also used as a design load for these elements. Because the applied load on the infill, mesh, or spindles was much, much less than for the posts and beams, the design of these elements would not control the shape or appearance of the pedestrian rail design and thus were not considered for the initial concepts. Furthermore, these components did not provide any structural support to the pedestrian rail.

4.2 Material Selection

4.2.1 Material Consideration

The materials considered for the initial design of the pedestrian-only rail structure included: (1) steel, (2) aluminum, (3) FRP, (4) PVC, (5) HDPE, and (6) wood. All material types had benefits and disadvantages. General properties of each material were ranked Very Low, Low, Medium, High, Very High, or Not Applicable (NA) or listed as Yes or No, as shown in Table 3. Steel, aluminum, and FRP provided high material strength, and the polymer options had

lower strengths and were assumed to act more brittle during impacts. A summary of all relevant material properties is shown in Table 4.

Table 3. General Material Comparisons

Consideration/ Condition	Material					
	Steel ¹	Aluminum ²	PVC	FRP	HDPE	Wood
Bending Strength (f_b)	Very High	High	Low	Medium	Very Low	Very Low
Modulus of Elasticity (E)	Very High	High	Low	Medium	Very Low	Medium
Brittleness	Low	Medium	High	High	Medium	High
Formability	Very High	Low	NA	NA	NA	NA
Cost	Medium	High	Medium	Very High	Medium	Low
Component Weight ³	Medium	Very Low	High	Low	High	Very High
Prefabricated Connections	Yes	Yes	Yes	Yes	No	No
Corrosion Resistance	Medium	Very High	Very High	Very High	Very High	Low
Temperature Degradation	Very Low	Very Low	High	Low	Very High	Very Low
UV Exposure Degradation	Very Low	Very Low	High ⁴	High ⁴	High ⁴	Very Low

1 – ASTM A992 Steel

2 – 6061-T6 Aluminum

3 – Weight of cross sections which meet load requirements

4 – Can be treated or painted to resist UV degradation

Table 4. Relevant Material Properties [37]

Material	Bending Strength (f_b)		Young's Modulus (E)		Density	
	(psi)	(kPa)	(ksi)	(MPa)	(lb/ft ³)	(kg/m ³)
Steel ¹	50,000	345,000	29,000	199,950	503	8,060
Aluminum ²	40,000	276,000	10,000	68,950	169	2,710
FRP	24,000	165,000	2,320	16,000	108	1,730
PVC	14,450	100,000	400	2,760	90	1,440
HDPE	4,800	33,000	200	1,380	59	950
Wood	1,550	11,000	1,700	11,720	31	500

1 – ASTM A992 Steel

2 – 6061-T6 Aluminum

Further evaluation of each material type was necessary to determine which material would provide the greatest benefits while keeping the initial designs to a manageable set. Although many variables should be considered when choosing the most efficient material, the primary selection criteria were aesthetics, strength, weight, cost, and workability.

4.2.2 Aluminum

Aluminum had many properties which were desirable for the fabrication of a pedestrian rail. Aluminum has a very high strength-to-density ratio and is highly resistant to corrosion. Depending on the rail design, prefabricated aluminum fittings are also available. One disadvantage is that aluminum is difficult to weld, and when welded, aluminum loses much of its strength near the site of the weld. However, aluminum may be heat-treated at an additional cost to retain its original strength. Another disadvantage is that aluminum is a relatively expensive material and may be a target for theft.

4.2.3 Steel

Steel has very high strength material properties and is about three times denser than aluminum. Steel is easily welded and formed to a desired shape with little to no loss in material strength. Prefabricated steel fittings are available. To reduce the effects of corrosion, the steel must be galvanized. The cost of steel is typically cheaper than aluminum.

4.2.4 Polyvinyl Chloride (PVC)

PVC is a very common material used for plumbing and private property fencing. PVC has a low material strength when compared to aluminum and steel, and is about one-sixth the density of steel. PVC is corrosion-resistant, but the material properties and appearance degrade with Ultra Violet (UV) exposure. The PVC material must be treated or painted to reduce the effects of UV exposure. PVC material strength is also affected by temperature. The stiffness of the PVC material is reduced at high temperatures, potentially resulting in large deformations at

warm temperatures. To reduce the temperature effects, PVC should be painted with a light color, preferably white. PVC has prefabricated fittings used for pipes, which may allow the material to work as a handrail system. PVC is very brittle under impact loading, specifically at low temperatures. The cost of PVC is in the medium range when compared to other materials.

4.2.5 Fiber-Reinforced Polymer (FRP)

The material strengths of FRP are much higher than other polymers due to the added strength from the internal reinforcing fibers of the material. FRP has about one-fifth the density of steel. It is corrosion-resistant and acts brittle under impact loading. The cost of FRP is much higher than all other materials considered.

4.2.6 High Density Polyethylene (HDPE)

HDPE is very similar to PVC, but the material strengths are lower. HDPE is corrosion-resistant and has about one-ninth the density of steel. It must be protected from UV degradation with paint or an additive. HDPE material strength is also affected by temperature. At high temperatures, the stiffness decreases. This could potentially result in large deformations at warm temperatures. To reduce the temperature effects, HDPE should be painted with a light color, preferably white.

4.2.7 Wood (Douglas Fir)

Douglas fir was considered for this project because of its high strength properties. Douglas fir has about one-sixteenth the density of steel. Wood has a low ultimate bending strength due to variability in the cross section from imperfections, such as cracks and knots. Wood is readily available and relatively inexpensive.

5 INITIAL CONCEPT DEVELOPMENT

5.1 Preliminary Concept

After a comprehensive literature review was completed on existing pedestrian rail systems and other commercially available railings, twenty-five pedestrian rail concepts were considered, as shown in Appendix B. The geometry of the pedestrian rail was the main focus, such that all concepts met the AASHTO *LRFD Bridge Design Specifications* loading criteria required for a pedestrian barrier. As stated previously, various materials were considered and included steel, aluminum, PVC, wood, HDPE, and FRP. Material types were considered based on aesthetics, strength, weight, cost, and workability. The handrail, infill, and connections were not designed during the initial development phase. Only one rail segment is shown for each concept. However, all preliminary concepts could later be designed as either a long, continuous railing system or as individual segments.

5.2 Refined Concepts

Following a review of the preliminary concepts, several concepts and materials were eliminated. Further investigation showed that the cost of aluminum was comparable to steel. Thus, since aluminum would fracture upon impact more easily than steel is lighter weight, aluminum options were added. Due to the significant cost of FRP, it was eliminated. HDPE was eliminated due to its limited application and having a low material strength, especially at high temperatures. Many designs were not pursued based on aesthetics and feasibility of fabrication.

Seven preliminary concepts were further developed and included: two modular aluminum concepts (designated AM-1 and AM-2), one welded aluminum concept (designated AW2), two PVC concepts (designated PVC1 and PVC2), and two wood concepts (designated WOOD1 and WOOD2). The system details are described in the following sections, and components were obtained to fabricate prototype segments of each concept. Connections were specified, but

further development, such as weld details for applicable systems, were not designed during this phase.

5.2.1 Design Concept AM-1

Concept AM-1 consisted of a modular aluminum system with vertical spindles welded to the horizontal rail. The modular assembly simplified installation. The aluminum material was lightweight for transportation and fabrication. The spindles may be solid or hollow aluminum cross sections. It was recommended that the spindles be clipped in or welded to both the center and bottom rails in order to reduce flying debris when impacted. Details of design concept AM-1 are shown in Figures 30 through 34. Photographs of the fabricated design are shown in Figures 35 and 36.

5.2.2 Design Concept AM-2

Concept AM-2 was very similar to concept AM-1. The only change for this design was to use a 2-in. x 2-in. (51-mm x 51-mm) steel mesh in place of the vertical aluminum spindles. The mesh would require panel clips or welds at the connections to the center and bottom rail components in order to secure it in place. This option was presented to provide variability in aesthetics of this structural design. Details of design concept AM-2 are shown in Figures 37 through 41. This concept was not fabricated due to the similarity between concepts AM-1 and AM-2.

5.2.3 Design Concept AW2

Concept AW2 utilized aluminum posts and rails with rectangular cross sections. Post-to-rail connections were welded at the connection surface. The connections were tack welded for illustrative purposes only. The aluminum material was lightweight for transportation and fabrication. The spindles may be solid or hollow aluminum cross sections. Spindles will need to be welded at both connections to the center and bottom rails. Details of design concept AW2 are

shown in Figures 42 through 46. Photographs of the fabricated design are shown in Figures 47 and 48.

5.2.4 Design Concept PVC1

Concept PVC1 consisted of a modular PVC system. The modular assembly simplified installation. Initial fabrication at the Midwest Roadside Safety Facility (MwRSF) utilized available plastic base connections, but it was determined that this base connection would not be as stable as desired. Thus, the base connection would need to be redesigned. The rail elements were overdesigned, as T-shaped PVC fittings for the connection between posts and rails were not available with two different diameters between the vertical and horizontal connection slots. It was noted during fabrication that the girth of concept PVC1 may reduce needed visibility near the side of the road. Details of design concept PVC1 are shown in Figures 49 through 53. Photographs of the fabricated design are shown in Figures 54 and 55.

5.2.5 Design Concept PVC2

Concept PVC2 utilized PVC posts and rails, with circular cut-out sections in the post at each post-to-rail connection. Horizontal rail elements were attached with a vertical steel reinforcing bar through the ends inside the PVC post to ensure that the rail elements did not shift individually within the system. A base connection for design concept PVC2 was not designed or fabricated. Fabrication of the PVC2 system was simplistic. Three variations utilized the same post-to-rail connection method with different post and rail sizes and segment geometry.

5.2.5.1 Design Concept PVC2-a

Concept PVC2-a was the original design that was fabricated with 4½-in. (114-mm) diameter rails. Details of design concept PVC2-a are shown in Figures 56 through 59. Photographs of the fabricated design are shown in Figures 60 and 61.

5.2.5.2 Design Concept PVC2-b

Concept PVC2-b decreased the rail diameter to $2\frac{7}{8}$ in. (73 mm). The reduced cross section of the system resulted in an extra rail element added to meet the AASHTO requirement of 6-in. (152-mm) minimum spacing between elements. This alteration allowed for the post spacing to be increased from 54 in. (1,372 mm) to 60 in. (1,524 mm). Details of design concept PVC2-b are shown in Figures 62 through 66. Concept PVC2-b was not fabricated due to its similarity to PVC2-a, and to the $2\frac{1}{2}$ -in. (64-mm) diameter PVC pipe not being readily available at the time of fabrication.

5.2.5.3 Design Concept PVC2-c

The design of concept PVC2-c altered that of concept PVC2-b to utilize local, readily-available material, since the $2\frac{7}{8}$ -in. (73-mm) diameter PVC was not readily available. The post diameter was reduced from $6\frac{5}{8}$ in. (168 mm) to $4\frac{1}{2}$ in. (114 mm), and the rail diameter was reduced from $2\frac{7}{8}$ in. (73 mm) to $2\frac{3}{8}$ in. (60 mm). The cross section changes resulted in a post spacing reduction from 60 in. (1,524 mm) to 48 in. (1,219 mm) to maintain strength requirements. Details of design concept PCV2-c are shown in Figures 67 through 71. Photographs of the fabricated design are shown in Figures 72 and 73.

5.2.6 Design Concept WOOD1

Concept WOOD1 consisted of Douglas Fir wood post and rail elements. The design details specified that a steel fitting be used for the post-to-rail connection, but this connection was not readily available and was altered during fabrication. Instead of a steel bracket, $1\frac{1}{2}$ -in. (38-mm) diameter steel conduit was used as a post-to-rail connection. The post and rail were auger-drilled, and then the conduit was set approximately $1\frac{1}{2}$ in. (38 mm) deep within these holes to secure the connection. The solid steel spindles were replaced with a $\frac{1}{2}$ -inch (13-mm) steel conduit during fabrication to reduce weight and cost of the section. Details of design

concept WOOD1 are shown in Figures 74 through 78. Photographs of the fabricated design are shown in Figures 79 and 80.

5.2.7 Design Concept WOOD2

Concept WOOD2 utilized Douglas Fir for post and rail elements. Although a square cutout was initially considered for inserting the rails into the posts, fabrication would be more difficult than circular cutouts. Thus, 3½-in. (89-mm) round holes were drilled into the post, and the square rail ends were cut down to a 3½-in. (89-mm) diameter head for easy insertion into the post cutout. Details of design concept WOOD2 are shown in Figures 81 through 85. Photographs of the fabricated design are shown in Figures 86 and 87.

5.3 Discussion

The initial pedestrian rail concepts were submitted to the project sponsor for review and comment as well as to select preferred concepts based on aesthetics, cost, installation, maintenance, and sight lines. Some of the sponsor's concerns included the possibility for the rail to obstruct a driver's visual line of sight at critical locations (such as near intersections), the need to treat a wood railing system on a regular basis to prevent degradation, the labor of heat-treating welded aluminum, and the possibility of system components fracturing away from the frame and becoming projectile hazards to pedestrians or drivers. The comments were considered and applied to eliminate numerous concepts. The concepts made from PVC material were eliminated mainly due to lack of aesthetic appeal, difficulty in the design and fabrication of post and rail connections, and instability of each PVC segment. The Douglas Fir wood concepts were eliminated due to the concern of long-term durability, warping of the wood sections, and splinter hazards to pedestrians, vehicle occupants, and bystanders. After eliminating the concepts configured with PVC and Douglas Fir materials, both modular and welded aluminum railing systems were pursued further.

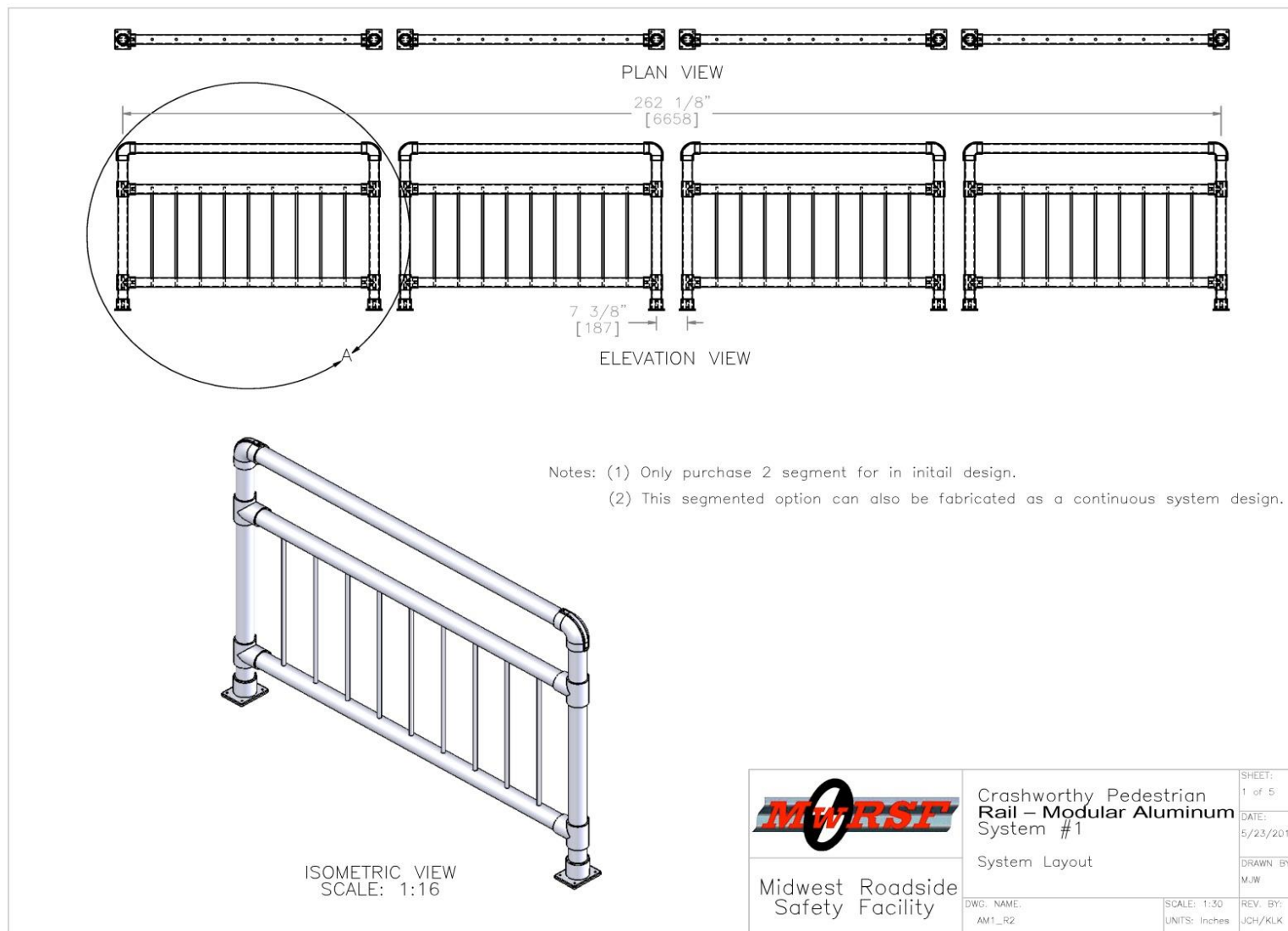


Figure 30. Aluminum Modular Rail with Spindles, Design Concept AM-1 (Sheet 1 of 5)

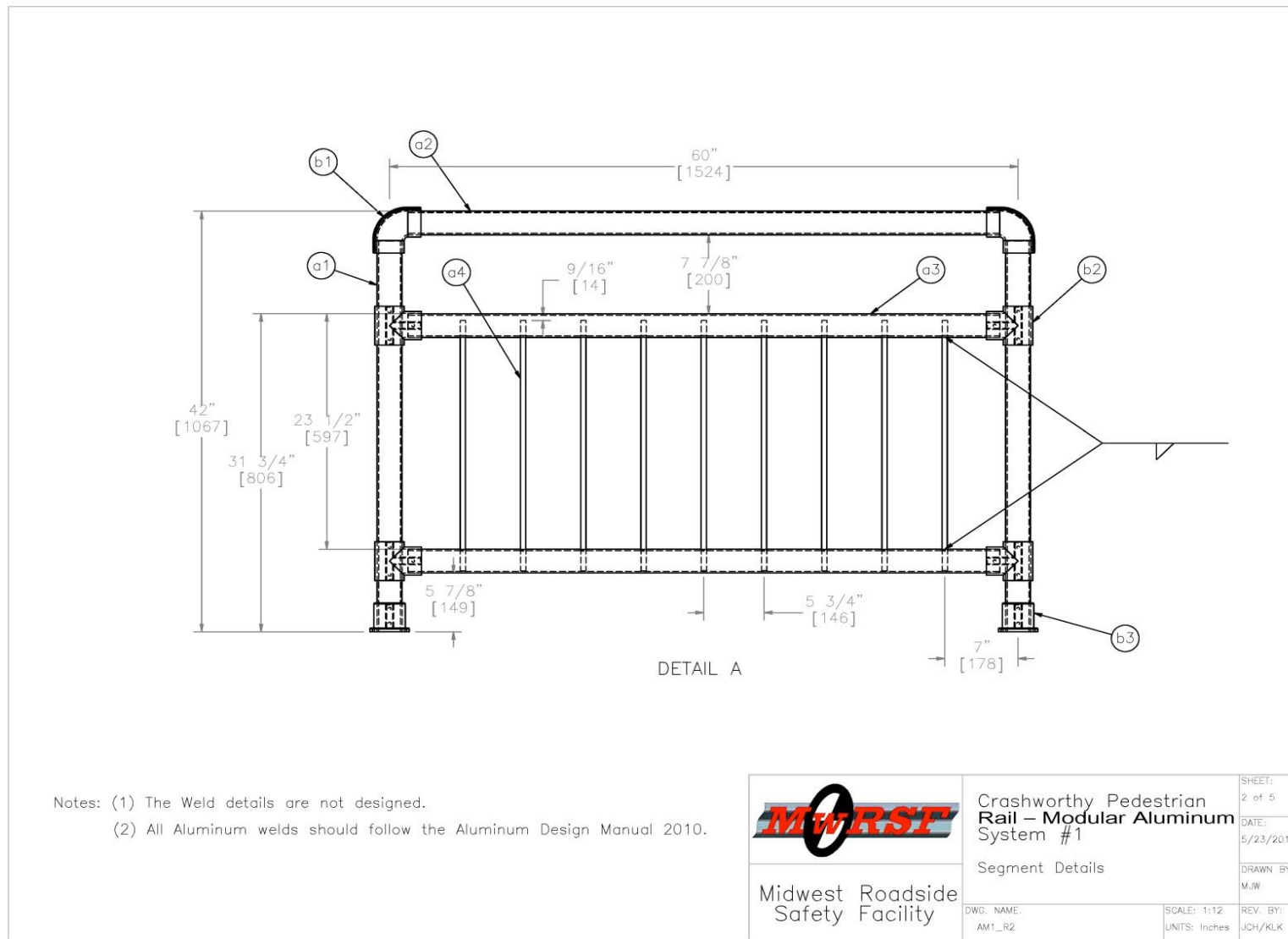


Figure 31. Aluminum Modular Rail with Spindles, Design Concept AM-1 (Sheet 2 of 5)

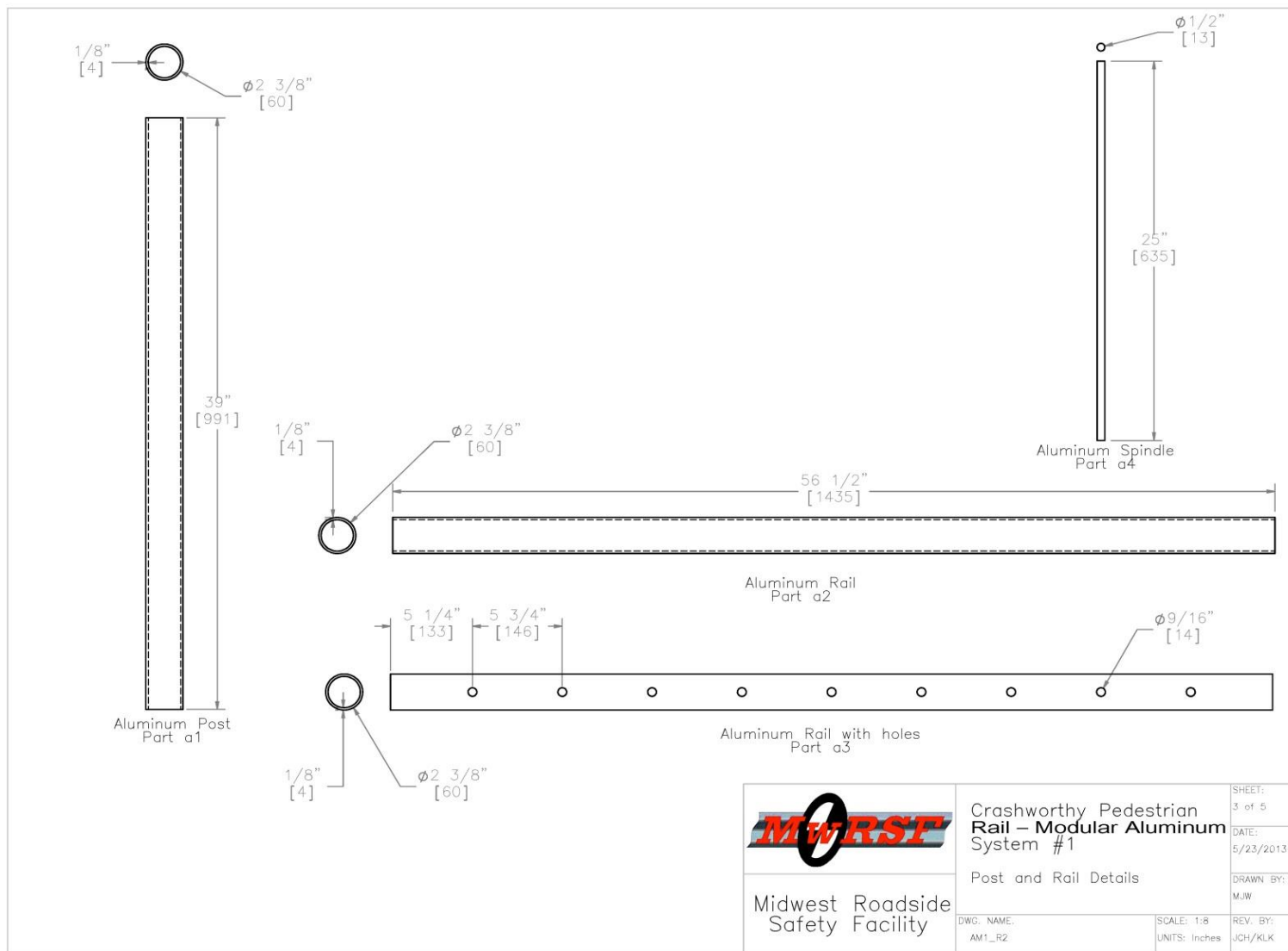


Figure 32. Aluminum Modular Rail with Spindles, Design Concept AM-1 (Sheet 3 of 5)

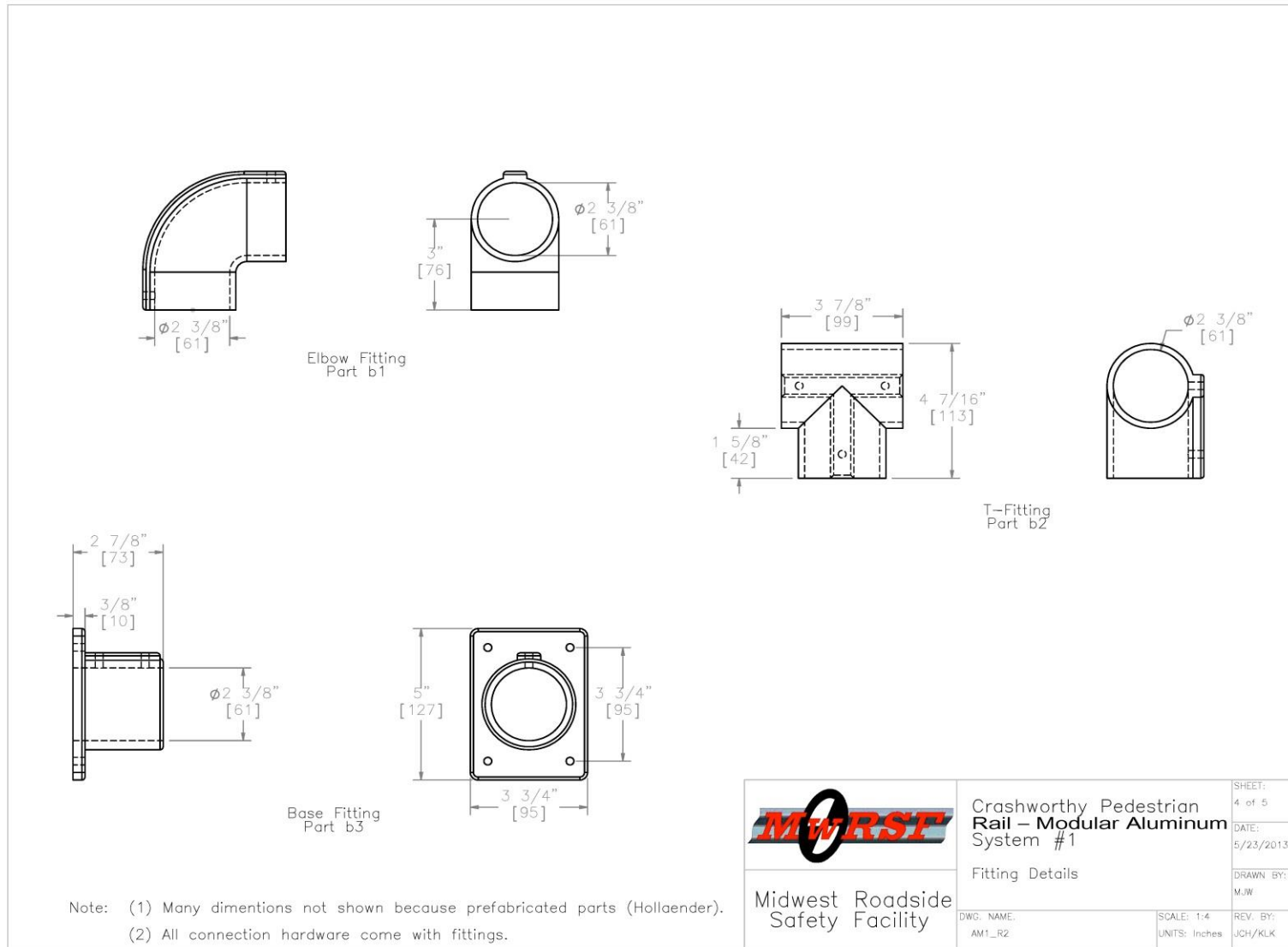


Figure 33. Aluminum Modular Rail with Spindles, Design Concept AM-1 (Sheet 4 of 5)

Crashworthy Pedestrian Rail – Segmented Aluminum Pipe with Fittings with Spindles					
Item No.	QTY.	Description	Material Spec	Hollander Part	Hardware Guide
a2	4	2" Dia. Schedule 40 Pipe Rail, 56 1/2" long	6061-T6 Aluminum	–	
a1	8	2" Dia. Schedule 40 Pipe Post, 39" long	6061-T6 Aluminum	–	–
a3	8	2" Dia. Schedule 40 Pipe Rail with Holes, 56 1/2" long	6061-T6 Aluminum	–	
a4	36	1/2" Dia. Spindle, 25" long	6061-T6 Aluminum	–	
b1	8	2" Elbow-Fitting	6061-T6 Aluminum	No. 3 Elbow	
b2	16	2" T-Fitting	6061-T6 Aluminum	No. 5 Tee	
b3	8	2" Base-Fitting	6061-T6 Aluminum	No. 47 Base	

Notes: (1) All aluminum pipe properties, dimensions, and prices came from Metals Depot (www.metalsdepot.com/).
 (2) All aluminum fittings are prefabricated components from Hollaender Speed-Rail (www.hollaender.com/?page=speedrail).
 (3) There are alternate (heavy duty) fittings for stability if needed.
 (4) Hollaender may prefabricate the rail with spindles.



Crashworthy Pedestrian Rail – Modular Aluminum System #1

Description of View

Midwest Roadside Safety Facility

DWG. NAME: AM1_R2	SCALE: 1:12 UNITS: Inches	REV. BY: JCH/KLK
----------------------	------------------------------	---------------------

SHEET: 5 of 5
DATE: 5/23/2013
DRAWN BY: MJW

Figure 34. Aluminum Modular Rail with Spindles, Design Concept AM-1 (Sheet 5 of 5)



Figure 35. Aluminum Modular Rail with Spindles, Design Concept AM-1



Figure 36. Aluminum Modular Rail with Spindles, Design Concept AM-1

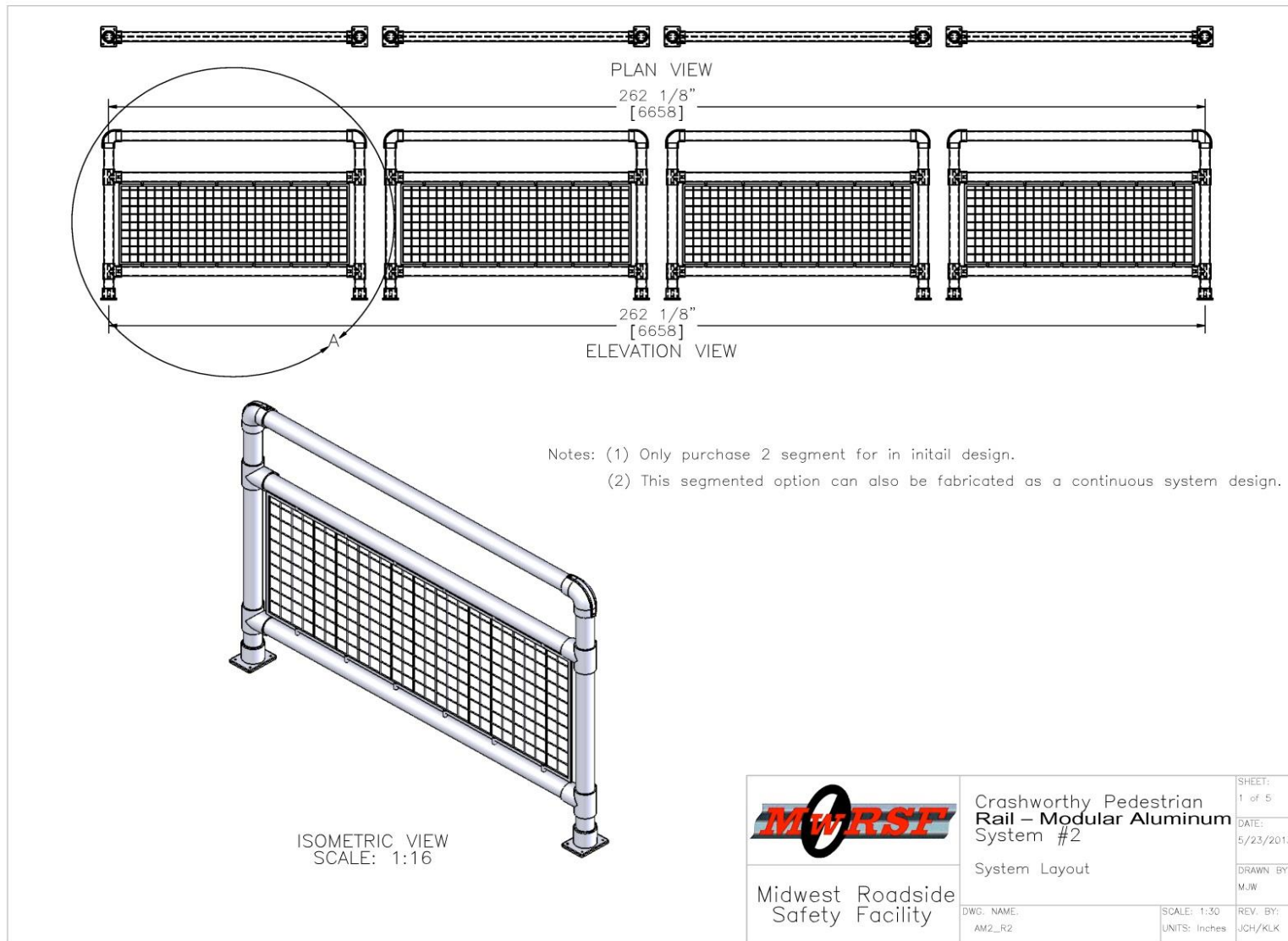
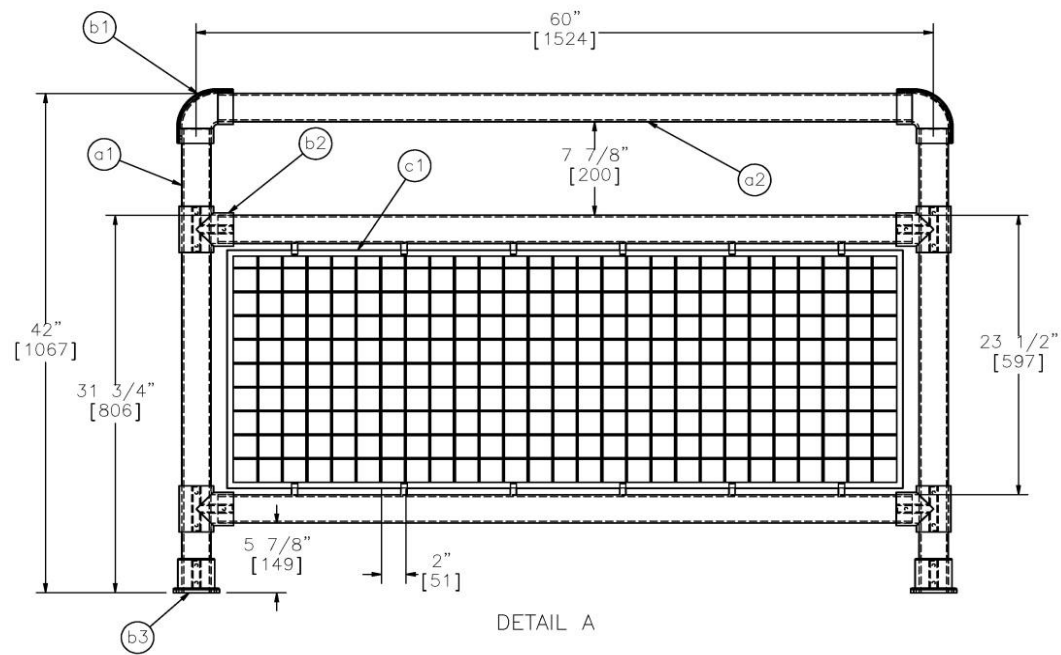


Figure 37. Aluminum Modular Rail with Wire Mesh, Design Concept AM-2 (Sheet 1 of 5)



	Crashworthy Pedestrian Rail – Modular Aluminum System #2		SHEET: 2 of 5
	Segment Details		DATE: 5/23/2013
Midwest Roadside Safety Facility	DWG. NAME: AM2_R2	SCALE: 1:12 UNITS: Inches	DRAWN BY: M.W.
			REV. BY: JCH/KLK

Figure 38. Aluminum Modular Rail with Wire Mesh, Design Concept AM-2 (Sheet 2 of 5)

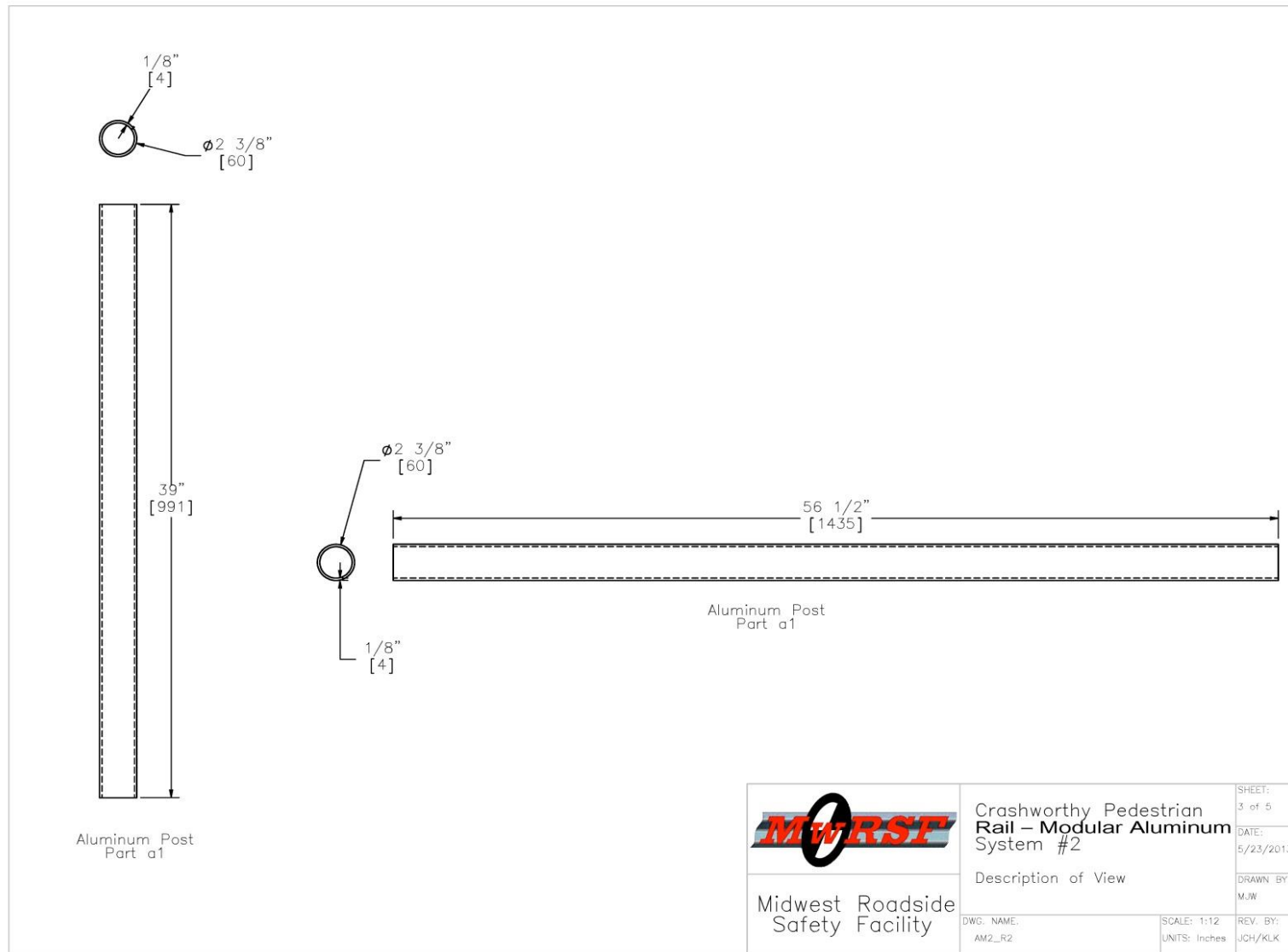


Figure 39. Aluminum Modular Rail with Wire Mesh, Design Concept AM-2 (Sheet 3 of 5)

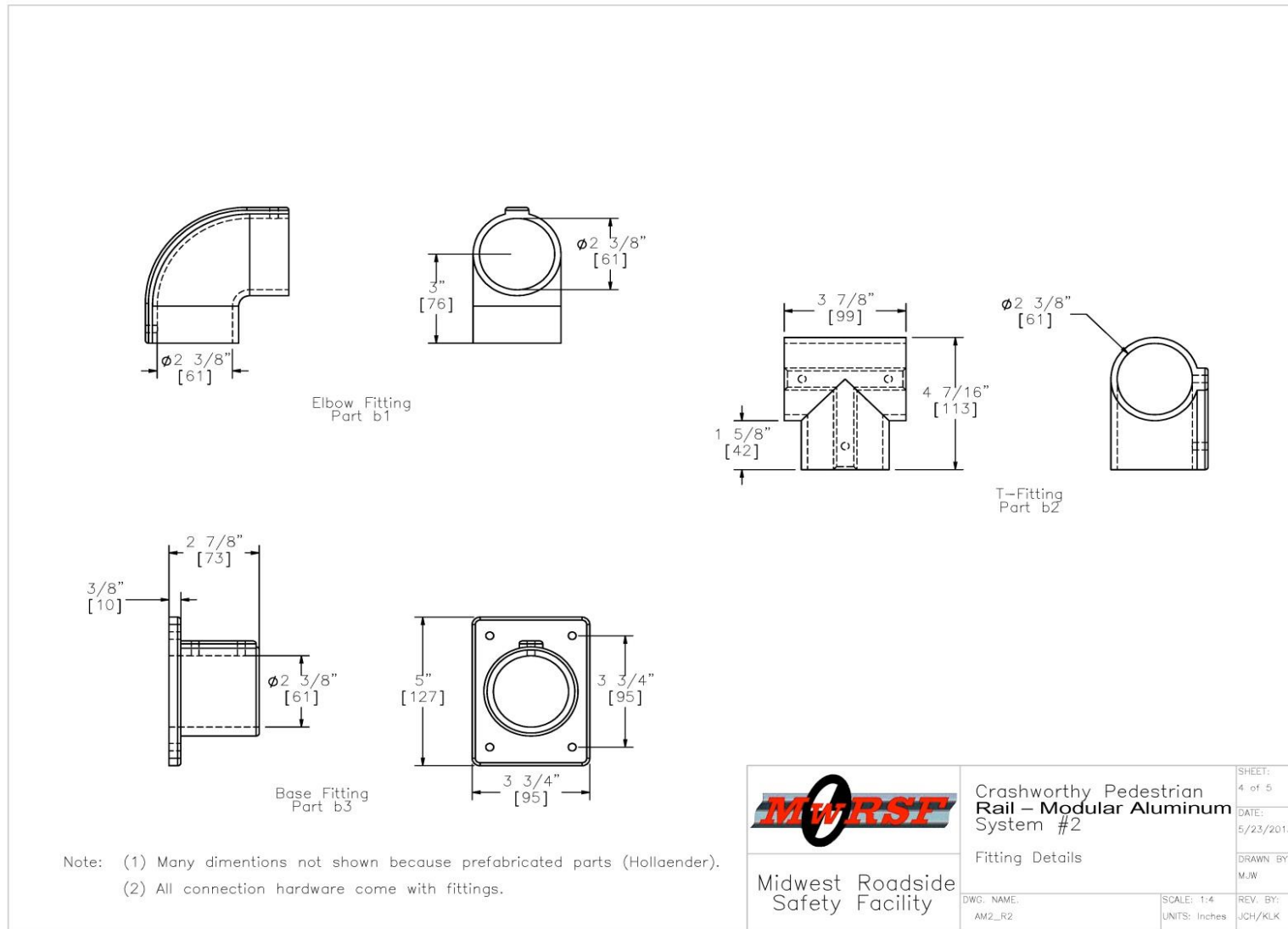


Figure 40. Aluminum Modular Rail with Wire Mesh, Design Concept AM-2 (Sheet 4 of 5)

Figure 41. Aluminum Modular Rail with Wire Mesh, Design Concept AM-2 (Sheet 5 of 5)

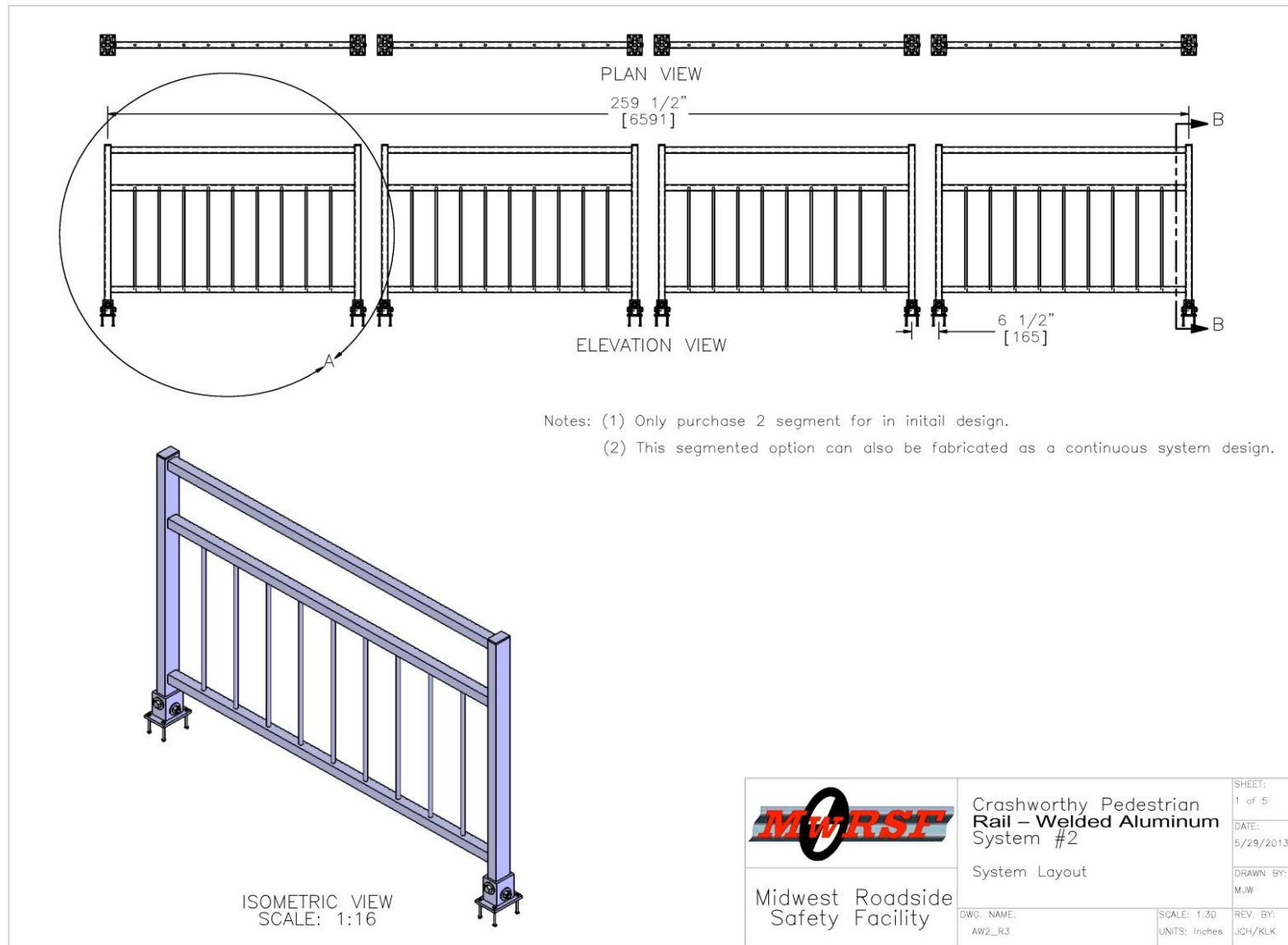


Figure 42. Welded Aluminum Rail, Design Concept AW2 (Sheet 1 of 5)

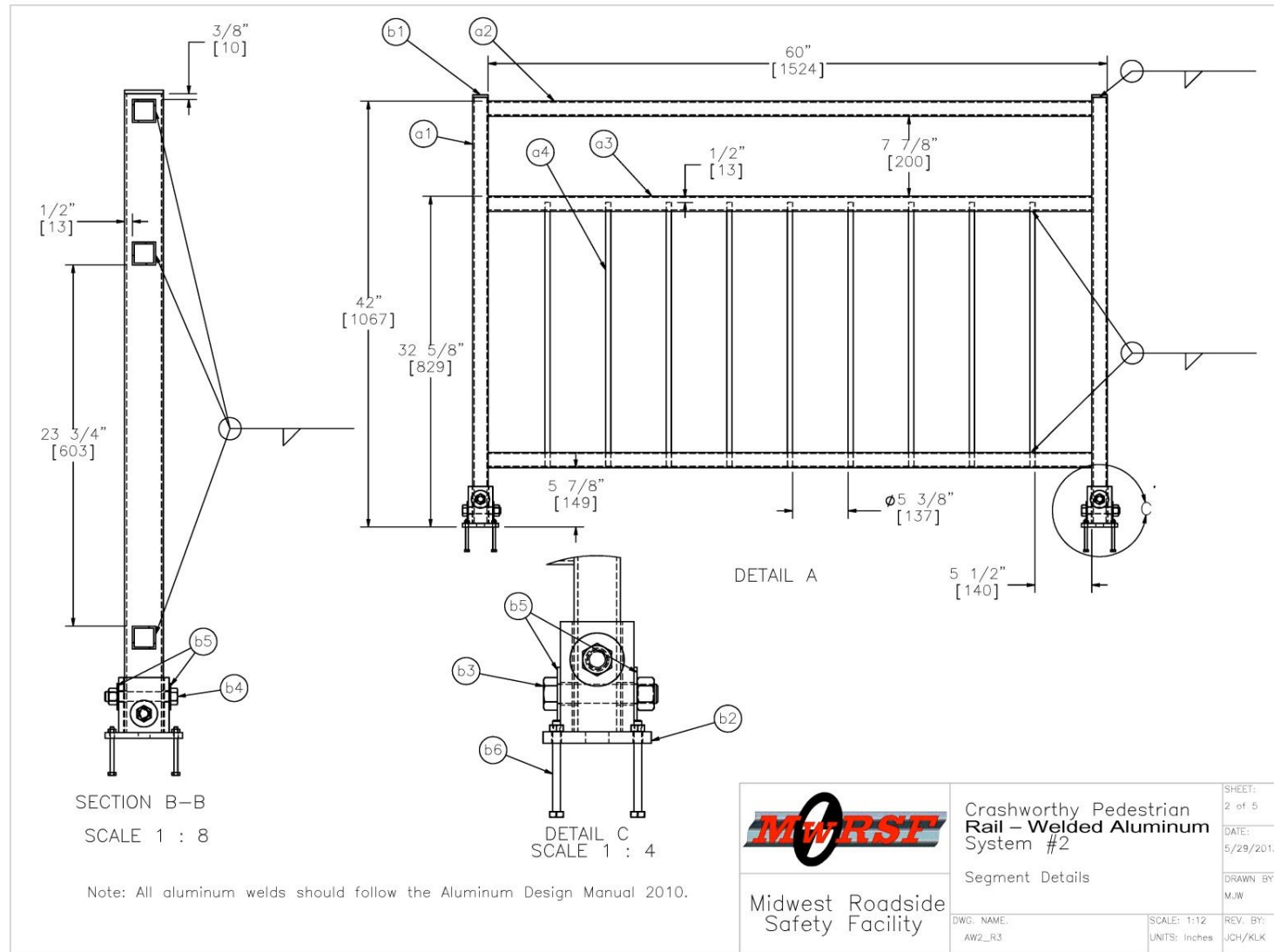


Figure 43. Welded Aluminum Rail, Design Concept AW2 (Sheet 2 of 5)

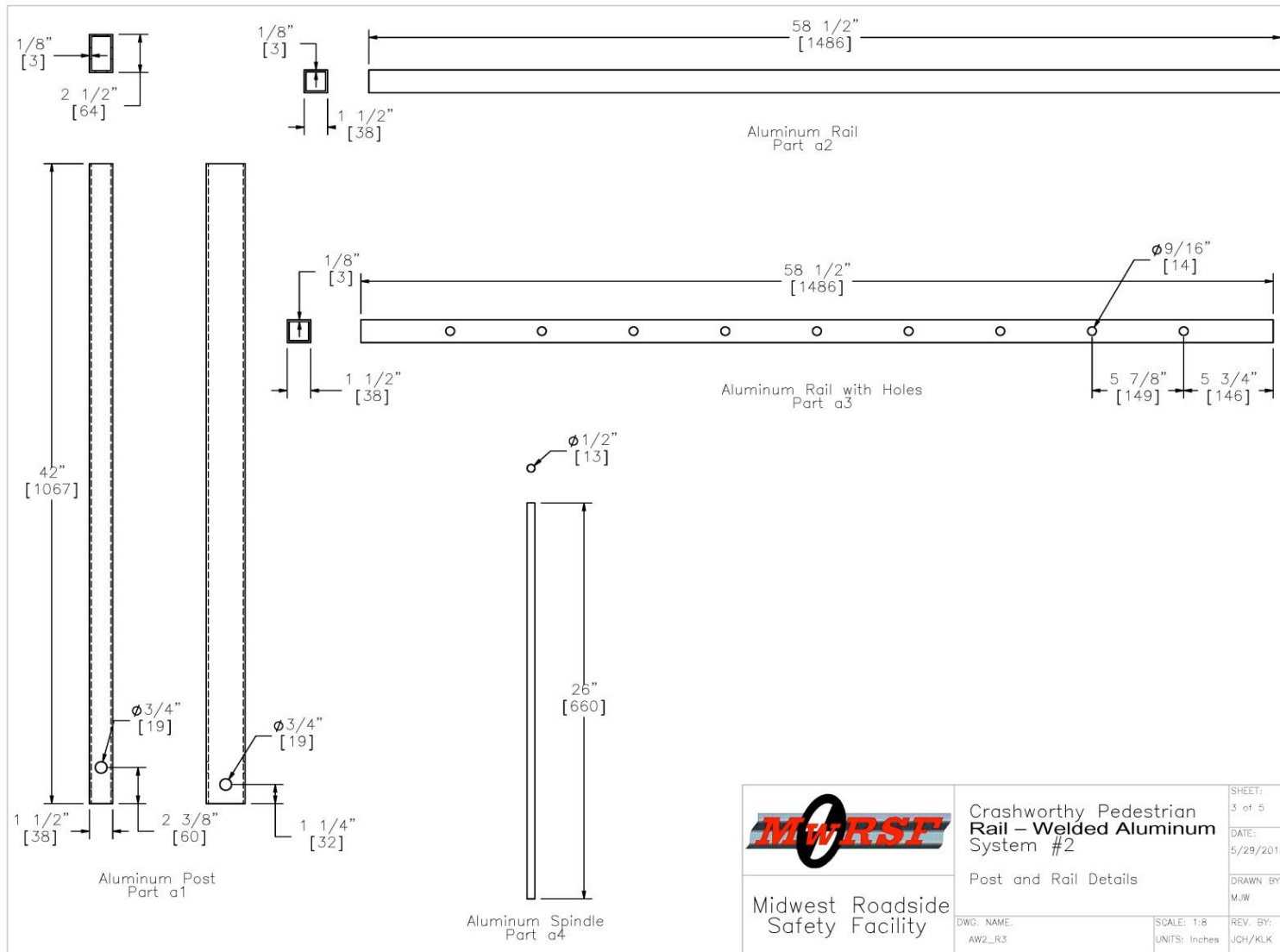


Figure 44. Welded Aluminum Rail, Design Concept AW2 (Sheet 3 of 5)

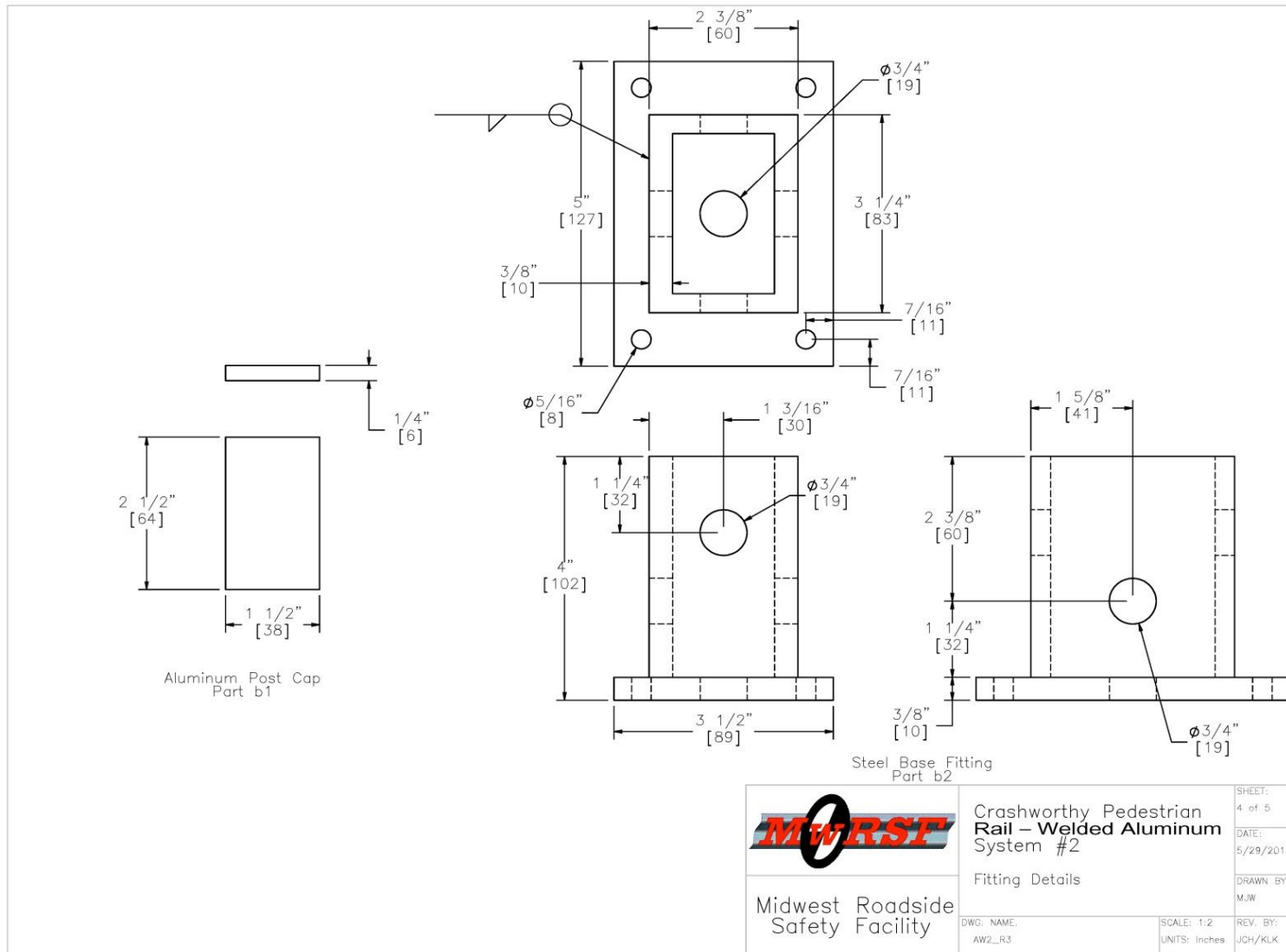


Figure 45. Welded Aluminum Rail, Design Concept AW2 (Sheet 4 of 5)


	Crashworthy Pedestrian Rail – Welded Aluminum System #2		SHEET: 5 of 5
	Bill of Materials		DATE: 5/29/2013
Midwest Roadside Safety Facility	DWG. NAME: AW2_R3	SCALE: None UNITS: Inches	DRAWN BY: M.J.W REV. BY: JCH/KLK

Figure 46. Welded Aluminum Rail, Design Concept AW2 (Sheet 5 of 5)



Figure 47. Welded Aluminum Rail, Design Concept AW2

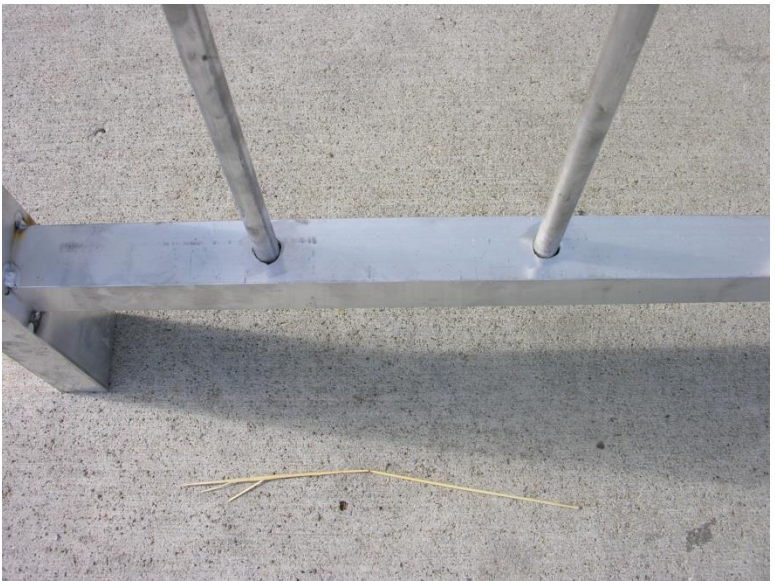


Figure 48. Welded Aluminum Rail, Design Concept AW2

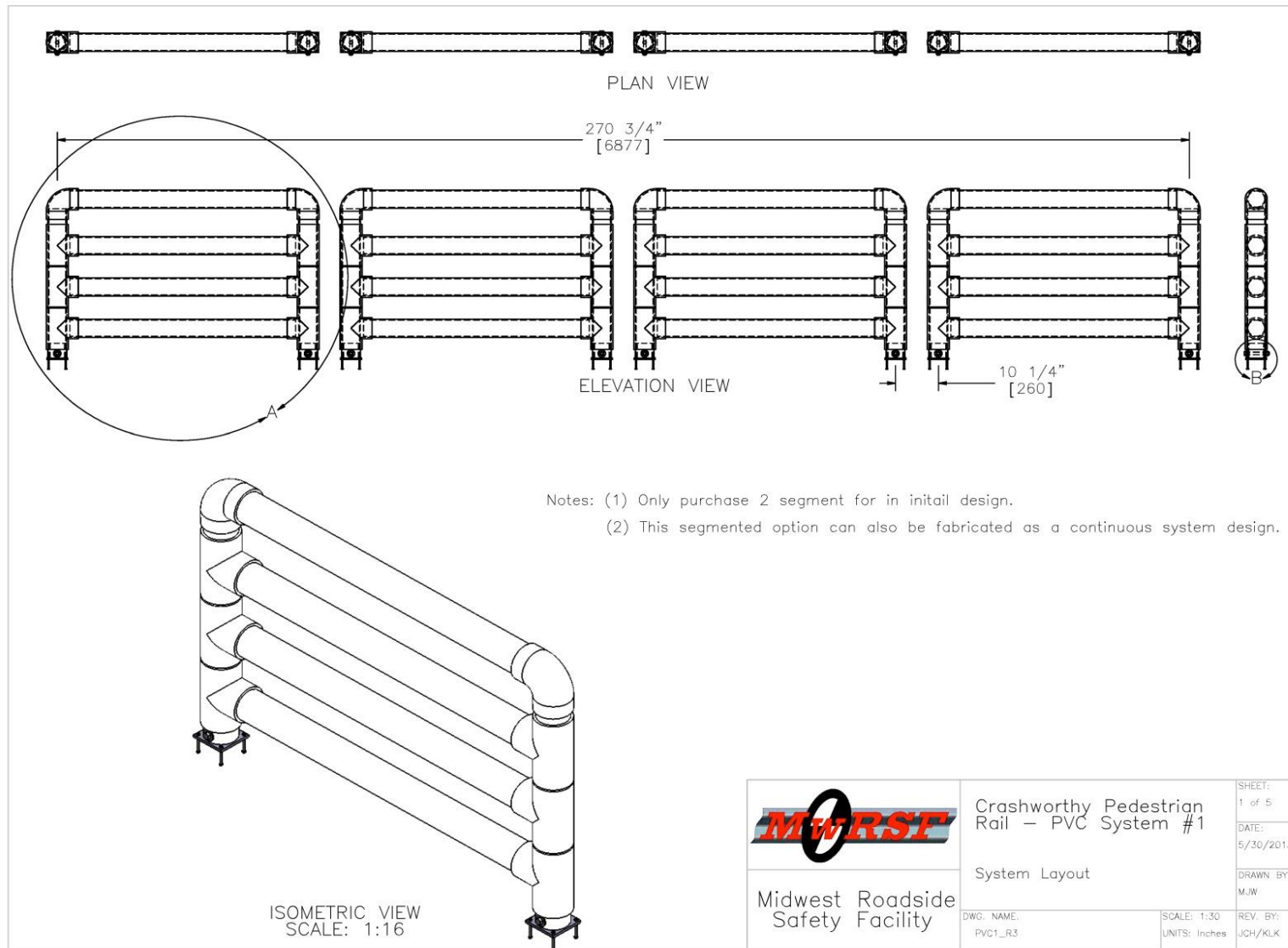


Figure 49. Modular PVC Rail, Design Concept PVC1 (Sheet 1 of 5)

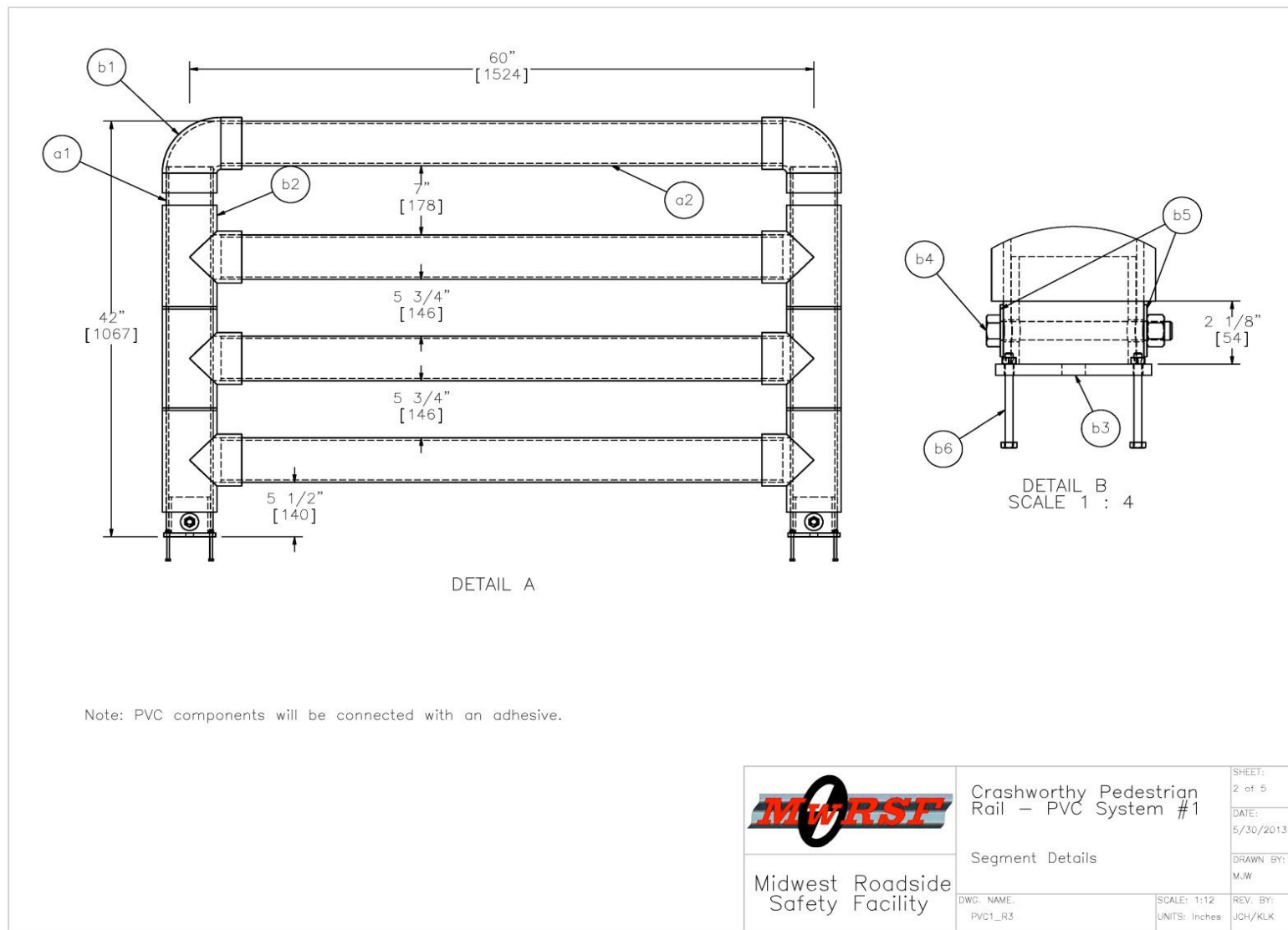


Figure 50. Modular PVC Rail, Design Concept PVC1 (Sheet 2 of 5)

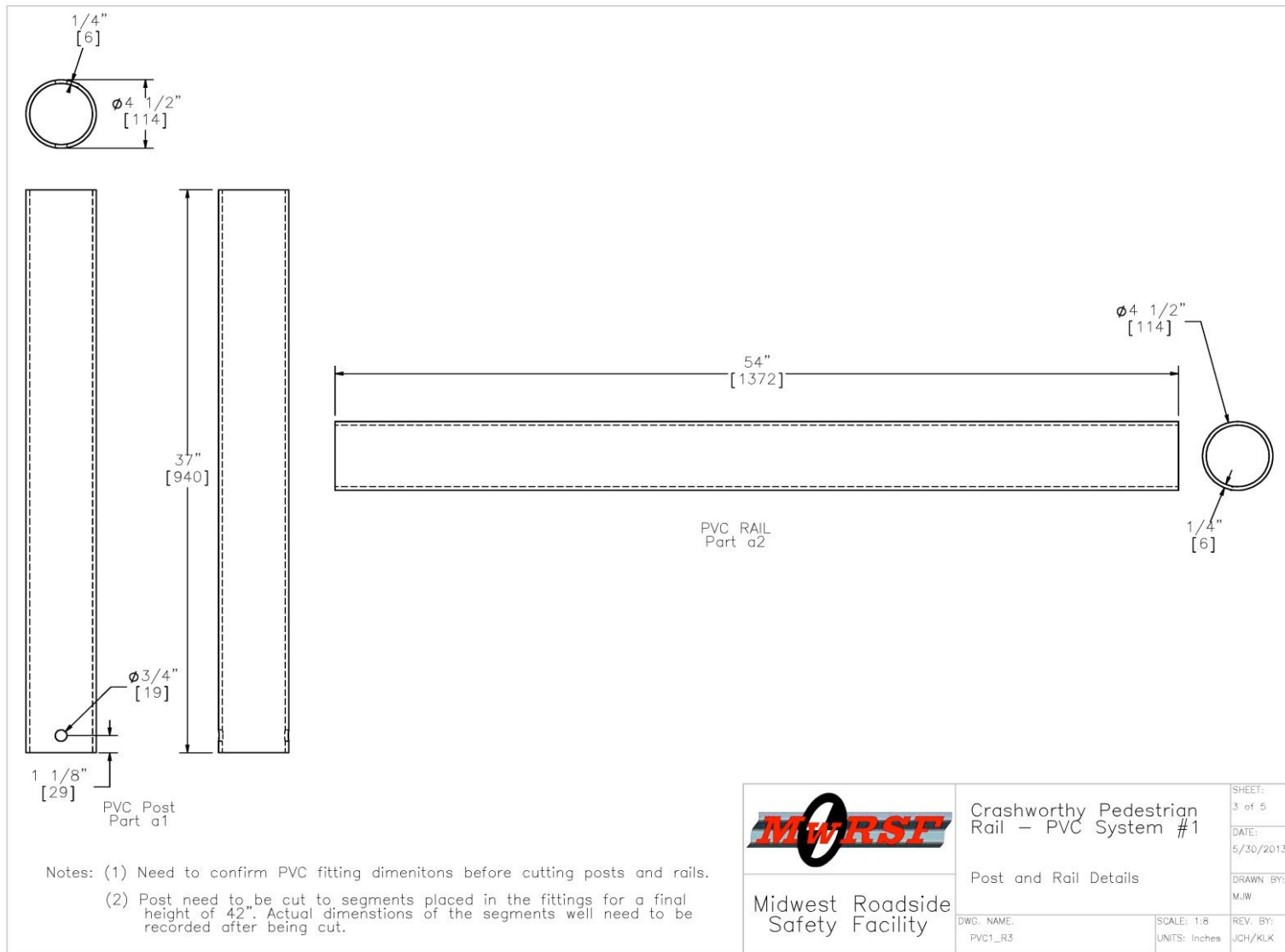


Figure 51. Modular PVC Rail, Design Concept PVC1 (Sheet 3 of 5)



Crashworthy Pedestrian Rail – Segmented PVC with Fittings					
Item No.	QTY.	Description	Material Spec	U.S. Plastic Parts	Hardware Guide
a1	8	4" Dia. Schedule 40 Post Pipe, 37" long	PVC		
a2	16	4" Dia. Schedule 40 Rail Pipe, 54" long	PVC		
b1	8	4" Dia. Elbow–Fitting	PVC	#28410	
b2	24	4" Dia. Tee Fitting	PVC	#28434	
b3	8	Post Base Fitting	A36		
b4	8	5/8" Dia. x 5 1/2" Long Hex Head Bolt and Nut	A307		FBX16a
b5	16	5/8" Dia. Flat Washer	ASTM F844 or Grade 2 Steel		FWC16a
b6	32	1/4" Dia. 3" long Hex Bolt and Nut	A307		FBX06a

Notes: (1) All PVC pipe and fitting properties, dimensions, and prices came from U.S. Plastic (www.usplastic.com).

(2) All pipe and fitting were designed with schedule 40. Schedule 80 is also available if needed.

	Crashworthy Pedestrian Rail – PVC System #1		SHEET: 5 of 5
	Bill of Materials		DATE: 5/30/2013
Midwest Roadside Safety Facility	DWG. NAME: PVC1_R3	SCALE: None UNITS: Inches	DRAWN BY: M.J.W.
			REV. BY: JCH/KLK

Figure 53. Modular PVC Rail, Design Concept PVC1 (Sheet 5 of 5)



Figure 54. Modular PVC Rail, Design Concept PVC1



Figure 55. Modular PVC Rail, Design Concept PVC1

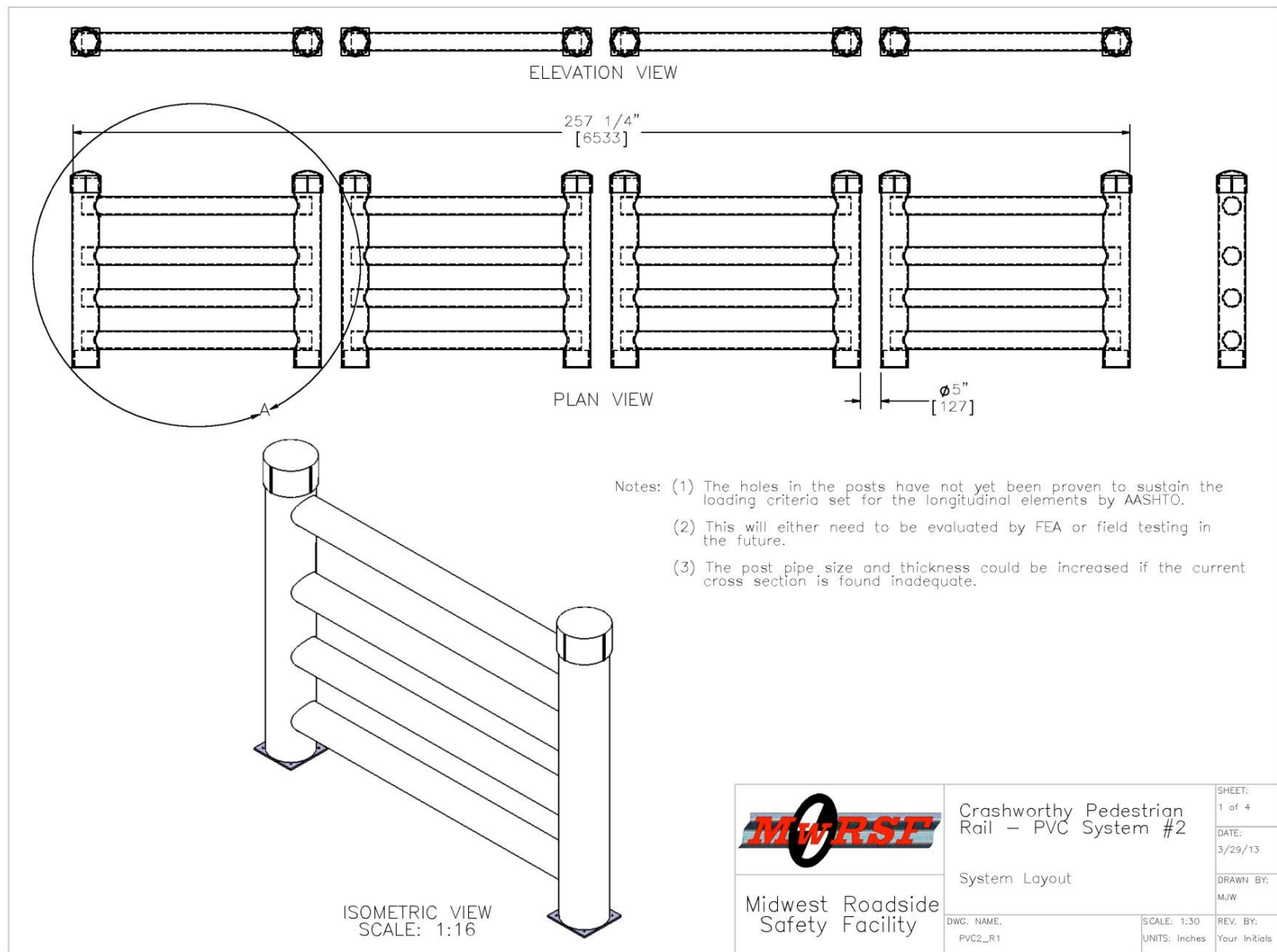
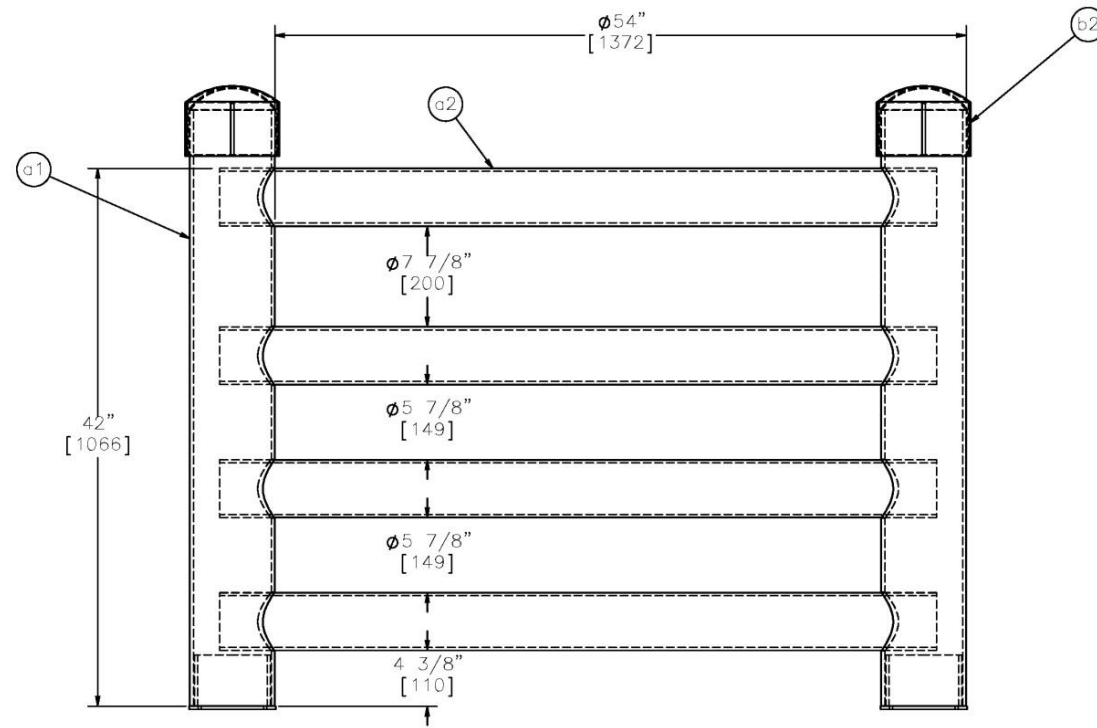


Figure 56. Modular PVC Rail, Design Concept PVC2-a (Sheet 1 of 4)



DETAIL A

	Crashworthy Pedestrian Rail — PVC System #2		SHEET: 2 of 4
	Segment Details		DATE: 3/29/13
Midwest Roadside Safety Facility	DWG. NAME: PVC2_R1		DRAWN BY: MJW
	SCALE: 1:12 UNITS: Inches		REV. BY: Your Initials

Figure 57. Modular PVC Rail, Design Concept PVC2-a (Sheet 2 of 4)

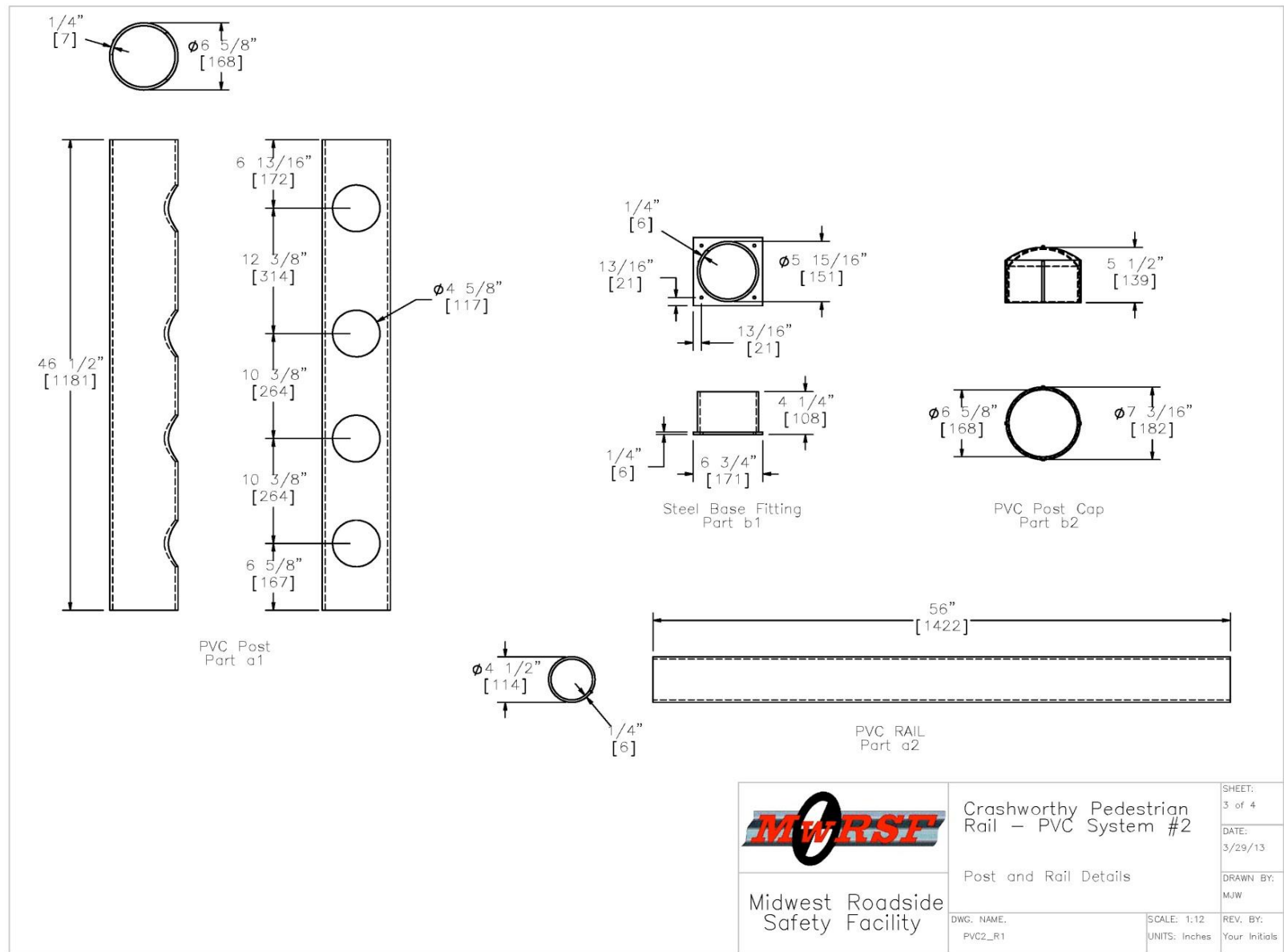


Figure 58. Modular PVC Rail, Design Concept PVC2-a (Sheet 3 of 4)

Notes: (1) All PVC pipe and fitting properties, dementions, and prices came from U.S. Plastic (www.usplastic.com).
(2) All pipe and fitting were desined with schedule 40. Schedule 80 is also available if needed.

Figure 59. Modular PVC Rail, Design Concept PVC2-a (Sheet 4 of 4)



Figure 60. Modular PVC Rail, Design Concept PVC2-a



Figure 61. Modular PVC Rail, Design Concept PVC2-a

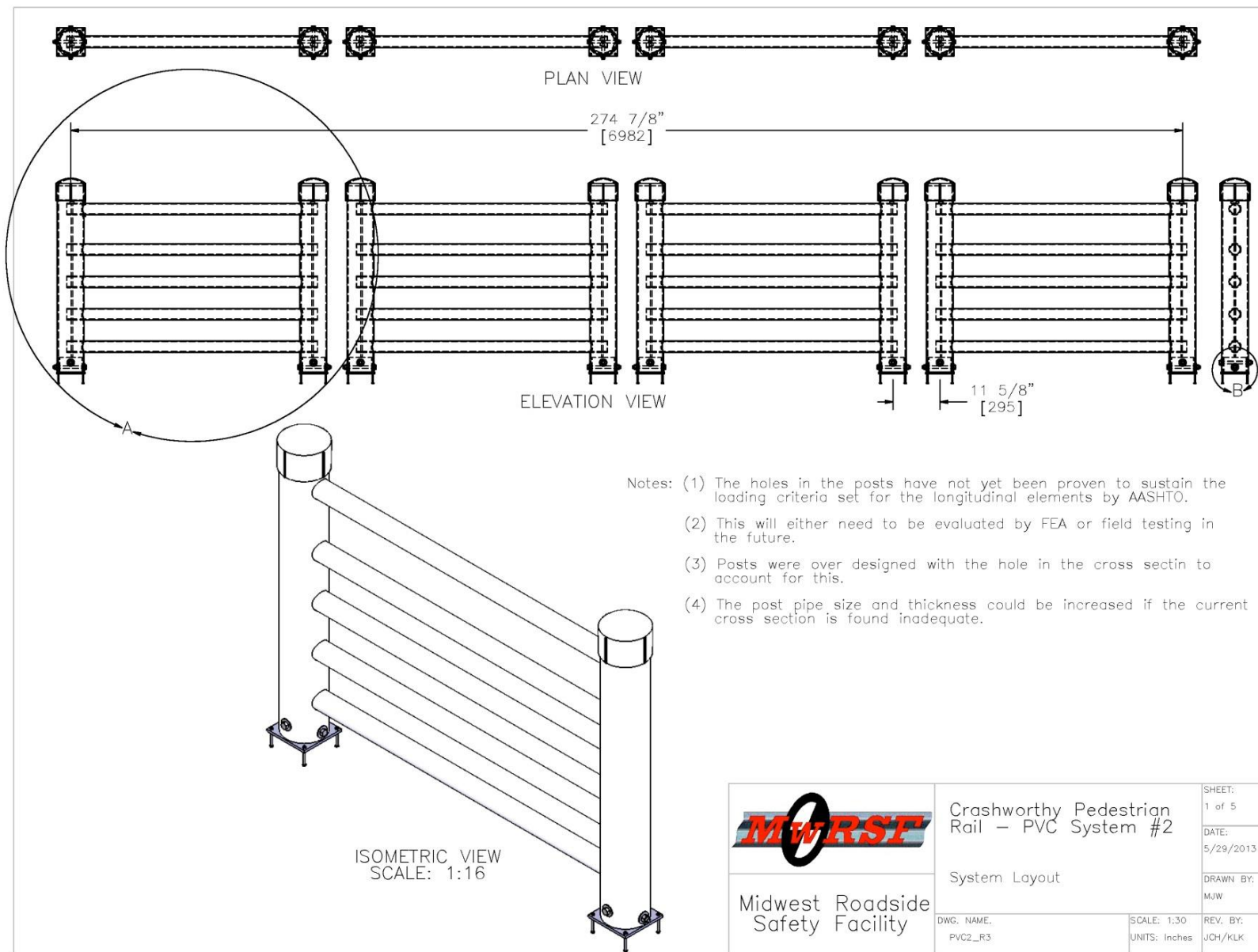


Figure 62. Modular PVC Rail, Design Concept PVC2-b (Sheet 1 of 5)

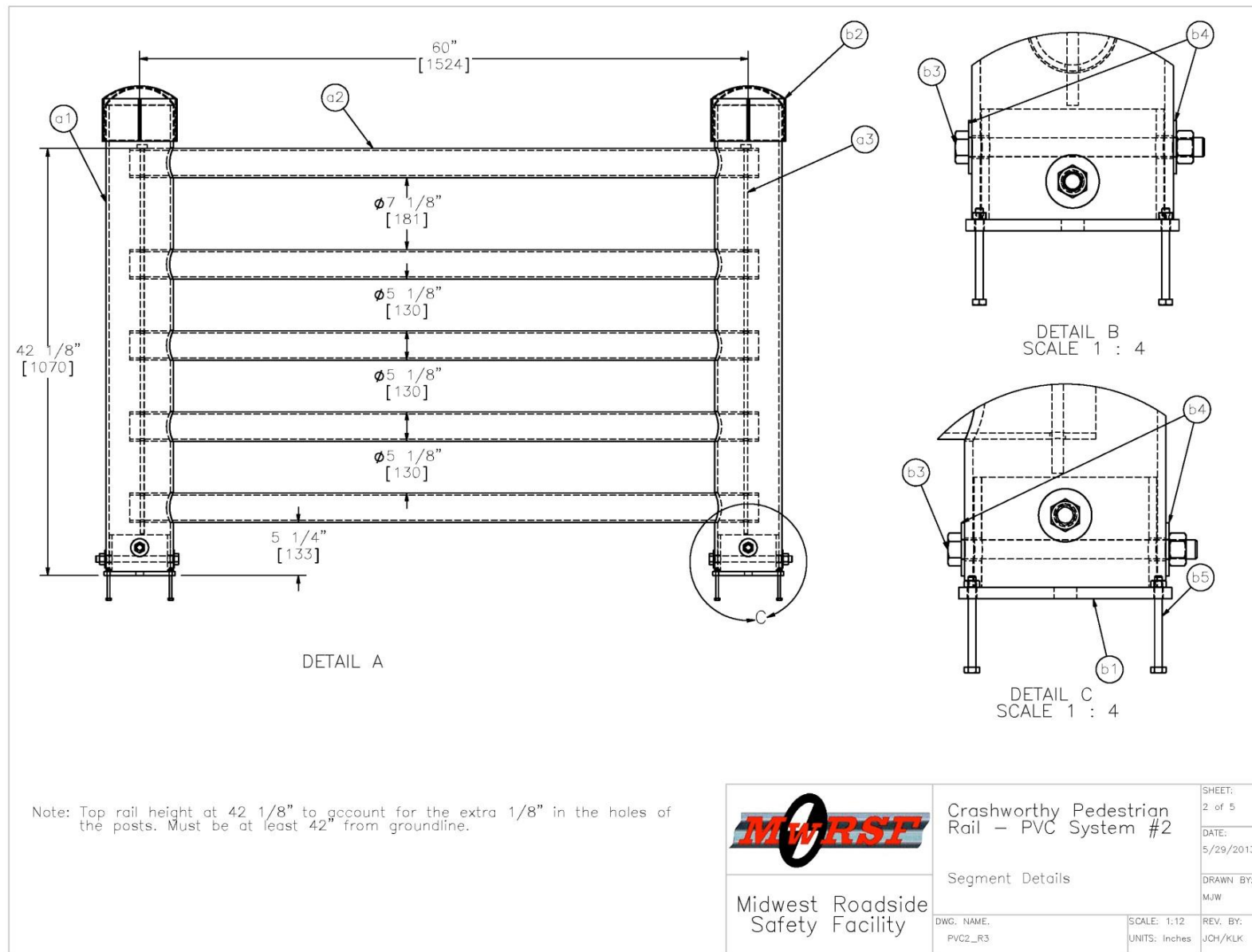


Figure 63. Modular PVC Rail, Design Concept PVC2-b (Sheet 2 of 5)

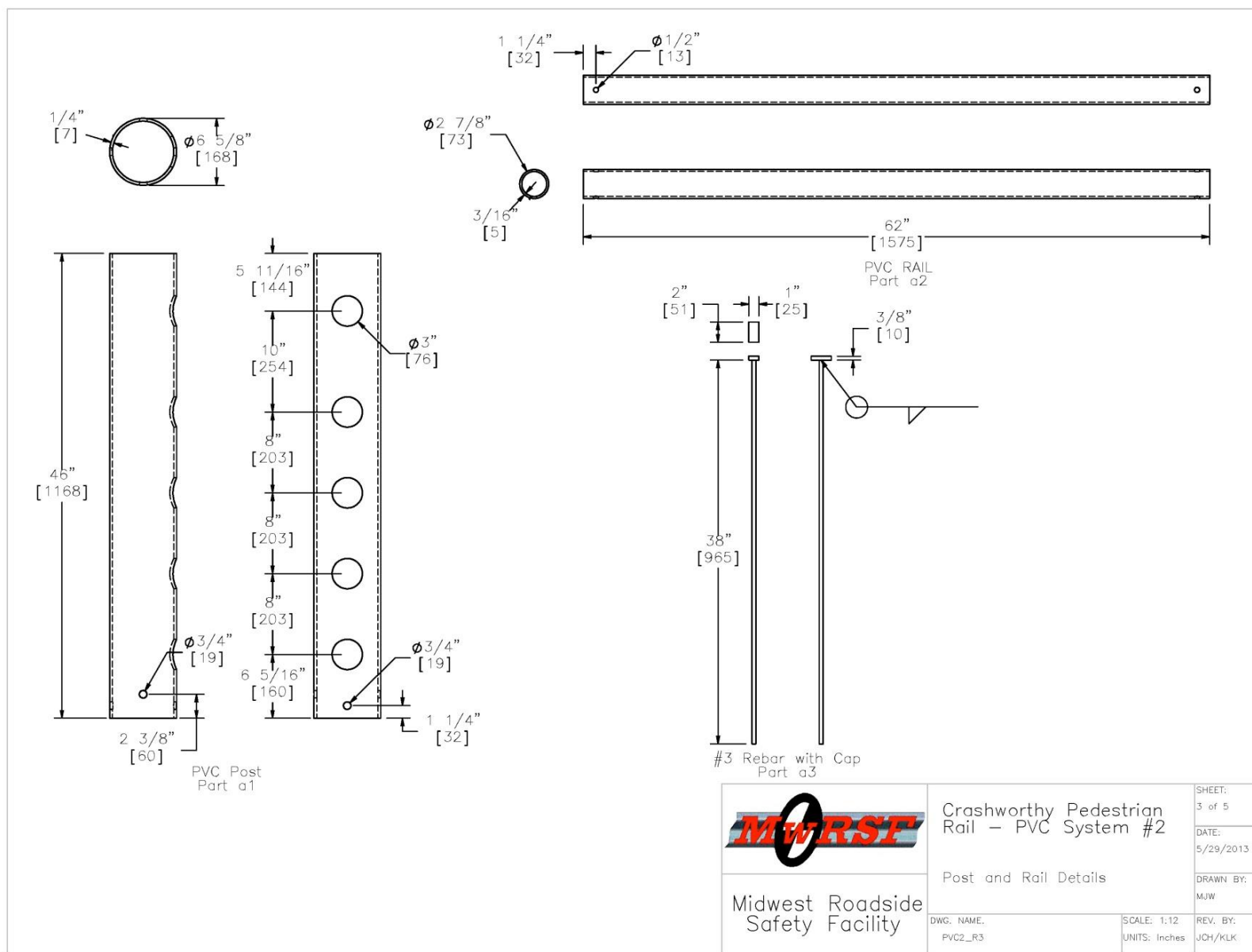


Figure 64. Modular PVC Rail, Design Concept PVC2-b (Sheet 3 of 5)

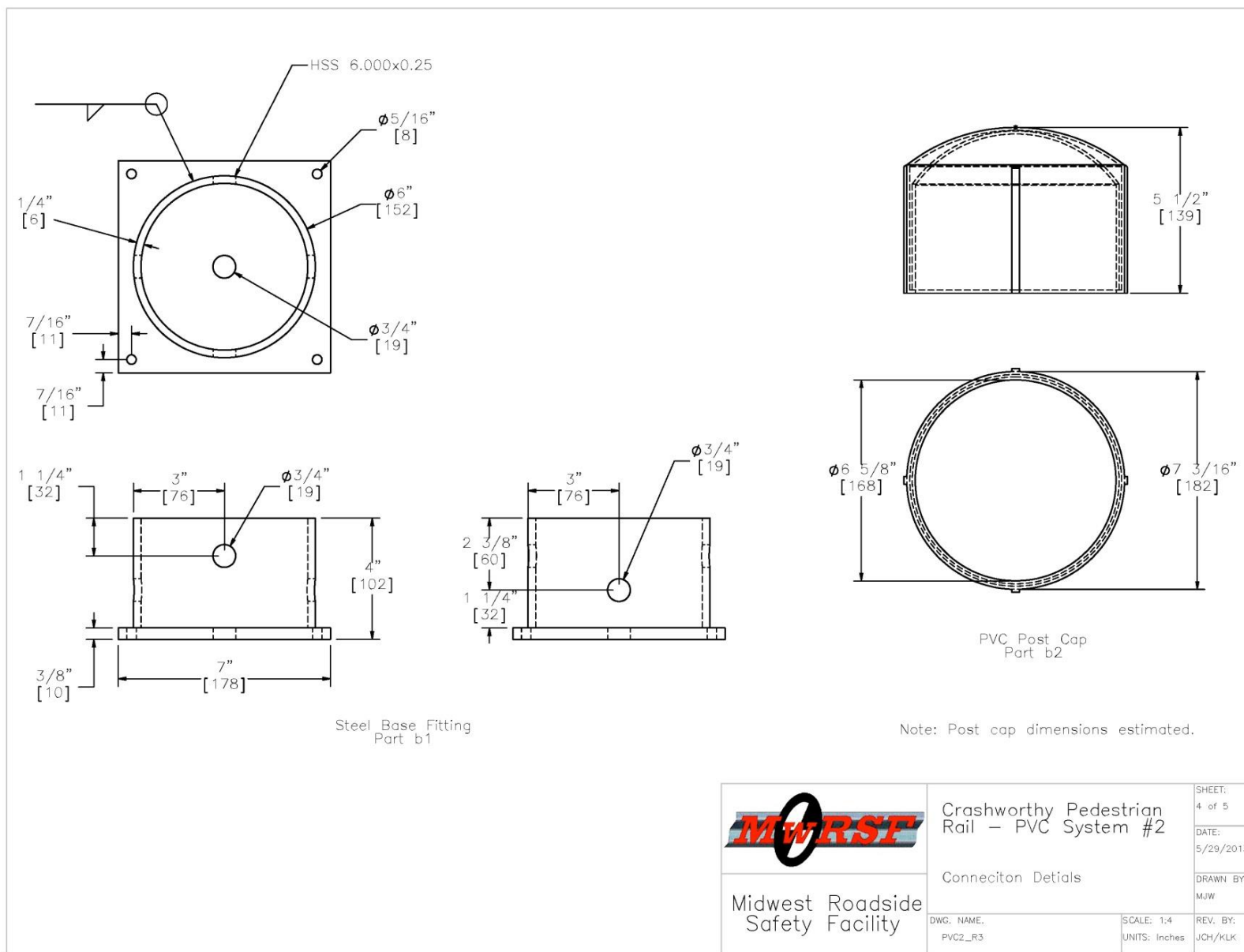


Figure 65. Modular PVC Rail, Design Concept PVC2-b (Sheet 4 of 5)

Crashworthy Pedestrian Rail – Segmented PVC					
Item No.	QTY.	Description	Material Spec	U.S. Plastic Parts	Hardware Guide
a1	8	6" Dia. Schedule 40 End Post Pipe, 46" long	PVC	#26508	
a2	20	2 1/2" Dia. Schedule 40 Rail Pipe, 62" long	PVC	#26511	
a3	8	#3 Straight Rebar with cap, 38" long	Grade 60		
b1	8	Post Base Fitting	A36	—	
b2	8	6" Dia. Post-Cap-Fitting	PVC	#28447	
b3	16	5/8" Dia. x 7 5/8" Long Hex Head Bolt and Nut	A307		FBX16a
b4	32	5/8" Dia. Flat Washer	ASTM F844 or Grade 2 Steel		FWC16a
b5	32	1/4" Dia. 3" long Hex Bolt and Nut	A307		FBX06a

Notes: (1) All PVC pipe and fitting properties, dimensions, and prices came from U.S. Plastic (www.usplastic.com).
 (2) All pipe and fitting were designed with schedule 40. Schedule 80 is also available if needed.

 Midwest Roadside Safety Facility	Crashworthy Pedestrian Rail – PVC System #2		SHEET: 5 of 5
	Bill of Materials		DATE: 5/29/2013
DWG. NAME: PVC2_R3	SCALE: None UNITS: Inches	REV. BY: JCH/KLK	

Figure 66. Modular PVC Rail, Design Concept PVC2-b (Sheet 5 of 5)

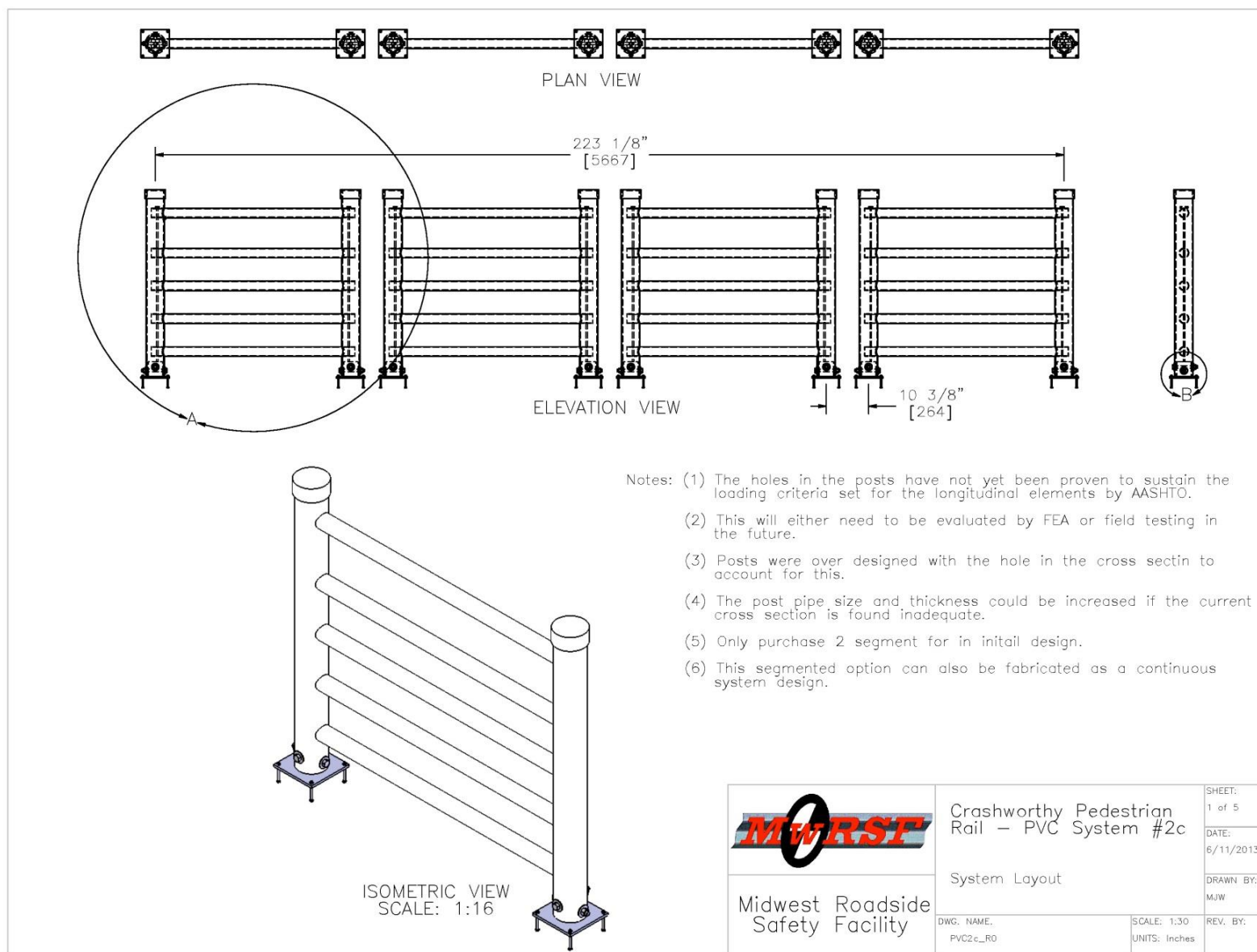


Figure 67. Modular PVC Rail, Design Concept PVC2-c (Sheet 1 of 5)

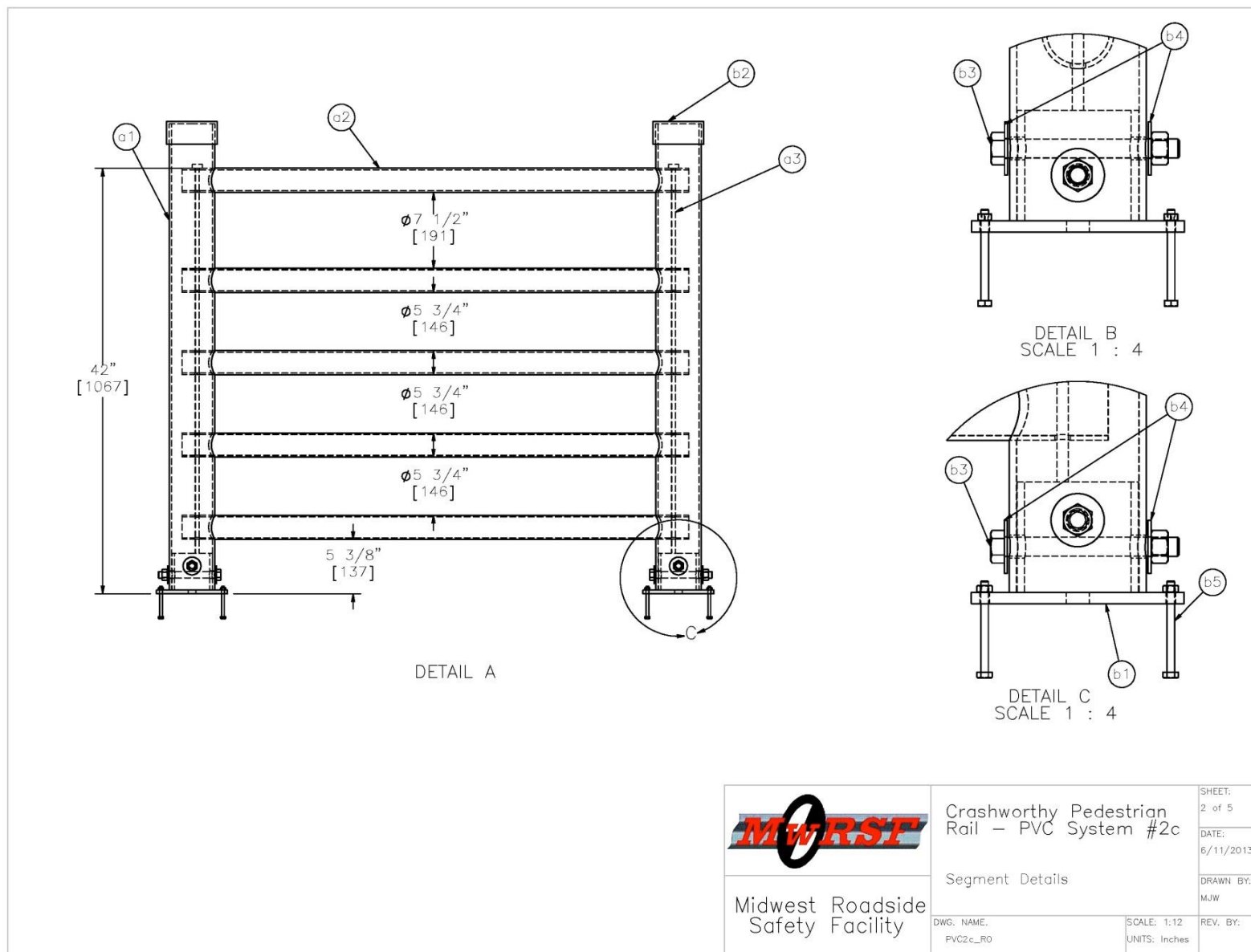


Figure 68. Modular PVC Rail, Design Concept PVC2-c (Sheet 2 of 5)

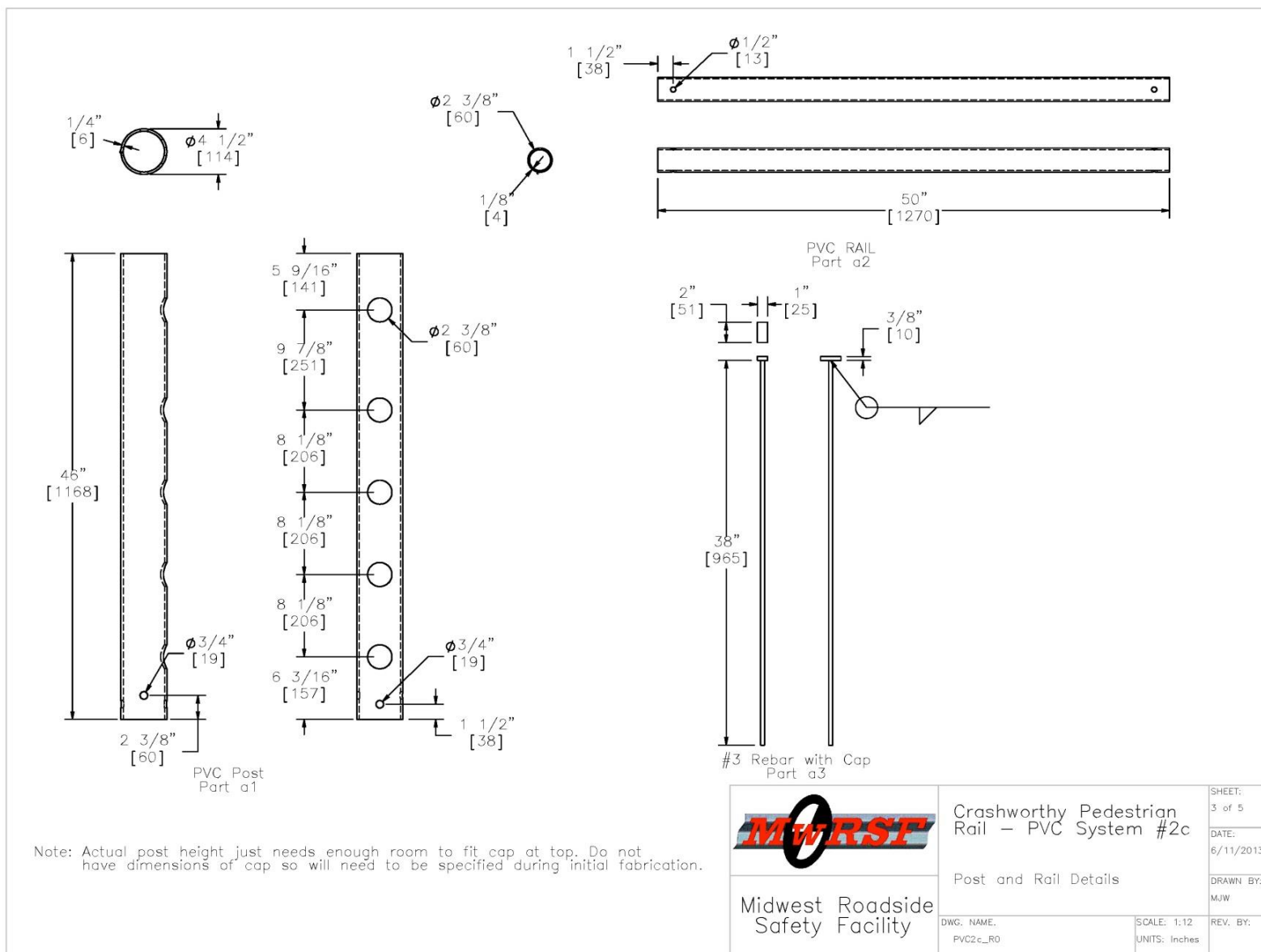


Figure 69. Modular PVC Rail, Design Concept PVC2-c (Sheet 3 of 5)

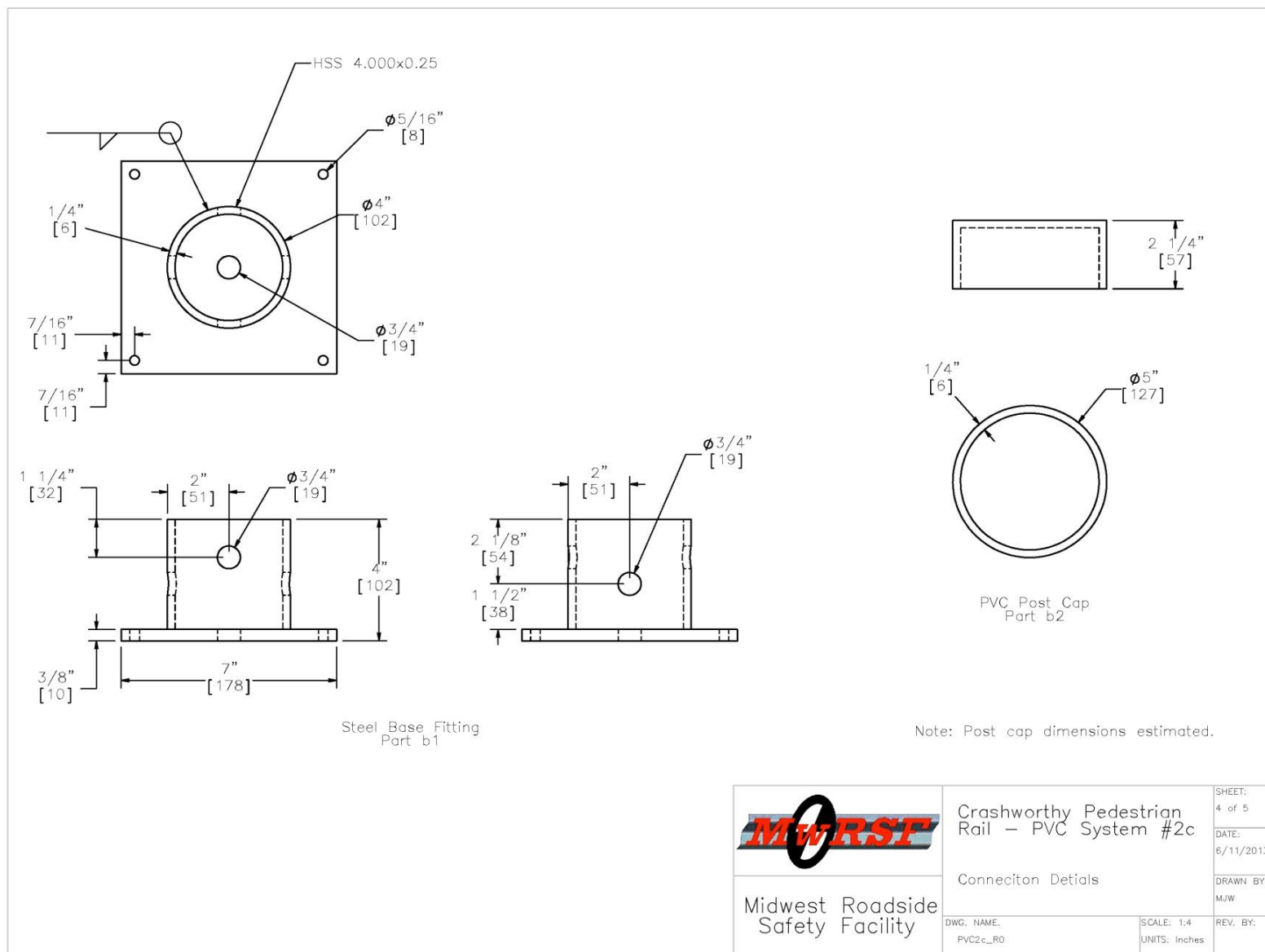


Figure 70. Modular PVC Rail, Design Concept PVC2-c (Sheet 4 of 5)

Crashworthy Pedestrian Rail – Segmented PVC				
Item No.	QTY.	Description	Material Spec	Hardware Guide
a1	8	4" Dia. Schedule 40 End Post Pipe, 46" long	PVC	
a2	20	2 1/2" Dia. Schedule 40 Rail Pipe, 50" long	PVC	
a3	8	#3 Straight Rebar with cap, 38" long	Grade 60	
b1	8	Post Base Fitting	A36	
b2	8	6" Dia. Post-Cap-Fitting	PVC	
b3	16	5/8" Dia. x 6 5/8" Long Hex Head Bolt and Nut	A307	FBX16a
b4	32	5/8" Dia. Flat Washer	ASTM F844 or Grade 2 Steel	FWC16a
b5	32	1/4" Dia. 3" long Hex Bolt and Nut	A307	FBX06a

Notes: (1) All PVC pipe and fitting properties, dimensions, and prices came from U.S. Plastic (www.usplastic.com).
 (2) All pipe and fitting were designed with schedule 40. Schedule 80 is also available if needed.

 Midwest Roadside Safety Facility	Crashworthy Pedestrian Rail – PVC System #2c	SHEET: 5 of 5
	Bill of Materials	DATE: 6/11/2013
DWG. NAME: PVC2c_R0	SCALE: None UNITS: Inches	DRAWN BY: MJW REV. BY:

Figure 71. Modular PVC Rail, Design Concept PVC2-c (Sheet 5 of 5)



Figure 72. Modular PVC Rail, Design Concept PVC2-c



Figure 73. Modular PVC Rail, Design Concept PVC2-c

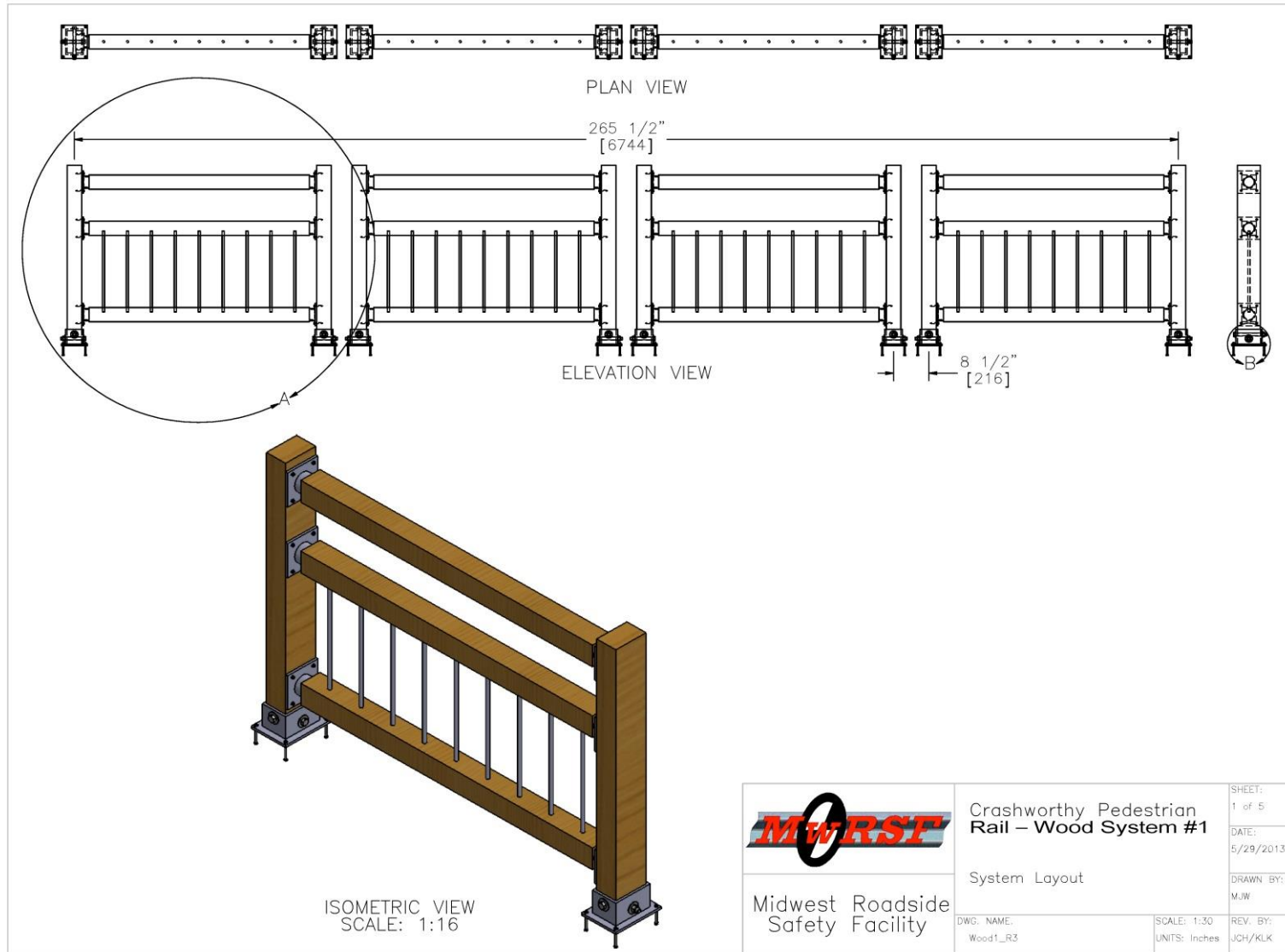


Figure 74. Modular Wood Rail, Design Concept WOOD1 (Sheet 1 of 5)

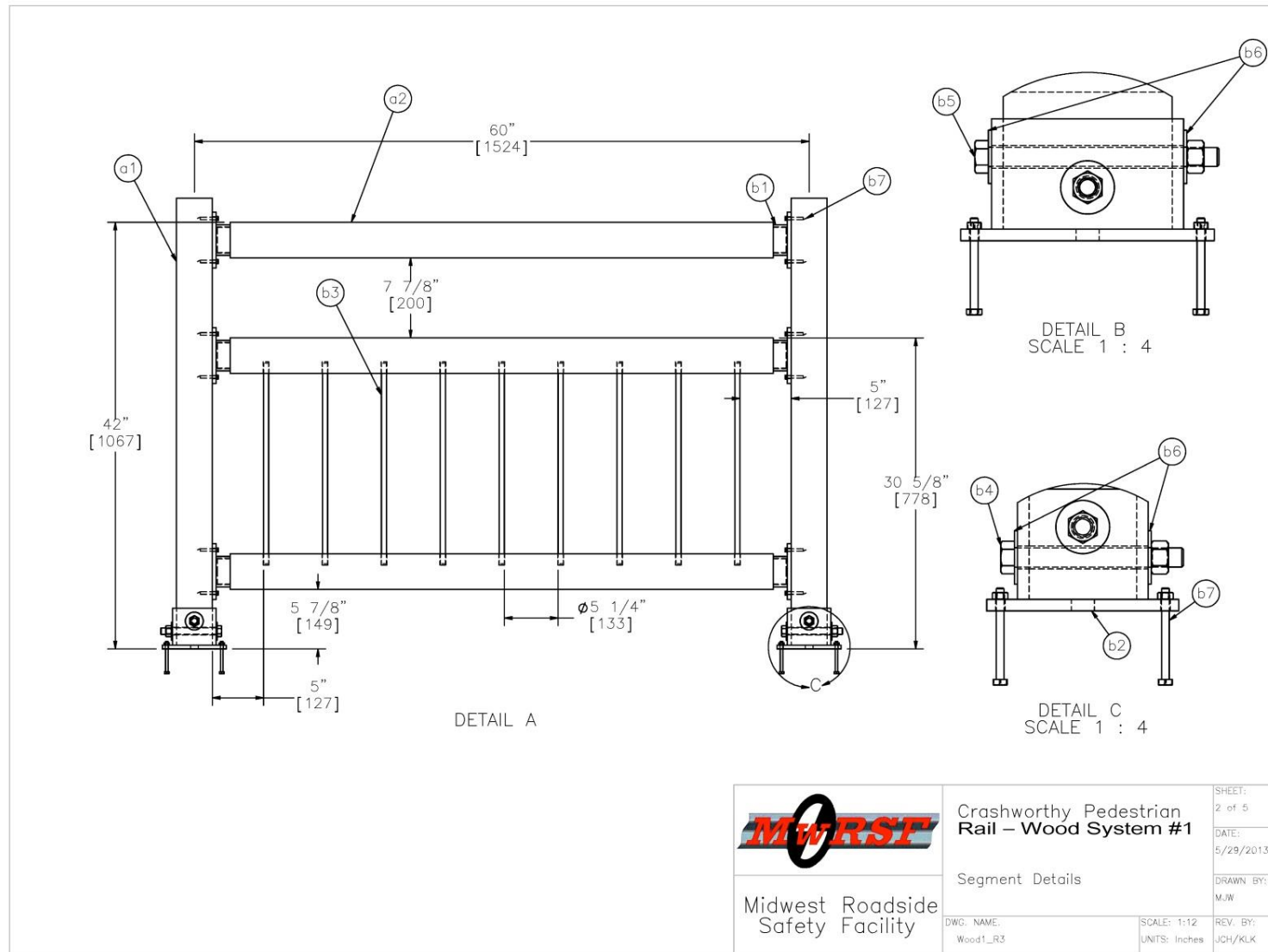


Figure 75. Modular Wood Rail, Design Concept WOOD1 (Sheet 2 of 5)

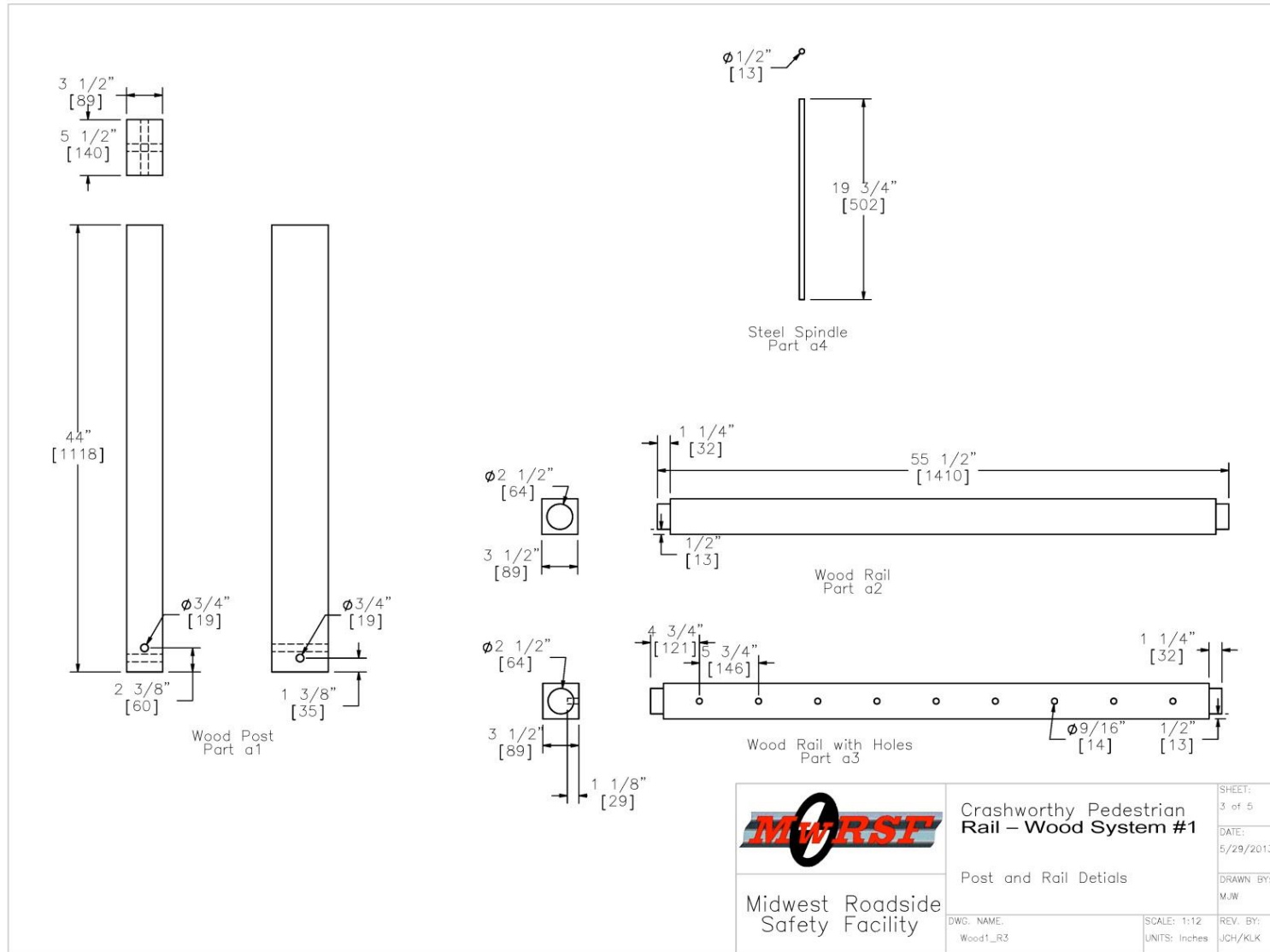


Figure 76. Modular Wood Rail, Design Concept WOOD1 (Sheet 3 of 5)

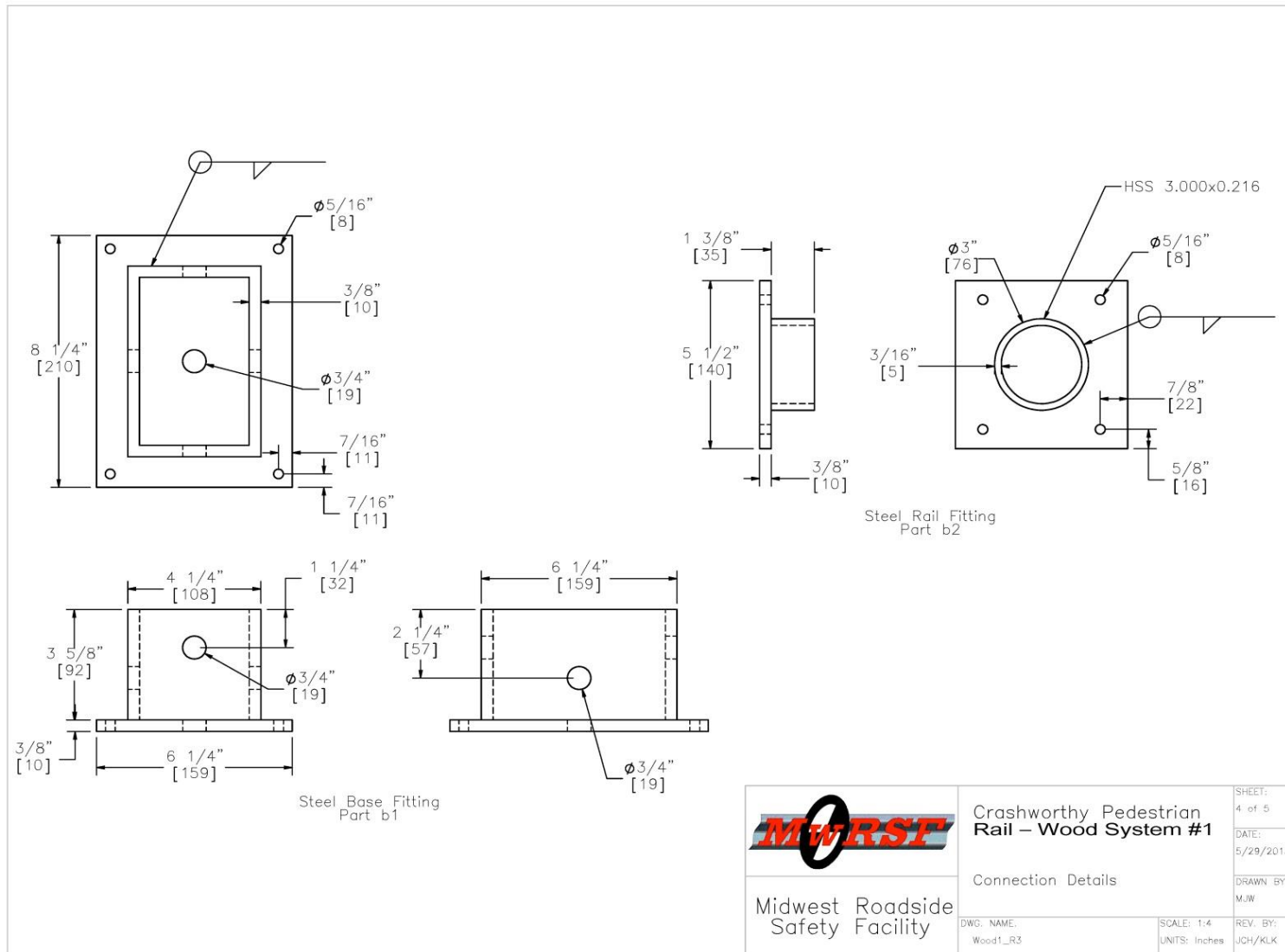


Figure 77. Modular Wood Rail, Design Concept WOOD1 (Sheet 4 of 5)


	Crashworthy Pedestrian Rail – Wood System #1		SHEET: 5 of 5
	Bill of Materials	DATE: 5/29/2013	DRAWN BY: M.J.W
Midwest Roadside Safety Facility	DWG. NAME: Wood1_R3	SCALE: None UNITS: Inches	REV. BY: JCH/KLK

Figure 78. Modular Wood Rail, Design Concept WOOD1 (Sheet 5 of 5)



Figure 79. Fabricated Refined Design Concept WOOD1

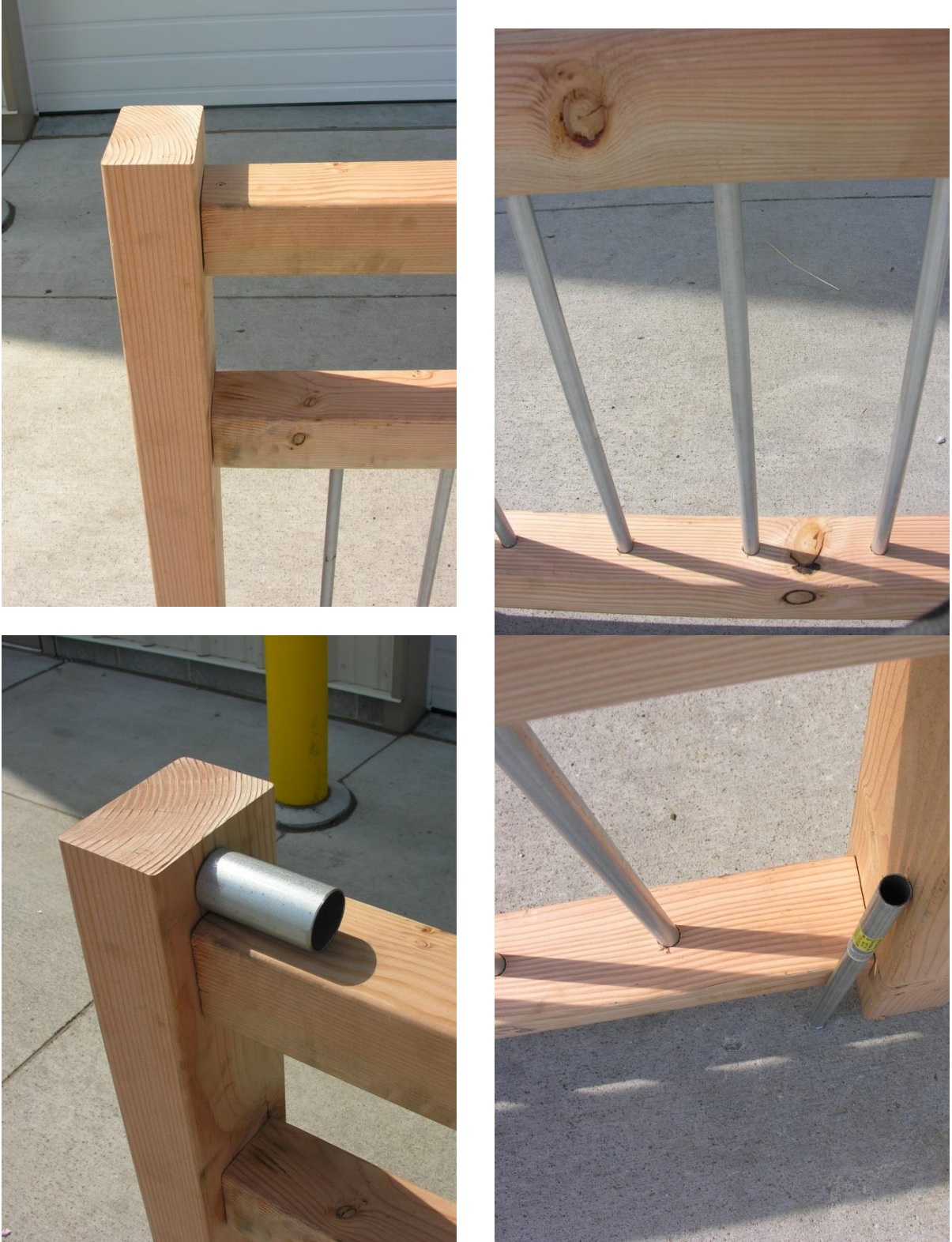


Figure 80. Fabricated Refined Design Concept WOOD1

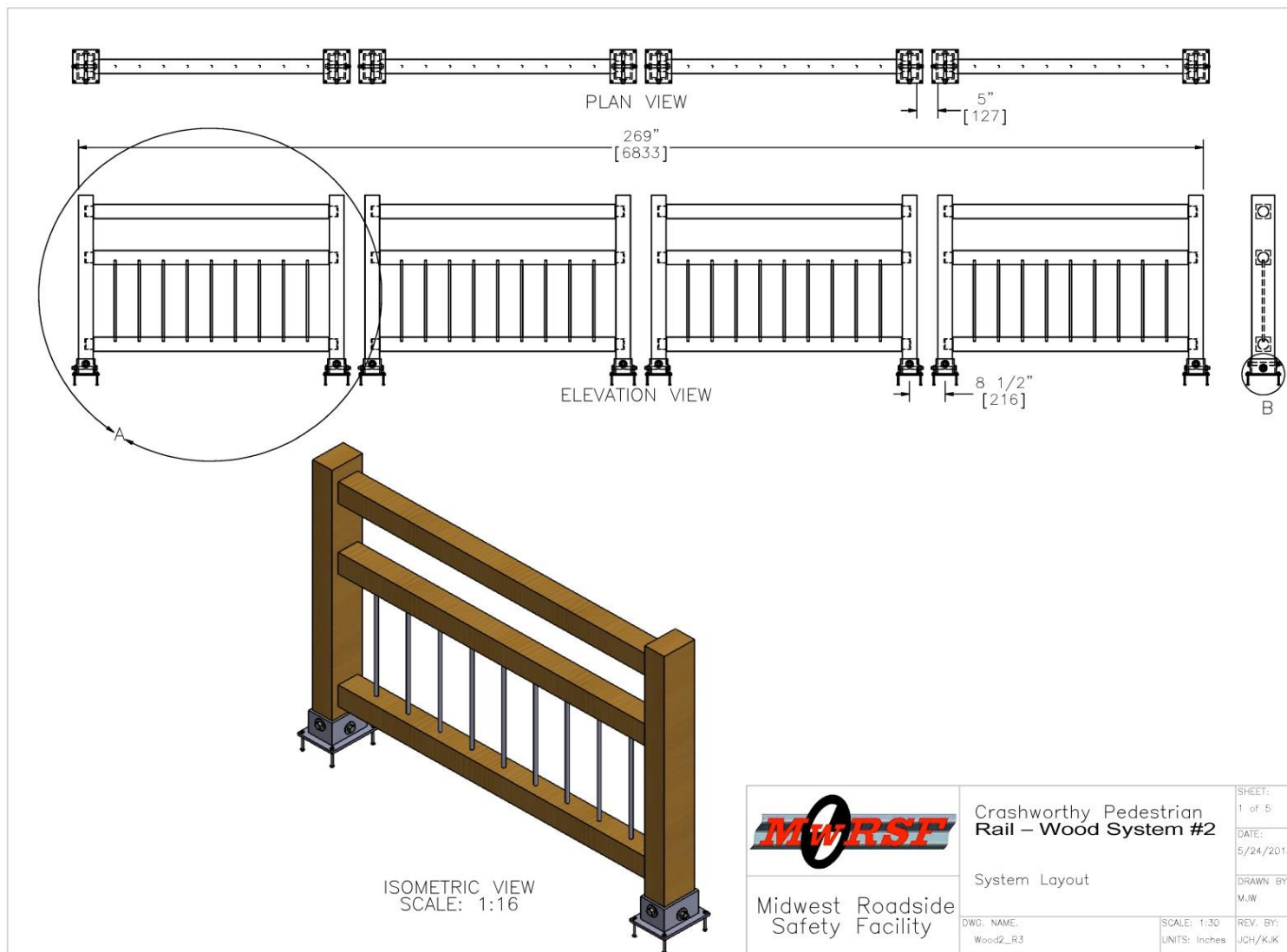


Figure 81. Cutout Wood Rail, Design Concept WOOD2 (Sheet 1 of 5)

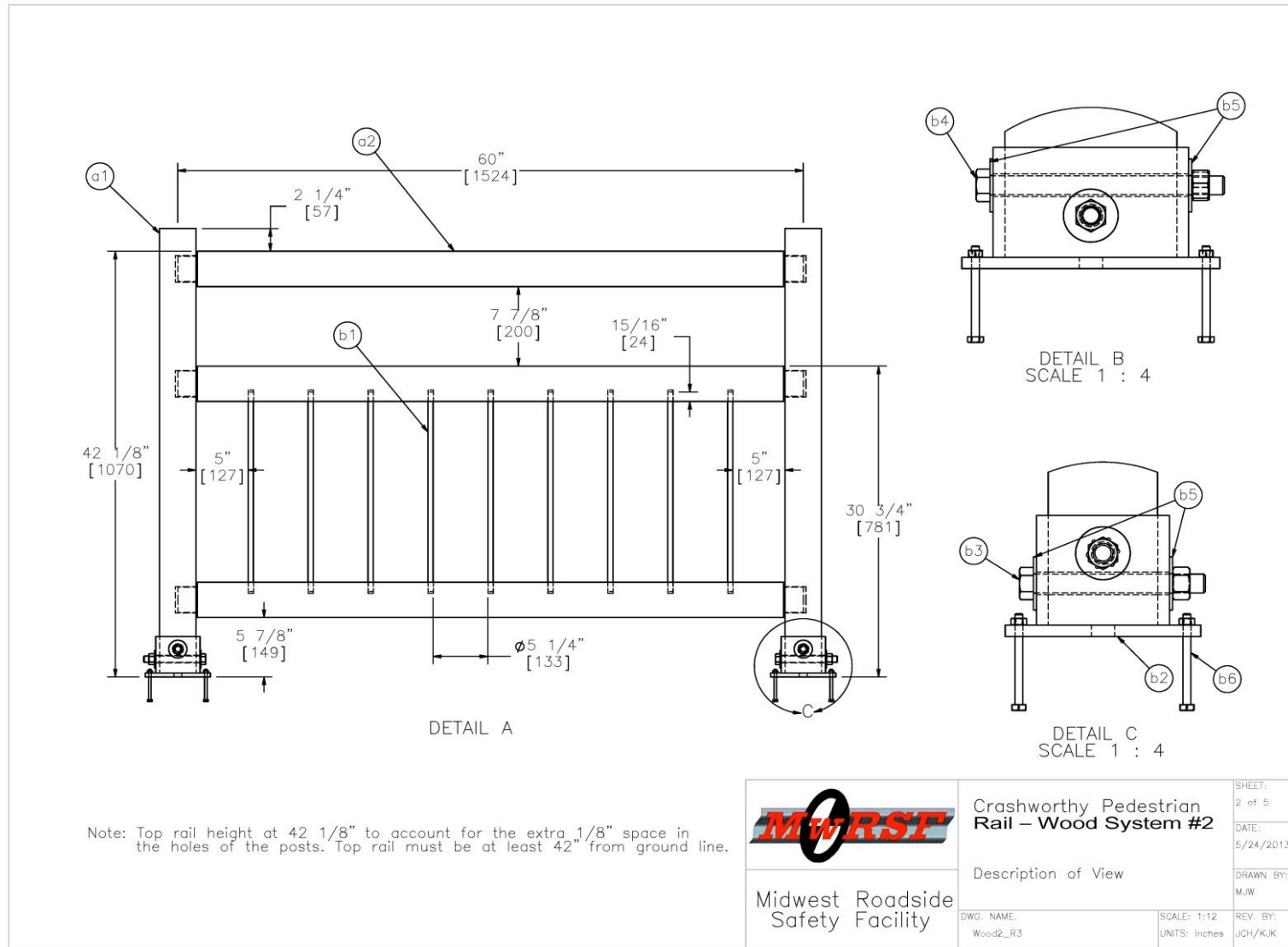


Figure 82. Cutout Wood Rail, Design Concept WOOD2 (Sheet 2 of 5)

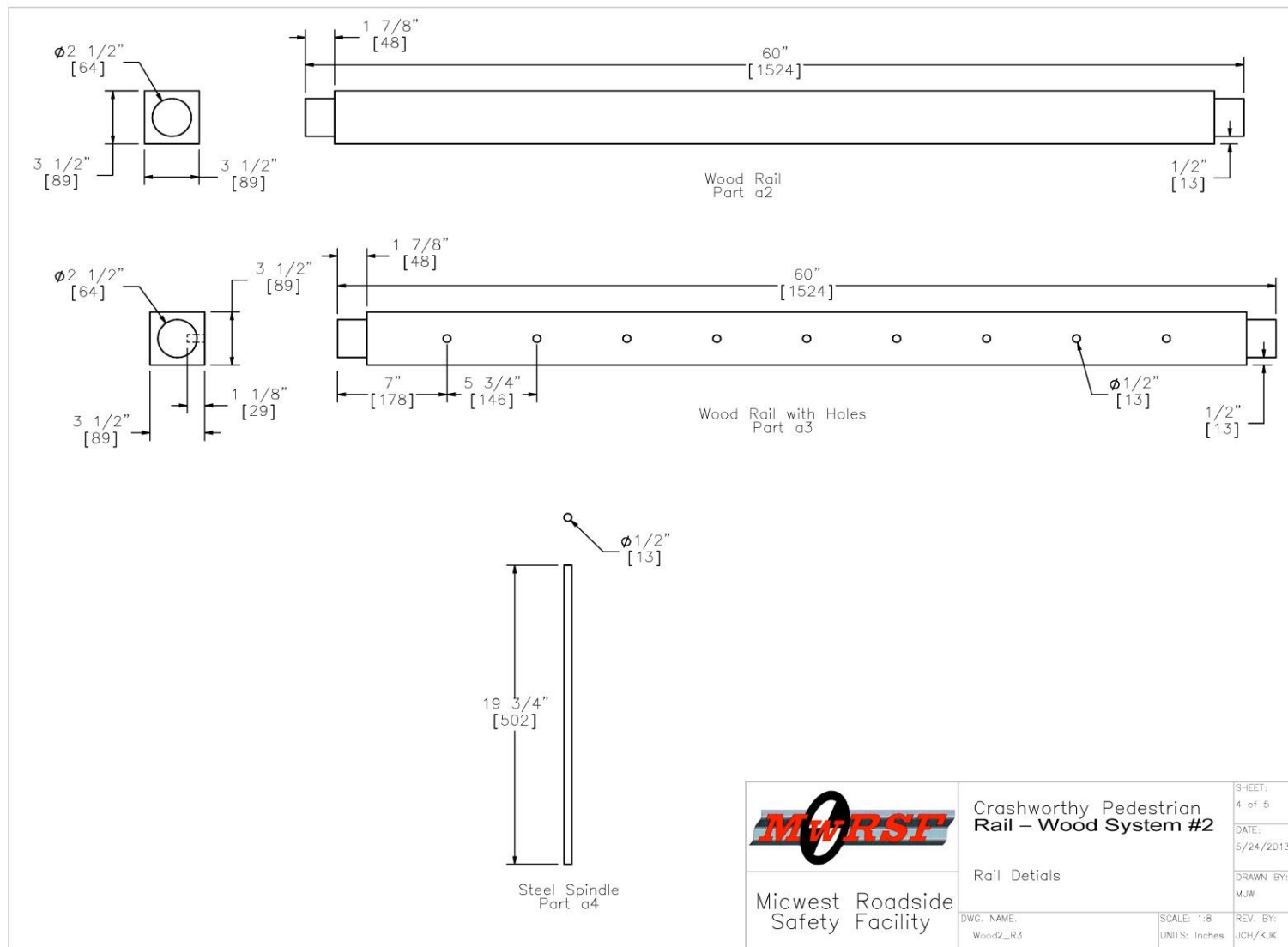


Figure 83. Cutout Wood Rail, Design Concept WOOD2 (Sheet 3 of 5)

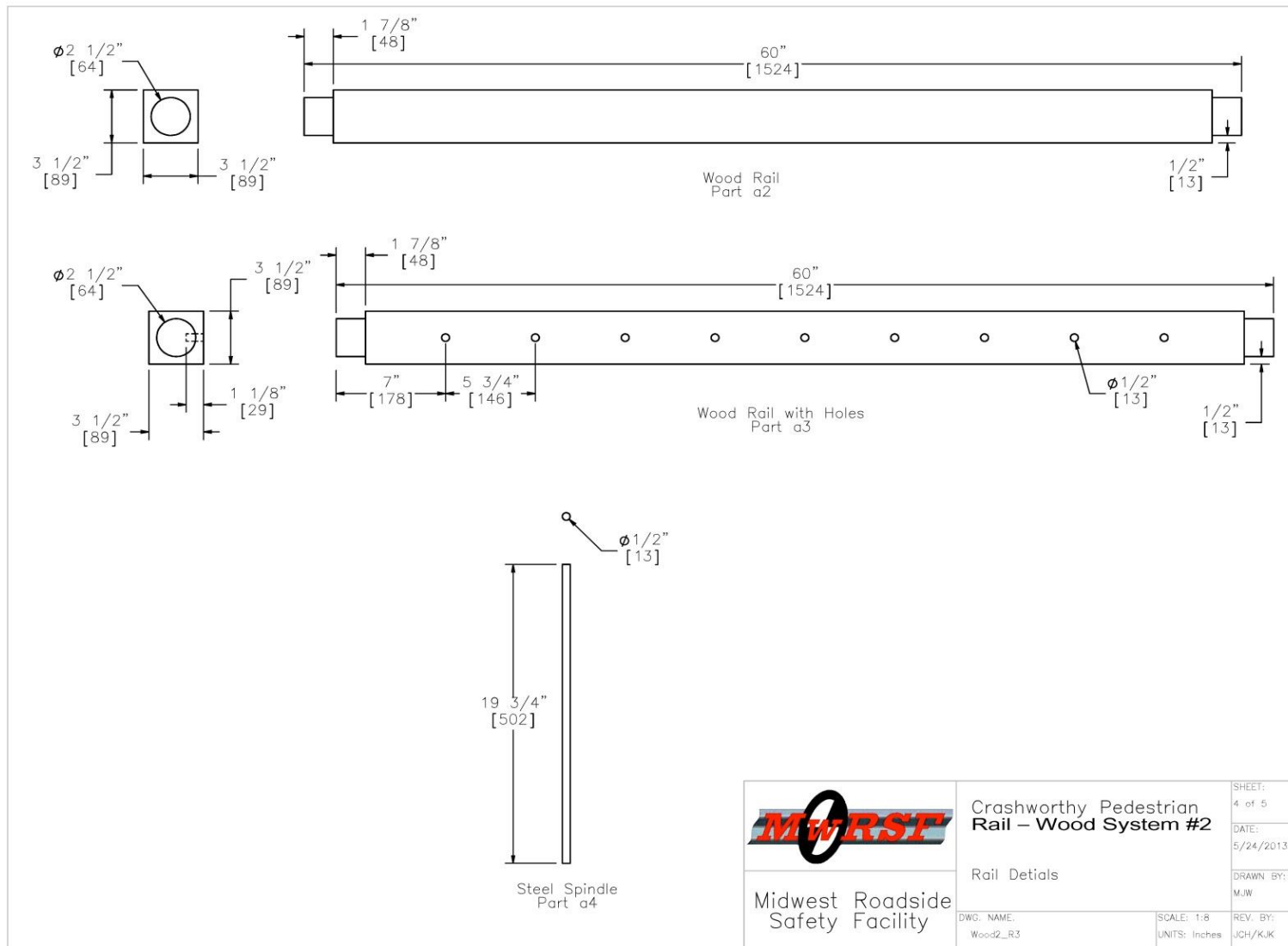


Figure 84. Cutout Wood Rail, Design Concept WOOD2 (Sheet 4 of 5)


	<p>Crashworthy Pedestrian Rail – Wood System #2</p>		<p>SHEET: 5 of 5</p>
	<p>Bill of Materials</p>		<p>DATE: 5/24/2013</p>
<p>Midwest Roadside Safety Facility</p>	<p>DWG. NAME: Wood2_R3</p>	<p>SCALE: None UNITS: Inches</p>	<p>DRAWN BY: MJW</p> <p>REV. BY: JCH/KJK</p>

Figure 85. Cutout Wood Rail, Design Concept WOOD2 (Sheet 5 of 5)



Figure 86. Fabricated Refined Design Concept WOOD2



Figure 87. Fabricated Refined Design Concept WOOD2

6 PEDESTRIAN RAIL DESIGNS

For the initial design, simplified load cases were assumed. The AASHTO *LRFD Bridge Design Specifications* denote design live loads on the longitudinal rail, vertical post, and any infill components of a pedestrian rail [6]. Additional load scenarios and assumptions were considered to determine detailed designs for: (1) rail member, (2) post member, (3) infill member, (4) post-to-rail connection, (5) post-to-base connection, (6) infill-to-rail, and (7) anchor ages.

6.1 Rail Component

The AASHTO *LRFD Bridge Design Specifications* specifies that the design live load of each longitudinal element shall include the application of two uniform loads of 50 lb/ft (730 N/m) or 4.17 lb/in. (730 N/m) and a concentrated load of 200 lb (890 N), acting simultaneously. Superposition of forces should be used to replicate loads in two principal directions based on the use of a doubly symmetric beam. The uniform loads shall be applied both vertically and transversely. The concentrated load may be applied in any direction to maximize the forces in the member. The system was designed with the concentrated load applied vertically on the rail, as shown in Figure 29. Simply supported and fixed-end configurations were assumed, and the maximum shears and moments were determined for design purposes. The length used for the rail design was 60 in. (1,524 mm).

6.1.1 Concentrated Load

The concentrated load applied at the support of the longitudinal element produced the maximum shear in the rail. The shear in the rail is shown in Figure 88. The maximum shear stress in a simply supported beam with a concentrated load was calculated using Equation 6. A 200-lb (890 N) concentrated load applied at either support of the longitudinal element produced a

maximum shear of approximately 200 lb (890 N) at either support with no shear elsewhere along the rail.

$$R_1 = V_{max}(\text{when } a < b) = \frac{Pb}{L} = \frac{(200 \text{ lb})(60 \text{ in.})}{(60 \text{ in.})} = 200 \text{ lb} \quad (6)$$

Where:

- R_1 = Support Reaction of Simply Supported Beam under a Point Load [lb]
- V_{max} = Maximum Shear Force in Rail due to Point Load, Virtually at One Support [lb] – 200 lb
- a = Distance from Concentrated Load to End of Rail [in.] – 0 in.
- b = Location of Concentrated Load Relative to End of Rail Component [in.] – 60 in.
- P = Concentrated Live Load for Rails [lb]
- L = Rail Length [in.] – 60 in.

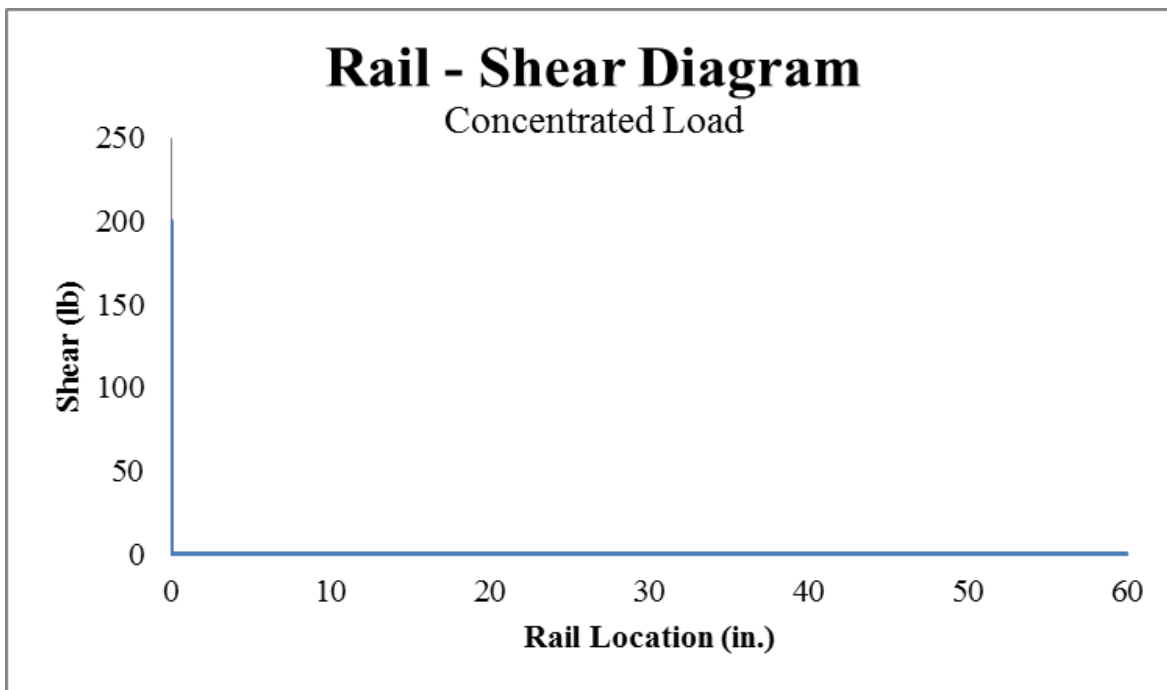


Figure 88. Rail Shear Diagram – Concentrated Load Virtually at Support

The concentrated load placed at the midspan of the beam maximizes the moment at the midspan in the rail when the ends are simply supported, as shown in Figure 89. The maximum moment at the midspan was calculated using Equation 7. The maximum moment resulting from

a 200-lb (890-N) concentrated load applied in any direction at the midspan of a 60-in. (1.5-m) rail span was calculated to be 3,000 lb-in. (339 N-m).

$$M_{max} = \frac{PL}{4} = \frac{(200 \text{ lb})(60 \text{ in.})}{4} = 3,000 \text{ lb-in. or } 250 \text{ lb-ft} \quad (7)$$

Where: M_{max} = Maximum Bending Moment in Rail due to Midspan Point Load [lb-in.]
P = Concentrated Midspan Live Load for Rails [lb] – 200 lb
L = Rail Length [in.] – 60 in.

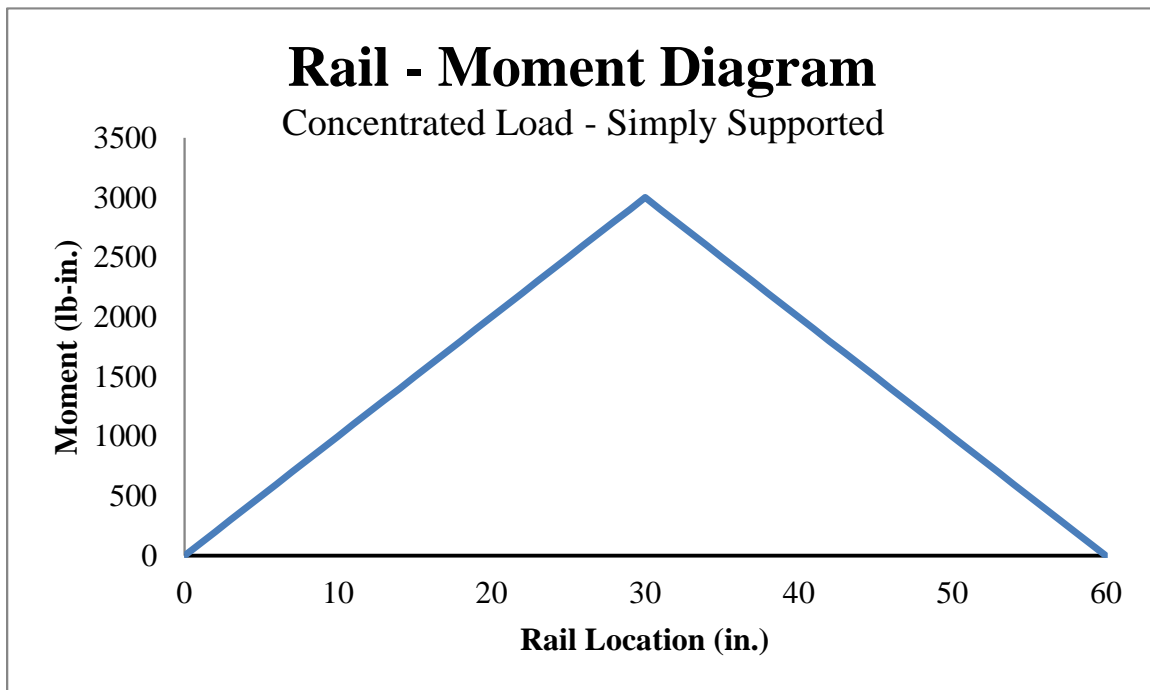


Figure 89. Rail Moment Diagram – Concentrated Load, Simply Supported Ends

6.1.2 Uniform Load

The shear in a simply supported the rail due to a uniformly distributed load is shown in Figure 90, with the maximum shear force occurring at the ends. The maximum shear force is equal to the support reaction, which can be calculated using Equation 8. The maximum shear force in a rail element with a 4.17-lb/in. (730-N/m) uniform load over a span of 60 in. (1.5 m) was calculated to be 125 lb (556 N).

$$R = V_{max} = \frac{wL}{2} = \frac{(4.17 \frac{lb}{in.})(60 in.)}{2} = 125 lb \quad (8)$$

Where: R= Support Reaction of Simply Supported Beam due to Uniform Load [lb]
 V_{max} = Maximum Shear Force in Rail due to Uniform Load [lb]
w= Distributed Live Load [lb/in.] – 4.17 lb/in.
L= Rail Length [in.] – 60 in.

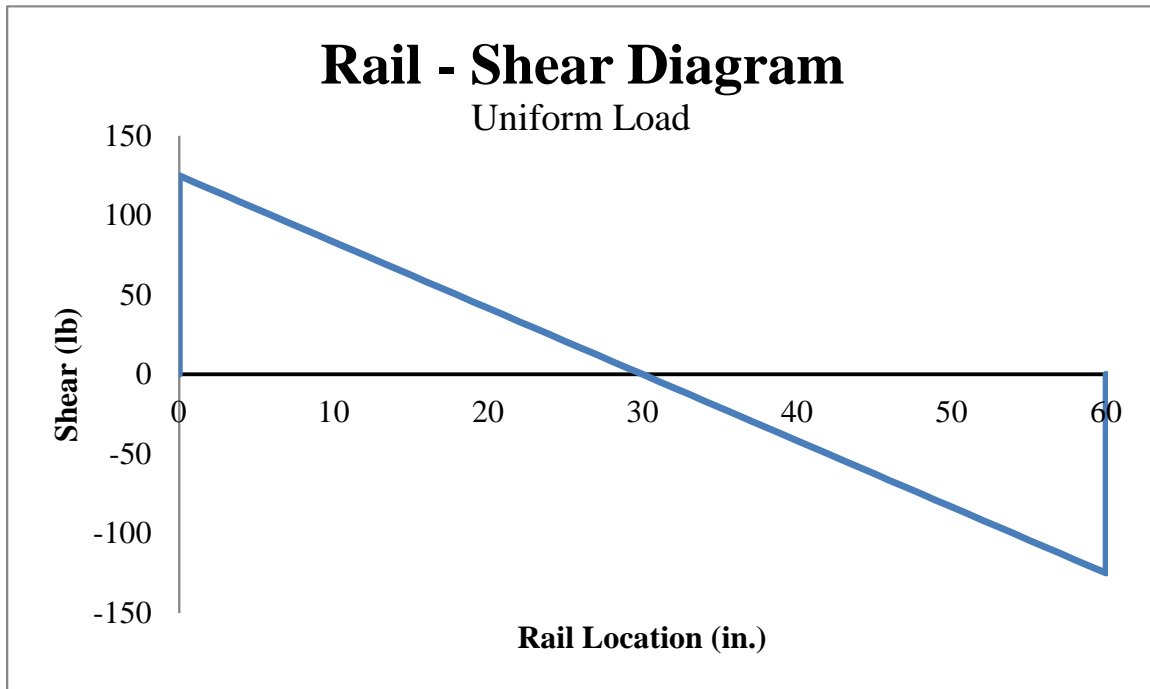


Figure 90. Rail Shear Diagram – Uniformly Distributed Load, Simply Supported Ends

When the ends are assumed to be simply supported, the maximum moment from a uniformly distributed load occurs at the midspan, as shown in Figure 91. The maximum moment, calculated using Equation 9 with a 4.17-lb/in. (730-N/m) uniform load over a 60-in. (1.5-m) span, was 1,876.5 lb-in. (213.4 N-m), which was located at the midpoint of the longitudinal member.

$$M_{max} = \frac{wL^2}{8} = \frac{(4.17 \frac{lb}{in.})(60 in.)^2}{8} = 1,876.5 lb - in. \text{ or } 156.25 lb - ft \quad (9)$$

Where: M_{max} = Maximum Bending Moment in Rail due to Uniform Load [lb-in.]
 w = Uniform Design Live Load [lb/in.] – 4.17 lb/in.
 L = Rail Length [in.] – 60 in.

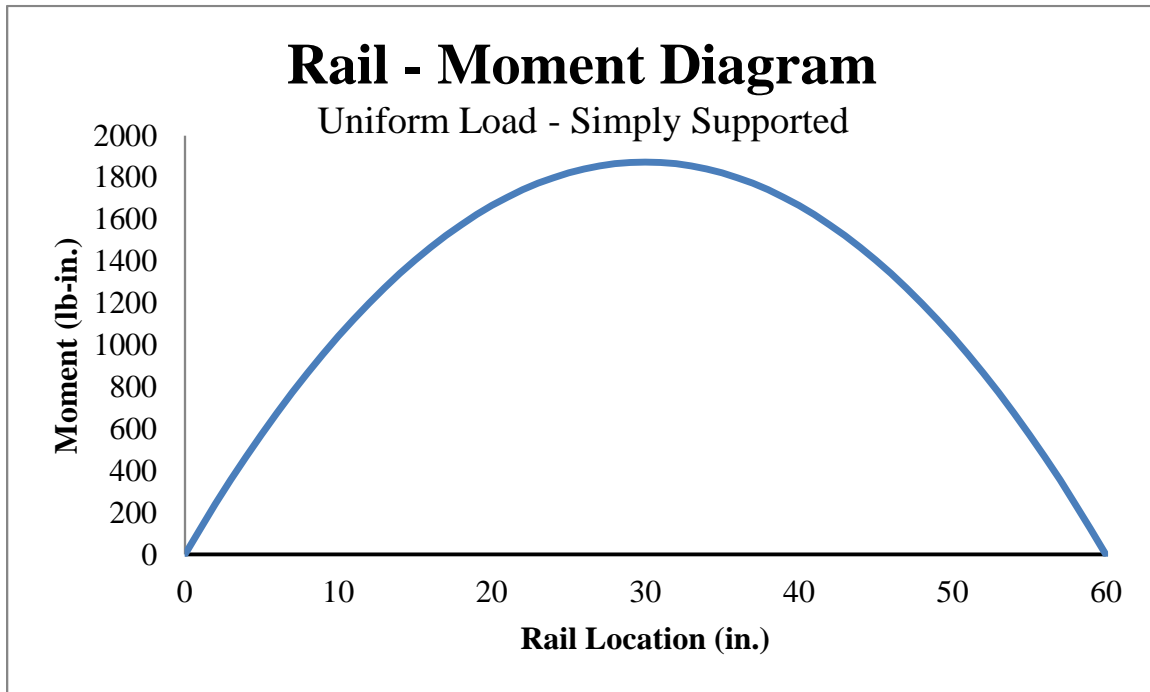


Figure 91. Rail Moment Diagram – Uniformly Distributed Load, Simply Supported Ends

6.1.3 Combined Concentrated and Uniform Loads

The total design loads for the longitudinal rail element must consider the combination of loading in two directions. AASHTO criteria specify that the two uniform loads must be applied vertically and transversely, but the concentrated load may be applied at any point and in any direction on the rail element [6]. The maximum shear and bending effect of the combined loading from the two uniform loads (ie., transverse and vertical) and the concentrated load acting in either the vertical (z-axis) or transverse (y-axis) directions. For the purposes of this design, the

concentrated load was assumed to act in the vertical direction (z-axis). However, since it could be applied transversely, a doubly symmetric section would be most efficient.

The maximum shear force for both the concentrated and uniform loads occurs at the end of the rail. Using results from Figures 88 and 90, these loads can be combined into a resultant shear force using Equation 10 and a maximum shear force of 348.2 lb (1,549 N).

$$V = \sqrt{V_z^2 + V_y^2} = \sqrt{325^2 + 125^2} = 348.2 \text{ lb} \quad (10)$$

Where:

V_z = Maximum Vertical Shear at End of Rail [lb] = 200 lb + 125 = 325 lb

V_y = Maximum Transverse Shear Force at End of Rail [lb] = 125 lb

The combined bending moment resulting from the three separate loads acting on the longitudinal member can be calculated using the combined bending formula shown in Equation 11. The rail element was designed as a doubly symmetric member, meaning $I_{zz} = I_{yy} = I$, $y = z = C$, and the product of inertia value, I_{yz} , is equal to zero. Elimination of the I_{yz} terms and simple algebra were used to obtain the form shown in Equation 12. To simplify this equation and acquire the maximum tensile or compressive stress in Equation 13, either y and z or M_y and M_z need to have opposite signs. Using the relation of section properties given in Equation 14, the formula can be further simplified to Equation 15. This relationship implies that moments acting about two orthogonal axes over a doubly symmetric cross section can be combined to determine a maximum bending stress in the cross section. In this case, the maximum applied moment would be determined as the sum of the maximum bending moments from the loads applied both vertically and transversely and used to size the symmetric beam section. Assuming the point load is acting in the same plane as one of the distributed loads to maximize reactions, then the maximum bending moment in the rail element would be the combination of the maximum

bending moment for two distributed loads, plus the bending moment from a concentrated load applied at the center of the rail span, or 6,750 lb-in. (762.8 N-m) using Equation 16 and shown in Figure 92.

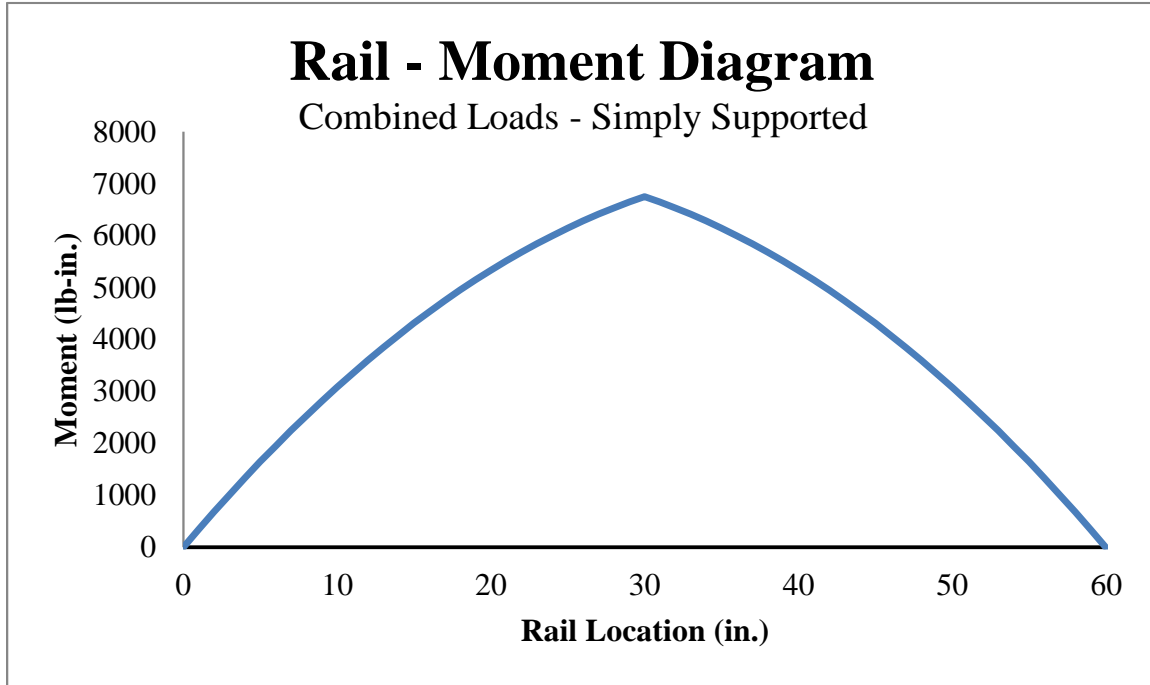


Figure 92. Rail Moment Diagram – Combined Loads, Simply Supported Ends

$$\sigma_{xx} = \frac{(M_y I_{zz} + M_z I_{yz})z - (M_z I_{yy} + M_y I_{yz})y}{(I_{yy} I_{zz} - I_{yz}^2)} \quad (11)$$

$$\sigma_{xx} = \frac{M_y z}{I_{yy}} - \frac{M_z y}{I_{zz}} \quad (12)$$

$$\sigma_{xx,max} = \frac{M_y C}{I} - \frac{M_z C}{I} \quad (13)$$

$$S = \frac{I}{C} \quad (14)$$

$$\sigma_{xx,max} = \frac{|M_y|}{S} + \frac{|M_z|}{S} \quad (15)$$

$$M = |M_y| + |M_z| \quad (16)$$

Where:

σ_{xx} = Tensile or Compressive Stress Acting on Surface Perpendicular to the X-Direction [psi]
 $\sigma_{xx,max}$ = Maximum Tensile or Compressive Stress Acting on Surface Perpendicular to the X-Direction [psi]
 M = Combined Moment [lb-ft]
 M_y = Moment in the Y-Direction [lb-ft]
 M_z = Moment in the Z-Direction [lb-ft]
 I_{zz} = Moment of Inertia with Respect to the Z-Axis [in.⁴]
 I_{yz} = Products of Inertia with Respect to the X- and Y-Axes [in.⁴]
 I_{yy} = Moment of Inertia with Respect to the Y-Axis [in.⁴]
 z = Distance from the Neutral Axis in the Z-Direction [in.]
 y = Distance from the Neutral Axis in the Y-Direction [in.]
 S = Section Modulus [in.³]
 I = Moment of Inertia $I_{yy} = I_{zz}$ [in.⁴]
 C = Distance from Neutral Axis $|y| = |z|$ [in.]

6.2 Post Component

The vertical member of a pedestrian rail must be designed for a concentrated live load, P_{LL} , applied transversely on the post at the center of gravity of the uppermost longitudinal element. P_{LL} is determined from Equation 13.8.2-1 in the AASHTO *LRFD Bridge Design Specifications* [6] and is shown in Equation 17. The magnitude of P_{LL} with a 60-in. (1.5-m) post spacing is 450 lb (2,000 N).

$$P_{LL} = 200 + 50L = 200 \text{ lb} + 4.17 \frac{\text{lb}}{\text{in.}} (60 \text{ in.}) = 450 \text{ lb} \quad (17)$$

Where P_{LL} = Concentrated Live Load for Posts [lb]
 L = Post Spacing [in.] – 60 in.

The post members were analyzed as a cantilever beam, with the fixed end represented by a rigid anchorage at the base of the post. The shear and moment diagrams correspond to a concentrated load, P_{LL} , applied transversely to the post element at the mid-height of the top rail [41 in. (1,041 mm) above ground], as shown in Figure 93 and Figure 94, respectively. Both the maximum shear load and bending moment in the post component is located at the base of the post, nearest the connection to the baseplate. The maximum shear in the post is equal to P_{LL} =

450 lb (2,000 N). The maximum bending moment in the post behaving as a fixed-end cantilever element was determined with Equation 18 and is 18,450 lb-in. (2,085 N-m).

$$M_{max} = P_{LL}h = (450 \text{ lb})(41 \text{ in.}) = 18,450 \text{ lb-in. or } 1,537.5 \text{ lb-ft.} \quad (18)$$

Where M_{max} = Maximum Bending Moment in Post [lb-in.]
 P_{LL} = Concentrated Live Load for Posts [lb] – 450 lb
 h = Height at which Transverse Point Load is Applied [in.] – 41 in.

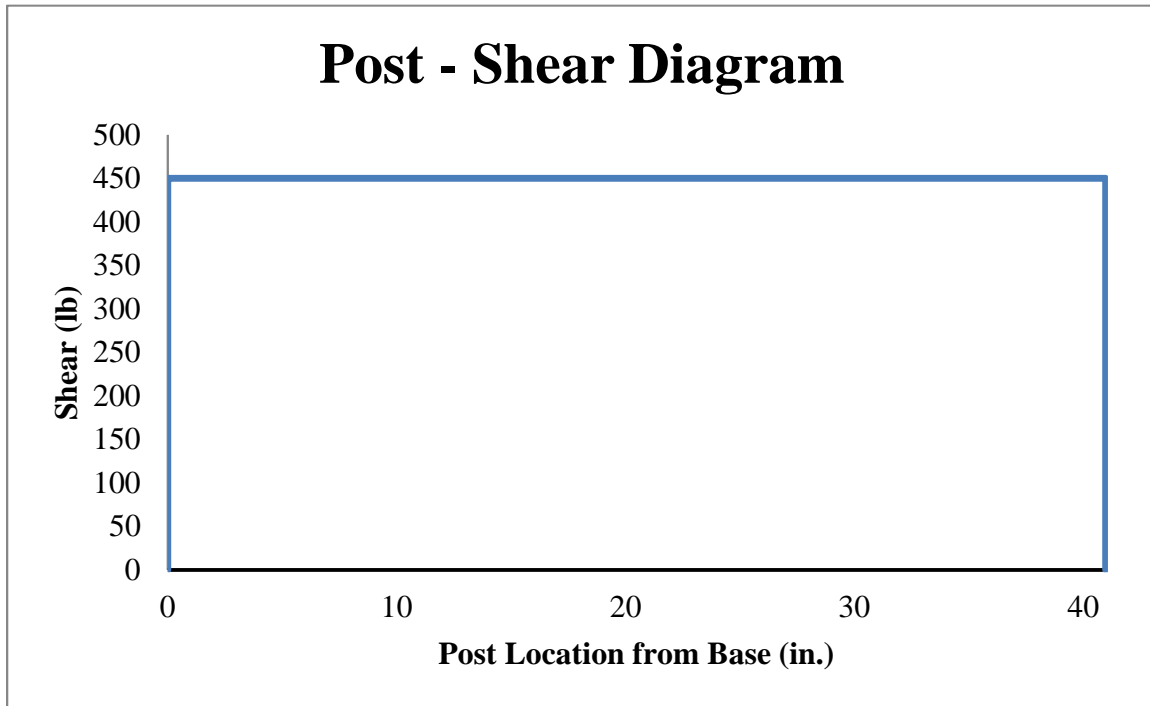


Figure 93. Post Shear Diagram

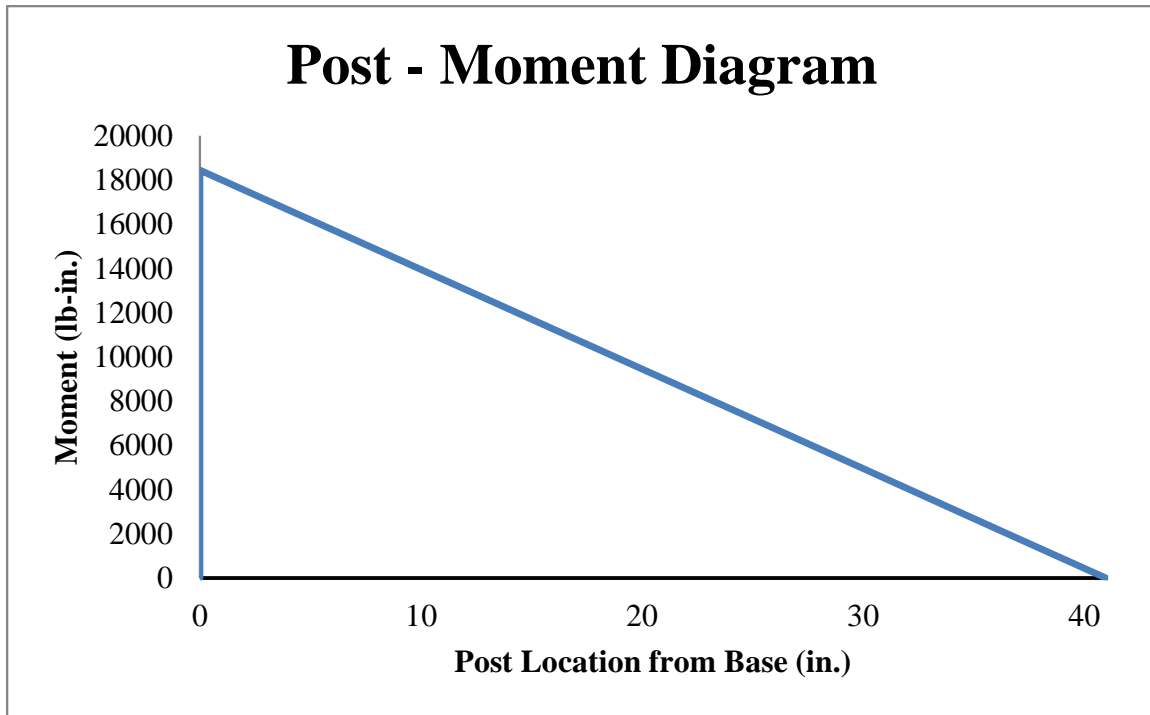


Figure 94. Post Moment Diagram

6.3 Infill

The infill region of a pedestrian rail system is the area between two vertical posts and longitudinal rails where mesh or spindle designs may be implemented to meet maximum opening requirements and add aesthetic characteristics to the rail system. The AASHTO *LRFD Bridge Design Specifications* specify that the members or panel within this area must support a 15-lb/ft² (718-N/m²) load over the entire infill area [6]. With a rail span of 60 in. (1,524 mm), nine ½-in. (13-mm) spindles would be required with a 5¾-in. (146-mm) maximum gap width [6]. The maximum spindle length between rail components was assumed to be 2¼ in. (616 mm), based on the preliminary designs. The average tributary area for each of the nine spindles was 151.56 in.² (0.098 m²). The 15-lb/ft² (718-N/m²) load distributed over the tributary area of the spindle equates to a uniform load, w , of 0.651 lb/in. (114 N/m) over the 2¼-in. (616-mm) length of the spindle member. The shear diagram is shown in Figure 95. The maximum shear force in a

spindle was calculated with Equation 19 based on an assumption of simply supported ends. The maximum midspan moment in the spindles was calculated with Equation 20. The moment diagram is shown in Figure 96.

When evaluating a mesh infill panel, the capacity needs to exceed 15 lb/ft² (718 N/m²). The maximum shear and moment is dependent on the types of mesh panel selected.

$$V_{max} = \frac{wL}{2} = \frac{(0.651 \frac{lb}{in.})(24.25 in.)}{2} = 7.9 lb \quad (19)$$

$$M_{max} = \frac{wL^2}{8} = \frac{(0.651 \frac{lb}{in.})(24.25 in.)^2}{8} = 47.85 lb - in. = 4.0 lb - ft \quad (20)$$

Where: V_{max} = Maximum Shear Force in Spindle [lb]
 M_{max} = Maximum Bending Moment in Spindle [lb-in.]
 L = Length of the Spindle Member [in.] - 24.25 in.
 w = Uniform Load [lb/in.] - 0.651 lb/in.

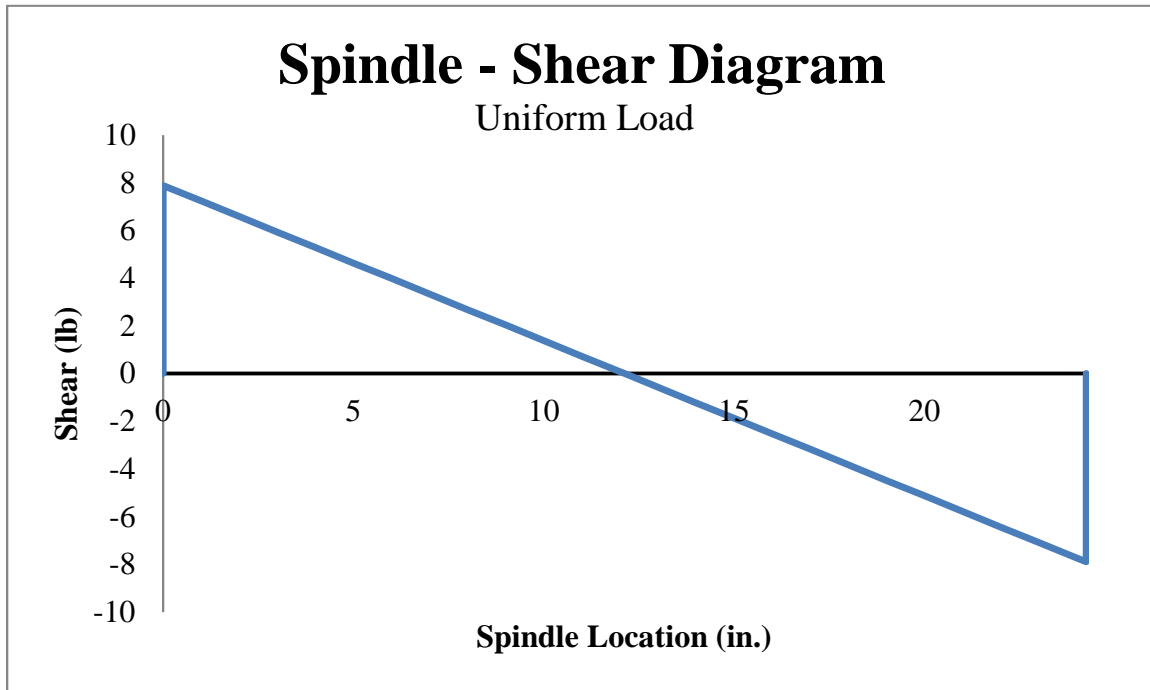


Figure 95. Spindle Shear Diagram – Uniform Load, Simply Supported Ends

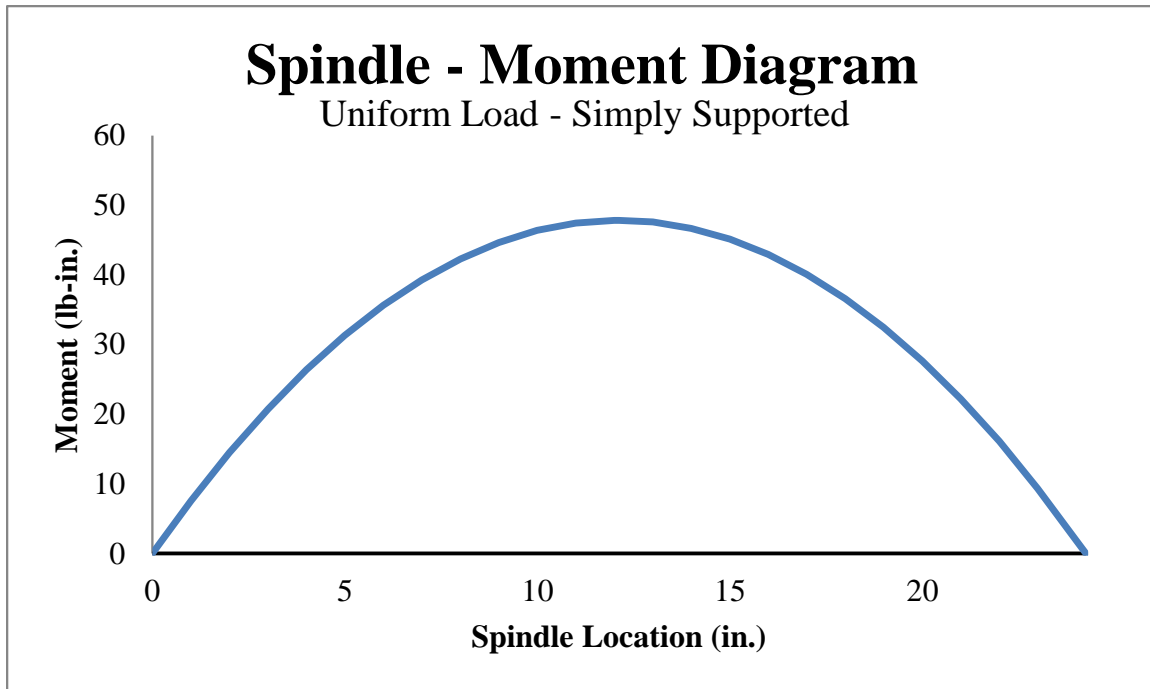


Figure 96. Spindle Moment Diagram – Uniform Load, Simply Supported Ends

6.4 Connections

The connections between the rail, post, and base components are essential for transferring loads between elements and to the anchoring system. It was assumed that the reactions at each joint would be fully transferred through the connection. Therefore, the shear and moment capacity of each connection must be greater than the calculated reactions at the member ends. The connections that were evaluated included post-to-rail, post-to-base, infill-to-rail, and concrete anchors.

6.4.1 Post-to-Rail Connection

While the rail member designs utilized an assumption of simply supported ends to maximize midspan moments, the ends were assumed to be fixed for connection design to maximize applied moment at the ends. This assumption was also more realistic, as a welded or fitted connection would likely be used. When the ends are fixed, the maximum moment at the

ends of the rail due to a concentrated load is shown in Figure 97. When the ends are fixed, the maximum moment at the ends of the rail from the uniform load is shown in Figure 98.

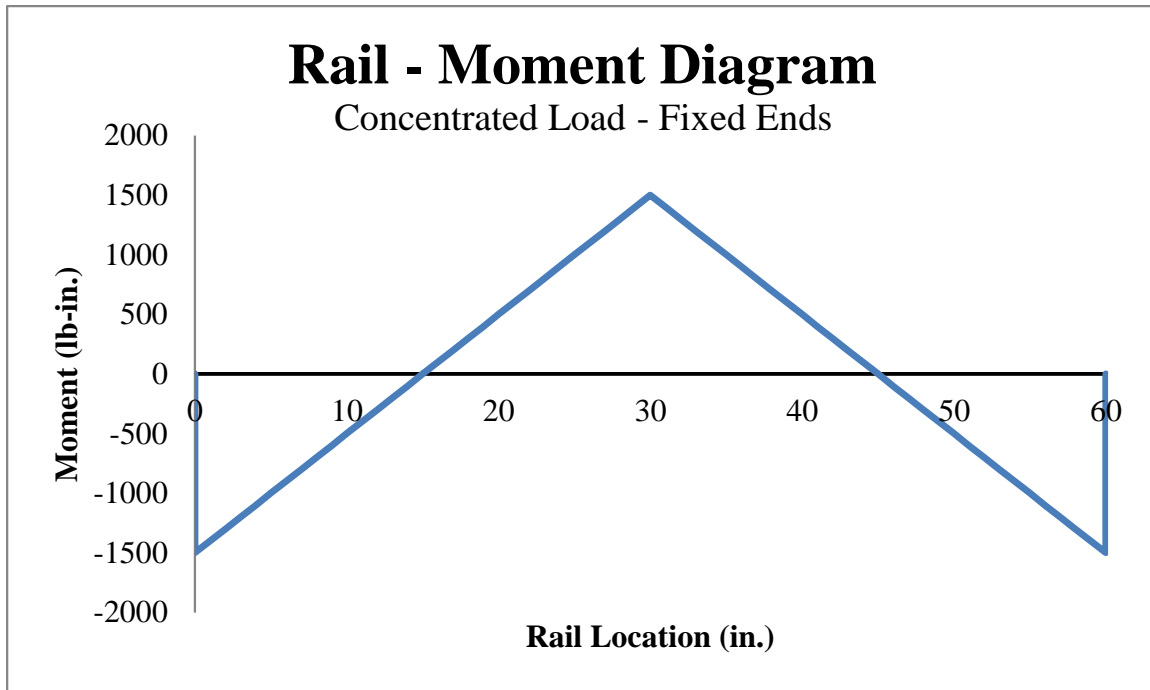


Figure 97. Rail Moment Diagram – Concentrated Load, Fixed-Fixed Ends

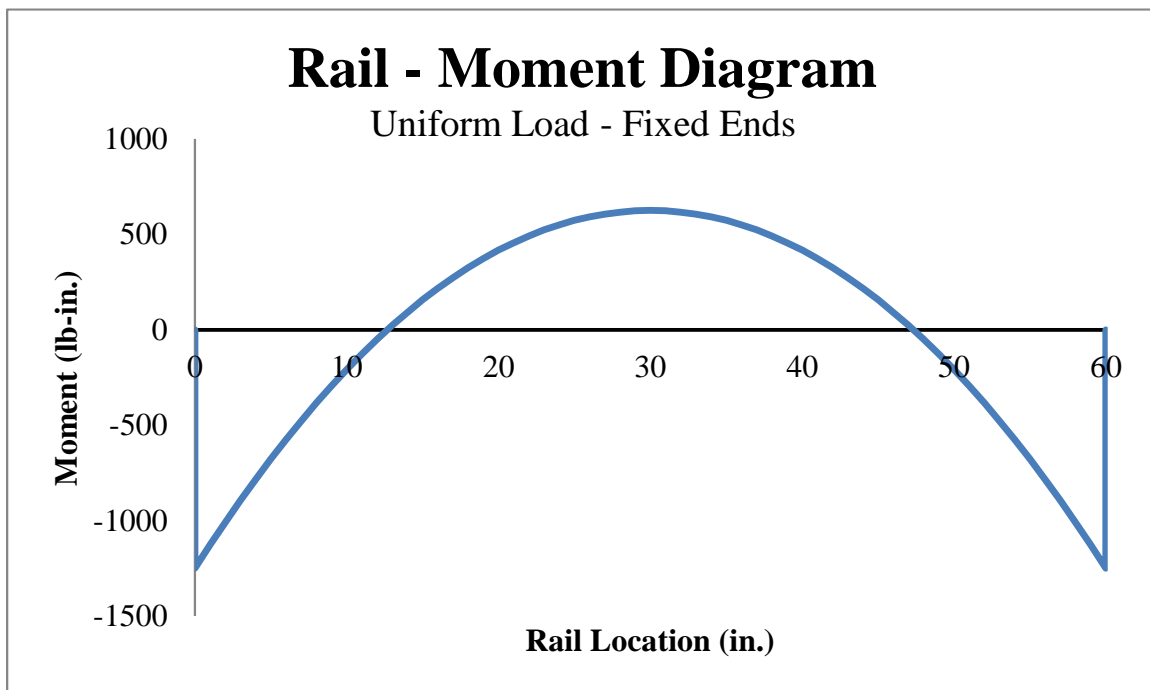


Figure 98. Rail Moment Diagram – Uniformly Distributed Load, Fixed-Fixed Ends

6.4.1.1 Maximum Shear Force

The required strength of the post-to-rail connection was calculated using shear and bending moments at the supported ends of the longitudinal rail element. The shear at the end of a fixed-fixed beam was calculated using Equation 10 and found to be 348.2 lb (1,549 N) at the post-to-rail connection.

6.4.1.2 Maximum Bending Moment

The bending moment at the support of a fixed-fixed beam from the distributed load along the entire beam is given in Equation 21. Using $w = 4.17 \text{ lb/in.}$ (730 N/m) and $L = 60 \text{ in.}$ (1,524 mm), Equation 21 yielded a maximum moment of 1,251 lb-in. (141.3 N-m) at each end of the longitudinal rail member, the location of the post-to-rail connection.

$$M_{end} = \frac{wL^2}{12} = \frac{(4.17 \frac{\text{lb}}{\text{in.}})(60 \text{ in.})^2}{12} = 1,251 \text{ lb-in. or } 104.2 \text{ lb-ft.} \quad (21)$$

Where: M_{end} = End Moment Reaction due to Distributed Load [lb-in.]
 w = Distributed Design Live Load [lb/in.] – 4.17 lb/in.
 L = Rail length [in.] – 60 in.

The shear reaction at the support of a fixed-fixed beam due to a 200-lb (890-N) concentrated load was calculated using Equation 22. The design bending moment was determined by Equation 23. The shear and bending moment depends on the longitudinal distance, a , away from the support to the concentrated load, which can be applied at any point on the longitudinal member. To maximize the moment due to point load, the differential of the bending moment in Equation 23 was set to zero to determine the longitudinal distance between the fixed end support to the concentrated point load. This calculation yielded a longitudinal distance of $a=(2/3)L$ and $b=(1/3)L$. Applying the corresponding values to the equation, the maximum bending moment formed at the fixed end was 1,778 lb-in. (201 N-m).

$$V(\text{max when } a > b) = \frac{Pa^2}{L^3}(a + 3b) \quad (22)$$

$$M(\text{max when } a > b) = \frac{Pa^2b}{L^2} \quad (23)$$

Where: V = Shear Moment due to Concentrated Load [lb]
 a = Longitudinal Distance between Concentrated and Load Considered Support [in.]
 b = $L - a$ [in.]
 L = Post Spacing [in.]
 M = End Moment due to Concentrated Load [lb-in.]

The combined shear loading in the post-to-rail connection was the same as the maximum shear load in the rail, which was 348.2 lb (1,549 N). The same concept of combining vertical and transverse bending moments for the rail applies at the connection as well. The combination of a reaction in the post-to-rail connection from the uniform and concentrated loads in the vertical plane plus a transverse uniform load was 4,280 lb-in. (483.6 N-m), as shown in Figure 99.

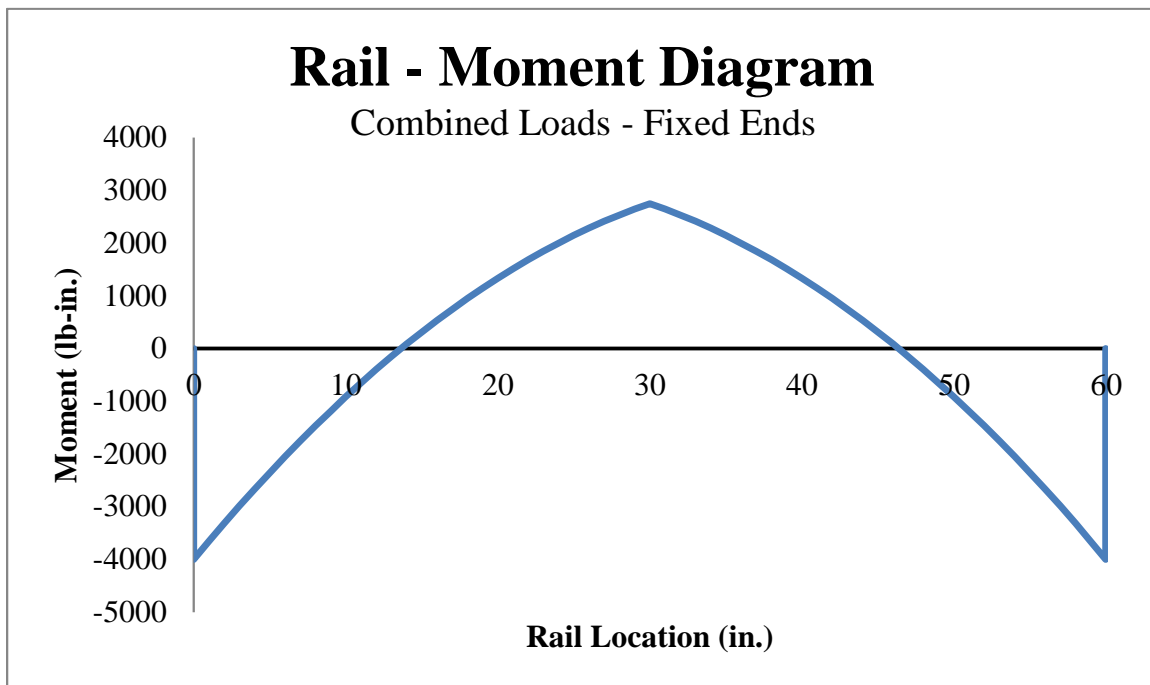


Figure 99. Rail Moment Diagram – Combined Loads, Fixed-Fixed Ends

6.4.2 Post-to-Base Assembly Connection

The required strength of the post-to-base connection was calculated using the design shear and bending moment at the base of the post element from the design loading conditions from Section 6.2. The shear and moment reactions at the post-to-base connection were 450 lb (2,000 N) and 18,450 lb-in. (2,085 N-m), respectively.

In addition to the applied shear and moment, each baseplate would be subjected to an axial force based on the sum of the rail loads that each post experiences. Each concept had three rail members, and based on the pedestrian rail loads defined by the AASHTO LRFD Bridge Specifications [6], one would have a concentrated load and all three would have a uniform load in the lateral and vertical directions. The resultant shear forces from these applied loads on the rails produced the maximum axial force on the baseplate, calculated to be $200 \text{ lb} + [125 \text{ lb} * 3] = 575 \text{ lb}$.

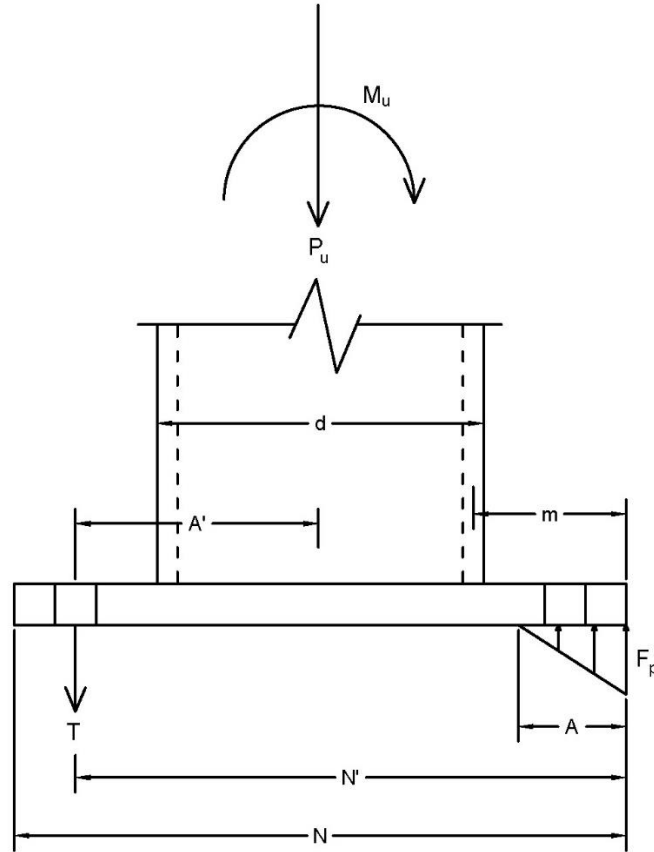
The maximum vertical force imparted to the baseplate can be determined from the maximum moment experienced at the base, 18,450 lb-in. (2,085 N-m), divided by the depth of the post. The maximum vertical force is calculated using Equation 24.

$$P_{max} = \frac{M_{max}}{d} = \frac{18,450 \text{ lb-in.}}{d} \quad (24)$$

Where: P_{max} = Maximum Vertical Force on Baseplate [in.]
 M_{max} = Maximum Moment at Base of Post [lb-in.]
 d = Depth of Post [in.]

Also, from the American Institute of Steel Construction (AISC) Steel Design Guide Series 1, the required bending moment of the baseplate with a large eccentricity is based upon a combined loading of the axial force, 575 lb (2,557 N), and the moment 18,450 lb-in. (2,085 N-m), on the baseplate [41-42]. The free-body diagram of this system is shown in Figure 100. The required bending moment per width, M_{pl} , for the baseplate design is shown in Equation 25. The

supporting concrete under the baseplate is assumed to have dimensions at least twice each dimension of the baseplate. While this equation was derived for steel baseplates, the variables were modified for an aluminum baseplate and should produce similar results.



M_u = Moment at Base of Post = 1,537.5 ft-lb

P_u = Axial Force on Post = 575 lb

d = Depth of Post [in.]

N = Length of Baseplate [in.]

N' = Distance from Edge of Plate to Far Bolt [in.]

A' = Distance from Bolt to Center of Post [in.]

T = Tensile Force in Bolt [lb]

m = Location of Critical Section [in.] = $\frac{N - 0.95d}{2}$

F_p = Maximum Design Bearing Stress [psi] = $0.85\phi f'_c \sqrt{A_2/A_1} \leq 1.7f'_c$

f'_c = Compressive Strength of Concrete [psi]

A_1 = Area of Baseplate

A_2 = Area of Supporting Concrete Foundation = $4A_1$

Figure 100. Baseplate Loads with Combined Axial Force and Bending Moment with Large Eccentricity

$$M_{pl} = \sum M_m \quad (25)$$

Where: M_{pl} = Required Bending Moment on Baseplate [in.-lb/in.]
 M_m = Maximum Moment at Location m, which is the Critical Section [in.-lb]

6.4.3 Infill-to-Rail Connection

The infill between the rail components varied by design concept and included aluminum spindles between the rail components, or a mesh infill between the post and rail members. To maximize the moment at the midspan of the spindle, a simply supported end connection was assumed in Section 6.3 for the spindle member design. However, for the connection between the spindle and rail, the ends were assumed to be fixed-fixed to maximize the moment at the connections, which would also be more representative of a welded or fitted connection. With a 24¼-in. (616-mm) long spindle and a uniform load of 0.651 lb/in. (114 N/m), the moment diagram is shown in Figure 101. Maximum shear at the spindle connection was the same as for the spindle member, 7.89 lb (35.1 N). The maximum bending moment located at the end of the spindle-to-rail connection was 31.9 lb-in. (3.6 N-m), as calculated by Equation 26.

$$M_{end} = \frac{wL^2}{12} = \frac{(0.651 \frac{lb}{in.})(24.25 \text{ in})^2}{12} = 31.9 \text{ lb} - \text{in.} = 2.66 \text{ lb} - \text{ft} \quad (26)$$

Where: M_{end} = Maximum Bending Moment at End of Spindle [lb-in.]
 L = Spindle Location [in.] – 24.25 in.
 w = Uniform Load [lb/in.] – 0.651 lb/in.

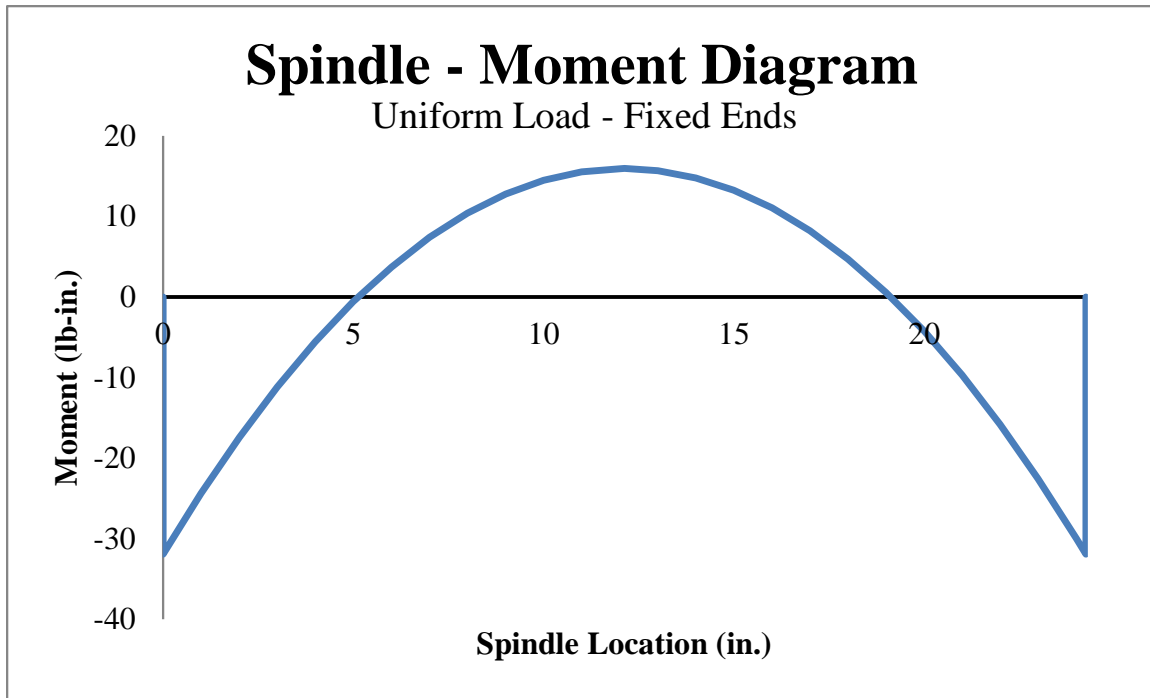


Figure 101. Spindle Moment Diagram – Uniformly Distributed Load, Fixed-Fixed Ends

6.4.4 Concrete Anchorage

The base of the post was previously assumed to have a fixed-end condition. In order for this assumption to be true, the base of the post was rigidly fixed to a concrete foundation with anchors. Wedge anchors would not likely allow a damaged system to be removed and reinstalled multiple times. Therefore, a threaded rod secured through the base fitting with an epoxy adhesive anchoring system was selected. The shear and bending moment induced at the base of the post were calculated in Sections 6.2 and 6.3.2 to be 450 lb (2,000 N) and 18,450 lb-in. (2,085 N-m), respectively.

If two bolts were utilized, the required shear load on each bolt was 225 lb (1,000 N). The bending moment at the base of the post transfers into a tensile force prying up on the bolt. The size of the baseplate and length of the moment arm between the anchor bolts influence the

magnitude of the tensile stress on the bolts' cross sections. The general equation for the magnitude of tensile force is shown in Equation 27.

$$P_{max} = \frac{M_{max}}{x} = \frac{(18,450 \text{ lb-in.})}{x \text{ in.}} \quad (27)$$

Where: P_{max} = Tensile Force Acting Upward on Anchor Bolts [lb]
 M_{max} = Moment at the Base of the Post [lb-in.]
 x = Distance between Anchor Bolts [in.]

7 DESIGN OF PROTOTYPE PEDESTRIAN RAILS

7.1 Introduction

The mechanical properties of aluminum can vary depending on the alloy, shape, thickness, and existence of weld-affected zones. The process of welding aluminum at a connection location significantly reduces the strength of the material surrounding the weld location. While heat treatment can be applied to regain most of the material strength in weld-affected zones, the heat treatment was not desired. Thus, the pedestrian rail was designed using the lower weld-affected material strengths. A common aluminum alloy, 6061-T6, was selected for all of the pedestrian rail designs. The mechanical properties of non-welded 6061-T6 aluminum were provided in Table A.3.4 in the Aluminum Design Manual (ADM) [38] and are shown in Table 5 for extrusions, sheets, and plates. The mechanical properties of weld-affected 6061-T6 aluminum were provided in Table A.3.5 in the ADM and are shown in Table 5 for all shapes and plate/sheet thicknesses, t , less than and greater than $\frac{3}{8}$ in. (10 mm).

Table 5. Aluminum Alloy 6061-T6 Material Strengths [38]

Non-welded Strength Extrusions, All Thicknesses ksi (MPa)		Non-Welded Strength Sheet & Plate, $0.010 \leq t \leq 4.000$ in. ksi (MPa)		Weld-Affected Strength All Shapes, $t \leq 0.375$ in. ksi (MPa)		Weld-Affected Strength All Shapes, $t > 0.375$ in. ksi (MPa)	
F_{tu}	38 (260)	F_{tu}	42 (290)	F_{tuw}	24 (165)	F_{tuw}	24 (165)
F_{ty}	35 (240)	F_{ty}	35 (240)	F_{tyw}	15 (105)	F_{tyw}	11 (80)
F_{cy}	35 (240)	F_{cy}	35(240)	F_{cyw}	15 (105)	F_{cyw}	11 (80)
F_{su}	24 (165)	F_{su}	27 (185)	F_{suw}	15 (105)	F_{suw}	15 (105)

Where: F_{tu} = Tensile Ultimate Strength
 F_{ty} = Tensile Yield Strength
 F_{cy} = Compressive Yield Strength
 F_{su} = Shear Ultimate Strength
 F_{tuw} = Tensile Ultimate Strength of Weld-Affected Zones
 F_{tyw} = Tensile Yield Strength of Weld-Affected Zones
 F_{cyw} = Compressive Yield Strength of Weld-Affected Zones
 F_{suw} = Shear Ultimate Strength of Weld-Affected Zones

Each component was designed using Load and Resistance Factor Design (LRFD) equations from the ADM in which the required strength, R_u , needs to be less than or equal to the design strength, ϕR_n , from equation B.3-1 in the ADM, as given in Equation 28 [38].

$$R_u \leq \phi R_n \quad (28)$$

Where R_u = Required Strength
 R_n = Nominal Strength
 ϕ = Resistance Factor
 ϕR_n = Design Strength

7.2 Section Capacities

The shear and flexural capacities of each rail, post, and spindle cross section were determined for limit states using equations in the ADM.

7.2.1 Shear

7.2.1.1 Rectangular tubes

The shear capacity of a non-welded section of a flat web support on both edges (e.g. rectangular tube) from Section G.2 of the ADM is given in Equation 29.

$$\phi V_n = \phi F_s A_w \quad (29)$$

Where ϕV_n = Nominal Shear Capacity [kip]
 F_s = Shear Stress Corresponding to Shear Strength from Table 6 [ksi]
 A_w = Area of Web = $d \cdot t$ [in.]
 ϕ = 0.90

Table 6. Rectangular Tubes Shear Strength [38]

Limit State	F_s	b/t	Slenderness Limits
yielding	F_{sy}	$b/t \leq S_1$	$S_1 = \frac{B_s - F_{sy}}{1.25D_s}$
inelastic buckling	$B_s - 1.25D_s b/t$	$S_1 < b/t < S_2$	
elastic buckling	$\frac{\pi^2 E}{(1.25b/t)^2}$	$b/t \geq S_2$	$S_2 = \frac{C_s}{1.25}$

F_{sy} = Shear Yield Strength [ksi]

D_s = Buckling Constant Slope [ksi]

B_s = Buckling Constant Intercept [ksi]

C_s = Buckling Constant Intersection

b = Clear Height of the Web for Unstiffened Webs [in.]

t = Web Thickness [in.]

d = Full Depth of Section [in.]

$F_{sy} = F_{sy}$ if Non-Welded and F_{syw} if Welded

For non-welded 6061-T6 aluminum extrusions, the buckling constants can be calculated using equations provided in Table 1-1 in the ADM, as follows:

$$\begin{aligned} B_s &= 27.2 \text{ ksi} \\ D_s &= 0.141 \text{ ksi} \\ C_s &= 79 \end{aligned}$$

The slenderness limits S_1 and S_2 were then calculated for non-welded sections using the relationship $F_{sy} = 0.6F_{ty} = 0.6 * 35 \text{ ksi} = 21 \text{ ksi}$ from Table A.3.1 in ADM and Equations 30 and 31.

$$S_1 = \frac{B_s - F_{sy}}{1.25D_s} = \frac{27.2 - 21}{1.25 * 0.141} = 35 \quad (30)$$

$$S_2 = \frac{C_s}{1.25} = \frac{79}{1.25} = 63.2 \quad (31)$$

The slenderness limits S_1 and S_2 were then calculated for welded sections using the relationship $F_{syw} = 0.6F_{tyw} = 0.6 * 15 \text{ ksi} = 9 \text{ ksi}$ from Table A.3.1 in ADM and Equations 32 and 33.

$$S_1 = \frac{B_s - F_{syw}}{1.25D_s} = \frac{12 - 9}{1.25 \times 0.051} = 47 \quad (32)$$

$$S_2 = \frac{C_s}{1.25} = \frac{158}{1.25} = 126 \quad (33)$$

For weld-affected zones of 6061-T6 aluminum extrusions, the buckling constants can be calculated using equations provided in Table 1-2 in the ADM, as follows:

If thickness is less than or equal to 0.375 in. (10 mm):

$$\begin{aligned} B_s &= 12 \text{ ksi} \\ D_s &= 0.051 \text{ ksi} \\ C_s &= 158 \end{aligned}$$

If thickness is greater than 0.375 in. (10 mm):

$$\begin{aligned} B_s &= 8.6 \text{ ksi} \\ D_s &= 0.031 \text{ ksi} \\ C_s &= 187 \end{aligned}$$

7.2.1.2 Round and Oval Tubes

The shear capacity of round or oval tubes from Section G.3 of the ADM is given in Equation 34.

$$\phi V_n = \phi F_s A_g / 2 \quad (34)$$

Where:

- ϕV_n = Nominal Shear Capacity [kip]
- F_s = Shear Stress Corresponding to Shear Strength from Table 7 [ksi]
- A_g = Gross Area [in.²]
- ϕ = 0.90

Since the buckling constants are dependent on the material type and slenderness limits, these values are the same as rectangular tubes in Section 7.2.1.1.

Table 7. Round or Oval Tubes Shear Strength [38]

Limit State	F_s	λ_t	Slenderness Limits
yielding	F_{sy}	$\lambda_t \leq S_1$	$S_1 = \frac{1.3B_s - F_{sy}}{1.63D_s}$
inelastic buckling	$1.3B_s - 1.63D_s \lambda_t$	$S_1 < \lambda_t < S_2$	
elastic buckling	$\frac{1.3\pi^2 E}{(1.25 \lambda_t)^2}$	$\lambda_t \geq S_2$	$S_2 = \frac{C_s}{1.25}$

$$\lambda_t = 2.9 \left(\frac{R_b}{t} \right)^{5/8} \left(\frac{L_v}{R_b} \right)^{1/4}$$

R_b = Mid-Thickness Radius of a Round Tube or Maximum Mid-Thickness Radius of an Oval Tube [in.]

t = Thickness of Tube [in.]

L_v = Length of Tube from Maximum to Zero Shear Force [in.]

$F_{sy} = F_{sy}$ if Non-Welded and F_{syw} if Welded

7.2.1.3 Solid Sections

For solid sections, the nominal shear capacity was not provided in the ADM but calculated using Equation 35.

$$\phi V_n = \phi F_{sy} A_g \quad (35)$$

Where:

ϕV_n = Nominal Shear Capacity [kip]

F_{sy} = Shear Yield Strength [ksi] = F_{sy} if Non-Welded and F_{syw} if Welded

$$F_{sy} = 0.6F_{ty} = 0.6 * 35 \text{ ksi} = 21 \text{ ksi}$$

$$F_{syw} = 0.6F_{tyw} = 0.6 * 15 \text{ ksi} = 9 \text{ ksi}$$

A_g = Gross Area [in.^2]

$$\phi = 0.90$$

7.2.2 Flexure

7.2.2.1 Rectangular Tubes

The general equation for the nominal flexural capacity of a closed-shape aluminum section, excluding pipes and round tubes, for the limit states of tensile yielding and tensile rupture is defined in Section F.8 in the ADM and shown in Equation 36. The flexural strength is

a function of the section modulus on the tension side of the neutral axis, S_t . In pure bending, half of a rectangular cross section is subjected to tension, while the other half is subjected to compression. This relation leads to the assumption that S_t of an aluminum tube section is half of the corresponding section modulus for the full section.

$$\phi M_n = \phi F_b S_t \quad (36)$$

Where: ϕM_n = Nominal Flexural Capacity [kip-ft]
 F_b = Flexural Strength [ksi]
 S_t = Section Modulus on the Tension Side of the Neutral Axis [in.³]
 ϕ = 0.90 for Yielding, 0.75 for Rupture

The flexural strength, F_b , for non-welded members in the yielding and rupture limit states is given by Equations 37 and 38. The flexural strength of a member within a weld-affected zone is defined differently and is explained in the next section. The tension coefficient, k_t , of the 6061 alloy with T6 temper is specified in the ADM as 1.0.

$$F_{b-yielding} = 1.30 F_{ty} \quad (37)$$

$$F_{b-rupture} = 1.42 F_{tu} / k_t \quad (38)$$

Where: $F_{b-yielding}$ = Flexural Strength in Yielding Limit State [ksi]
 $F_{b-rupture}$ = Flexural Strength in Rupture Limit State [ksi]
 F_{ty} = Tensile Yield Strength [ksi]
 k_t = Tension Coefficient

A section which has been welded uses a flexural strength, F_b , in yielding and rupture limit states determined by Equations 39 and 40. These equations use a combination of the tensile yield or ultimate strengths and the weld-affected yield or ultimate strength, with each contribution based on the proportion of the cross section in tension affected by the weld (A_{wzt}) to the gross cross-sectional area of the member in tension (A_{gt}). The ADM defines the weld-affected zone as any part within 1 in. (25.4 mm) of the centerline of the weld [38]. If the entire

cross section is in the weld-affected zone, then $A_{wzt}=A_{gt}$ and the equations simplify to include only the tensile yield or ultimate strength of welded aluminum.

$$F_{b-yielding} = 1.30[F_{ty} \left(1 - \frac{A_{wzt}}{A_{gt}}\right) + F_{tyw} \left(\frac{A_{wzt}}{A_{gt}}\right)] \quad (39)$$

$$F_{b-rupture} = 1.42[F_{tu} \frac{\left(1 - \frac{A_{wzt}}{A_{gt}}\right)}{k_t} + F_{tuw} \left(\frac{A_{wzt}}{A_{gt}}\right)] \quad (40)$$

Where:

$F_{b-yielding}$ =	Flexural Strength in Yielding Limit State [ksi]
$F_{b-rupture}$ =	Flexural Strength in Rupture Limit State [ksi]
F_{ty} =	Tensile Yield Strength [ksi]
F_{tyw} =	Tensile Yield Strength of Weld-Affected Zone [ksi]
F_{tu} =	Tensile Ultimate Strength [ksi]
F_{tuw} =	Tensile Ultimate Strength of Weld-Affected Zone [ksi]
A_{wzt} =	Cross-Sectional Area of the Weld-Affected Zone in Tension [in. ²]
A_{gt} =	Gross Cross-Sectional Area of Element in Tension [in. ²]
k_t =	Tension Coefficient

7.2.2.2 Pipe and Round Tubes

The nominal flexural capacity of pipes and round tubes should be calculated for the limit states of compressive yielding, tensile yielding, tensile rupture, and local buckling, as defined in Section F.6 in the ADM. For the compressive yielding limit state, nominal flexural capacity is given in Equation 41. For the tensile yielding limit state, nominal flexural capacity is given in Equation 42. For the tensile rupture limit state, nominal flexural capacity is given in Equation 43. For the local buckling limit state, the nominal flexural capacity is given in Equation 44.

$$\phi M_n = \phi 1.17 F_{cy} S \quad (41)$$

Where:

ϕM_n =	Nominal Capacity in Flexural Compressive Yielding [kip-ft]
F_{cy} =	Compressive Yield Strength [ksi]
S =	Section Modulus [in. ³]
ϕ =	0.90

$$\phi M_n = \phi 1.17 F_{ty} S \quad (42)$$

Where: ϕM_n = Nominal Capacity in Flexural Tensile Yielding [kip-ft]
 F_{ty} = Tensile Yield Strength [ksi]
 S = Section Modulus [in.³]
 ϕ = 0.90

$$\phi M_n = \phi 1.24 \frac{F_{tu} S}{k_t} \quad (43)$$

Where: ϕM_n = Nominal Capacity in Flexural Tensile Rupture [kip-ft]
 F_{tu} = Tensile Yield Strength [ksi]
 S = Section Modulus [in.³]
 k_t = Tension Coefficient
 ϕ = 0.75

$$\phi M_n = \phi F_b S \quad (44)$$

Where: ϕM_n = Nominal Capacity in Flexural Local Buckling [kip-ft]
 F_b = Flexural Strength as Determined by Table 8 [ksi]
 S_t = Section Modulus on the Tension Side of the Neutral Axis [in.³]
 ϕ = 0.90

Table 8. Pipe Flexural Local Buckling Strength [38]

Limit State	F_b	$\frac{R_b}{t}$	Slenderness Limits
upper inelastic buckling	$B_{tb} - D_{tb} \sqrt{\frac{R_b}{t}}$	$\frac{R_b}{t} \leq S_1$	$S_1 = \left(\frac{B_{tb} - B_t}{D_{tb} - D_t} \right)^2$
lower inelastic buckling	$B_t - D_t \sqrt{\frac{R_b}{t}}$	$S_1 < \frac{R_b}{t} < S_2$	
elastic buckling	$\frac{\pi^2 E}{16 \left(\frac{R_b}{t} \right) \left(1 + \sqrt{\frac{R_b}{t}} \right)^2}$	$\frac{R_b}{t} \geq S_2$	$S_2 = C_t$

D_t = Buckling Constant Slope [ksi]
 B_t = Buckling Constant Intercept [ksi]
 C_t = Buckling Constant Intersection
 D_{tb} = Buckling Constant [ksi]
 B_{tb} = Buckling Constant Intercept [ksi]
 R_b = Mid-Thickness Radius of a Round Tube or Maximum Mid-Thickness Radius of an Oval Tube [in.]
 t = Thickness of Tube [in.]

For non-welded 6061-T6 aluminum pipe, the buckling constants can be calculated using equations provided in Tables B.4.2 and Table 1-1 in the ADM, as follows:

$$\begin{aligned}B_t &= 43.2 \text{ ksi} \\D_t &= 1.558 \text{ ksi} \\C_t &= 141 \\B_{tb} &= 64.8 \text{ ksi} \\D_{tb} &= 4.458 \text{ ksi}\end{aligned}$$

The corresponding slenderness limits for non-welded pipe are shown in Equations 45 and 46.

$$S_1 = \left(\frac{B_{tb} - B_t}{D_{tb} - D_t} \right)^2 = \left(\frac{64.8 - 43.2}{4.458 - 1.558} \right)^2 = 55.48 \quad (45)$$

$$S_2 = C_t = 141 \quad (46)$$

For weld-affected zones of 6061-T6 aluminum pipe, the buckling constants can be calculated using equations provided in Tables B.4.2 and Table 1-2 in the ADM, as follows:

If thickness is less than or equal to 0.375 in. (10 mm):

$$\begin{aligned}B_t &= 19.5 \text{ ksi} \\D_t &= 0.654 \text{ ksi} \\C_t &= 390 \\B_{tb} &= 29.2 \text{ ksi} \\D_{tb} &= 1.539 \text{ ksi}\end{aligned}$$

If thickness is greater than 0.375 in. (10 mm):

$$\begin{aligned}B_t &= 14.1 \text{ ksi} \\D_t &= 0.425 \text{ ksi} \\C_t &= 524 \\B_{tb} &= 21.1 \text{ ksi} \\D_{tb} &= 0.999 \text{ ksi}\end{aligned}$$

The corresponding slenderness limits for welded pipe with thicknesses less than 0.375 in. (10 mm) are shown in Equations 47 and 48.

$$S_1 = \left(\frac{B_{tb} - B_t}{D_{tb} - D_t} \right)^2 = \left(\frac{29.2 - 19.5}{1.539 - 0.654} \right)^2 = 120.1 \quad (47)$$

$$S_2 = C_t = 390 \quad (48)$$

The corresponding slenderness limits for welded pipe with thicknesses greater than 0.375 in. (10 mm) are shown in Equations 49 and 50.

$$S_1 = \left(\frac{B_{tb} - B_t}{D_{tb} - D_t} \right)^2 = \left(\frac{21.1 - 14.1}{0.999 - 0.425} \right)^2 = 148.7 \quad (49)$$

$$S_2 = C_t = 524 \quad (50)$$

7.3 Connection Capacity

7.3.1 Welds

The filler material used in welding two aluminum elements together is dependent on the alloy specification of the two elements being welded. Table M.9.1 in the ADM specifies the desired filler alloy to be used for a welded connection, which is 5356 aluminum alloy for welds between two elements of the 6061 alloy. The corresponding tensile ultimate strength, F_{tuw} , and shear ultimate strength, F_{suw} , of the 5356 filler alloy from Table J.2.1 in the ADM are 35 ksi (240 MPa) and 17 ksi (115 MPa), respectively. The ADM considers the stress on an aluminum weld to be a shear stress, so weld capacities are calculated as a nominal shear strength from Section J.2.2.2 in the ADM, as shown in Equation 51.

$$\phi R_n = \phi F_{sw} L_{we} \quad (51)$$

Where

ϕR_n = Nominal Weld Shear Strength [lb]

F_{sw} = Shear Strength of Weld [psi], which is the Least of:

- The Product of the Weld Filler's Shear Ultimate Strength and the Effective Throat = $F_{suw(filler)} * e = 17,000 \text{ psi} * e$
- For Base Metal in Shear at the Weld-Base Metal Joint, the Product of the Base Metal's Welded Shear Ultimate Strength and the Fillet Size S_w at the Joint = $F_{suw(base metal)} * S_w = 15,000 \text{ psi} * S_w$
- For Base Metal in Tension at the Weld-Base Metal Joint, the Product of the Base Metal's Welded Tensile Ultimate Strength and the Fillet Size S_w at the Joint = $F_{tuw(base metal)} * S_w = 24,000 \text{ psi} * S_w$

L_{we} = Weld Effective Length [in.]

$\Phi = 0.75$

The ADM did not provide a specific method for calculating the flexural capacity of a weld, so a calculation was derived based on the nominal shear strength of the weld and moment of inertia of the weld group, as shown in Equation 52. Detailed calculations of the nominal shear strength and moment capacity are provided in Appendix C.

$$\phi M_n = \frac{\phi F_{suw} I}{c} \quad (52)$$

Where: ϕM_n = Moment Capacity of Weld [ft-lb]
 F_{suw} = Shear Ultimate Strength of the Weld Filler, $F_{suw}(\text{filler})$
 c = Distance to Neutral Axis [in.]
 $\phi = 0.75$

7.3.2 Baseplate

The aluminum design manual does not specify a design procedure for baseplates. Therefore, two steel baseplate design equations were utilized as specified in the AISC *Steel Construction Manual* and *Steel Design Guide Series 1* [41-42]. Method no. 1 was from Page 14-6 in the *Steel Construction Manual*, describing how the minimum baseplate thickness can be determined using the maximum tensile force acting on the baseplate with Equation 53.

Using Equation 53, the nominal capacity of the baseplate is calculated with Equation 54. An example of the baseplate design for Concept AW2-A is shown in Appendix C.

$$t_{min} = l \sqrt{\frac{2P_u}{\phi F_y B N}} \quad (53)$$

Where: t_{min} = Minimum Baseplate Thickness [in.]
 l = The Greater of m and n [in.]:
 $m = \frac{N - 0.95d}{2}$
 $n = \frac{B - 0.80b_f}{2}$
 B = Baseplate Width [in.]
 N = Baseplate Depth [in.]
 b_f = Post Flange Width [in.]
 d = Post Depth [in.]
 F_y = Yield Stress [psi]
 P_u = Maximum Vertical Force from Equation (24 [lb])
 $\phi = 0.90$

$$\phi P_n = \phi \frac{F_y B N}{2} \left(\frac{t}{l} \right)^2 \quad (54)$$

Where: ϕP_n = Nominal Baseplate Strength [lb]
 t = Baseplate Thickness [in.]
 l = The Greater of m and n [in.]:
 $m = \frac{N - 0.95d}{2}$
 $n = \frac{B - 0.80b_f}{2}$
 B = Baseplate Width [in.]
 N = Baseplate Depth [in.]
 b_f = Post Flange Width [in.]
 d = Post Depth [in.]
 F_y = Yield Stress [psi]
 $\phi = 0.90$

An alternative equation from the AISC *Steel Design Guide Series 1* [41-42] combines the axial force and moment on the baseplate, and the minimum can be determined using the required bending moment on the baseplate with Equation 55. Using method no. 2, the nominal capacity of the baseplate is calculated with Equation 56. An example of the baseplate design for Concept AW2-A is shown in Appendix C.

$$t_{min} = \sqrt{\frac{4M_{pl}}{\phi F_y}} \quad (55)$$

Where: t_{min} = Minimum Baseplate Thickness [in.]
 F_y = Yield Stress [psi]
 M_{pl} = Required Bending Moment per Width from Equation (25)
[lb-in./in.]
 $\phi = 0.90$

$$\phi M_n = \frac{\phi F_y t^2}{4} \quad (56)$$

Where: M_n = Nominal Bending Moment per Width [lb-in./in.]
 t = Baseplate Thickness [in.]
 F_y = Yield Stress [psi]
 $\phi = 0.90$

For the welded aluminum concepts, the base of the post or a sleeve was welded to the baseplate; therefore, F_y was set equal to $F_{tyw} = 15,000$ psi. For the modular concept, the baseplate was a cast aluminum part made from aluminum alloy 535. According to Table A.3.6 in the ADM, the tensile yield strength for alloy 535 is 13,500 psi (93 MPa).

7.3.3 Anchors

Steel bolts were preferred over aluminum due to availability. Certain types of steel react with aluminum; therefore, the grade of anchor bolts was selected to be compatible with 6061-T6 aluminum. Threaded anchor rods that were embedded into a concrete foundation using an epoxy adhesive were selected as they are the easiest to install and would allow the rail system to be repaired without replacing anchors. The threaded rod was configured with ASTM A193 Grade B7 steel.

The shear and flexural stresses have two different effects on the anchor. The shear stress that is transferred to the anchor is resisted completely by the shear capacity of the anchor bolts, while the flexural stress is assumed to concentrate about a moment arm, resulting in an upward tension on the anchorage rods. The procedure in the *Building Code Requirements for Structural Concrete (ACI 318-11)* [40] was used to determine the appropriate size and strength required of the anchor bolts while using Powers Fasteners AC100+ Gold epoxy. The minimum bond strength of the Powers Fastener epoxy is 1,450 psi (10.0 MPa) for threaded rods up to 7/8 in. (22 mm) in diameter. The equations to find the compared required strength of the steel, concrete, and bond are shown in Table D.4.1.1 in ACI 318-11 [40] and in Table 9. The concrete foundation has a minimum compressive strength of 2,500 psi (17.2 MPa), a minimum thickness of 7 in. (178 mm), and outer dimensions at least 10 in. (254 mm) away from the nearest anchor.

Table 9. Strength of Anchors [40]

Failure mode	Single anchor	Anchor group*	
		Individual anchor in a group	Anchors as a group
Steel strength in tension (D.5.1)	$\phi N_{sa} \geq N_{ua}$	$\phi N_{sa} \geq N_{ua,i}$	
Concrete breakout strength in tension (D.5.2)	$\phi N_{cb} \geq N_{ua}$		$\phi N_{cbg} \geq N_{ua,g}$
Pullout strength in tension (D.5.3)	$\phi N_{pn} \geq N_{ua}$	$\phi N_{pn} \geq N_{ua,i}$	
Concrete side-face blowout strength in tension (D.5.4)	$\phi N_{sb} \geq N_{ua}$		$\phi N_{sbg} \geq N_{ua,g}$
Bond strength of adhesive anchor in tension (D.5.5)	$\phi N_a \geq N_{ua}$		$\phi N_{ag} \geq N_{ua,g}$
Steel strength in shear (D.6.1)	$\phi V_{sa} \geq V_{ua}$	$\phi V_{sa} \geq V_{ua,i}$	
Concrete breakout strength in shear (D.6.2)	$\phi V_{cb} \geq V_{ua}$		$\phi V_{cbg} \geq V_{ua,g}$
Concrete pryout strength in shear (D.6.3)	$\phi V_{cp} \geq V_{ua}$		$\phi V_{cpg} \geq V_{ua,g}$
*Required strengths for steel and pullout failure modes shall be calculated for the most highly stressed anchor in the group.			

7.3.3.1 Tension

The designs that were considered in Section 5.2 utilized rails spanning between two posts. One anchor plate was attached to each post, as shown in Figure 29. Calculations were performed to determine whether or not a two-bolt anchor plate design was sufficient to withstand the design loads. Assuming a nearly rigid system and worst-case loading conditions means that nearly all bending load is applied to one anchor, meaning that one anchor rod (e.g., front anchor rod) would support all of the tension load and one anchor rod (e.g., rear anchor rod) would not be loaded, due to bending loads on the frame. Thus, each anchor was treated independently in the calculations.

ACI318-11 compares five different failure criteria for the anchorage system under tensile loading to determine the final capacity of the anchor: steel strength (N_{sa}), concrete breakout

strength (N_{cb}), pullout strength (N_{pn}), concrete side-face blowout strength (N_{sb}), and bond strength of adhesive anchor (N_a) [40].

The equation used to determine the steel strength of an anchor rod in tension is calculated with Equation D-2 in ACI 318-11 [40] and is shown in Equation 57.

$$\phi N_{sa} = \phi A_{se,N} f_{uta} \quad (57)$$

Where: ϕN_{sa} = Nominal Strength of an Anchor in Tension [in.^2]
 $A_{se,N}$ = Effective Cross-Sectional Area of an Anchor in Tension [in.^2]
 f_{uta} = Steel Strength, Minimum [$1.9f_{ya}$, 125,000 psi]
 f_{ya} = Yield Strength of Anchor [psi]
 $\phi = 0.75$

Determination of the concrete breakout strength is given in equation D-3 in ACI 318-11 [40] and by Equation 58. The project concrete failure area, A_{nc} , is estimated as the base of the rectilinear geometrical figure that results from projecting the failure surface outward $1.5h_{ef}$ from the centerlines of the anchor.

$$\phi N_{cb} = \phi \frac{A_{Nc}}{A_{Nco}} \Psi_{ed,N} \Psi_{c,N} \Psi_{cp,N} N_b \quad (58)$$

Where: ϕN_{cb} = Nominal concrete breakout strength in Tension of a Single Anchor [lb]
 A_{nc} = Projected Concrete Failure Area of a Single Anchor or Group of Anchors [in.^2]
 A_{Nco} = Projected Concrete Failure Area of a Single Anchor [in.^2]
 $= 9h_{ef}^2$
 h_{ef} = Anchor Embedment Depth [in.]
 $\Psi_{ed,N}$ = Modification Factor for Edge Effects for Single Anchor or Anchor Groups Tension in Tension (≤ 1.0)
If $c_{a,min} \geq 1.5h_{ef}$, $\Psi_{ed,N} = 1.0$
If $c_{a,min} < 1.5h_{ef}$, $\Psi_{ed,N} = 0.7 + 0.3 \frac{c_{a,min}}{1.5h_{ef}}$
 c_{a1} = Distance from the Center of an Anchor to the Edge of the Concrete in one Direction [in.]
 c_{a2} = Distance from the Center of an Anchor to the Edge of the Concrete in Direction Perpendicular to c_{a1} [in.]
 $c_{a,min}$ = Minimum Distance from the Center of an Anchor to the Edge of the Concrete [in.]

$$\begin{aligned}
 \Psi_{c,N} &= \text{Modification Factor Based on Presence or Absence of Cracks in Concrete} \\
 &= 1.25 \text{ for Cast-In Anchors} \\
 &= 1.4 \text{ for Post-Installed Anchors} \\
 \Psi_{cp,N} &= \text{Modification Factor for Post-Installed Anchors for Uncracked Concrete without Supplementary Reinforcement} \\
 &\text{If } c_{a,min} \geq c_{ac}, \Psi_{cp,N} = 1.0 \\
 &\text{If } c_{a,min} < c_{ac}, \Psi_{cp,N} = \frac{c_{a,min}}{c_{ac}} \\
 c_{ac} &= \text{Critical Edge Distance [in.]} = 2h_{ef} \text{ (for Adhesive Anchors)} \\
 N_b &= \text{Basic Concrete Breakout Strength of a Single Anchor in Tension} = k_c \lambda_a \sqrt{f'_c} h_{ef}^{1.5} \\
 k_c &= 24 \text{ for Cast-In Anchors} \\
 &= 17 \text{ for Post-Installed Anchors} \\
 f'_c &= \text{Compressive Strength of Concrete [psi]} = 2,500 \text{ psi} \\
 \phi &= 0.65
 \end{aligned}$$

The pullout strength (N_{pn}) is not applicable for adhesive anchors, according to Section D.5.3 in ACI 318-11. The concrete side-face blowout strength (N_{sb}) is not applicable unless deep anchors exist (where $h_{ef} > 2.5c_{a1}$), which is not the case for these designs. The bond strength of an adhesive anchor in tension is given by equation D-18 in ACI 318-11 [40] and is shown in Equation 59.

$$\phi N_a = \phi \frac{A_{Na}}{A_{Na0}} \Psi_{ed,Na} \Psi_{cp,Na} N_{ba} \quad (59)$$

Where:

$$\begin{aligned}
 \phi N_a &= \text{Nominal Bond Strength in Tension of a Single Anchor [lb]} \\
 A_{Na} &= \text{Projected Influence Area of a Single Anchor or Group of Anchors [in.}^2\text{]} \\
 A_{Na0} &= \text{Projected Influence Area of a Single Adhesive Anchor with an Edge Distance Equal to or Greater than } c_{Na} \text{ [in.}^2\text{]}, \\
 &\quad A_{Na0} = (2c_{Na})^2 \\
 c_{Na} &= \text{Critical Distance} = 10d_a \sqrt{\frac{\tau_{uncr}}{1100}} \\
 d_a &= \text{Diameter of Anchor [in.]} \\
 \tau_{uncr} &= \text{Uncracked Shear Stress [psi]} \\
 \Psi_{ed,Na} &= \text{Modification Factor for Edge Effects for Single Anchors or Anchor Groups Loaded in Tension} \\
 &\text{If } c_{a,min} \geq c_{Na}, \Psi_{ed,Na} = 1.0 \\
 &\text{If } c_{a,min} < c_{Na}, \Psi_{ed,Na} = 0.7 + 0.3 \frac{c_{a,min}}{c_{Na}} \\
 c_{a1} &= \text{Distance from the Center of an Anchor to the Edge of the Concrete in one Direction [in.]}
 \end{aligned}$$

c_{a2} = Distance from the Center of an Anchor to the Edge of the Concrete in Direction Perpendicular to c_{a1} [in.]
 $c_{a,min}$ = Minimum Distance from the Center of an Anchor to the Edge of the Concrete [in.]
 $\Psi_{cp,Na}$ = Modification Factor for Adhesive Anchors in Uncracked Concrete without Supplementary Reinforcement
 If $c_{a,min} \geq c_{ac}$, $\Psi_{cp,Na} = 1.0$
 If $c_{a,min} < c_{ac}$, $\Psi_{cp,Na} = \frac{c_{a,min}}{c_{ac}}$
 c_{ac} = Critical Edge Distance [in.]
 $N_{ba} = \lambda_a \tau_{cr} \pi d_a h_{ef}$
 h_{ef} = Anchor Embedment Depth [in.]
 τ_{cr} = Characteristic Bond Stress [psi]
 $\lambda_a = 1.0$ for Normal-Weight Concrete
 $\phi = 0.65$

7.3.3.2 Shear

ACI318-11 compares three different failure criteria of the anchorage system under shear loading to determine the final capacity of the anchor: steel strength (V_{sa}), concrete breakout strength (V_{cb}), and concrete pryout strength (V_{cp}) [40]. Two anchors with a spacing, s , can be loaded in shear at the same time, so the two anchors should be considered a group.

The equation used to determine the steel strength of an anchor rod in tension is calculated with Equation D-29 in ACI318-11 [40] and is shown in Equation 60.

$$\phi V_{sa} = \phi 0.6 A_{se,V} f_{uta} \quad (60)$$

Where:
 ϕV_{sa} = Nominal Strength of an Anchor in Shear [lb]
 $A_{se,V}$ = Effective Cross-Sectional Area of an Anchor in Shear [in.²]
 f_{uta} = Steel Strength, Minimum [$1.9f_{ya}$, 125,000 psi]
 f_{ya} = Yield Strength of Anchor [psi]
 $\phi = 0.75$

Determination of the concrete breakout strength is given in equation D-31 in ACI318-11 [40] and by Equation 61. The project concrete failure area, A_{vc} , is estimated as the base of the rectilinear geometrical figure that results from projecting the failure surface outward $1.5c_{a1}$ from the centerline of the anchors.

$$\phi V_{cbg} = \phi \frac{A_{vc}}{A_{vco}} \Psi_{ec,v} \Psi_{ed,v} \Psi_{c,v} \Psi_{h,v} V_b \quad (61)$$

Where:

- ϕV_{cbg} = Nominal Concrete Breakout Strength in Shear of a Group of Anchors [lb]
- A_{vc} = Projected Concrete Failure Area of a Single Anchor or Group of Anchors [in.²]
- A_{vco} = Projected Concrete Failure Area of a Single Anchor [in.²] = $4.5(c_{a1})^2$
- h_a = Depth of Concrete Foundation [in.]
- $\Psi_{ec,v}$ = Modification Factor for Anchors Based on Eccentricity of Applied Loads = $\frac{1}{\left(1 + \frac{2e'_v}{3c_{a1}}\right)}$
- e'_v = Eccentricity of Applied Shear Force [in.] = 0
- $\Psi_{ed,v}$ = Modification Factor for Edge Effects for Single Anchor or Anchor Groups Loaded in Shear
 - If $c_{a2} \geq 1.5c_{a1}$, $\Psi_{ed,v} = 1.0$
 - If $c_{a2} < 1.5c_{a1}$, $\Psi_{ed,v} = 0.7 + 0.3 \frac{c_{a2}}{1.5c_{a1}}$
- c_{a1} = Distance from the Center of an Anchor to the Edge of the Concrete in one Direction [in.]
- c_{a2} = Distance from the Center of an Anchor to the Edge of the Concrete in Direction Perpendicular to c_{a1} [in.]
- $c_{a,min}$ = Minimum Distance from the Center of an Anchor to the Edge of the Concrete [in.]
- $\Psi_{c,v}$ = Modification Factor Based on Presence or Absence of Cracks in Concrete
 - = 1.4 for No Cracking at Service Loads
 - = 1.0 for Anchors in Cracked Concrete without Supplementary Reinforcement
 - = 1.2 for Anchors in Cracked Concrete with Supplementary Reinforcement
 - = 1.4 for Anchors in Cracked Concrete with Supplementary Reinforcement Enclosed within Stirrups
- $\Psi_{h,v}$ = Modification Factor for Anchors Located in Concrete
 - If $h_a < 1.5c_{a1}$, $\Psi_{h,v} = \sqrt{\frac{1.5c_{a1}}{h_a}} \geq 1.0$
 - Otherwise $\Psi_{h,v} = 1.0$
- V_b = Basic Concrete Breakout Strength of a Single Anchor in Shear is Equal to the Smaller of:
 - $V_b = \left(7 \left(\frac{l_e}{d_a}\right)^{0.2} \sqrt{d_a}\right) \lambda_a \sqrt{f'_c} (c_{a1})^{1.5}$
 - $V_b = 9 \lambda_a \sqrt{f'_c} (c_{a1})^{1.5}$
- l_e = h_{ef} for Anchors with a Constant Stiffness over the Length of Embedded Section

d_a = Diameter of Anchor [in.]
 f_c' = Compressive Strength of Concrete [psi] = 2,500 psi
 $\phi = 0.75$

The concrete pryout of an adhesive anchor in shear is given by equation D-41 in ACI318-11 [40] and is shown in Equation 62.

$$\phi V_{cpg} = \phi k_{cp} N_{cpg} \quad (62)$$

Where: ϕV_{cpg} = Nominal Concrete Pryout Strength in Shear of Anchor Group [lb]

k_{cp} = Coefficient for Pryout Strength
 = 1.0 for $h_{ef} < 2.5$ in.
 = 2.0 for $h_{ef} \geq 2.5$ in.

h_{ef} = Anchor Embedment Depth [in.]

N_{cpg} = Concrete Pryout Strength for Adhesive Anchors is Lesser of

$$N_{ag} = \frac{A_{Na}}{A_{Na0}} \Psi_{ec,Na} \Psi_{ed,Na} \Psi_{cp,Na} N_{ba}$$

$$N_{cbg} = \frac{A_{Nc}}{A_{Nco}} \Psi_{ec,N} \Psi_{ed,N} \Psi_{c,N} \Psi_{cp,N} N_b$$

N_{ag} = Nominal Bond Strength in Tension of an Anchor Group

A_{Na} = Projected Influence Area of a Single Anchor or Group of Anchors [in.²]

A_{Na0} = Projected Influence Area of a Single Anchor with an Edge Distance Equal to or Greater than c_{Na} [in.²], $A_{Na0} = (2c_{Na})^2$

$$c_{Na} = \text{Critical Distance} = 10d_a \sqrt{\frac{\tau_{uncr}}{1100}}$$

d_a = Diameter of Anchor [in.]

τ_{uncr} = Uncracked Shear Stress [psi]

$\Psi_{ec,Na}$ = Modification Factor for Anchors Based on Eccentricity of

$$\text{Applied Loads} = \frac{1}{\left(1 + \frac{2e'_N}{3c_{a1}}\right)}$$

e'_N = Eccentricity of Applied Tension Force [in.] = 0

$\Psi_{ed,Na}$ = Modification Factor for Edge Effects for Single Anchors or Anchor Groups Loaded in Tension

If $c_{a,min} \geq c_{Na}$, $\Psi_{ed,Na} = 1.0$

If $c_{a,min} < c_{Na}$, $\Psi_{ed,Na} = 0.7 + 0.3 \frac{c_{a,min}}{c_{Na}}$

c_{a1} = Distance from the Center of an Anchor to the Edge of the Concrete in One Direction [in.]

c_{a2} = Distance from the Center of an Anchor to the Edge of the Concrete in Direction Perpendicular to c_{a1} [in.]

$c_{a,min}$ = Minimum Distance from the Center of an Anchor to the Edge of the Concrete [in.]

$\Psi_{cp,Na}$ = Modification Factor for Adhesive Anchors in uncracked Concrete without Supplementary Reinforcement

If $c_{a,min} \geq c_{ac}$, $\Psi_{cp,Na} = 1.0$

If $c_{a,min} < c_{ac}$, $\Psi_{cp,Na} = \frac{c_{a,min}}{c_{ac}}$

c_{ac} = Critical Edge Distance [in.]

$N_{ba} = \lambda_a \tau_{cr} \pi d_a h_{ef}$

h_{ef} = Anchor Embedment Depth [in.]

τ_{cr} = Characteristic Bond Stress [psi]

$\lambda_a = 1.0$ for Normal-Weight Concrete

N_{cbg} = Nominal Concrete Breakout Strength in Tension of Anchor Group [lb]

A_{nc} = Projected Concrete Failure Area of a Single Anchor or Group of Anchors [in.²]

A_{Nco} = Projected Concrete Failure Area of a Single Anchor [in.²] = $9h_{ef}^2$

h_{ef} = Anchor Embedment Depth [in.]

$\Psi_{ec,N}$ = Modification Factor for Anchors Based on Eccentricity of Applied Loads = $\frac{1}{\left(1 + \frac{2e'_N}{3c_{a1}}\right)}$

$\Psi_{ed,N}$ = Modification Factor for Edge Effects for Single Anchors or Anchor Groups Loaded in Tension in Tension (≤ 1.0)

If $c_{a,min} \geq 1.5h_{ef}$, $\Psi_{ed,N} = 1.0$

If $c_{a,min} < 1.5h_{ef}$, $\Psi_{ed,N} = 0.7 + 0.3 \frac{c_{a,min}}{1.5h_{ef}}$

$\Psi_{c,N}$ = Modification Factor Based on Presence or Absence of Cracks in Concrete

= 1.25 for Cast-In Anchors

= 1.4 for Post-Installed Anchors

$\Psi_{cp,N}$ = Modification Factor for Post-Installed Anchors for Uncracked Concrete without Supplementary Reinforcement

If $c_{a,min} \geq c_{ac}$, $\Psi_{cp,N} = 1.0$

If $c_{a,min} < c_{ac}$, $\Psi_{cp,N} = \frac{c_{a,min}}{c_{ac}}$

c_{ac} = Critical Edge Distance = $2h_{ef}$ (for Adhesive Anchors)

N_b = Basic Concrete Breakout Strength of a Single Anchor in Tension = $k_c \lambda_a \sqrt{f'_c} h_{ef}^{1.5}$

$k_c = 24$ for Cast-In Anchors

= 17 for Post-Installed Anchors

f'_c = Compressive Strength of Concrete [psi] = 2,500 psi

$\phi = 0.75$

The calculations for determining the nominal capacities of the anchors for each concept are shown in Appendix C, while details are provided in Section 7.4.

7.3.4 Modular Cast Aluminum

For the modular system, cast aluminum connections including tees and elbows were provided with the system. Since these connections are specialized parts based on the selected rail and post sizes, the capacities of these parts were not evaluated.

7.4 Final Designs

7.4.1 Introduction

Two concepts from Section 5.2 were further refined into four concepts and had final design calculations completed. Those concepts included the Modular Aluminum AM-1 design (Section 5.2.1) and three variations of the Welded Aluminum AW2 design (Section 5.2.3). The capacity of each component of the final four rail designs to be tested (AW2-A, AW2-C, AM-1, and AW2-D), as well as the required design loads, are shown in Appendix C. The system drawings for each of the concepts are shown in Figures 102 through 121.

The smallest section that met the required design loads was determined for each component. The sections were then evaluated to determine if they were commonly available by aluminum suppliers. If not, the next smallest section that was commonly available was selected for the final design. In some cases, the thickness of the section was optimized to match the minimum base metal thickness for a given weld size.

For the three AW2 concepts, a $\frac{3}{8}$ -in. (10-mm) thick baseplate was selected, even though Concept AW2-C did not meet the required design loads based on the method no. 1 equations for the nominal capacity. None of the concepts met the baseplate design with method no. 2 equations, and since these equations were derived with columns with a large axial force, they may not be applicable to this situation. However, the smaller baseplate dimensions were selected for two reasons. First, the baseplate capacity equations were derived for steel connections and are

believed to be inherently conservative. Second, it was not desired that the anchor bolts incur damage when impacted dynamically. If a larger and/or thicker baseplate were selected, the greater plate capacity may cause a greater load imparted to the anchor bolts, which could cause permanent deformation. The researchers believed that a $\frac{3}{8}$ -in. (10-mm) thick baseplate was sufficient to sustain the AASHTO *LRFD Bridge Design Specifications* pedestrian rail live loads and had the ability to verify the loads with a static component test, if necessary.

7.4.2 AW2-A Welded Aluminum

Concept AW2-A designated 2-in. x 4-in. x $\frac{1}{4}$ -in. x 43-in. tall (51-mm x 102-mm x 6-mm x 1,029-mm tall) posts with three 2-in. x 2-in. x $\frac{1}{8}$ -in. (51-mm x 51-mm x 3-mm) rail components at heights of 42 in. (1,067 mm), $34\frac{1}{8}$ in. (867 mm), and $7\frac{7}{8}$ in. (200 mm). The rails were secured to the posts with $\frac{1}{8}$ -in. (3-mm) fillet welds at each connection. Nine $\frac{1}{2}$ -in. x $\frac{1}{2}$ -in. x $24\frac{1}{4}$ -in. (13-mm x 13-mm x 616-mm) square spindles were used as the infill design between the mid and bottom rail components, connected with $\frac{1}{8}$ -in. (3-mm) fillet welds. Each post member was welded to a 3-in. x $7\frac{1}{2}$ -in. x $\frac{3}{8}$ -in. (76-mm x 191-mm x 9.5-mm) baseplate with a $\frac{1}{4}$ -in. (6-mm) fillet weld at the connection. The baseplate had two $\frac{1}{2}$ -in. (13-mm) holes spaced at 6 in. (152 mm) to accommodate two $\frac{3}{8}$ -in. (9.5-mm) threaded anchor rods, each embedded 5 in. (127 mm) into 1,450-psi (10.0-MPa) minimum bond strength epoxy adhesive secured through the baseplate with a $\frac{3}{8}$ -in. (9.5-mm) dia. ASTM A194 Grade 8M nut. The concrete foundation has a minimum compressive strength of 2,500 psi (17.2 MPa), a minimum thickness of 7 in. (178 mm), and outer dimensions at least 10 in. (254 mm) away from the nearest anchor. The static post deflection was estimated to be 0.19 in. (4.8 mm), and the static rail deflection was estimated to be 0.32 in. (8 mm). Detailed schematic drawings of design AW2-A are shown in Figures 102 through 105, 109, and 114. A photograph of design AW2-A is shown in Figure 122.

7.4.3 AW2-C Welded Aluminum

Concept AW2-C designated 2-in. x 3-in. x $\frac{1}{8}$ -in. x 43-in. tall (51-mm x 76-mm x 3-mm x 1,029-mm tall) posts with three 2-in. x 2-in. x $\frac{1}{8}$ -in. (51-mm x 51-mm x 3-mm) rail components at heights of 42 in. (1,067 mm), $34\frac{1}{8}$ in. (867 mm), and $7\frac{7}{8}$ in. (200 mm). The rails were secured to the posts with $\frac{1}{8}$ -in. (3-mm) fillet welds at each connection. Nine $\frac{1}{2}$ -in. x $\frac{1}{2}$ -in. x $24\frac{1}{4}$ -in. (13-mm x 13-mm x 616-mm) square spindles were used as the infill design between the mid and bottom rail components, connected with $\frac{1}{8}$ -in. (3-mm) fillet welds. Each post member was connected to a $3\frac{1}{2}$ -in. x $7\frac{1}{2}$ -in. x $\frac{3}{8}$ -in. (89-mm x 191-mm x 9.5-mm) baseplate with a retention sleeve. The $3\frac{1}{2}$ -in. (89-mm) tall retention sleeve was constructed using $\frac{1}{4}$ -in. (6-mm) aluminum plates to form a sleeve for the post. The outer dimensions of the sleeve were $2\frac{5}{8}$ in. x $3\frac{3}{8}$ in. (67 mm x 92 mm), and the inner dimensions were $2\frac{1}{8}$ in. x $3\frac{1}{8}$ in. (54 mm x 79 mm). The sleeve was completely welded to the baseplate with a $\frac{3}{16}$ -in. (4.8-mm) fillet weld. A $\frac{3}{8}$ -in. (9.5-mm) hole was drilled longitudinally through both the sleeve and post components at a height of 2 in. (51 mm) from the surface of the baseplate, so a $\frac{1}{4}$ -in. dia. x 3-in. long (6-mm dia. x 76-mm long) ASTM A193 Grade B8M bolt could be fastened through the post and sleeve together, secured with a $\frac{1}{4}$ -in. (6-mm) dia. ASTM A194 Grade 8M nut. The baseplate had two $\frac{1}{2}$ -in. (13-mm) holes spaced at 6 in. (152 mm) to accommodate two $\frac{3}{8}$ -in. (9.5-mm) threaded anchor rods, each embedded 5 in. (127 mm) into 1,450-psi (10.0-MPa) minimum bond strength epoxy adhesive and secured through the baseplate with a $\frac{3}{8}$ -in. (9.5-mm) dia. ASTM A194 Grade 8M nut. The concrete foundation has a minimum compressive strength of 2,500 psi (17.2 MPa), a minimum thickness of 7 in. (178 mm), and outer dimensions at least 10 in. (254 mm) away from the nearest anchor. The static post deflection was estimated to be 0.70 in. (18 mm), and the static rail deflection was estimated to be 0.32 in. (8 mm). Detailed drawings of design AW2-C are shown

in Figures 102, 103, 106 through 109, and 114. A photograph of design AW2-C is shown in Figure 123.

7.4.4 AM-1 Modular Aluminum

Concept AM-1 was a standard modular system, the Speed Rail® that is available through Hollaender. The system was designed by Hollaender according to the AASHTO pedestrian rail loads [6] and the rail, post, spindle, and baseplate were verified by MwRSF in Appendix C. Hollaender's Speed-Rail® system is composed of 6061-T6 aluminum circular tube rail and post members, with tee, elbow, and cross fittings utilized as connections. Various standard bases are available depending on the combination of the required strength and anchoring options [35].

The Hollaender modular system uses 2-in. dia. x 39-in. long (51-mm dia. x 991-mm long) schedule 80 posts, with 2-in. dia. x 56½-in. long (51-mm dia. x 1,435-mm long) schedule 40 rails, and standard bases for anchoring, depending on the style and required capacity. Hollaender's two-hole No. 48 Heavy-Duty Base Flange was selected as the base connection bracket for anchoring the system to the concrete. Two ⅜-in. (9.5-mm) threaded anchor rods were embedded 5 in. (127 mm) into 1,450-psi (10.0-MPa) minimum bond strength epoxy adhesive and secured through the baseplate with a ⅜-in. (9.5-mm) dia. ASTM A194 Grade 8M nut. The concrete foundation has a minimum compressive strength of 2,500 psi (17.2 MPa), a minimum thickness of 7 in. (178 mm), and outer dimensions at least 10 in. (254 mm) away from the nearest anchor. The static post deflection was estimated to be 1.18 in. (30 mm), and the static rail deflection was estimated to be 0.26 in. (7 mm). Detailed drawings of design AM-1 are shown in Figures 102, 103, 110 through 113, and 115. A photograph of design AM-1 is shown in Figure 124.

7.4.5 AW2-D Welded Aluminum

Concept AW2-D was similar to Concept AW2-A, with differences in the rail locations and spindle length. Concept AW2-D designated 2-in. x 4-in. x 1/4-in. x 43-in. tall (51-mm x 102-mm x 6-mm x 1,029-mm tall) posts with three 2-in. x 2-in. x 1/8-in. (51-mm x 51-mm x 3-mm) rail components at heights of 42 in. (1,067 mm), $24^{15}/_{16}$ in. (633 mm), and $7^{7}/_{8}$ in. (200 mm). The rails were inserted into cutouts in the posts at each rail location and secured to the face of the posts with 1/8-in. (3-mm) fillet welds at each connection. The post-to-rail connection was more rigid than Concept AW2-A due to the interaction of the end of the rail with both post faces. Nine 1/2-in. x 1/2-in. x $32^{1}/_{8}$ -in. (13-mm x 13-mm x 816-mm) square spindles were spanned between the top and bottom rail and were inserted through the middle rail. The spindles were welded with 1/8-in. (3-mm) fillet welds at each rail location. Each post member was welded to a 3-in. x $7^{3}/_{4}$ -in. x 3/8-in. (76-mm x 191-mm x 9.5-mm) baseplate with a 1/4-in. (6-mm) fillet weld at the connection. The baseplate had two 5/8-in. (16-mm) holes spaced at $6^{1}/_{4}$ in. (159 mm) to accommodate two 1/2-in. (13-mm) diameter threaded anchor rods, each embedded 5 in. (127 mm) into 1,450-psi (10.0-MPa) minimum bond strength epoxy adhesive and secured through the baseplate with a 1/2-in. (13-mm) diameter ASTM A194 Grade 8M nut. The concrete foundation has a minimum compressive strength of 2,500 psi (17.2 MPa), a minimum thickness of 7 in. (178 mm), and outer dimensions at least 10 in. (254 mm) away from the nearest anchor. The static post deflection was estimated to be 0.19 in. (4.8 mm), and the static rail deflection was estimated to be 0.32 in. (8 mm). Detailed drawings of design AW2-D are shown in Figures 116 through 121. A photograph of design AW2-D is shown in Figure 125.

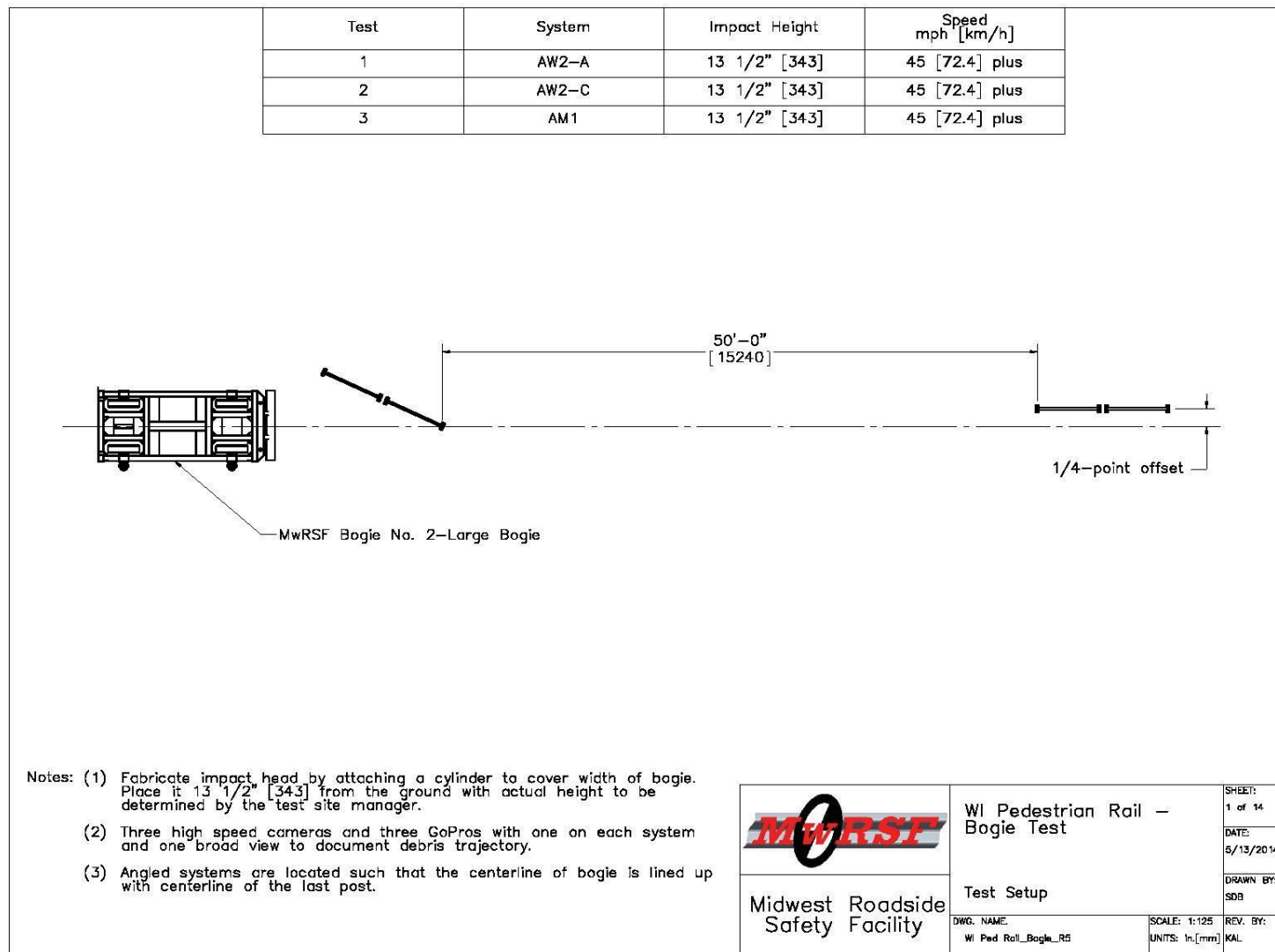


Figure 102. Pedestrian Rail Test Setup, Designs AW2-A, AW2-C and AM-1

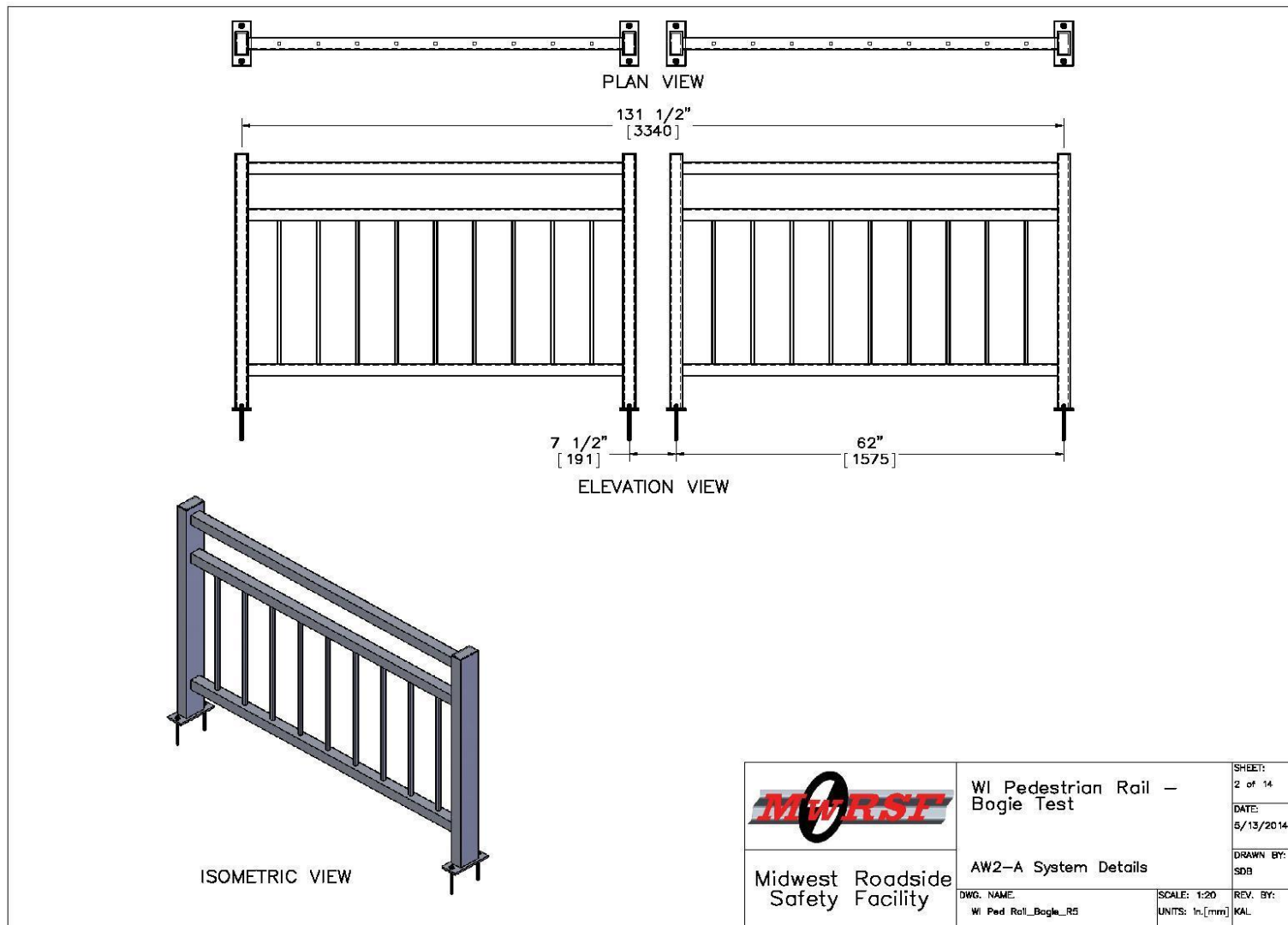


Figure 103. Pedestrian Rail Test Setup, Designs AW2-A, AW2-C and AM-1

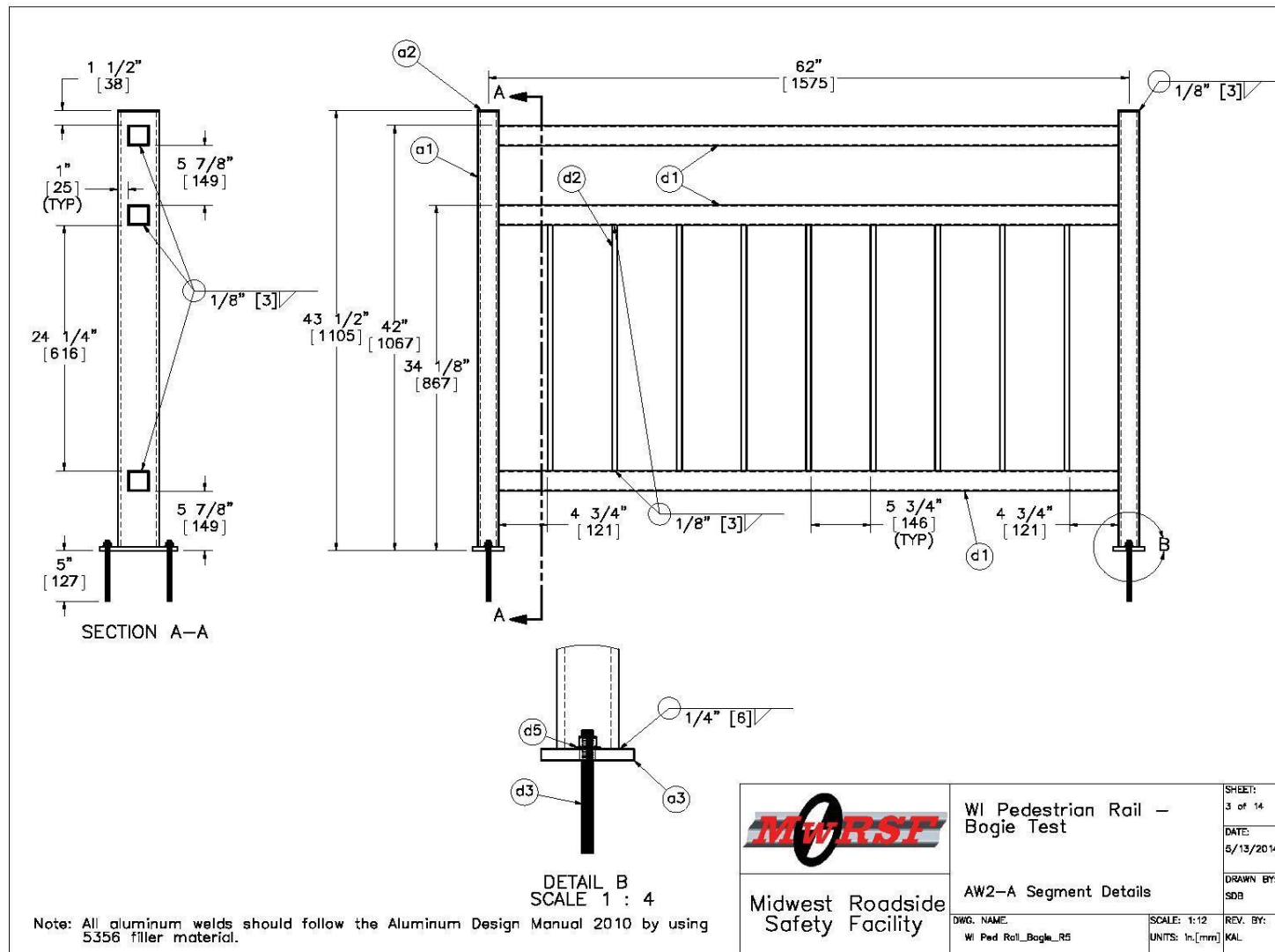


Figure 104. Pedestrian Rail Design AW2-A

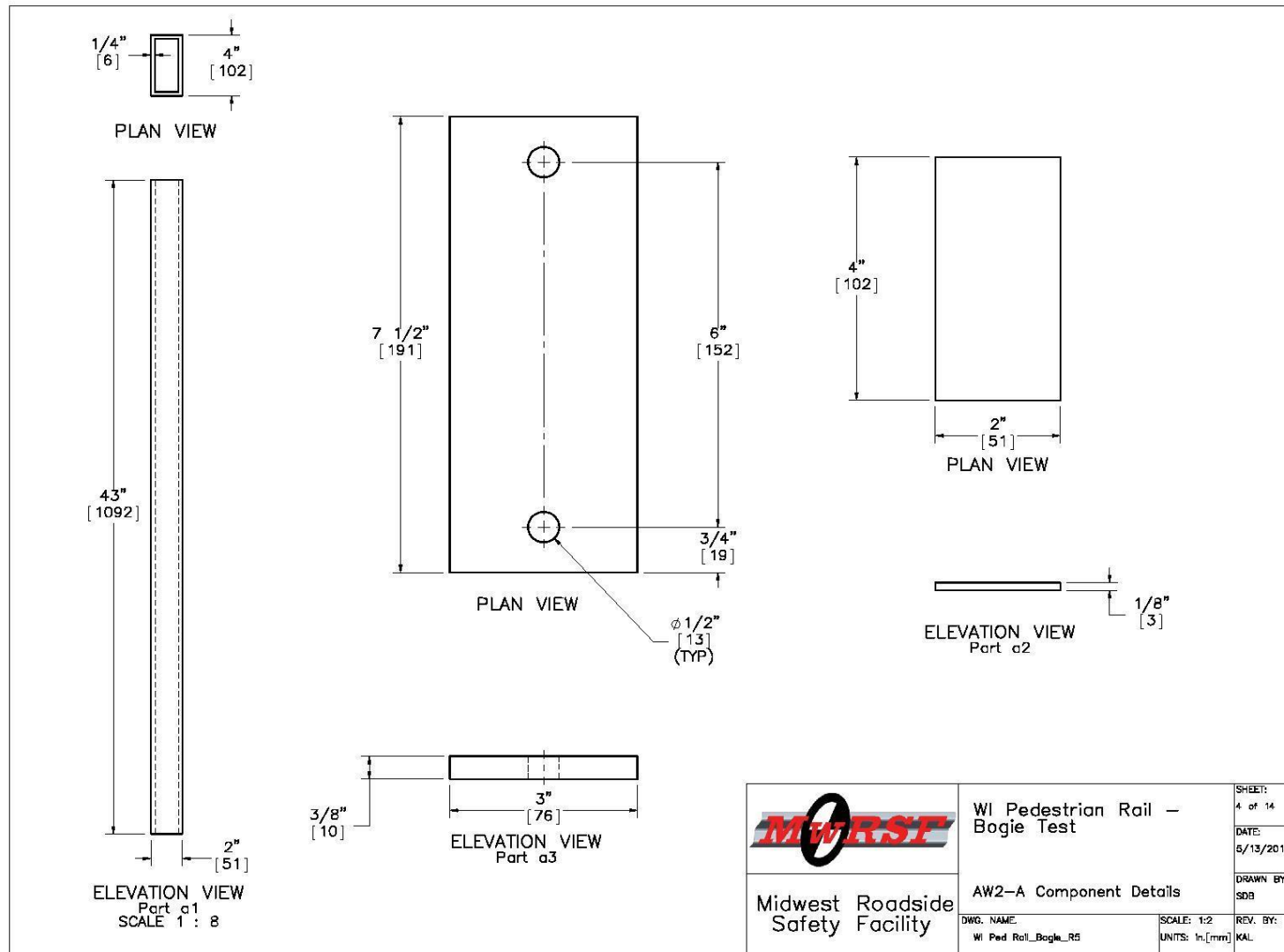


Figure 105. Pedestrian Rail Design AW2-A

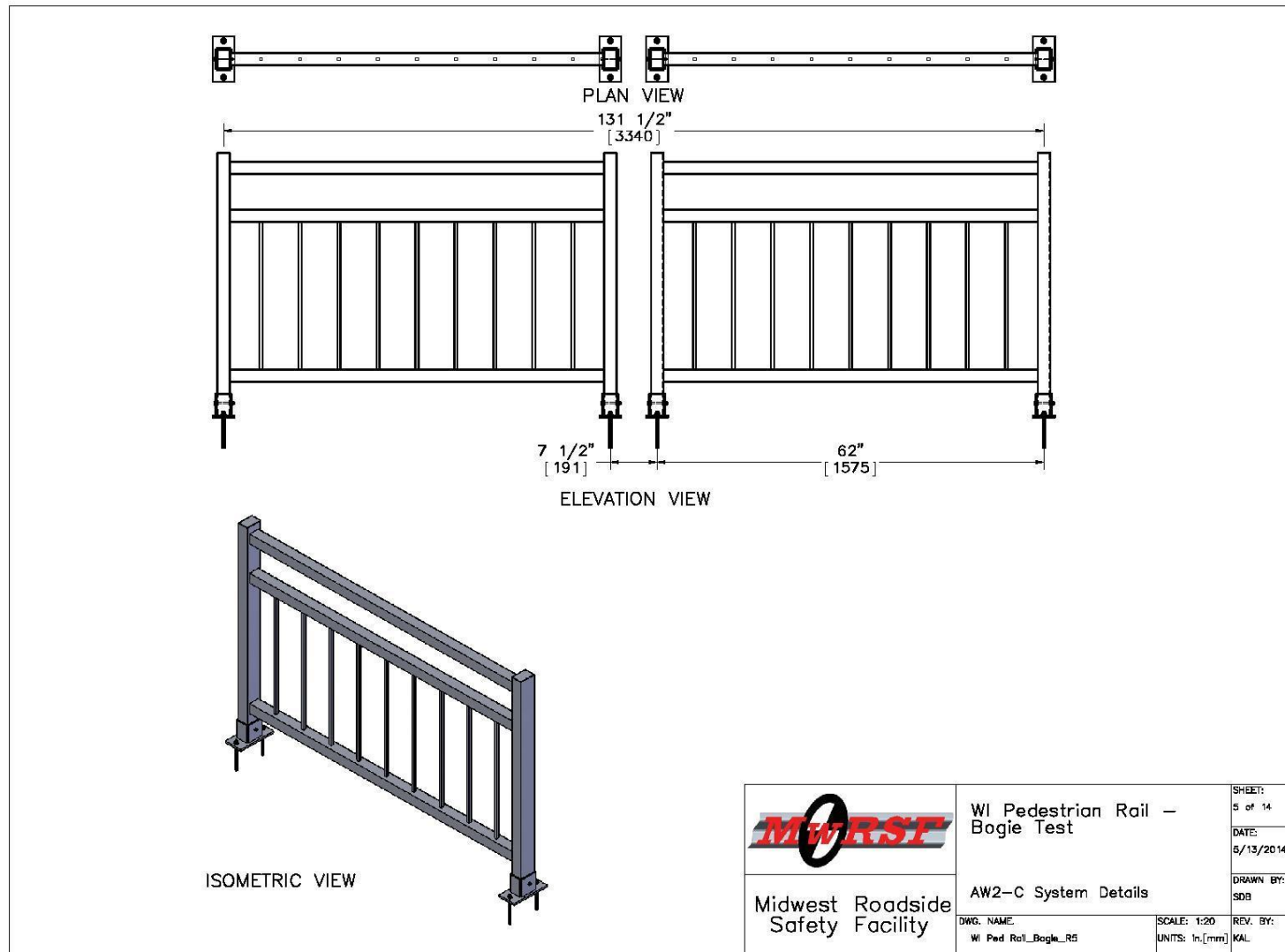


Figure 106. Pedestrian Rail Design AW2-C

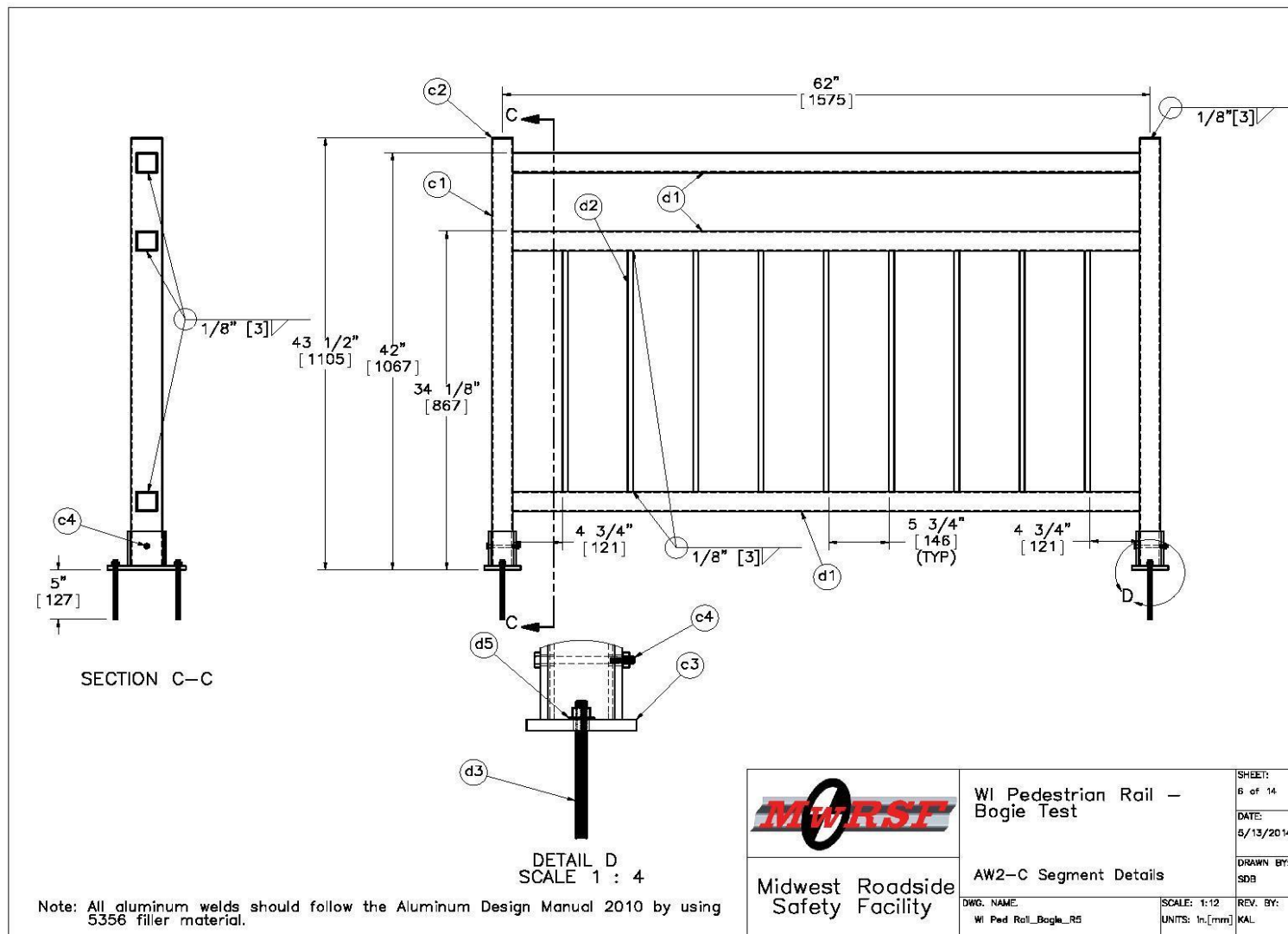


Figure 107. Pedestrian Rail Design AW2-C

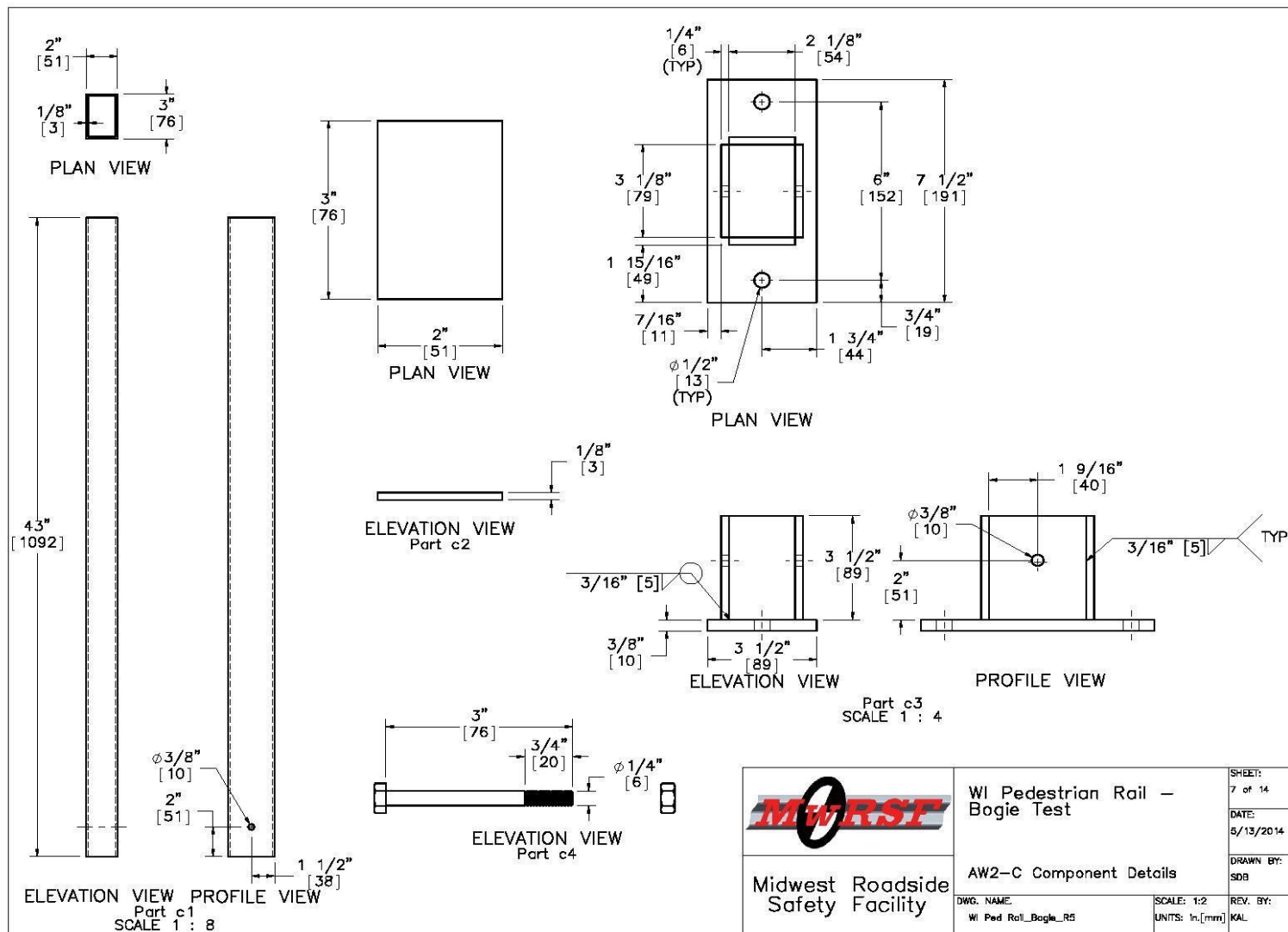


Figure 108. Pedestrian Rail Design AW2-C

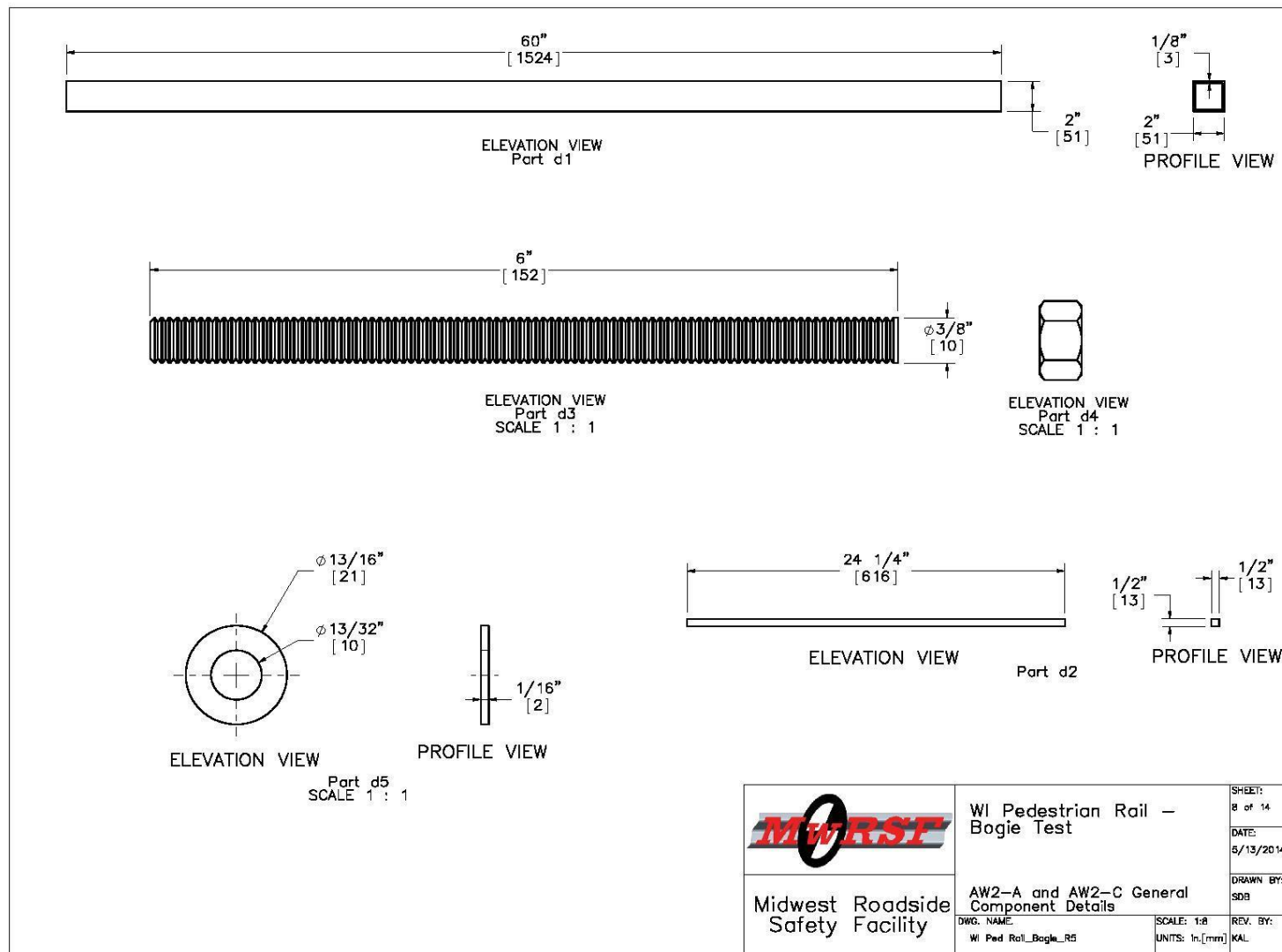


Figure 109. General Components, Pedestrian Rail Designs AW2-A and AW2-C

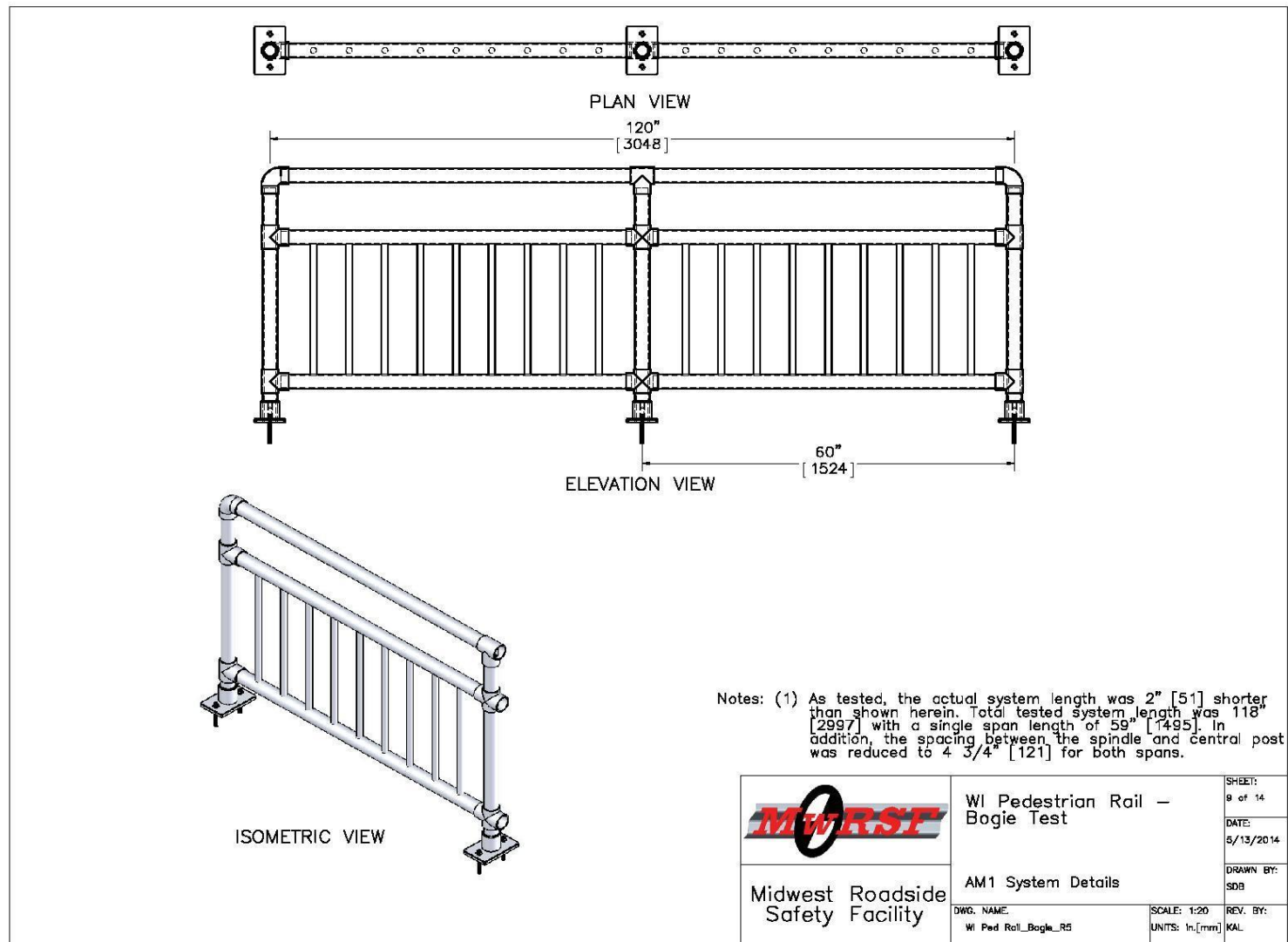


Figure 110. Pedestrian Rail Design AM-1

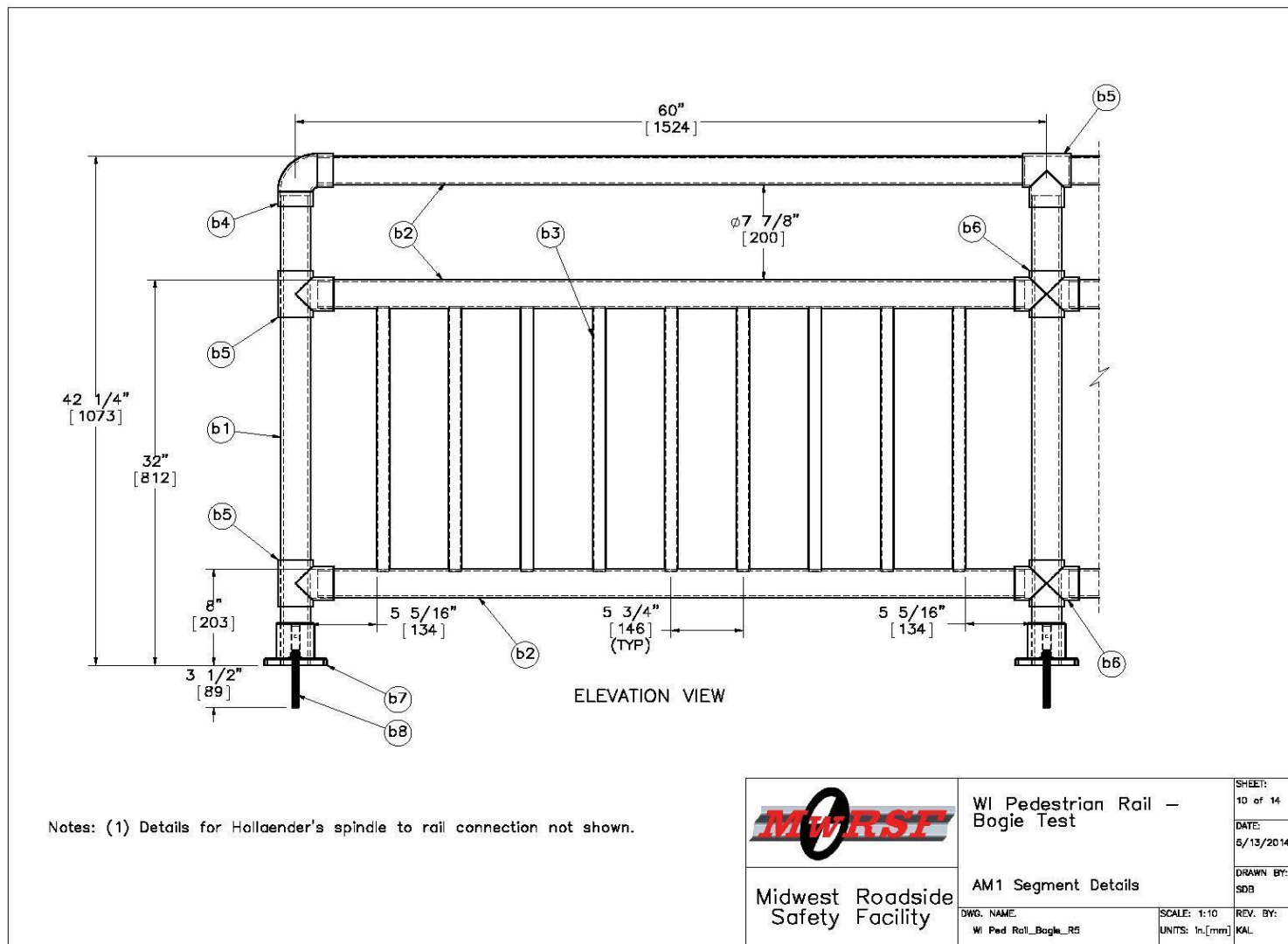


Figure 111. Pedestrian Rail Design AM-1

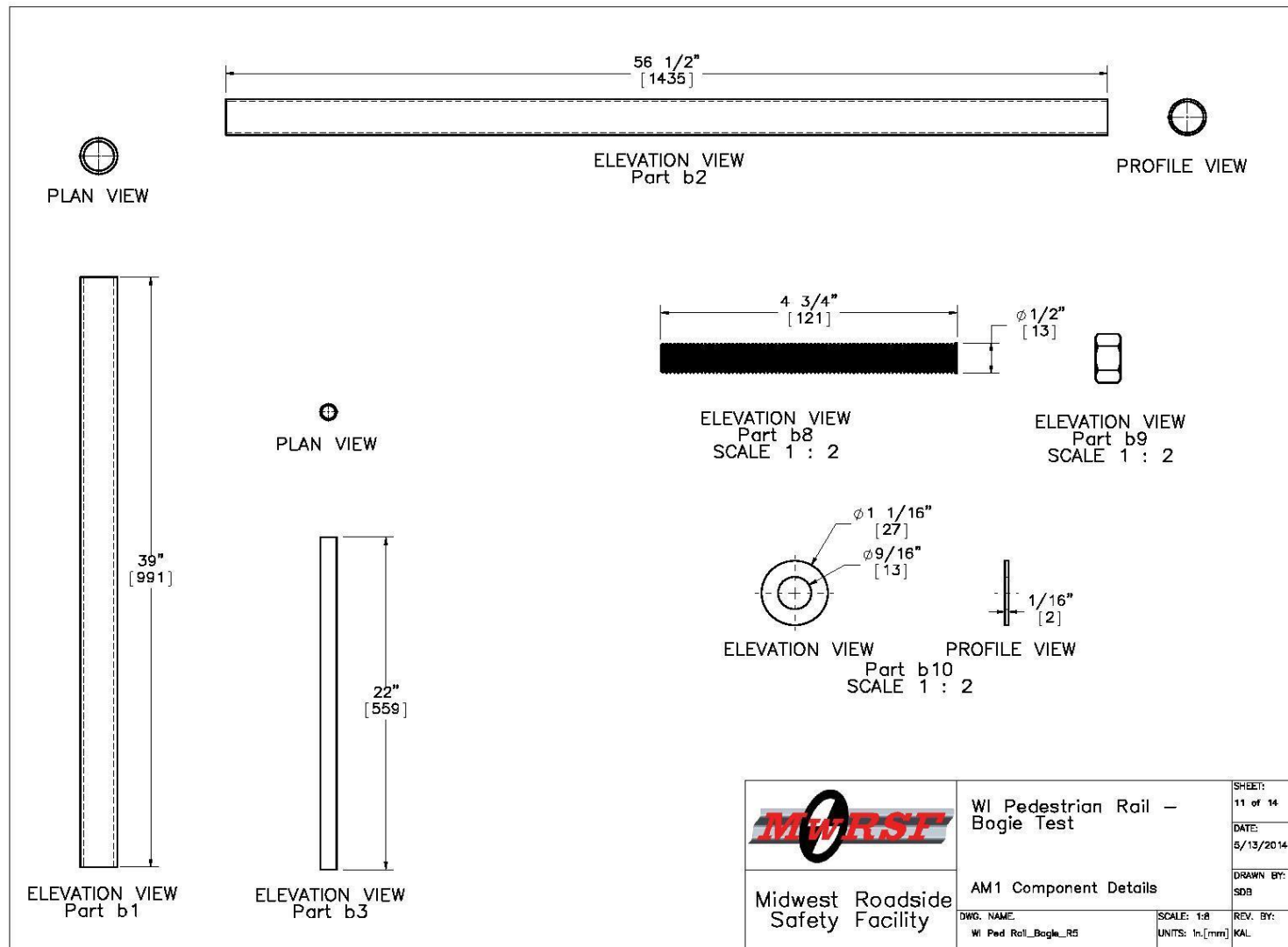


Figure 112. Pedestrian Rail Design AM-1

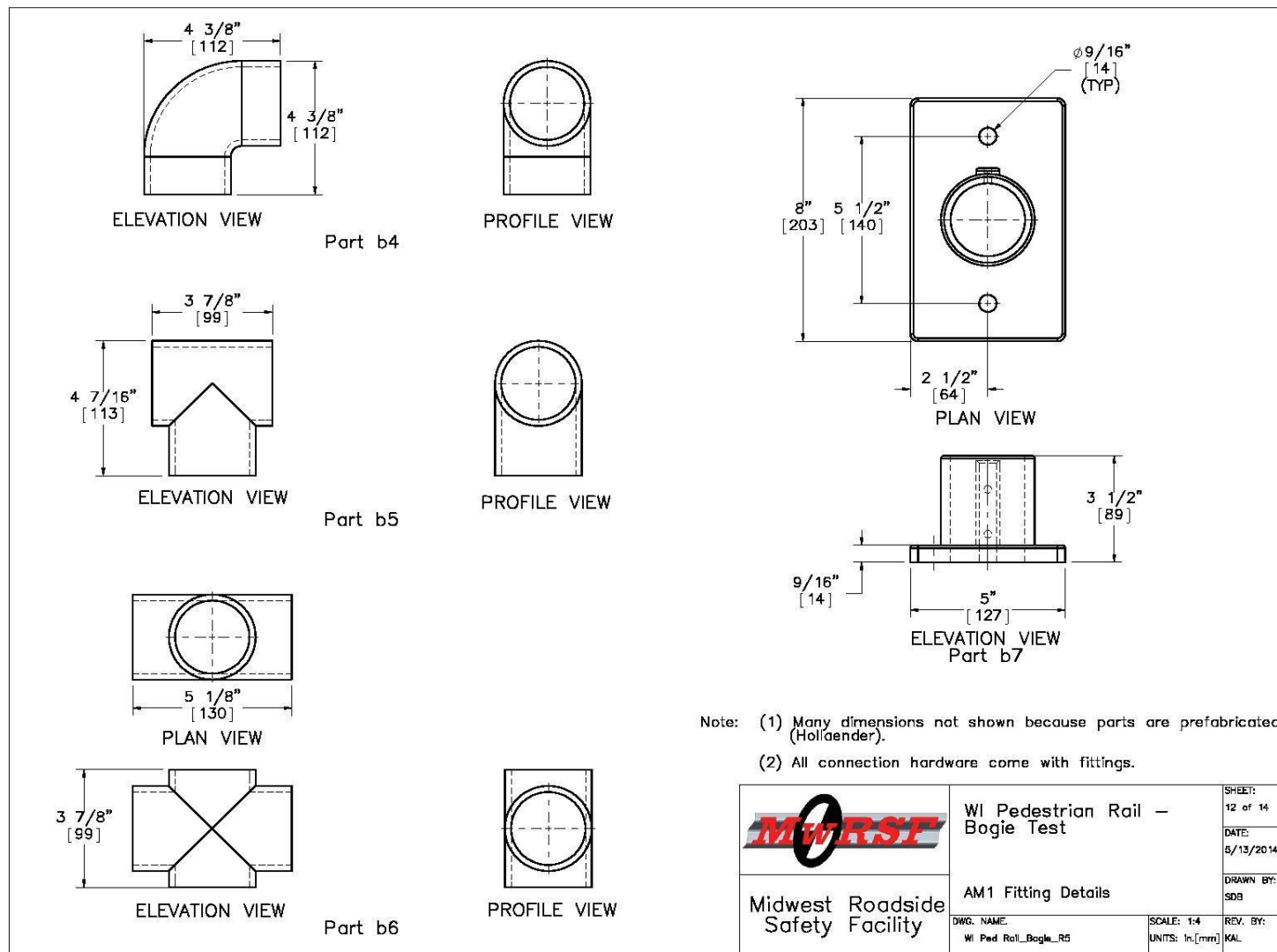


Figure 113. Pedestrian Rail Design AM-1

Item No.	QTY.	Description	Material Spec
a1	8	2"x4"x1/4" [51x102x6] Aluminum Post, 43" [1092] long	6061-T6
a2	8	Aluminum Post Cap – 1/8" [3] Plate	6061-T6
a3	8	Aluminum Post Base	6061-T6
d1	12	2"x2"x1/8" [51x51x3] Aluminum Rail – 60" [1524] long	6061-T6
d2	36	1/2"x1/2" [13x13] Square Aluminum Spindle – 24 1/4" [616] long	6061-T6
d3	16	3/8" [10] Dia. Threaded Rod	ASTM A193 Grade B7 Galv.
d4	16	3/8" [10] Dia. Nut	ASTM A194 Grade 8M Galv.
d5	16	3/8" [10] Dia. SAE Flat Washer	ASTM F436 Type 1 Galv.
d6	—	Epoxy	Powers Fasteners AC100+ Gold Minimum bond strength = 1,450 psi [10.0 MPa]
Item No.	QTY.	Description	Material Spec
c1	8	2"x3"x1/8" [51x76x3] Aluminum Post, 43" [1092] long	6061-T6
c2	8	Aluminum Post Cap – 1/8" [3] Plate	6061-T6
c3	8	Aluminum Post Base	6061-T6
c4	8	1/4" [6] Dia., 3" [76] Long Bolt and Nut	Bolt ASTM A193 Grade B8M Class 2, Nut ASTM A194 Grade 8M
d1	12	2"x2"x1/8" [51x51x3] Aluminum Rail – 60" [1524] long	6061-T6
d2	36	1/2"x1/2" [13x13] Square Aluminum Spindle – 24 1/4" [616] long	6061-T6
d3	16	3/8" [10] Dia. Threaded Rod	ASTM A193 Grade B7 Galv.
d4	16	3/8" [10] Dia. Nut	ASTM A194 Grade 8M Galv.
d5	16	3/8" [10] Dia. SAE Flat Washer	ASTM F436 Type 1 Galv.
d6	—	Epoxy	Powers Fasteners AC100+ Gold Minimum bond strength = 1,450 psi [10.0 MPa]
			 Midwest Roadside Safety Facility
			WI Pedestrian Rail – Bogie Test AW2–A and AW2–C Bill of Materials
			SHEET: 13 of 14 DATE: 5/13/2014 DRAWN BY: SDB REV. BY: KAL
			DWG. NAME: WI Ped Rail_Bogie_RS SCALE: None UNITS: In./mm

Figure 114. Bill of Materials, Pedestrian Rail Designs AW2-A and AW2-C

Item No.	QTY.	Description	Material Specification	Hollaender Part No.
b1	6	2" [51] Dia. Schedule 80 post, 39" [991] long	6061-T6 Aluminum	99231
b2	12	2" [51] Dia. Schedule 40 rail, 56 1/2" [1435] long	6061-T6 Aluminum	98221
b3	36	3/4" [19] Dia. Schedule 10 picket, 22" [559] long	6063-T6 Aluminum	—
b4	4	No. 3 Elbow (2" [51])	6061-T6 Aluminum	09020
b5	10	No. 5 Tee (2" [51])	6061-T6 Aluminum	09040
b6	4	No. 7 Cross (2" [51])	6061-T6 Aluminum	09090
b7	6	No. 48 Heavy-Duty Base Flange (2" [51], 2-hole)	6061-T6 Aluminum	28200
b8	12	1/2" [13] Dia. Threaded Rod	ASTM A193 Grade B7 Galv.	—
b9	12	1/2" [13] Dia. Nut	ASTM A194 Grade 8M Galv.	—
b10	12	1/2" [13] Dia. SAE Flat Washer	ASTM F436 Type 1 Galv.	—
b11	—	Epoxy	Powers Fasteners AC100+ Gold Minimum bond strength = 1,450 psi [10.0 MPa]	—

Notes: (1) All aluminum fittings are prefabricated components from Hollaender Speed-Rail (www.hollaender.com/?page=speedrail).

(2) All aluminum pipe properties and dimensions from Hollaender.

(3) Order as Hollaender picket rail system.

(4) Pickets (Part b3) may be substituted for comparable aluminum tube.


 Midwest Roadside Safety Facility	WI Pedestrian Rail — Bogie Test		SHEET: 14 of 14
	AM1 Bill of Materials		DATE: 5/13/2014
DWG. NAME: WI Ped Rail_Bogie_R5		SCALE: NONE UNITS: in.[mm]	DRAWN BY: SDB
			REV. BY: KAL

Figure 115. Bill of Materials, Continued, Pedestrian Rail Design AM-1

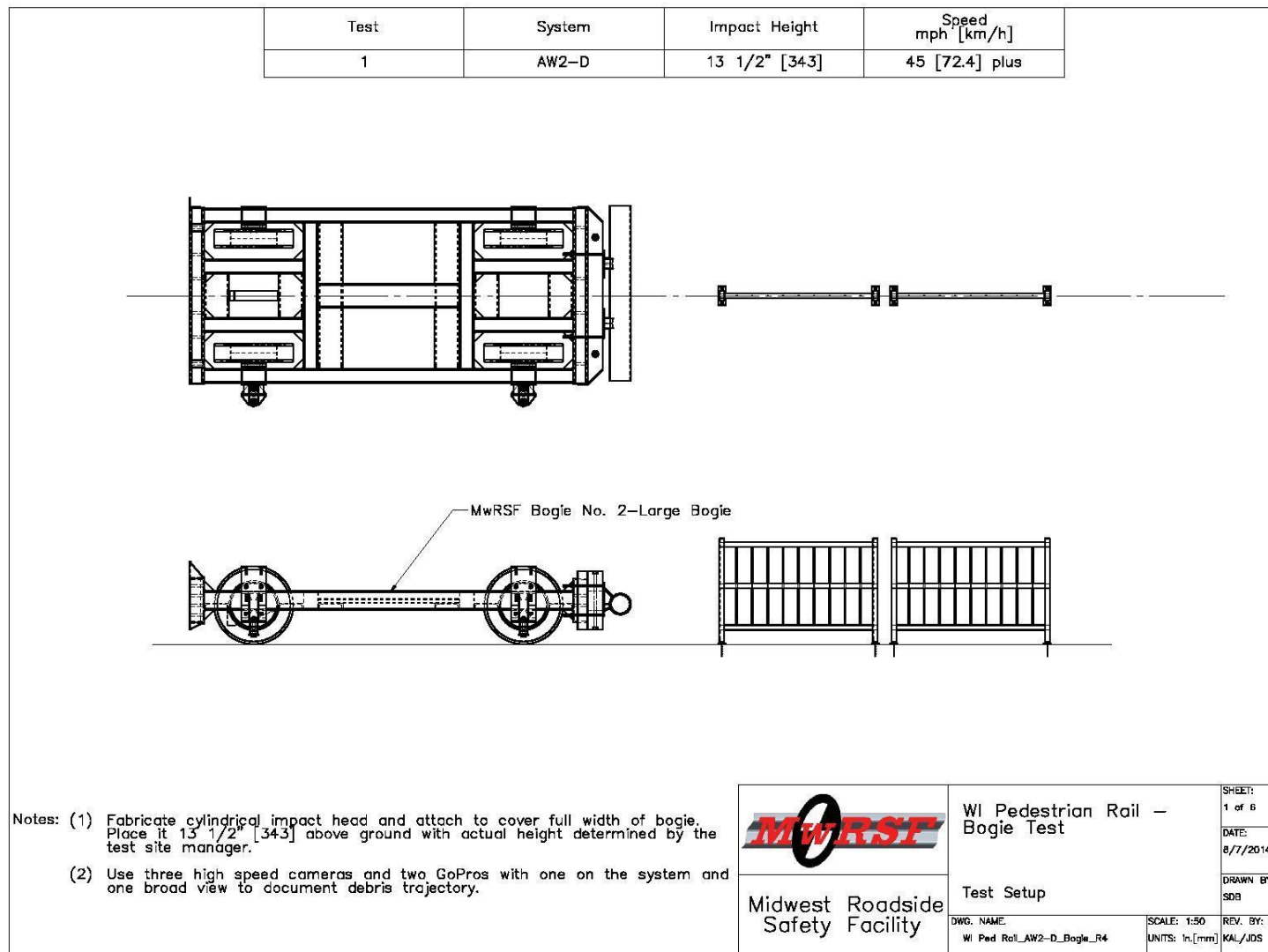


Figure 116. Pedestrian Rail Test Setup, Design AW2-D

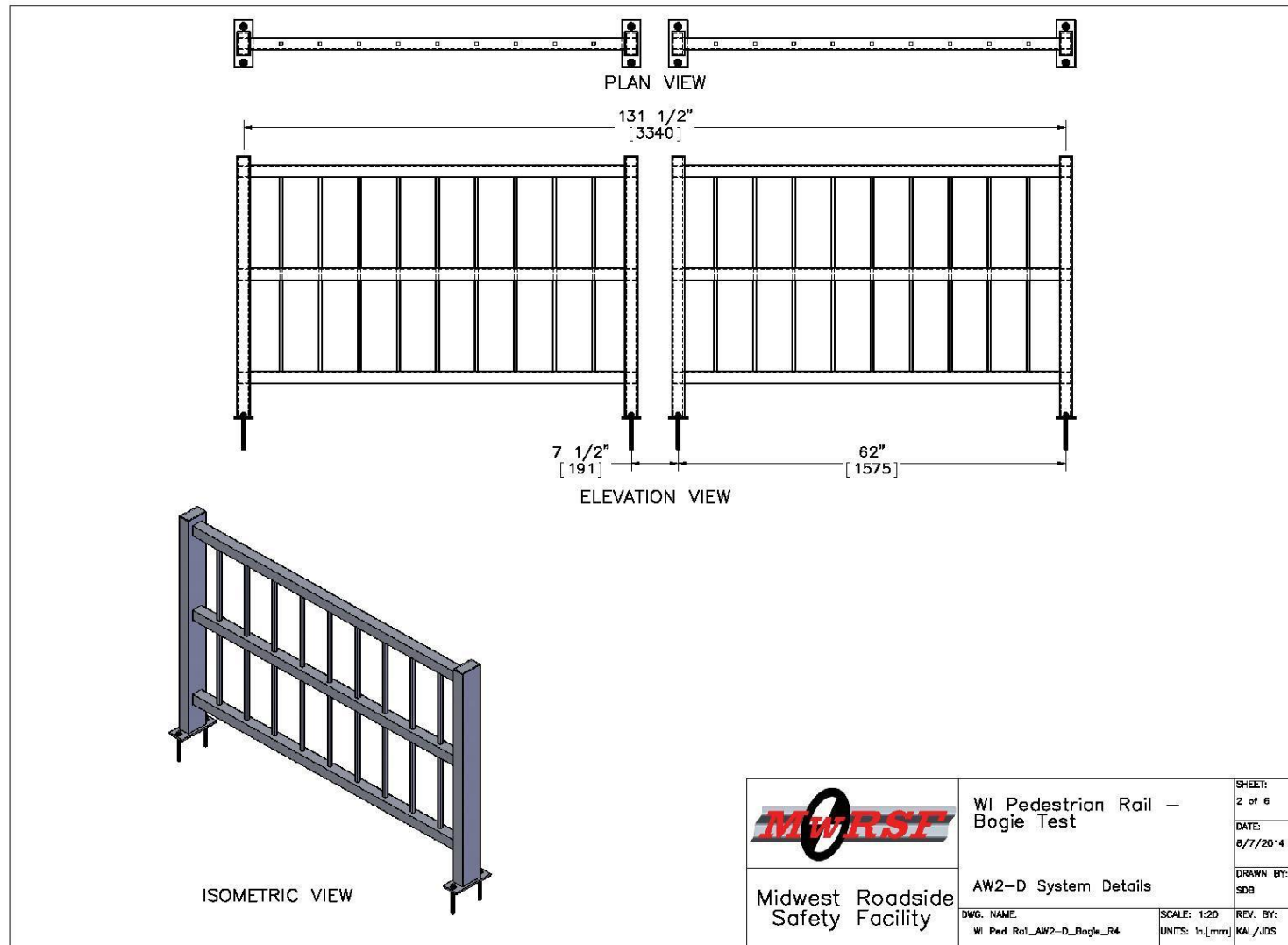


Figure 117. Pedestrian Rail Design AW2-D

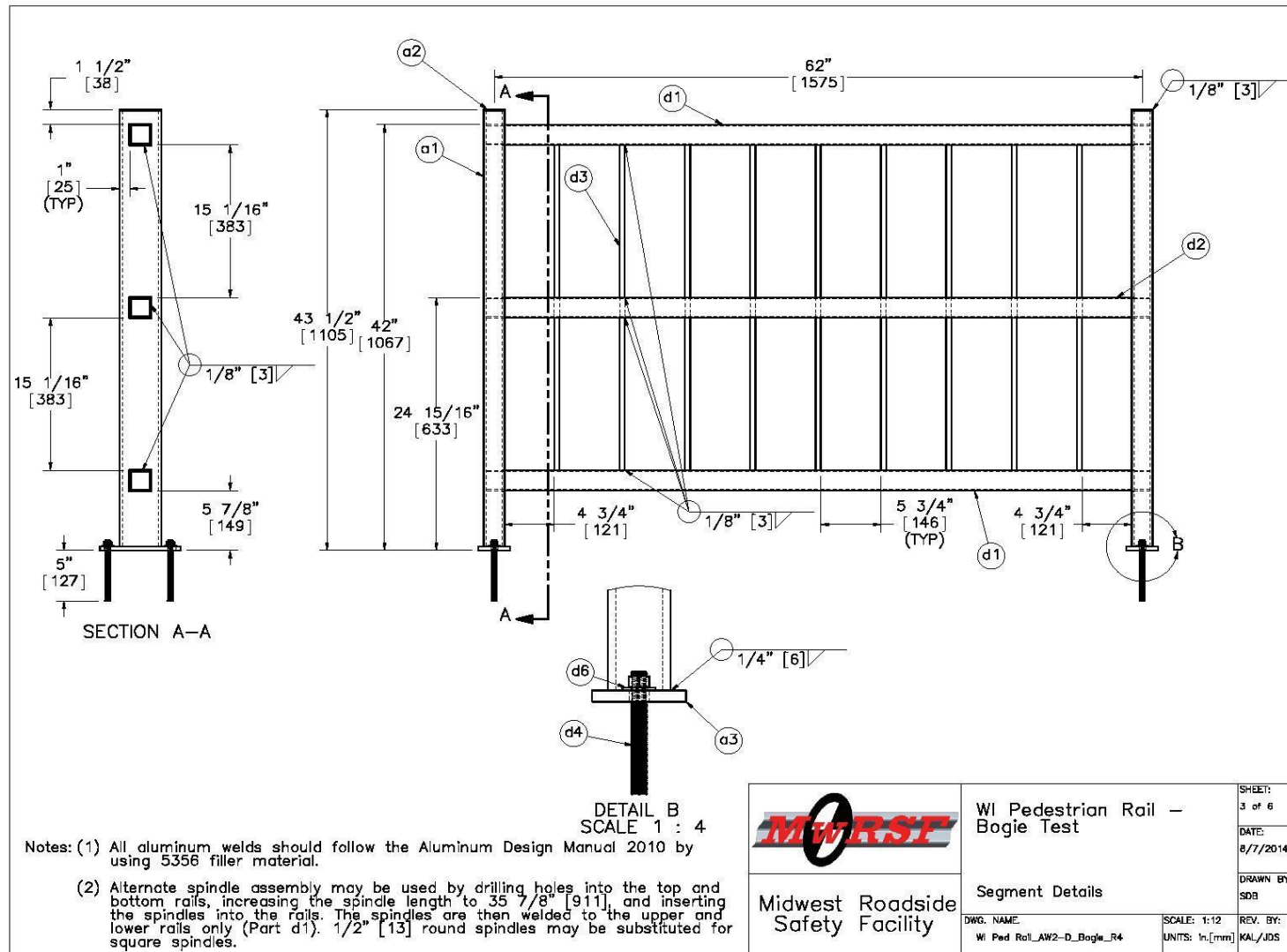


Figure 118. Pedestrian Rail Design AW2-D

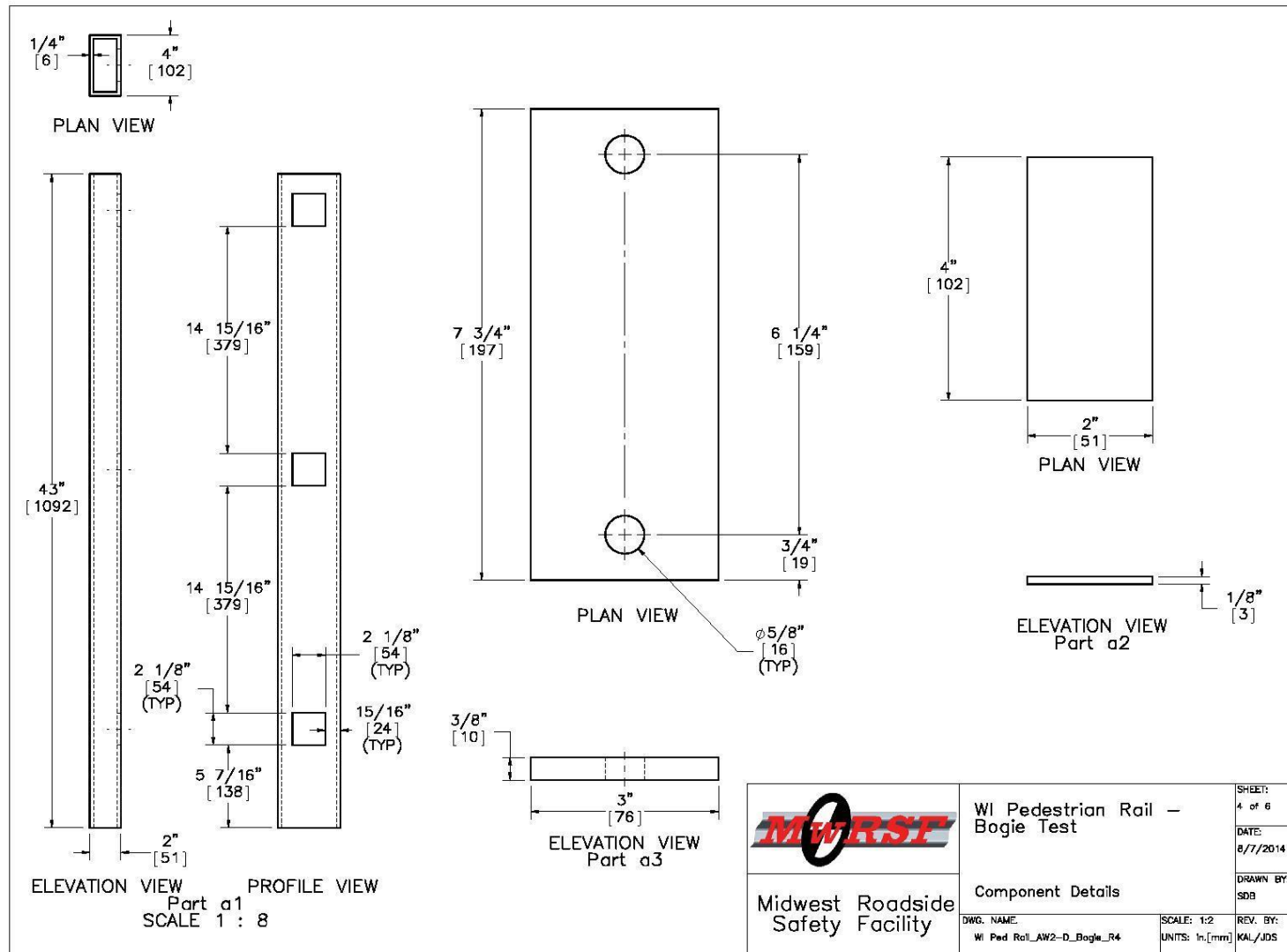


Figure 119. Pedestrian Rail Design AW2-D

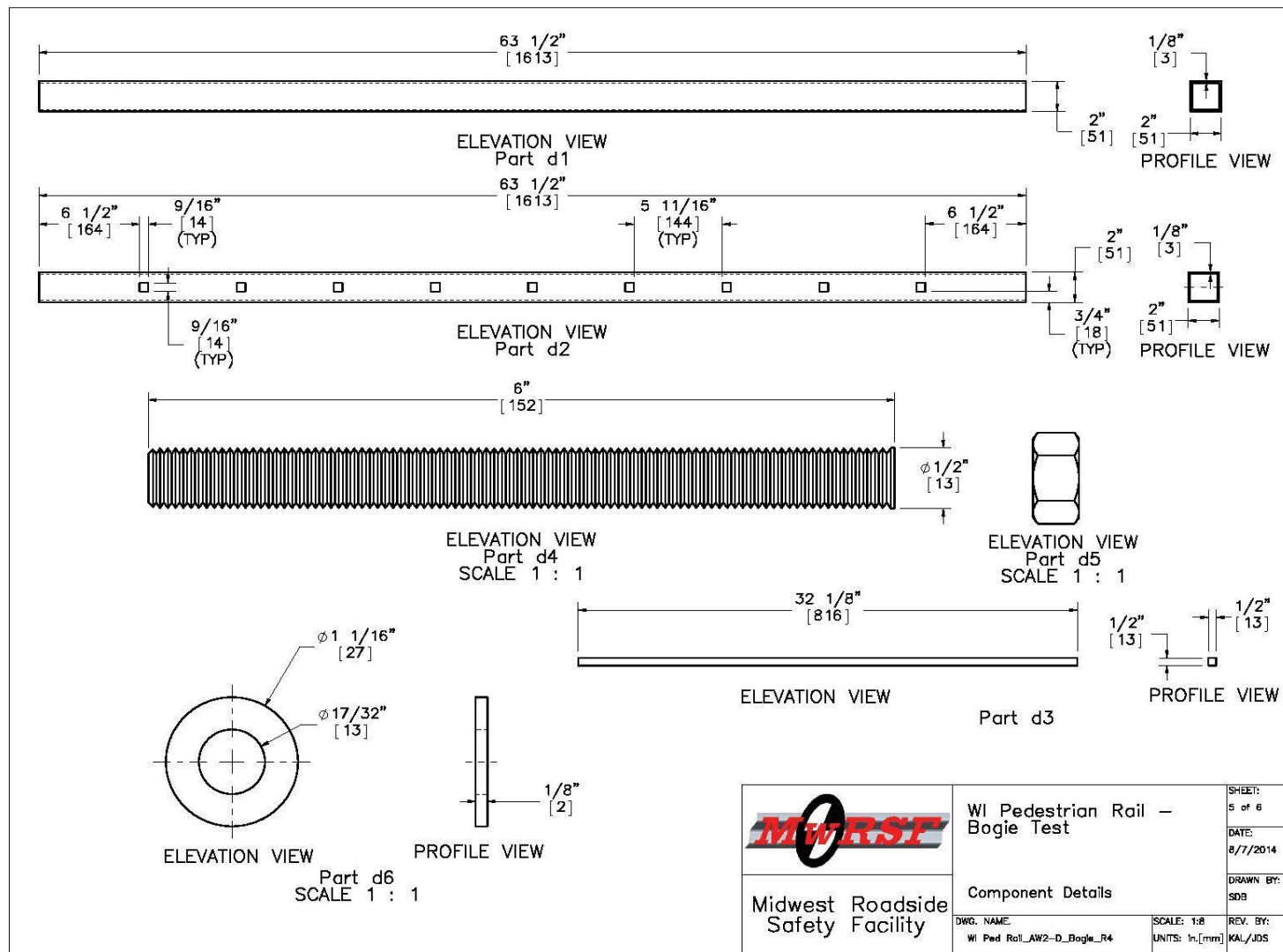


Figure 120. Pedestrian Rail Design AW2-D


Item No.	QTY.	Description	Material Spec
a1	4	2"x4"x1/4" [51x102x6] Aluminum Post, 43" [1092] long	6061-T6
a2	4	Aluminum Post Cap – 1/8" [3] Plate	6061-T6
a3	4	Aluminum Post Base	6061-T6
d1	4	2"x2"x1/8" [51x51x3] Aluminum Rail – 63 1/2" [1613] long	6061-T6
d2	2	2"x2"x1/8" [51x51x3] Aluminum Rail – 63 1/2" [1613] long with holes	6061-T6
d3	18	1/2"x1/2" [13x13] Square Aluminum Spindle – 32 1/8" [816] long	6061-T6
d4	8	1/2" [13] Dia. Steel Threaded Rod	ASTM A193 Grade B7 Galv.
d5	8	1/2" [13] Dia. Steel Nut	ASTM A194 Grade 8M Galv.
d6	8	1/2" [13] Dia. Steel SAE Flat Washer	ASTM F436 Type 1 Galv.
d7	–	Epoxy	Powers Fasteners AC100+ Gold Minimum bond strength = 1,450 psi [10.0 MPa]
<div>  <div> <div>WI Pedestrian Rail – Bogie Test</div> <div>Bill of Materials</div> </div> <div> <div>Midwest Roadside Safety Facility</div> <div> <div>DWG. NAME: WI Ped Rail_AW2-D_Bogie_R4</div> <div>SCALE: None UNITS: In./mm</div> <div>REV. BY: KAL/JDS</div> </div> </div> <div> <div>SHEET: 6 of 6</div> <div>DATE: 8/7/2014</div> <div>DRAWN BY: SDB</div> </div> </div>			

Figure 121. Bill of Materials, Pedestrian Rail Design AW2-D

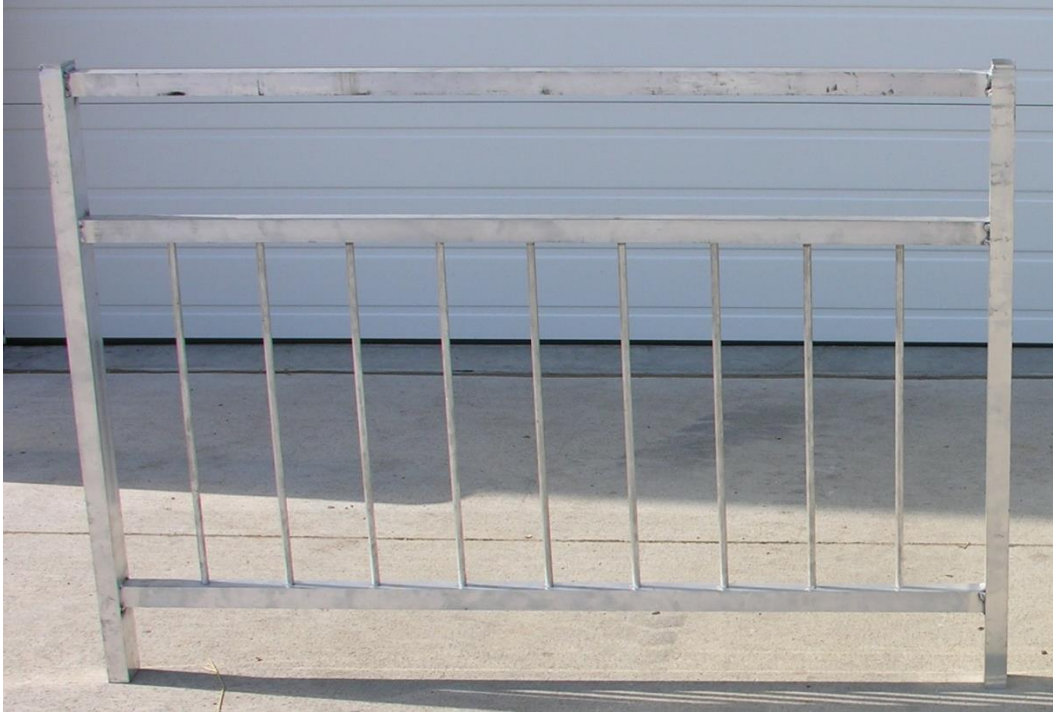


Figure 122. Pedestrian Rail AW2-A



Figure 123. Pedestrian Rail AW2-C



Figure 124. Pedestrian Rail AM-1

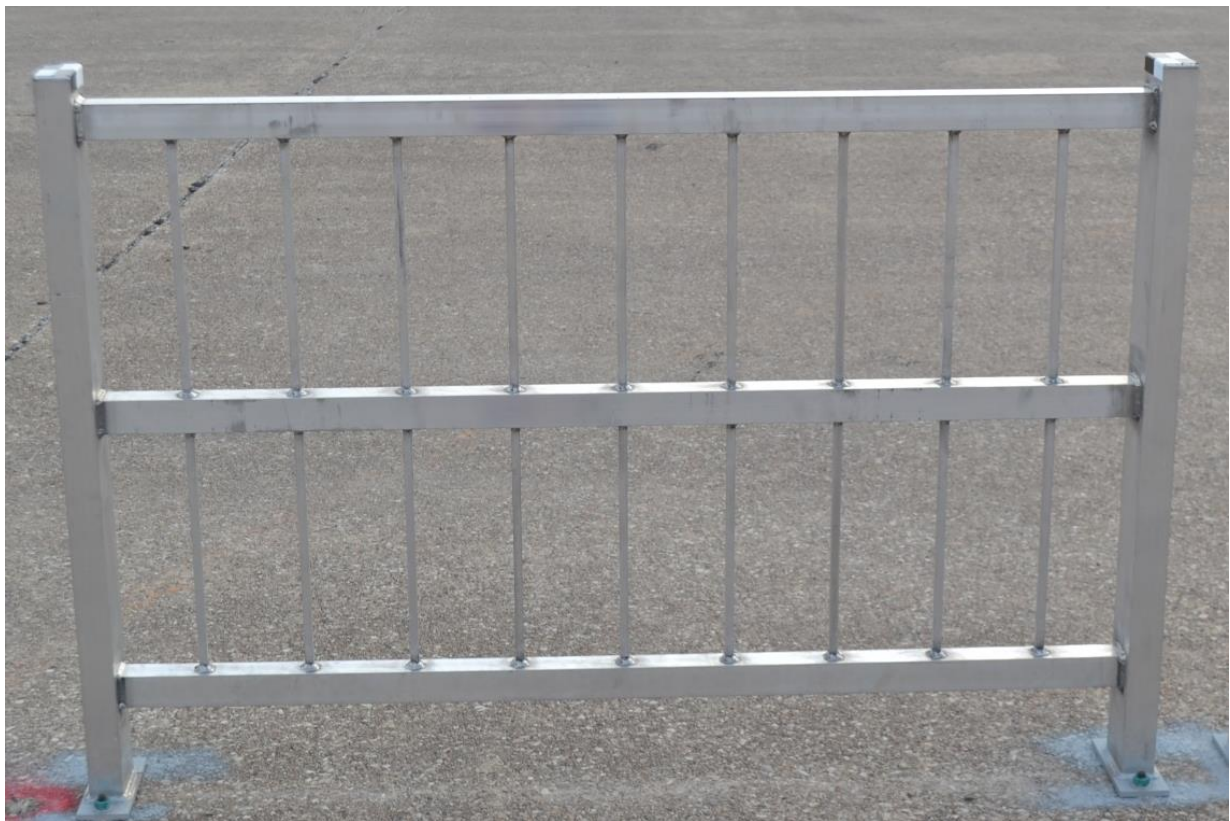


Figure 125. Pedestrian Rail AW2-D

8 COMPONENT TESTING CONDITIONS

8.1 Purpose

According to TL-2 of MASH, longitudinal channelizing systems must be subjected to two full-scale vehicle crash tests which include impacts with both a passenger car and a pickup truck at a nominal speed of 44 mph (70 km/h) and a critical angle between 0 and 25 degrees. In order to evaluate the four pedestrian rail concepts, bogie test were undertaken and impacting similar to the MASH TL-2 test conditions in lieu of full-scale crash testing. The bogie was configured with a bumper similar in height and shape to the 1100C small car to evaluate how the pedestrian rails fracture upon impact with a low impact height. Ideal impact performance characteristics for the pedestrian rails included: clean and consistent component fracture, no anchor damage, component trajectory away from the windshield and undercarriage, and the potential for no vehicle instability and low occupant risk. Although the bogie was not configured with a windshield, floorpan, or body panels, the trajectory of components was evaluated to determine if the potential for occupant compartment or windshield deformation or penetration existed.

8.2 Scope

Four test runs, consisting of seven bogie tests were conducted on four pedestrian rail concepts, as described in Section 7.4. Each concept was mounted to the existing concrete tarmac and was configured as a two-panel system. The target impact conditions included a speed of 45 mph (72 km/h) and two different impact orientations: 25 degrees and within the spindle region of the first panel, or 0 degrees for an end-on impact. The fourth concept (AW2-D) was only evaluated in the end-on orientation, due to its similarity to the first concept (AW2-A). The systems were impacted 13 $\frac{5}{8}$ in. (346 mm) above the groundline. The seven crash tests are

summarized in Table 10. The test setups are shown in Figure 102 through Figure 121. Photographs from a typical test set up are shown in Figure 126. Material specifications, mill certifications, and certificates of conformity for the pedestrian rail concepts are shown in Appendix D.



Figure 126. Typical Bogie Testing Setup

Table 10. Bogie Testing Matrix

Run No.	Test No.	Design Concept	Target Impact Velocity mph (km/h)	Impact Angle (deg)
WIPR-1	WIPR-1-1	AW2-A	45 (72)	25
	WIPR-1-2	AW2-A	45 (72)	0 (end-on)
WIPR-2	WIPR-2-1	AW2-C	45 (72)	25
	WIPR-2-2	AW2-C	45 (72)	0 (end-on)
WIPR-3	WIPR-3-1	AM-1	45 (72)	25
	WIPR-3-2	AM-1	45 (72)	0 (end-on)
WIPR-4	WIPR-4	AW2-D	45 (72)	0 (end-on)

8.3 Test Facility

Physical testing of the pedestrian rail concepts was conducted at the MwRSF Proving Grounds, which is located at the Lincoln Air Park on the northwest side of the Lincoln Municipal Airport in Lincoln, Nebraska. The facility is approximately 5 miles (8 km) northwest from the University of Nebraska-Lincoln's city campus.

8.4 Equipment and Instrumentation

Several pieces of equipment and instrumentation were utilized to collect and record data during the dynamic bogie tests, including a bogie vehicle, accelerometers, a retroreflective speed trap, high-speed and standard-speed digital video, and still cameras.

8.4.1 Bogie Vehicle

A rigid-frame bogie vehicle was used to impact the rail prototypes. A variable-height, detachable impact head was used in the testing program. The bogie head was constructed of 6-in. (152-mm) diameter, 1/4-in. (13-mm) thick standard steel pipe. The impact head was bolted to the bogie vehicle, creating a rigid frame with an impact height of 13⁵/₈ in. (346 mm). The bogie with the impact head is shown in Figure 127. The bogie weight, including the mountable impact head and accelerometers, was 5,166 lb (2,343 kg).



Figure 127. Rigid-Frame Bogie Vehicle on Guidance Track

A pickup truck with a reverse cable tow system was used to propel the bogie to a target impact speed of 45 mph (72 km/h). When the bogie approached the end of the guidance system, it was released from the tow cable, allowing it to be free-rolling when it impacted the system. A remote-control braking system was installed on the bogie, allowing it to be brought safely to rest after the test.

8.4.2 Accelerometers

No accelerometer readings were recorded for run nos. WIPR-1 or WIPR-2. For run nos. WIPR-3 and WIPR-4, an accelerometer system was mounted on the bogie vehicle near its center of gravity to measure the acceleration in the longitudinal, lateral, and vertical directions. However, only the longitudinal acceleration data was processed and reported.

The SLICE-2 unit was a modular data acquisition system manufactured by Diversified Technical Systems, Inc. (DTS) of Seal Beach, California. The acceleration sensors were mounted inside the body of a custom built SLICE 6DX event data recorder and recorded data at 10,000 Hz to the onboard microprocessor. The SLICE 6DX was configured with 7 GB of non-volatile flash

memory, a range of ± 500 g's, a sample rate of 10,000 Hz, and a 1,650 Hz (CFC 1000) anti-aliasing filter. The "SLICEWare" computer software program and a customized Microsoft Excel worksheet were used to analyze and plot the accelerometer data.

8.4.3 Retroreflective Optic Speed Trap

The retroreflective optic speed trap was used to determine the speed of the bogie vehicle before impact. Five retroreflective targets, spaced at approximately 18-in. (457-mm) intervals, were applied to the side of the vehicle. When the emitted beam of light was reflected by the targets and returned to the Emitter/Receiver, a signal was sent to the data acquisition computer, recording at 10,000 Hz, as well as the external LED box activating the LED flashes. The speed was then calculated using the spacing between the retroreflective targets and the time between the signals. LED lights and high-speed digital video analysis are only used as a backup in the event that vehicle speeds cannot be determined from the electronic data.

8.4.4 Digital Photography

No photographic documentation was collected for run no. WIPR-1. For run nos. WIPR-2 and WIPR-3, three AOS high-speed digital video cameras, four GoPro digital video cameras, and one JVC digital camera were used to document each test. For run no. WIPR-4, two AOS high-speed digital video cameras, three GoPro digital video cameras, and one JVC digital camera were used to document the test. The AOS high-speed cameras had a frame rate of 500 frames per second, the GoPro video cameras had a frame rate of 120 frames per second, and the JVC digital video cameras had a frame rate of 29.97 frames per second. The cameras were placed laterally away from the prototype pedestrian rails, with a view perpendicular to the bogie's direction of travel. A Nikon D50 digital still camera was used to document pre- and post-test conditions for all tests.

8.5 Data Processing

The electronic accelerometer data obtained in dynamic testing was filtered using the SAE Class 60 Butterworth filter conforming to the SAE J211/1 specifications [43]. The pertinent acceleration signal was extracted from the bulk of the data signals. The processed acceleration data was then multiplied by the mass of the bogie to get the impact force using Newton's Second Law. Next, the acceleration trace was integrated to find the change in velocity versus time. The initial velocity of the bogie, as calculated from the retroreflective optical speed trap data, was then used to determine the bogie velocity as a function of time, using the change in velocity data. The calculated velocity trace was integrated to find the bogie's displacement. This displacement was also used as the system displacement. Combining the previous results, a force versus deflection curve was plotted for each test. Finally, integration of the force versus deflection curve provided the energy versus deflection curve for each test.

9 DYNAMIC BOGIE TESTING RESULTS AND DISCUSSION

9.1 Run No. WIPR-1 (Test Nos. WIPR-1-1 and WIPR-1-2)

Run no. WIPR-1 was conducted during a practice run when the brakes malfunctioned. This run consisted of test nos. WIPR-1-1 and WIPR-1-2 occurring successively. For test no. WIPR-1-1, the bogie impacted the pedestrian rail concept AW2-A oriented at an angle to the vehicle, at an unknown speed and an angle of 25 degrees. For test no. WIPR-1-2, the bogie then impacted the pedestrian rail concept AW2-A oriented end-on to the vehicle, at an unknown speed and an angle of 0 degrees. These two tests were conducted without collecting videos, speed trap data, or accelerometer data. The systems prior to impact are shown in Figures 128 and 129.

Damage to the systems impacted during test nos. WIPR-1-1 and WIPR-1-2 is shown in Figures 130 through 133. The systems impacted during test nos. WIPR-1-1 and WIPR-1-2 encountered damage to both the first and second panels.

The damage to the first panel in test no. WIPR-1-1 consisted of:

- fractured welds between (1) downstream post and its baseplate (2) bottom and middle horizontal rails and the downstream post, and (3) top rail and both posts;
- downstream post baseplate bent due to prying;
- upstream post twisted and bent downstream;
- spindles detached from the horizontal rails; and
- all threaded anchors deformed slightly.

The damage to the second panel in test no. WIPR-1-1 consisted of:

- fractured welds between both posts and their baseplates,
- partially fractured welds between (1) top and middle horizontal rails and both posts and (2) bottom horizontal rail and downstream post,
- both post baseplates bent due to prying, and

- all threaded anchors deformed slightly.

The damage to the first panel in test no. WIPR-1-2 consisted of:

- fractured welds between (1) both posts and their baseplates and (2) all three horizontal rails and both posts,
- both post baseplates bent due to prying,
- upstream post bent above bottom horizontal rail (or at bumper height),
- some spindles detached from middle horizontal rail, and
- all threaded anchors deformed slightly.

The damage to the second panel in test no. WIPR-1-2 consisted of:

- fractured welds between (1) both posts and their baseplates, (2) the middle and bottom horizontal rails and both posts, and (3) the top rail and the downstream post;
- both post baseplates bent due to prying;
- some spindles detached from middle and bottom horizontal rails; and
- all threaded anchors deformed slightly.

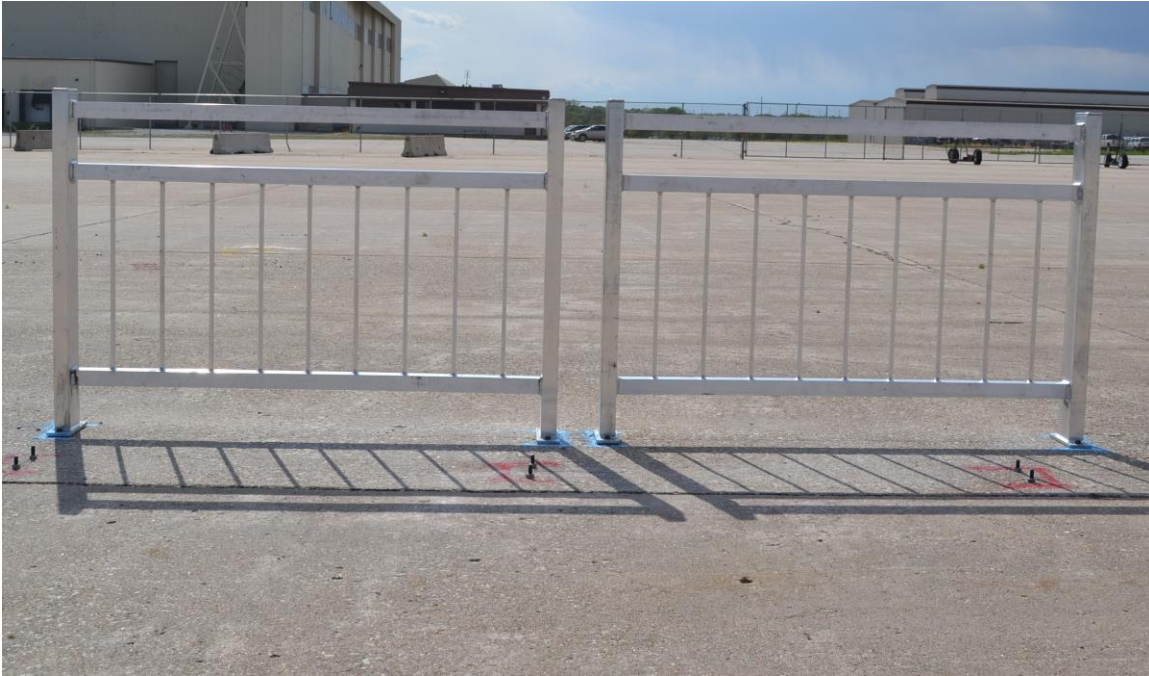


Figure 128. System Panels and Anchor, Run No. WIPR-1

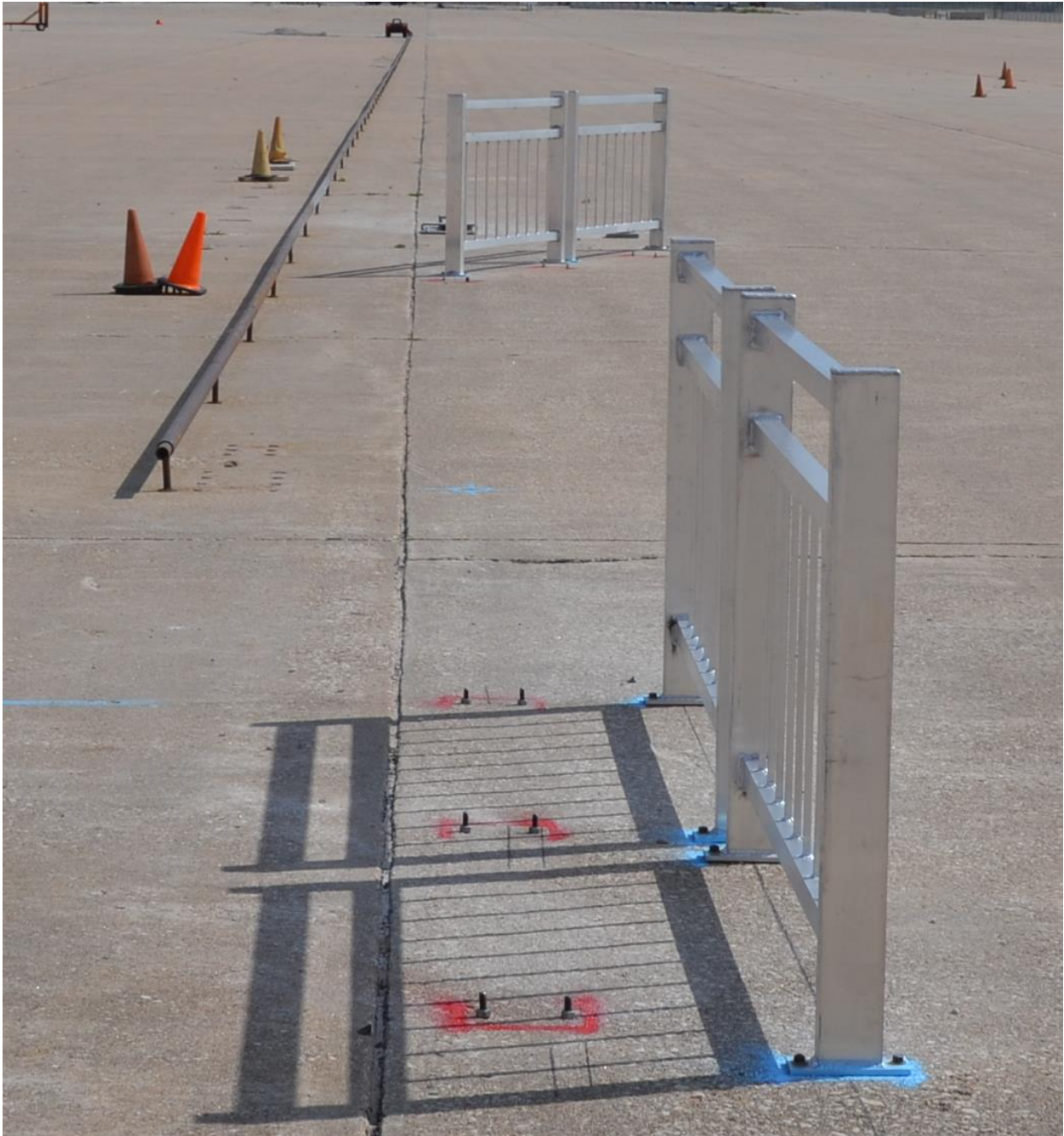


Figure 129. System Installation, Run No. WIPR-1

189

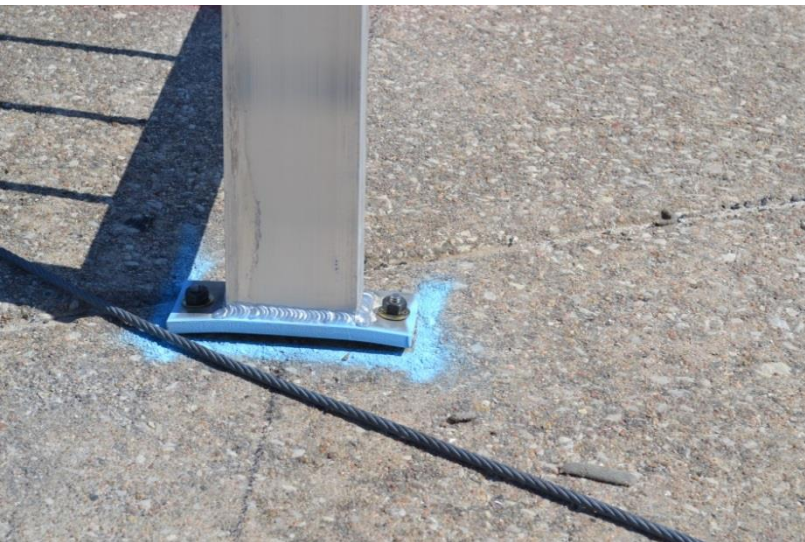


Figure 130. First Panel Damage, Run No. WIPR-1, Test No. WIPR-1-1

190



Figure 131. Second Panel Damage, Run No. WIPR-1, Test No. WIPR-1-1

191

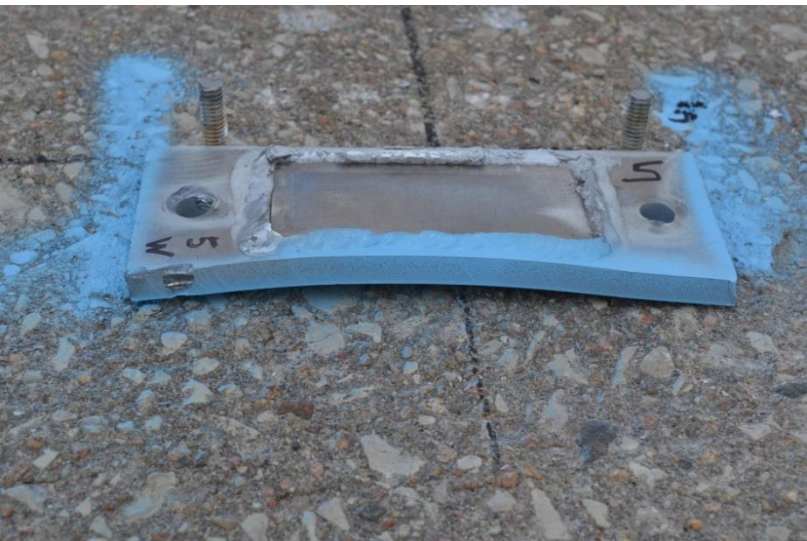


Figure 132. First Panel Damage, Run No. WIPR-1, Test No. WIPR-1-2



Figure 133. Second Panel Damage, Run No. WIPR-1, Test No. WIPR-1-2

9.2 Run No. WIPR-2 (Test Nos. WIPR-2-1 and WIPR-2-2)

Run no. WIPR-2 consisted of two tests conducted successively, with test no. WIPR-2-1 followed by test no. WIPR-2-2. During test no. WIPR-2-1, the bogie, traveling at a speed of 50.7 mph (81.6 km/h), impacted the pedestrian rail concept AW2-C oriented at a 25-degree angle to the vehicle. For test no. WIPR-2-2, the bogie then impacted the pedestrian rail concept AW2-C at a speed of 48.5 mph (78.1 km/h), with the rail oriented end-on to the vehicle (i.e., 0 degrees). The systems prior to impact are shown in Figures 134 and 135.

Time-sequential photographs are shown in Figures 136 and 137. Damage to system nos. WIPR-2-1 and WIPR-2-2 is shown in Figures 138 through 141. The systems impacted during test nos. WIPR-2-1 and WIPR-2-2 encountered damage to both the first and second panels.

The damage to the first panel in test no. WIPR-2-1 consisted of:

- fractured welds between downstream post socket and its baseplate,
- downstream post sheared below middle horizontal rail,
- upstream post bent downstream at its base,
- all three horizontal rails bent at upstream post,
- some spindles were deformed and some detached from horizontal rails, and
- all threaded anchors deformed slightly.

The damage to the second panel in test no. WIPR-2-1 consisted of:

- fractured welds between both post sockets and their baseplates,
- upstream post bent above bottom horizontal rail,
- downstream post bent at middle and bottom horizontal rails,
- bottom horizontal rail bent, and
- some spindles deformed.

The damage to the first panel in test no. WIPR-2-2 consisted of:

- fractured welds between (1) both post sockets and their baseplates and (2) bottom horizontal rail and both posts,
- upstream post bent and fractured below middle horizontal rail,
- downstream post fractured between middle and bottom horizontal rails, and
- some spindles detached from horizontal rails and encountered deformations.

The damage to the second panel in test no. WIPR-2-2 consisted of:

- fractured welds between (1) downstream post socket and its baseplate, (2) top horizontal rail and upstream post, (3) middle horizontal rail and downstream post, and (4) the bottom horizontal rail and both posts;
- upstream post socket fractured and tore;
- upstream post bent above bottom horizontal rail (at bumper height) and tore below bottom horizontal rail; and
- downstream post bent below bottom horizontal rail.

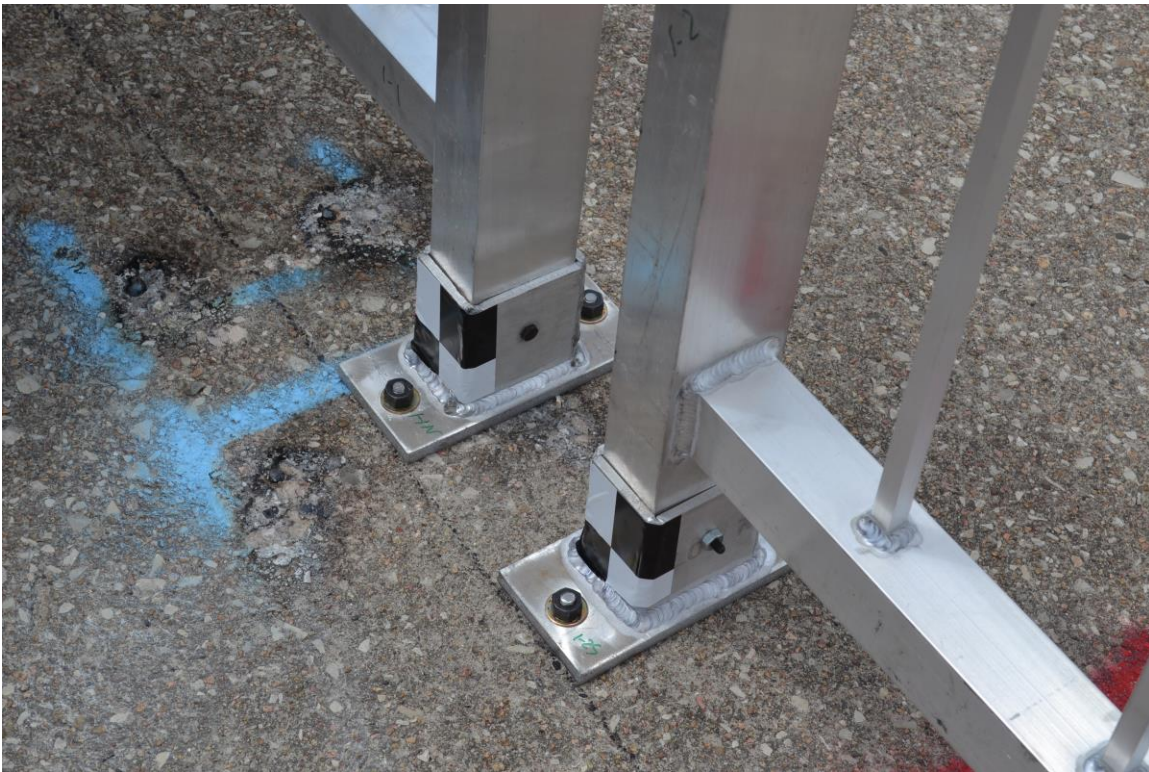
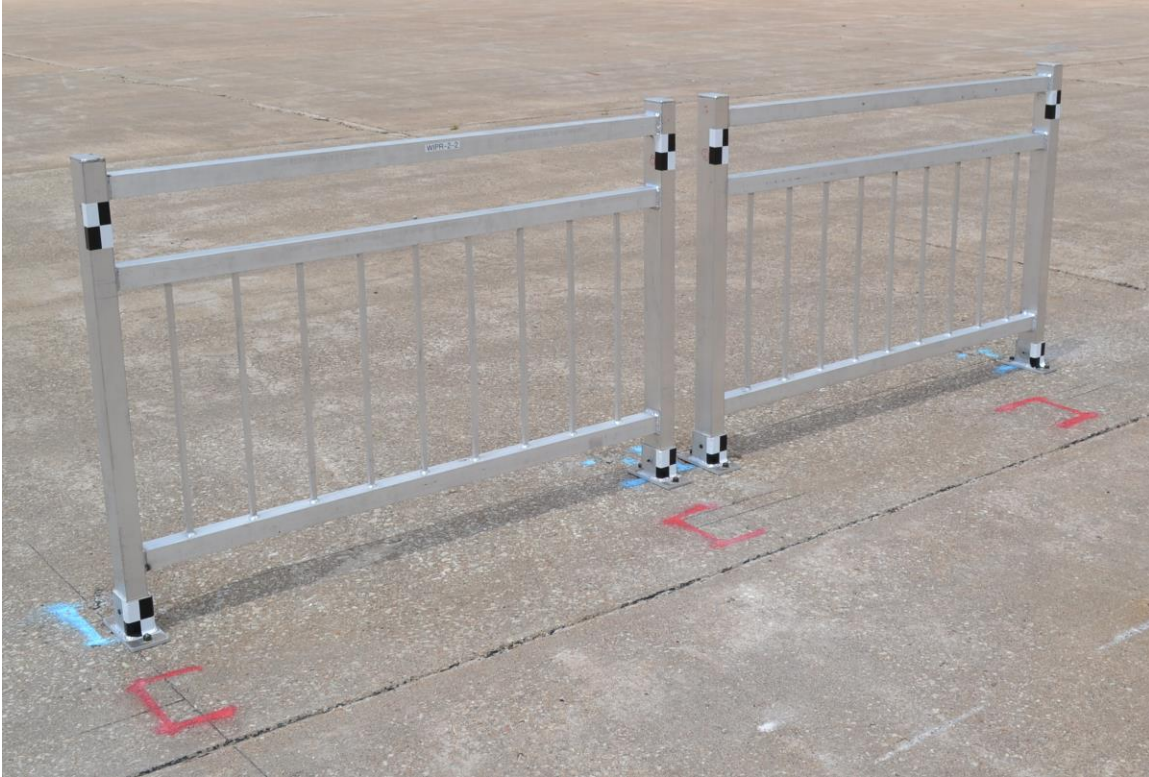


Figure 134. System Panels and Anchors, Run No. WIPR-2



Figure 135. System Installation, Run No. WIPR-2

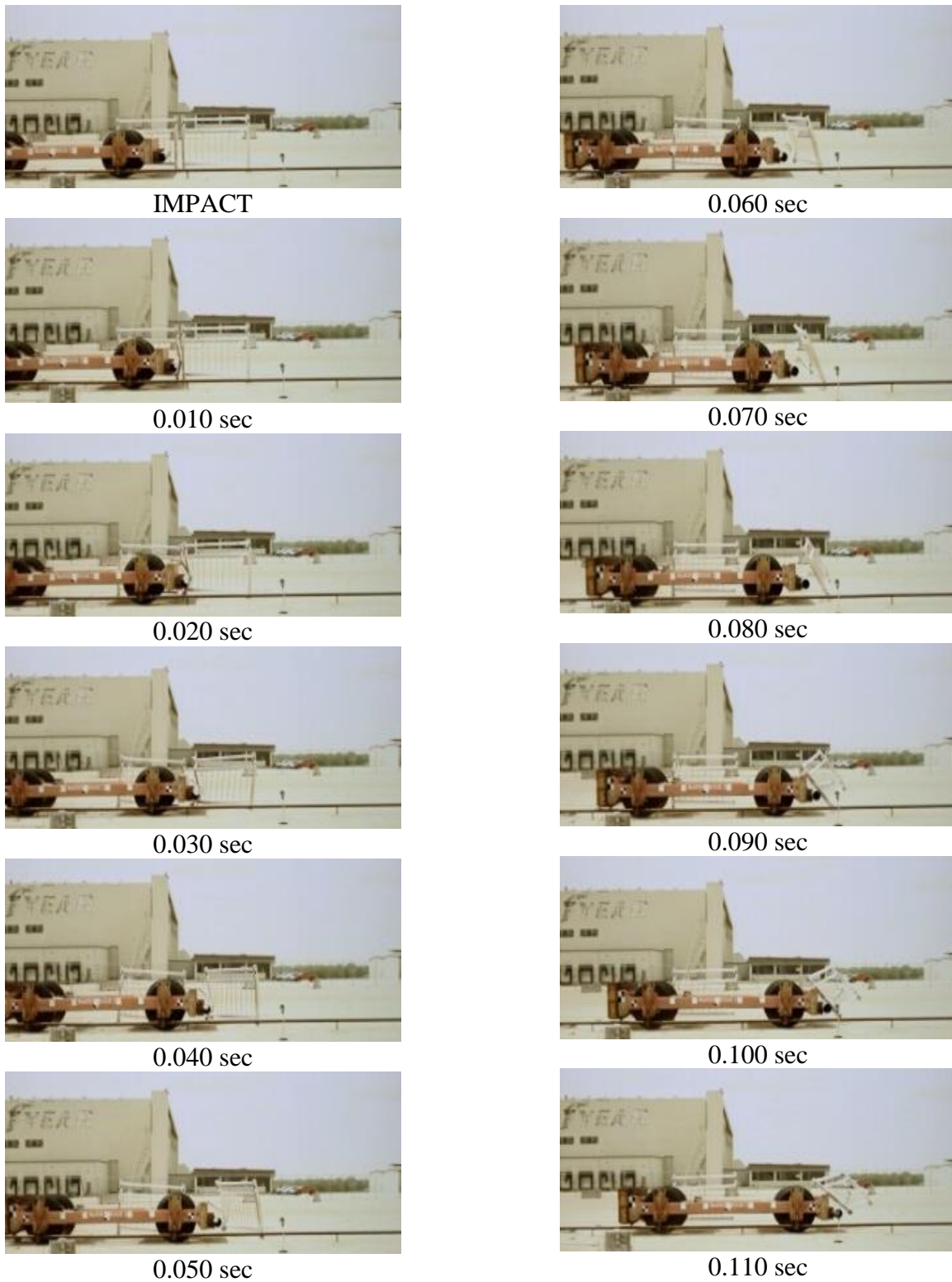


Figure 136. Time-Sequential Photographs, Run No. WIPR-2, Test No. WIPR-2-1



Figure 137. Time-Sequential Photographs, Run No. WIPR-2, Test No. WIPR-2-2



Figure 138. First Panel Damage, Run No. WIPR-2, Test No. WIPR-2-1



Figure 139. Second Panel Damage, Run No. WIPR-2, Test No. WIPR-2-1



Figure 140. First Panel Damage, Run No. WIPR-2, Test No. WIPR-2-2



Figure 141. Second Panel Damage, Run No. WIPR-2, Test No. WIPR-2-2

9.3 Run No. WIPR-3 (Test Nos. WIPR-3-1 and WIPR-3-2)

Run no. WIPR-3 consisted of two tests conducted successively, with test no. WIPR-3-1 followed by test no. WIPR-3-2. During test no. WIPR-3-1, the bogie, traveling at a speed of 46.6 mph (75.0 km/h), impacted the pedestrian rail concept AM-1 oriented at a 25-degree angle to the vehicle. For test no. WIPR-3-2, the bogie then impacted the pedestrian rail concept AM-1 at a speed of 43.3 mph (68.1 km/h), with the rail oriented end-on to the vehicle (i.e., 0 degrees). The systems prior to impact are shown in Figures 142 and 143.

Time-sequential photographs are shown in Figures 144 and 145. Damage to the pedestrian rail concepts impacted during test nos. WIPR-3-1 and WIPR-3-2 is shown in Figures 146 through 149. The posts, rails, and spindles from test nos. WIPR-3-1 and WIPR-3-2 disengaged, thus generating a fair amount of debris and concerns of flying projectiles. Damage to the systems consisted of fractured post socket couplers and post-to-rail connection joints, as well as deformed posts.

Force versus displacement and energy versus displacement curves created from the DTS-SLICE accelerometer data are shown in Figures 150 and 151 for test nos. WIPR-3-1 and WIPR-3-2, respectively. A total of 387.8 kip-in. (42.8 kJ) of energy was absorbed by the system in test no. WIPR-3-1 through 80.7 in. (2,050 mm) of displacement, while a total of 452.5 kip-in. (51.1 kJ) of energy was absorbed by the system in test no. WIPR-3-2 through 78.2 in. (1,986 mm).



Figure 142. System Panels and Anchor, Run No. WIPR-3



Figure 143. System Installation, Run No. WIPR-3



Figure 144. Time-Sequential Photographs, Run No. WIPR-3, Test No. WIPR-3-1



Figure 145. Time-Sequential Photographs, Run No. WIPR-3, Test No. WIPR-3-2

208



Figure 146. System Damage, Run No. WIPR-3, Test No. WIPR-3-1



Figure 147. System Damage, Run No. WIPR-3, Test No. WIPR-3-1



Figure 148. System Damage, Run No. WIPR-3, Test No. WIPR-3-2



Figure 149. System Damage, Run No. WIPR-3, Test No. WIPR-3-2

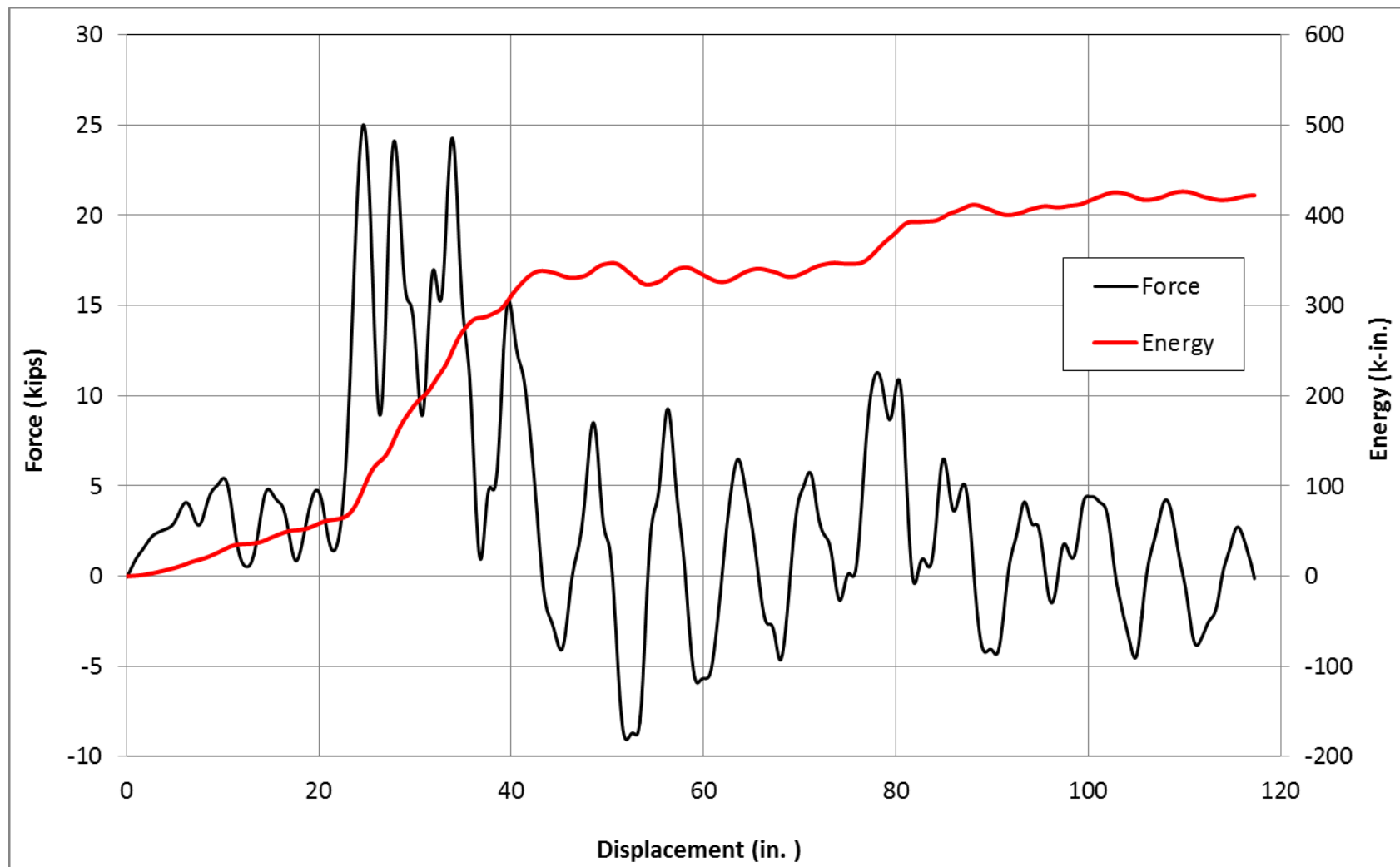


Figure 150. Force vs. Displacement and Energy vs. Displacement, Run No. WIPR-3, Test No. WIPR-3-1

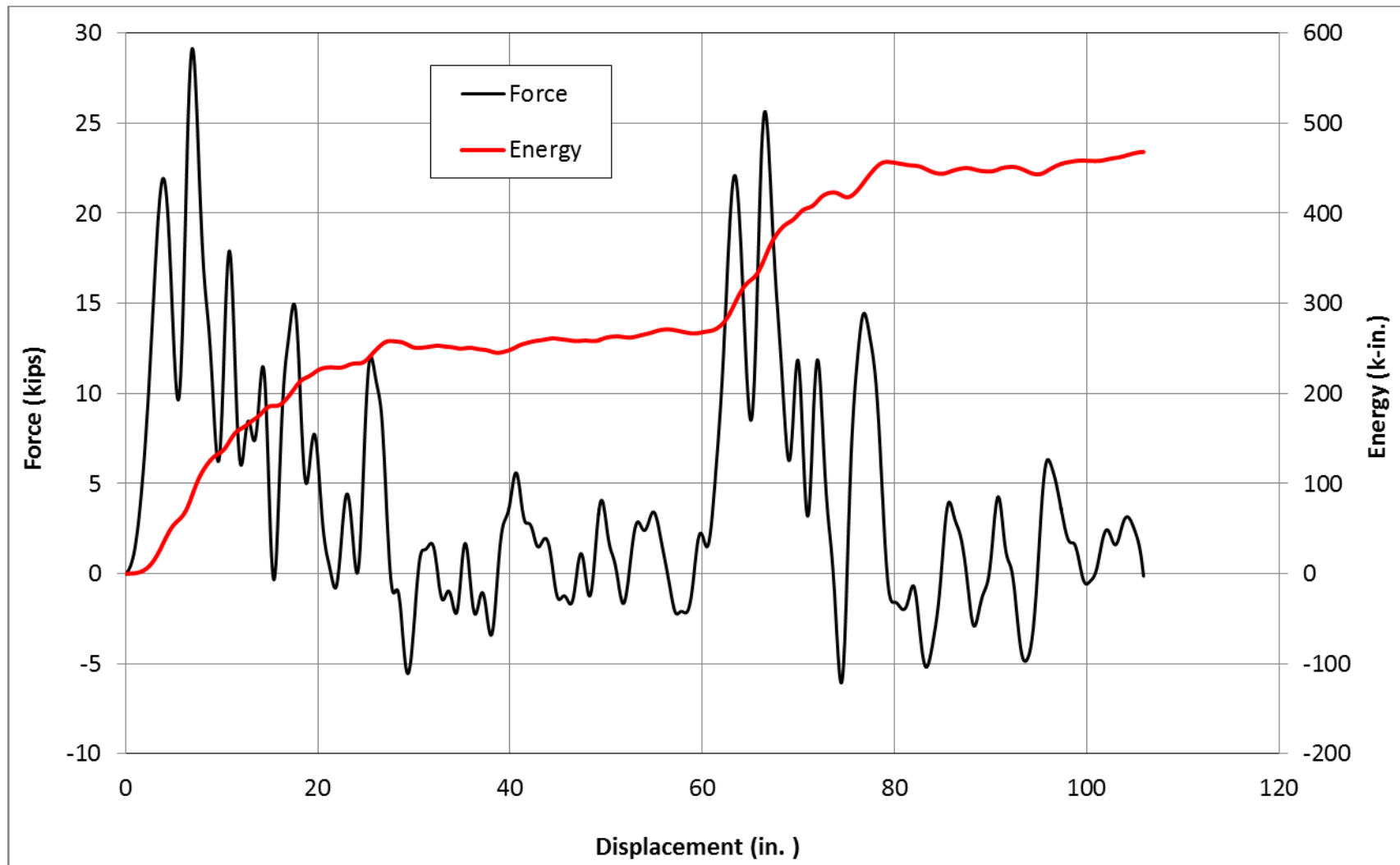


Figure 151. Force vs. Displacement and Energy vs. Displacement, Run No. WIPR-3, Test No. WIPR-3-2

9.4 Run No. WIPR-4 (Test No. WIPR-4)

Run no. 4 consisted of a single test, test no. WIPR-4, during which the bogie impacted the pedestrian rail concept AW2-D at a speed of 45.8 mph (73.8 km/h), with the rail oriented end-on to the vehicle (i.e., 0 degrees). The system prior to impact are shown in Figures 152 and 153.

Time-sequential photographs are shown in Figure 154. Damage incurred during test no. WIPR-4 is shown in Figures 155 and 156. The rail encountered damage to both the first and second panels. The damage to the first panel consisted of:

- fractured welds between both posts and their baseplates,
- all baseplates deformed,
- upstream post bent above bottom horizontal rail,
- downstream post bent at the middle horizontal rail,
- some spindles deformed, and
- upstream end of bottom horizontal rail crushed and bent.

The damage to the second panel consisted of:

- both posts bent at middle horizontal rail,
- some spindles deformed, and
- downstream end of bottom horizontal rail bent.

Force versus displacement and energy versus displacement curves created from the DTS-SLICE accelerometer data are shown in Figure 157. A total of 310.4 kip-in. (35.1 kJ) of energy was absorbed by the system in test no. WIPR-4 through 78.1 in. (1,984 mm) of displacement. However, a total of 306.8 kip-in. (34.7 kJ) of energy was absorbed by the system through 18.0 in. (457 mm) of displacement when all posts had fractured from their baseplates and the system was moving out in front of the bogie vehicle.

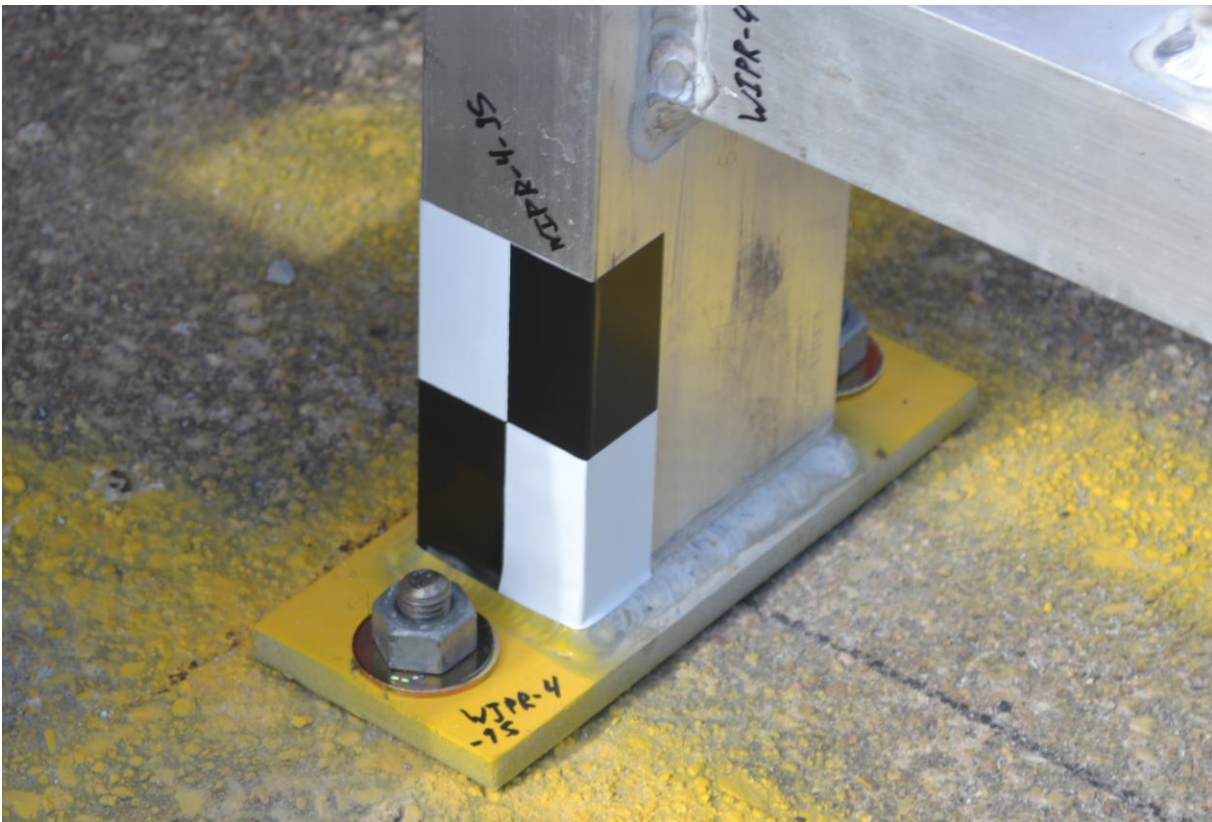


Figure 152. System Panels and Anchor, Run No. WIPR-4

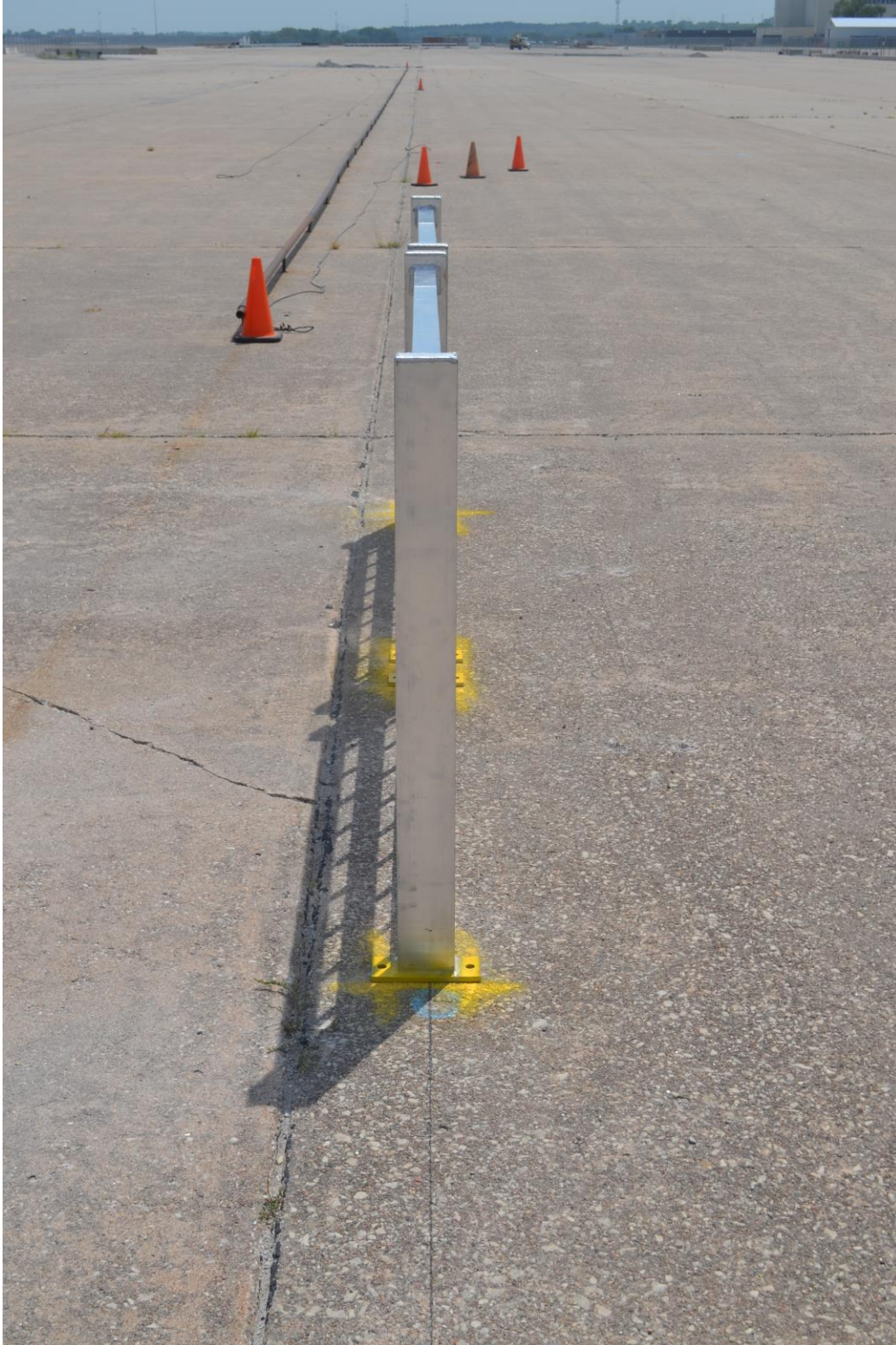


Figure 153. System Installation, Run No. WIPR-4



Figure 154. Time-Sequential Photographs, Run No. WIPR-4, Test No. WIPR-4



Figure 155. First Panel Damage, Run No. WIPR-4, Test No. WIPR-4



Figure 156. Second Panel Damage, Run No. WIPR-4, Test No. WIPR-4

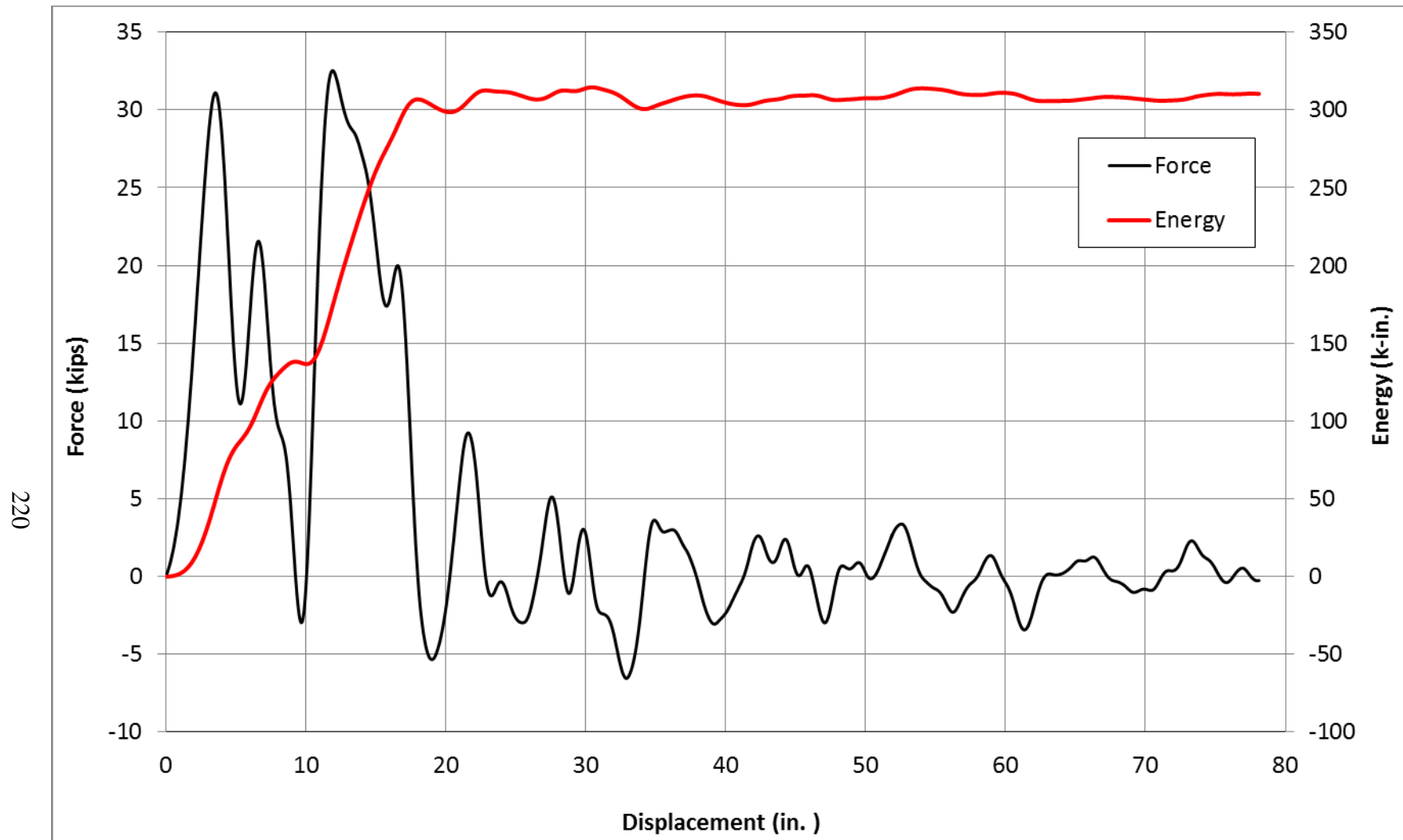


Figure 157. Force vs. Displacement and Energy vs. Displacement, Run No. WIPR-4, Test No. WIPR-4

9.5 Discussion

Four runs of seven bogie tests were conducted on four pedestrian rail concepts. Each concept was configured as a two-panel system. They were impacted at approximately 45 mph (72.4 km/h) and evaluated in two different impact orientations, except for the fourth concept (run no. WIPR-4). First, each concept was impacted at a 25-degree angle and within the spindle region of the first panel. Second, each concept was impacted using an end-on orientation. For run no. WIPR-4, only the end-on orientation was evaluated.

The performance of the post with welded baseplate (run no. WIPR-1 and WIPR-4) appeared to provide a cleaner fracture compared to the concept involving a post inserted into a socket that was welded to a baseplate (run no. WIPR-2). Minor deformation was found on all the baseplates. Permanent deformations of the baseplates could be eliminated by increasing the baseplate thickness. The $\frac{3}{8}$ -in. (9.5-mm) diameter anchors exhibited slight permanent deformations during the tests of the two welded concepts (run nos. WIPR-1 and WIPR-2). Increasing anchor diameter to $\frac{1}{2}$ -in. (12.7-mm) eliminated this permanent deformation, as shown in run nos. WIPR-3 and WIPR-4.

The upper and middle horizontal rails fractured or disengaged from the posts, rode over the top of the bogie, and posed the potential for windshield penetration and deformation during the first three system configurations when impacted end-on. In addition, based on the results of the first six bogie tests, the critical orientation was believed to occur under end-on impacts. All of the systems fractured cleanly when impacted at a 25-degree angle broke away and did not exhibit much potential for vehicle intrusion. Therefore, the last bogie test was only conducted using an end-on orientation.

The middle rail was lowered to more closely align with the bumper heights of the pickup truck and small car in order to improve dynamic impact behavior, as shown in test no. WIPR-4.

The change helped the system behave more rigidly instead of as individual posts and included: (1) lowering the middle horizontal rail, (2) extending the spindles from the top to bottom rail and passing the spindles through the middle rail, (3) increasing the anchor size to ½ in. (12.7 mm), and (4) inserting the rails into the posts. Therefore, design concept AW2-D (test no. WIPR-4) was recommended to be evaluated through full-scale vehicle crash testing according to the AASHTO MASH TL-2 safety performance criteria for longitudinal channelizers.

10 FULL-SCALE TEST REQUIREMENTS AND EVALUATION CRITERIA

10.1 Test Requirements

Longitudinal channelizers, such as pedestrian rail, must satisfy impact safety standards in order to be declared eligible for federal reimbursement by the Federal Highway Administration (FHWA) for use on the National Highway System (NHS). For new hardware, these safety standards consist of the guidelines and procedures published in MASH [7]. According to TL-2 of MASH, longitudinal channelizing systems must be subjected to two full-scale vehicle crash tests. The two required full-scale crash tests are noted below:

1. Test Designation No. 2-90 consists of a 2,425-lb (1,100-kg) passenger car impacting the system at a nominal speed of 44 mph (70 km/h) and a critical angle between 0 and 25 degrees.
2. Test Designation No. 2-91 consists of a 5,000-lb (2,268-kg) pickup truck impacting the system at a nominal speed of 44 mph (70 km/h) and a critical angle between 0 and 25 degrees.

The test conditions of TL-2 longitudinal barriers are summarized in Table 11. According to MASH, the critical impact angle for channelizers should be selected to maximize the risk of vehicle rollover and/or excessive vehicle decelerations. During discussions with FHWA personnel, the 0-degree impact angle would likely provide the greatest risk of excessive vehicle decelerations, and could also cause vehicle instability and windshield and occupant compartment deformation and/or penetration. The 25-degree impact angle could cause vehicle instability and windshield and occupant compartment deformation and/or penetration. Therefore, impact angles of 0- and 25-degrees were both deemed critical as vehicle instability and occupant risk could occur with either impact angle. Other impact angles between those values would likely be less critical.

Table 11. MASH TL-2 Crash Test Conditions

Test Article	Test Designation No.	Test Vehicle	Impact Conditions			Evaluation Criteria ¹
			Speed		Angle (deg)	
			mph	km/h		
Longitudinal Channelizer	2-90	1100C	44	70	0-25	C,D,F,H,I,N
	2-91	2270P	44	70	0-25	C,D,F,H,I,N

¹ Evaluation criteria explained in Table 12.

Test no. 2-90 was deemed most critical as the small car has a greater potential for excessive vehicle decelerations, due to its smaller mass, and vehicle instability, due to overriding components. The small car also has lower hood, windshield, and floorpan heights, which would make it more susceptible to occupant compartment and windshield penetration and deformation with the channelizer. Therefore, after discussion with FHWA personnel, two tests with the small car were deemed critical initially: test no. 2-90 with an 1100C small car impacting at 0 degrees and test no. 2-90 with an 1100C small car impacting at 25 degrees. If the results of either test no. 2-90 test indicated that channelizer had the potential to cause excessive vehicle deceleration, vehicle instability, or occupant compartment or windshield penetration or deformation with the 2270P pickup truck, then additional test no. 2-91 tests would be conducted.

MASH is unclear in regards to the use of a centerline impact versus a quarter-point impact when testing channelizers. Therefore, the choice was made to use a centerline impact scenario for all full-scale tests, as the vehicle would likely interact with a greater number of panels with a greater risk of excessive vehicle deceleration. Further, a quarter-point impact typically is used to evaluate the potential for vehicle rollover and this is not as large of a concern for the channelizer system.

10.2 Evaluation Criteria

Evaluation criteria for full-scale vehicle crash testing are based on three appraisal areas: (1) structural adequacy, (2) occupant risk, and (3) vehicle trajectory after collision. Criteria for structural adequacy are intended to evaluate the ability of the longitudinal channelizer to perform acceptably through either redirection, controlled penetration, or controlled vehicle stopping. Occupant risk evaluates the degree of hazard to occupants in the impacting vehicle. Post-impact vehicle trajectory is a measure of the potential of the vehicle to result in a secondary collision with other vehicles and/or fixed objects, thereby increasing the risk of injury to the occupants of the impacting vehicle and/or other vehicles. For longitudinal channelizers, penetration of the vehicle behind the test article is acceptable. These evaluation criteria are summarized in Table 12 and defined in greater detail in MASH. All full-scale vehicle crash tests were conducted and reported in accordance with the procedures provided in MASH.

In addition to the standard occupant risk measures, the Post-Impact Head Deceleration (PHD), the Theoretical Head Impact Velocity (THIV), and the Acceleration Severity Index (ASI) were determined and reported on the test summary sheet. Additional discussion on PHD, THIV and ASI is provided in MASH.

Table 12. MASH Evaluation Criteria for Longitudinal Channelizers

Structural Adequacy	C.	Acceptable test article performance may be by redirection, controlled penetration, or controlled stopping of the vehicle.		
Occupant Risk	D.	Detached elements, fragments or other debris from the test article should not penetrate or show potential for penetrating the occupant compartment, or present an undue hazard to other traffic, pedestrians, or personnel in a work zone. Deformations of, or intrusions into, the occupant compartment should not exceed limits set forth in Section 5.3 and Appendix E of MASH.		
	F.	The vehicle should remain upright during and after collision. The maximum roll and pitch angles are not to exceed 75 degrees.		
	H.	Occupant Impact Velocity (OIV) (see Appendix A, Section A5.3 of MASH for calculation procedure) should satisfy the following limits:		
	Occupant Impact Velocity Limits			
	Component	Preferred	Maximum	
	Longitudinal and Lateral	30 ft/s (9.1 m/s)	40 ft/s (12.2 m/s)	
I.	The Occupant Ridedown Acceleration (ORA) (see Appendix A, Section A5.3 of MASH for calculation procedure) should satisfy the following limits:			
Occupant Ridedown Acceleration Limits				
Component	Preferred	Maximum		
Longitudinal and Lateral	15.0 g's	20.49 g's		
Vehicle Trajectory	N.	Vehicle trajectory behind the test article is acceptable.		

11 TEST CONDITIONS

11.1 Test Facility

The testing facility is located at the Lincoln Air Park on the northwest side of the Lincoln Municipal Airport and is approximately 5 miles (8.0 km) northwest of the University of Nebraska-Lincoln city campus.

11.2 Vehicle Tow and Guidance System

A reverse cable tow system with a 1:2 mechanical advantage was used to propel the test vehicle. The distance traveled and the speed of the tow vehicle were one-half those of the test vehicle. The test vehicle was released from the tow cable before impact with the longitudinal channelizer system. A digital speedometer on the tow vehicle increased the accuracy of the test vehicle impact speed.

A vehicle guidance system developed by Hinch [44] was used to steer the test vehicle. A guide flag, attached to the left-front wheel and the guide cable, was sheared off before impact with the system. The $\frac{3}{8}$ -in. (9.5-mm) diameter guide cable was tensioned to approximately 3,500 lb (15.6 kN) and supported both laterally and vertically every 100 ft (30.5 m) by hinged stanchions. The hinged stanchions stood upright while holding up the guide cable, but as the vehicle was towed down the line, the guide flag struck and knocked each stanchion to the ground.

11.3 Test Vehicles

For test no. APR-1, a 2006 Kia Rio was used as the test vehicle. The curb, test inertial, and gross static vehicle weights were 2,421 lb (1,098 kg), 2,428 lb (1,101 kg), and 2,599 lb (1,179 kg), respectively. The test vehicle and vehicle dimensions are shown in Figure 158 and Figure 159, respectively.

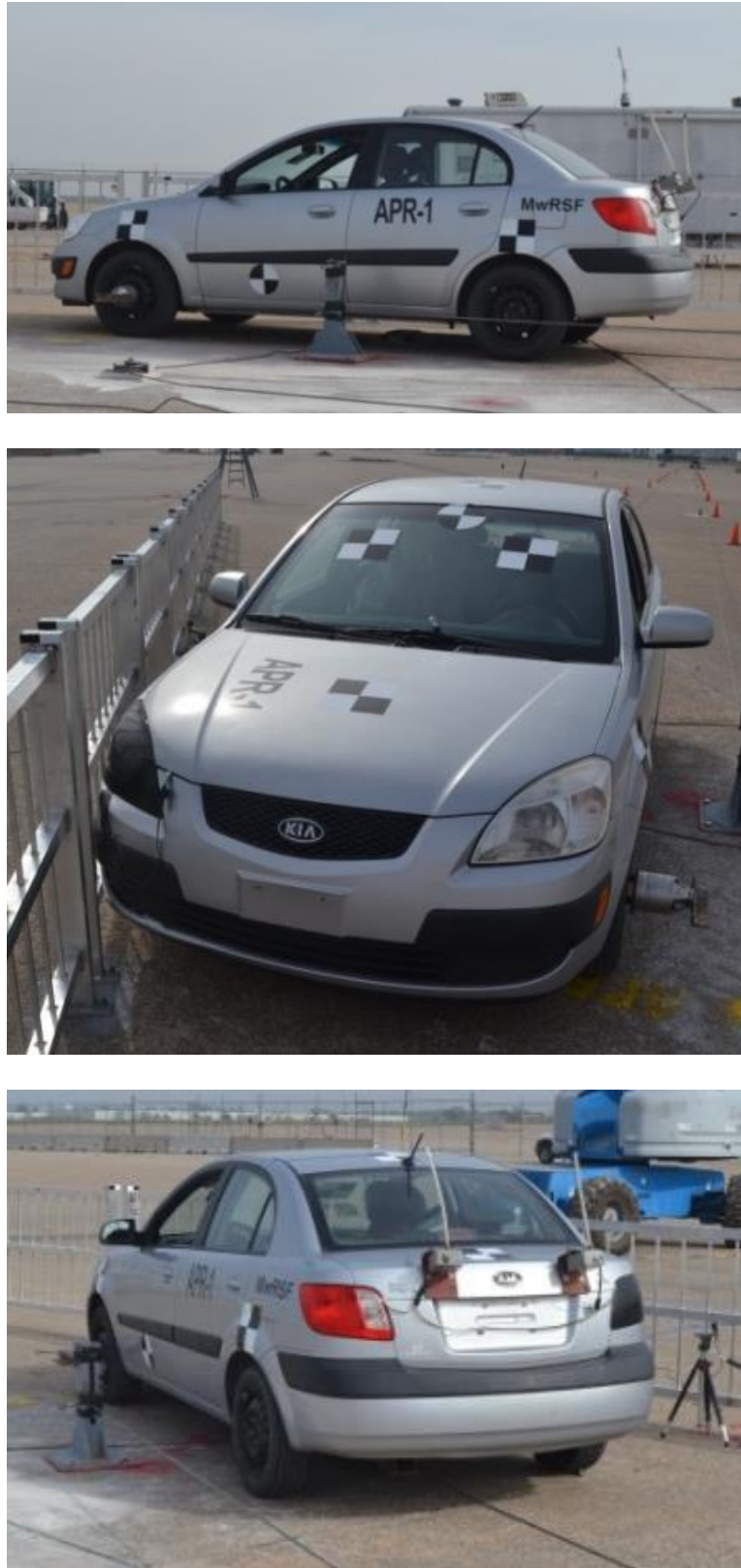


Figure 158. Test Vehicle, Test No. APR-1

Date: <u>10/23/2014</u>	Test Number: <u>APR-1</u>	Model: <u>Rio</u>
Make: <u>Kia</u>	Vehicle I.D.#: <u>knade123576194884</u>	
Tire Size: <u>P186/65/R14</u>	Year: <u>2006</u>	Odometer: <u>138090</u>
Tire Inflation Pressure: <u>32psi</u>		

*(All Measurements Refer to Impacting Side)

Vehicle Geometry -- in. (mm)

a	<u>65</u>	<u>(1651)</u>	b	<u>57 1/2</u>	<u>(1461)</u>
c	<u>167</u>	<u>(4242)</u>	d	<u>35 1/2</u>	<u>(902)</u>
e	<u>98 3/4</u>	<u>(2508)</u>	f	<u>32 3/4</u>	<u>(832)</u>
g	<u>16 1/2</u>	<u>(419)</u>	h	<u>36 4/9</u>	<u>(926)</u>
i	<u>15</u>	<u>(381)</u>	j	<u>21</u>	<u>(533)</u>
k	<u>12</u>	<u>(305)</u>	l	<u>24</u>	<u>(610)</u>
m	<u>56 1/2</u>	<u>(1435)</u>	n	<u>57 3/4</u>	<u>(1467)</u>
o	<u>35</u>	<u>(889)</u>	p	<u>2</u>	<u>(51)</u>
q	<u>23 1/2</u>	<u>(597)</u>	r	<u>15 1/4</u>	<u>(387)</u>
s	<u>11 3/4</u>	<u>(298)</u>	t	<u>63 1/4</u>	<u>(1607)</u>

Wheel Center Height Front	<u>10 3/4</u>	<u>(273)</u>
Wheel Center Height Rear	<u>11 1/4</u>	<u>(286)</u>
Wheel Well Clearance (F)	<u>3</u>	<u>(76)</u>
Wheel Well Clearance (R)	<u>2 1/2</u>	<u>(64)</u>
Frame Height (F)	<u>6</u>	<u>(152)</u>
Frame Height (R)	<u>15 3/4</u>	<u>(400)</u>

Engine Type Gasoline

Engine Size 1.6L

Transmission Type:

☒ Automatic ☐ Manual
☒ FWD ☐ RWD ☐ 4WD

Mass Distribution lb (kg)			
Gross Static	LF	<u>800</u>	<u>(363)</u>
	LR	<u>484</u>	<u>(220)</u>
	RF	<u>826</u>	<u>(375)</u>
	RR	<u>489</u>	<u>(222)</u>

Weights lb (kg)	Curb	Test Inertial	Gross Static
W-front	<u>1580</u>	<u>(717)</u>	<u>1626</u>
W-rear	<u>841</u>	<u>(381)</u>	<u>973</u>
W-total	<u>2421</u>	<u>(1098)</u>	<u>2599</u>

GVWR Ratings	Dummy Data
Front <u>1918</u>	Type: <u>Hybrid II</u>
Rear <u>1874</u>	Mass: <u>171 lb</u>
Total <u>3638</u>	Seat Position: <u>Passenger</u>

Note any damage prior to test: Minor small dents

Figure 159. Vehicle Dimensions, Test No. APR-1

For test no. APR-2, a 2006 Kia Rio was used as the test vehicle. The curb, test inertial, and gross static vehicle weights were 2,424 lb (1,100 kg), 2,437 lb (1,105 kg), and 2,599 lb (1,179 kg), respectively. The test vehicle and vehicle dimensions are shown in Figure 160 and Figure 161, respectively.

The longitudinal component of the center of gravity (c.g.) was determined using the measured axle weights. The vertical component of the c.g. for the 1100C vehicle was determined utilizing a procedure published by SAE [45]. The location of the final c.g. for each test vehicle is shown in Figures 159 and 161. Data used to calculate the location of the c.g. and ballast information are shown in Appendix E.

Square, black- and white-checkered targets were placed on the vehicle for reference to be viewed from the high-speed digital video cameras and aid in the video analysis. Round, checkered targets were placed on the center of gravity on the left-side door, the right-side door, and the roof of the vehicle. Target locations are shown for each vehicle in Figures 162 and 163.

The front wheels of the test vehicle were aligned to vehicle standards, except the toe-in value was adjusted to zero so that the vehicles would track properly along the guide cable. A 5B flash bulb was mounted on each vehicle's dash and was fired by a pressure tape switch mounted at the impact corner of the bumper. The flash bulb was fired upon initial impact with the test article to create a visual indicator of the precise time of impact on the high-speed videos. A remote controlled brake system was installed in the test vehicle, so the vehicle could be brought safely to a stop after the test.

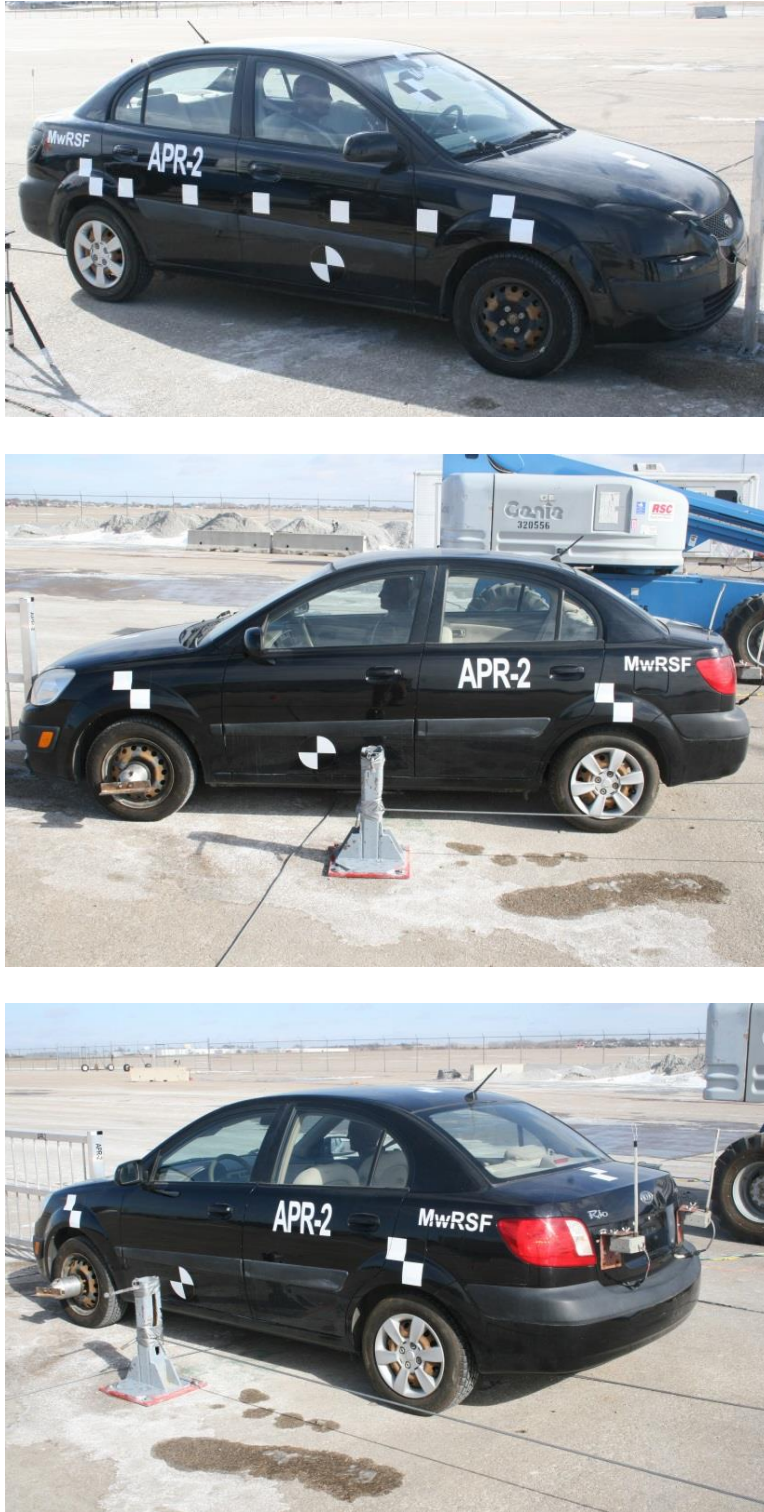


Figure 160. Test Vehicle, Test No. APR-2

Date: <u>11/12/2014</u>	Test Number: <u>APR-2</u>	Model: <u>Rio</u>
Make: <u>Kia</u>	Vehicle I.D.#: <u>knade123166085031</u>	
Tire Size: <u>P186/65/R14</u>	Year: <u>2006</u>	Odometer: <u>128514</u>
Tire Inflation Pressure: <u>32psi</u>		

*(All Measurements Refer to Impacting Side)

Vehicle Geometry -- in. (mm)

a	<u>64 1/4</u>	<u>(1632)</u>	b	<u>57 1/4</u>	<u>(1454)</u>
c	<u>166 3/4</u>	<u>(4235)</u>	d	<u>35 1/2</u>	<u>(902)</u>
e	<u>98 1/2</u>	<u>(2502)</u>	f	<u>32 3/4</u>	<u>(832)</u>
g	<u>16 1/4</u>	<u>(413)</u>	h	<u>37 2/3</u>	<u>(957)</u>
i	<u>8 1/2</u>	<u>(216)</u>	j	<u>21</u>	<u>(533)</u>
k	<u>12 1/4</u>	<u>(311)</u>	l	<u>23 1/4</u>	<u>(591)</u>
m	<u>57 1/2</u>	<u>(1461)</u>	n	<u>57 3/4</u>	<u>(1467)</u>
o	<u>35</u>	<u>(889)</u>	p	<u>1 3/4</u>	<u>(44)</u>
q	<u>23</u>	<u>(584)</u>	r	<u>15 1/4</u>	<u>(387)</u>
s	<u>11 1/2</u>	<u>(292)</u>	t	<u>63 1/2</u>	<u>(1613)</u>

Wheel Center Height Front	<u>10 1/2</u>	<u>(267)</u>
Wheel Center Height Rear	<u>11</u>	<u>(279)</u>
Wheel Well Clearance (F)	<u>3 1/4</u>	<u>(83)</u>
Wheel Well Clearance (R)	<u>3 1/4</u>	<u>(83)</u>
Frame Height (F)	<u>7 1/4</u>	<u>(184)</u>
Frame Height (R)	<u>15 1/2</u>	<u>(394)</u>

Mass Distribution lb (kg)			
Gross Static	LF	<u>799</u>	<u>(362)</u>
	RF	<u>793</u>	<u>(360)</u>
	LR	<u>475</u>	<u>(215)</u>
	RR	<u>532</u>	<u>(241)</u>

Weights lb (kg)	Curb	Test Inertial	Gross Static
W-front	<u>1527</u>	<u>(693)</u>	<u>1592</u>
W-rear	<u>897</u>	<u>(407)</u>	<u>1007</u>
W-total	<u>2424</u>	<u>(1100)</u>	<u>2599</u>

GVWR Ratings	Dummy Data
Front <u>1918</u>	Type: <u>Hybrid II</u>
Rear <u>1874</u>	Mass: <u>162 lb</u>
Total <u>3638</u>	Seat Position: <u>Passenger</u>

Note any damage prior to test: Hail dents, small dent on rear deck lid.

Engine Type: Gasoline

Engine Size: 1.6L

Transmission Type: Automatic Manual

FWD RWD 4WD

Figure 161. Vehicle Dimensions, Test No. APR-2

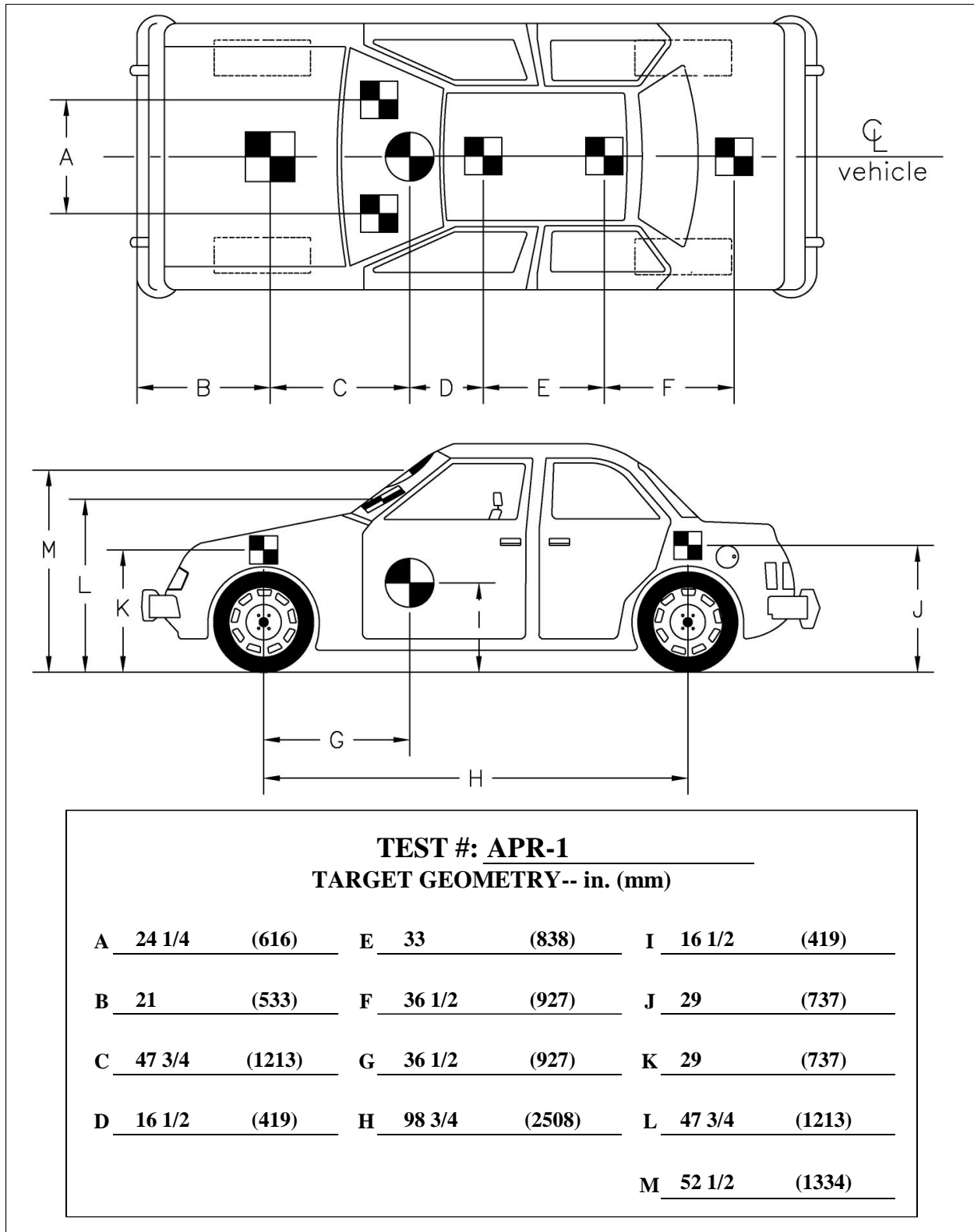


Figure 162. Target Geometry, Test No. APR-1

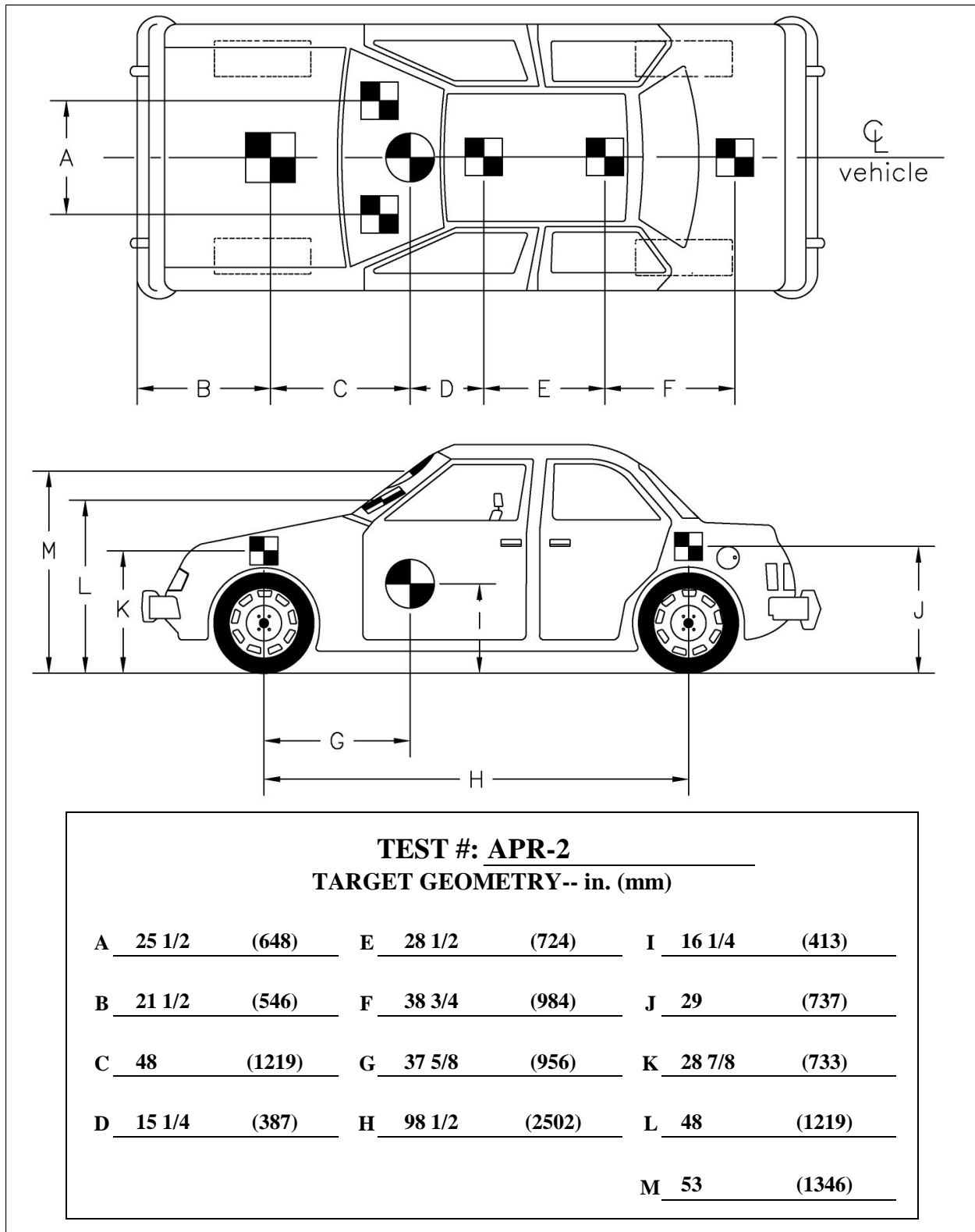


Figure 163. Target Geometry, Test No. APR-2

11.4 Simulated Occupant

For test nos. APR-1 and APR-2, a Hybrid II 50th-Percentile, Adult Male Dummy, equipped with clothing and footwear, was placed in the right-front seat of the test vehicle with the seat belt fastened. The dummy, which had an approximate weight of 170 lb (77 kg), was represented by model no. 572, serial no. 451, and was manufactured by Android Systems of Carson, California. As recommended by MASH, the dummy was not included in calculating the c.g location.

11.5 Data Acquisition Systems

11.5.1 Accelerometers

Two environmental shock and vibration sensor/recorder systems were used to measure the accelerations in the longitudinal, lateral, and vertical directions. All of the accelerometers were mounted near the center of gravity of each test vehicle. The electronic accelerometer data obtained in dynamic testing was filtered using the SAE Class 60 and the SAE Class 180 Butterworth filters conforming to SAE J211/1 specifications [43].

The first accelerometer system, DTS, was a two-arm piezoresistive accelerometer system manufactured by Endevco of San Juan Capistrano, California. Three accelerometers were used to measure each of the longitudinal, lateral, and vertical accelerations independently at a sample rate of 10,000 Hz. The accelerometers were configured and controlled using a system developed and manufactured by Diversified Technical Systems, Inc. (DTS) of Seal Beach, California. More specifically, data was collected using a DTS Sensor Input Module (SIM), Model TDAS3-SIM-16M. The SIM was configured with 16 MB SRAM and eight sensor input channels with 250 kB SRAM/channel. The SIM was mounted on a TDAS3-R4 module rack. The module rack was configured with isolated power/event/communications, 10BaseT Ethernet and RS232 communication, and an internal backup battery. Both the SIM and module rack were

crashworthy. The “DTS TDAS Control” computer software program and a customized Microsoft Excel worksheet were used to analyze and plot the accelerometer data.

The second system, SLICE-2, was a modular data acquisition system manufactured by DTS. The acceleration sensors were mounted inside the body of the custom-built SLICE 6DX event data recorder and recorded data at 10,000 Hz to the onboard microprocessor. The SLICE 6DX was configured with 7 GB of non-volatile flash memory, a range of ± 500 g's, a sample rate of 10,000 Hz, and a 1,650 Hz (CFC 1000) anti-aliasing filter. The “SLICEWare” computer software program and a customized Microsoft Excel worksheet were used to analyze and plot the accelerometer data.

11.5.2 Rate Transducers

An angle rate sensor, the ARS-1500, with a range of 1,500 degrees/sec in each of the three directions (roll, pitch, and yaw) was used to measure the rates of rotation of the test vehicles. The angular rate sensor was mounted on an aluminum block inside the test vehicle near the center of gravity and recorded data at 10,000 Hz to the DTS SIM. The raw data measurements were then downloaded, converted to the proper Euler angles for analysis, and plotted. The “DTS TDAS Control” computer software program and a customized Microsoft Excel worksheet were used to analyze and plot the angular rate sensor data.

A second angle rate sensor system, mounted inside the body of the SLICE-2 event data recorder was used to measure the rates of rotation of the test vehicle. The SLICE MICRO Triax ARS had a range of 1,500 degrees/sec in each of the three directions (roll, pitch, and yaw) and recorded data at 10,000 Hz to the onboard microprocessor. The raw data measurements were then downloaded, converted to the proper Euler angles for analysis, and plotted. The “SLICEWare” computer software program and a customized Microsoft Excel worksheet were used to analyze and plot the angular rate sensor data.

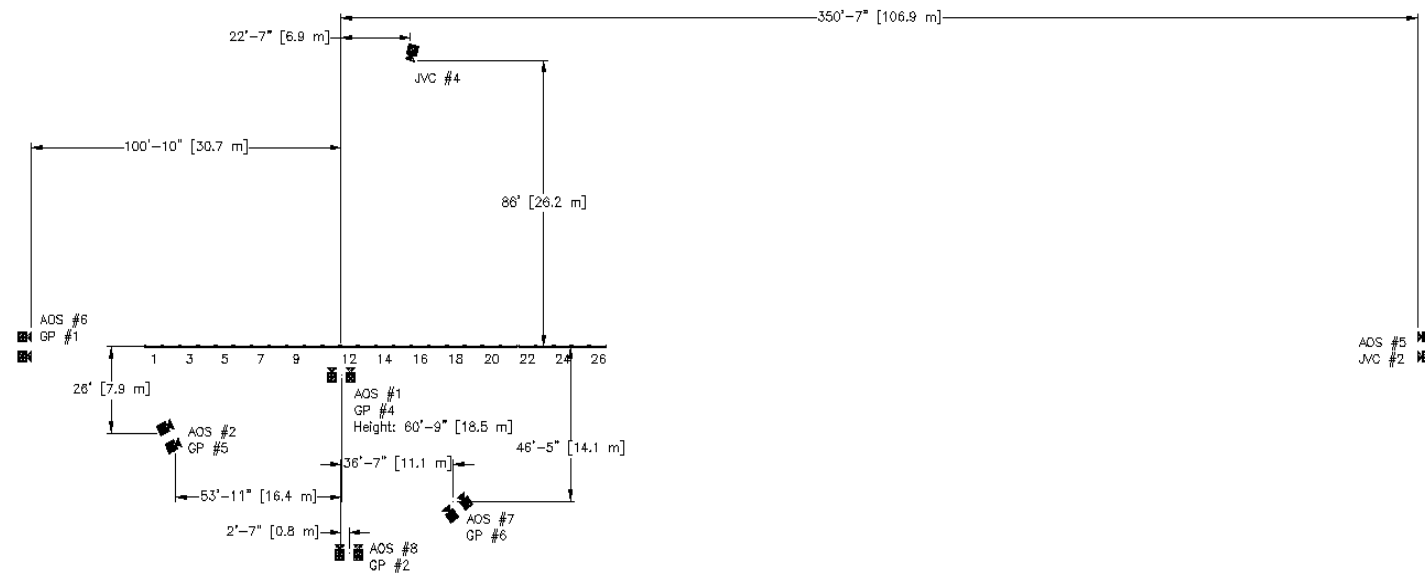
11.5.3 Retroreflective Optic Speed Trap

The retroreflective optic speed trap was used to determine the speed of the bogie vehicle before impact. Five retroreflective targets, spaced at approximately 18-in. (457-mm) intervals, were applied to the side of the vehicle. When the emitted beam of light was reflected by the targets and returned to the Emitter/Receiver, a signal was sent to the data acquisition computer, recording at 10,000 Hz, and activated the External LED box. The speed was then calculated using the spacing between the retroreflective targets and the time between the signals. LED lights and high-speed digital video analysis are only used as backups in the event that vehicle speeds cannot be determined from the electronic data.

11.5.4 Digital Photography

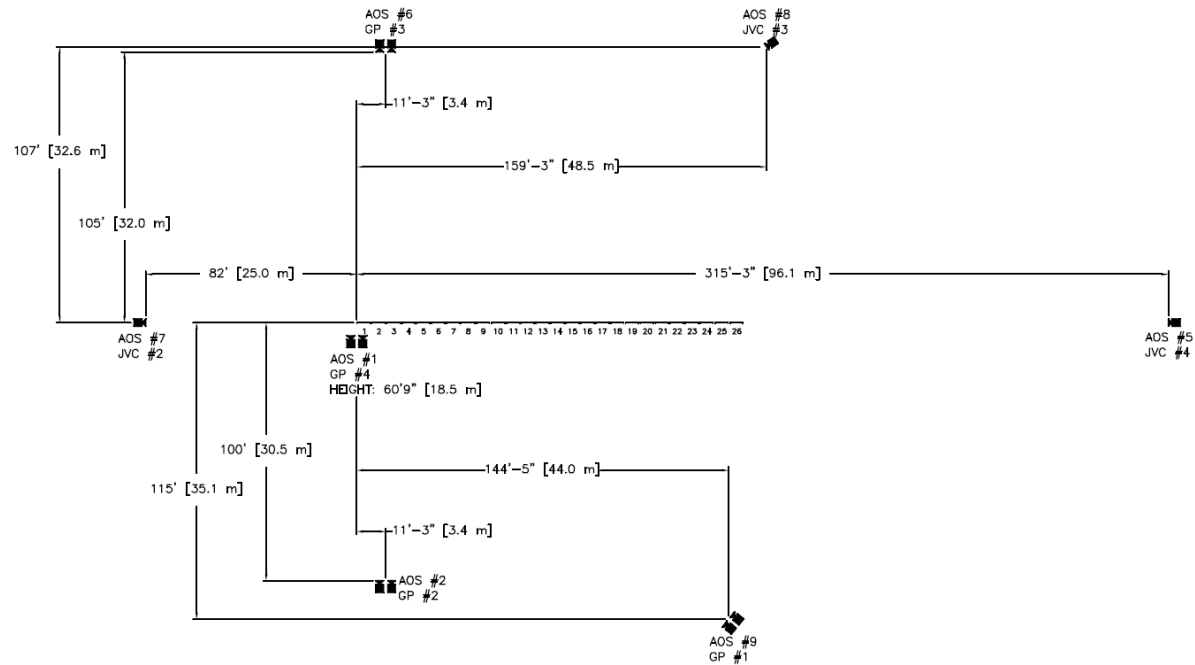
Six AOS high-speed digital video cameras, five GoPro digital video cameras, and two JVC digital video cameras were utilized to film test no. APR-1. Seven AOS high-speed digital video cameras, four GoPro digital video cameras, and three JVC digital video cameras were utilized to film test no. APR-2. Camera details, camera operating speeds, lens information, and a schematic of the camera locations relative to the system for each crash test are shown in Figures 164 and 165 for test nos. APR-1 and APR-2, respectively.

The high-speed videos were analyzed using ImageExpress MotionPlus and RedLake MotionScope software programs. Actual camera speed and camera divergence factors were considered in the analysis of the high-speed videos. A Nikon D50 digital still camera was used to document pre- and post-test conditions for all tests.



No.	Type	Operating Speed (frames/sec)	Lens	Lens Setting
1	AOS Vitcam CTM	500	Cosmicar 12.5mm fixed	-
2	AOS Vitcam CTM	500	Sigma 28-70mm	28
5	AOS X-PRI Gigabit	500	Canon 200m	102
6	AOS X-PRI Gigabit	500	Fujinon-50mm fixed	-
7	AOS X-PRI Gigabit	500	Nikkor 28mm fixed	-
8	AOS S-Vit 1531	500	Sigma UC 200m 28-70mm	35
2	JVC – GZ-MC27u (Everio)	29.97		
4	JVC – GZ-MG27u (Everio)	29.97		
1	GoPro Hero 3	120		
2	GoPro Hero 3	120		
4	GoPro Hero 3+	120		
5	GoPro Hero 3+	120		
6	GoPro Hero 3+	120		

Figure 164. Camera Locations, Speeds, and Lens Settings, Test No. APR-1



No.	Type	Operating Speed (frames/sec)	Lens	Lens Setting
1	AOS Vitcam CTM	500	Cosmicar 12.5mm fixed	-
2	AOS Vitcam CTM	500	Sigma 28-70mm	28
5	AOS X-PRI Gigabit	500	TV 200m 17-102	102
6	AOS X-PRI Gigabit	500	Nikkor 20mm fixed	-
7	AOS X-PRI Gigabit	500	Fujinon 50 fixed	-
8	AOS S-Vit 1531	500	Sigma UC 200m 28-70mm	50
9	AOS TRI-Vit	1000	Sigma 24-135	70
2	JVC-GZ-MC27u (Everio	29.97		
3	JVC-GZ-MC27u (Everio	29.97		
4	JVC-GZ-MC27u (Everio	29.97		
1	GoPro Hero 3	120		
2	GoPro Hero 3	120		
3	GoPro Hero 3+	120		
4	GoPro Hero 3+	120		

Figure 165. Camera Locations, Speeds, and Lens Settings, Test No. APR-2

12 DESIGN DETAILS

The 150-ft (45.7-m) long channelizer system was comprised of twenty-six aluminum pedestrian rail panels. Design details for test nos. APR-1 and APR-2 are shown in Figures 166 through 171. Photographs of the as-tested system are shown in Figures 172 through 174. Material specifications, mill certifications, and certificates of conformity for the system materials are shown in Appendix D.

Each panel utilized 2-in. x 4-in. x 1/4-in. x 43-in. tall (51-mm x 102-mm x 6-mm x 1,029-mm tall) posts with three 2-in. x 2-in. x 1/8-in. (51-mm x 51-mm x 3-mm) rail components at heights of 42 in. (1,067 mm), $24^{15}/_{16}$ in. (633 mm), and $7^{7}/_{8}$ in. (200 mm). The rails were inserted into cutouts in the posts at each rail location and secured to the face of the posts with 1/8-in. (3-mm) fillet welds at each connection. Nine 1/2-in. x 1/2-in. x $32^{1}/_{8}$ -in. (13-mm x 13-mm x 816-mm) square spindles spanned between the top and bottom rails and were inserted through the middle rail. The spindles were welded with 1/8-in. (3-mm) fillet welds at each rail location. Each post member was welded to a 3-in. x $7^{3}/_{4}$ -in. x $3^{3}/_{8}$ -in. (76-mm x 191-mm x 9.5-mm) baseplate with a 1/4-in. (6-mm) fillet weld at the connection. The baseplate had two $5^{5}/_{8}$ -in. (16-mm) holes spaced at $6^{1}/_{4}$ in. (159 mm) to accommodate two 1/2-in. (13-mm) diameter threaded anchor rods, each embedded 5 in. (127 mm) into 1,450-psi (10.0-MPa) minimum bond strength epoxy adhesive and secured through the baseplate with a 1/2-in. (13-mm) diameter ASTM A194 Grade 8M nut. The concrete foundation had a minimum compressive strength of 2,500 psi (17.2 MPa), a minimum thickness of 7 in. (178 mm), and outer dimensions at least 10 in. (254 mm) away from the nearest anchor. The panels were spaced $5^{1}/_{2}$ in. (140 mm) away from each other.

During baseplate fabrication, jigs were built and slots were cut into the baseplates to aid in welding. Note, these slots do not appear in the system drawings. Examples of these slots are shown in Figure 174. Drawings from the fabricator are shown in Appendix F.

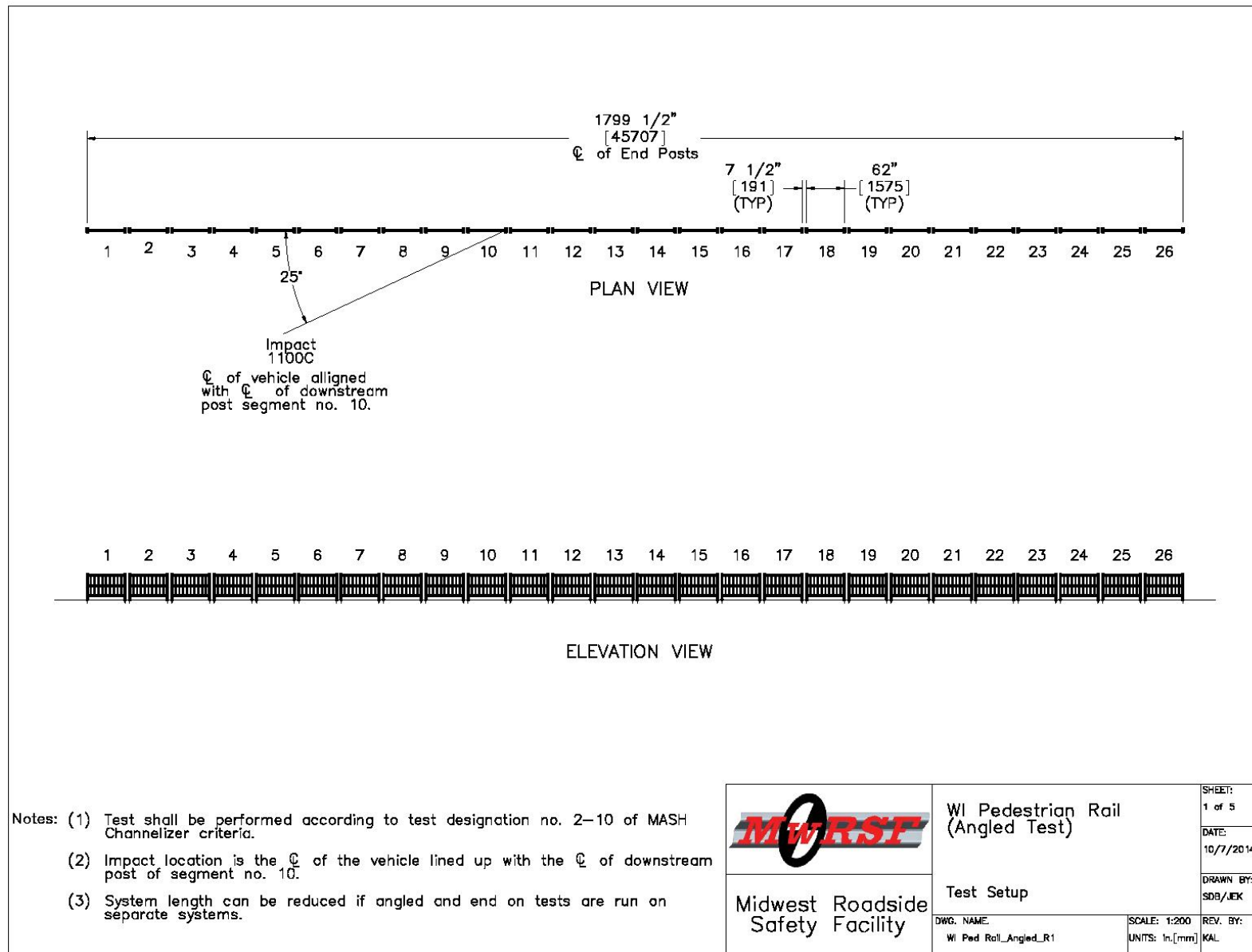


Figure 166. Test Installation Layout, Test No. APR-1

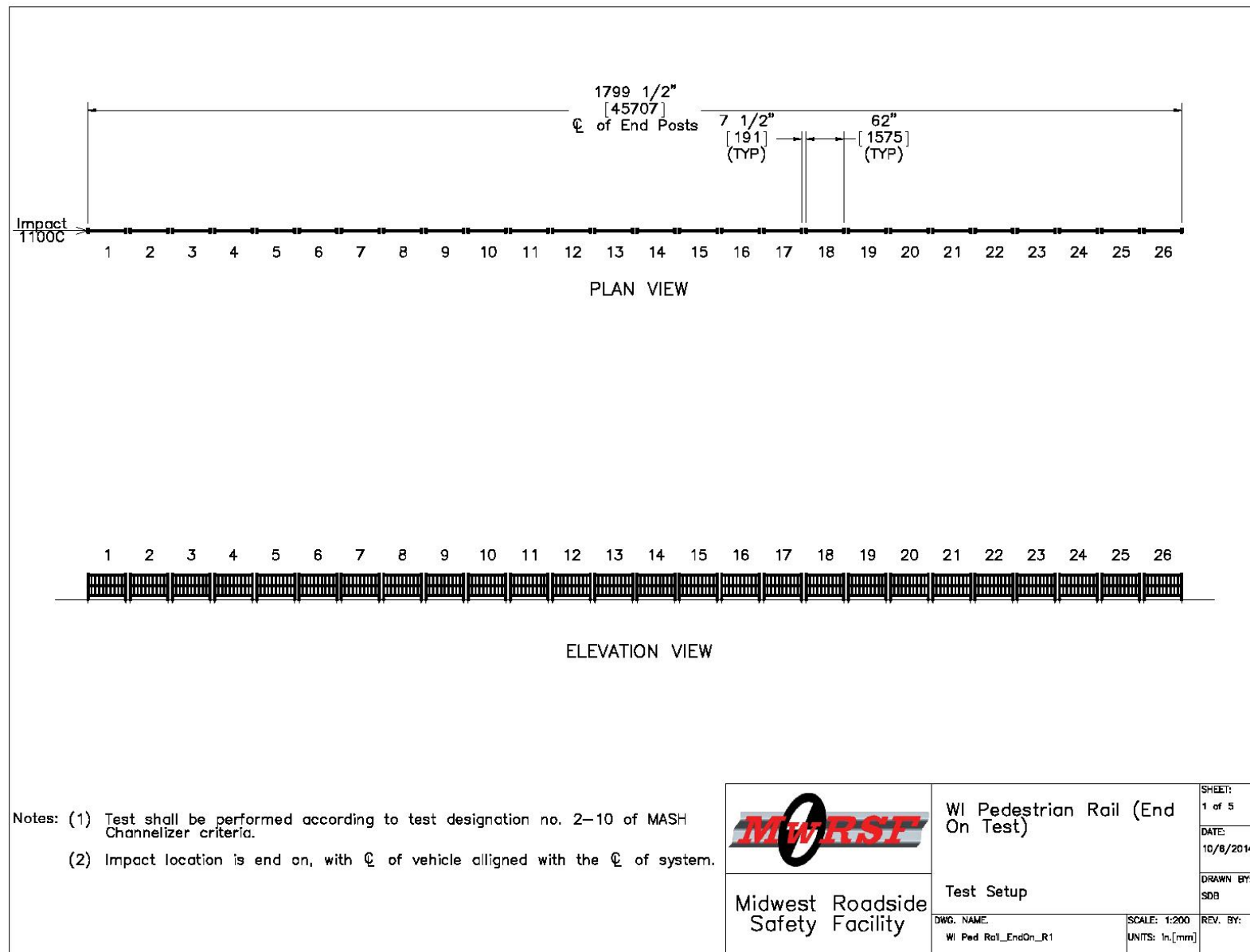


Figure 167. Test Installation Layout, Test No. APR-2

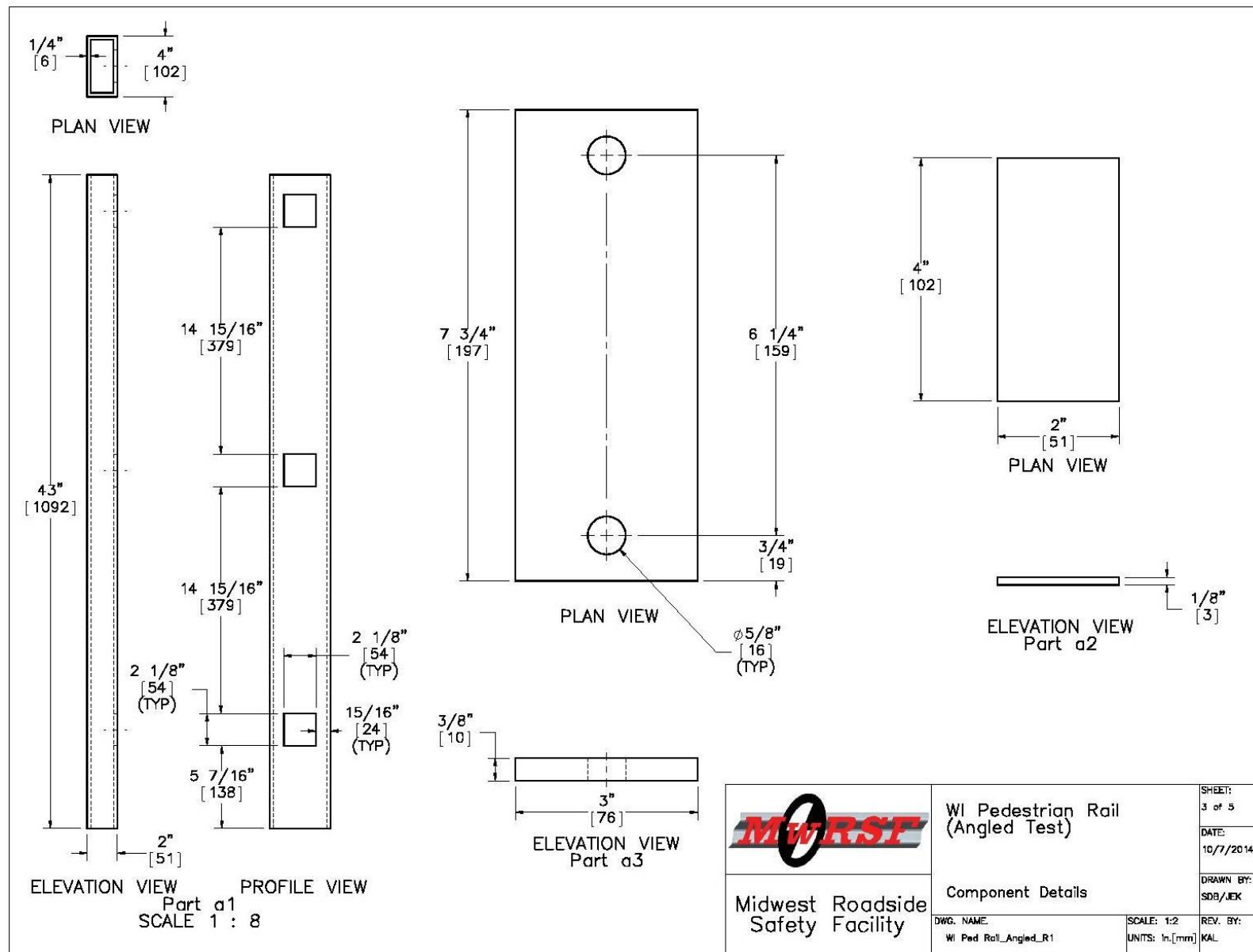


Figure 168. Component Details, Test Nos. APR-1 and APR-2

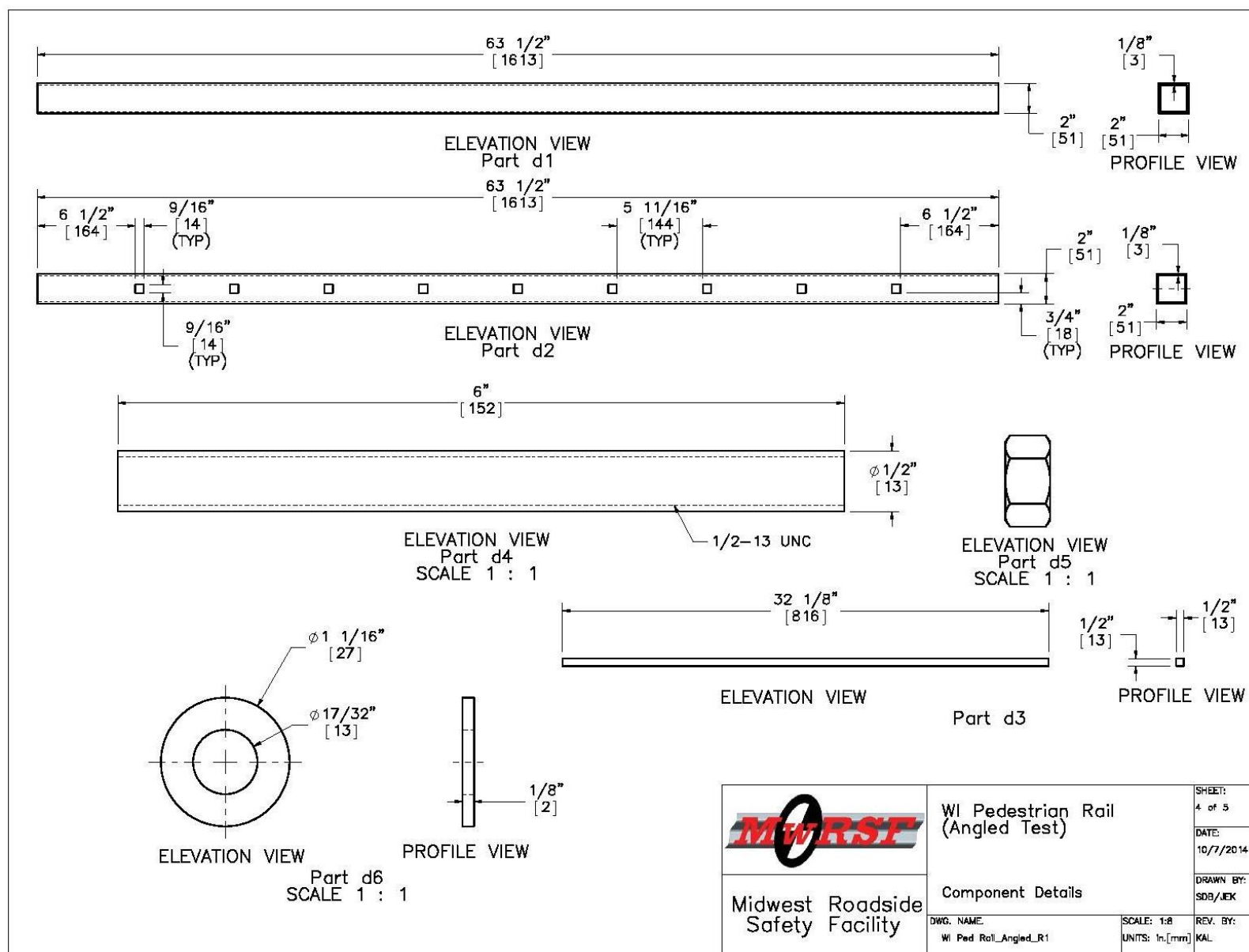


Figure 169. Component Details, Test Nos. APR-1 and APR-2

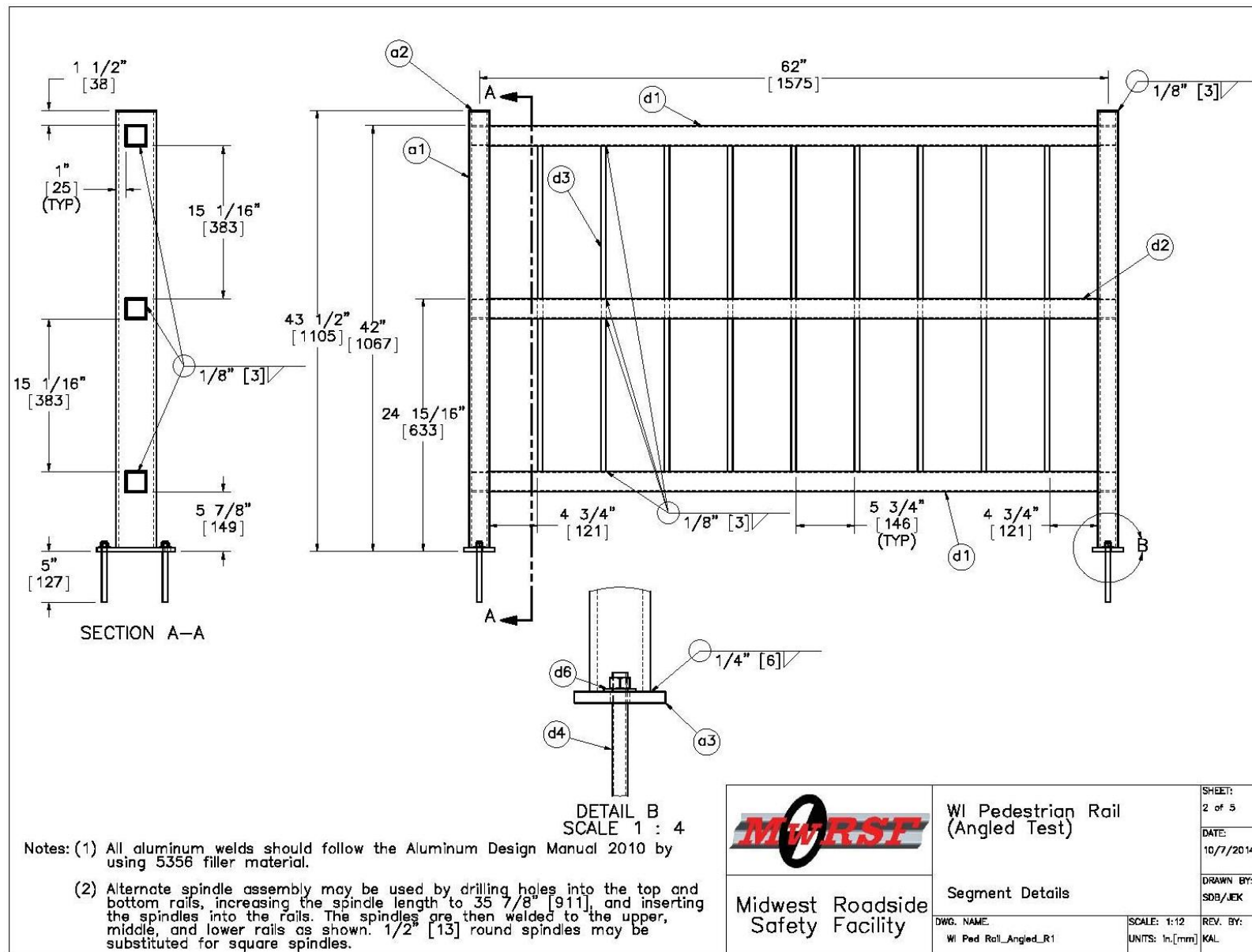


Figure 170. Pedestrian Rail Panel Details, Test Nos. APR-1 and APR-2


Item No.	QTY.	Description	Material Spec
a1	52	2"x4"x1/4" [51x102x6] Aluminum Post, 43" [1092] long	6061-T6
a2	52	Aluminum Post Cap - 1/8" [3] Plate	6061-T6
a3	52	Aluminum Post Base	6061-T6
d1	52	2"x2"x1/8" [51x51x3] Aluminum Rail - 63 1/2" [1613] long	6061-T6
d2	26	2"x2"x1/8" [51x51x3] Aluminum Rail - 63 1/2" [1613] long with holes	6061-T6
d3	234	1/2"x1/2" [13x13] Square Aluminum Spindle - 32 1/8" [816] long	6061-T6
d4	104	1/2" [13] Dia. UNC, 6" [152] Long Threaded Rod	ASTM A193 Grade B7
d5	104	1/2" [13] Dia. Steel Nut	ASTM A194 Grade 8M Galv.
d6	104	1/2" [13] Dia. Steel SAE Flat Washer	ASTM F436 Type 1 Galv.
d7	-	Epoxy	Powers Fasteners AC100+ Gold Minimum bond strength = 1,450 psi [10.0 MPa]
<div>  <div> <div>WI Pedestrian Rail (Angled Test)</div> <div>Bill of Materials</div> <div>Midwest Roadside Safety Facility</div> </div> <div> <div>DWG. NAME: WI Ped Rail_Angled_R1</div> <div>SCALE: None UNITS: In./mm</div> <div>REV. BY: KAL</div> </div> <div> <div>SHEET: 5 of 5</div> <div>DATE: 10/7/2014</div> <div>DRAWN BY: SDB/JEK</div> </div> </div>			

Figure 171. Bill of Materials, Test Nos. APR-1 and APR-2



Figure 172. Pedestrian Rail Test Installation



Figure 173. System Panels and Anchors, Test No. APR-1



Figure 174 Slots Cut in Baseplates to Aid in Rail Fabrication

13 FULL-SCALE CRASH TEST NO. APR-1

13.1 Test No. APR-1

The 2,428-lb (1,101-kg) small car impacted the aluminum pedestrian rail at a speed of 45.2 mph (72.7 km/h) and an angle of 25.1 degrees. A summary of the test results and sequential photographs are shown in Figure 175. Additional sequential photographs are shown in Figures 176 and 177. Documentary photographs of the crash test are shown in Figure 178.

13.2 Weather Conditions

Test no. APR-1 was conducted on October 24, 2014, at approximately 1:30 p.m. The weather conditions, as per the National Oceanic and Atmospheric Administration (station 14939/LNK), were reported and are shown in Table 13.

Table 13. Weather Conditions, Test No. APR-1

Temperature	74° F
Humidity	56%
Wind Speed	9 mph
Wind Direction	230° from True North
Sky Conditions	Partly Cloudy
Visibility	10.00 Statute Miles
Pavement Surface	Dry
Previous 3-Day Precipitation	0.66 in.
Previous 7-Day Precipitation	0.66 in.

13.3 Test Description

Initial vehicle impact was to occur with the centerline of the vehicle aligned with the centerline of the downstream post of panel no. 12, as shown in Figures 166 and 179. This location was selected in order to evaluate the potential for windshield damage as the result of a panel sliding up the hood and the debris field. The first point of vehicle contact was the second spindle upstream from the downstream post of panel no. 11. A sequential description of the impact events is contained in Table 14. The vehicle came to rest upright and 45.5 ft (13.9 m)

behind the centerline of panel no. 26. The vehicle trajectory and final position are shown in Figures 175 and 180.

Table 14. Sequential Description of Impact Events, Test No. APR-1

TIME (sec)	EVENT
0	Right side of front bumper contacted downstream end of panel no. 11
0.002	Right side of front bumper began to deform
0.010	Right fender began to deform
0.036	Vehicle began to yaw toward channelizer
0.042	Right-front tire overrode downstream end of panel no. 11
0.052	Panel no. 11 disengaged from post baseplates
0.056	Panel no. 12 disengaged from post baseplates
0.074	Front bumper contacted panel no. 13
0.082	Hood began to deform
0.102	Left fender began to deform
0.110	Right rear tire became airborne
0.114	Panel no. 13 disengaged from post baseplates
0.128	Panel no. 14 disengaged from post baseplates
0.138	Vehicle pitched downward
0.144	Upstream post of panel no. 15 disengaged from upstream post baseplate
0.176	Vehicle rolled slightly toward barrier
0.218	Left fender contacted panel no. 15
0.312	Right-rear tire contacted ground

13.4 System Damage

Damage to the pedestrian rail is shown in Figures 181 through 186. The welds fractured between the posts and baseplates on panel nos. 11 through 15, resulting in the panels disengaging from the baseplates. All anchors remained undamaged. The final locations of the disengaged panels are shown in Table 15.

All components of panel no. 11 remained intact, except the post welds fractured and the posts disengaged from the baseplates. The entire panel twisted slightly. The welds partially fractured at the upstream and downstream ends of the bottom and top horizontal rails, the downstream end of the middle horizontal rail, and around some of the spindles of panel no. 11. The upstream end of the middle rail and downstream end of the top rail partially ruptured. The post baseplates encountered minor deformations. Contact marks were found on the lower portion of the downstream post.

Panel no. 12 remained intact, except the post welds fractured and the posts disengaged from the baseplates and five spindles disengaged. The entire panel twisted slightly. The welds partially fractured on panel no. 12 at the upstream end of the bottom and middle horizontal rails, the downstream end of the middle horizontal rail, and around some of the spindles. The bottom horizontal rail tore at spindle locations. The post baseplates were bent. Contact marks were found on the upstream and front faces of the upstream post.

All components of panel no. 13 remained intact, except the post welds fractured and the posts disengaged from the baseplates. The panel was bent. The welds partially fractured at both the upstream and downstream ends of all three horizontal rails and the downstream post cap of panel no. 13. The downstream end of the bottom rail partially ruptured. The post baseplates were bent, and the downstream slot in the downstream post baseplate sheared. Dents were found on the upstream face of the upstream post and on the back face of the top rail. Contact marks were found on the top of the upstream post and on the upstream face of the upstream post near the bottom and middle horizontal rails.

All components of panel no. 14 remained intact, except the post welds fractured and the posts disengaged from the baseplates. The panel was bent. The welds fractured at both the

upstream and downstream ends of all three horizontal rails of panel no. 14. The post baseplates were bent.

All components of panel no. 15 remained intact, except the post welds fractured and the posts disengaged from the baseplates. The panel was bent. The welds fractured at both the upstream and downstream ends of all three horizontal rails and around some of the spindles of panel no. 15. The downstream end of the top rail tore. Some spindles were bent. The post baseplates were bent, and the downstream slot in the upstream post baseplate sheared.

All components of panel no. 16 remained intact. The panel was bent. The welds partially fractured at both the upstream and downstream ends of all three horizontal rails, except the downstream end of the top rail. Welds between the posts and the baseplates began to fracture; however, the posts remained attached to the baseplates. The downstream post baseplate was bent.

Table 15. Final Locations of Disengaged Panels, Test No. APR-1

Panel No.	Final Location	Reference Location
11	55 ft (16.8 m) behind system	Centerline of panel no. 13 (initial location)
12	70 ft (21.3 m) behind system	Centerline of panel no. 20
13	6 ft (1.8 m) behind system	Centerline of panel no. 23
14	29 ft (8.8 m) in front of system	Joint between panel nos. 13 and 14
15	13.5 ft (4.1 m) in front of system	Centerline of panel no. 15 (initial location)

13.5 Vehicle Damage

The damage to the vehicle was moderate, as shown in Figures 187 and 189. The maximum occupant compartment deformations are listed in Table 16 along with the deformation limits established in MASH for various areas of the occupant compartment. Note that none of the MASH-established deformation limits were violated. Occupant compartment damage is shown in Figure 189. Complete occupant compartment and vehicle deformations and the corresponding locations are provided in Appendix G.

The majority of the damage was concentrated on the front of the vehicle. The front plastic bumper disengaged and was fractured. The hood and front bumper were dented and deformed backward into the radiator. The right-front fender deformed outward, and the right headlight fractured. The right-front rim was dented, and the tire was torn and deflated. The right-front A-arm disengaged from the wheel. The left-front fender was dented and encountered contact marks behind the tire. The left headlight disengaged but remained attached by the cable. All window glass remained undamaged.

Table 16. Maximum Occupant Compartment Deformations by Location

LOCATION	MAXIMUM DEFORMATION in. (mm)	MASH ALLOWABLE DEFORMATION in. (mm)
Wheel Well & Toe Pan	¼ (6)	≤ 9 (229)
Floorpan & Transmission Tunnel	¼ (6)	≤ 12 (305)
Side Front Panel (in Front of A-Pillar)	½ (13)	≤ 12 (305)
Side Door (Above Seat)	½ (13)	≤ 9 (229)
Side Door (Below Seat)	¼ (6)	≤ 12 (305)
Roof	0 (0)	≤ 4 (102)
Windshield	0 (0)	≤ 3 (76)

13.6 Occupant Risk

The calculated occupant impact velocities (OIVs) and maximum 0.010-sec occupant ridedown accelerations (ORAs) in both the longitudinal and lateral directions are shown in Table 17. Note that the OIVs and ORAs were within the suggested limits provided in MASH. The calculated THIV, PHD, and ASI values are also shown in Table 17. The results of the occupant risk analysis, as determined from the accelerometer data, are summarized in Figure 175. The recorded data from accelerometers and rate transducers are shown graphically in Appendix H.

Note, the DTS unit was designated as the primary unit during this test, as it was mounted closer to the c.g. of the vehicle.

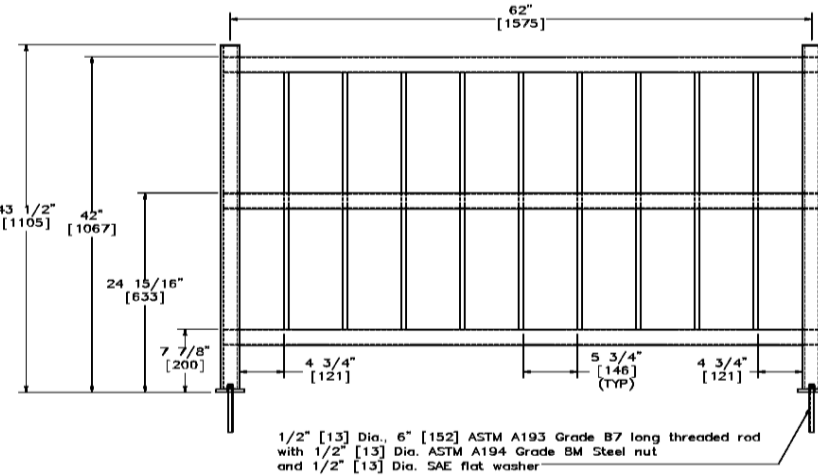
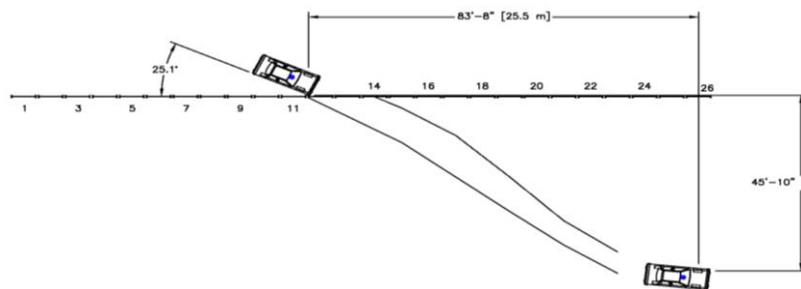
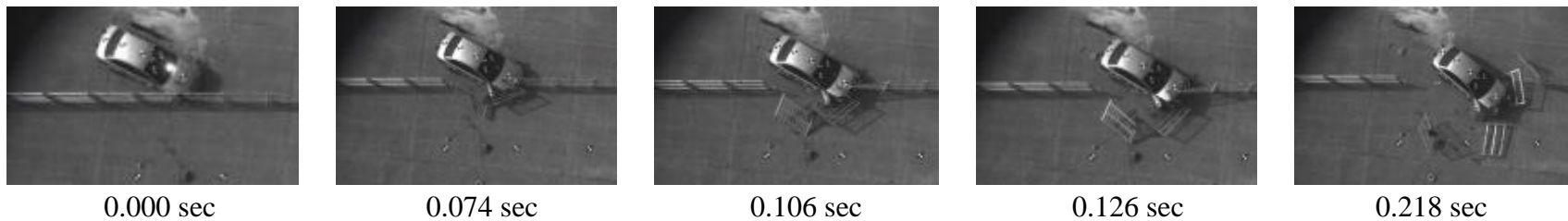
Table 17. Summary of OIV, ORA, THIV, PHD, and ASI Values, Test No. APR-1

Evaluation Criteria		Transducer		MASH Limits
		DTS (Primary)	SLICE-2	
OIV ft/s (m/s)	Longitudinal	-19.08 (-5.82)	-18.79 (-5.73)	≤ 40 (12.2)
	Lateral	3.89 (1.19)	2.89 (0.88)	≤40 (12.2)
ORA g's	Longitudinal	-1.85	-2.11	≤ 20.49
	Lateral	-3.33	-3.35	≤ 20.49
MAX. ANGULAR DISPL. deg.	Roll	10.61	-5.64	≤75
	Pitch	7.99	-1.82	≤75
	Yaw	50.72	51.33	not required
THIV ft/s (m/s)		20.26 (6.17)	20.08 (6.12)	not required
PHD g's		3.65	3.79	not required
ASI		0.62	0.60	not required

13.7 Discussion

The analysis of the test results for test no. APR-1 showed that the pedestrian rail allowed controlled penetration of the 1100C vehicle through the longitudinal channelizer. Neither detached elements nor fragments showed potential for penetrating the occupant compartment or for presenting undue hazard to other traffic. Note, none of the pedestrian rail panels went over the hood, near the windshield, or underneath the vehicle. Deformations of, or intrusions into, the occupant compartment that could have caused serious injury did not occur. The OIVs and ORAs were within the suggested limits provided in MASH. The test vehicle remained upright during

and after the collision. Vehicle roll, pitch, and yaw angular displacements, as shown in Appendix I, were deemed acceptable, because they did not adversely influence occupant risk safety criteria or cause rollover. After impact, the vehicle penetrated behind the channelizer. Therefore, test no. APR-1 was determined to be acceptable according to the MASH safety performance criteria for longitudinal channelizers, test designation no. 2-90.



- Test AgencyMwRSF
- Test Number.....APR-1
- Date.....10/24/14
- MASH Test Designation2-90
- Test Article.....Aluminum Pedestrian Rail
- Total Length150 ft (45.7 m)
- Vehicle Make /Model.....2006 Kia Rio
 - Curb.....2,421 lb (1,098 kg)
 - Test Inertial.....2,428 lb (1,101 kg)
 - Gross Static.....2,599 lb (1,179 kg)
- Impact Conditions
 - Speed45.2 mph (72.7 km/h)
 - Angle25.1 deg
 - Impact Location.....Spindle no. 8 of panel no. 11
- Impact Severity (IS)29.8 kip-ft (40.5 kJ) > 25 kip-ft (34.2 kJ)
- Exit Conditions
 - SpeedNot Applicable, Longitudinal Channelizer
 - AngleNot Applicable, Longitudinal Channelizer
- Vehicle Stability.....Satisfactory
- Vehicle Stopping Distance83 ft – 8 in. (25.5 m) downstream of impact
 -45 ft – 10 in. (14.0 m) laterally behind
- Vehicle DamageModerate
 - VDS [46]1-FR-5
 - CDC [47]01-FRLN-1
 - Maximum Interior Deformation1/2 in. (13 mm)
- Test Article Damage.....Moderate
- Maximum Test Article Deflections
 - Permanent Set.....Not Applicable, Longitudinal Channelizer
 - DynamicNot Applicable, Longitudinal Channelizer
 - Working Width.....Not Applicable, Longitudinal Channelizer

• Transducer Data

Evaluation Criteria		Transducer		MASH Limit
		DTS (Primary)	SLICE-2	
OIV ft/s (m/s)	Longitudinal	-19.08 (-5.82)	-18.79 (-5.73)	≤ 40 (12.2)
	Lateral	3.89 (1.19)	2.89 (0.88)	≤ 40 (12.2)
ORA g's	Longitudinal	-1.85	-2.11	≤ 20.49
	Lateral	-3.33	-3.35	≤ 20.49
MAX ANGULAR DISP. deg.	Roll	10.61	-5.64	≤ 75
	Pitch	7.99	-1.82	≤ 75
	Yaw	50.72	51.33	Not required
THIV – ft/s (m/s)		20.26 (6.17)	20.08 (6.12)	Not required
PHD – g's		3.65	3.79	Not required
ASI		0.62	0.60	Not required

Figure 175. Summary of Test Results and Sequential Photographs, Test No. APR-1



0.000 sec



0.040 sec



0.060 sec



0.130 sec



0.312 sec



0.502 sec



0.000 sec



0.042 sec



0.094 sec



0.122 sec



0.176 sec



0.502 sec

Figure 176. Additional Sequential Photographs, Test No. APR-1



0.000 sec



0.036 sec



0.060 sec



0.110 sec



0.176 sec



0.502 sec



0.000 sec



0.040 sec



0.082 sec



0.128 sec



0.176 sec



0.312 sec

Figure 177. Additional Sequential Photographs, Test No. APR-1



Figure 178. Documentary Photographs, Test No. APR-1

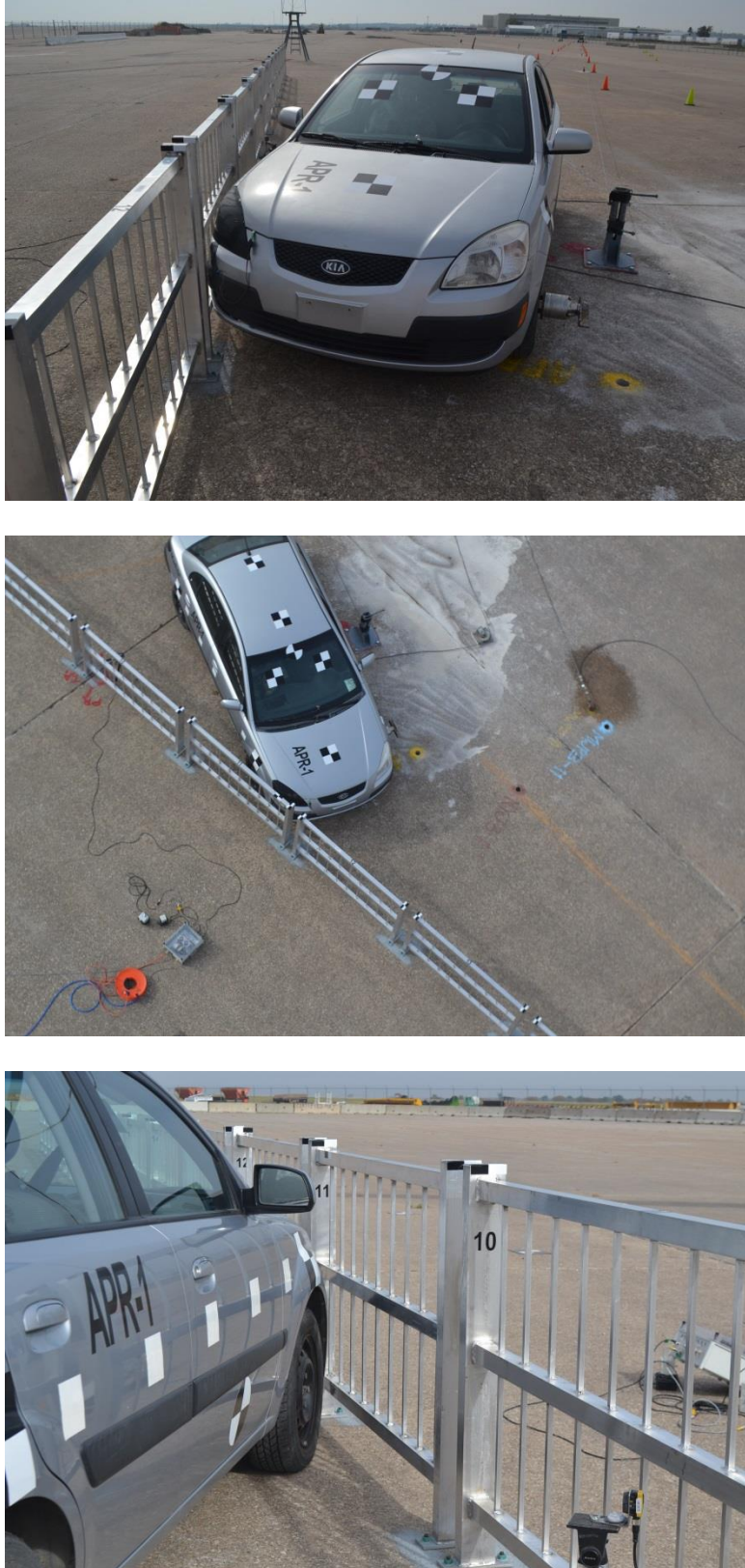


Figure 179. Impact Location, Test No. APR-1



Figure 180. Vehicle Final Position and Trajectory Marks, Test No. APR-1



Figure 181. System Damage, Test No. APR-1



Figure 182. Panel No. 11 Damage, Test No. APR-1



Figure 183. Panel No. 12 Damage, Test No. APR-1



Figure 184. Panel No. 13 Damage, Test No. APR-1



Figure 185. Panel No. 14 Damage, Test No. APR-1



Figure 186. Panel No. 15 Damage, Test No. APR-1

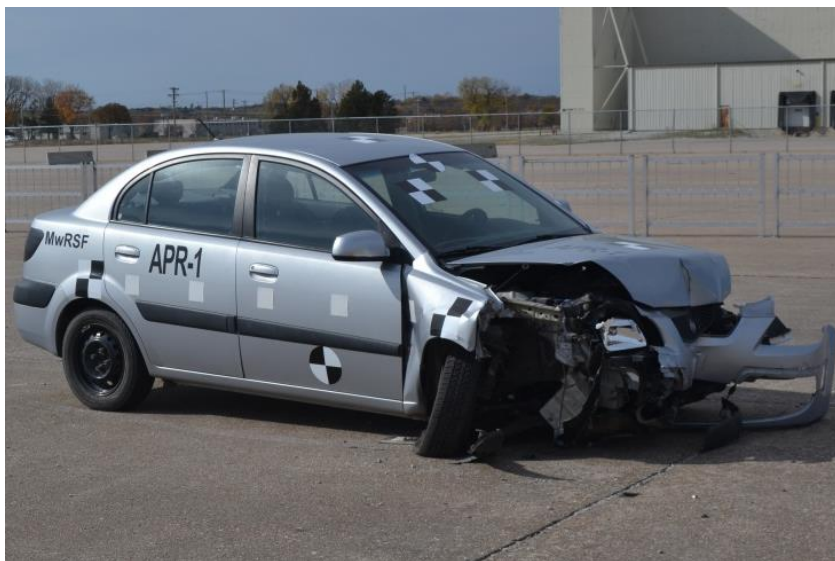


Figure 187. Vehicle Damage, Test No. APR-1

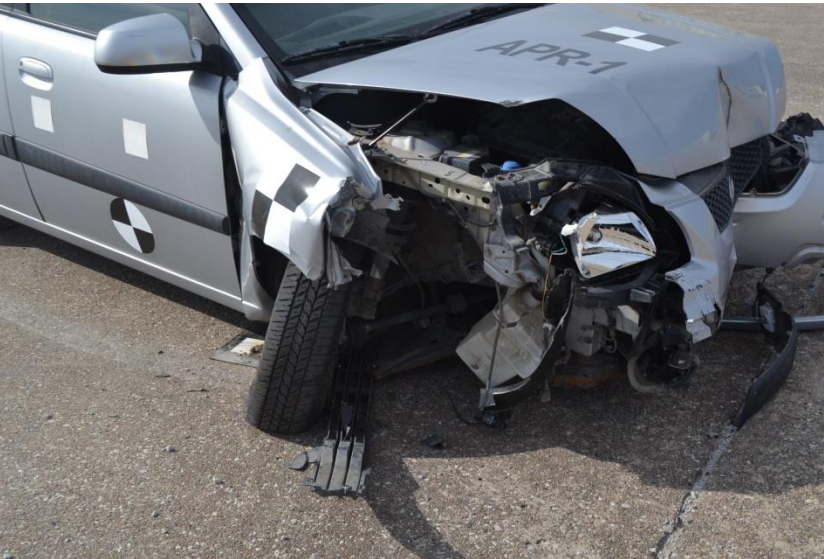


Figure 188. Vehicle Damage, Test No. APR-1

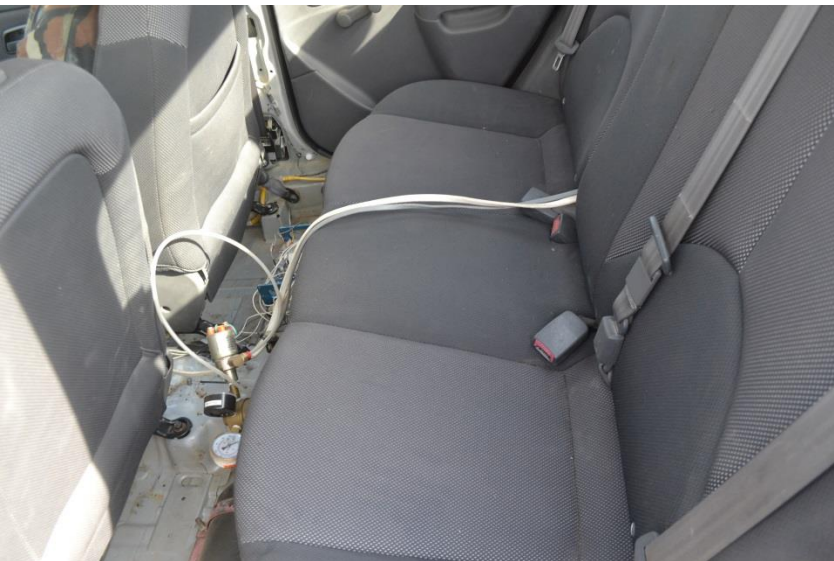
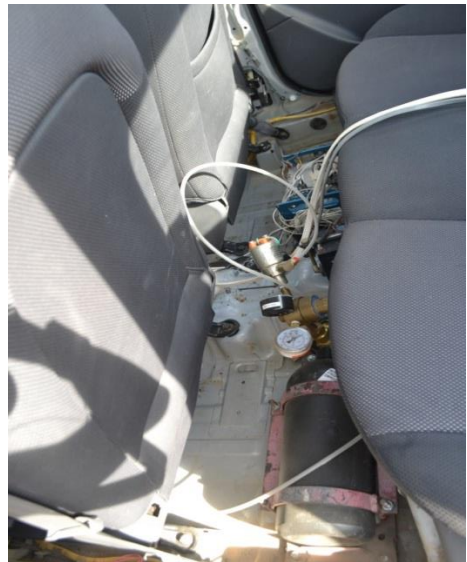


Figure 189. Occupant Compartment Damage, Test No. APR-1

14 FULL-SCALE CRASH TEST NO. APR-2

14.1 Test No. APR-2

The 2,437-lb (1,105-kg) small car impacted the aluminum pedestrian rail at a speed of 44.5 mph (71.6 km/h) and an angle of 0 degrees. A summary of the test results and sequential photographs are shown in Figure 190. Additional sequential photographs are shown in Figures 191 and 192. Documentary photographs of the crash test are shown in Figure 193.

14.2 Weather Conditions

Test no. APR-2 was conducted on November 12, 2014, at approximately 2:15 p.m. The weather conditions, as per the National Oceanic and Atmospheric Administration (station 14939/LNK), were reported and are shown in Table 18.

Table 18. Weather Conditions, Test No. APR-2

Temperature	23° F
Humidity	48%
Wind Speed	20 mph
Wind Direction	320° from True North
Sky Conditions	Sunny
Visibility	10.00 Statute Miles
Pavement Surface	Dry
Previous 3-Day Precipitation	0.06 in.
Previous 7-Day Precipitation	0.07 in.

14.3 Test Description

Initial vehicle impact was to occur with the centerline of the vehicle aligned with the centerline of the upstream post of panel no. 1, as shown in Figures 167 and 194. This location was selected in order to evaluate the potential for windshield and roof damage, vehicle instability, occupant risk, and the debris field. The actual point of impact was the centerline of the upstream post of panel no. 1. A sequential description of the impact events is contained in Table 19. The vehicle came to rest 15 ft – 11 in. (4.9 m) upstream from the upstream post of

panel no. 10 and parallel to the centerline of the system. The vehicle trajectory and final position are shown in Figures 190 and 195.

Table 19. Sequential Description of Impact Events, Test No. APR-2

TIME (sec)	EVENT
0	Front bumper contacted upstream post of panel no. 1
0.002	Front bumper deformed
0.006	Hood deformed
0.014	Downstream post of panel no. 1 contacted upstream post of panel no. 2
0.024	Panel no. 1 disengaged from post baseplates
0.030	Downstream post of panel no. 2 contacted upstream post of panel no. 3
0.038	Downstream post of panel no. 3 contacted upstream post of panel no. 4
0.044	Panel no. 2 disengaged from post baseplates
0.050	Downstream post of panel no. 4 contacted upstream post of panel no. 5
0.054	Panel no. 3 disengaged from post baseplates
0.060	Downstream post of panel no. 5 contacted upstream post of panel no. 6
0.068	Panel no. 4 disengaged from post baseplates
0.070	Downstream post of panel no. 6 contacted upstream post of panel no. 7
0.078	Panel no. 5 disengaged from post baseplates
0.088	Downstream post of panel no. 7 contacted upstream post of panel no. 8
0.216	Panel no. 1 overrode hood
0.268	Panel no. 2 overrode hood
0.342	Panel no. 3 overrode hood
0.364	Front bumper contacted upstream post of panel no. 4
0.476	Front bumper contacted upstream post of panel no. 5
0.684	Panel no. 6 disengaged from post baseplates
0.710	Downstream post of panel no. 8 contacted upstream post of panel no. 9
0.872	Panel no. 7 disengaged from post baseplates
0.892	Downstream post of panel no. 9 contacted upstream post of panel no. 10
0.908	Panel no. 8 disengaged from post baseplates
1.580	Front bumper contacted upstream post of panel no. 9
1.592	Panel no. 9 disengaged from post baseplates
1.774	Vehicle stopped and began to roll backward

14.4 System Damage

Damage to the pedestrian rail is shown in Figures 196 through 206. The welds fractured between the posts and baseplates for panel nos. 1 through 9, resulting in the panels disengaging away from the baseplates. Panel nos. 1 through 9 otherwise remained intact and were bent. All anchors remained undamaged. The final locations of the disengaged panels are shown in Table 20.

Panel no. 1 had fractured welds at the downstream end of the middle and top rails and the bottom of the vertical spindles. The upstream post fractured above the bottom rail. The downstream post also fractured, but this occurred below the middle rail. The downstream end of the bottom rail tore. All spindles bent.

Panel nos. 2, 3, 4, and 5 had fractured welds at the upstream end of the bottom, middle, and top horizontal rails, the downstream end of the middle and top rails, and the bottom of some vertical spindles. The upstream and downstream posts fractured below the middle rail on panel nos. 2 through 5. The downstream end of the bottom rail tore on panel nos. 2 through 5. All spindles on panel nos. 2 through 5 bent. Gouges were found on the bottom rail of panel no. 5.

Panel no. 6 had fractured welds at the upstream end of the bottom, middle, and top rails and the downstream end of the middle and top rails. The upstream post fractured below the middle rail. The downstream post bent at the middle rail. The downstream end of the bottom rail tore. The middle of all three rails bent and tore. The top rail had a $\frac{5}{8}$ -in. (16-mm) diameter hole near the downstream post. All spindles bent and one spindle fractured.

The downstream post of panel no. 7 fractured and bent below the middle rail. The upstream post bent at the middle rail. The upstream and downstream ends of the bottom, middle, and top rails tore. Gouges were found on the upstream face of the downstream post. All spindles bent.

Panel no. 8 had fractured welds at the upstream end of the bottom, middle, and top rails and the downstream end of the middle and top rails. The downstream end of the bottom rail tore. The upstream and downstream posts bent at the middle rail. All spindles bent.

The horizontal rails of panel no. 9 buckled near their midspans. The bottom and middle rails tore near the middle. Welds fractured at the upstream end of the bottom, middle, and top rails and the downstream end of the middle rail. The downstream post bent at the middle rail. Significant gouging was found on the upstream post. All spindles bent.

Panel no. 10 remained intact, and the panel remained attached to both baseplates. The entire panel was bent. The welds partially fractured at the upstream and downstream ends of the bottom, middle, and top rails and at the upstream and downstream baseplates. The upstream and downstream posts were bent.

Table 20. Final Location of Disengaged Panels, Test No. APR-2

Panel No.	Final Location	Reference Location Centerline of upstream post on panel no. 10
1	39 ft (11.9 m) right of system	35 ft (10.7 m) upstream
2	4 ft (1.2 m) right of system	30 ft (9.1 m) upstream
3	5 ft (1.5 m) left of system	30 ft (9.1 m) upstream
4	21 ft (6.4 m) right of system	16 ft (4.9 m) downstream
5	6 ft (1.8 m) left of system	6 ft (1.8 m) upstream
6	8.5 ft (2.6 m) right of system	2 ft (0.6 m) downstream
7	30 ft (9.1 m) right system	5 ft (1.5 m) downstream
8	32 ft (9.8 m) right of system	7 ft (2.1 m) upstream
9	2.5 ft (0.8 m) left of system	2.7 ft (0.8 m) upstream

14.5 Vehicle Damage

The damage to the vehicle was moderate, as shown in Figures 207 through 210. The maximum occupant compartment deformations are listed in Table 21 along with the deformation limits established in MASH for various areas of the occupant compartment. Note that none of the MASH-established deformation limits were violated. Occupant compartment damage is shown

in Figure 209. Complete occupant compartment and vehicle deformations and the corresponding locations are provided in Appendix G.

The majority of the damage was concentrated on the front of the vehicle. The front plastic bumper disengaged and fractured. The entire front end, including the radiator supports and steel bumper, crushed inward. The hood was bent and deformed upward. Both the right-front and left-front fenders were bent, deformed, and dented. Both headlights were fractured and disengaged but remained attached by the cables. Contact marks were found on the hood and on the undercarriage of the vehicle. The lower-right corner of the windshield was cracked.

Table 21. Maximum Occupant Compartment Deformations by Location

LOCATION	MAXIMUM DEFORMATION in. (mm)	MASH ALLOWABLE DEFORMATION in. (mm)
Wheel Well & Toe Pan	$\frac{3}{8}$ (9.5)	≤ 9 (229)
Floorpan & Transmission Tunnel	$\frac{1}{4}$ (6.4)	≤ 12 (305)
Side Front Panel (in Front of A-Pillar)	$\frac{1}{4}$ (6.4)	≤ 12 (305)
Side Door (Above Seat)	0 (0)	≤ 9 (229)
Side Door (Below Seat)	$\frac{1}{4}$ (6.4)	≤ 12 (305)
Roof	0 (0)	≤ 4 (102)
Windshield	0 (0)	≤ 3 (76)

14.6 Occupant Risk

The calculated occupant impact velocities (OIVs) and maximum 0.010-sec occupant ridedown accelerations (ORAs) in both the longitudinal and lateral directions are shown in Table 22. The calculated THIV, PHD, and ASI values are also shown in Table 22. The results of the occupant risk analysis, as determined from the accelerometer data, are summarized in Figure 190. The recorded data from the accelerometers and the rate transducers are shown graphically in Appendix I. Note, the DTS unit was designated as the primary unit during this test as it was mounted closer to the c.g. of the vehicle.

Table 22. Summary of OIV, ORA, THIV, PHD, and ASI Values, Test No. APR-2

Evaluation Criteria		Transducer		MASH Limits
		SLICE-2	DTS (Primary)	
OIV ft/s (m/s)	Longitudinal	-21.95 (-6.69)	-21.69 (-6.61)	≤ 40 (12.2)
	Lateral	-0.23 (-0.07)	-1.19 (-0.36)	≤40 (12.2)
ORA g's	Longitudinal	-20.91	-19.41	≤ 20.49
	Lateral	-6.74	-3.87	≤ 20.49
MAX. ANGULAR DISPL. deg.	Roll	-2.07	8.63	≤75
	Pitch	3.93	17.68	≤75
	Yaw	-1.88	9.57	not required
THIV ft/s (m/s)		21.95 (6.69)	21.79 (6.64)	not required
PHD g's		20.91	19.5	not required
ASI		0.9	0.87	not required

14.7 Discussion

The analysis of the test results for test no. APR-2 showed that the pedestrian rail allowed controlled penetration of the 1100C vehicle through the longitudinal channelizer. Neither detached elements nor fragments showed potential for penetrating the occupant compartment or for presenting undue hazard to other traffic. Deformations of, or intrusions into, the occupant compartment that could have caused serious injury did not occur. The test vehicle remained upright during and after the collision and came to rest within the longitudinal line of the channelizer. Vehicle roll, pitch, and yaw angular displacements, as shown in Appendix I, were deemed acceptable, because they did not adversely influence occupant risk safety criteria or cause rollover.

The longitudinal ORA for the backup accelerometer unit was greater than the specified MASH limit. The test results revealed that the pedestrian rail system imparted a high longitudinal ORA to the hypothetical vehicle occupants when struck end-on. The longitudinal ORA from the DTS (the primary accelerometer unit) was 19.41 g's, while the longitudinal ORA from the SLICE-2 (the backup accelerometer unit) was 20.91 g's.

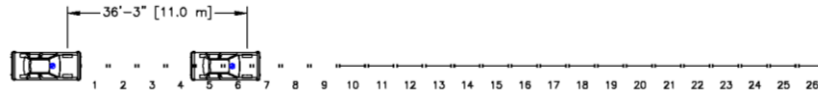
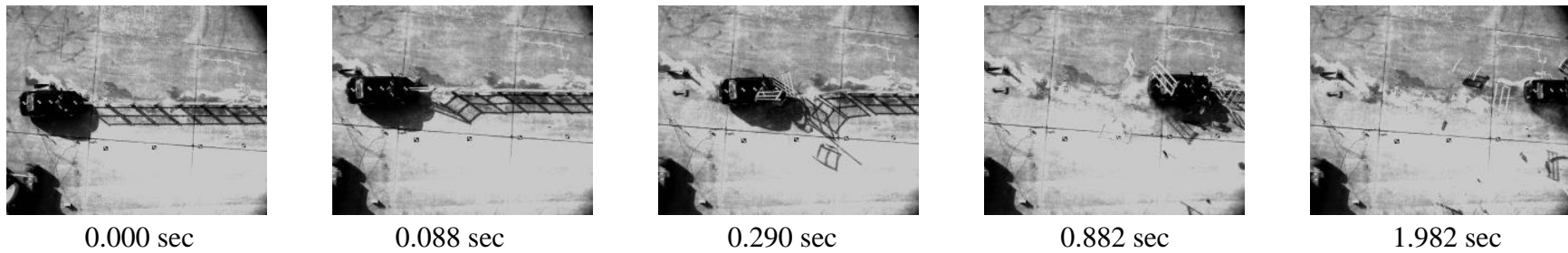
During this testing program, there was no existing guidance or policy within the crash test laboratories regarding comparison of accelerations from different transducer units used during the same test near the c.g. of a test vehicle or which value to choose if the values varied. Consequently, feedback was sought from FHWA in February 2015. Following the discussion with FHWA and quoting them directly,

“We’ve not seen this situation before (i.e., 2 conflicting accel readings). After review of video, we certainly agree with your detailed assessment of test in regards to acceleration spike. As there is no existing policy for comparing accelerations from different transducer units on same test, we feel it best to recognize the implication of a higher value.”

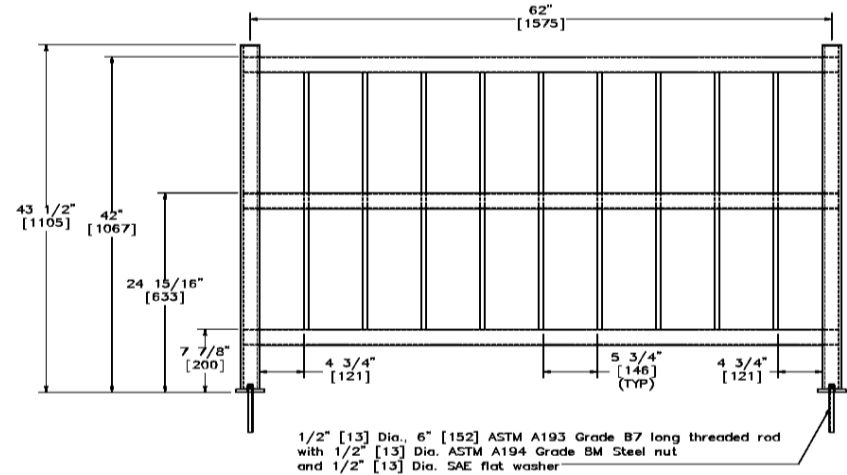
The documentation of the correspondence with FHWA is shown in Appendix J. Based on the FHWA response, test no. APR-2 was initially determined to be unacceptable according to the MASH safety performance criteria for longitudinal channelizers, test designation no. 2-90.

Cases where varying occupant risk results were acquired from different accelerometer systems was addressed with other crash test laboratories during the AASHTO Task Force 13 Subcommittee #7 meeting on April 30, 2015 in Lincoln, Nebraska. During this discussion, the crash test laboratories and FHWA came to a consensus that the results from the primary accelerometer unit would be reported. The primary accelerometer unit is defined as the unit placed closest to the c.g. More detailed information on this discussion can be found in the minutes from the April 2015 AASHTO Task Force 13 Subcommittee #7 meeting shown in Appendix J. Under this guidance, the primary accelerometer unit provided a longitudinal ORA

value below the MASH limit. Therefore, test no. APR-2 was subsequently determined to be acceptable according to the MASH safety performance criteria for longitudinal channelizers, test designation no. 2-90.



- Test AgencyMwRSF
- Test Number.....APR-2
- Date11/12/14
- MASH Test Designation2-90
- Test Article.....Aluminum Pedestrian Rail
- Total Length150 ft (45.7 m)
- Vehicle Make /Model.....2006 Kia Rio
 - Curb.....2,424 lb (1,100 kg)
 - Test Inertial.....2,437 lb (1,105 kg)
 - Gross Static.....2,599 lb (1,179 kg)
- Impact Conditions
 - Speed44.5 mph (71.6 km/h)
 - Angle0 deg
 - Impact Location.....Upstream post of Panel No. 1
- Impact Severity (IS)161.1 kip-ft (218.4 kJ) > 141 kip-ft (191 kJ)
- Exit Conditions
 - SpeedNot Applicable, Longitudinal Channelizer
 - AngleNot Applicable, Longitudinal Channelizer
- Vehicle Stability.....Satisfactory
- Vehicle Stopping Distance36 ft – 3 in. (11.05 m) downstream of impact
- Vehicle Damage.....Moderate
 - VDS [46]12-FC-7
 - CDC [47]12-FCLN-2
 - Maximum Interior Deformation $\frac{3}{8}$ in. (9.5 mm)
- Test Article Damage.....Moderate
- Maximum Test Article Deflections
 - Permanent Set.....Not Applicable, Longitudinal Channelizer
 - DynamicNot Applicable, Longitudinal Channelizer
 - Working Width.....Not Applicable, Longitudinal Channelizer



• Transducer Data

Evaluation Criteria		Transducer		MASH Limit
		SLICE-2	DTS (primary)	
OIV ft/s (m/s)	Longitudinal	-21.95 (-6.69)	-21.69 (-6.61)	≤ 40 (12.2)
	Lateral	-0.23 (-0.07)	-1.19 (-0.36)	≤ 40 (12.2)
ORA g's	Longitudinal	-20.91	-19.41	≤ 20.49
	Lateral	-6.74	-3.87	≤ 20.49
MAX ANGULAR DISP. deg.	Roll	-2.07	8.63	≤ 75
	Pitch	3.93	17.68	≤ 75
	Yaw	-1.88	9.57	not required
THIV – ft/s (m/s)		21.95 (6.69)	21.79 (6.64)	not required
PHD – g's		20.91	19.5	not required
ASI		0.9	0.87	not required

Figure 190. Summary of Test Results and Sequential Photographs, Test No. APR-2



0.000 sec



0.088 sec



0.426 sec



0.684 sec



0.972 sec



1.172 sec



0.000 sec



0.096 sec



0.324 sec



0.724 sec



1.424 sec



1.824 sec

Figure 191. Additional Sequential Photographs, Test No. APR-2



0.000 sec



0.070 sec



0.326 sec



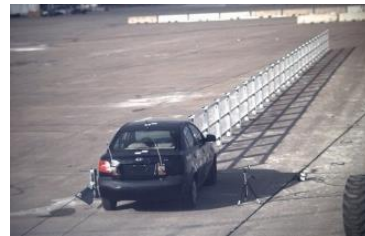
0.892 sec



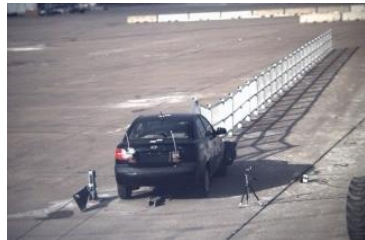
1.408 sec



1.874 sec



0.000 sec



0.078 sec



0.278 sec



0.626 sec



1.126 sec



1.626 sec

Figure 192. Additional Sequential Photographs, Test No. APR-2

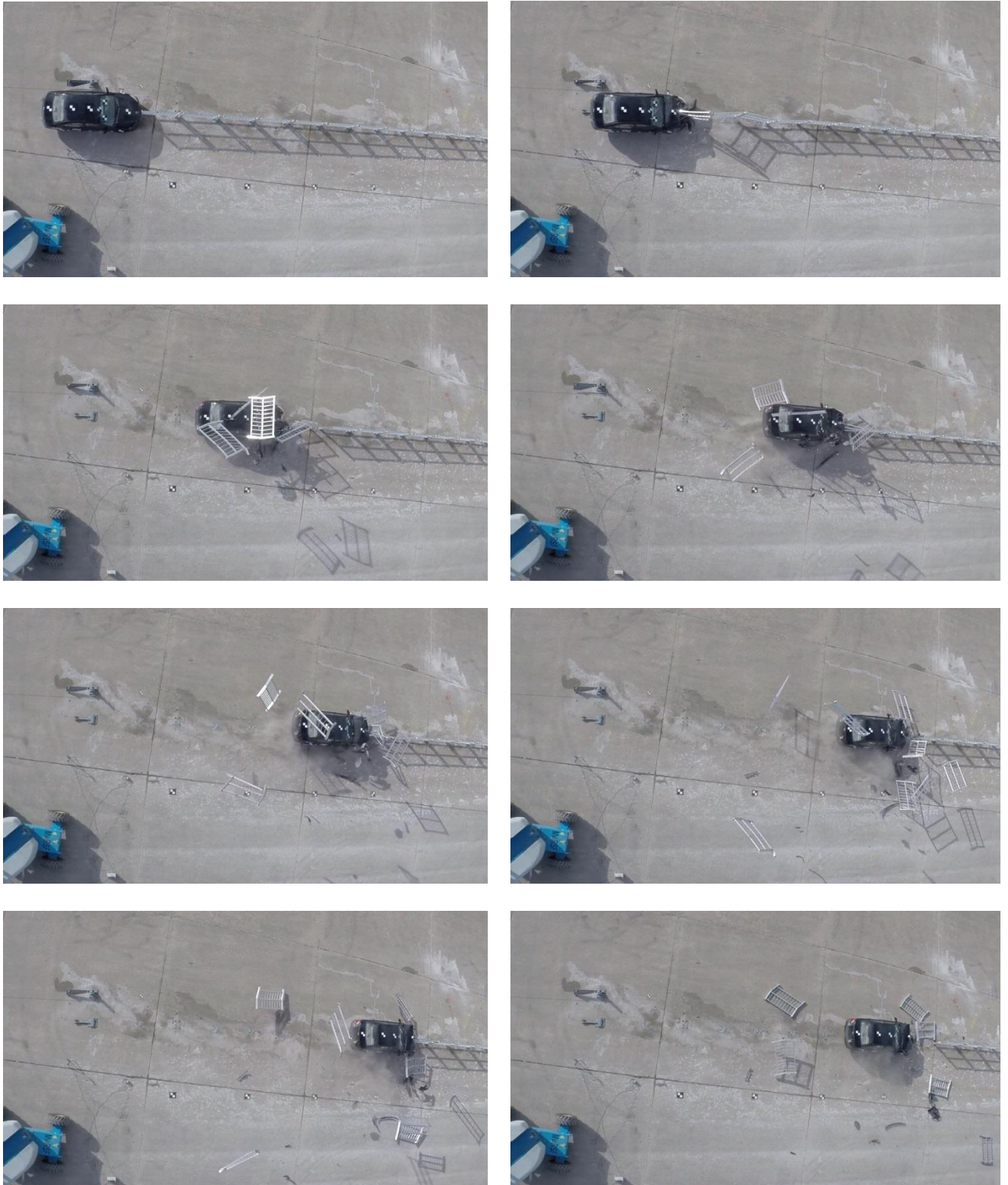


Figure 193. Documentary Photographs, Test No. APR-2



Figure 194. Impact Location, Test No. APR-2



Figure 195. Vehicle Final Position and Trajectory Marks, Test No. APR-2



Figure 196. System Damage, Test No. APR-2



Figure 197. Panel No. 1 Damage, Test No. APR-2



Figure 198. Panel No. 2 Damage, Test No. APR-2



Figure 199. Panel No. 3 Damage, Test No. APR-2



Figure 200. Panel No. 4 Damage, Test No. APR-2



Figure 201. Panel No. 5 Damage, Test No. APR-2



Figure 202. Panel No. 6 Damage, Test No. APR-2



Figure 203. Panel No. 7 Damage, Test No. APR-2



Figure 204. Panel No. 8 Damage, Test No. APR-2

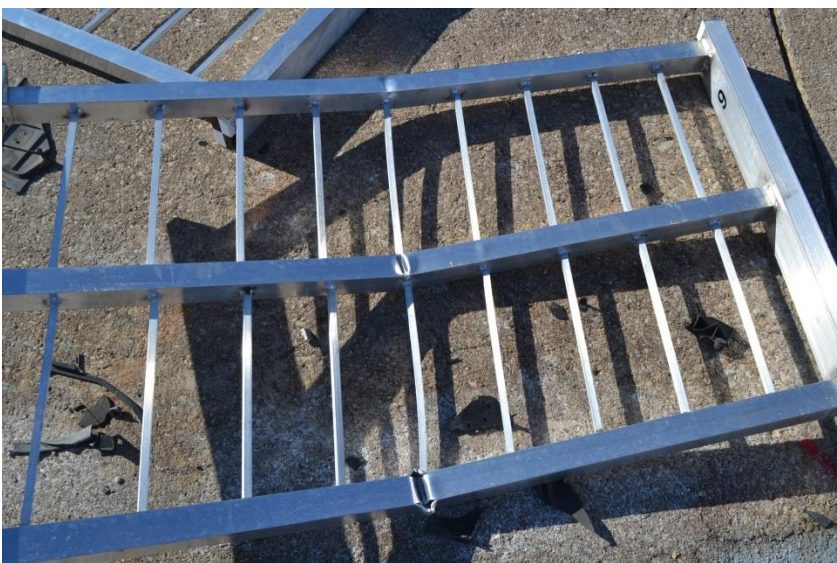


Figure 205. Panel No. 9 Damage, Test No. APR-2



Figure 206. Panel No. 10 Damage, Test No. APR-2



Figure 207. Vehicle Damage, Test No. APR-2



Figure 208. Vehicle Damage, Test No. APR-2



Figure 209. Occupant Compartment Damage, Test No. APR-2



Figure 210. Vehicle Undercarriage Damage, Test No. APR-2

15 SUMMARY, CONCLUSIONS, AND RECOMMENDATIONS

The objective of this study was to design a crashworthy pedestrian rail that will protect pedestrians from hazards while not posing undue safety risk to motorists and pedestrians. The new pedestrian rail was to meet the design standards of the ADA, the AASHTO *LRFD Bridge Design Specifications*, and the AASHTO MASH TL-2 safety performance evaluation criteria for longitudinal channelizers.

After a literature review was completed on existing pedestrian rail systems and commercially-available railings, twenty-five pedestrian rail concepts were considered and included various materials, such as steel, PVC, wood, HDPE, and FRP. During this design phase, the geometry and structural capacity of the pedestrian rail concepts were investigated to meet the AASHTO *LRFD Bridge Design Specifications*.

After sponsor review of the original concepts, several prototypes and material options were eliminated. Concepts were refined based on aesthetics, strength, weight, cost, and workability. Eight concepts, including two modular aluminum, two welded aluminum, two PVC, and two wood, were further developed using simplified load cases. After sponsor review, the aluminum concepts were further refined into four concepts and designed. Each component of the systems, including rails, posts, and infill members, post-to-rail, post-to-base, and infill-to-rail connections, and anchorages, were configured.

Seven dynamic bogie tests were conducted on four aluminum pedestrian rail concepts. Each system was configured as a two-panel system, impacted at approximately 45 mph (72.4 km/h) and evaluated in two different impact orientations, except for the fourth concept (test no. WIPR-4). Each system was impacted at a 25-degree angle and within the spindle region of the first panel. Next, each system was impacted using an end-on orientation. For test no. WIPR-4, only the end-on orientation was evaluated.

Each system broke away as designed. The concept of a post welded to a baseplate seemed to fracture more cleanly at the base than the concept involving a post inserted into a socket that was welded to the baseplate. Minor permanent deformation was found on all the baseplates. An increased anchor diameter of ½ in. (12.7 mm) eliminated permanent anchor deformations. Shifting the middle rail downward, closer toward the bumper heights of the pickup truck and small car, minimized component damage and allowed the system to behave more like a rigid frame. The factors that helped to improve system behavior included: (1) lowering the middle horizontal rail; (2) extending the spindles from the top to bottom rails and passing the spindles through the middle rail; (3) increasing anchor diameter to ½ in. (12.7 mm); and (4) inserting the rails into cutouts in the posts. Thus, design concept AW2-D (test no. WIPR-4) was recommended to be evaluated through full-scale vehicle crash testing according to the MASH TL-2 safety performance criteria for longitudinal channelizers.

Two full-scale vehicle crash tests were conducted on the pedestrian rail according to the TL-2 safety performance criteria found in MASH for longitudinal channelizers. Test no. APR-1, test designation no. 2-90, consisted of an 1100C small car impacting the pedestrian rail at a speed of 45.2 mph (72.7 km/h) and an angle of 25.1 degrees within the system. The pedestrian rail allowed controlled penetration of the 1100C vehicle through the longitudinal channelizer. Neither detached elements nor fragments showed potential for penetrating the occupant compartment or for presenting undue hazard to other traffic. Note, none of the pedestrian rail panels went over the hood, near the windshield, or underneath the vehicle. Deformations of, or intrusions into, the occupant compartment that could have caused serious injury did not occur. The OIVs and ORAs were within the suggested limits provided in MASH. The test vehicle remained upright during and after the collision. After impact, the vehicle penetrated behind the

channelizer. Therefore, test no. APR-1 was determined to be acceptable according to the MASH safety performance criteria for longitudinal channelizers, test designation no. 2-90.

Test no. APR-2, test designation no. 2-90, consisted of an 1100C small car impacting the pedestrian rail on its upstream end at a speed of 44.5 mph (71.6 km/h) and an angle of 0 degrees. The test vehicle remained upright during and after the collision and came to rest within the longitudinal line of the channelizer. The test results revealed that the pedestrian rail system imparted a high longitudinal ORA to the hypothetical vehicle occupants when struck end-on. The longitudinal ORA from the DTS (the primary accelerometer unit) was 19.41 g's, while the longitudinal ORA from the SLICE-2 (the backup accelerometer unit) was 20.91 g's. Thus, the primary accelerometer produced an acceptable longitudinal ORA according to MASH, while the backup accelerometer was unacceptable.

During this testing program, there was no existing guidance or policy within the crash test laboratories regarding comparison of accelerations from different transducer units used within the same test vehicle or which value to choose if the values varied. Consequently, feedback was sought from FHWA in February 2015. Following the discussion with FHWA and quoting them directly,

“We’ve not seen this situation before (i.e., 2 conflicting accel readings). After review of video, we certainly agree with your detailed assessment of test in regards to acceleration spike. As there is no existing policy for comparing accelerations from different transducer units on same test, we feel it best to recognize the implication of a higher value.”

The documentation of the correspondence with FHWA is shown in Appendix J. Therefore, test no. APR-2 was initially determined to be unacceptable according to the MASH safety performance criteria for longitudinal channelizers, test designation no. 2-90.

Cases where varying occupant risk results were acquired from different accelerometer systems was addressed with other crash test laboratories during the AASHTO Task Force 13

Subcommittee #7 meeting on April 30, 2015 in Lincoln, Nebraska. During the discussion, the crash test laboratories and FHWA came to a consensus that the results from the primary accelerometer unit would be reported. The primary accelerometer unit is defined as the unit placed closest to the c.g. More detailed information on this discussion can be found in the minutes from the April 2015 AASHTO Task Force 13 Subcommittee #7 meeting. Under this guidance, the accelerometer unit that was considered the primary unit provided a longitudinal ORA below the MASH limit. As such, test no. APR-2 was subsequently determined to be acceptable according to the MASH safety performance criteria for longitudinal channelizers. A summary of the safety performance evaluation for each test is provided in Table 23.

The results from both test designation no. 2-90 crash tests were analyzed to determine if any test no. 2-91 crash tests would be required for the pedestrian rail system. In test no. 2-90 with an impact angle of 25 degrees (test no. APR-1), the small car did not have any instability or accelerations that were of concern. Thus, there were no concerns for excessive accelerations with the larger, more massive pickup truck conducted under test designation no. 2-91 at a 25-degree impact angle. Also, the pedestrian rails panels did not get above the hood, near the windshield, or traverse under the car, so occupant compartment deformation or penetration was not a concern given the geometry of the pickup truck.

In test no. 2-90 with an impact angle of 0 degrees (test no. APR-2), the small car did not have any instability concerns, although the accelerations were higher than desired. However, there were no concerns for excessive accelerations with the larger, more massive pickup truck conducted under test designation no. 2-91 at a 0-degree impact angle. In test no. APR-2, some panels shifted downstream, compressed against one another end-on, and buckled upward as a series. As a result, some panels were propelled upward, passing over the top of the small car, while other panels contacted the front of the engine hood. The front-end geometry of the pickup

truck is taller than that provided by the small car. Both the engine hood and bumper are higher relative to the ground. Thus, it is not believed that the pedestrian rail panels would become airborne as easily during an end-on, pickup truck crash event as compared to small car end-on impacts. With a higher load height, it is expected that the panels may displace more sideways rather than vertically. Even if some vertical panel displacement occurred, the panels would not likely be propelled at the windshield. Thus, there is no concern for occupant compartment penetration or deformation in tests with the pickup truck. Therefore, it is believed that test designation no. 2-91 is not necessary for this channelizer system.

The current as-tested system did not include ADA-compliant handrails, which may be required for some roadside applications. As such, further design and crash testing may be required to investigate the use of ADA-compliant handrails. In addition, the current system was tested on level terrain. Consequently, no information was ascertained as to the safety performance of this pedestrian rail placed on top of and behind roadside curbs as well as on sloped terrain. If this pedestrian rail is desired for use near curbs or sloped terrain, then it is recommended that further investigation and crash testing be performed.

Initially, it was believed that the pedestrian rail system could be configured with segmented panels with gaps or as a continuous system. The researchers configured and tested a segmented panel system as it was believed to be easier to install. However, the researchers do not currently recommend that this system be installed continuously due to concerns for loading multiple posts simultaneously and the potential for higher longitudinal ORAs when impacted end-on.

Although the pedestrian rail system met the requirements in MASH, it is recommended that the system be modified to improve its safety performance and lower the occupant risk measures. It may be useful to reduce the amount of flying debris that could cause additional risk

to pedestrians. However, it should be noted that channelizers do not provide positive protection between pedestrians and errant vehicles. Thus, the errant vehicle itself also poses a risk to pedestrians. In addition, it may be beneficial to consider other design modifications that reduce the tendency for panel segment to contact one another in the form of a longer compressed column. Such modifications may include staggered placement or post sections that allow for improved shedding of the upstream panel section under end-on impact events. Finally, future considerations should be directed toward inclusion of an ADA-compliant handrail that does not pose undue safety risk to motorists and pedestrians. Further crash testing may be required to accommodate these modifications.

Table 23. Summary of Safety Performance Evaluation Results

Evaluation Factors	Evaluation Criteria	Test No. APR-1	Test No. APR-2		
Structural Adequacy	C. Acceptable test article performance may be by redirection, controlled penetration, or controlled stopping of the vehicle.	S	S		
Occupant Risk	D. Detached elements, fragments or other debris from the test article should not penetrate or show potential for penetrating the occupant compartment, or present an undue hazard to other traffic, pedestrians, or personnel in a work zone. Deformations of, or intrusions into, the occupant compartment should not exceed limits set forth in Section 5.3 and Appendix E of MASH.	S	S		
	F. The vehicle should remain upright during and after collision. The maximum roll and pitch angles are not to exceed 75 degrees.	S	S		
	H. Occupant Impact Velocity (OIV) (see Appendix A, Section A5.3 of MASH for calculation procedure) should satisfy the following limits:	S	S		
	Occupant Impact Velocity Limits				
	Component			Preferred	Maximum
	Longitudinal and Lateral			30 ft/s (9.1 m/s)	40 ft/s (12.2 m/s)
	I. The Occupant Ridedown Acceleration (ORA) (see Appendix A, Section A5.3 of MASH for calculation procedure) should satisfy the following limits:	S	S*		
Occupant Ridedown Acceleration Limits					
Component	Preferred			Maximum	
Longitudinal and Lateral	15.0 g's			20.49 g's	
Vehicle Trajectory	N. Vehicle trajectory behind the test article is acceptable.	S	S		
MASH Test Designation		2-90	2-90		
PASS/FAIL		Pass	Pass*		

S – Satisfactory U – Unsatisfactory NA - Not Applicable

*The primary accelerometer unit provided a longitudinal ORA below the MASH limit, and the backup accelerometer unit provided a longitudinal ORA above the MASH limit.

16 REFERENCES

1. *Traffic Safety Facts 2010 Data: Pedestrians*, United States Department of Transportation, National Highway Traffic Safety Administration, 2010.
2. Leaf, W.A., and Preusser, D.F., *Literature Review on Vehicle Travel Speeds and Pedestrian Injuries*, United States Department of Transportation, National Highway Traffic Safety Administration, October 1999.
3. Zegeer, C.V., Seiderman, C., Lagerwey, P., Cynecki, M., Ronkin, M., and Schneider, R., *Pedestrian Facilities Users Guide-Providing Safety and Mobility*, Report No. FHWA-RD-01-102, Submitted to the Office of Safety and Traffic Operations R&D, Federal Highway Administration, Performed by Highway Safety Research Center, University of North Carolina, Chapel Hill, North Carolina, March 2002.
4. Zegeer, C.V., Stewart, J.R., Huang, H.H., and Lagerwey, P.A., *Safety Effects of Marked vs. Unmarked Crosswalks at Uncontrolled Locations: Executive Summary and Recommended Guidelines*, Report No. FHWA-RD-01-075, Submitted by the Office of Safety Research and Development, Federal Highway Administration, Performed by Highway Safety Research Center, University of North Carolina, Chapel Hill, North Carolina, February 2002.
5. *2010 ADA Standards for Accessible Design*, United States Department of Justice, September 2010.
6. *AASHTO Load and Resistance Factor Design (LRFD) Bridge Design Specifications*, American Association of State Highway and Transportation Officials (AASHTO), 2010.
7. *Manual for Assessing Safety Hardware (MASH)*, American Association of State Highway and Transportation Officials (AASHTO), Washington, D.C., 2009.
8. *2012 International Building Code (IBC)*, International Code Council, Country Club Hills, Illinois, June 2011.
9. *Part 1910 – Occupational Safety and Health Standards (OSHA)*, United States Department of Labor, June 2012.
10. Polivka, K.A., Faller, R.K., Keller, E.A., Sicking, D.L., Rohde, J.R., and Holloway, J.C., *Design and Evaluation of the TL-4 Minnesota Combination Traffic/Bicycle Bridge Rail*, Final Report to the Midwest Regional Pooled Fund Program, Transportation Research Report No. TRP-03-74-98, Project No. SPR-3(17), Midwest Roadside Safety Facility, University of Nebraska-Lincoln, Lincoln, Nebraska, November 1998.
11. Ross, H.E., Sicking, D.L., Zimmer, R.A. and Michie, J.D., *Recommended Procedures for the Safety Performance Evaluations of Highway Features*, National Cooperative Research Program (NCHRP) Report No. 350, Transportation Research Board, Washington, D.C., 1993.

12. *Post and Rail Fence: Wind River Post & Rail, Split Rail Fence*, Austintown Fence Company, Austintown, Ohio, <<http://www.afencecompany.com/Windriver%20post%20and%20rail.htm>>.
13. *HDPE Fencing*, Amberway Equine Solutions, Midway, Kentucky, <<http://www.amberwayequine.com/products/hdpe-fencing-2>>.
14. *Horse Fences Picture 236*, CJ Distributing, <<http://fencepictures.org/p/236/horse-fences/picture-236>>.
15. *Railing Type C, Fiber Reinforced Polymer (FRP)*, Modi Safety, Mumbai, India, <<http://www.modisafety.com/wp-content/uploads/2012/12/Railing-Type-C.jpg>>.
16. *Crossovers, Fibergrate: Molded Fiberglass Products*, 949 Supplies Co., Ltd., Bangkok, Thailand, <http://www.949supplies.com/fibergrate_products_en.html>.
17. *SAFRAIL Industrial Handrail: Industrial Fiberglass Handrail Systems*, Brochure, Strongwell, Bristol, Virginia, <<http://www.strongwell.com/wp-content/uploads/2013/04/SAFRAIL-Industrial-Handrail-Brochure.pdf>>.
18. *Zucchi Vinyl Fence*, Zucchi, Mondovi, Italy, <<http://www.recinzionipvc.com/fr/gallery/category/1.html>>.
19. *Vinyl Fences Vancouver*, Cedar Fencing Vancouver, Vancouver, British Columbia, Canada, <<http://cedarfencingvancouver.com/vinyl-fences-vancouver>>.
20. *Plastic Fence Post Covers*, Lasiroc Pictures Gallery, Lasiroc, <<http://www.lasiroc.com/plastic-fence-post-covers>>.
21. *Post and Rail Fencing, Guardian Timber Fencing*, Guardian Security Fencing, Basildon, Essex, England, <<http://gsfencing.com/guardian-fencing.htm#>>.
22. *Split Rail, Ritter Fence*, Middletown, Maryland, <<http://www.ritterfence.com/#!about/stackercoverflowalbum0=2>>.
23. *Wooden Fences*, Pure Fence LLC, Battle Creek, Michigan, <<http://purefencellc.com/wooden-fences>>.
24. *First Class Fencing*, Renoback.com, <<https://www.renoback.com/landscaping/for-sale-in-calgary/dont-pay-for-6-months-residential-acreage-fencing-1427751374>>.
25. *Technical Direction for Road Safety Practitioners: Pedestrian Fencing*, New South Wales Centre for Road Safety, Sidney, New South Wales, October 2010, <http://www.rta.nsw.gov.au/roadsafety/downloads/tds/td2010_sr02.pdf>.
26. Stewart, D., *Pedestrian Guardrails and Accidents*, Faculty of Engineering, Aberdeen University, Aberdeen, United Kingdom, 1988.

27. *VISIFLEX, All – Purpose Pedestrian Guardrail*, Pell & Baldwin (Fabrications) LTD. *VISIFLEX* [Brochure]. Peterborough, UK.
28. *352'-0 x Variable Height Reinforced Concrete Retaining Wall Steel Pipe Rail Details*, Iowa Department of Transportation, Highway Division, 2008.
29. *Pedestrian Railing*, Washington State Department of Transportation, Bridge and Structures Office, February 2011.
30. *Bridge Railing Manual*, Texas Department of Transportation, May 2006, <http://www.scribd.com/doc/26903479/Bridge-Railing-Manual#outer_page_22>.
31. *Metal Framed Cable Railings*, Ultra-tec Cable Railing Systems, Carson City, Nevada, <<http://www.thecableconnection.com/metal-framed-railings.html>>.
32. *Aluminum Pedestrian/Bicycle Railing*, Florida Department of Transportation, 2013 FDOT Design Standards, Index No. 862, 2013.
33. *Instructions for Design Standards – Aluminum Pedestrian/Bicycle Railing*, Florida Department of Transportation, 2013 FDOT Design Standards, Index No. 862, 2013.
34. *Hollaender Component Catalog*, Hollaender Manufacturing Company, Cincinnati, OH, <<http://www.hollaender.com/?page=catalog>>.
35. *Speed-Rail, ADA Railing, Handrails, Panels & Pipe Fittings. Hollaender Component Catalog*, Hollaender Manufacturing Company, Cincinnati, OH, <<http://www.hollaender.com/?page=speedrail>>.
36. *National Safety Council Injury Facts*. National Safety Council (NSC), 2011 edition.
37. Beer, F.P., Johnston, E.R., DeWolf, J.T., and Mazurek, D.F., *Mechanics of Materials*, McGraw Hill, Seventh Edition, 2015.
38. *2010 Aluminum Design Manual*. The Aluminum Association, 2010.
39. *Combined Bending of Unsymmetrical Beams*. EM 424: Intermediate Mechanics of Materials. Iowa State University. Web, <http://www.public.iastate.edu/~e_m.424/unsymm%20bending.pdf>.
40. *Building Code Requirements for Structural Concrete (ACI-318-11) and Commentary*. American Concrete Institute, Committee 318. 2011. “Appendix D: Anchoring to Concrete”.
41. American Institute of Steel Construction (AISC), *Steel Construction Manual, 13th Edition*, Third Printing, April 2007.
42. American Institute of Steel Construction (AISC), *Steel Design Guide Series 1: Column Base Plates*, Third Printing, October 2003.

43. Society of Automotive Engineers (SAE), *Instrumentation for Impact Test – Part 1 – Electronic Instrumentation*, SAE J211/1 MAR95, New York City, NY, July, 2007.
44. Hinch, J., Yang, T.L., and Owings, R., *Guidance Systems for Vehicle Testing*, ENSCO, Inc., Springfield, Virginia, 1986.
45. MacInnis, D., Cliff, W., and Ising, K., *A Comparison of the Moment of Inertia Estimation Techniques for Vehicle Dynamics Simulation*, SAE Technical Paper Series – 970951, Society of Automotive Engineers, Inc., Warrendale, Pennsylvania, 1997.
46. *Vehicle Damage Scale for Traffic Investigators*, Second Edition, Technical Bulletin No. 1, Traffic Accident Data (TAD) Project, National Safety Council, Chicago, Illinois, 1971.
47. *Collision Deformation Classification – Recommended Practice J224 March 1980*, Handbook Volume 4, Society of Automotive Engineers (SAE), Warrendale, Pennsylvania, 1985.

17 APPENDICES

Appendix A. Pooled Fund Survey for Pedestrian Rail Highest Priority Need

3/28/12

Wisconsin Department of Transportation
Hill Farms State Transportation Building
4802 Sheboygan Avenue
P.O. Box 7910
Madison, WI 53707-7910

Dear Erik Emerson,

The Midwest Roadside Safety Facility (MwRSF) is working on the initial phase of a pedestrian rail project that will ultimately lead to the development of a crashworthy ADA-compliant pedestrian-only rail. The project has been sponsored by the Wisconsin Department of Transportation, who has requested the input from the member states of the Pooled Fund.

Situations arise where a barrier or rail is required to prevent pedestrians from crossing or dropping into an area which may be acceptable for an errant vehicle. These types of pedestrian rails are located (1) on top of short culverts and retaining walls (less than 8 ft tall); (2) next to high pedestrian and vehicle facilities to prevent jaywalking; and (3) to keep pedestrians off public/private property such as train tracks. Examples are shown in Figures 1 through 3. It is important to keep pedestrians from entering these locations, but it is not feasible to install a crashworthy barrier as shown in Figure 4. These rails would not need to redirect or stop an errant vehicle, and they must not present additional hazards to the motoring public. In addition, pedestrian rails must comply with the Americans with Disabilities Act (ADA). Currently, no permanent pedestrian-only rails have been crash tested and accepted for use on roadsides.



Figure 1. Rail over Culvert



Figure 2. Rail Restricting Jaywalkers



Figure 3. Rail around Private Property



Figure 4. Concrete Traffic/Pedestrian Rail

Since only a small number of rails will actually be developed and tested, identifying the most prominent need is required. To complete the initial phase of the project, the researchers at MwRSF need to establish which pedestrian rails provide the greatest value to the state of Wisconsin and the member states of the Pooled Fund. Thus, MwRSF researchers are seeking input on what rails are the most common, what they are being used for, and what additional/updated standard plans or drawing details have been established for pedestrian-only permanent rails.

The compiled pedestrian rail needs will be organized into a limited number of design categories that will result in the smallest number of full-scale crash tests as possible. It is anticipated these rails will be tested under TL-2 criteria since they are not used on high-speed facilities. Priorities for the project will be assigned based on (1) the importance of the pedestrian rail to the states participating; (2) the number of different system configurations that can be addressed simultaneously; and (3) the potential for the development of a successful design under MASH.

A review of the WisDOT website was done to find current pedestrian-only rail standards. The details of pedestrian-type railings obtained from the website were limited to (1) wire and (2) chain link fences. The acquired drawings found are attached. Drawing standards for a true pedestrian-only barrier were not found. Please respond with the most recent/additional pedestrian rail standards which are used in the state of Wisconsin.

Please reply no later than 4/13/2012 with the following information:

- A completed copy of the attached survey
- Any additional/updated details, state standards, or plans concerning any type of pedestrian-only rail installed near a roadway
- Any photographs of these pedestrian rails currently in use

Questions should be directed to Mitch Wiebelhaus, MwRSF graduate research assistant, at mitchw1@huskers.unl.edu or (402) 472-9043 or Karla Lechtenberg at kpolivka2@unl.edu or (402) 472-9070. The completed form and all additional documents may be e-mailed, faxed, or mailed to:

Mitch Wiebelhaus
mitchw1@huskers.unl.edu
130 Whittier Building
2200 Vine Street
Lincoln, Nebraska 68583-0853
Fax: (402) 472-2022

Once again your response is requested no later than 4/13/2012. Thank you for your efforts and time.

Sincerely,
Mitch Wiebelhaus, B.S.C.E., E.I.
Graduate Research Assistant

Usage Summary for Permanent Pedestrian-Only Rail

- (1) Identify how useful the development of the listed pedestrian rails would be to your state by putting an X in the box.
- (2) Include the approximate percentage of pedestrian rails which are comprised of the rails implemented in your state.
- (3) Rank the pedestrian rail location/circumstance in order of their benefit to your state with 1 being the most beneficial.
- (4) List additional location/situation your state has for pedestrian rails and indicate its usefulness, percentage of rails, and benefit to your state.
- (5) Include pictures, details, and drawings of current pedestrian rails installed near roadways in your state.

Pedestrian Rail Locations/Situation	Usefulness (1)					Percent (2)	Rank (3)
	Not Useful	Somewhat Useful		Very Useful			
On top of culverts							
On top of retaining walls							
To prevent jaywalking							
Around private/public property							
Additional Locations/Situations (4)							

Please direct questions and return the completed form with the additional materials to:

Mitch Wiebelhaus
mitchw1@huskers.unl.edu
 130 Whittier Building
 2200 Vine Street
 Lincoln, Nebraska 68583-0853
 (402) 472-9043
 Fax: (402) 472-2022

Appendix B. Original Design Concepts

Material properties for Concepts 1 through 19 and Designs 1 through 6 are shown in Table B-1 and Table B-2, respectively. These values may vary from nominal to account for temperature or degradation variations.

Table B-1. Material Properties, Concepts 1 through 19

Material	σ_y (psi)	E (ksi)	ρ (lb/ft³)
Steel	50,000	29,000	503
PVC	7,000	300	90
Wood	12,000	1,600	28

Table B-2. Material Properties, Designs 1 through 6

Material	σ_y (psi)	E (ksi)
PVC	4,500	300
Wood	12,000	1,600
HDPE	2,175	1,600
FRP	24,000	2,320

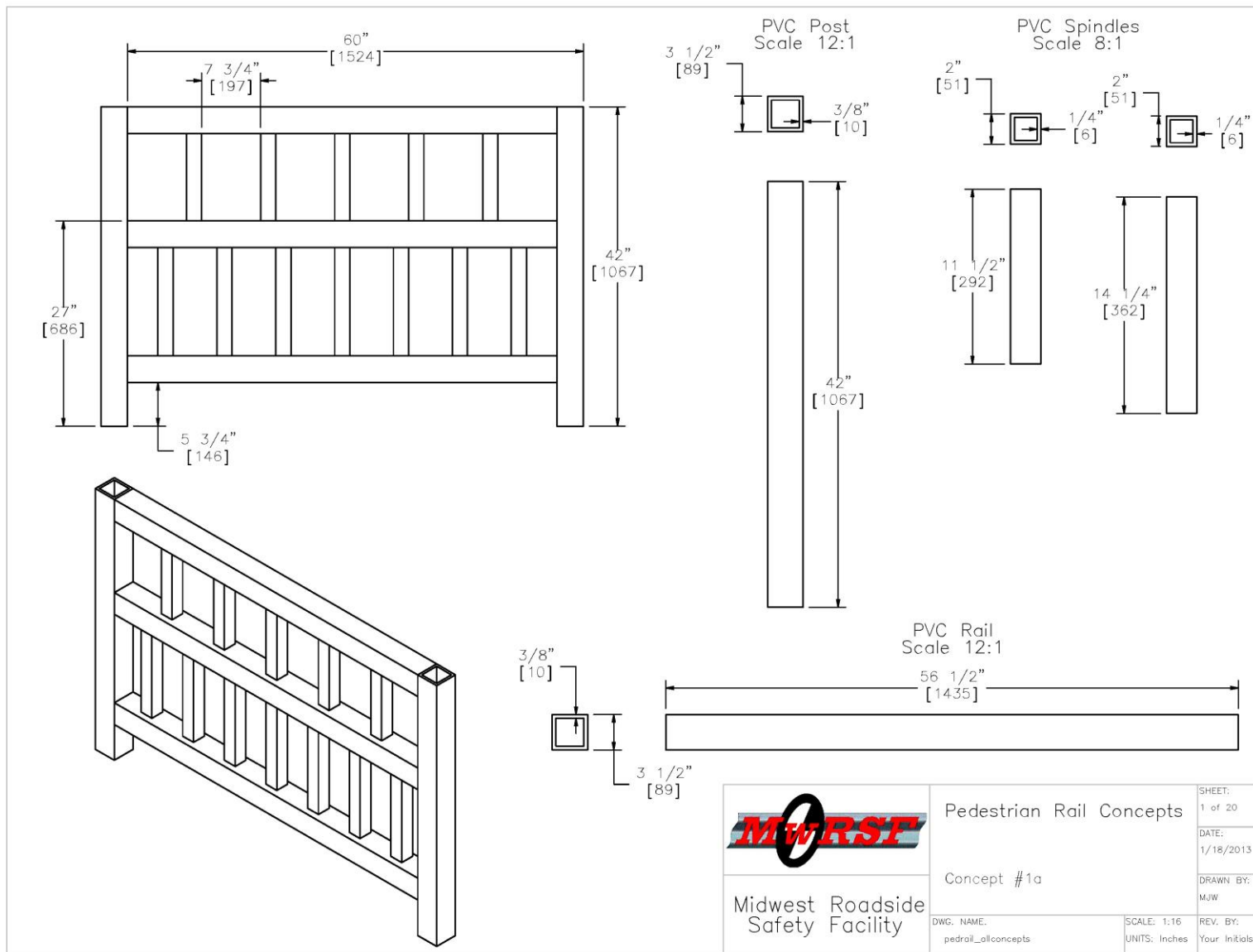


Figure B-1. Concept 1: PVC Posts, Rails, and Spindles

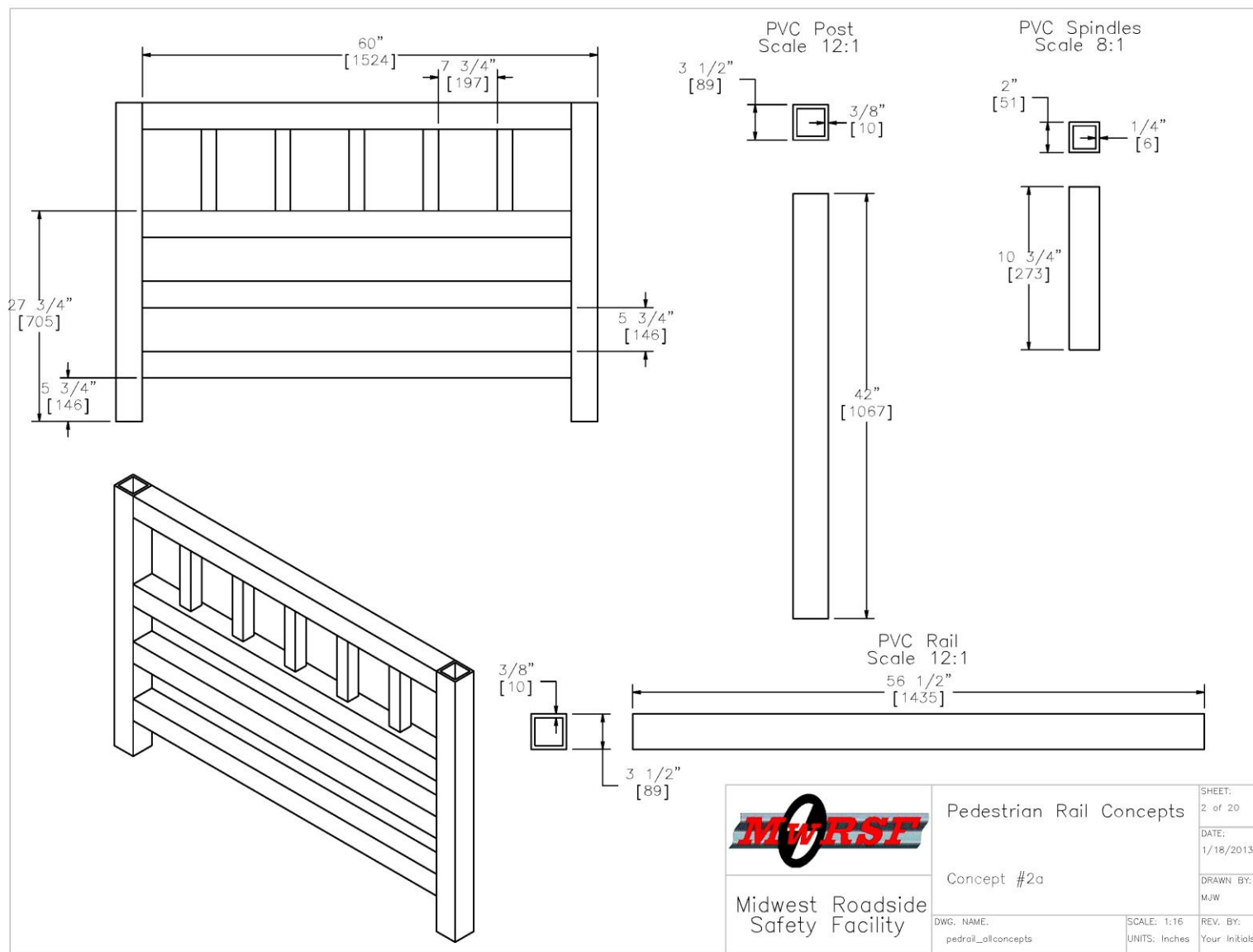


Figure B-2. Concept 2: PVC Posts, Rails, and Spindles

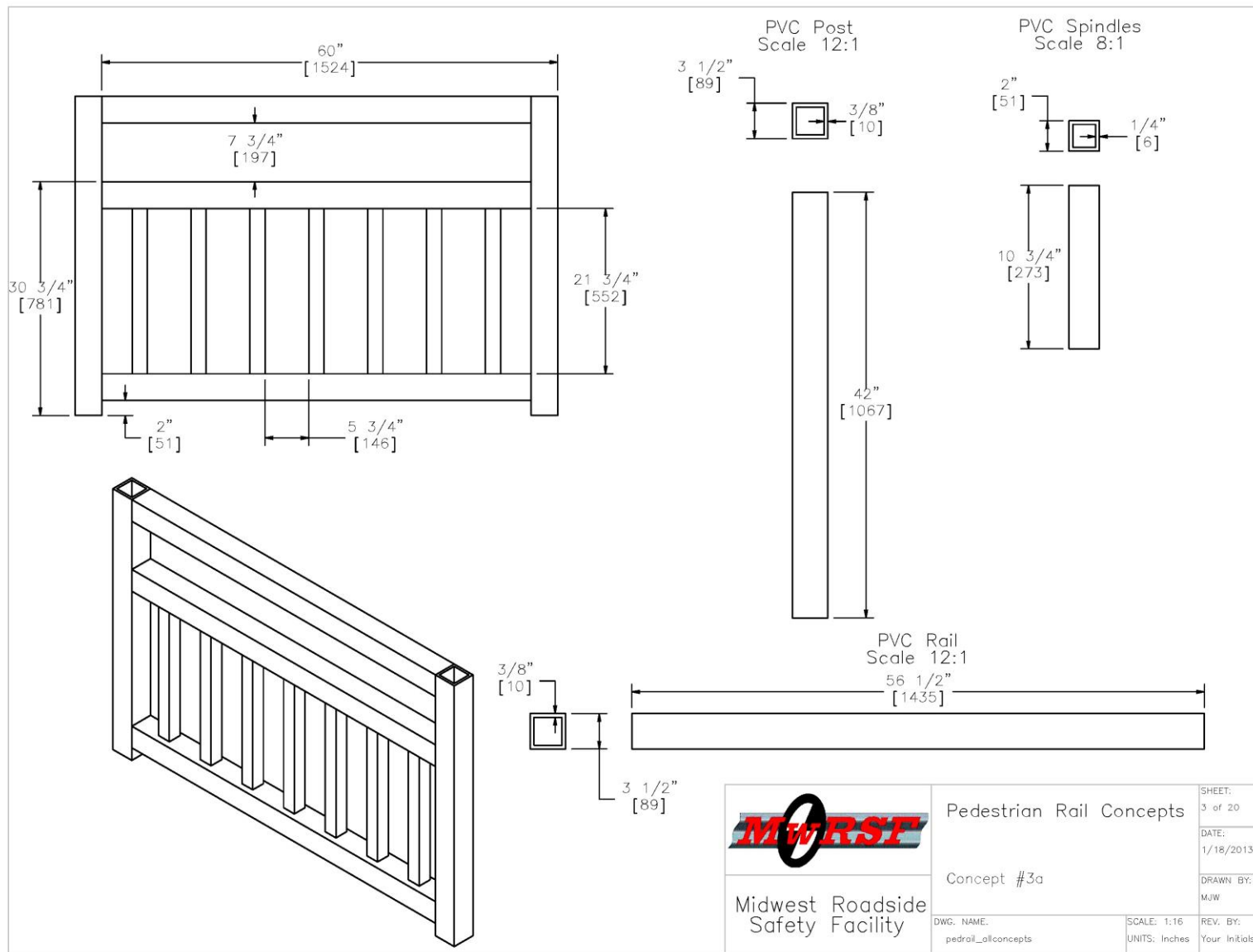


Figure B-3. Concept 3: PVC Posts, Rails, and Spindles

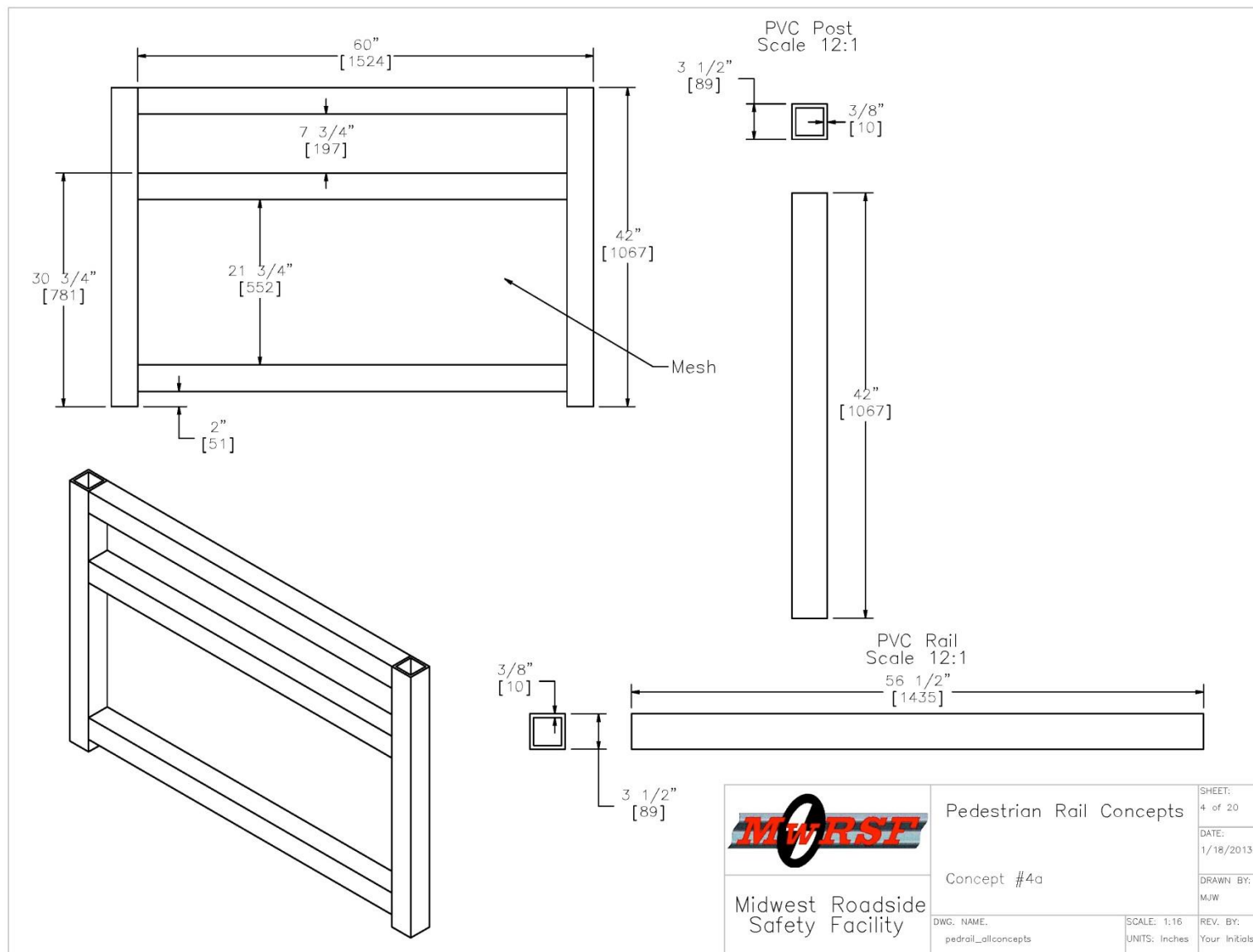


Figure B-4. Concept 4: PVC Posts and Rails with Mesh

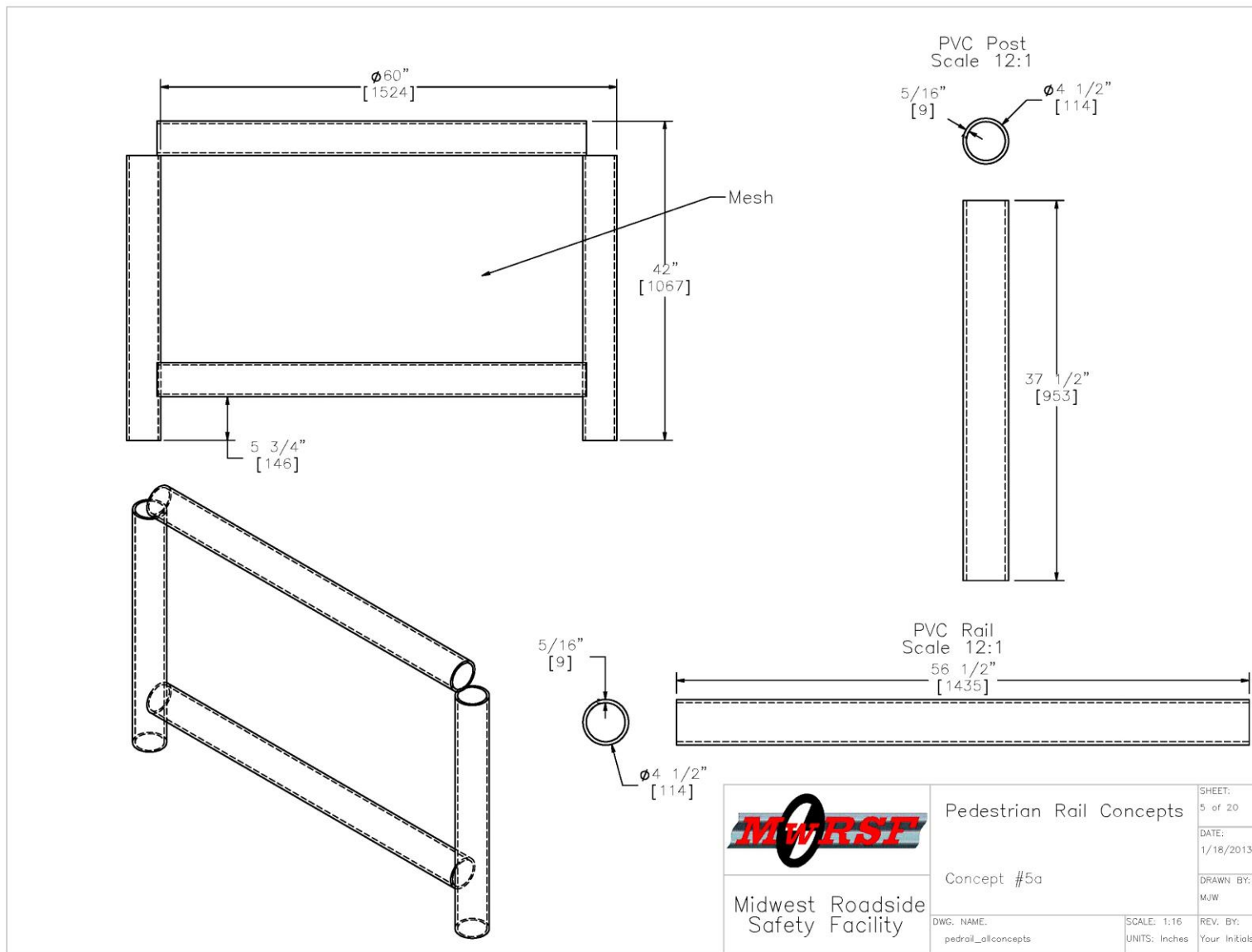


Figure B-5. Concept 5: PVC Posts and Rails with Mesh

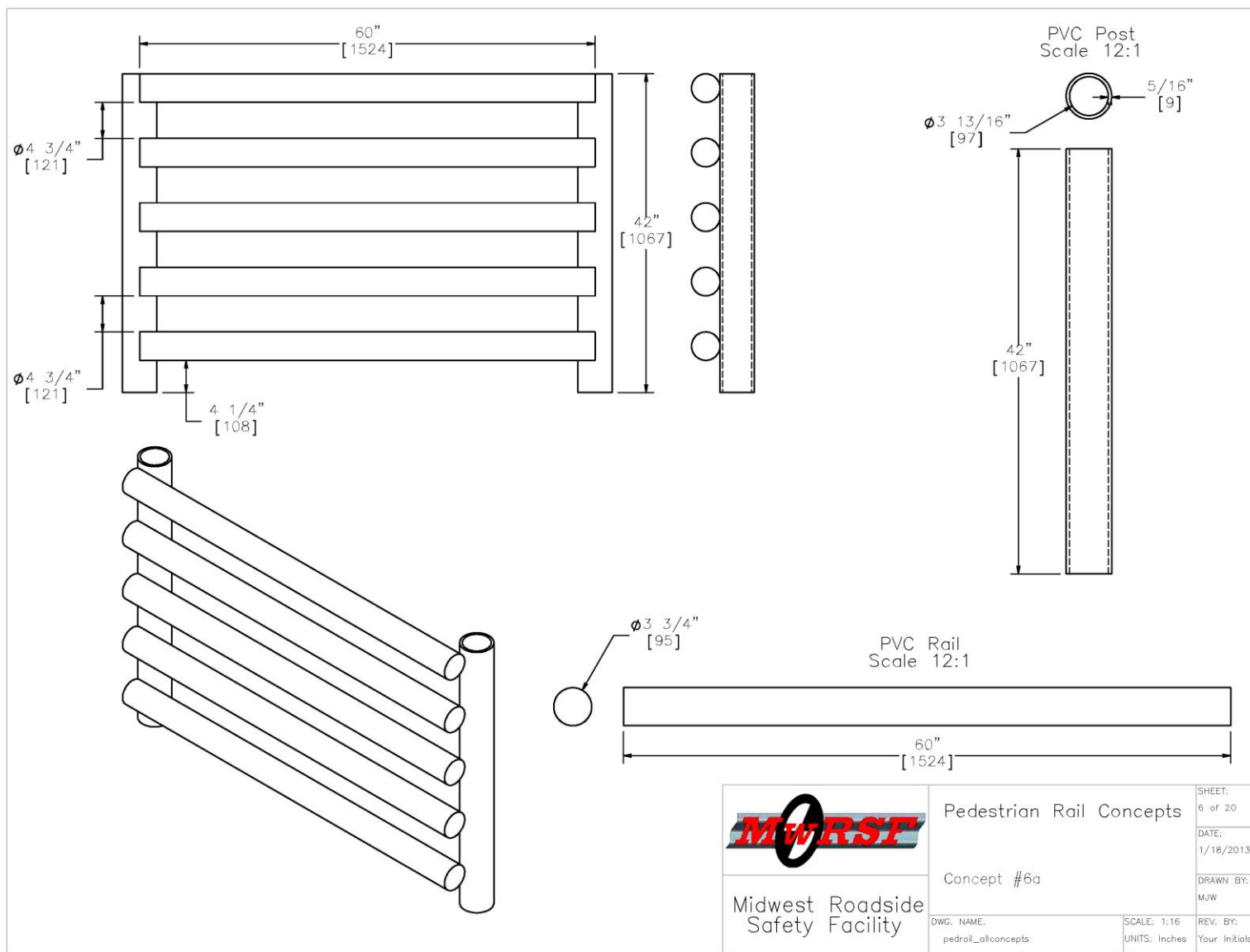


Figure B-6. Concept 6: PVC Posts and Rails

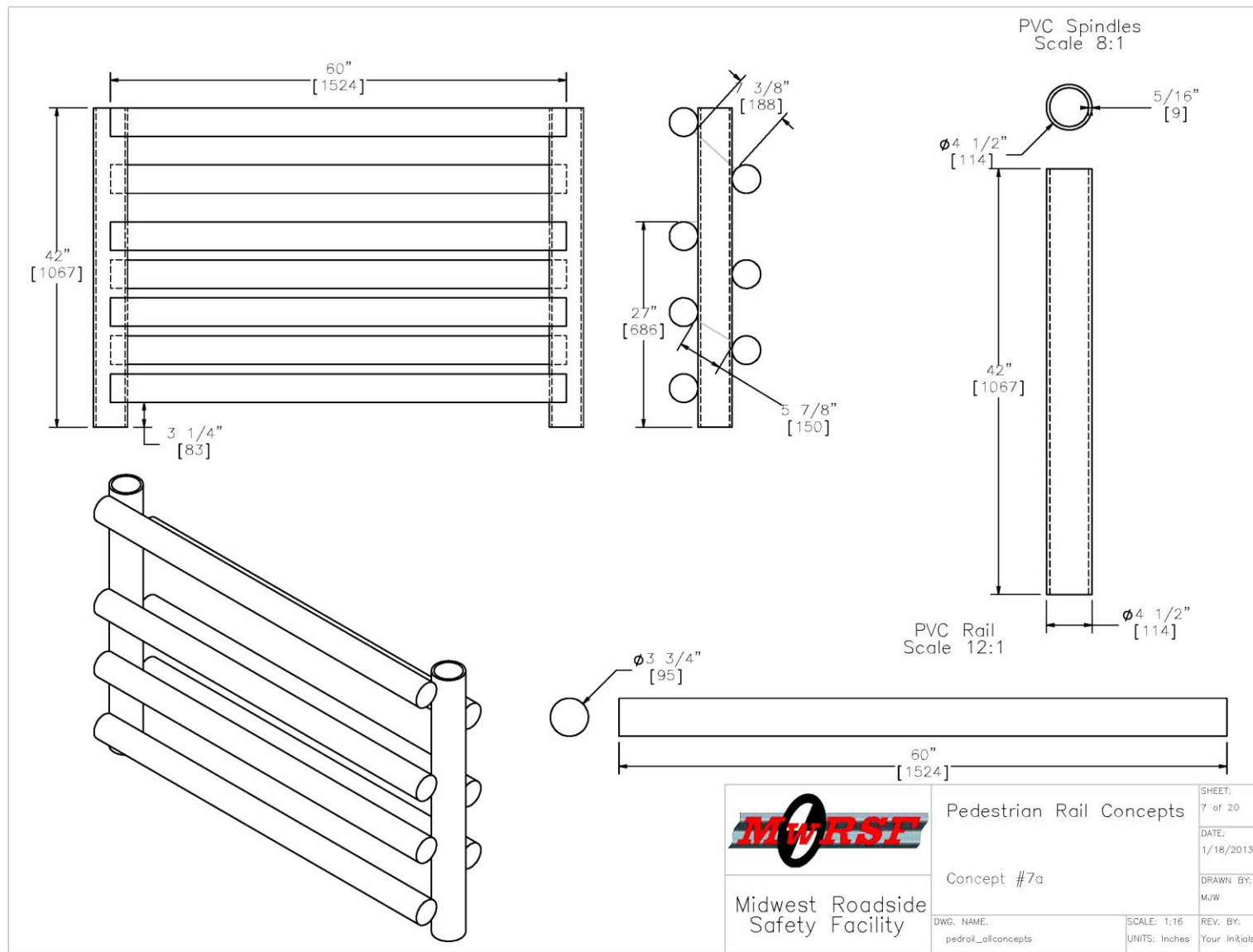


Figure B-7. Concept 7: PVC Posts and Rails

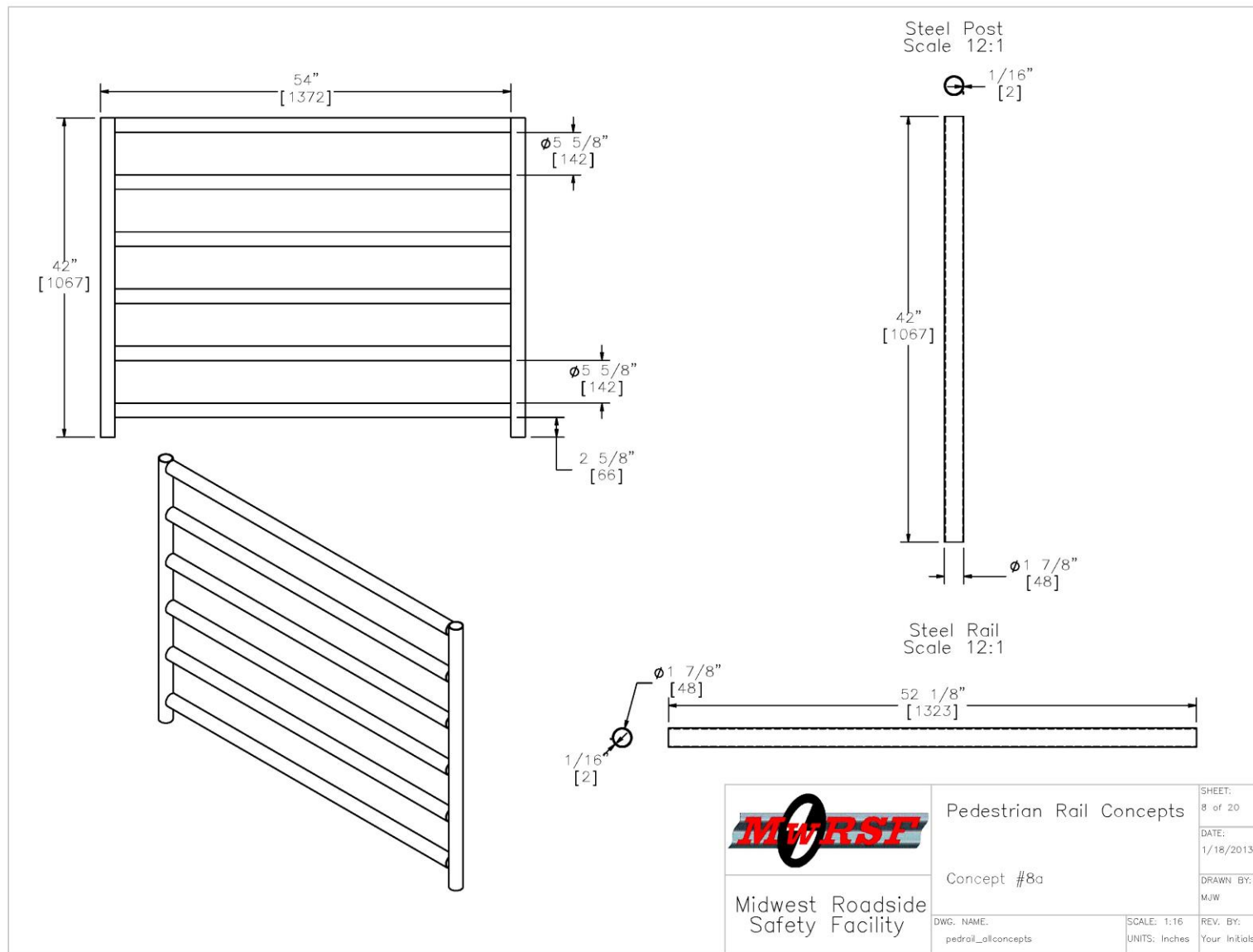


Figure B-8. Concept 8: Steel Posts and Rails

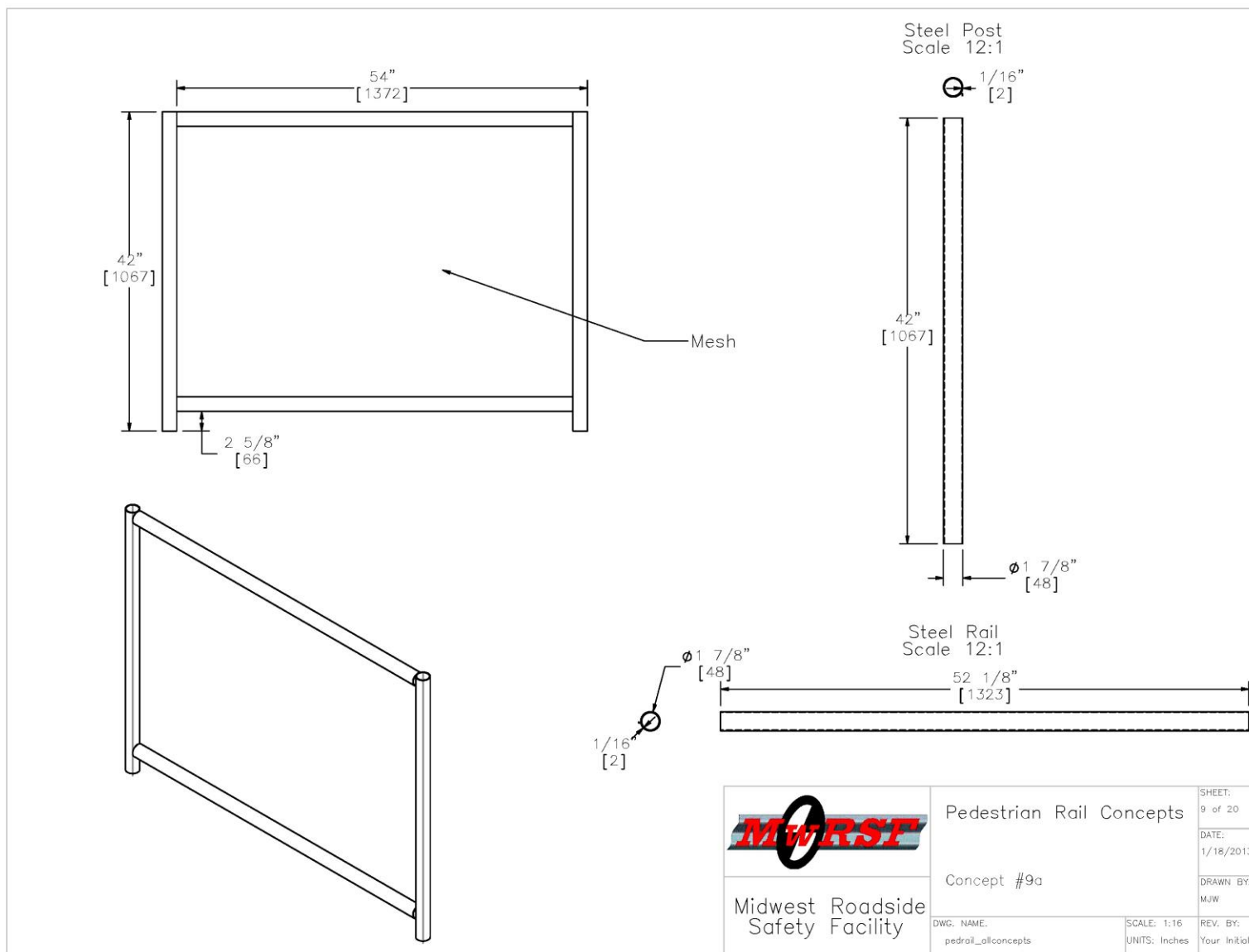


Figure B-9. Concept 9: Steel Posts and Rails with Mesh

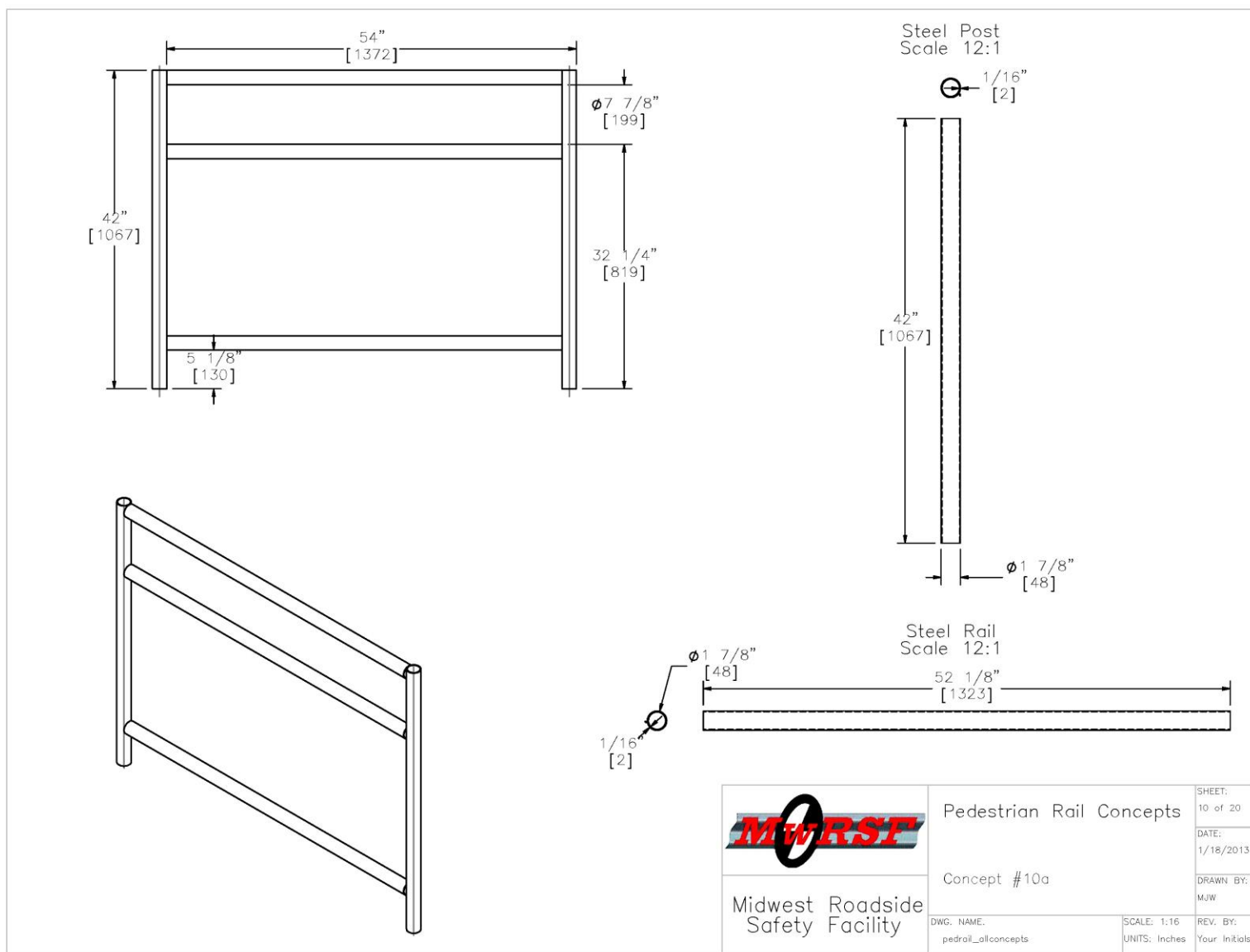


Figure B-10. Concept 10: Steel Posts and Rails with Mesh

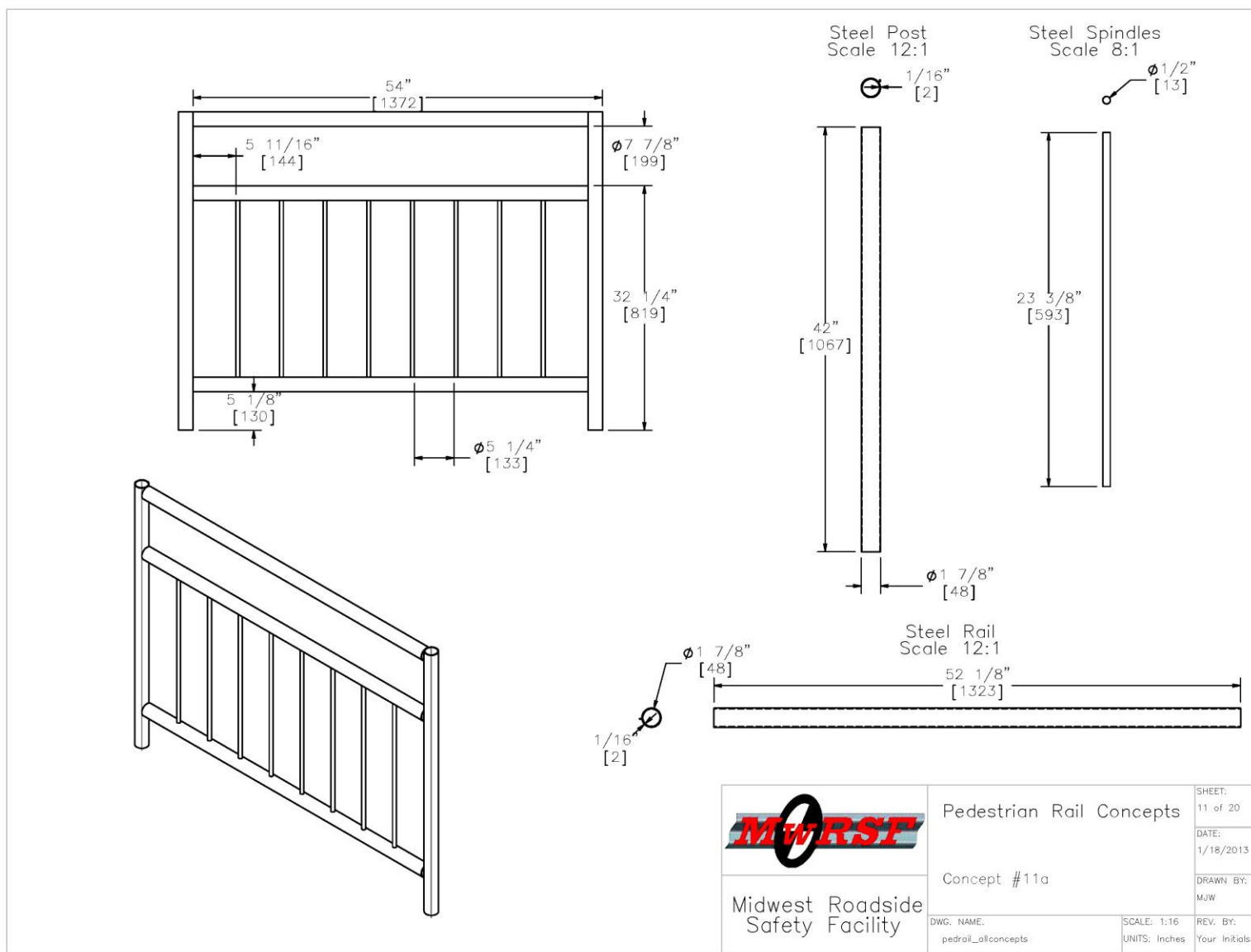


Figure B-11. Concept 11: Steel Posts, Rails, and Spindles

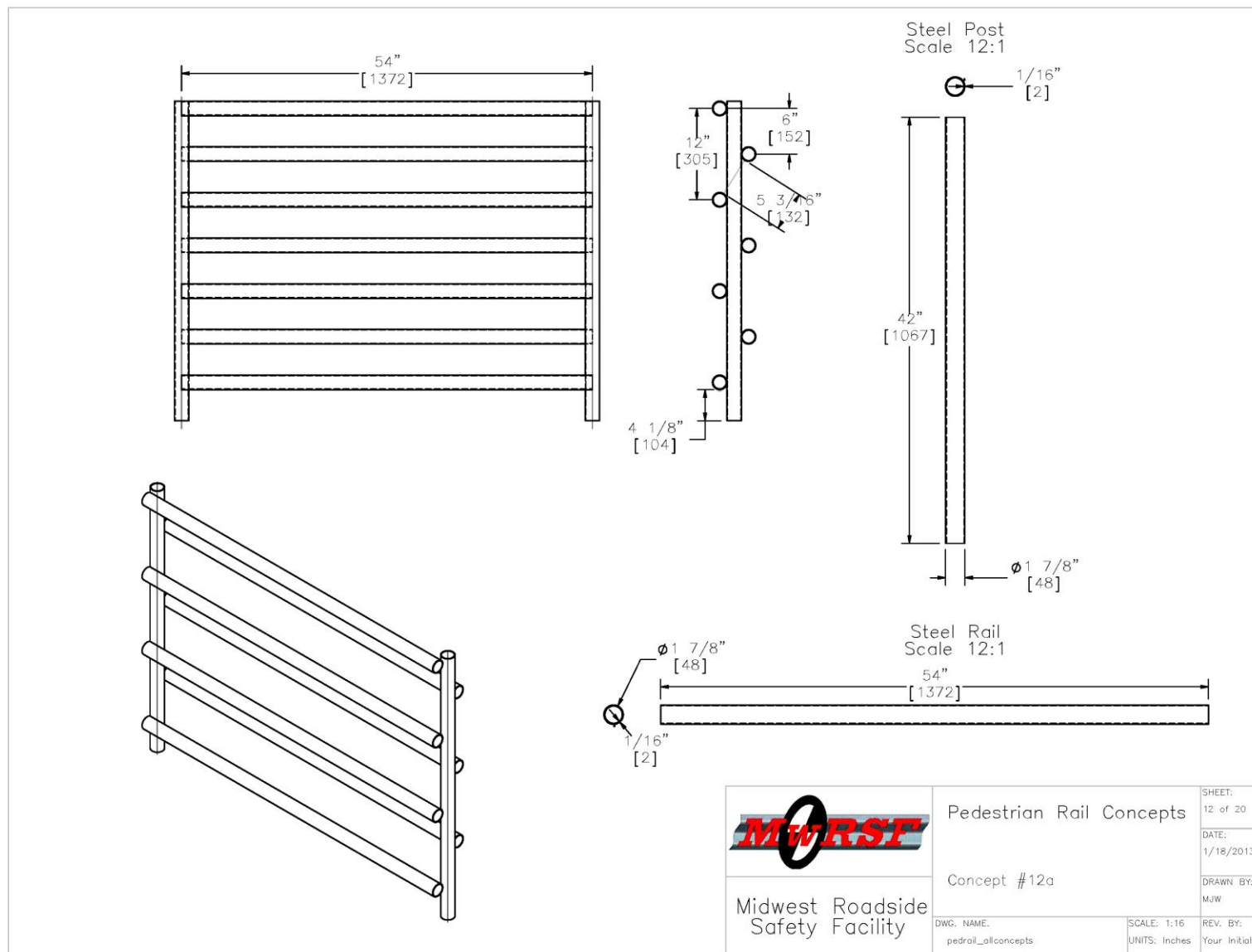


Figure B-12. Concept 12: Steel Posts and Rails

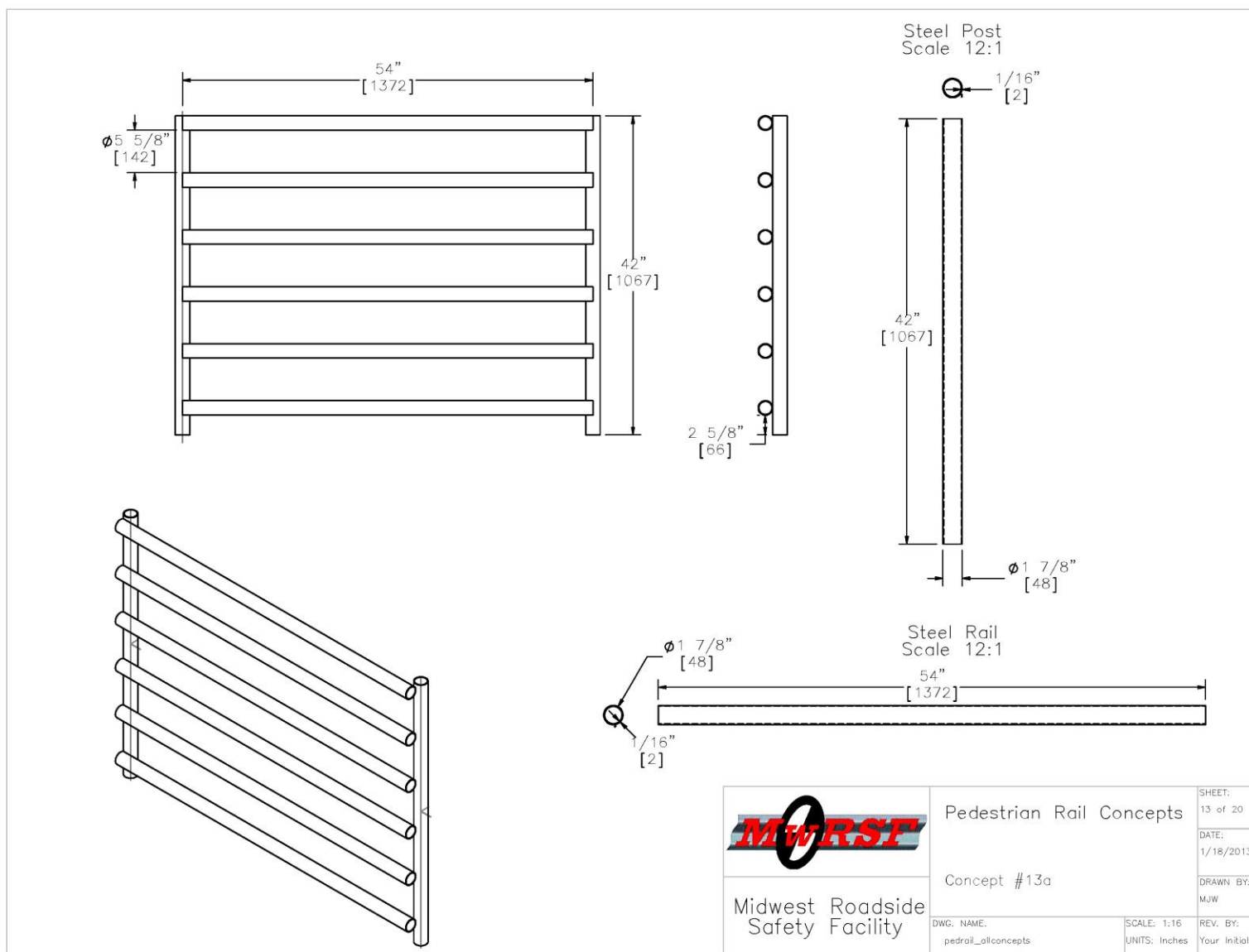


Figure B-13. Concept 13: Steel Posts and Rails

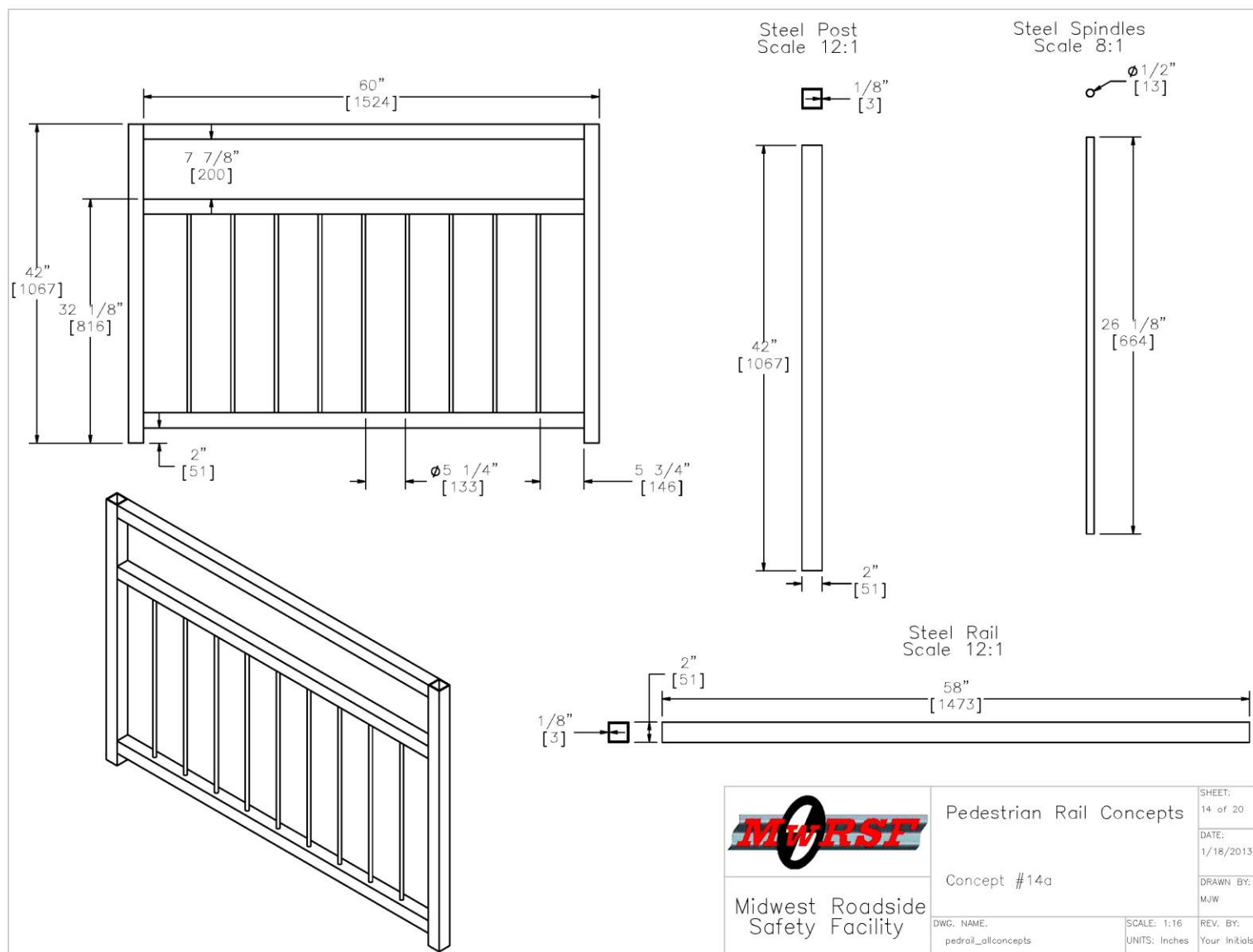


Figure B-14. Concept 14: Steel Posts, Rails, and Spindles

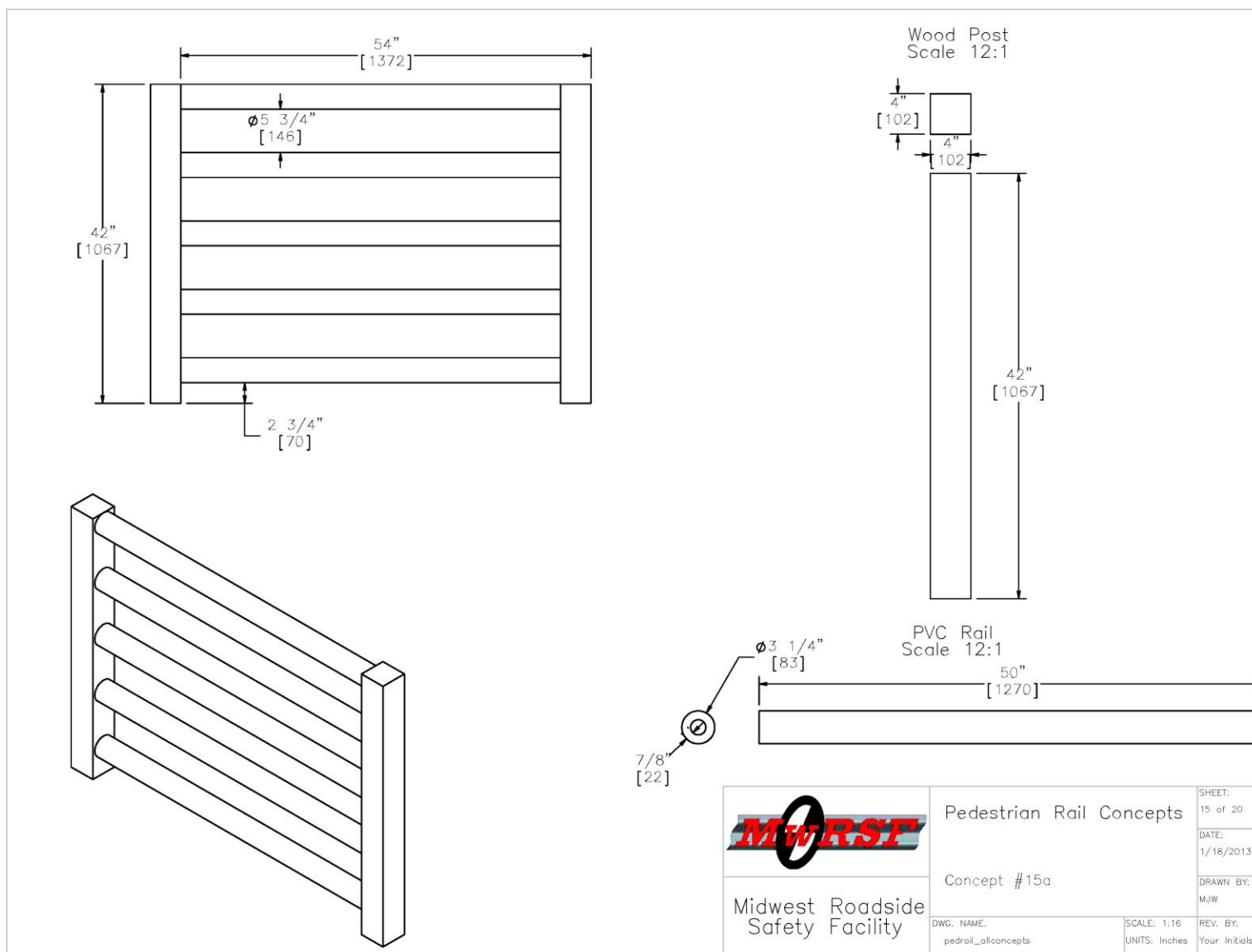


Figure B-15. Concept 15: Wood Posts and PVC Rails

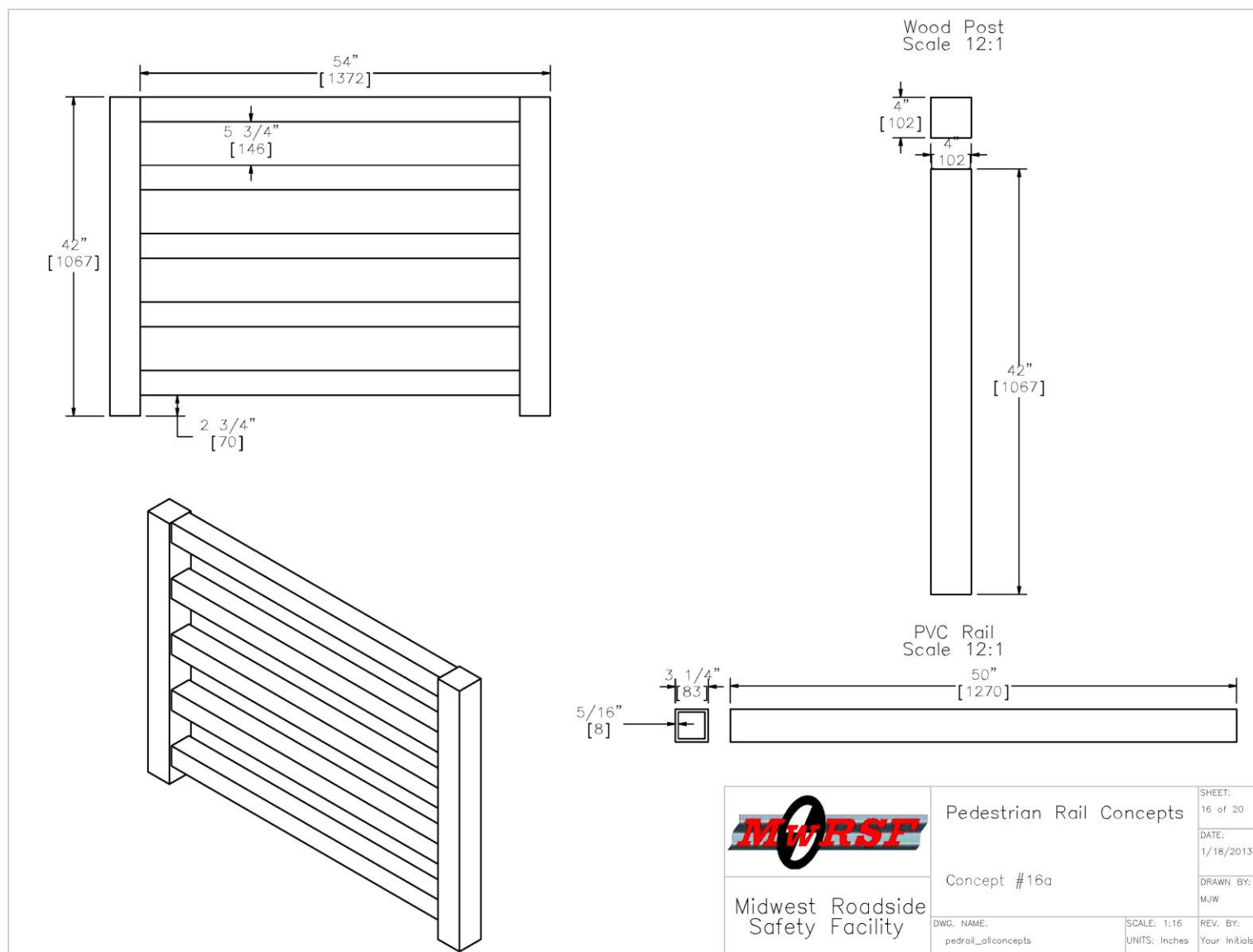


Figure B-16. Concept 16: Wood Posts and PVC Rails

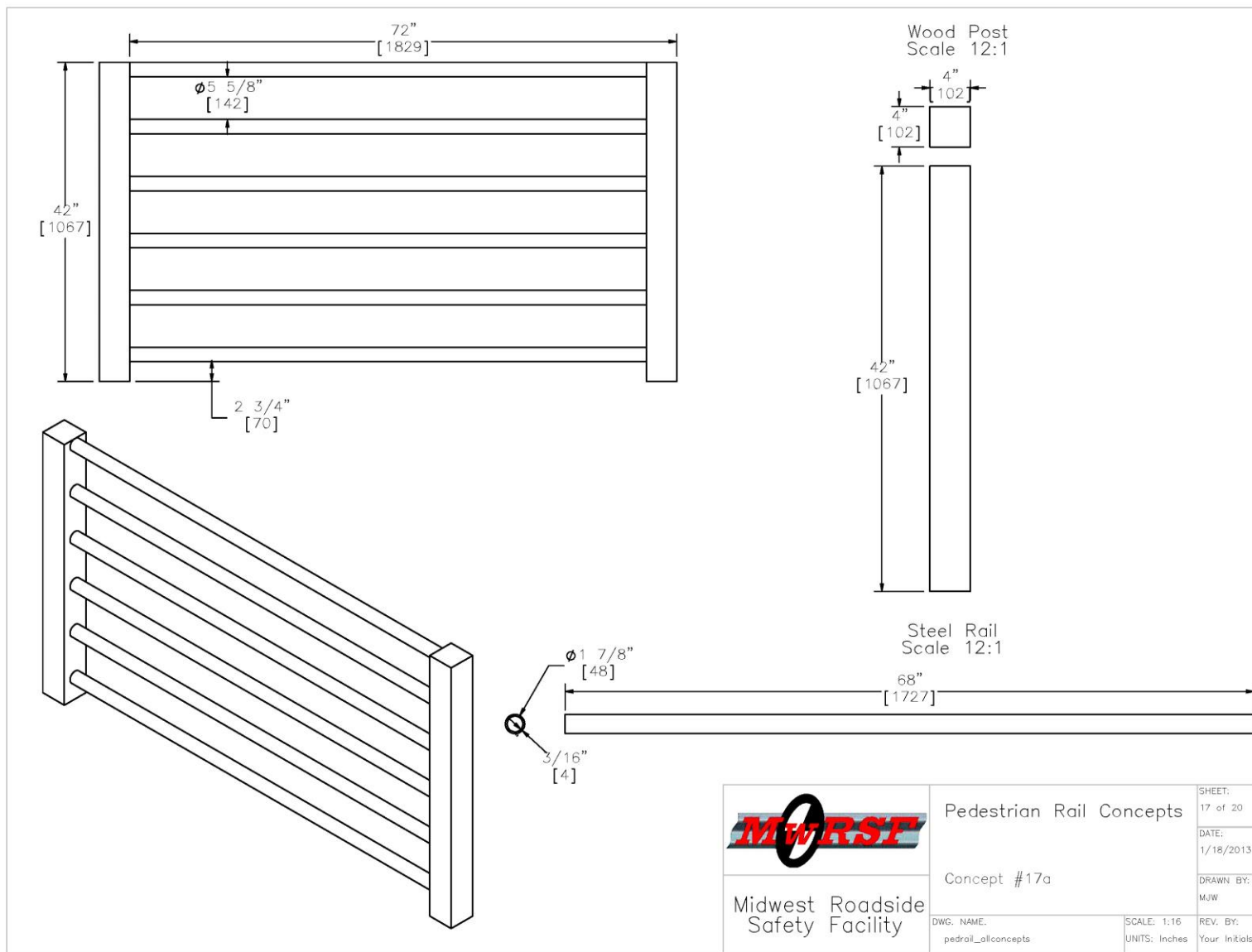


Figure B-17. Concept 17: Wood Posts and Steel Rails

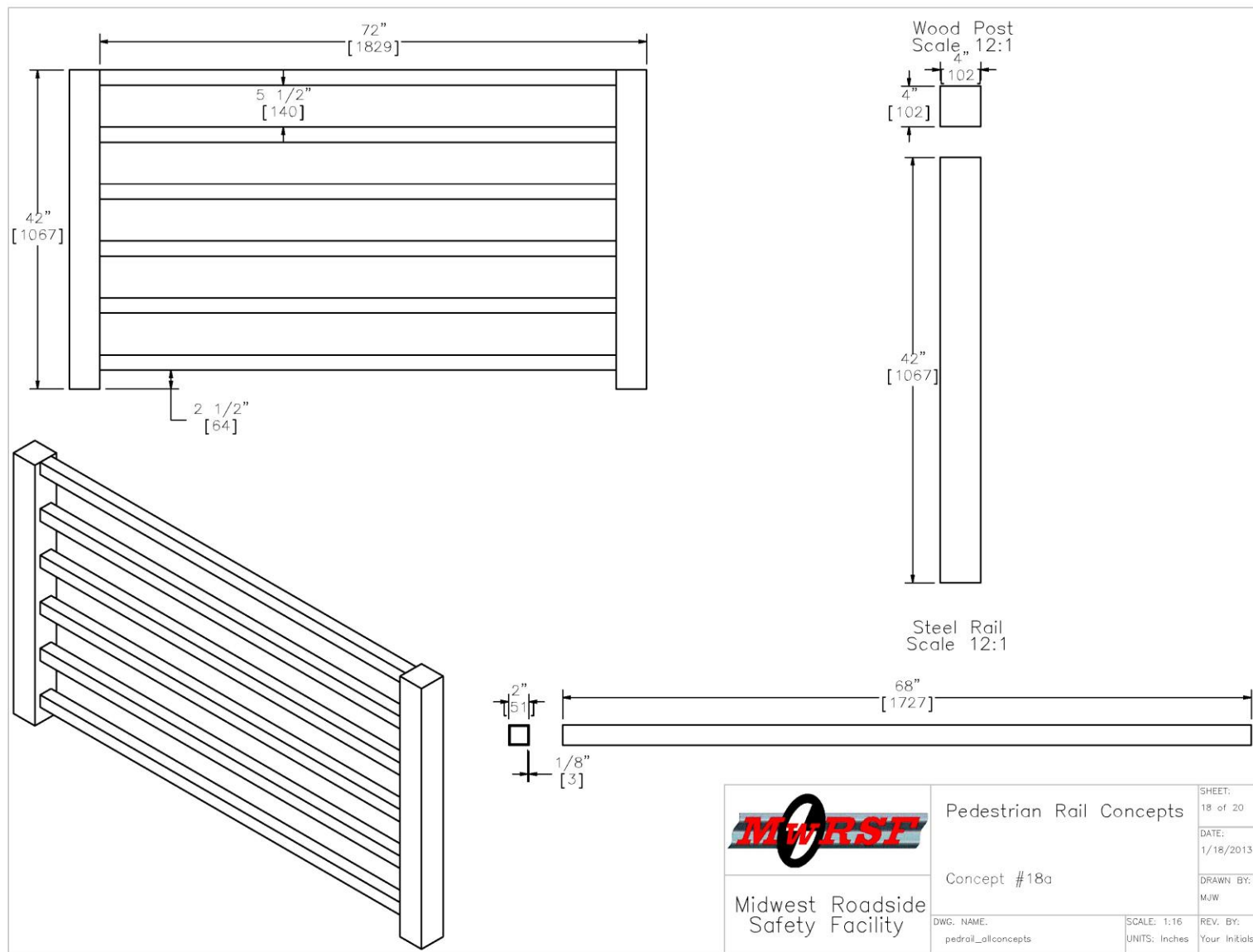


Figure B-18. Concept 18: Wood Posts and Steel Rails

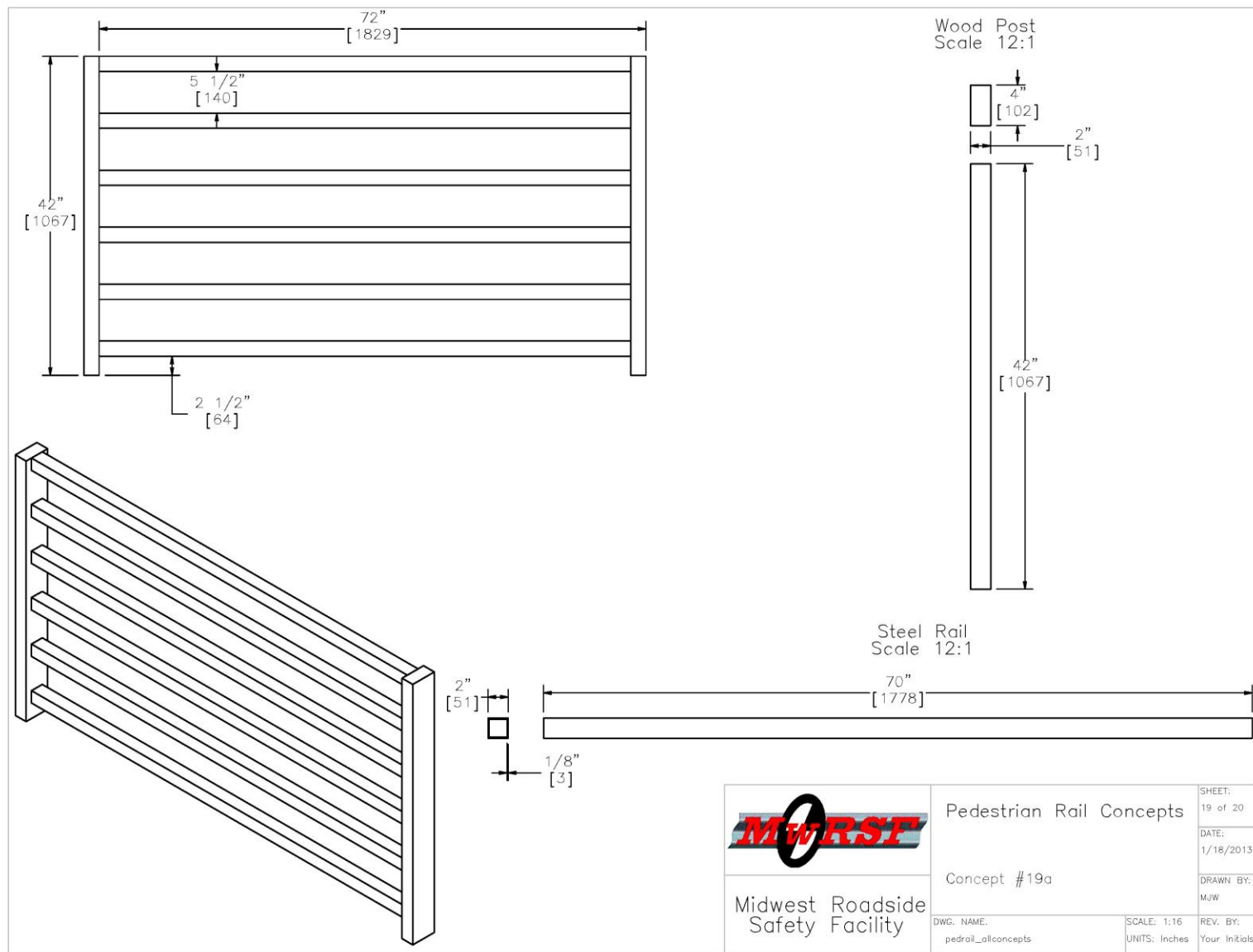


Figure B-19. Concept 19: Wood Posts and Steel Rails

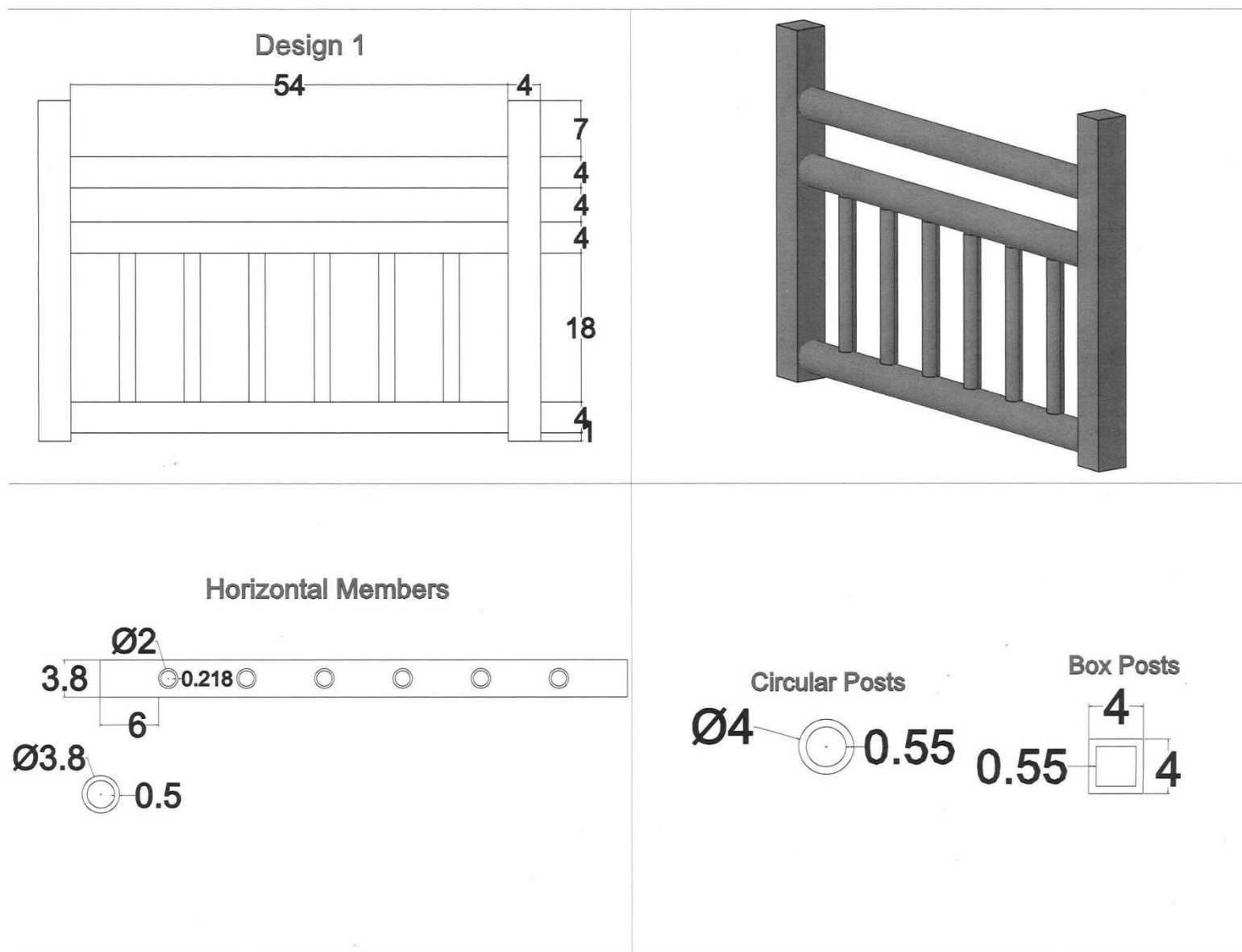


Figure B-20. Design 1: PVC Posts, Rails, and Spindles

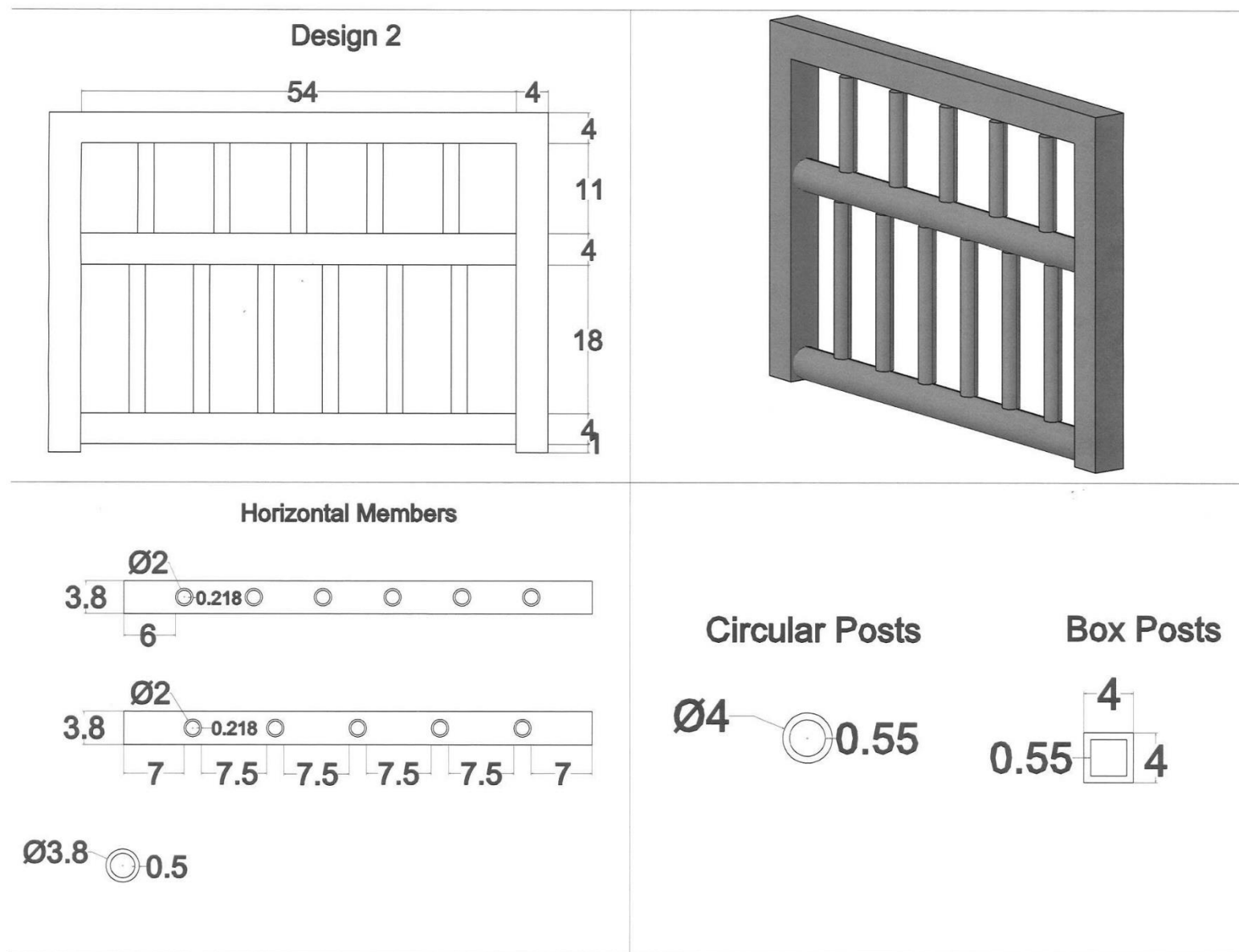


Figure B-21. Design 2: PVC Posts, Rails, and Spindles

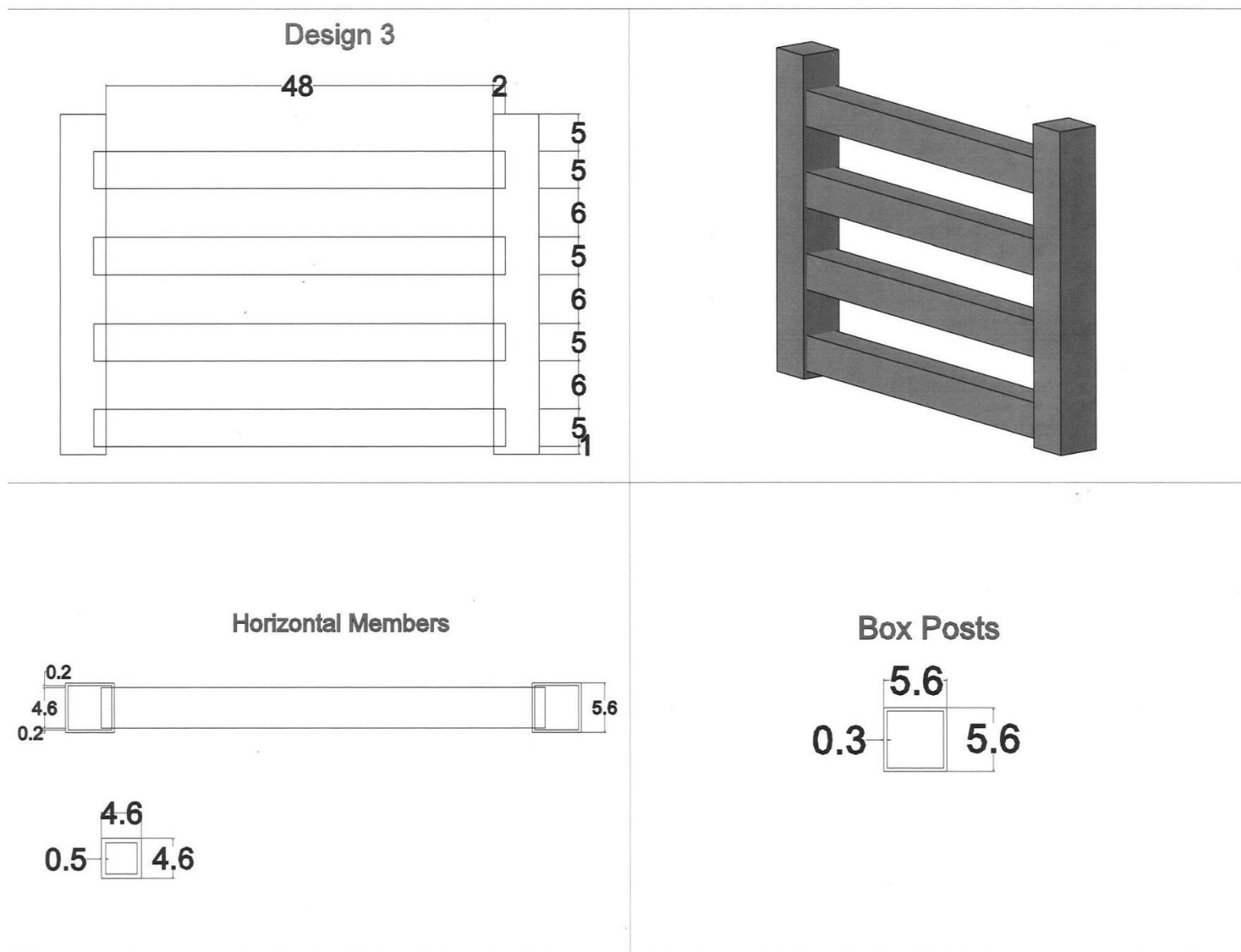


Figure B-22. Design 3: HDPE Posts and Rails

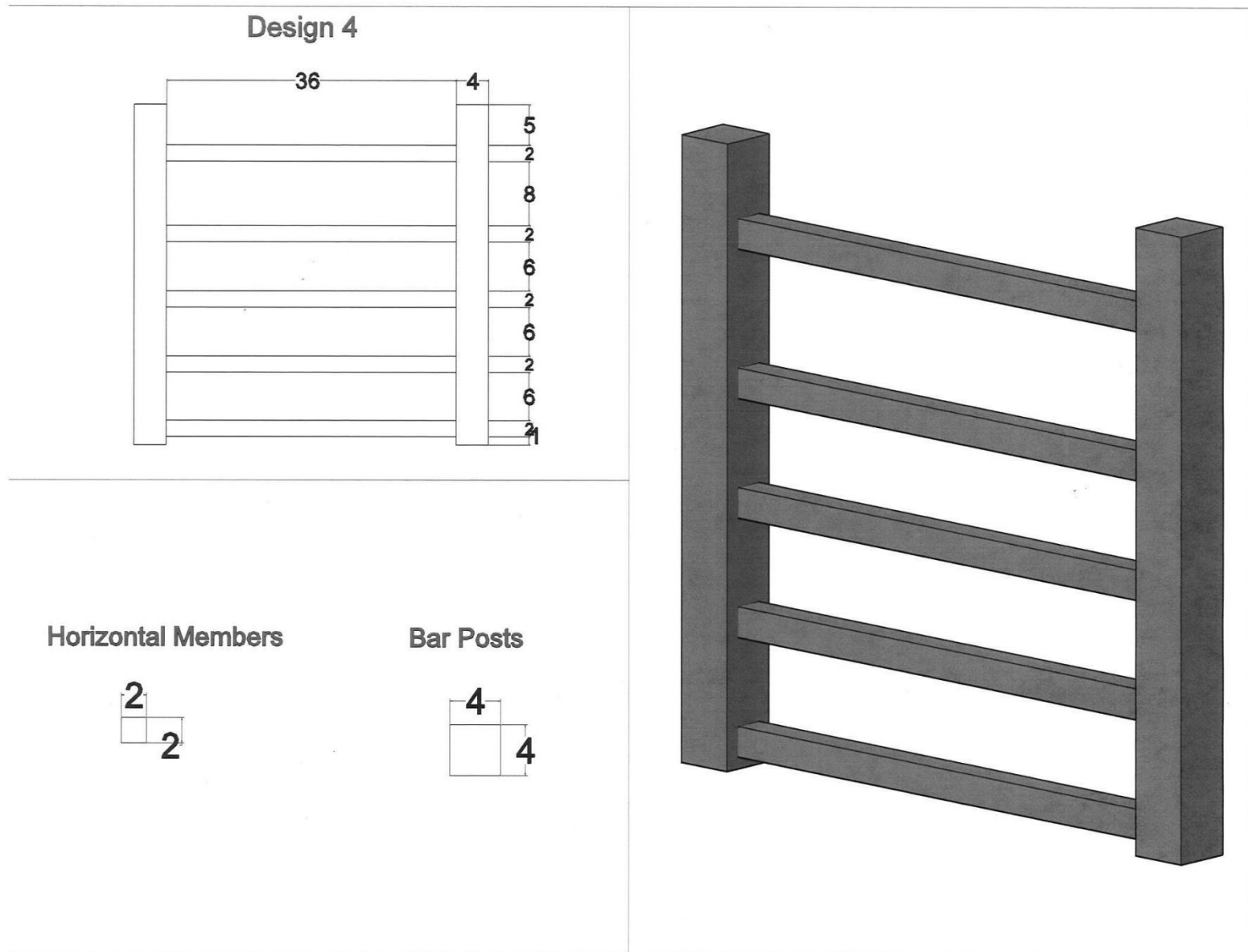


Figure B-23. Design 4: Wood Posts and Rails

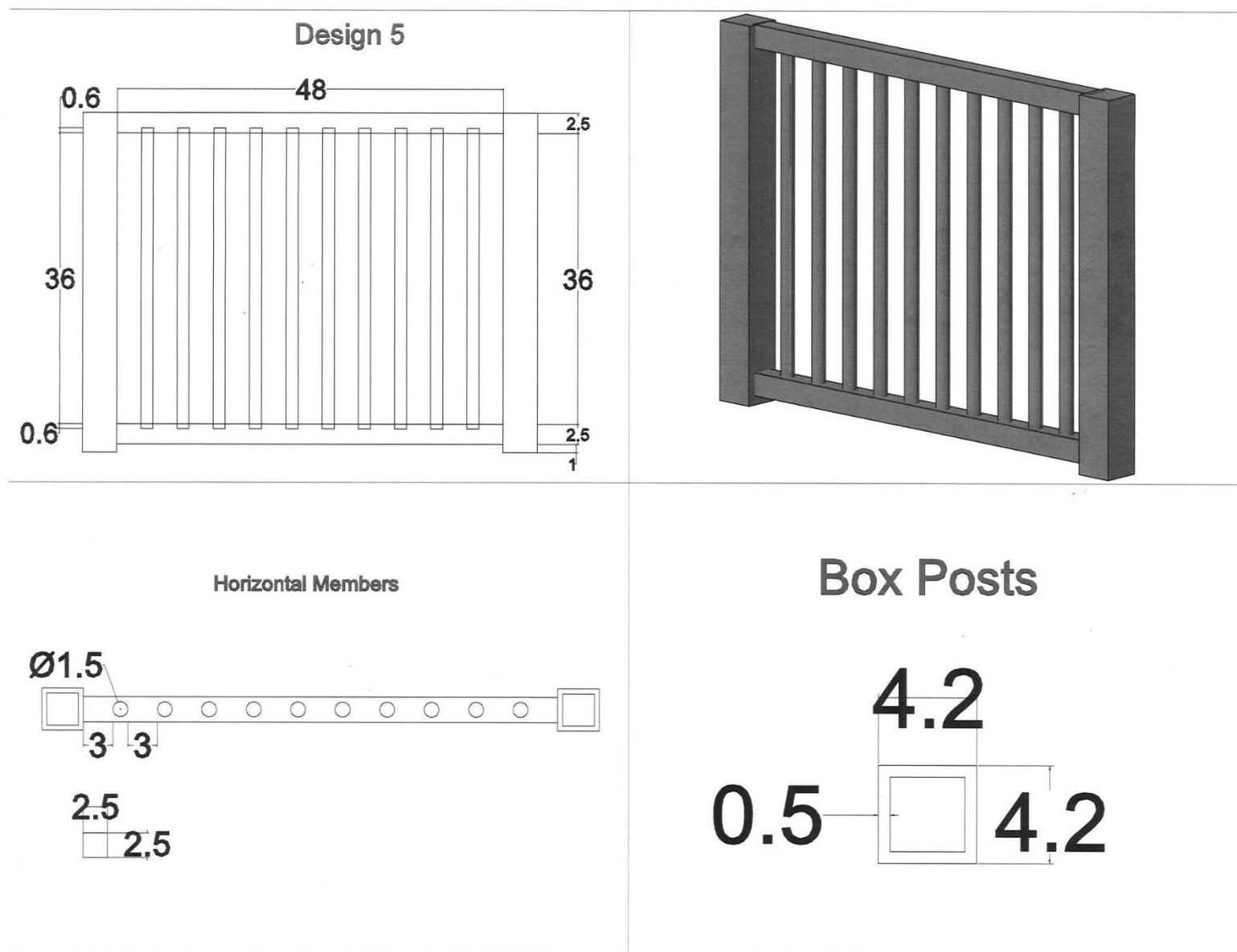


Figure B-24. Design 5: HDPE Posts, Wood Rails, FRP Spindles

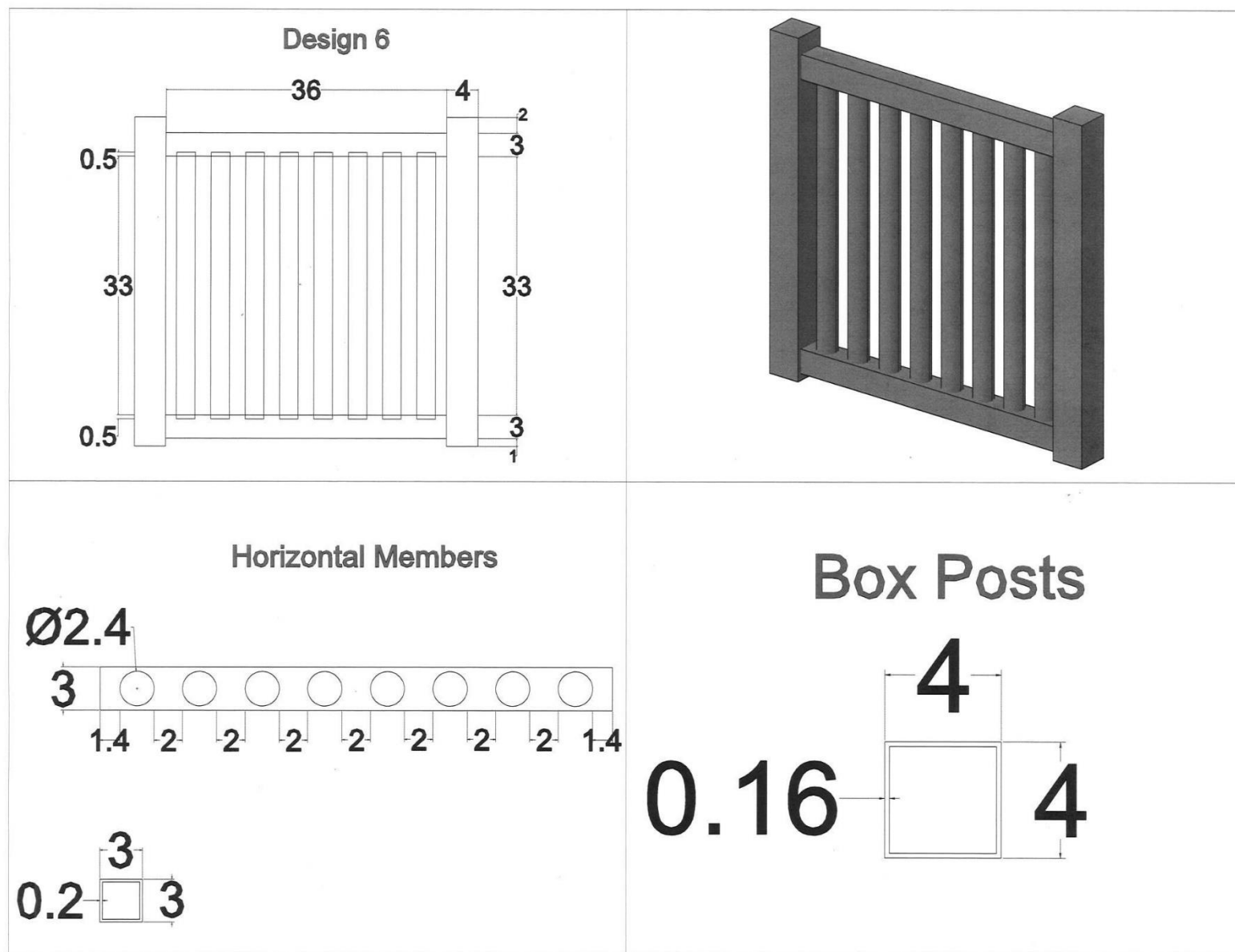


Figure B-25. Design 6: FRP Posts, HDPE Rails, PVC Spindles

Appendix C. Design Calculations

The material strengths for 6061-T6 aluminum, 5356 aluminum weld filler, and 535 aluminum alloy castings that were used in the example calculations are shown in Tables C-1, C-2, and C-3, respectively.

Table C-1. Material Strengths for 6061-T6 Aluminum from Tables A.3.4, A.3.5, and A3.1 in ADM [38]

Non-Welded Strength Extrusions, All Thicknesses ksi (MPa)		Non-Welded Strength Sheet & Plate, 0.010 ≤ t ≤ 4.000 in. ksi (MPa)		Weld-Affected Strength All Shapes, t ≤ 0.375 in. ksi (MPa)		Weld-Affected Strength All Shapes, t > 0.375 in. ksi (MPa)	
F _{tu}	38 (260)	F _{tu}	42 (290)	F _{tuw}	24 (165)	F _{tuw}	24 (165)
F _{ty}	35 (240)	F _{ty}	35 (240)	F _{tyw}	15 (105)	F _{tyw}	11 (80)
F _{cy}	35 (240)	F _{cy}	35(240)	F _{cyw}	15 (105)	F _{cyw}	11 (80)
F _{su}	24 (165)	F _{su}	27 (185)	F _{suw}	15 (105)	F _{suw}	15 (105)
F _{sy}	21(145)	F _{sy}	21 (145)	F _{syw}	9 (62)	F _{syw}	6.6 (46)

Where:

F_{tu} = Tensile Ultimate Strength
F_{ty} = Tensile Yield Strength
F_{cy} = Compressive Yield Strength
F_{su} = Shear Ultimate Strength
F_{tuw} = Tensile Ultimate Strength of Weld-Affected Zones
F_{tyw} = Tensile Yield Strength of Weld-Affected Zones
F_{cyw} = Compressive Yield Strength of Weld-Affected Zones
F_{suw} = Shear Ultimate Strength of Weld-Affected Zones
F_{sy} = Shear Yield Strength
F_{syw} = Shear Yield Strength of Weld-Affected Zones

Table C-2. Material Strengths for 5356 Aluminum Weld Filler from Table J.2.1 in ADM [38]

Weld Strength ksi (MPa)	
F _{tuw}	35 (240)
F _{suw}	17 (115)

Table C-3. Material Strengths for 535 Aluminum Alloy Castings from Table A.3.6 in ADM [38]

Weld Strength ksi (MPa)	
F _{tu}	26.2 (180)
F _{ty}	13.5 (93)

The capacity of a weld was determined for four different connections: Concepts AW2-A and AW2-D post-to-base; Concept AW2-C sleeve-to-base; Concepts AW2-A, AW2-C, and AW2-D rail-to-post; and Concepts AW2-A, AW2-C, and AW2-D spindle-to-post. An example of determining the moment of inertia of the weld group and all the calculations is shown in Figure C-1 for Concept AW2-A post-to-base weld. The weld calculations are shown in Figures C-2 through C-5 for all concepts.

Example calculations of the baseplate by Method nos. 1 and 2 are shown for Concept AW2-A in Figures C-6 and C-7. The calculations for all baseplate designs are shown in C-8 through C-15.

The calculations for the anchor capacity in both tension and shear for all concepts is shown in Figures C-16 through C-21.

The final design calculations are shown in Figures C-22 through C-25.

Weld Capacity

Inputs: S_w (Weld Size) = ¼ in.
 $F_{suw}(\text{filler}) = 17,000$ psi
 $F_{suw}(\text{base metal}) = 15,000$ psi
 $F_{tuw}(\text{base metal}) = 24,000$ psi
 b (Flange Width) = 2 in.
 h (Web Width) = 4 in.
 $\phi = 0.75$
 e (Effective Throat) = $S_w * \cos 45^\circ = 0.25 * \cos 45^\circ = 0.1768$ in.

From Equation 32, $\phi R_n = \phi F_{sw} L_{we}$

F_{sw} = Shear Strength of Weld [psi], which is the Least of:

$$F_{suw}(\text{filler}) * e = 17,000 \text{ psi} * e = 17,000 * 0.1768 = 3,005 \text{ psi}$$

$$F_{suw}(\text{base metal}) * S_w = 15,000 \text{ psi} * S_w = 15,000 * 0.25 = 3,750 \text{ psi}$$

$$F_{tuw}(\text{base metal}) * S_w = 24,000 \text{ psi} * S_w = 24,000 * 0.25 = 6,000 \text{ psi}$$

Therefore, $F_{sw} = 3,005$ psi.

$$L_{we} \text{ (Weld Effective Length)} = 2 * 2 \text{ in.} + 2 * 4 \text{ in.} = 12 \text{ in.}$$

$$\phi R_n = \phi F_{sw} L_{we} = 0.75 * 3,005 \text{ psi} * 12 \text{ in.} = 27,047 \text{ lb}$$

From Equation 33, $\phi M_n = \frac{\phi F_{suw}(\text{filler}) I}{c}$

I (Moment of Inertia, Weld Group)

$$= 2(I_{flange} + A_{flange} d_{flange}^2) + 2(I_{web} + A_{web} d_{web}^2)$$

$$I_{flange} = \frac{be^3}{12} = \frac{2 * 0.1768^3}{12} = 0.00092 \text{ in.}^4$$

$$I_{web} = \frac{eh^3}{12} = \frac{0.1768 * 4^3}{12} = 0.9428 \text{ in.}^4$$

$$A_{flange} = be = 2 * 0.1768 = 0.3536 \text{ in.}^2$$

$$A_{web} = eh = 0.1768 * 4 = 0.7071 \text{ in.}^3$$

$$d_{flange} = \left(\frac{h}{2}\right) + \left(\frac{e}{2}\right) \cos 45^\circ = \left(\frac{4}{2}\right) + \left(\frac{0.1768}{2}\right) \cos 45^\circ = 2.0625 \text{ in.}$$

$$d_{web} = 0$$

$$I = 2(0.00092 + 0.3536 * 2.0625^2) + 2(0.9428 + 0.7071 * 0^2) = 4.895 \text{ in.}^4$$

$$c(\text{Distance to Neutral Axis}) = \left(\frac{h}{2}\right) + \left(\frac{e}{2}\right) \cos 45^\circ = \left(\frac{4}{2}\right) + \left(\frac{0.1768}{2}\right) \cos 45^\circ = 2.0625 \text{ in.}$$

$$\phi M_n = \frac{\phi F_{suw(filler)} I}{c} = \frac{0.75 * 17,000 \text{ psi} * 4.895 \text{ in.}^4}{2.0625 \text{ in.}} = 30,363 \text{ in.} - \text{lb}$$

$$= 2,522 \text{ ft} - \text{lb}$$

Figure C-1. Example Calculation of Weld, Concept AW2-A

Connection: 2" x 4" x 1/4" Post-to-Base Plate, 1/4" Weld

Input Name	Input Value	Units
S _w (weld size)	1/4	in.
F _{suw} (filler)	17000	psi
F _{suw} (base metal)	15000	psi
F _{tuw} (base metal)	24000	psi
b flange width	2	in.
h web width	4	in.
Φ	0.75	

Output Name	Output Value	Units
e (effective throat)	0.176776695	in.
F _{sw}	3005.20382	lb/in.
L _{we} (effective weld length)	12	in.
R _n (nominal shear capacity)	27046.83438	lb
M _n (nominal moment capacity)	30262.63013	in.-lb
M _n (nominal moment capacity)	2521.885845	ft-lb
c (distance to neutral axis (NA))	2.0625	in.
I (moment of inertia of weld group)	4.895425463	in. ⁴
I _{flange} (moment of inertia of flange)	0.000920712	in. ⁴
I _{web} (moment of inertia of web)	0.942809042	in. ⁴
A _{flange} (area of one flange)	0.353553391	in. ²
A _{web} (area of one web)	0.707106781	in. ²
d _{flange} (distance from NA section to NA flange)	2.0625	in.
d _{web} (distance from NA section to NA web)	0	in.

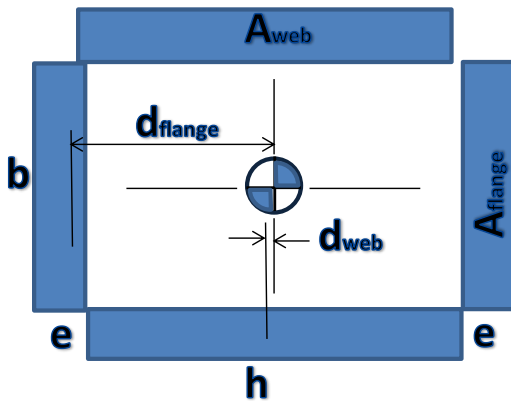


Figure C-2. Post-to-Base Weld, Concepts AW2-A and AW2-D

Connection: 2 1/8" x 3 1/8" x 1/4" Sleeve-to-Base Plate, 3/16" Weld

Input Name	Input Value	Units
S_w (weld size)	3/16	in.
F_{suw} (filler)	17000	psi
F_{suw} (base metal)	15000	psi
F_{tuw} (base metal)	24000	psi
b flange width	2 1/8	in.
h web width	3 1/8	in.
Φ	0.75	

Output Name	Output Value	Units
e (effective throat)	0.132582521	in.
F_{sw}	2253.902865	lb/in.
L_{we} (effective weld length)	10 1/2	in.
R_n (nominal shear capacity)	17749.48506	lb
M_n (nominal moment capacity)	16911.21663	in.-lb
M_n (nominal moment capacity)	1409.268053	ft-lb
C (distance to neutral axis)	1.609375	in.
I (moment of inertia of weld group)	2.134626609	in. ⁴
I_{flange} (moment of inertia of flange)	0.000412702	in. ⁴
I_{web} (moment of inertia of web)	0.337174788	in. ⁴
A_{flange} (area of one flange)	0.281737858	in. ²
A_{web} (area of one web)	0.41432038	in. ²
d_{flange} (distance from NA section to NA flange)	1.609375	in.
d_{web} (distance from NA section to NA web)	0	in.

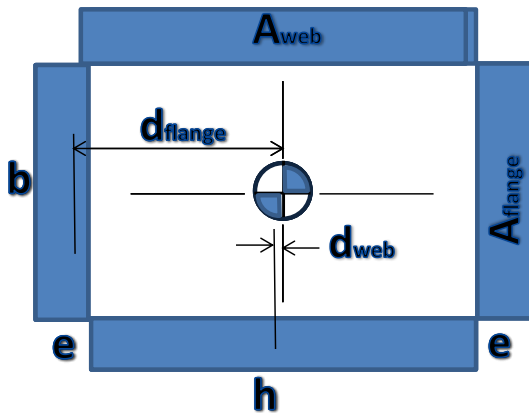


Figure C-3. Post-to-Base Weld, Concept AW2-C

Connection: 2" x 2" x 1/8" Rail-to-Post, 1/8" Weld

Input Name	Input Value	Units
S_w (weld size)	1/8	in.
F_{suw} (filler)	17000	psi
F_{suw} (base metal)	15000	psi
F_{tuw} (base metal)	24000	psi
b flange width	2	in.
h web width	2	in.
Φ	0.75	

Output Name	Output Value	Units
e (effective throat)	0.088388348	in.
F_{sw}	1502.60191	lb/in.
L_{we} (effective weld length)	8	in.
R_n (nominal shear capacity)	9015.61146	lb
M_n (nominal moment capacity)	6108.589015	in.-lb
M_n (nominal moment capacity)	509.0490846	ft-lb
C (distance to neutral axis)	1.03125	in.
I (moment of inertia of weld group)	0.494077053	in. ⁴
I_{flange} (moment of inertia of flange)	0.000115089	in. ⁴
I_{web} (moment of inertia of web)	0.058925565	in. ⁴
A_{flange} (area of one flange)	0.176776695	in. ²
A_{web} (area of one web)	0.176776695	in. ²
d_{flange} (distance from NA section to NA flange)	1.03125	in.
d_{web} (distance from NA section to NA web)	0	in.

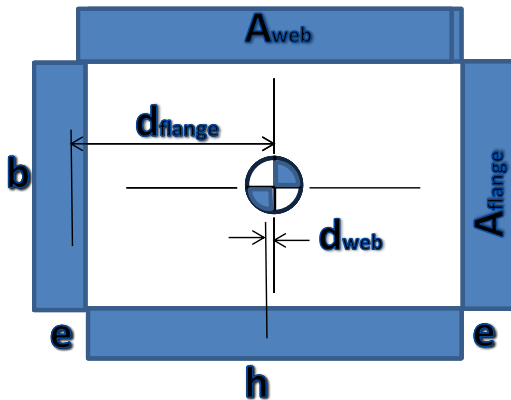


Figure C-4. Rail-to-Post Weld, Concepts AW2-A, AW2-C, and AW2-D

Connection: 1/2" x 1/2" Spindle-to-Rail, 1/8" Weld

Input Name	Input Value	Units
S_w (weld size)	1/8	in.
F_{suw} (filler)	17000	psi
F_{suw} (base metal)	15000	psi
F_{tuw} (base metal)	24000	psi
b flange width	1/2	in.
h web width	1/2	in.
Φ	0.75	

Output Name	Output Value	Units
e (effective throat)	0.088388348	in.
F_{sw}	1502.60191	lb/in.
L_{we} (effective weld length)	2	in.
R_n (nominal shear capacity)	2253.902865	lb
M_n (nominal moment capacity)	403.0416582	in.-lb
M_n (nominal moment capacity)	33.58680485	ft-lb
C (distance to neutral axis)	0.28125	in.
I (moment of inertia of weld group)	0.008890625	in. ⁴
I_{flange} (moment of inertia of flange)	2.87722E-05	in. ⁴
I_{web} (moment of inertia of web)	0.000920712	in. ⁴
A_{flange} (area of one flange)	0.044194174	in. ²
A_{web} (area of one web)	0.044194174	in. ²
d_{flange} (distance from NA section to NA flange)	0.28125	in.
d_{web} (distance from NA section to NA web)	0	in.

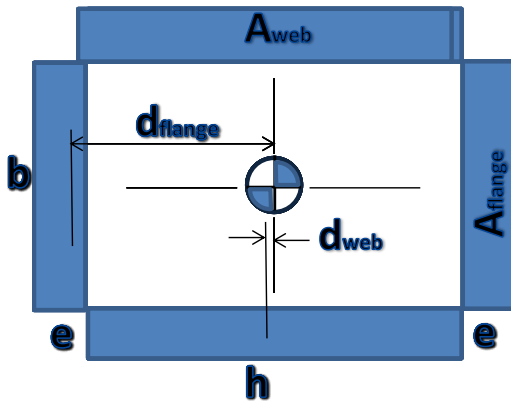


Figure C-5. Spindle-to-Rail Weld, Concepts AW2-A, AW2-C, and AW2-D

Baseplate Capacity

Inputs:

B=3 in. (Width of Baseplate)

N=7.5 in. (Depth of Baseplate)

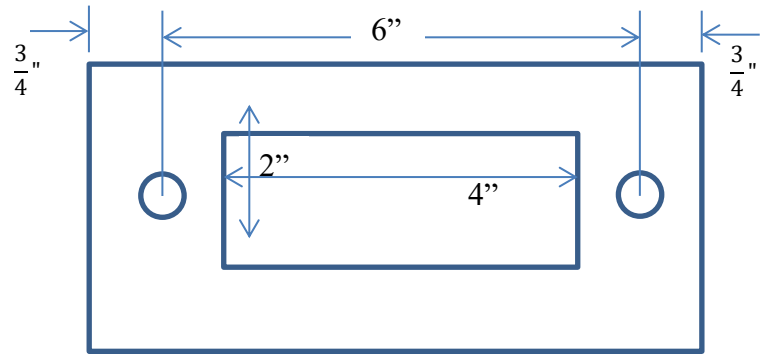
b_f= 2 in. (Width of Flange)

d=4 in. (Depth of Web)

M_u= 1,537.5 lb-ft (Moment on Baseplate)

F_y = yield stress [psi] = F_{tyw} = 15,000 psi

φ = 0.90



$$m = \frac{N - 0.95d}{2} = \frac{7.5 - 0.95(4)}{2} = 1.85 \text{ in.}$$

$$n = \frac{B - 0.80b_f}{2} = \frac{3 - 0.80(2)}{2} = 0.7 \text{ in.}$$

l = Greater of m and n = 1.85 in.

$$P_u = \frac{M_u}{d} = \frac{1,537.5 \text{ ft} \cdot \text{lb} \left(12 \frac{\text{in.}}{\text{ft}} \right)}{4 \text{ in.}} = 4,613 \text{ lb}$$

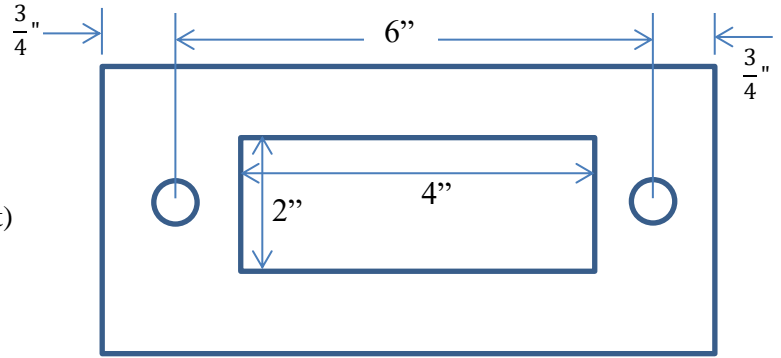
$$t_{min} = l \sqrt{\frac{2P_u}{\phi F_y B N}} = 1.85 \text{ in.} \sqrt{\frac{2 * 4,613 \text{ lb}}{0.9 * 15,000 \text{ psi} * 3 \text{ in.} * 7.5 \text{ in.}}} = 0.322 \text{ in.}$$

Choose a baseplate thickness of t = 3/8 in. The nominal capacity, φP_n, of a 3/8-in. baseplate is:

$$\phi P_n = \phi \frac{F_y B N}{2} \left(\frac{t}{l} \right)^2 = 0.90 \frac{15,000 \text{ psi} * 3 \text{ in.} * 7.5 \text{ in.}}{2} \left(\frac{\frac{3}{8} \text{ in.}}{1.85 \text{ in.}} \right)^2 = 6,240 \text{ lb}$$

φP_n = 6,240 lb > P_u = 4,613 lb , so the design is adequate.

Figure C-6. Example Calculation of Baseplate – Method No. 1, Concept AW2-A



Inputs:

$B = 3$ in. (Width of Baseplate)

$N = 7.5$ in. (Depth of Baseplate)

$N' = 6.75$ in.

$A' = 3$ in. (Distance from Bolt to Center of Post)

$b_f = 2$ in. (Width of Flange)

$d = 4$ in. (Depth of Web)

$M_u = 1,537.5$ lb-ft $\times 12$ in/ft = 18,450 lb-in.

$P_u = 575$ lb

$\Phi = 0.90$

$$A_1 = B * N = 3 * 7.5 = 22.5 \text{ in.}^2$$

$$A_2 = 4 * A_1 = 90 \text{ in.}^2$$

$$m = \frac{N - 0.95d}{2} = \frac{7.5 - 0.95(4)}{2} = 1.85 \text{ in.}$$

$$e = \frac{M_u}{P_u} = \frac{18,450 \text{ lb-in}}{575 \text{ lb}} = 32.1 \text{ in.} \quad e_{crit} = \frac{N}{2} = \frac{7.5}{2} = 3.75 \text{ in.}$$

$e > e_{crit}$, so use design with a large eccentricity

$$F_p = 0.65 \times 0.85 f_c' \sqrt{\frac{A_2}{A_1}} \leq 0.65 \times 1.7 f_c' = 0.65 \times 0.85 (2500) (4) \leq 0.65 \times 1.7 (2500) = 2,762.5 \text{ psi}$$

$$f' = \frac{F_p B N'}{2} = \frac{2,762.5 * 3 * 6.75}{2} = 27,970.3 \text{ lb}$$

$$A = \frac{f' \pm \sqrt{(f')^2 - 4 \left(\frac{F_p B}{6} \right) (P A' + M)}}{\frac{F_p B}{3}}$$

$$= \frac{27,970.3 \text{ lb} \pm \sqrt{(27,970.3 \text{ lb})^2 - 4 \left(\frac{2,762.5 \text{ psi} * 3 \text{ in.}}{6} \right) (575 \text{ lb} * 3 \text{ in.} + 1,537.5 \text{ ft-lb} * 12 \text{ in./ft})}}{\frac{2,762.5 \text{ psi} * 3 \text{ in.}}{3}}$$

$$= 0.749 \text{ in.}$$

$$T = \frac{F_p A B}{2} - P = \frac{2,762.5 \text{ psi} * 0.749 \text{ in.} * 3 \text{ in.}}{2} - 575 \text{ lb} = 3,104 \text{ lb}$$

$$M_{pl} = \frac{F_p A}{2} \left(m - \frac{1}{3} A \right) = \frac{2,762.5 \text{ psi} * 0.749 \text{ in.}}{2} \left(1.85 - \frac{1}{3} * 0.749 \right) = 1,655 \text{ lb-in./in.}$$

$$t_{min} = \sqrt{\frac{4 M_{pl}}{0.9 F_y}} = \sqrt{\frac{4 * 1,655 \text{ lb-in./in.}}{0.9 * 15,000 \text{ psi}}} = 0.7 \text{ in.}$$

Even though this method requires a minimum 0.7 in. thick, t_{min} , baseplate, a $t = 3/8$ -in. thick baseplate was selected for the design. According to this method, the nominal bending capacity of the plate is:

$$\phi M_n = \frac{\phi F_y t^2}{4} = \frac{0.9 * 15,000 \text{ psi} * (.375 \text{ in.})^2}{4} = 474.6 \text{ lb-in./in.}$$

$$\phi M_n = 474.6 \text{ lb-in./in.} < M_{pl} = 1,655 \text{ lb-in./in.}$$

Figure C-7. Example Calculation of Baseplate – Method No. 2, Concept AW2-A

Concept: AW2-A

Variable	Input	Unit	Description	
b	2	in.	width of post	
d	4	in.	depth of post	
B	3	in.	width of base plate	
N	7.5	in.	depth of base plate	
F _{tyw}	15000	psi	tensile yield strength	
M _u	1537.5	ft-lb	moment at base of post	
φ	0.9			
Variable	Calculation	Unit	Equation	Description
P _u	4612.5	lb	=M _u /d	maximum vertical force on base plate
m	1.85	in.	=(N-0.95d)/2	location of critical section along N
n	0.7	in.	=(B-0.80b)/2	location of critical section along B
l	1.85	in.		the greater of m and n
t _{min}	0.322	in.	=l*sqrt(2P _u /(φF _{tyw} BN))	minimum base plate thickness
t	0.375	in.		actual base plate thickness
φP _n	6240.3	lb	=φF _{tyw} BN/2*(t/l)^2	nominal base plate capacity

$\phi P_n > P_u$ so design is good

Figure C-8. Capacity of Baseplate – Method No. 1, Concept AW2-A

Concept: AW2-C

Variable	Input	Unit	Description	
b	2	in.	width of post	
d	3	in.	depth of post	
B	3.5	in.	width of base plate	
N	7.5	in.	depth of base plate	
F _{tyw}	15000	psi	tensile yield strength	
M _u	1537.5	ft-lb	moment at base of post	
φ	0.9			
Variable	Calculation	Unit	Equation	Description
P _u	6150	lb	=M _u /d	maximum vertical force on base plate
m	2.325	in.	=(N-0.95d)/2	location of critical section along N
n	0.95	in.	=(B-0.80b)/2	location of critical section along B
l	2.325	in.		the greater of m and n
t _{min}	0.433	in.	=l*sqrt(2P _u /(φF _{tyw} BN))	minimum base plate thickness
t	0.375	in.		actual base plate thickness
φP _n	4609.5	lb	=φF _{tyw} BN/2*(t/l)^2	nominal base plate capacity

$\phi P_n < P_u$ so design is not good

Figure C-9. Capacity of Baseplate – Method #No. 1, Concept AW2-C

Concept: AM-1

Variable	Input	Unit	Description	
b	2.375	in.	width of post	
d	2.375	in.	depth of post	
B	5	in.	width of base plate	
N	8.5	in.	depth of base plate	
F _{ty}	13500	psi	tensile yield strength	
M _u	1537.5	ft-lb	moment at base of post	
φ	0.9			
Variable	Calculation	Unit	Equation	Description
P _u	7768.4	lb	=M _u /d	maximum vertical force on base plate
m	3.122	in.	=(N-0.95d)/2	location of critical section along N
n	1.55	in.	=(B-0.80b)/2	location of critical section along B
l	3.122	in.		the greater of m and n
t _{min}	0.542	in.	=l*sqrt(2P _u /(φF _{ty} BN))	minimum base plate thickness
t	0.5625	in.		actual base plate thickness
φP _n	8382.0	lb	=φF _{ty} BN/2*(t/l)^2	nominal base plate capacity

φP_n>P_u so design is good

Figure C-10. Capacity of Baseplate – Method No. 1, Concept AM-1

Concept: AW2-D

Variable	Input	Unit	Description	
b	2	in.	width of post	
d	4	in.	depth of post	
B	3	in.	width of base plate	
N	7.75	in.	depth of base plate	
F _{tyw}	15000	psi	tensile yield strength	
M _u	1537.5	ft-lb	moment at base of post	
φ	0.9			
Variable	Calculation	Unit	Equation	Description
P _u	4612.5	lb	=M _u /d	maximum vertical force on base plate
m	1.975	in.	=(N-0.95d)/2	location of critical section along N
n	0.7	in.	=(B-0.80b)/2	location of critical section along B
l	1.975	in.		the greater of m and n
t _{min}	0.339	in.	=l*sqrt(2P _u /(φF _{tyw} BN))	minimum base plate thickness
t	0.375	in.		actual base plate thickness
φP _n	5657.9	lb	=φF _{tyw} BN/2*(t/l)^2	nominal base plate capacity

φP_n>P_u so design is good

Figure C-11. Capacity of Baseplate – Method No. 1, Concept AW2-D

Concept: AW2-A

Variable	Input	Unit	Description	
M _u	18450	in-lb	max moment at base of post	
P _u	575	lb	axial load on base plate	
B	3	in	width of BP	
N	7.5	in	length of BP	
N'	6.75	in	distance from edge of plate to far bolt along N	
A'	3	in	distance from anchor to centerline of post along N	
b	2	in	flange of post	
d	4	in	web of post	
f _c '	2500	psi	compression strength of concrete	
A ₁	22.5	in. ²	area of base plate	
A ₂	90	in. ²	area of supporting concrete foundation	
F _{tyw}	15000	psi	tensile yield strength	
φ	0.9			
φ _c	0.65			
Variable	Output	Unit	Calculation	Description
e	32.08696	in.	M _u /P _u	eccentricity
e _{crit}	3.75	in	N/2	critical eccentricity
			e>e _{crit}	therefore use large eccentricity base plate design
m	1.85	in.	(N-0.95d)/2	location of critical section along N
F _p	2762.5	psi	φ _c 0.85f _c '*sqrt(A ₂ /A ₁)	maximum design bearing stress
	2762.5	psi	≤φ _c 1.7f _c '	maximum design bearing stress
f'	27970.3	lb		
A	0.749	in.	(f'±sqrt((f')^2-4*(F _p B/6)(P _u A'+M)))/(F _p B/3)	length of bearing stress block along N
T	2528.7	lb	F _p AB/2-P _u	tension in bolt
M _{pl}	1655.6	lb-in./in.	0.5*F _p A(m-1/3A)	required bending moment per width
t _{min}	0.700	in.	sqrt(4*M _{pl} /(φF _{tyw}))	minimum base plate thickness
t	0.375	in.		actual base plate thickness
φM _n	474.6	lb-in./in.	φF _{tyw} t ² /4	nominal moment capacity

$\phi M_n < M_{pl}$ so design is not good

Figure C-12. Capacity of Baseplate – Method No. 2, Concept AW2-A

Concept: AW2-C

Variable	Input	Unit	Description	
M _u	18450	in-lb	max moment at base of post	
P _u	575	lb	axial load on base plate	
B	3.5	in	width of BP	
N	7.5	in	length of BP	
N'	6.75	in	distance from edge of plate to far bolt along N	
A'	3	in	distance from anchor to centerline of post along N	
b	2	in	flange of post	
d	3	in	web of post	
f _c '	2500	psi	compression strength of concrete	
A ₁	26.25	in. ²	area of base plate	
A ₂	105	in. ²	area of supporting concrete foundation	
F _{tyw}	15000	psi	tensile yield strength	
φ	0.9			
φ _c	0.65			
Variable	Output	Unit	Calculation	Description
e	32.08696	in.	M _u /P _u	eccentricity
e _{crit}	3.75	in	N/2	critical eccentricity
			e>e _{crit}	therefore use large eccentricity base plate design
m	2.325	in.	(N-0.95d)/2	location of critical section along N
F _p	2762.5	psi	φ _c 0.85f _c '*sqrt(A ₂ /A ₁)	maximum design bearing stress
	2762.5	psi	≤φ _c 1.7f _c '	maximum design bearing stress
f'	32632.0	lb		
A	0.638	in.	(f'±sqrt((f')^2-4*(F _p B/6)(P _u A'+M)))/(F _p B/3)	length of bearing stress block along N
T	2511.2	lb	F _p AB/2-P _u	tension in bolt
M _{pl}	1862.5	lb-in./in.	0.5*F _p A(m-1/3A)	required bending moment per width
t _{min}	0.743	in.	sqrt(4*M _{pl} /(φF _{tyw}))	minimum base plate thickness
t	0.375	in.		actual base plate thickness
φM _n	474.6	lb-in./in.	φF _{tyw} t ² /4	nominal moment capacity

$\phi M_n < M_{pl}$ so design is not good

Figure C-13. Capacity of Baseplate – Method No. 2, Concept AW2-C

Concept: AM-1

Variable	Input	Unit	Description	
M _u	18450	in-lb	max moment at base of post	
P _u	575	lb	axial load on base plate	
B	5	in	width of BP	
N	8.5	in	length of BP	
N'	6.75	in	distance from edge of plate to far bolt along N	
A'	2.75	in	distance from anchor to centerline of post along N	
b	2.375	in	flange of post	
d	2.375	in	web of post	
f _c '	2500	psi	compression strength of concrete	
A ₁	42.5	in. ²	area of base plate	
A ₂	170	in. ²	area of supporting concrete foundation	
F _{ty}	13500	psi	tensile yield strength	
φ	0.9			
φ _c	0.65			
Variable	Output	Unit	Calculation	Description
e	32.08696	in.	M _u /P _u	eccentricity
e _{crit}	4.25	in	N/2	critical eccentricity
			e>e _{crit}	therefore use large eccentricity base plate design
m	3.121875	in.	(N-0.95d)/2	location of critical section along N
F _p	2762.5	psi	φ _c 0.85f _c '*sqrt(A ₂ /A ₁)	maximum design bearing stress
	2762.5	psi	≤φ _c 1.7f _c '	maximum design bearing stress
f'	46617.2	lb		
A	0.439	in.	(f'±sqrt((f')^2-4*(F _p B/6)(P _u A'+M)))/(F _p B/3)	length of bearing stress block along N
T	2458.4	lb	F _p AB/2-P _u	tension in bolt
M _{pl}	1805.1	lb-in./in.	0.5*F _p A(m-1/3A)	required bending moment per width
t _{min}	0.731	in.	sqrt(4*M _{pl} /(φF _{ty}))	minimum base plate thickness
t	0.5625	in.		actual base plate thickness
φM _n	961.1	lb-in./in.	φF _{ty} t ² /4	nominal moment capacity

$\phi M_n < M_{pl}$ so design is not good

Figure C-14. Capacity of Baseplate – Method No. 2, Concept AM-1

Concept: AW2-D

Variable	Input	Unit	Description	
M _u	18450	in-lb	max moment at base of post	
P _u	575	lb	axial load on base plate	
B	3	in	width of BP	
N	7.75	in	length of BP	
N'	7	in	distance from edge of plate to far bolt along N	
A'	3.125	in	distance from anchor to centerline of post along N	
b	2	in	flange of post	
d	4	in	web of post	
f _c '	2500	psi	compression strength of concrete	
A ₁	23.25	in. ²	area of base plate	
A ₂	93	in. ²	area of supporting concrete foundation	
F _{tyw}	15000	psi	tensile yield strength	
φ	0.9			
φ _c	0.65			
Variable	Output	Unit	Calculation	Description
e	32.08696	in.	M _u /P _u	eccentricity
e _{crit}	3.875	in	N/2	critical eccentricity
			e>e _{crit}	therefore use large eccentricity base plate design
m	1.975	in.	(N-0.95d)/2	location of critical section along N
F _p	2762.5	psi	φ _c 0.85f _c '*sqrt(A ₂ /A ₁)	maximum design bearing stress
	2762.5	psi	≤φ _c 1.7f _c '	maximum design bearing stress
f'	29006.3	lb		
A	0.723	in.	(f'±sqrt(((f')^2-4*(F _p B/6)(P _u A'+M))))/(F _p B/3)	length of bearing stress block along N
T	2420.5	lb	F _p AB/2-P _u	tension in bolt
M _{pl}	1731.4	lb-in./in.	0.5*F _p A(m-1/3A)	required bending moment per width
t _{min}	0.716	in.	sqrt(4*M _{pl} /(φF _{tyw}))	minimum base plate thickness
t	0.375	in.		actual base plate thickness
φM _n	474.6	lb-in./in.	φF _{tyw} t ² /4	nominal moment capacity

$\phi M_n < M_{pl}$ so design is not good

Figure C-15. Capacity of Baseplate – Method No. 2, Concept AW2-D

Anchor Capacity

Anchor Design - Concept AW2-A and AW2-C			
TENSION ANCHORS (FRONT FACE)			
Embedment Depth, h_{ef} :	5	in.	
Steel Bar Diameter, d_a :	0.375	in.	
Area of Steel, A_s :	0.078	in. ²	
Front (Tension) Anchor Spacing, s :	6	in.	
Front (Tension) Anchor to deck edge, $c_{a,min}$:	10	in.	
Bond Strength, $\tau_{uncr} = \tau_{cr}$:	1450	psi	
Steel Strength, f_{uta} :	125000	psi	
Concrete Strength, f'_c :	2500	psi	
Foundation Reinforced? (γ/n):	n		
λ_u :	1		
		Tension Strengths	
		Failure Mode	Load (kips)
		Steel Fracture:	7313
		Concrete Breakout:	8648
		Bond Failure:	5552
		Tension	Shear
ACI Steel Strength Reduction Factor, ϕ_s :	0.75	0.65	
ACI Concrete Strength Reduction Factor, ϕ_c :	0.65	0.75	
ACI Adhesive Strength Reduction Factor, ϕ_a :	0.65	NA	
Required Capacity	$\approx 1537.5 \times 12/s$	3075	lb
TENSION CAPACITY			
Steel Fracture: $\phi N_{sa} = A_{se,N} f_{uta}$			
		$\phi N_{sa} =$	7312.50 lb
Concrete Breakout: $\phi N_{cb} = A_{Nc}/A_{Nco} * \psi_{ed,N} \psi_{c,N} \psi_{cp,N} * N_b$			
		$N_b = k_c * \lambda_u h_{ef}^{1.5} \sqrt{f'_c}$	
		k_c :	17 (24 for cast in place, 17 for post installed)
		$\psi_{c,N}$:	1.4 (1.25 for cast in anchors, 1.4 for post installed)
		$N_b =$	9503.29 lb
		c_{ac} :	10
		$\psi_{cp,N}$:	1
		$\psi_{ed,N}$:	1
		$A_{Nco} = 9 * h_{ef}^2$:	225 in. ²
		A_{Nc} :	225 in. ²
		A_{Nc}/A_{Nco} :	1
		$\phi N_{cb} =$	8647.99 lb
Adhesive / Bond Failure: $\phi N_a = A_{Na}/A_{Na0} * \psi_{ed,Na} \psi_{cp,Na} * N_{ba}$			
		$N_{ba} = \tau_{cr} \pi d_s h_{ef}$	
		$N_{ba} =$	8541.21 lb
		$A_{Na0} = (2 * C_{Na})^2$	
		$C_{Na} = 10 * d_s * \sqrt{(\tau_{cr}/1100)}$	
		$C_{Na} =$	4.31 in.
		$A_{Na0} =$	74.15 in. ²
		$A_{Na} =$	74.15 in. ²
		A_{Na}/A_{Na0} :	1
		$\psi_{cp,Na}$:	1 (should be the same as $\psi_{cp,N}$)
		$\psi_{ed,Na}$:	1
		$\phi N_a =$	5551.78 lb

Figure C-16. Capacity of Anchors-Tension, Concepts AW2-A and AW2-C

Anchor Design - Concept AW2-A and AW2-C		
SHEAR ANCHORS (BACK FACE)		
Embedment Depth, h_{ef} :	5	in.
Steel Bar Diameter, d_b :	0.375	in.
Area of Steel, A_s :	0.078	in. ²
Anchor Spacing, s :	6	in.
Anchor to Deck Edge Distance, c_{a1} :	10	in.
Steel Strength, f_{uta} :	125000	psi
Concrete Strength, f'_c :	2500	psi
Foundation Thickness, h_f :	7	in.
Foundation Reinforced? (y/n):	n	
Bond Strength, τ_{cr} :	1450	psi
λ_a	1	
Required Capacity	225	lb
SHEAR CAPACITY		
Steel Fracture: $\phi V_{sa} = 0.6 * A_{se} * f_{uta}$		
$\phi V_{sa} =$	3802.50	lb
Concrete Breakout: $\phi V_{cbg} = A_{vc}/A_{vco} * \psi_{ec,v} \psi_{ed,v} \psi_{c,v} \psi_{h,v} * V_b$		
$V_{b1} = 7 * (l_e/d_a)^{0.2} * \sqrt{d_a} * \sqrt{f'_c} * C_{a1}^{1.5}$		
$l_e:$	3.00	
$V_{b1} =$	10273.10	lb
$V_{b2} = 9 * \lambda_a C_{a1}^{1.5} * \sqrt{f'_c}$		
	14230.25	lb
$V_b = \min(V_{b1}, V_{b2}) =$	10273.10	lb
$\psi_{ec,v}:$	1	
$\psi_{ed,v}:$	1	
$\psi_{c,v}:$	1.4	(1.4 for uncracked, 1.2 for cracked reinforced, 1.0 for cracked unreinforced)
$\psi_{h,v}:$	1.463850	
$\psi_{ec,v}:$	1	
$A_{vco} = 4.5 * (c_{a1})^2 =$	450	in. ²
$A_{vc} =$	336	in. ²
$A_{vco}/A_{vc} =$	0.746667	
$\phi V_{cb} =$	11790.01	lb
Concrete Pryout Strength: $\phi V_{cpb} = k_{cp} * N_{cpb}$		
$k_{cp} =$	2	
$N_{cpb} = \text{Min}(N_{cbg}, N_{ag})$		
$N_{cbg} = A_{Nc}/A_{Nco} * \psi_{ec,N} \psi_{ed,N} \psi_{c,N} \psi_{cp,N} * N_b$		
$N_b = k_c * h_{ef}^{1.5} * \sqrt{f'_c}$		
$k_c:$	17	
$\psi_{c,N}:$	1.4	
$N_b =$	9503.29	lb
$c_{ac}:$	10	
$\psi_{cp,N}:$	1	
$\psi_{ed,N}:$	1	
$\psi_{ec,N}:$	1	
$A_{Nco} = 9 * h_{ef}^2:$	225	in. ²
$A_{Nc}:$	225	in. ²
$A_{Nc}/A_{Nco}:$	1	
$N_{cb} =$	13304.60	lb
$N_{cpb} =$	8541.21	lb
$\phi V_{cp} =$	12811.81	lb
$N_{ag} = A_{Na}/A_{Na0} * \psi_{ec,Na} \psi_{ed,Na} \psi_{cp,Na} * N_{ba}$		
$N_{ba} = \tau_{cr} * \pi * d_b * h_{ef}$		
$N_{ba} =$	8541.21	lb
$A_{Na0} = (2 * C_{Na})^2$		
$C_{Na} = 10 * d_a * \sqrt{v(\tau_{cr}/1100)}$		
$C_{Na} =$	4.31	
$A_{Na0} =$	74.15	in. ²
$A_{Na} =$	74.14773	in. ²
$A_{Na}/A_{Na0}:$	1	
$\psi_{ec,Na}:$	1	
$\psi_{cp,Na}:$	1	(should be the same as $\psi_{cp,N}$)
$\psi_{ed,Na}:$	1	
$N_{ag} =$	8541.21	lb

Figure C-17. Capacity of Anchors-Shear, Concepts AW2-A and AW2-C

Anchor Design - Concept AW2-D			
TENSION ANCHORS (FRONT FACE)			
Embedment Depth, h_{ef} :	5	in.	
Steel Bar Diameter, d_a :	0.5	in.	
Area of Steel, A_s :	0.142	in. ²	
Front (Tension) Anchor Spacing, s :	6.25	in.	
Front (Tension) Anchor to deck edge, $c_{a,min}$:	10	in.	
Bond Strength, $\tau_{uncr} = \tau_{cr}$:	1450	psi	
Steel Strength, f_{uta} :	125000	psi	
Concrete Strength, f'_c :	2500	psi	
Foundation Reinforced? (γ/n):	n		
λ_a :	1		
		Tension	Shear
ACI Steel Strength Reduction Factor, ϕ_s :	0.75	0.65	
ACI Concrete Strength Reduction Factor, ϕ_c :	0.65	0.75	
ACI Adhesive Strength Reduction Factor, ϕ_a :	0.65	NA	
Required Capacity	=1537.5*12/s	2952	lb
TENSION CAPACITY			
Steel Fracture: $\phi N_{sa} = A_{se,N} f_{uta}$			
	$\phi N_{sa} =$	13312.50	lb
Concrete Breakout: $\phi N_{cb} = A_{Nc}/A_{Nco} * \psi_{ed,N} \psi_{c,N} \psi_{cp,N} * N_b$			
	$N_b = k_c * \lambda_a h_{ef}^{1.5} \sqrt{f'_c}$		
	k_c :	17	(24 for cast in place, 17 for post installed)
	$\psi_{c,N}$:	1.4	(1.25 for cast in anchors, 1.4 for post installed)
	$N_b =$	9503.29	lb
	C_{ac} :	10	
	$\psi_{cp,N}$:	1	
	$\psi_{ed,N}$:	1	
	$A_{Nco} = 9 * h_{ef}^2$:	225	in. ²
	A_{Nc} :	225	in. ²
	A_{Nc}/A_{Nco} :	1	
	$\phi N_{cb} =$	8647.99	lb
Adhesive / Bond Failure: $\phi N_a = A_{Na}/A_{NaO} * \psi_{ed,Na} \psi_{cp,Na} * N_{ba}$			
	$N_{ba} = \tau_{cr} \pi d_a h_{ef}$		
	$N_{ba} =$	11388.27	lb
	$A_{NaO} = (2 * C_{Na})^2$		
	$C_{Na} = 10 * d_a * \sqrt{(\tau_{cr}/1100)}$		
	$C_{Na} =$	5.74	in.
	$A_{NaO} =$	131.82	in. ²
	$A_{Na} =$	131.82	in. ²
	A_{Na}/A_{NaO} :	1	
	$\psi_{cp,Na}$:	1	(should be the same as $\psi_{cp,N}$)
	$\psi_{ed,Na}$:	1	
	$\phi N_a =$	7402.38	lb

Figure C-18. Capacity of Anchors-Tension, Concept AW2-D

Anchor Design - Concept AW2-D											
SHEAR ANCHORS (BACK FACE)											
Embedment Depth, h_{ef} :	5 in.	Shear Strengths <table border="1"> <thead> <tr> <th>Failure Mode</th> <th>Load (kips)</th> </tr> </thead> <tbody> <tr> <td>Steel Fracture:</td> <td>6923</td> </tr> <tr> <td>Concrete Breakout:</td> <td>11016</td> </tr> <tr> <td>Concrete Pryout:</td> <td>17082</td> </tr> </tbody> </table>		Failure Mode	Load (kips)	Steel Fracture:	6923	Concrete Breakout:	11016	Concrete Pryout:	17082
Failure Mode	Load (kips)										
Steel Fracture:	6923										
Concrete Breakout:	11016										
Concrete Pryout:	17082										
Steel Bar Diameter, d_s :	0.5 in.										
Area of Steel, A_s :	0.142 in. ²										
Anchor Spacing, s :	6.25 in.										
Anchor to Deck Edge Distance, c_{a1} :	10 in.										
Steel Strength, f_{uta} :	125000 psi										
Concrete Strength, f'_c :	2500 psi										
Foundation Thickness, h_f :	7 in.										
Foundation Reinforced? (y/n):	n										
Bond Strength, τ_{cr} :	1450 psi										
λ_o :	1										
Required Capacity	225 lb										
SHEAR CAPACITY											
Steel Fracture: $\phi V_{sa} = 0.6 A_s N_{f_{uta}}$											
$\phi V_{sa} = 6922.50 \text{ lb}$											
Concrete Breakout: $\phi V_{cbg} = A_{vc}/A_{vco} \cdot \psi_{ec,v} \psi_{ed,v} \psi_{c,v} \psi_{h,v} \cdot V_b$											
$V_{b1} = 7 \cdot (l_e/d_s)^{0.2} \cdot \sqrt{d_s} \cdot \sqrt{f'_c} \cdot c_{a1}^{1.5}$											
$l_e = 4.00$											
$V_{b1} = 11862.36 \text{ lb}$											
$V_{b2} = 9 \cdot c_{a1}^{1.5} \cdot \sqrt{f'_c}$											
14230.25 lb											
$V_b = \min(V_{b1}, V_{b2}) = 11862.36 \text{ lb}$											
$\psi_{ed,v} = 1$ (only reduced for anchor adjacent to deck discontinuity)											
$\psi_{c,v} = 1.4$ (1.4 for uncracked deck, 1.2 for cracked reinforced, 1.0 for cracked unreinforced deck)											
$\psi_{h,v} = 1.46$											
$\psi_{ec,v} = 1$											
$A_{vco} = 4.5 \cdot (c_{a1})^2 = 450 \text{ in.}^2$											
$A_{vc} = 271.875 \text{ in.}^2$											
$A_{vco}/A_{vc} = 0.604167$											
$\phi V_{cb} = 11015.74 \text{ lb}$											
Concrete Pryout Strength: $\phi V_{cpg} = k_{cp} N_{cpg}$											
$k_{cp} = 2$											
$N_{cpg} = \min(N_{cbg}, N_{ag})$											
$N_{cbg} = A_{Nc}/A_{Nco} \cdot \psi_{ec,N} \psi_{ed,N} \psi_{c,N} \psi_{cp,N} \cdot N_b$		$N_{ag} = A_{Na}/A_{Nao} \cdot \psi_{ec,Na} \psi_{ed,Na} \psi_{cp,Na} \cdot N_{ba}$									
$N_b = k_c \cdot h_{ef}^{1.5} \cdot \sqrt{f'_c}$		$N_{ba} = \tau_{cr} \cdot \pi \cdot d_s \cdot h_{ef}$									
$k_c = 17$		$N_{ba} = 11388.27 \text{ lb}$									
$\psi_{c,N} = 1.4$											
$N_b = 9503.29 \text{ lb}$											
$c_{ac} = 10$		$A_{Nao} = (2 \cdot C_{Na})^2$									
$\psi_{cp,N} = 1$		$C_{Na} = 10 \cdot d_s \cdot \sqrt{(\tau_{cr}/1100)}$									
$\psi_{ed,N} = 1$		$C_{Na} = 5.74$									
$\psi_{ec,N} = 1$		$A_{Nao} = 131.82 \text{ in.}^2$									
$A_{Nco} = 9 \cdot h_{ef}^2 = 225 \text{ in.}^2$		$A_{Na} = 131.8182 \text{ in.}^2$									
$A_{Nc} = 225 \text{ in.}^2$		$A_{Na}/A_{Nao} = 1$									
$A_{Nc}/A_{Nco} = 1$		$\psi_{ec,Na} = 1$									
		$\psi_{cp,Na} = 1$ (should be the same as $\psi_{cp,N}$)									
		$\psi_{ed,Na} = 1$									
$N_{cb} = 13304.60 \text{ lb}$		$N_{ag} = 11388.27 \text{ lb}$									
		$N_{cpg} = 11388.27 \text{ lb}$									
$\phi V_{cp} = 17082.41 \text{ lb}$											

Figure C-19. Capacity of Anchors-Shear, Concept AW2-D

Anchor Design - Concept AM-1			
TENSION ANCHORS (FRONT FACE)			
Embedment Depth, h_{ef} :	3.5	in.	
Steel Bar Diameter, d_a :	0.5	in.	
Area of Steel, A_s :	0.142	in. ²	
Front (Tension) Anchor Spacing, s :	5.5	in.	
Front (Tension) Anchor to deck edge, $c_{a,min}$:	10	in.	
Bond Strength, $\tau_{uncr} = \tau_{cr}$:	1450	psi	
Steel Strength, f_{uta} :	125000	psi	
Concrete Strength, f'_c :	2500	psi	
Foundation Reinforced? (y/n):	n		
λ_a :	1		
		Tension	Shear
ACI Steel Strength Reduction Factor, ϕ_s :	0.75	0.65	
ACI Concrete Strength Reduction Factor, ϕ_c :	0.65	0.75	
ACI Adhesive Strength Reduction Factor, ϕ_a :	0.65	NA	
Required Capacity	=1537.5*12/s	3355	lb
TENSION CAPACITY			
Steel Fracture: $\phi N_{sa} = A_{se} N_{f_{uta}}$			
	$\phi N_{sa} =$	13312.50	lb
Concrete Breakout: $\phi N_{cb} = A_{Nc}/A_{Nco} * \psi_{ed,N} \psi_{c,N} \psi_{cp,N} * N_b$			
	$N_b = k_c * \lambda_a h_{ef}^{1.5} \sqrt{f'_c}$		
	k_c :	17	(24 for cast in place, 17 for post installed)
	$\psi_{c,N}$:	1.4	(1.25 for cast in anchors, 1.4 for post installed)
	$N_b =$	5565.72	lb
	C_{ac} :	7	
	$\psi_{cp,N}$:	1	
	$\psi_{ed,N}$:	1	
	$A_{Nco} = 9 * h_{ef}^2$:	110.25	in. ²
	A_{Nc} :	110.25	in. ²
	A_{Nc}/A_{Nco} :	1	
	$\phi N_{cb} =$	5064.80	lb
Adhesive / Bond Failure: $\phi N_a = A_{Na}/A_{Nao} * \psi_{ed,Na} \psi_{cp,Na} * N_{ba}$			
	$N_{ba} = \tau_{cr} \pi d_a h_{ef}$		
	$N_{ba} =$	7971.79	lb
	$A_{Nao} = (2 * C_{Na})^2$		
	$C_{Na} = 10 * d_a * \sqrt{(\tau_{cr}/1100)}$		
	$C_{Na} =$	5.74	in.
	$A_{Nao} =$	131.82	in. ²
	$A_{Na} =$	131.82	in. ²
	A_{Na}/A_{Nao} :	1	
	$\psi_{cp,Na}$:	1	(should be the same as $\psi_{cp,N}$)
	$\psi_{ed,Na}$:	1	
	$\phi N_a =$	5181.66	lb

Figure C-20. Capacity of Anchors-Tension, Concept AM-1

Anchor Design - Concept AM-1			
SHEAR ANCHORS (BACK FACE)			
Embedment Depth, h_{ef} :	3.5 in.	Shear Strengths	
Steel Bar Diameter, d_s :	0.5 in.		
Area of Steel, A_s :	0.142 in. ²	Failure Mode	Load (kips)
Anchor Spacing, s :	5.5 in.	Steel Fracture:	6923
Anchor to Deck Edge Distance, c_{a1} :	10 in.	Concrete Breakout:	10504
Steel Strength, f_{uta} :	125000 psi	Concrete Pryout:	11688
Concrete Strength, f'_c :	2500 psi		
Foundation Thickness, h_f :	7 in.		
Foundation Reinforced? (y/n):	n		
Bond Strength, τ_{cr} :	1450 psi		
λ :	1		
Required Capacity	225 lb		
SHEAR CAPACITY			
Steel Fracture: $\phi V_{sa} = 0.6 A_s N_{f_{uta}}$			
$\phi V_{sa} = 6922.50 \text{ lb}$			
Concrete Breakout: $\phi V_{cbg} = A_{vc}/A_{vco} \cdot \psi_{ec,v} \psi_{ed,v} \psi_{c,v} \psi_{h,v} \cdot V_b$			
$V_{b1} = 7 \cdot (l_e/d_s)^{0.2} \cdot \sqrt{d_s} \cdot \sqrt{f'_c} \cdot C_{a1}^{1.5}$			
$l_e = 3.50$			
$V_{b1} = 11549.75 \text{ lb}$			
$V_{b2} = 9 \cdot C_{a1}^{1.5} \cdot \sqrt{f'_c}$			
14230.25 lb			
$V_b = \min(V_{b1}, V_{b2}) = 11549.75 \text{ lb}$			
$\psi_{ed,v} = 1$ (only reduced for anchor adjacent to deck discontinuity)			
$\psi_{c,v} = 1.4$ (1.4 for uncracked deck, 1.2 for cracked reinforced, 1.0 for cracked unreinforced deck)			
$\psi_{h,v} = 1.46385$			
$\psi_{ec,v} = 1$			
$A_{vco} = 4.5 \cdot (c_{a1})^2 = 450 \text{ in.}^2$			
$A_{vc} = 266.25 \text{ in.}^2$			
$A_{vco}/A_{vc} = 0.591667$			
$\phi V_{cb} = 10503.54 \text{ lb}$			
Concrete Pryout Strength: $\phi V_{cpg} = k_{cp} N_{cpg}$			
$k_{cp} = 2$			
$N_{cpg} = \min(N_{cbg}, N_{ag})$			
$N_{cbg} = A_{Nc}/A_{Nco} \cdot \psi_{ec,N} \psi_{ed,N} \psi_{c,N} \psi_{cp,N} \cdot N_b$		$N_{ag} = A_{Na}/A_{Nao} \cdot \psi_{ec,Na} \psi_{ed,Na} \psi_{cp,Na} \cdot N_{ba}$	
$N_b = k_c \cdot h_{ef}^{1.5} \cdot \sqrt{f'_c}$		$N_{ba} = \tau_{cr} \cdot \pi \cdot d_s \cdot h_{ef}$	
$k_c = 17$		$N_{ba} = 7971.79 \text{ lb}$	
$\psi_{c,N} = 1.4$			
$N_b = 5565.72 \text{ lb}$			
$c_{ac} = 7$		$A_{Nao} = (2 \cdot C_{Na})^2$	
$\psi_{cp,N} = 1$		$C_{Na} = 10 \cdot d_s \cdot \sqrt{(\tau_{cr}/1100)}$	
$\psi_{ed,N} = 1$		$C_{Na} = 5.74$	
$\psi_{ec,N} = 1$		$A_{Nao} = 131.82 \text{ in.}^2$	
$A_{Nco} = 9 \cdot h_{ef}^2 = 110.25 \text{ in.}^2$		$A_{Na} = 131.8182 \text{ in.}^2$	
$A_{Nc} = 110.25 \text{ in.}^2$		$A_{Na}/A_{Nao} = 1$	
$A_{Nc}/A_{Nco} = 1$		$\psi_{ec,Na} = 1$	
		$\psi_{cp,Na} = 1$ (should be the same as $\psi_{cp,N}$)	
		$\psi_{ed,Na} = 1$	
$N_{cb} = 7792.00 \text{ lb}$		$N_{ag} = 7971.79 \text{ lb}$	
$N_{cpg} = 7792.00 \text{ lb}$			
$\phi V_{cp} = 11688.00 \text{ lb}$			

Figure C-21. Capacity of Anchors-Shear, Concept AM-1

Variables	Condition	Load Case	Equation		Calculation		Nominal Capacity	Required Design Load
Rail - 2" x 2" x 1/4" 6061 Aluminum Tube								
A _w = 0.4375 in ² b = 1.75 in. t = 0.25 in. b/t = 7 < S ₁ F _s = F _{sy} or F _{syw} S _t = 0.2759 in ³ A _{wzt} = 0.25 in ² A _g = 0.4688 in ²	No Welding	Shear	φV _n = φF _c A _w	= 0.9*21000*0.4375	=	8268.8 lb	> 348.2 lb	
		Flexural Yielding	φM _n = φ1.3F _{ly} S _t	= 0.9*1.3*35000*0.2759/12	=	941.5 ft-lb	> 562.5 ft-lb	
		Flexural Rupture	φM _n = φ1.42F _{tu} S _t	= 0.75*1.42*38000*0.2759/12	=	930.5 ft-lb	> 562.5 ft-lb	
	Fully Welded	Shear	φV _n = φF _c A _w	= 0.9*9000*0.4375	=	3543.8 lb	> 348.2 lb	
		Flexural Yielding	φM _n = φ1.3F _{lyw} S _t	= 0.9*1.3*15000*0.2759/12	=	403.5 ft-lb	> 356.5 ft-lb	
		Flexural Rupture	φM _n = φ1.42F _{tuw} S _t	= 0.75*1.42*24000*0.2759/12	=	587.7 ft-lb	> 356.5 ft-lb	
	One-side welded	Flexural Yielding	φM _n = φ1.30[F _{ly} (1 - ^{A_{wzt}} / _{A_g}) + F _{lyw} (^{A_{wzt}} / _{A_g})]S _t	= 0.9*1.3*(35000*(1-.25/.4688)+15000*0.25/0.4688)*0.2759/12	=	654.6 ft-lb	> 562.5 ft-lb	
		Flexural Rupture	φM _n = φ1.42[F _{tu} (1 - ^{A_{wzt}} / _{A_g})/k _t + F _{tuw} (^{A_{wzt}} / _{A_g})]S _t	= 0.75*1.42*(38000*(1-.25/.4688)/1.0+24000*0.25/0.4688)*0.2759/12	=	747.7 ft-lb	> 562.5 ft-lb	
Post - 2" x 4" x 1/4" 6061 Aluminum Tube								
A _w = 2 in ² b = 3.5 in. t = 0.5 in. b/t = 7 < S ₁ F _s = F _{sy} or F _{syw} S _t = 1.3268 in ³	No Welding	Shear	φV _n = φF _c A _w	= 0.9*21000*2	=	37800 lb	> 450 lb	
		Flexural Yielding	φM _n = φ1.3F _{ly} S _t	= 0.9*1.3*35000*1.3268/12	=	4527.7 ft-lb	> 1537.5 ft-lb	
		Flexural Rupture	φM _n = φ1.42F _{tu} S _t	= 0.75*1.42*38000*1.3268/12	=	4474.6 ft-lb	> 1537.5 ft-lb	
	Fully Welded	Shear	φV _n = φF _c A _w	= 0.9*9000*2	=	16200 lb	> 450 lb	
		Flexural Yielding	φM _n = φ1.3F _{lyw} S _t	= 0.9*1.3*15000*1.3268/12	=	1940.4 ft-lb	> 1537.5 ft-lb	
		Flexural Rupture	φM _n = φ1.42F _{tuw} S _t	= 0.75*1.42*24000*1.3268/12	=	2826.1 ft-lb	> 1537.5 ft-lb	
Spindles - 1/2" x 1/2" solid square								
A _g = 0.25 in ² S _t = 0.0104 in ³	No Welding	Shear	φV _n = φF _{sy} A _g	= 0.9*21000*0.25	=	4725 lb	> 7.9 lb	
		Flexural Yielding	φM _n = φ1.3F _{ly} S _t	= 0.9*1.3*35000*0.0104/12	=	35.5 ft-lb	> 4.0 ft-lb	
		Flexural Rupture	φM _n = φ1.42F _{tu} S _t	= 0.75*1.42*38000*0.0104/12	=	35.1 ft-lb	> 4.0 ft-lb	
	Fully Welded	Shear	φV _n = φF _{syw} A _g	= 0.9*9000*0.25	=	2025 lb	> 7.9 lb	
		Flexural Yielding	φM _n = φ1.3F _{lyw} S _t	= 0.9*1.3*15000*0.0104/12	=	15.2 ft-lb	> 2.7 ft-lb	
		Flexural Rupture	φM _n = φ1.42F _{tuw} S _t	= 0.75*1.42*24000*0.0104/12	=	22.2 ft-lb	> 2.7 ft-lb	
Base Plate - 7 1/2" x 3" x 3/4" 6061 Aluminum Plate								
B = 3 in. t = 3/4 in. N = 7.5 in. l = 1.85 in.	Fully Welded	Method #1 - Vertical Force	φP _n =φF _{lyw} BN/2*(t/l) ²	= 0.9*15000*3*7.5/2*(.375/1.85) ²	=	6240.3 lb	> 4612.5 lb	
		Method #2 - Moment	φM _n = φF _{lyw} t ² /4	= 0.9*15000*(.375) ² /4	=	474.6 in.-lb/in.	< 1656 in.-lb/in.	
Post to Base Plate Weld - 1/4" 5356 Filler								
e = 0.1768 in. L _{we} = 12 in. I = 4.8954 in. ⁴ c = 2.0625 in.	Weld	Shear	φR _n =φF _{sw} L _{we}	= 0.75*17000*0.1768*12	=	27046.8 lb	> 450 lb	
		Moment	φM _n = φF _{sw} *I/c	= 0.75*17000*4.8954/2.0625/12	=	2521.9 ft-lb	> 1537.5 ft-lb	
Rail to Post Weld - 1/4" 5356 Filler								
e = 0.0884 in. L _{we} =8 in. I = 0.4941 in. ⁴ c = 1.03125 in.	Weld	Shear	φR _n =φF _{sw} L _{we}	= 0.75*17000*0.0884*8	=	9015.6 lb	> 348.2 lb	
		Moment	φM _n = φF _{sw} *I/c	= 0.75*17000*0.4941/1.03125/12	=	509.0 ft-lb	> 356.5 ft-lb	
Spindles to Rail Weld - 1/4" 5356 Filler								
e = 0.0884 in. L _{we} = 2 in. I = 0.0089 in. ⁴ c = 0.28125 in.	Weld	Shear	φR _n =φF _{sw} L _{we}	= 0.75*17000*0.0884*2	=	2253.9 lb	> 7.9 lb	
		Moment	φM _n = φF _{sw} *I/c	= 0.75*17000*0.0089/0.28125/12	=	33.6 ft-lb	> 2.7 ft-lb	
Anchor Bolts - 3/4" Diameter A193 B7 Threaded Rod, Embedded 5", at 6" spacing								
A _{sc,N} =A _{sc,V} = 0.078 in. ² f _{ua} = 125,000 psi A _{Nc} /A _{Nco} = 1 Ψ _{ed,N} = 1 Ψ _{ed,V} = 1 Ψ _{c,N} = 1.4 Ψ _{c,V} = 1.4 Ψ _{cp,N} = 1 Ψ _{h,V} = 1.46 N _b = 9503 lb V _b = 10273 lb Ψ _{ed,Na} = 1 k _{cp} = 2 Ψ _{cp,Na} = 1 N _{cp} = 8541 lb	Anchor	Tension (Steel)	φN _{sa} =φA _{sc,N} f _{ua}	= 0.75*0.078*125000	=	7313 lb	> 3075 lb	
		Tension (Concrete Breakout)	φN _{cb} =φA _{Nc} /A _{Nco} Ψ _{ed,N} Ψ _{c,N} Ψ _{cp,N} N _b	= 0.65*1*1.4*1*9503	=	8648 lb	> 3075 lb	
		Tension (Adhesive Bond)	φN _a =φA _{Nc} /A _{Nco} Ψ _{ed,Na} Ψ _{cp,Na} N _b	= 0.65*1*1*1*8541	=	5552 lb	> 3075 lb	
		Shear (Steel)	φN _{sa} =φ0.6A _{sc,V} f _{ua}	= 0.65*0.6*0.078*125000	=	3803 lb	> 225 lb	
		Shear (Concrete Breakout)	φV _{cbg} = A _{Vc} /A _{Vco} *Ψ _{ec,V} Ψ _{ed,V} Ψ _{c,V} Ψ _{h,V} * V _b	= 0.75*0.7467*1*1*1.4*1.46*10273	=	11790 lb	> 225 lb	
		Shear (Concrete Pryout)	φV _{cpb} = k _{cp} N _{cpb}	= 0.75*2*8541	=	12812 lb	> 225 lb	

Figure C-22. Final Design Calculations, Concept AW2-A

Variables	Condition	Load Case	Equation	Calculation	Nominal Capacity	Required Design Load
Rail - 2" x 2" x 1/4" 6061 Aluminum Tube						
$A_w = 0.4375 \text{ in}^2$ $b = 1.75 \text{ in.}$ $t = 0.25 \text{ in.}$ $b/t = 7 < S_1$ $F_s = F_{sy} \text{ or } F_{syw}$ $S_t = 0.2759 \text{ in}^3$ $A_{wzt} = 0.25 \text{ in}^2$ $A_{zg} = 0.4688 \text{ in}^2$	No Welding	Shear	$\phi V_n = \phi F_u A_w$	$= 0.9 * 21000 * 0.4375$	$= 8268.8 \text{ lb}$	$> 348.2 \text{ lb}$
		Flexural Yielding	$\phi M_n = \phi 1.3 F_{ly} S_t$	$= 0.9 * 1.3 * 35000 * 0.2759 / 12$	$= 941.5 \text{ ft-lb}$	$> 562.5 \text{ ft-lb}$
		Flexural Rupture	$\phi M_n = \phi 1.42 F_{tu} S_t$	$= 0.75 * 1.42 * 38000 * 0.2759 / 12$	$= 930.5 \text{ ft-lb}$	$> 562.5 \text{ ft-lb}$
	Fully Welded	Shear	$\phi V_n = \phi F_u A_w$	$= 0.9 * 9000 * 0.4375$	$= 3543.8 \text{ lb}$	$> 348.2 \text{ lb}$
		Flexural Yielding	$\phi M_n = \phi 1.3 F_{lyw} S_t$	$= 0.9 * 1.3 * 15000 * 0.2759 / 12$	$= 403.5 \text{ ft-lb}$	$> 356.5 \text{ ft-lb}$
		Flexural Rupture	$\phi M_n = \phi 1.42 F_{tuw} S_t$	$= 0.75 * 1.42 * 24000 * 0.2759 / 12$	$= 587.7 \text{ ft-lb}$	$> 356.5 \text{ ft-lb}$
	One-side welded	Flexural Yielding	$\phi M_n = \phi 1.30 [F_{ly} (1 - \frac{A_{wzt}}{A_g}) + F_{lyw} (\frac{A_{wzt}}{A_g})] S_t$	$= 0.9 * 1.3 * (35000 * (1 - .25 / .4688) + 15000 * 0.25 / 0.4688) * 0.2759 / 12$	$= 654.6 \text{ ft-lb}$	$> 562.5 \text{ ft-lb}$
		Flexural Rupture	$\phi M_n = \phi 1.42 [F_{tu} (1 - \frac{A_{wzt}}{A_g}) / k_t + F_{tuw} (\frac{A_{wzt}}{A_g})] S_t$	$= 0.75 * 1.42 * (38000 * (1 - .25 / .4688) / 1.0 + 24000 * 0.25 / 0.4688) * 0.2759 / 12$	$= 747.7 \text{ ft-lb}$	$> 562.5 \text{ ft-lb}$
Post - 2" x 3" x 1/4" 6061 Aluminum Tube						
$A_w = 0.75 \text{ in}^2$ $b/t = 11 < S_1$ $b = 2.75 \text{ in.}$ $t = 0.25 \text{ in.}$ $F_s = F_{sy} \text{ or } F_{syw}$ $S_t = 0.4890 \text{ in}^3$	No Welding	Shear	$\phi V_n = \phi F_u A_w$	$= 0.9 * 21000 * 0.75$	$= 14175 \text{ lb}$	$> 450 \text{ lb}$
		Flexural Yielding	$\phi M_n = \phi 1.3 F_{ly} S_t$	$= 0.9 * 1.3 * 35000 * 0.4890 / 12$	$= 1668.7 \text{ ft-lb}$	$> 1537.5 \text{ ft-lb}$
		Flexural Rupture	$\phi M_n = \phi 1.42 F_{tu} S_t$	$= 0.75 * 1.42 * 38000 * 0.4890 / 12$	$= 1649.2 \text{ ft-lb}$	$> 1537.5 \text{ ft-lb}$
Spindles - 1/2" x 1/2" solid square						
$A = 0.25 \text{ in}^2$ $S_t = 0.0104 \text{ in}^3$	No Welding	Shear	$\phi V_n = \phi F_{sy} A_g$	$= 0.9 * 21000 * 0.25$	$= 4725 \text{ lb}$	$> 7.9 \text{ lb}$
		Flexural Yielding	$\phi M_n = \phi 1.3 F_{ly} S_t$	$= 0.9 * 1.3 * 35000 * 0.0104 / 12$	$= 35.5 \text{ ft-lb}$	$> 4.0 \text{ ft-lb}$
		Flexural Rupture	$\phi M_n = \phi 1.42 F_{tu} S_t$	$= 0.75 * 1.42 * 38000 * 0.0104 / 12$	$= 35.1 \text{ ft-lb}$	$> 4.0 \text{ ft-lb}$
	Fully Welded	Shear	$\phi V_n = \phi F_{syw} A_g$	$= 0.9 * 9000 * 0.25$	$= 2025 \text{ lb}$	$> 7.9 \text{ lb}$
		Flexural Yielding	$\phi M_n = \phi 1.3 F_{lyw} S_t$	$= 0.9 * 1.3 * 15000 * 0.0104 / 12$	$= 15.2 \text{ ft-lb}$	$> 2.7 \text{ ft-lb}$
		Flexural Rupture	$\phi M_n = \phi 1.42 F_{tuw} S_t$	$= 0.75 * 1.42 * 24000 * 0.0104 / 12$	$= 22.2 \text{ ft-lb}$	$> 2.7 \text{ ft-lb}$
Base Plate - 7 1/2" x 3 1/2" x 1/4" 6061 Aluminum Plate						
$B = 3.5 \text{ in.}$ $N = 7.5 \text{ in.}$ $t = 3/8 \text{ in.}$ $l = 2.325 \text{ in.}$	Fully Welded	Method #1 - Vertical Force	$\phi P_n = \phi F_{lyw} B N / 2 * (t/l)^2$	$= 0.9 * 15000 * 3.5 * 7.5 / 2 * (.375 / 2.325)^2$	$= 4609.5 \text{ lb}$	$< 6150 \text{ lb}$
		Method #2 - Moment	$\phi M_n = \phi F_{lyw} l^2 / 4$	$= 0.9 * 15000 * (.375)^2 / 4$	$= 474.6 \text{ in.-lb/in.}$	$< 1862.5 \text{ in.-lb/in.}$
Sleeve - 3 5/8" x 2 5/8" x 1/4" 6061 Aluminum Plate						
$A_w = 1.5625 \text{ in}^2$ $b = 3.125 \text{ in.}$ $t = 0.5 \text{ in.}$ $b/t = 6.25 < S_1$ $F_s = F_{sy} \text{ or } F_{syw}$ $S_t = 1.3837 \text{ in}^3$	Fully Welded	Shear	$\phi V_n = \phi F_u A_w$	$= 0.9 * 9000 * 1.5625$	$= 12656.3 \text{ lb}$	$> 450 \text{ lb}$
		Flexural Yielding	$\phi M_n = \phi 1.3 F_{lyw} S_t$	$= 0.9 * 1.3 * 15000 * 1.3837 / 12$	$= 2023.7 \text{ ft-lb}$	$> 1537.5 \text{ ft-lb}$
		Flexural Rupture	$\phi M_n = \phi 1.42 F_{tuw} S_t$	$= 0.75 * 1.42 * 24000 * 1.3837 / 12$	$= 2947.3 \text{ ft-lb}$	$> 1537.5 \text{ ft-lb}$
Sleeve to Base Plate Weld - 3/16" 5356 Filler						
$e = 0.1326 \text{ in.}$ $L_{we} = 10.5 \text{ in.}$ $I = 2.1346 \text{ in.}^4$ $c = 1.6094 \text{ in.}$	Weld	Shear	$\phi R_n = \phi F_{sw} L_{we}$	$= 0.75 * 17000 * 0.1326 * 10.5$	$= 17749.5 \text{ lb}$	$> 450 \text{ lb}$
		Moment	$\phi M_n = \phi F_{su} * I / c$	$= 0.75 * 17000 * 2.1346 / 1.6094 / 12$	$= 1409.2 \text{ ft-lb}$	$< 1537.5 \text{ ft-lb}$
Rail to Post Weld - 1/4" 5356 Filler						
$e = 0.0884 \text{ in.}$ $L_{we} = 8 \text{ in.}$ $I = 0.4938 \text{ in.}^4$ $c = 1.03125 \text{ in.}$	Weld	Shear	$\phi R_n = \phi F_{sw} L_{we}$	$= 0.75 * 17000 * 0.0884 * 8$	$= 9015.6 \text{ lb}$	$> 348.2 \text{ lb}$
		Moment	$\phi M_n = \phi F_{su} * I / c$	$= 0.75 * 17000 * 0.4941 / 1.03125 / 12$	$= 509.0 \text{ ft-lb}$	$> 356.5 \text{ ft-lb}$
Spindles to Rail Weld - 1/4" 5356 Filler						
$e = 0.0884 \text{ in.}$ $L_{we} = 2 \text{ in.}$ $I = 0.0089 \text{ in.}^4$ $c = 0.28125 \text{ in.}$	Weld	Shear	$\phi R_n = \phi F_{sw} L_{we}$	$= 0.75 * 17000 * 0.0884 * 2$	$= 2253.9 \text{ lb}$	$> 7.9 \text{ lb}$
		Moment	$\phi M_n = \phi F_{su} * I / c$	$= 0.75 * 17000 * 0.0089 / 0.28125 / 12$	$= 33.6 \text{ ft-lb}$	$> 2.7 \text{ ft-lb}$
Anchor Bolts - 3/4" Diameter A193 B7 Threaded Rod, Embedded 5", at 6" spacing						
$s_N = A_{se,V} = 0.078 \text{ in.}^2$ $N_{ba} = 8541 \text{ lb}$ $f_{tba} = 125,000 \text{ psi}$ $A_{Nc} / A_{Nco} = 1$ $\psi_{ec,N} = 1$ $\psi_{ed,N} = 1$ $\psi_{c,N} = 1.4$ $\psi_{cp,N} = 1$ $N_b = 9503 \text{ lb}$ $V_b = 10273 \text{ lb}$ $\psi_{ed,Nb} = 1$ $\psi_{cp,Nb} = 1$ $k_{cp} = 2$ $N_{cpb} = 8541 \text{ lb}$	Anchor	Tension (Steel)	$\phi N_{sa} = \phi A_{se,N} f_{tba}$	$= 0.75 * 0.078 * 125000$	$= 7313 \text{ lb}$	$> 3075 \text{ lb}$
		Tension (Concrete Breakout)	$\phi N_{cb} = \phi A_{Nc} / A_{Nco} \psi_{ed,N} \psi_{c,N} \psi_{cp,N} N_b$	$= 0.65 * 1 * 1.4 * 1 * 9503$	$= 8648 \text{ lb}$	$> 3075 \text{ lb}$
		Tension (Adhesive Bond)	$\phi N_a = \phi A_{Nc} / A_{Nco} \psi_{ed,Nb} \psi_{c,Nb} N_{ba}$	$= 0.65 * 1 * 1 * 1 * 8541$	$= 5552 \text{ lb}$	$> 3075 \text{ lb}$
		Shear (Steel)	$\phi N_{sa} = \phi 0.6 A_{se,V} f_{tba}$	$= 0.65 * 0.6 * 0.078 * 125000$	$= 3803 \text{ lb}$	$> 225 \text{ lb}$
		Shear (Concrete Breakout)	$\phi V_{cbg} = A_{Nc} / A_{Nco} * \psi_{ec,V} \psi_{ed,V} \psi_{c,V} \psi_{h,V} * V_b$	$= 0.75 * 0.7467 * 1 * 1 * 1.4 * 1.46 * 10273$	$= 11790 \text{ lb}$	$> 225 \text{ lb}$
		Shear (Concrete Pryout)	$\phi V_{cpb} = k_{cp} N_{cpb}$	$= 0.75 * 2 * 8541$	$= 12812 \text{ lb}$	$> 225 \text{ lb}$

Figure C-23. Final Design Calculations, Concept AW2-C

Variables	Condition	Load Case	Equation	Calculation	Nominal Capacity	Required Design Load
Rail - 2" x 2" x 1/8" 6061 Aluminum Tube						
A _w = 0.4375 in ² b = 1.75 in. t = 0.25 in. b/t = 7 < S ₁ F _s = F _{sy} or F _{syw} S ₁ = 0.2759 in ³ A _{wzt} = 0.25 in ² A _{gt} = 0.4688 in ²	No Welding	Shear	ϕV _n = ϕF _s A _w	= 0.9*21000*0.4375	= 8268.8 lb	> 348.2 lb
		Flexural Yielding	ϕM _n = ϕ1.3F _{ty} S _t	= 0.9*1.3*35000*0.2759/12	= 941.5 ft-lb	> 562.5 ft-lb
		Flexural Rupture	ϕM _n = ϕ1.42F _{tu} S _t	= 0.75*1.42*38000*0.2759/12	= 930.5 ft-lb	> 562.5 ft-lb
	Fully Welded	Shear	ϕV _n = ϕF _s A _w	= 0.9*9000*0.4375	= 3543.8 lb	> 348.2 lb
		Flexural Yielding	ϕM _n = ϕ1.3F _{tyw} S _t	= 0.9*1.3*15000*0.2759/12	= 403.5 ft-lb	> 356.5 ft-lb
		Flexural Rupture	ϕM _n = ϕ1.42F _{tw} S _t	= 0.75*1.42*24000*0.2759/12	= 587.7 ft-lb	> 356.5 ft-lb
One-side welded	Flexural Yielding	ϕMn = ϕ1.30[F _{ty} (1-(A _{wzt} /A _g) + F _{tyw} (A _{wzt} /A _g)]S _t	= 0.9*1.3*(35000*(1-.25/4688)+15000*0.25/0.4688)*0.2759/12	= 654.6 ft-lb	> 562.5 ft-lb	
	Flexural Rupture	ϕMn = ϕ1.42[F _{tu} (1-(A _{wzt} /A _g)/k _t + F _{tw} (A _{wzt} /A _g)]S _t	= 0.75*1.42*(38000*(1-.25/4688)/1.0+24000*0.25/0.4688)*0.2759/12	= 747.7 ft-lb	> 562.5 ft-lb	
Post - 2" x 4" x 1/4" 6061 Aluminum Tube						
A _w = 2 in ² b = 3.5 in. t = 0.5 in. b/t = 7 < S ₁ F _s = F _{sy} or F _{syw} S _t = 1.3268 in ³	No Welding	Shear	ϕV _n = ϕF _s A _w	= 0.9*21000*2	= 37800 lb	> 450 lb
		Flexural Yielding	ϕM _n = ϕ1.3F _{ty} S _t	= 0.9*1.3*35000*1.3268/12	= 4527.7 ft-lb	> 1537.5 ft-lb
		Flexural Rupture	ϕM _n = ϕ1.42F _{tu} S _t	= 0.75*1.42*38000*1.3268/12	= 4474.6 ft-lb	> 1537.5 ft-lb
	Fully Welded	Shear	ϕV _n = ϕF _s A _w	= 0.9*9000*2	= 16200 lb	> 450 lb
		Flexural Yielding	ϕM _n = ϕ1.3F _{tyw} S _t	= 0.9*1.3*15000*1.3268/12	= 1940.4 ft-lb	> 1537.5 ft-lb
		Flexural Rupture	ϕM _n = ϕ1.42F _{tw} S _t	= 0.75*1.42*24000*1.3268/12	= 2826.1 ft-lb	> 1537.5 ft-lb
Spindles - 1/2" x 1/2" solid square						
A = 0.25 in ² S _t = 0.0104 in ³	No Welding	Shear	ϕV _n = ϕF _{sy} A _g	= 0.9*21000*0.25	= 4725 lb	> 10.5 lb
		Flexural Yielding	ϕM _n = ϕ1.3F _{ty} S _t	= 0.9*1.3*35000*0.0104/12	= 35.5 ft-lb	> 7.0 ft-lb
		Flexural Rupture	ϕM _n = ϕ1.42F _{tu} S _t	= 0.75*1.42*38000*0.0104/12	= 35.1 ft-lb	> 7.0 ft-lb
	Fully Welded	Shear	ϕV _n = ϕF _{syw} A _g	= 0.9*9000*0.25	= 2025 lb	> 10.5 lb
		Flexural Yielding	ϕM _n = ϕ1.3F _{tyw} S _t	= 0.9*1.3*15000*0.0104/12	= 15.2 ft-lb	> 4.7 ft-lb
		Flexural Rupture	ϕM _n = ϕ1.42F _{tw} S _t	= 0.75*1.42*24000*0.0104/12	= 22.2 ft-lb	> 4.7 ft-lb
Base Plate - 7 3/4" x 3" x 3/8" 6061 Aluminum Plate						
B = 3 in. t = 3/8 in. N = 7.75 in. l = 1.975 in.	Fully Welded	Method #1 - Vertical Force	ϕP _n =ϕF _{tyw} BN/2*(t/l) ²	= 0.9*15000*3*7.75/2*(.375/1.975) ²	= 5657.9 lb	> 4312.5 lb
		Method #2 - Moment	ϕM _n = ϕF _{tyw} t ² /4	= 0.9*15000*(.375) ² /4	= 474.6 in.-lb/in.	< 1731.4 in.-lb/in.
Post to Base Plate Weld - 1/4" 5356 Filler						
e = 0.1768 in. I = 4.8961 in. ⁴ L _{we} = 12 in. c = 2.0625 in.	Weld	Shear	ϕR _n =ϕF _{sw} L _{we}	= 0.75*17000*0.0884*8	= 9015.6 lb	> 450 lb
		Moment	ϕM _n = ϕF _{su} *I/c	= 0.75*17000*0.4941/1.03125/12	= 509.0 ft-lb	> 1537.5 ft-lb
Rail to Post Weld - 3/8" 5356 Filler						
e = 0.0884 in. I = 0.4938 in. ⁴ L _{we} = 8 in. c = 1.03125 in.	Weld	Shear	ϕR _n =ϕF _{sw} L _{we}	= 0.75*17000*0.0884*8	= 9016.8 lb	> 348.2 lb
		Moment	ϕM _n = ϕF _{su} *I/c	= 0.75*17000*0.4938/1.03125/12	= 508.8 ft-lb	> 356.5 ft-lb
Spindles to Rail Weld - 3/8" 5356 Filler						
e = 0.0884 in. I = 0.0089 in. ⁴ L _{we} = 2 in. c = 0.28125 in.	Weld	Shear	ϕR _n =ϕF _{sw} L _{we}	= 0.75*17000*0.0884*2	= 2253.9 lb	> 7.9 lb
		Moment	ϕM _n = ϕF _{su} *I/c	= 0.75*17000*0.0089/0.28125/12	= 33.6 ft-lb	> 2.7 ft-lb
Anchor Bolts - 1/2" Diameter A193 B7 Threaded Rod, Embedded 5", at 6 1/4" spacing						
=A _{sc,v} = 0.142 in. ² N _{ba} = 11388 lb f _{uta} = 125,000 psi√v _c /A _{vco} = 0.6042 A _{Nc} /A _{Nco} = 1 √ _{ec,v} = 1 √ _{ed,N} = 1 √ _{ed,v} = 1 √ _{c,N} = 1.4 √ _{c,v} = 1.4 √ _{cp,N} = 1 √ _{h,v} = 1.46 N _b = 9503 lb V _b = 11862 lb √ _{ed,Na} = 1 k _{cp} = 2 √ _{cp,Na} = 1 N _{cpg} = 11388 lb	Anchor	Tension (Steel)	ϕN _{sa} =ϕA _{sc,N} f _{uta}	= 0.75*0.142*125000	= 13313 lb	> 3075 lb
		Tension (Concrete Breakout)	ϕN _{cb} =ϕA _{Nc} /A _{Nco} √ _{ed,N} √ _{c,N} √ _{cp,N} N _b	= 0.65*1*1.4*1*9503	= 8648 lb	> 3075 lb
		Tension (Adhesive Bond)	ϕN _a =ϕA _{Nc} /A _{Nco} √ _{ed,Na} √ _{cp,Na} N _{ba}	= 0.65*1*1*1*11388	= 7402 lb	> 3075 lb
		Shear (Steel)	ϕN _{sa} =ϕ0.6A _{sc,v} f _{uta}	= 0.65*0.6*0.142*125000	= 6923 lb	> 225 lb
		Shear (Concrete Breakout)	ϕV _{cbg} = A _{vc} /A _{vco} *√ _{ec,v} √ _{ed,v} √ _{c,v} √ _{h,v} *V _b	= 0.75*0.6042*1*1*1.4*1.46*11862	= 11016 lb	> 225 lb
		Shear (Concrete Pryout)	ϕV _{cpb} = k _{cp} N _{cpg}	= 0.75*2*11388	= 17082 lb	> 225 lb

Figure C-24. Final Design Calculations, Concept AW2-D

Variables	Condition	Load Case	Equation	Calculation	Nominal Capacity	Required Design Load
Rail - 2" Dia. Schedule 40 6061 Aluminum Pipe						
$A_g = 1.0745 \text{ in}^2$ $F_s = F_{sy}$ $R_b = 2.22 \text{ in.}$ $S = 0.5606 \text{ in}^3$ $t = 0.31 \text{ in.}$ $R_b/t = 7.16 \leq S_1$ $L_v = 60 \text{ in.}$ $F_b = 52.87 \text{ ksi}$ $\lambda_1 = 22.63 \leq S_1$	No Welding	Shear	$\phi V_n = \phi F_s A_g/2$	$= 0.9*21000*1.0745/2$	$= 10154.0 \text{ lb}$	$> 348.2 \text{ lb}$
		Flexural Tensile Yielding	$\phi M_n = \phi 1.17 F_{1y} S$	$= 0.9*1.17*35000*0.5606/12$	$= 1721.7 \text{ ft-lb}$	$> 562.5 \text{ ft-lb}$
		Flexural Tensile Rupture	$\phi M_n = \phi 1.24 F_{1u} S/k_t$	$= 0.75*1.24*38000*0.5606/12$	$= 1651.0 \text{ ft-lb}$	$> 562.5 \text{ ft-lb}$
		Flexural Compressive Yielding	$\phi M_n = \phi 1.17 F_{cy} S$	$= 0.9*1.17*35000*0.5606/12$	$= 1721.7 \text{ ft-lb}$	$> 562.5 \text{ ft-lb}$
		Flexural Local Buckling	$\phi M_n = \phi F_b S$	$= 0.9*(52.87*1000)*0.5606/12$	$= 2222.9 \text{ ft-lb}$	$> 562.5 \text{ ft-lb}$
Post - 2" Dia. Schedule 80 6061 Aluminum Pipe						
$A_g = 1.4773 \text{ in}^2$ $F_s = F_{sy}$ $R_b = 2.16 \text{ in.}$ $S = 0.7309 \text{ in}^3$ $t = 0.44 \text{ in.}$ $R_b/t = 4.91 \leq S_1$ $L_v = 41 \text{ in.}$ $F_b = 54.92 \text{ ksi}$ $\lambda_1 = 18.64 \leq S_1$	No Welding	Shear	$\phi V_n = \phi F_s A_g/2$	$= 0.9*21000*1.4773/2$	$= 13960.5 \text{ lb}$	$> 450 \text{ lb}$
		Flexural Tensile Yielding	$\phi M_n = \phi 1.17 F_{1y} S$	$= 0.9*1.17*35000*0.7309/12$	$= 2244.8 \text{ ft-lb}$	$> 1537.5 \text{ ft-lb}$
		Flexural Tensile Rupture	$\phi M_n = \phi 1.24 F_{1u} S/k_t$	$= 0.75*1.24*38000*0.7309/12$	$= 2152.5 \text{ ft-lb}$	$> 1537.5 \text{ ft-lb}$
		Flexural Compressive Yielding	$\phi M_n = \phi 1.17 F_{cy} S$	$= 0.9*1.17*35000*0.7309/12$	$= 2244.8 \text{ ft-lb}$	$> 1537.5 \text{ ft-lb}$
		Flexural Local Buckling	$\phi M_n = \phi F_b S$	$= 0.9*(54.92*1000)*0.7309/12$	$= 3010.6 \text{ ft-lb}$	$> 1537.5 \text{ ft-lb}$
Spindles - 3/4" Dia. Schedule 10 6061 Aluminum Pipe						
$A_g = 0.2577 \text{ in}^2$ $F_s = F_{sy}$ $R_b = 0.97 \text{ in.}$ $S_1 = 0.0566 \text{ in}^3$ $t = 0.083 \text{ in.}$ $R_b/t = 11.69 \leq S_1$ $L_v = 12.125 \text{ in.}$ $F_b = 49.56 \text{ ksi}$ $\lambda_1 = 13.99 \leq S_1$	No Welding	Shear	$\phi V_n = \phi F_s A_g/2$	$= 0.9*21000*0.2577/2$	$= 2435.3 \text{ lb}$	$> 7.9 \text{ lb}$
		Flexural Tensile Yielding	$\phi M_n = \phi 1.17 F_{1y} S$	$= 0.9*1.17*35000*0.0566/12$	$= 98.3 \text{ ft-lb}$	$> 4.0 \text{ ft-lb}$
		Flexural Tensile Rupture	$\phi M_n = \phi 1.24 F_{1u} S/k_t$	$= 0.75*1.24*38000*0.0566/12$	$= 97.1 \text{ ft-lb}$	$> 4.0 \text{ ft-lb}$
		Flexural Compressive Yielding	$\phi M_n = \phi 1.17 F_{cy} S$	$= 0.9*1.17*35000*0.0566/12$	$= 98.3 \text{ ft-lb}$	$> 4.0 \text{ ft-lb}$
		Flexural Local Buckling	$\phi M_n = \phi F_b S$	$= 0.9*(49.56*1000)*0.0566/12$	$= 210.4 \text{ ft-lb}$	$> 4.0 \text{ ft-lb}$
Base Plate - 7 1/2" x 3" x 3/8" 535 Aluminum Alloy Casting						
$B = 5 \text{ in.}$ $t = 9/16 \text{ in.}$ $N = 8.5 \text{ in.}$ $l = 3.122 \text{ in.}$	Fully Welded	Method #1 - Vertical Force	$\phi P_n = \phi F_{1y} B N / 2 * (t/l)^2$	$= 0.9*13500*5*8.5/2*(0.5625/3.122)^2$	$= 8381.4 \text{ lb}$	$> 7768.4 \text{ lb}$
		Method #2 - Moment	$\phi M_n = \phi F_{1y} t^2 / 4$	$= 0.9*13500*(0.5625)^2/4$	$= 961.1 \text{ in.-lb/in.}$	$< 1805.1 \text{ in.-lb/in.}$
Anchor Bolts - 1/2" Diameter A193 B7 Threaded Rod, Embedded 3 1/2", at 5 1/2" spacing						
$A_{sc,N} = A_{sc,V} = 0.142 \text{ in.}^2$ $N_{ba} = 7972 \text{ lb}$ $f_{uta} = 125,000 \text{ psi}$ $A_{Vc}/A_{Vco} = 0.5917$ $A_{Nc}/A_{Nco} = 1$ $\psi_{ec,V} = 1$ $\psi_{ed,N} = 1$ $\psi_{ed,V} = 1$ $\psi_{c,N} = 1.4$ $\psi_{c,V} = 1.4$ $\psi_{cp,N} = 1$ $\psi_{h,V} = 1.46$ $N_b = 5566 \text{ lb}$ $V_b = 11550 \text{ lb}$ $\psi_{ed,Na} = 1$ $k_{cp} = 2$ $\psi_{cp,Na} = 1$ $N_{cpg} = 7792 \text{ lb}$	Anchor	Tension (Steel)	$\phi N_{sa} = \phi A_{sc,N} f_{uta}$	$= 0.75*0.142*125000$	$= 13313 \text{ lb}$	$> 3075 \text{ lb}$
		Tension (Concrete Breakout)	$\phi N_{cb} = \phi A_{Nc}/A_{Nco} \psi_{ed,N} \psi_{c,N} \psi_{cp,N} N_b$	$= 0.65*1*1.4*1*5566$	$= 5065 \text{ lb}$	$> 3075 \text{ lb}$
		Tension (Adhesive Bond)	$\phi N_a = \phi A_{Nc}/A_{Nco} \psi_{ed,Na} \psi_{cp,Na} N_{ba}$	$= 0.65*1*1*1*7972$	$= 5182 \text{ lb}$	$> 3075 \text{ lb}$
		Shear (Steel)	$\phi N_{sa} = \phi 0.6 A_{sc,V} f_{uta}$	$= 0.65*0.6*0.142*125000$	$= 6923 \text{ lb}$	$> 225 \text{ lb}$
		Shear (Concrete Breakout)	$\phi V_{cb} = A_{Vc}/A_{Vco} * \psi_{ec,V} \psi_{ed,V} \psi_{c,V} \psi_{h,V} * V_b$	$= 0.75*0.5917*1*1*1.4*1.46*11550$	$= 10504 \text{ lb}$	$> 225 \text{ lb}$
		Shear (Concrete Pryout)	$\phi V_{cp} = k_{cp} N_{cpg}$	$= 0.75*2*7792$	$= 11688 \text{ lb}$	$> 225 \text{ lb}$

Figure C-25. Final Design Calculations, Concept AM-1

Appendix D. Material Specifications

Pedestrian Rail Design AW2-A and AW2-D (WIPR-1 and WIPR-4)			
Item No.	Description	Material Spec	Reference
a1	2"x4"x1/4" [51x102x6] Aluminum Post, 43" [1092] long	6061-T6	H# 21311648
a2	Aluminum Post Cap - 1/8" [3] Plate	6061-T6	R# 14-0473 L# 21635829
a3	Aluminum Post Base	6061-T6	R# 14-0473 L# 212073 & 539961
d1	2"x2"x1/8" [51x51x3] Aluminum Rail - 60" [1524] long	6061-T6	H# 201405597
d2	1/2"x1/2" [13x13] Square Aluminum Spindle - 24 1/4" [616] long	6061-T6	H# 201405836
d3	3/8" [10] Dia. Threaded Rod	ASTM A193 Grade B7 Galv.	Grainger COC R# 14-0433 - 4FHG3
d4	3/8" [10] Dia. Nut	ASTM A194 Grade 8M Galv	Grainger COC R# 14-0433 - 1XA24
d5	3/8" [10] Dia. SAE Flat Washer	ASTM F436 Type 1 Galv.	Grainger COC R# 14-0433 - 6PE80
d6	Epoxy	Minimum bond strength = 1,450 psi [10.0 MPa]	June 2014 C300

Pedestrian Rail Design AW2-C (WIPR-2)			
Item No.	Description	Material Spec	Reference
c1	2"x3"x1/8" [51x76x3] Aluminum Post, 43" [1092] long	6061-T6	H# 21393458
c2	Aluminum Post Cap - 1/8" [3] Plate	6061-T6	R# 14-0473 L# 21635829
c3	Aluminum Post Base	6061-T6	R# 14-0473 L# 212073 & 539961
c4	1/4" [6] Dia., 3" [76] Long Bolt and Nut Bolt	ASTM A193 Grade B8M Class 2, Nut ASTM A194 Grade 8M	Grainger COC - IVZA6
d1	2"x2"x1/8" [51x51x3] Aluminum Rail - 60" [1524] long	6061-T6	H# 201405597
d2	1/2"x1/2" [13x13] Square Aluminum Spindle - 24 1/4" [616] long	6061-T6	H# 201405836
d3	3/8" [10] Dia. Threaded Rod	ASTM A193 Grade B7 Galv.	Grainger COC R# 14-0433 - 4FHG3
d4	3/8" [10] Dia. Nut	ASTM A194 Grade 8M Galv.	Grainger COC R# 14-0433 - 1XA24
d5	3/8" [10] Dia. SAE Flat Washer	ASTM F436 Type 1 Galv.	Grainger COC R# 14-0433 - 6PE80
d6	Epoxy	Minimum bond strength = 1,450 psi [10.0 MPa]	June 2014 C300

Figure D-1. Bill of Materials and Material Reference, Test Nos. WIPR-1, WIPR-2, and WIPR-4

Pedestrian Rail Design AM-1 (WIPR-3)			
Item No.	Description	Material Spec	Reference
b1	2" [51] Dia. Schedule 80 post, 39" [991] long	6061-T6 Aluminum	Item# G00369485 L# 21684972 H# S14033401
b2	2" [51] Dia. Schedule 40 rail, 56 1/2" [1435] long	6061-T6 Aluminum	Item# G03369473 L# 21633667 H# S14010202
b3	3/4" [19] Dia. Schedule 10 picket, 22" [559] long	6063-T6 Aluminum	Cast# 34391
b4	No. 3 Elbow (2" [51])	6061-T6 Aluminum	See Alex
b5	No. 5 Tee (2" [51])	6061-T6 Aluminum	See Alex
b6	No. 7 Cross (2" [51])	6061-T6 Aluminum	See Alex
b7	No. 48 Heavy-Duty Base Flange (2" [51], 2-hole)	6061-T6 Aluminum	See Alex
b8	1/2" [13] Dia. Threaded Rod ASTM	A193 Grade B7 Galv.	Grainger COC R# 14-0433 - 4FHF3
b9	1/2" [13] Dia. Nut	ASTM A194 Grade 8M Galv.	Ken
b10	1/2" [13] Dia. SAE Flat Washer	ASTM F436 Type 1 Galv.	Ken
b11	Epoxy	Minimum bond strength = 1,450 psi [10.0 MPa]	June 2014 C300

Pedestrian Rail Design (APR-1 and APR-2)			
Item No.	Description	Material Spec	Reference
a1	2"x4"x1/4" [51x102x6] Aluminum Post, 43" [1092] long	6061-T6	R#15-0098 H# 21550443
a2	Aluminum Post Cap - 1/8" [3] Plate	6061-T6	R#15-0098 No Definite Heat #
a3	Aluminum Post Base	6061-T6	R#15-0098 L# 2307073D0
d1	2"x2"x1/8" [51x51x3] Aluminum Rail - 63 1/2" [1613] long	6061-T6	R#15-0098 H# 21836702
d2	2"x2"x1/8" [51x51x3] Aluminum Rail - 63 1/2" [1613] long with holes	6061-T6	R#15-0098 H# 21836702
d3	1/2"x1/2" [13x13] Square Aluminum Spindle - 32 1/8" [816] long	6061-T6	R#15-0098 H# 201408541
d4	1/2" [13] Dia. UNC, 6" [152] long Threaded Rod	ASTM A193 Grade B7 Galv.	R# 15-0188 H# E21306214 L# 1401071935C
d5	1/2" [13] Dia. Steel Nut	ASTM A194 Grade 8M Galv	R# 15-0188 H# NF12104365 L# 325254B
d6	1/2" [13] Dia. SAE Steel Flat Washer	ASTM F436 Type 1 Galv.	R# 15-0188 H# 342288 L# C7313D
d7	Epoxy	Minimum bond strength = 1,450 psi [10.0 MPa]	TECHNICAL DATA AVAILABLE ONLINE

Figure D-2. Bill of Materials and Material Reference, Test Nos. WIPR-3, APR-1, and APR-2

CERTIFICATE OF TEST



Page 01 of 01

Certification Date
10-APR-2014

CUSTOMER ORDER NUMBER

39584

EARLE M. JORGENSEN COMPANY
1800 N UNIVERSAL AVENUE
KANSAS CITY MO 64120

Invoice Number
S107282

CUSTOMER PART NUMBER

0001

116661

SOLD TO: RIVERS METAL PRODUCTS

3100 N 38TH
LINCOLN NE 68504

SHIP TO:

RIVERS METAL PRODUCTS

3100 NORTH 38TH
LINCOLN NE 68504

Description: 6061-T6 EXTRUDED PORTHOLE TUBING -ASTM B221 Q
2 X 4 X .250 W X 20' Line Total: 39.2703 FT
HEAT: 21311648 ITEM: 116661

Specifications:

ASTM B221 12
EN 10204 3.1

QQ-A-200/8

AMS QQ A 200/8 97

ALUMINIUM CHEMICAL ANALYSIS

DESCRIPTION:

	SI	FE	CU	MN	MG	CR	ZN	TI
MIN	0.4		0.15		0.8	0.04		
MAX	0.8	0.7	0.4	0.15	1.2	0.35	0.25	0.15

OTHERS : EACH TOTAL
0.05 0.15 AL REMAINDER

RCPT: R911497

VENDOR: SAPA PROFILES NORTH AMERICA COUNTRY OF ORIGIN : USA

MECHANICAL PROPERTIES

DESCRIPTION	YLD STR KSI	ULT TEN KSI	%ELONG IN 02 IN	%RED IN AREA	HARDNESS
	44.1	47.0	13.5		
	45.5	48.9	14.0		

The above data were transcribed from the manufacturer's Certificate of Test after verification for completeness and specification requirements of the information on the certificate. All test results remain on file subject to examination.

We hereby certify that the material covered by this report will meet the applicable requirements described herein, including any specification forming a part of the description.

The willful recording of false, fictitious, or fraudulent statements in connection with test results may be punishable as a felony under federal statutes.

Material did not come in contact with mercury while in our possession.

LARRY BUSICK

Larry A. Busick
Manager, Quality Assurance

Figure D-3. 2"x4"x1/4" Aluminum Post Material Certificate, Test Nos. WIPR-1 and WIPR-4

sapa: Sapa Industrial Extrusions
1550 KIRBY LANE
SPANISH FORK, UT
84660-1349

Sapa Extrusions Inc., a Subsidiary of Sapa AB

Invokes To Customer
METALS USA
2840 E HEARTLAND DRIVE
LIBERTY, MO - 64068

Ship To Customer
METALS USA
2840 E HEARTLAND DR.
LIBERTY, MO - 64068

Certified Inspection Report

Sales Order Number 1100709644	Line No. 8	Customer P/O LIB-26723-008
-----------------------------------------	----------------------	--------------------------------------

Cert Number SAPA907749	Page 1 of 2
Cert Creation Date 24-JAN-14	Cert Print Date 24-JAN-14

Quantity Shipped 531	Date Shipped 24-JAN-14	Item Description Extruded Rectangular Bar 0.125 TK x 2.000 W RAD 144,000 IN LN FIN M-MILL W/P 0.294 P 14 CS 2 6061/T6511 Marking CONTINUOUS;	Specification ASTMB221 REV 13 AMS-QQ-A-2008 REV 1997 ASMESB221 REV 09 UNSPA96061 REV
B/L 498453	Item No. Q03361053		
Delivery Id 4505720	Item No. Rev ---		
Customer Part No. .125X2			

Applicable Specifications, Revisions and Exceptions

COMPOSITION NOTE: The values for 'Others Each' and 'Others Total' have met the limits as shown on this certified inspection report. Remainder is Aluminum.

Legal Statement
We hereby certify that, unless otherwise indicated, the material covered by this report has been manufactured, inspected, and tested in accordance with, and has been found to meet, the applicable requirements described herein, including any specifications forming a part of the description and that samples representative of the material met the composition and had the mechanical properties shown on the face of this certification. Also, note that mercury is not a normal contaminant in aluminum alloys and neither it nor any of its compounds are used in the manufacture of our product. This certification is not to be reproduced in partial form without prior written approval of our Quality Assurance Dept.

Signature And Title
Brian Pike
Brian Pike
Quality Control Manager
24-JAN-14

Quantities per Lot / Packages

Package Number	Lot Number	Quantity	UOM	Weight
G14-FKO1510952	21635829	146	PCS	537

Composition Limits

Alloy	Si		Fe		Cu		Mn		Mg		Cr		Zn	
	Min	Max	Min	Max	Min	Max	Min	Max	Min	Max	Min	Max	Min	Max
6061	0.40	0.80	—	0.70	0.15	0.40	—	0.15	0.80	1.20	0.04	0.35	—	0.25

Certificate of Mill Test Results
Fig 1/2
12MM14
BL LIB-270655-002

METALS USA - FLAT ROLLED
NBK
FOUR 39412

METALS USA - FLAT ROLLED
6061 Aluminum Rect Bar 16
1.25 x 2.000 x 12
PART NO.

Figure D-4. 1/8" thick Aluminum Post Cap Material Certificate (Sheet 1 of 2), Test Nos. WIPR-1, WIPR-2, and WIPR-4

CERTIFIED INSPECTION REPORT

Alcoa Inc.

DAVENPORT WORKS 4879 State Street Bettendorf, IA 52722

We hereby certify that the material covered by this certificate has been inspected with, and has been found to meet the applicable requirements described therein, including any specifications forming a part of the description and that samples representative of the material met the composition limits and had the mechanical properties shown on the face of this sheet.

This test report shall not be reproduced except in full, without the written approval of the Quality Department. No alteration, addition or other change is authorized to be made to this certificate. The recording of false, fictitious, or otherwise fraudulent statements or entries on this certificate by any recipient may be punished as a felony under applicable law.

Per:

Rob Woodall

Rob Woodall
Director of Manufacturing Davenport Works

Terrence Thom

Terrence Thom
Quality Assurance Manager

Page 1 of 4

Ship To: RYERSON PROCUREMENT CORP
4404 S 134TH ST
OMAHA 68137 NE

Item Description
0.375 IN TK (+.017 -0.000) X 48.5 IN W (+.375 -
0.000) X 144.5 IN LN (+.5 -0.0) CAT X 160001705 (N) A/T 6061-
T651 TYPE 200 WROUGHT TOOLING PLATE MILL
FINISH. AMS4027 REV N ANSIN35.2 REV 2009 EXC_MRK ASME-SB-
209 REV 11 EXC_MRK ASTM209 REV 10
(MARKED)) KRAFT PAPER INTERLEAVED
MAX GROSS SKID WGT: 4500 LB QUAN TOL +/-
40 % CQR D164057 REV 08 CUST REQ 12-11-
11 *** W/E 12-11-17 ***

Num	Package Ticket	Lot	Weight	Quantity	UOM	Inspector Clock Numbers
1	466854	212821	1348	3	PC	47419
2	466854	632492	808	3	PC	47408 47419
3	466854	632493	2156	8	PC	47368 47408 47419
4	469053	107026	535	2	PC	47338
5	469053	107027	1066	4	PC	47338
6	469053	107028	799	3	PC	47338
			6712	25		

Notes for CQR: D164057.8
PRODUCT PRODUCED TO THE REQUIREMENTS OF AMS4027 REV N ALSO MEET THE REQUIREMENTS OF AMS-QQ-A-250_11 ORIGINAL REVISIO N DATED 1997-08-01.

CQR: D164057.8 -Specification Limits -----

		UTS	TYS	EL4D
Temp	Dir	KSI	KSI	PCT
T651	Long Transv.	Max		
		Min	42.0	35.0 10

Figure D-5. 1/8" thick Aluminum Post Cap Material Certificate (Sheet 2 of 2), Test Nos. WIPR-1, WIPR-2, and WIPR-4

CERTIFIED INSPECTION REPORT

Alcoa Inc.

DAVENPORT WORKS 4879 State Street Bettendorf, IA 52722

Ship From: RIVERDALE, IA.

We hereby certify that the material covered by this certificate has been inspected with, and has been found to meet the applicable requirements described therein, including any specifications forming a part of the description and that samples representative of the material met the composition limits and had the mechanical properties shown on the face of this sheet.

This test report shall not be reproduced except in full, without the written approval of the Quality Department. No alteration, addition or other change is authorized to be made to this certificate. The recording of false, fictitious, or otherwise fraudulent statements or entries on this certificate by any recipient may be punished as a felony under applicable law.

Per:

Rob Woodall

Rob Woodall
Director of Manufacturing Davenport Works

Terrence Thom

Terrence Thom
Quality Assurance Manager

1436681	0			
Ship Date	B.L. No.	Invoice No.	Alcoa No.	Item
2012-09-30	7388421	00000	1000404652-1	DP-04652-1
P.O. No./Govt Contract No.	Customer	Alcoa Item		
4500504158 Ln#: 0000	RYERSON - COON RAP	G041107416R08		

Page 2 of 4

CQR: D164055.8 -Specification Limits -----

Temp	Dir	UTS	TYS	EL4D
		KSI	KSI	PCT
T651	Long Transv.	Max		
		Min	42.0	35.0 10

Chemical Composition		Max	SI	FE	CU	MN	MG	CR	ZN	TI	Other		Total Aluminum
											Each	Other	
Alloy 6061		Min	0.40	0.7	0.40	0.15	1.2	0.35	0.25	0.15	0.05	0.15	
Lot: 212073	- Mechanical, Physical, Metallography, Quantometer Results -----												

Temp	Dir	No->	UTS	TYS	EL4D
		Test	KSI	KSI	PCT
T651	Long Transv.	2	48.1	43.7	14.1
			48.2	43.8	14.5

Cast Number	Chemical - OES	SI	FE	CU	MN	MG	CR	ZN	TI
12L02301	Actuals	0.66	0.5	0.24	0.01	1.0	0.16	0.01	0.05

Lot: 539961 - Mechanical, Physical, Metallography, Quantometer Results -----

Temp	Dir	No->	UTS	TYS	EL4D
		Test	KSI	KSI	PCT
T651	Long Transv.	2	48.1	43.6	14.5
			48	43.5	14.6

Cast Number	Chemical - OES	SI	FE	CU	MN	MG	CR	ZN	TI
H2122011	Actuals	0.64	0.4	0.25	0.05	0.9	0.15	0.03	0.03

376

Figure D-6. Aluminum Post Base Material Certificate (Sheet 1 of 2), Test Nos. WIPR-1, WIPR-2, and WIPR-4

CERTIFIED INSPECTION REPORT

Alcoa Inc.

DAVENPORT WORKS 4879 State Street Bettendorf, IA 52722

Ship From: RIVERDALE, IA.

We hereby certify that the material covered by this certificate has been inspected with, and has been found to meet the applicable requirements described therein, including any specifications forming a part of the description and that samples representative of the material met the composition limits and had the mechanical properties shown on the face of this sheet.

This test report shall not be reproduced except in full, without the written approval of the Quality Department. No alteration, addition or other change is authorized to be made to this certificate. The recording of false, fictitious, or otherwise fraudulent statements or entries on this certificate by any recipient may be punished as a felony under applicable law.

Per:

Rob Woodall

Rob Woodall
Director of Manufacturing Davenport Works

Terrence Thom

Terrence Thom
Quality Assurance Manager

1436681	0			
Ship Date	B.L. No.	Invoice No.	Alcoa No.	Item
2012-09-30	7388421	00000	1000404652-1	DP-04652-1
P.O. No./Govt Contract No.	Customer	Alcoa Item		
4500504158 Ln#: 0000	RYERSON - COON RAP	G041107416R08		

Page 1 of 4

Ship To: RYERSON PROCUREMENT CORP
455 85TH AVE NW
COON RAPIDS 55433 MN

Item Description
0.25 IN TK (+.014 -0.000) X 48.5 IN W (+.375 -
0.000) X 144.5 IN LN (+.5 -0.0) CAT X 160001700 (N) A/T 6061-
T651 TYPE 200 WROUGHT TOOLING PLATE MILL
FINISH. AMS4027 REV N ANSIIH35.2 REV 2009 EXC_MRK ASME-SB-
209 REV 11 EXC_MRK ASTM B209 REV 10
((MARKED)) KRAFT PAPER INTERLEAVED
MAX GROSS SKID WGT: 4500 LB QUAN TOL +/-
30 % CQR D164055 REV 08 CUST REQ 12-09-
30 *** W/E 12-10-06 ***

Num	Package Ticket	Lot	Weight	Quantity	UOM	Inspector Clock Numbers
1	441631	212073	1068	6	PC	47200
2	441631	572941	1068	6	PC	47200
3	441631	572947	1068	6	PC	47200
4	441631	572948	1068	6	PC	47200
5	441634	212073	1068	6	PC	47200
6	441634	572941	1068	6	PC	47200
7	441634	572947	1068	6	PC	47200
8	441634	572948	1068	6	PC	47200
9	441753	539961	536	3	PC	47200
10	441753	539966	889	5	PC	47200
11	441753	539967	711	4	PC	47200
12	441753	539968	1067	6	PC	47200
13	441753	572941	1067	6	PC	47200
			12814	72		

Notes for CQR: D164055.8
PRODUCT PRODUCED TO THE REQUIREMENTS OF AMS4027 REV N ALSO MEET THE REQUIREMENTS OF AMS-QQ-A-250_11 ORIGINAL REVISIO N DATED 1997-08-01.

Figure D-7. Aluminum Post Base Material Certificate (Sheet 2 of 2), Test Nos. WIPR-1, WIPR-2, and WIPR-4

CERTIFICATE OF TEST



Page 01 of 01

Certification Date
10-APR-2014

CUSTOMER ORDER NUMBER

39584

EARLE M. JORGENSEN COMPANY
1800 N UNIVERSAL AVENUE
KANSAS CITY MO 64120

Invoice Number

S107283

CUSTOMER PART NUMBER

0001

107209

SOLD TO: RIVERS METAL PRODUCTS

3100 N 38TH
LINCOLN NE 68504

SHIP TO:

RIVERS METAL PRODUCTS

3100 NORTH 38TH
LINCOLN NE 68504

Description: 6061-T6 EXTRUDED PORTHOLE TUBING -ASTM B221 Q
2 X 2 X .125 W X 20' Line Total: 139.6207 FT
HEAT: 201405597 ITEM: 107209

Specifications:

ASTM B221 13

QQ-A-200/8

AMS QQ A 200/8 97

ALUMINIUM CHEMICAL ANALYSIS

DESCRIPTION:

	SI	FE	CU	MN	MG	CR	ZN	TI
MIN	0.4		0.15		0.8	0.04		
MAX	0.8	0.7	0.4	0.15	1.2	0.35	0.25	0.15

OTHERS : EACH TOTAL
0.05 0.15 AL REMAINDER

RCPT: R328024

VENDOR: SERVICE CENTER METALS

COUNTRY OF ORIGIN : USA

MECHANICAL PROPERTIES

DESCRIPTION	YLD STR KSI	ULT TEN KSI	%ELONG IN 02 IN	%RED IN AREA	HARDNESS
	40.3	42.6	11.5		
	42.7	44.9	14.85		

The above data were transcribed from the manufacturer's Certificate of Test after verification for completeness and specification requirements of the information on the certificate. All test results remain on file subject to examination.

We hereby certify that the material covered by this report will meet the applicable requirements described herein, including any specification forming a part of the description.

The willful recording of false, fictitious, or fraudulent statements in connection with test results may be punishable as a felony under federal statutes.

Material did not come in contact with mercury while in our possession.

LARRY BUSICK

Larry A Busick
Manager, Quality Assurance

Figure D-8. 2"x2"x1/8" Aluminum Rail Material Certificate, Test Nos. WIPR-1, WIPR-2, and WIPR-4

CERTIFICATE OF TEST



Page 01 of 01

Certification Date
NOT VALID

CUSTOMER ORDER NUMBER

39584

1800 N UNIVERSAL AVENUE
KANSAS CITY MO 64120

Invoice Number
S107281

CUSTOMER PART NUMBER

01 513315

SOLD TO: RIVERS METAL PRODUCTS
3100 N 38TH
LINCOLN NE 68504

SHIP TO: RIVERS METAL PRODUCTS
3100 NORTH 38TH
LINCOLN NE 68504

Description: 6061-T6511 EXTRUDED BAR AMS QQ-A-200/8
1/2 SQ X 12' Line Total 71.0000 LB
HEAT: 201405836 ITEM: 513315 CST 2.09LB 71.00LB

Specifications:

*** NO VALID TEST REPORT FOR ORDER
*** MESSAGE - DOES NOT EXIST

The above data were transcribed from the manufacturer's Certificate of Test after verification for completeness and specification requirements of the information on the certificate. All test results remain on file subject to examination.

We hereby certify that the material covered by this report will meet the applicable requirements described herein, including any specification forming a part of the description.
The willful recording of false, fictitious, or fraudulent statements in connection with test results may be punishable as a felony under federal statutes.

Material did not come in contact with mercury while in our possession.

Figure D-9. 1/2"x1/2" Aluminum Spindle Material Certificate, Test Nos. WIPR-1, WIPR-2, and WIPR-4



April 15 2014

W.W. Grainger, Inc.
100 Grainger Parkway
Lake Forest, IL. 60045-5201

Attn: KENNETH L KRENK
KENNETH L KRENK
29 WSEC
LINCOLN, NE, 68588-0000

Pedestrian Hardware
R# 14-0433

Fax #

Grainger Sales Order #: 1206167220
Customer PO #: E000137265

Dear KENNETH L KRENK

As you requested, we are providing you with the following information. We certify that, to the best of Grainger's actual knowledge, the products described below conform to the respective manufacturer's specifications as described and approved by the manufacturer.

Item #	Description	Vendor Part #	Catalog Page #	Order Quantity
4FHF3	Threaded Rod,B7,Yellow Zinc,1/2-13x3 ft	U22182.050.3600	2929	1.000
4FHG3	Threaded Rod,B7,Yellow Zinc,3/8-16x6 ft	U22182.037.7200	2929	1.000
4FHF1	Threaded Rod,B7,Yellow Zinc,3/8-16x3 ft	U22182.037.3600	2929	1.000
1XA24	Hex Nut,Grade 2H,3/8-16,PK50	SHY97	0000	1.000
6PE80	Flat Washer,Ylw Zinc,Fits 3/8 In,Pk 50	HU-0375USSHZYBAGGR	2825	1.000

Tim Phillips
Process Management Analyst
Compliance Team
Grainger Industrial Supply

Figure D-10. Certificate of Conformance – 3/8" and 1/2" Threaded Rods, 3/8" Nut, 3/8" Washer, Test Nos. WIPR-1 through WIPR-4

CERTIFICATE OF TEST



Page 01 of 01

Certification Date
14-APR-2014

CUSTOMER ORDER NUMBER

39584

EARLE M. JORGENSEN COMPANY
1800 N UNIVERSAL AVENUE
KANSAS CITY MO 64120

Invoice Number
T780976

CUSTOMER PART NUMBER

0001

116063

SOLD TO: RIVERS METAL PRODUCTS
3100 N 38TH
LINCOLN NE 68504

SHIP TO: RIVERS METAL PRODUCTS
3100 NORTH 38TH
LINCOLN NE 68504

Description: 6061-T6 EXTRUDED PORTHOLE TUBING -ASTM B221 Q
2 X 3 X .125 W X 20' Line Total: 40.5175 FT
HEAT: 21393458 ITEM: 116063

Specifications:
ASTM B221 12A

QQ-A-200/8

AMS QQ A 200/8 97

ALUMINIUM CHEMICAL ANALYSIS

DESCRIPTION:

	SI	FE	CU	MN	MG	CR	ZN	TI
MIN	0.4		0.15		0.8	0.04		
MAX	0.8	0.7	0.4	0.15	1.2	0.35	0.25	0.15

OTHERS : EACH TOTAL
0.05 0.15 AL REMAINDER

RCPT: R982552

VENDOR: SAPA PROFILES NORTH AMERICA COUNTRY OF ORIGIN : USA

MECHANICAL PROPERTIES

DESCRIPTION	YLD STR KSI	ULT TEN KSI	%ELONG IN 02 IN	%RED IN AREA	HARDNESS
	40.8	45.5	11.0		
	42.6	46.5	13.0		

The above data were transcribed from the manufacturer's Certificate of Test after verification for completeness and specification requirements of the information on the certificate. All test results remain on file subject to examination.

We hereby certify that the material covered by this report will meet the applicable requirements described herein, including any specification forming a part of the description.

The willful recording of false, fictitious, or fraudulent statements in connection with test results may be punishable as a felony under federal statutes.

Material did not come in contact with mercury while in our possession.

LARRY BUSICK

Larry A Busick
Manager, Quality Assurance

Figure D-11. 2"x3"x1/8" Aluminum Post Material Certificate, Test No. WIPR-2



W.W. Grainger, Inc.
100 Grainger Parkway
Lake Forest, IL. 60045-5201

April 25 2014

Attn: KENNETH L KRENK
KENNETH L KRENK
29 WSEC
LINCOLN, NE, 68588-0000

Pedestrian Rail
R# 14-0472
April 2014 SMT

Fax #

Grainger Sales Order #: 1206971310
Customer PO #: E000139790

Dear KENNETH L KRENK
As you requested, we are providing you with the following information. We certify that, to the best of Grainger's actual knowledge, the products described below conform to the respective manufacturer's specifications as described and approved by the manufacturer.

Item #	Description	Vendor Part #	Catalog Page #	Order Quantity
1VZA6	Hex Cap Screw,B7,1/4-20x3,PK10	HXCS.001609.50	2766	1.000

Tim Phillips
Process Management Analyst
Compliance Team
Grainger Industrial Supply

Figure D-12. Certificate of Conformance – 1/4" Dia. x 3" Bolt and 1/4" Nut, Test No. WIPR-2

METALS USA - FLAT ROLLED

NBK

Certificate of Mill Test Results

BL LIB-000000-000

Pg 1/2

PART NO:

Altir:

sapa:

Sapa Industrial Extrusions
1550 KIRBY LANE
SPANISH FORK, UT
84660-1349

Sapa Extrusions Inc., a Subsidiary of Sapa AB

Invoice To Customer

METALS USA
2840 E HEARTLAND DRIVE
LIBERTY, MO - 64068

Ship To Customer

METALS USA
2840 E HEARTLAND DR.
LIBERTY, MO - 64068

Certified Inspection Report

Sales Order Number	Line No.	Customer P/O	Cert Number	Page
1100729388	6	LIB-27207-006	SAPAS06804	Page 1 of 2
			Cert Creation Date	Cert Print Date
			14-MAR-14	14-MAR-14

Quantity Shipped	Date Shipped	Item Description	Specification
1166 LB	14-MAR-14	Extruded Structural Pipe 2.000 DIA x SCHEDULE 80	ASTMB429 REV 10 ASTMD221 REV 13
B/L	Item No.	240 IN LN FIN M-MILL	AMS-QQ-A-20008 REV 1997 MIL-DTL-25995 REV D UNSA96061 REV
512394	G00360485	W/F L737 F 08 CS 2.4 6061/T6	
Delivery Id	Item No. Rev	Marking CONTINUOUS	
4521272			
Customer Part No.			
2X80			

Applicable Specifications, Revisions and Exceptions

COMPOSITION NOTE: The values for 'Others Each' and 'Others Total' have met the limits as shown on this certified inspection report. Remainder is Aluminum.

Legal Statement

We hereby certify that, unless otherwise indicated, the material covered by this report has been manufactured, inspected, and tested in accordance with, and has been found to meet, the applicable requirements described herein, including any specifications forming a part of the description and that samples representative of the material met the composition and had the mechanical properties shown on the face of this certification. Also, note that mercury is not a normal contaminant in aluminum alloys and neither it nor any of its compounds are used in the manufacture of our product. This certification is not to be reproduced in partial form without prior written approval of our Quality Assurance Dept.

Signature And Title

Brian Pike

Brian Pike
Quality Control Manager

14-MAR-14

Quantities per Lot / Packages

Package Number	Lot Number	Quantity	UOM	Weight	
				Gross	Net
G14-PKG1528623	21684972	17	PCS	591	583
G14-PKG1528624	21684972	17	PCS	591	583

Composition Limits

Alloy	Si		Fe		Cu		Mn		Mg		Cr		Zn	
	Min	Max	Min	Max	Min	Max	Min	Max	Min	Max	Min	Max	Min	Max
6061	0.40	0.80	—	0.70	0.15	0.40	—	0.15	0.80	1.20	0.04	0.35	—	0.25

Doc No. 173119 Indexed 18Mar14 by 166dmh

Figure D-13. 2" Dia. Schedule 80 Aluminum Post Material Certificate (Sheet 1 of 2), Test No. WIPR-3

PART NO.

Attr:

sapa:

Sapa Industrial Extrusions
1550 KIRBY LANE
—
SPANISH FORK, UT
84660-1349

Certified Inspection Report

Sales Order Number
1100729388

Line No. 6

Customer PO
LIB-27207-006

Cert Number	Page
SAPA936804	Page 2 of 2
Cert Creation Date	Cert Print Date
14-MAR-14	14-MAR-14

Alloy	Ti		Others Each		Others Total	
	Min	Max	Min	Max	Min	Max
6061	—	0.15	—	0.05	—	0.15

Composition Results

Heat / Cast	Si	Pb	Cu	Mn	Mg	Cr	Zn	Ti	Others Each	Others Total
S14022301	0.75	0.37	0.23	0.08	0.85	0.07	0.07	0.03	—	—

Mechanical Property - Test Limits

Test Temper	Lot Number	# of Tests	TYS - L		TYS - L		EL 4D-Long	
			MIN Value	MAX Value	MIN Value	MAX Value	MIN Value	MAX Value
T6	21684972	2	47.7	48.5	41.4	44.6	13.5	18.9

Cert Notes

Material manufactured to T6511 specifications also meets T6 requirements.

All elements are represented in the chemical analysis section. The remainder is Aluminum.

All mill finish alloys produced at Sapa Industrial Extrusions comply with Directive 2011/65/EU (RoHS 2) with the exception of 6262 alloy.

In accordance with EN 10204, Test Report Type 2.2 and Certificate Type 3.1

Material produced in compliance to EN 10204 3.1

Manufactured in the USA

Made in USA

Figure D-14. 2" Dia. Schedule 80 Aluminum Post Material Certificate (Sheet 2 of 2), Test No. WIPR-3

METALS USA - FLAT ROLLED

NBK

Certificate of Mill Test Results

PO/Ref

BL11B-000000-000

Pg 1/2

PART NO.

Alt:

sapa: Sapa Industrial Extrusions
1550 KIRBY LANE

SPANISH FORK, UT
84660-1349

Sapa Extrusions Inc., a Subsidiary of Sapa AB

Invoice To Customer

METALS USA
2840 E HEARTLAND DRIVE

LIBERTY, MO - 64068

Ship To Customer

METALS USA
2840 E HEARTLAND DR.

LIBERTY, MO - 64068

Certified Inspection Report

Sales Order Number	Line No.	Customer P/O	Cert Number	Page
1100717538	2	LJB-26908-2	SAPA920186	1 of 2
			Cert Creation Date	Cert Print Date
			14-FEB-14	14-FEB-14

Quantity Shipped	Date Shipped	Item Description	Specification
505 LB	14-FEB-14	Extruded Structural Pipe 2.000 DIA x SCHEDULE 40	ASTM B429 REV 10 ASTM B221 REV 13
B/L	Item No.	240 IN LN	AMS-QQ-A-200/8 REV 1997
503983	G03369473	FIN M-MILL	MIL-DTL-25995 REV D
Delivery Id	Item No. Rev	W/F 1.264 F 11 CS 2.4	UNSA96061 REV
4512314	--	6061/T6	
Customer Part No.		Marking CONTINUOUS;	
2X40			

Applicable Specifications, Revisions and Exceptions

COMPOSITION NOTE: The values for 'Others Each' and 'Others Total' have met the limits as shown on this certified inspection report. Remainder is Aluminum.

Legal Statement

We hereby certify that, unless otherwise indicated, the material covered by this report has been manufactured, inspected, and tested in accordance with, and has been found to meet, the applicable requirements described herein, including any specifications forming a part of the description and that samples representative of the material met the composition and had the mechanical properties shown on the face of this certification. Also, note that mercury is not a normal contaminant in aluminum alloys and neither it nor any of its compounds are used in the manufacture of our product. This certification is not to be reproduced in partial form without prior written approval of our Quality Assurance Dept.

Signature And Title

Brian Pike

Brian Pike
Quality Control Manager

14-FEB-14

Quantities per Lot / Packages

Package Number	Lot Number	Quantity	COM.	Weight
G14-PKG1506843	21633667	20	PCS	Gross 509 Net 505

Composition Limits

Alloy	Si		Fe		Cu		Mn		Mg		Cr		Zn	
	Min	Max	Min	Max	Min	Max	Min	Max	Min	Max	Min	Max	Min	Max
6061	0.40	0.80	—	0.70	0.15	0.40	—	0.15	0.80	1.20	0.04	0.25	—	0.25

Doc No. 171386 Indexed 17Feb14 by 166dmh

385

Figure D-15. 2" Dia. Schedule 40 Aluminum Post Material Certificate (Sheet 1 of 2), Test No. WIPR-3

January 18, 2016
MWRSF Report No. TRP-03-321-15

PART NO.

Alt#:

sapa:Sapa Industrial Extrusions
1550 KIRBY LANE
SPANISH FORK, UT
84660-1349

Certified Inspection Report

Sales Order Number
1100717538Line No.
2Customer PO
LIS-26908-2Cert Number
SAPA920186
Cert Creation Date
14-FEB-14Page
1 of 2
Cert Print Date
14-FEB-14

Alloy	Ti		Others Each		Others Total	
	Min	Max	Min	Max	Min	Max
6061	---	0.15	---	0.05	---	0.15

Composition Results

Heat / Cast	Si	Pb	Cu	Mn	Mg	Ce	Zn	Ti	Others Each	Others Total
S14010202	0.77	0.36	0.24	0.05	0.85	0.06	0.08	0.02	---	---

Mechanical Property - Test Results

Test Temper	Lot Number	# of Tests	UTS - L		TYS - L		EL 40-Long	
			MIN Value	MAX Value	MIN Value	MAX Value	MIN Value	MAX Value
T6	21603667	3	46.7	48.7	44.3	46.6	11.9	12.0

Cert Notes

Material manufactured to T6511 specifications also meets T6 requirements.

All elements are represented in the chemical analysis section. The remainder is Aluminum.

All mill finish alloys produced at Sapa Industrial Extrusions comply with Directive 2011/65/EU (RoHS 2) with the exception of 6262 alloy.

In accordance with EN 10204, Test Report Type 2.2 and Certificate Type 3.1

Material produced in compliance to EN 10204 3.1

Melted and Manufactured in the USA

Made in USA

Figure D-16. 2" Dia. Schedule 40 Aluminum Post Material Certificate (Sheet 2 of 2), Test No. WIPR-3



CERTIFICATE OF TEST

Pedestrian Rail R#15-0098 TMC0
August/October 2014 SMT

Page 01 of 01

Certification Date
22-SEP-2014

CUSTOMER ORDER NUMBER

35316

EARLE M. JORGENSEN COMPANY
1800 N UNIVERSAL AVENUE
KANSAS CITY MO 64120

Invoice Number
S153306

CUSTOMER PART NUMBER

0001

894-02002

SOLD TO: TMC0 INC
ATTENTION ACCOUNTS PAYABLE
535 J STREET
LINCOLN NE 68508

SHIP TO:

TMC0 INC
701 S 6TH STREET
LINCOLN NE 68508

Description: 6061-T6 EXTRUDED PORTHOLE TUBING -ASTM B221 Q
2 X 4 X .250 W X 20' Line Total: 257.27 FT
HEAT: 21550443 ITEM: 116661

Specifications:
ASTM B221 13
EN 10204 3.1

QQ-A-200/8

AMS QQ A 200/8

ALUMINIUM CHEMICAL ANALYSIS

DESCRIPTION:

	SI	FE	CU	MN	MG	CR	ZN	TI
MIN	0.4		0.15		0.8	0.04		
MAX	0.8	0.7	0.4	0.15	1.2	0.35	0.25	0.15

OTHERS : EACH TOTAL
0.05 0.15 AL REMAINDER

RCPT: R197775

VENDOR: SAPA PROFILES NORTH AMERICA COUNTRY OF ORIGIN : USA

MECHANICAL PROPERTIES

DESCRIPTION	YLD STR KSI	ULT TEN KSI	%ELONG IN 02 IN	%RED IN AREA	HARDNESS
	44.3	46.7	14.0		

The above data were transcribed from the manufacturer's Certificate of Test after verification for completeness and specification requirements of the information on the certificate. All test results remain on file subject to examination.

We hereby certify that the material covered by this report will meet the applicable requirements described herein, including any specification forming a part of the description.

The willful recording of false, fictitious, or fraudulent statements in connection with test results may be punishable as a felony under federal statutes.

Material did not come in contact with mercury while in our possession.

LARRY BUSICK

Larry A Busick
Manager, Quality Assurance

Figure D-18. 2"x4"x1/4" Aluminum Post Material Certificate, Test Nos. APR-1 and APR-2

Pedestrian Rail 1/8" Post Cap
R#15-0098 No Definitive Heat No.
August/October 2014

ZHE JIANG GKO ALUMINIUM CO. LTD.
XINTAO, FENGJIANG, LUQIAO, TAIZHOU, ZHEJIANG, CHINA
TEL: +86 576 82696583 FAX: +86 576 82696589

MILL TEST REPORT

SMCL102546

BUYER:
TA CHEN INTERNATIONAL, INC
5855 ORISPO AVE.
LONG BEACH, CA 90805, USA

Date: 2014-5-6
Invoice: C106042-1
Contract No.: N06042
Loading Port: Ningbo, China
COUNTRY OF MELT & MANUFACTURE: CHINA

MATERIAL GRADE: 5052H32 AS PER ASTM B309-10 - AMS QQ-A 250/3 AND AMS 4016M

Destination: LA

B/L NO.: ECLV143486695000

ISF NO.: 8EFT698585508

ETD: 2014-5-4

No.	PO NO.	DESCRIPTION OF GOODS	ALLOY/T EMPER	Specification (inch)	Roller No.	N.W. (lb)	HEAT NO.	Chemical Composition (%)												Mechanical Properties		
								Al	Si	Fe	Cu	Mn	Mg	Zn	Pb	Ca	Ti	Other	Tensile Strength ksi	Yield Strength ksi	Elongation %	
1	N06042	COIL	5052H32	0.063*48	514032206	9678	514032206	96.87	0.113	0.134	0.011	0.010	2.490	0.225	0.018	0.008	0.013	0.000	32.6	28.7	10.2	
2	N06042	COIL	5052H32	0.063*48	514032207	9273	514032207	96.89	0.103	0.258	0.002	0.010	2.480	0.216	0.015	0.008	0.026	0.000	32.6	28.7	10.0	
3	N06042	COIL	5052H32	0.063*48	514032216	8942	514032216	96.57	0.104	0.250	0.002	0.010	2.450	0.231	0.007	0.009	0.018	0.019	31.9	28.6	12.4	
4	N06042	COIL	5052H32	0.063*48	514032310	9286	514032310	96.32	0.121	0.282	0.003	0.014	2.390	0.228	0.015	0.005	0.019	0.000	31.9	28.6	10.8	
5	N06042	COIL	5052H32	0.063*48	514032280	8792	514032280	96.96	0.121	0.277	0.003	0.013	2.390	0.225	0.012	0.007	0.028	0.000	32.6	28.3	11.2	
6	N06042	COIL	5052H32	0.063*48	514032311	9572	514032311	96.92	0.121	0.282	0.003	0.014	2.390	0.228	0.016	0.005	0.019	0.000	31.9	28.3	10.2	
7	N06042	COIL	5052H32	0.063*48	514032325	8294	514032325	96.91	0.125	0.281	0.011	0.009	2.419	0.211	0.020	0.008	0.016	0.019	28.7	10.8		
8	N06042	COIL	5052H32	0.063*60	514032451-1	7852	514032451	97.06	0.046	0.235	0.004	0.039	2.370	0.194	0.015	0.007	0.011	0.019	28.9	11.2		
9	N06042	COIL	5052H32	0.063*60	514032451-2	7665	514032451	97.06	0.065	0.235	0.004	0.039	2.370	0.194	0.015	0.007	0.011	0.019	28.9	11.2		
10	N06042	COIL	5052H32	0.063*60	514032489-1	7875	514032489	97.07	0.065	0.232	0.003	0.032	2.390	0.195	0.015	0.007	0.019	0.019	28.6	10.4		
11	N06042	COIL	5052H32	0.08*48	514032145	9775	514032145	96.90	0.095	0.253	0.007	0.053	2.436	0.212	0.012	0.021	0.021	0.000	32.6	28.7	11.6	
12	N06042	COIL	5052H32	0.08*48	514032331-2	9321	514032331	97.07	0.107	0.270	0.010	0.010	2.310	0.220	0.018	0.020	0.020	0.000	31.9	28.3	12.2	
13	N06042	COIL	5052H32	0.08*48	514032147-2	9762	514032147	96.99	0.083	0.262	0.003	0.013	2.390	0.230	0.018	0.011	0.014	0.019	28.9	11.8		
14	N06042	COIL	5052H32	0.08*48	514032190-2	8726	514032190	96.94	0.119	0.275	0.003	0.015	2.410	0.208	0.011	0.010	0.011	0.019	28.0	11.6		
15	N06042	COIL	5052H32	0.1*48	514032195-2	8902	514032195	96.88	0.099	0.265	0.003	0.030	2.450	0.216	0.016	0.028	0.014	0.026	28.7	11.8		
16	N06042	COIL	5052H32	0.1*48	514032196-2	8717	514032196	96.79	0.100	0.282	0.000	0.051	2.430	0.213	0.013	0.022	0.013	0.022	28.7	12.8		
17	N06042	COIL	5052H32	0.1*48	514032199-2	8016	514032199	96.85	0.091	0.300	0.011	0.044	2.410	0.202	0.012	0.008	0.021	0.019	28.6	13.0		
18	N06042	COIL	5052H32	0.1*48	514032248-2	8170	514032248	97.01	0.114	0.266	0.003	0.015	2.340	0.209	0.018	0.010	0.012	0.012	28.7	13.2		
19	N06042	COIL	5052H32	0.1*48	514032250-2	9612	514032250	97.04	0.030	0.134	0.003	0.010	2.380	0.216	0.012	0.010	0.014	0.019	28.7	12.2		
20	N06042	COIL	5052H32	0.1*48	514032251-2	9012	514032251	97.04	0.104	0.255	0.003	0.016	2.320	0.230	0.012	0.011	0.014	0.019	29.0	12.8		
21	N06042	COIL	5052H32	0.1*48	514032427-2	8394	514032427	97.06	0.075	0.235	0.005	0.061	2.320	0.198	0.009	0.007	0.018	0.019	28.7	11.2		

389

MILL TEST REPORT
Customer: PHOKAN PO#: 79516 SO#: LBY740
Item: 25485052H32 Bundle: 514032061-2 Heat#: 514032061
Item: 25485052H32 Bundle: 514033385-2 Heat#: 514033385
TA CHEN INTERNATIONAL, INC.
This MTR contains 2 pages (Page# 1)
MTR#: SMCL102546.GIF

Figure D-19. 1/8" thick Aluminum Post Cap Material Certificate (Sheet 1 of 2), Test Nos. APR-1 and APR-2

MILL TEST REPORT
Customer: PHOKAN PO#79516 SO#14BT40
Item: 125485052H32 Bundle: 514032061-2 Heat#: 514032061
Item: 125485052H32 Bundle: 514033385-2 Heat#: 514033385
TA CHEN INTERNATIONAL, INC.
This MTR contains 2 pages (Page# 2)
MTR#SMCL102546-2.GIT

SMCL102546-2

22	N06042	COIL	5052H32	0.125*48	514032213-2	9321	514032213	96.99	0.087	0.261	0.006	0.026	1.540	0.215	0.033	0.008	0.019	33.4	28.6	10.4
23	N06042	COIL	5052H32	0.1460	514033006-1	7840	514033006	96.56	0.110	0.250	0.016	0.040	1.390	0.200	0.014	0.010	0.020	31.8	28.3	14.0
24	N06042	COIL	5052H32	0.1460	514033006-2	13004	514033006	96.56	0.110	0.250	0.016	0.040	1.390	0.200	0.014	0.010	0.020	31.8	28.3	14.0
25	N06042	COIL	5052H32	0.1460	514033119-1	8042	514033119	96.92	0.110	0.230	0.010	0.020	2.460	0.200	0.018	0.010	0.020	32.6	28.4	11.8
26	N06042	COIL	5052H32	0.125*48	514032020	9317	514032020	96.91	0.096	0.300	0.011	0.070	2.370	0.196	0.020	0.007	0.022	33.4	28.3	10.2
27	N06042	COIL	5052H32	0.125*48	514032051-2	8188	514032051	96.92	0.086	0.300	0.011	0.070	2.370	0.196	0.012	0.007	0.022	33.4	28.7	12.2
28	N06042	COIL	5052H32	0.125*48	514032061-2	8364	514032061	96.84	0.091	0.300	0.011	0.094	2.410	0.202	0.020	0.008	0.022	32.6	28.9	12.2
29	N06042	COIL	5052H32	0.125*48	514033362-3	8968	514033362	96.94	0.130	0.280	0.010	0.010	2.410	0.190	0.012	0.010	0.020	32.6	28.7	12.2
30	N06042	COIL	5052H32	0.125*48	514033362-2	9458	514033362	97.06	0.080	0.220	0.010	0.020	2.360	0.210	0.016	0.010	0.010	31.2	28.6	13.6
31	N06042	COIL	5052H32	0.125*48	514033364-2	8735	514033364	96.99	0.080	0.280	0.010	0.020	2.400	0.210	0.013	0.010	0.020	32.6	28.3	12.2
32	N06042	COIL	5052H32	0.125*48	514033384-2	9766	514033384	96.96	0.130	0.280	0.010	0.010	2.400	0.190	0.021	0.010	0.020	31.9	28.4	13.6
33	N06042	COIL	5052H32	0.125*48	514033385-2	8721	514033385	96.92	0.140	0.240	0.010	0.020	2.420	0.190	0.017	0.020	0.020	31.2	28.9	12.2

ZHEJIANG GEO ALUMINUM CO., LTD.



Figure D-20. 1/8" thick Aluminum Post Cap Material Certificate (Sheet 2 of 2), Test Nos. APR-1 and APR-2

TEST CERTIFICATE



Certificate No : 1307LB8422

Hulamin Limited Reg. No. 1940/013924/06 VAT Reg. No. 4080149604
HEAD OFFICE: Moses Mabhidia Rd, Pietermaritzburg 3201, P.O. Box 74, Pietermaritzburg 3200, South Africa
Telephone: +27 33 395 6911 Telefax: +27 33 394 6335

BUYER: EMPIRE RESOURCES INC 10th FLOOR 1 PARKER PLAZA FORT LEE	Shipping File No: UR46949 Lot No: 23/07/073D0 P/List No: 2/1274813 Release No: RE112504	Product: 375" X 48.5" X 96.5" PLATE 6061, T651 Dimension: 0.375" X 48.5" X 96.5" Alloy - Temper: 6061 - T651
	Cust Order No: 6043-P.R142815 HULAMIN Order No: 247713E Item Part: 1/1	Certificate No: 1307LB8422 Cust Ref/Part No: Combined P/List No: R138732

Case No : PGW881,PGW882

MECHANICAL TEST RESULTS

Lot No.	Cast No.	Metal Id	Alloy	Spec No	Mechanical Properties							
					Yield Strength (Ksi)	UTS (Ksi)	Elongation A50 (%)	Earing (%)	Test Date	Gauge Length (Inches)	Bend Test	Actual Gauge (Inches)
Spec				Min	35.1	42.0	10					0.375
				Max						50		0.392
23/07/073D0	VNKK	59693083	6061	1	41.8	46.3	16		31/07/13	2		0.386
				2	41.8	46.3	16		31/07/13	2		0.386

CHEMICAL COMPOSITION

	Cast No.	Alloy	Si (%)	Fe (%)	Cu (%)	Mn (%)	Mg (%)	Cr (%)	Zn (%)	Ti (%)	Each (%)	Total (%)	Al (%)
Min			0.40		0.15		0.8	0.04					
Max			0.8	0.7	0.40	0.15	1.2	0.35	0.25	0.15	0.05	0.15	
	VNKK	6061	0.72	0.42	0.30	0.10	1.00	0.18	0.02	0.008			97.21

CONFORMS TO: ASME SB-209 ASTM B209/10 AMS 4027N AMS-QQA-250/11, 08.1997

For purposes of determining conformance with these specifications, an observed value or a calculated value shall be rounded "to the nearest unit" in the last right-hand digit used in expressing the specification limit, in accordance with the rounding method of ASTM Practice E29, for Using Significant Digits in Test Data to Determine Conformance with Specifications.

WE HEREBY CERTIFY, THAT THE MATERIAL DESCRIBED ABOVE HAS BEEN TESTED AND COMPLIES WITH THE TERMS OF THE ORDER CONTRACT. THE INSPECTION RESULTS INDICATED IN THE CHEMICAL COMPOSITION HAVE BEEN OBTAINED FROM CAST ANALYSIS.

Dr. A. Pitchford (HEAD OF CHEMICAL TESTING)

Ver 2 6 2

V. Maniram (HEAD OF PHYSICAL TESTING)

Printed Date : 31 Aug 2013

Melted, cast, rolled and processed in South Africa - meets Requirements of RoHS and REACH

1 of 1

Figure D-21. Aluminum Post Base Material Certificate, Test Nos. APR-1 and APR-2



CERTIFICATE OF TEST

Pedestrian Rail R#15-0098 TMC0
August/October 2014 SMT

Page 01 of 01

Certification Date
22-SEP-2014

CUSTOMER ORDER NUMBER

35316

EARLE M. JORGENSEN COMPANY
1800 N UNIVERSAL AVENUE
KANSAS CITY MO 64120

Invoice Number
S153305

CUSTOMER PART NUMBER

0001

884-02000

SOLD TO: TMC0 INC
ATTENTION ACCOUNTS PAYABLE
535 J STREET
LINCOLN NE 68508

SHIP TO:

TMC0 INC
701 S 6TH STREET
LINCOLN NE 68508

Description: 6061-T6 EXTRUDED PORTHOLE TUBING -ASTM B221 Q
2 X 2 X .125 W X 20' Line Total: 609.22 FT
HEAT: 21836702 ITEM: 107209

Specifications:
ASTM B221 13

QQ-A-200/8

AMS QQ A 200/8

ALUMINIUM CHEMICAL ANALYSIS

DESCRIPTION:

	SI	FE	CU	MN	MG	CR	ZN	TI
MIN	0.4		0.15		0.8	0.04		
MAX	0.8	0.7	0.4	0.15	1.2	0.35	0.25	0.15

OTHERS : EACH TOTAL
0.05 0.15 AL REMAINDER

RCPT: R431612

VENDOR: SAPA PROFILES NORTH AMERICA COUNTRY OF ORIGIN : USA

MECHANICAL PROPERTIES

DESCRIPTION	YLD STR KSI	ULT TEN KSI	%ELONG IN 02 IN	%RED IN AREA	HARDNESS
	36.6	44.1	11.5		
	40.6	48.0	13.0		

The above data were transcribed from the manufacturer's Certificate of Test after verification for completeness and specification requirements of the information on the certificate. All test results remain on file subject to examination.

We hereby certify that the material covered by this report will meet the applicable requirements described herein, including any specification forming a part of the description.

The willful recording of false, fictitious, or fraudulent statements in connection with test results may be punishable as a felony under federal statutes.

Material did not come in contact with mercury while in our possession.

LARRY BUSICK

Larry A Busick
Manager, Quality Assurance

Figure D-22. 2"x2"x1/8" Aluminum Rail Material Certificate, Test Nos. APR-1 and APR-2



CERTIFICATE OF TEST

Pedestrian Rail R#15-0098 TMCO
August/October 2014 SMT

Page 01 of 02

Certification Date
24-SEP-2014

CUSTOMER ORDER NUMBER

35349

EARLE M. JORGENSEN COMPANY
1800 N UNIVERSAL AVENUE
KANSAS CITY MO 64120

Invoice Number
S153835

CUSTOMER PART NUMBER

0001

854-00500

SOLD TO: TMCO INC
ATTENTION ACCOUNTS PAYABLE
535 J STREET
LINCOLN NE 68508

SHIP TO: TMCO INC
701 S 6TH STREET
LINCOLN NE 68508

Description: 6061-T6511 EXTRUDED BAR AMS QQ-A-200/8
1/2 SQ X 12' Line Total: 256 LB
HEAT: 201408541 ITEM: 513315

Specifications:

QQ A 200/8
AMS QQA 200/8 97

ASTM B221 13*
MEETS T6 TEMPER

*NO STENCIL

ALUMINIUM CHEMICAL ANALYSIS

DESCRIPTION:

	SI	FE	CU	MN	MG	CR	ZN	TI
MIN	0.4		0.15		0.8	0.04		
MAX	0.8	0.7	0.4	0.15	1.2	0.35	0.25	0.15

OTHERS : EACH TOTAL
0.05 0.15 AL REMAINDER

RCPT: R364734

VENDOR: SERVICE CENTER METALS

COUNTRY OF ORIGIN : USA

MECHANICAL PROPERTIES

DESCRIPTION	YLD STR KSI	ULT TEN KSI	%ELONG IN 02 IN	%RED IN AREA	HARDNESS
	46.8	49.1	11.1		
	47.5	49.8	18.1		

The above data were transcribed from the manufacturer's Certificate of Test after verification for completeness and specification requirements of the information on the certificate. All test results remain on file subject to examination.

We hereby certify that the material covered by this report will meet the applicable requirements described herein, including any specification forming a part of the description.

The willful recording of false, fictitious, or fraudulent statements in connection with test results may be punishable as a felony under federal statutes.

Material did not come in contact with mercury while in our possession.

LARRY BUSICK

Manager, Quality Assurance

Figure D-23. 1/2"x1/2" Aluminum Spindle Material Certificate (Sheet 1 of 2), Test Nos. APR-1 and APR-2

CERTIFICATE OF TEST



Page 02 of 02

Certification Date
24-SEP-2014

CUSTOMER ORDER NUMBER

35349

EARLE M. JORGENSEN COMPANY
1800 N UNIVERSAL AVENUE
KANSAS CITY MO 64120

Invoice Number
S153835

CUSTOMER PART NUMBER

0001

854-00500

SOLD TO: TMCO INC
ATTENTION ACCOUNTS PAYABLE
535 J STREET
LINCOLN NE 68508

SHIP TO: TMCO INC
701 S 6TH STREET
LINCOLN NE 68508

Description: 6061-T6511 EXTRUDED BAR AMS QQ-A-200/8
1/2 SQ X 12' Line Total: 256 LB
HEAT: 201408541 ITEM: 513315
COMMENTS
melt source usa
chemistry:
cast number 04191405 & g02061402
si 0.71/0.77
fe 0.35/0.36
cu 0.32/0.33
mn 0.10/0.11
mg 0.84/0.89
cr 0.09/0.09
zn 0.07/0.02
ti 0.02/0.02
al 97.50/97.41
others each 0.03/0.03 total 0.10/0.10

The above data were transcribed from the manufacturer's Certificate of Test after verification for completeness and specification requirements of the information on the certificate. All test results remain on file subject to examination.

We hereby certify that the material covered by this report will meet the applicable requirements described herein, including any specification forming a part of the description.

The willful recording of false, fictitious, or fraudulent statements in connection with test results may be punishable as a felony under federal statutes.

Material did not come in contact with mercury while in our possession.

LARRY BUSICK

Manager, Quality Assurance

Figure D-24. 1/2"x1/2" Aluminum Spindle Material Certificate (Sheet 2 of 2), Test Nos. APR-1 and APR-2

Pedestrian Rail Threaded Rods October 2014 R# 15-0188 SMT

CERTIFIED MATERIAL TEST REPORT

FOR ASTM A193-11 B7 STUDS

INSPECTION CERTIFICATE PER BS EN10204:2004 3.1

DATE: JAN.17.2014

FACTORY: ZHIEJIANG HIEITER MFG & TRADE CO.,LTD

ADDRESS: HAIYAN JIAXING ZHEJIANG CHINA

MFR LOT NO.: 1401071935C

CUSTOMER: BRIGHTON-BEST INTERNATIONAL(TAIWAN)INC.

QTY: 1350 PCS

PO NUMBER: U15971

SAMPLING PLAN PER ASTM A193-11 GR-B7

SIZE & DESCRIPTION: 1/2-13X6-1/4" PL.

PART NO: 775042

HEAD MARKS: NDF-B7

STEEL PROPERTIES:

STEEL GRADE: SAE 4140

STEEL SIZE: 0.472 "

HEAT NO: E21306214

CHEMISTRY COMPOSITION:

CHEMIST	C %	Mn %	Si %	P %	S %	Cr %	Mo %	Ni %	Cu %					OTHERS
SPEC.	0.37	0.65	0.15	MAX	MAX	0.75	0.15							
	0.49	1.10	0.35	0.035	0.040	1.20	0.25							
RESULTS	0.40	0.79	0.23	0.016	0.004	0.94	0.16							

MECHANICAL PROPERTIES:

SPECIFICATION: ASTM A193-11 B7

ITEM	TENSILE	YIELD	Elongation	Reduction	Tempering	Quenching	Hardness	MACRO
SPEC.	STRENGTH	STRENGTH		of Area			(HRC)	ETCH
	MIN(psi)	MIN(psi)	MIN(%)	MIN(%)	MIN(°C)	MIN(°C)	Max	TESTING
STANDARD	125,000	105,000	16	50	593	820-880	35	
RESULTS	Min	132,025	20	58	620	860	28	PASSED
	Max	134,228	21	60			32	
TIME (Minutes)					100	80		

MACRO ETCH

SPEC OF TEST METHOD: ASTM E381-01(2006)

DIVISION	SURFACE CONDITION	RANDOM CONDITION	CENTER SEGREGATION
SPEC	S2	R2	C3
RESULTS	S2	R2	C2

DIMENSION:

SPECIFICATION: IFI 136-02; ASME B1.1-2003

ITEM	Shank Dia	MAJOR DIA	GO	NO GO	T/Length	L/Tolerance	STRAIGHTNESS	ADD
STANDARD	Max	0.498"	2A	2A	6.00"±0.0625"	6.25"±0.0625"	MAX	
	Min	0.488"	GO	NO	6.00"-0.0625"	6.25"-0.0625"	0.038"	
TEST REPORT		OK	OK	OK	OK	OK	OK	OK

REPORT: ACCEPT

PARTS ARE MANUFACTURED AND TESTED IN ACCORDANCE WITH ASTM A193-11 B7

ALL TESTS IN ACCORDANCE WITH THE METHODS PRESCRIBED IN THE APPLICABLE ASTM SPECIFICATION,

ALSO MEET THE REQUIREMENTS OF ASME SA-95 SECTION 2.

WE CERTIFY THAT THIS DATA IS A TRUE REPRESENTATION OF INFORMATION PROVIDED BY

THE MATERIAL SUPPLIER AND OUR TESTING LABORATORY.

All parts meet the requirements of FQA and records of compliance are on file.

Marker's ISO#ISO9001:2008 SGS

CN11/20818

PLACE OF ORIGIN: CHINA



SIGNATURE: LAB MGR.

ZHIEJIANG NEW ORIENTAL FASTENER CO., LTD

Figure D-25. 1/2" Threaded Rod Material Certificate, Test Nos. APR-1 and APR-2

Pedestrian Rail Nuts October 2014 R# 15-0188 SMT

NUCOR
FASTENER DIVISION

LOT NO.
3252548

Post Office Box 6100
Saint Joe, Indiana 46785
Telephone 260/337-1600

CUSTOMER NO/NAME
8061 STRUCTURAL BOLT CO LLC
TEST REPORT SERIAL# FB410424
TEST REPORT ISSUE DATE 7/24/13
DATE SHIPPED 9/13/13
NAME OF LAB SAMPLER: JEFFREY HOERING, LAB TECHNICIAN
*****CERTIFIED MATERIAL TEST REPORT*****
NUCOR PART NO QUANTITY LOT NO. DESCRIPTION
175597 11600 3252548 1/2-13 GR DH HV HX NUT H.D.G.
MANUFACTURE DATE 5/14/13 HEX NUT H.D.G.

NUCOR ORDER # 839871
CUST PART #
CUSTOMER P.O. # 14790

---CHEMISTRY MATERIAL GRADE -1026L
MATERIAL HEAT **CHEMISTRY COMPOSITION (WT% HEAT ANALYSIS) BY MATERIAL SUPPLIER
NUMBER NUMBER C MN P S SI NUCOR STEEL - NEBRASKA
RM028016 NF12104365 .23 .75 .011 .021 .25
MIN .20 .60
MAX .55 .040 .050

---MECHANICAL PROPERTIES IN ACCORDANCE WITH ASTM A563-07a
SURFACE CORE PROOF LOAD TENSILE STRENGTH
HARDNESS HARDNESS 21300 LBS DEG-WEDGE STRESS (PSI)
(R30N) (RC) (LBS)
N/A 28.4 PASS N/A N/A
N/A 28.5 PASS N/A N/A
N/A 31.0 PASS N/A N/A
N/A 31.6 PASS N/A N/A
N/A 28.0 PASS N/A N/A
AVERAGE VALUES FROM TESTS
29.5
PRODUCTION LOT SIZE 98500 PCS


ROTATIONAL CAPACITY TESTED IN ACCORDANCE WITH A325-10, A563-07a
SAMPLE #1 PASSED SAMPLE #2 PASSED

---VISUAL INSPECTION IN ACCORDANCE WITH ASTM A563-07a 80 PCS. SAMPLED LOT PASSED

---COATING - HOT DIP GALVANIZED TO ASTM F2329-13 - GALVANIZING PERFORMED IN THE U.S.A.
1. 0.00283 2. 0.00916 3. 0.00335 4. 0.00213 5. 0.00217 6. 0.00295 7. 0.00455
8. 0.00635 9. 0.00243 10. 0.00343 11. 0.00384 12. 0.00337 13. 0.00251 14. 0.00235
15. 0.00249
AVERAGE THICKNESS FROM 15 TESTS .00359
HEAT TREATMENT - AUSTENITIZED, OIL QUENCHED & TEMPERED (MIN 800 DEG F)

---DIMENSIONS PER ASME B18.2.6-2012
CHARACTERISTIC #SAMPLES TESTED MINIMUM MAXIMUM
Width Across Corners 8 0.9790 0.9900
Thickness 32 0.4750 0.4810

ALL TESTS ARE IN ACCORDANCE WITH THE LATEST REVISIONS OF THE METHODS PRESCRIBED IN THE APPLICABLE SAE AND ASTM SPECIFICATIONS. THE SAMPLES TESTED CONFORM TO THE SPECIFICATIONS AS DESCRIBED/LISTED ABOVE AND WERE MANUFACTURED FREE OF MERCURY CONTAMINATION. NO INTENTIONAL ADDITIONS OF BISMUTH, SELENIUM, TELLURIUM, OR LEAD WERE USED IN THE STEEL USED TO PRODUCE THIS PRODUCT.
THE STEEL WAS MELTED AND MANUFACTURED IN THE U.S.A. AND THE PRODUCT WAS MANUFACTURED AND TESTED IN THE U.S.A.
PRODUCT COMPLIES WITH DFARS 252.225-7014. WE CERTIFY THAT THIS DATA IS A TRUE REPRESENTATION OF INFORMATION PROVIDED BY THE MATERIAL SUPPLIER AND OUR TESTING LABORATORY. THIS CERTIFIED MATERIAL TEST REPORT RELATES ONLY TO THE ITEMS LISTED ON THIS DOCUMENT AND MAY NOT BE REPRODUCED EXCEPT IN FULL.


MECHANICAL FASTENER
CERTIFICATE NO. A2LA 0139.01
EXPIRATION DATE 12/31/13


NUCOR FASTENER
A DIVISION OF NUCOR CORPORATION

JOHN W. FERGUSON
QUALITY ASSURANCE SUPERVISOR

Figure D-26. 1/2" Nut Material Certificate (Sheet 1 of 2), Test Nos. APR-1 and APR-2

Raw Material Cert for Lot 325254B

Nucor Steel

2/9/2013 9:27:41 AM PAGE 2/002 Fax Server

NUCOR
NUCOR CORPORATION
NUCOR STEEL NEBRASKA

Mill Certification
2/9/2013

28016
2911 East Nucor Road
NORFOLK, NE 68701
(402) 644-0200
Fax: (402) 644-0329

Sold To: NUCOR FASTENER INDIANA
PO BOX 6100
6730 COUNTY RD 60
ST JOE, IN 46785-0000
(260) 337-1600
Fax: (435) 734-4581

Ship To: NUCOR FASTENER INDIANA
COUNTY RD 60
ST JOE, IN 46785-0000

Customer P.O.	135757	Sales Order	126701.14
Product Group	Special Bar Quality	Part Number	31B00875000W680
Grade	1026L	Lot #	NF1210436511
Size	.8750-7/8 Round Coil	Heat #	NF12104365
Product	.8750-7/8 Round Coil 1026L	B.L. Number	N1-246876
Description	1026L	Load Number	N1-193067
Customer Spec		Customer Part #	CH5008

I hereby certify that the material described herein has been manufactured in accordance with the specifications and standards listed above and that it satisfies those requirements.

Roll Date: 2/6/2013 Melt Date: 12/5/2012 Qty Shipped LBS: 160,995 Qty Shipped Pcs: 32

C	Mn	V	Si	S	P	Cu	Cr	Ni	Mo	Al	Cb
0.23%	0.75%	0.003%	0.25%	0.021%	0.011%	0.08%	0.08%	0.04%	0.01%	0.001%	0.002%
Pb	Sn	Ca	B	Ti							
0.000%	0.005%	0.0007%	0.0002%	0.001%							

Reduction Ratio 73 :1

Specification Comments: Coarse Grain Practice

Selenium, Tellurium, Lead, Bismuth or Boron were not intentionally added to this heat.

1. All manufacturing processes of the steel materials in this product, including melting, have been performed in the United States.
2. All products produced are weld free.
3. Mercury, in any form, has not been used in the production or testing of this material.
4. Test conform to ASTM A29-12, ASTM E415 and ASTM E1018-resulphurized grades or applicable customer requirements.
5. All material melted at Nucor Steel Nebraska is produced in an Electric Arc Furnace
6. Strand Cast
7. ISO-17025 LAB accreditation cert. available upon request

Chemistry Verification Checks

Part# CH5008 RM# 28016

Checked By Date

Receiving OK: 297 2-18-13

Certifications OK: 375 2-18-13


Jim Hill

Jim Hill
Division Metallurgist

Figure D-27. 1/2" Nut Material Certificate (Sheet 2 of 2), Test Nos. APR-1 and APR-2

Pedestrian Rail Washers October 2014 R#15-0188 SMT

Prestige
Stamping,
Inc.



23513 Groesbeck Highway
Warren, Michigan 48089
(586) 773-2700 * Fax (586) 773-2298
www.PrestigeStamping.com

PRODUCT CERTIFICATION
CERTIFICATION NUMBER

119614

THIS IS TO CERTIFY THE PRODUCT STATED BELOW WAS FABRICATED AND PROCESSED TO THE ORDER AS INDICATED AND CONFORMS TO THE APPLICABLE SPECIFICATIONS AND STANDARDS.

Customer: THE STRUCTURAL BOLT CO
2140 CORNHUSKER HWY
LINCOLN, NE 68521

Customer Part: 1/2" F436 H/DIP
Prestige Part: P1088HP300
Part Name: 1/2" F436 H/DIP
Purchase Order: 15432-1
Shipment BOL: B173265
Shipment ID: A0184180
Quantity: 6400
Manufacturers Marking: "P"

Steel Supplier: HORIZON STEEL CO.
Grade: CF436 GRADE STEEL
Lot: C7313D
Heat: 342288
Carbon: .248 (.21 - .93)
Manganese: 1.059 (.43 - 1.6)
Phosphorous: .012 (.03 Max.)
Sulfur: .0016 (.05 Max.)
Silicon: .206

SPECIFICATIONS

HARDNESS: TEST METHOD: ASTM E18
HRC 38 - 45
CHECKED TO ASTM F606

PLATING: TEST METHOD: ASTM B499
0.0017" Min.
HOT DIP GALV TO ASTM F-2329

TEST RESULTS

HARDNESS:
HRC 41 - 43

PLATING:
0.0020" - 0.0030"

Chemistry is as reported from raw material certification and does not fall under Prestige Stamping's accreditation.
This product was produced under an ISO/TS 16949 Quality Assurance System.
ISO/TS 16949 Certification No: 0062933.
Material was melted and manufactured in the U.S.A.
This product was manufactured in Warren, Michigan U.S.A.
This product conforms to all requirements for washers as produced according to A.S.T.M. F-436-10.
Sampling Plan per P.S.I W.I. # 5.4.18.015.
The test results only apply to the items tested.
This test report must not be reproduced except in full without prior written approval.
Materials used to manufacture these products are mercury, asbestos and radio activity free.
No weld repairs made to material.



FRANK SCHUBERT
Quality Assurance Manager

Econ Information System

03/24/14

10:02

KGUZ

PAGE 1 of 1

Figure D-28. 1/2" Washer Material Certificate, Test Nos. APR-1 and APR-2

Appendix E. Vehicle Center of Gravity Determination

Test: APR-1

Vehicle: Rio

Vehicle CG Determination

VEHICLE	Equipment	Weight (lb)
+	Unbalasted Car (curb)	2421
+	Brake receivers/wires	6
+	Brake Frame	7
+	Brake Cylinder	28
+	Strobe Battery	6
+	Hub	20
+	CG Plate (SLICES)	10
+	DTS	19
-	Battery	-34
-	Oil	-10
-	Interior	-38
-	Fuel	0
-	Coolant	-8
-	Washer fluid	-8
BALLAST	Water	
	Misc.	
	Misc.	

Estimated Total Weight 2419 lb

wheel base 98.75 in.

MASH targets		Test Inertial	Difference
Test Inertial Wt (lb)	2420 (+/-)55	2428	8.0
Long CG (in.)	39 (+/-)4	36.44	-2.55848
Lateral CG (in.)	N/A	-0.63525	NA

Note: Long. CG is measured from front axle of test vehicle

Note: Lateral CG measured from centerline - positive to vehicle right (passenger) side

CURB WEIGHT (lb)		
	Left	Right
Front	800	780
Rear	429	412
FRONT	1580 lb	
REAR	841 lb	
TOTAL	2421 lb	

Dummy = 166lbs.

TEST INERTIAL WEIGHT (lb)		
(from scales)		
	Left	Right
Front	788	744
Rear	453	443
FRONT	1532 lb	
REAR	896 lb	
TOTAL	2428 lb	

Figure E-1. Vehicle Mass Distribution, Test No. APR-1

Test: APR-2

Vehicle: Rio

Vehicle CG Determination

VEHICLE	Equipment	Weight (lb)
+	Unbalasted Car (curb)	2424
+	Brake receivers/wires	6
+	Brake Frame	8
+	Brake Cylinder	28
+	Strobe Battery	6
+	Hub	20
+	CG Plate (SLICES)	10
+	DTS	19
-	Battery	-36
-	Oil	-6
-	Interior	-42
-	Fuel	0
-	Coolant	-7
-	Washer fluid	0
BALLAST	Water	
	Misc.	
	Misc.	
Estimated Total Weight		2430 lb

wheel base 98.5 in.

MASH targets		Test Inertial	Difference
Test Inertial Wt (lb)	2420 (+/-)55	2437	17.0
Long CG (in.)	39 (+/-)4	37.67	-1.32991
Lateral CG (in.)	N/A	-0.48474	NA

Note: Long. CG is measured from front axle of test vehicle

Note: Lateral CG measured from centerline - positive to vehicle right (passenger) side

CURB WEIGHT (lb)		
	Left	Right
Front	766	761
Rear	461	436
FRONT	1527 lb	
REAR	897 lb	
TOTAL	2424 lb	

Dummy = 166lbs.

TEST INERTIAL WEIGHT (lb)		
(from scales)		
	Left	Right
Front	769	736
Rear	470	462
FRONT	1505 lb	
REAR	932 lb	
TOTAL	2437 lb	

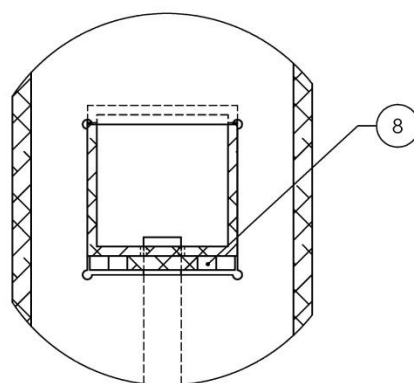
Figure E-2. Vehicle Mass Distribution, Test No. APR-2

Appendix F. Fabrication Drawings for Test Nos. APR-1 and APR-2

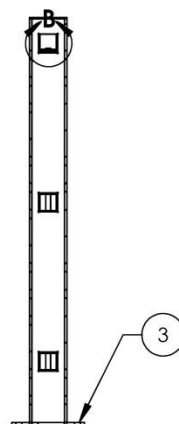
ITEM NO.	QTY.	PART NUMBER	DESCRIPTION
1	2	A1	ALUM. POST, 43" LONG
2	2	A2	POST CAP
3	2	A3	POST BASE
4	1	D2	AL. RAIL LONG
5	1	D1	AL. RAIL LONG
6	1	D1MOD	AL. RAIL LONG
7	9	D3	SQ. ALUM. SPINDLE
8	2	D1MOD2	AW2-D SHIM

REVISIONS		
REV.	DESCRIPTION	DATE

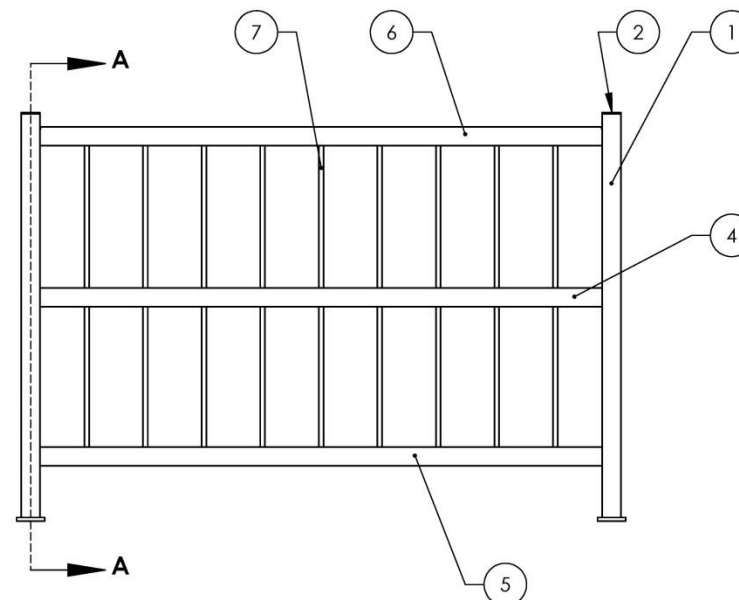
WELD SYMBOLS AND DIMS ON PG 2



DETAIL B
SCALE 1 : 2



SECTION A-A



NOTES:
1.) ALL ALUM. WELDS SHOULD FOLLOW AL. DESIGN MANUAL 2010
BY USING 5356 FILLER MATERIAL.

UNLESS OTHERWISE SPECIFIED:
DIMENSIONS ARE IN INCHES
TOLERANCES:
FRACTIONAL $\pm 1/8"$
ANGLE: MACH $\pm 1^\circ$ BEND $\pm 2^\circ$
.X $\pm .060$
.XX $\pm .030$
.XXX $\pm .010$
MATERIAL
ALUMINUM
FINISH
RAW
DO NOT SCALE DRAWING

NAME	DATE
FOLKERTS	10/1/14
DRAWN	CHECKED



DESCRIPTION:
WI PEDESTRIAN RAIL

SIZE	PART NO.	REV
A	AW2-D (IR)	
SCALE: 1:16	WEIGHT:	SHEET 1 OF 2

X:\MIDWEST ROADSIDE SAFETY\AW2-D\AW2-D (IR)

Figure F-1. Fabrication Drawings, Test Nos. APR-1 and APR-2

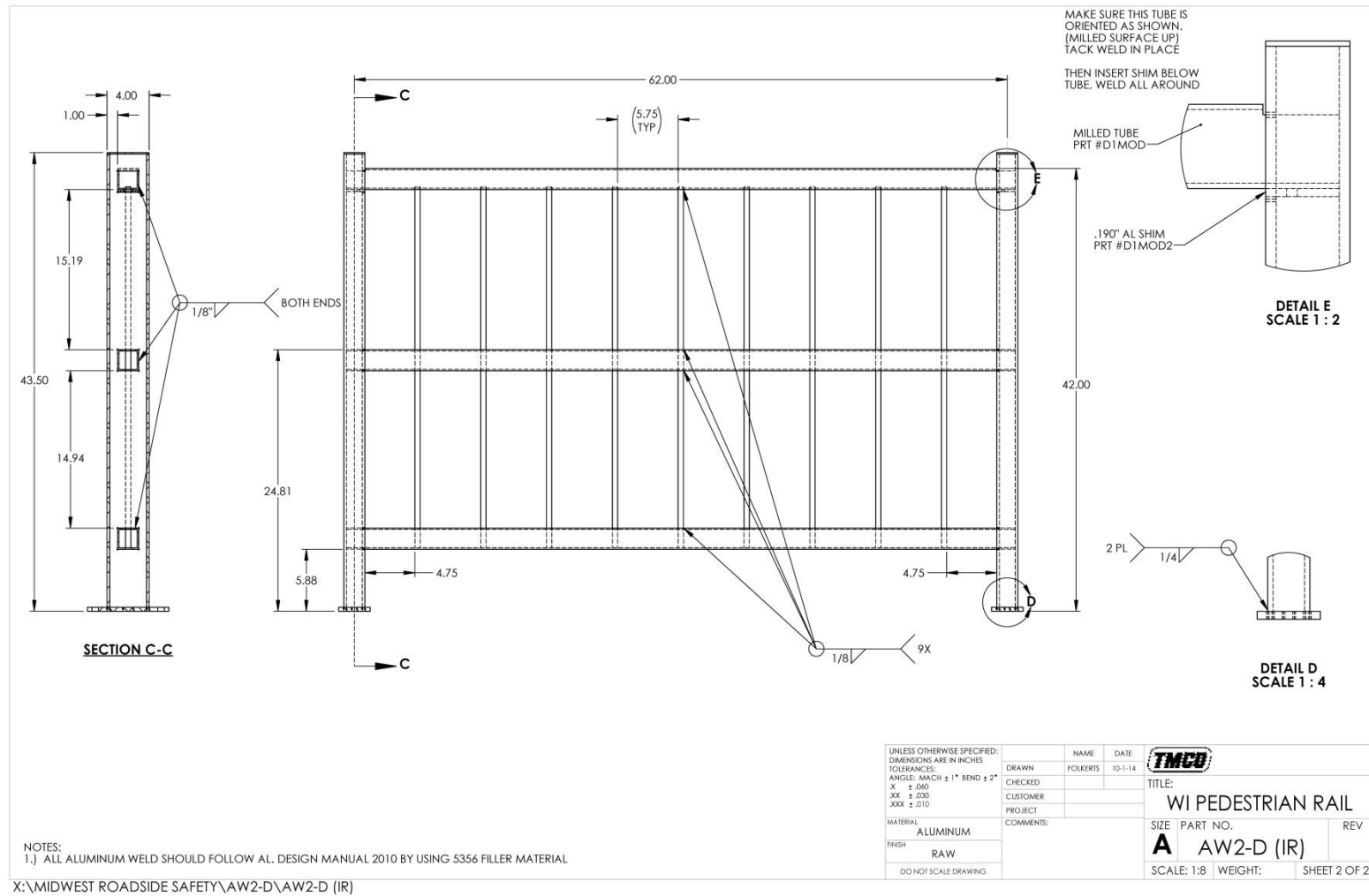
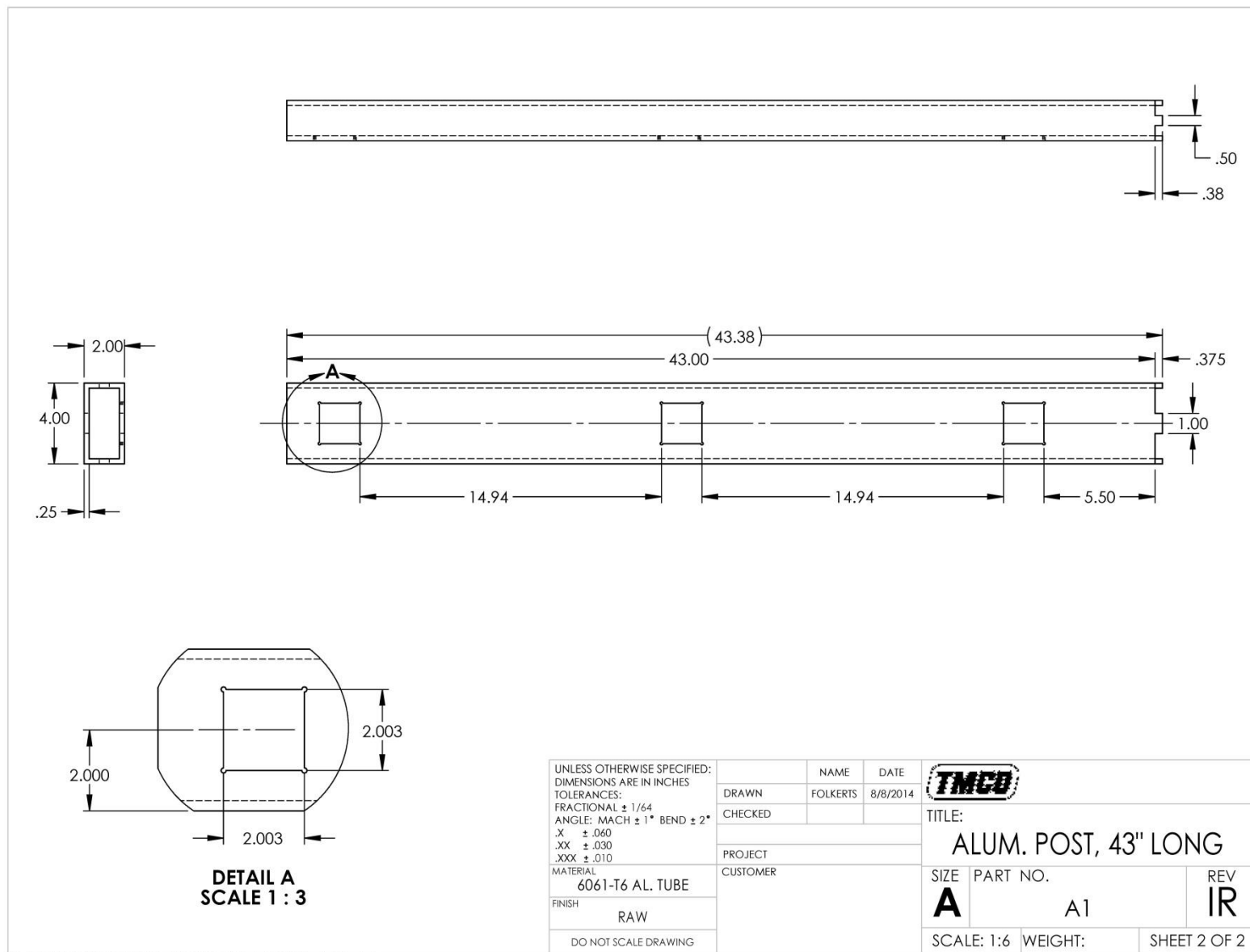
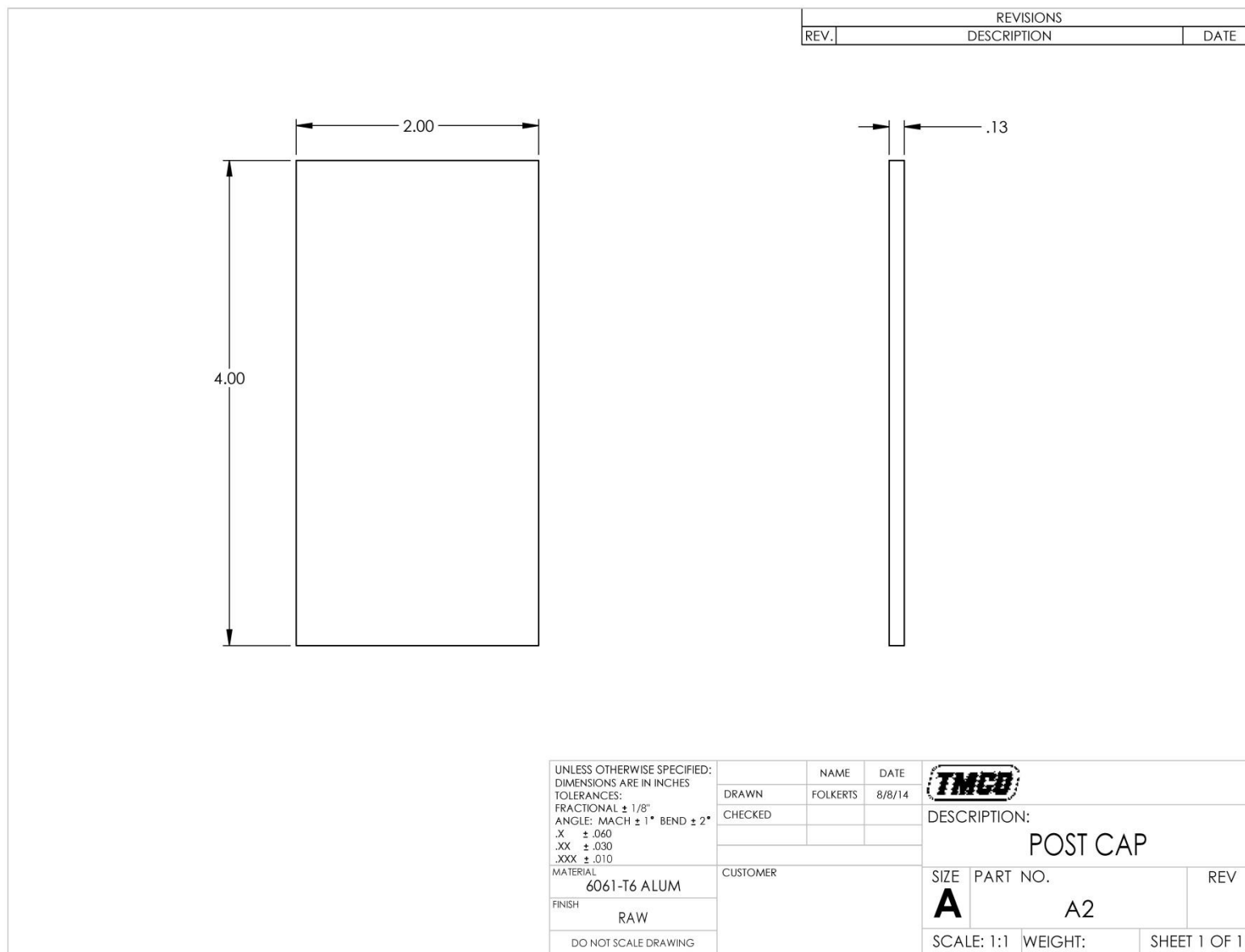


Figure F-2. Fabrication Drawings, Test Nos. APR-1 and APR-2



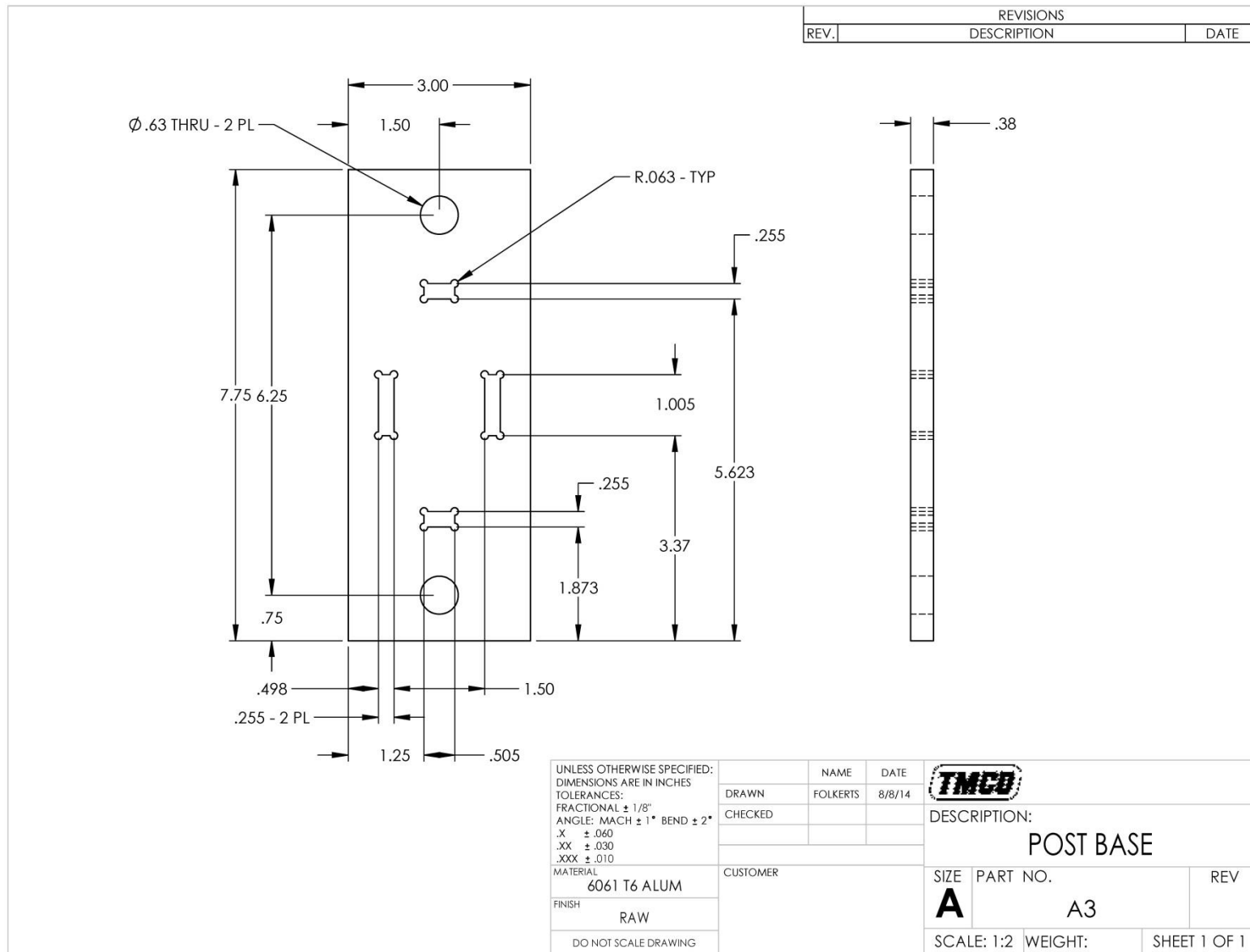
X:\MIDWEST ROADSIDE SAFETY\A1\A1

Figure F-3. Fabrication Drawings, Test Nos. APR-1 and APR-2

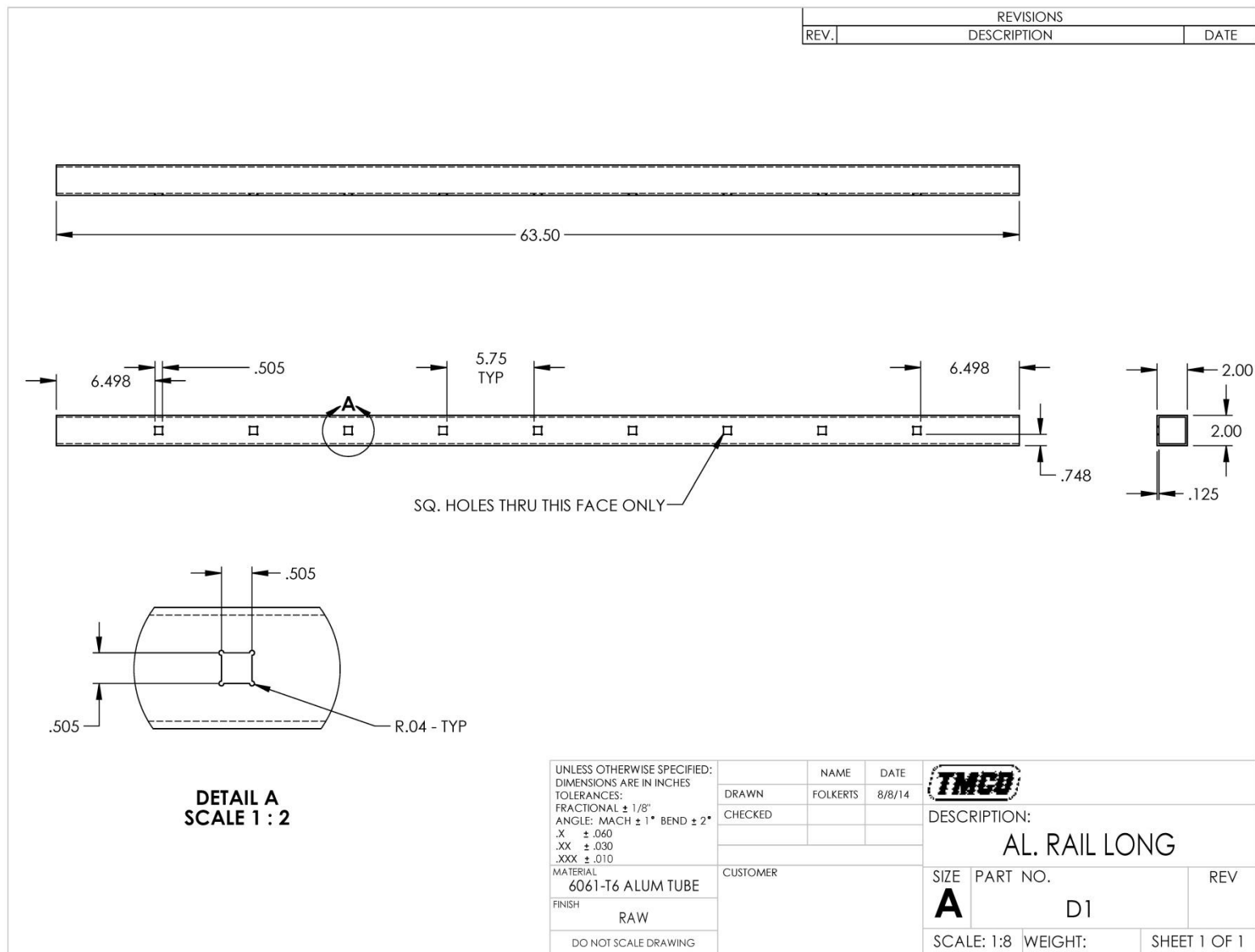


X:\MIDWEST ROADSIDE SAFETY\A2\A2

Figure F-4. Fabrication Drawings, Test Nos. APR-1 and APR-2

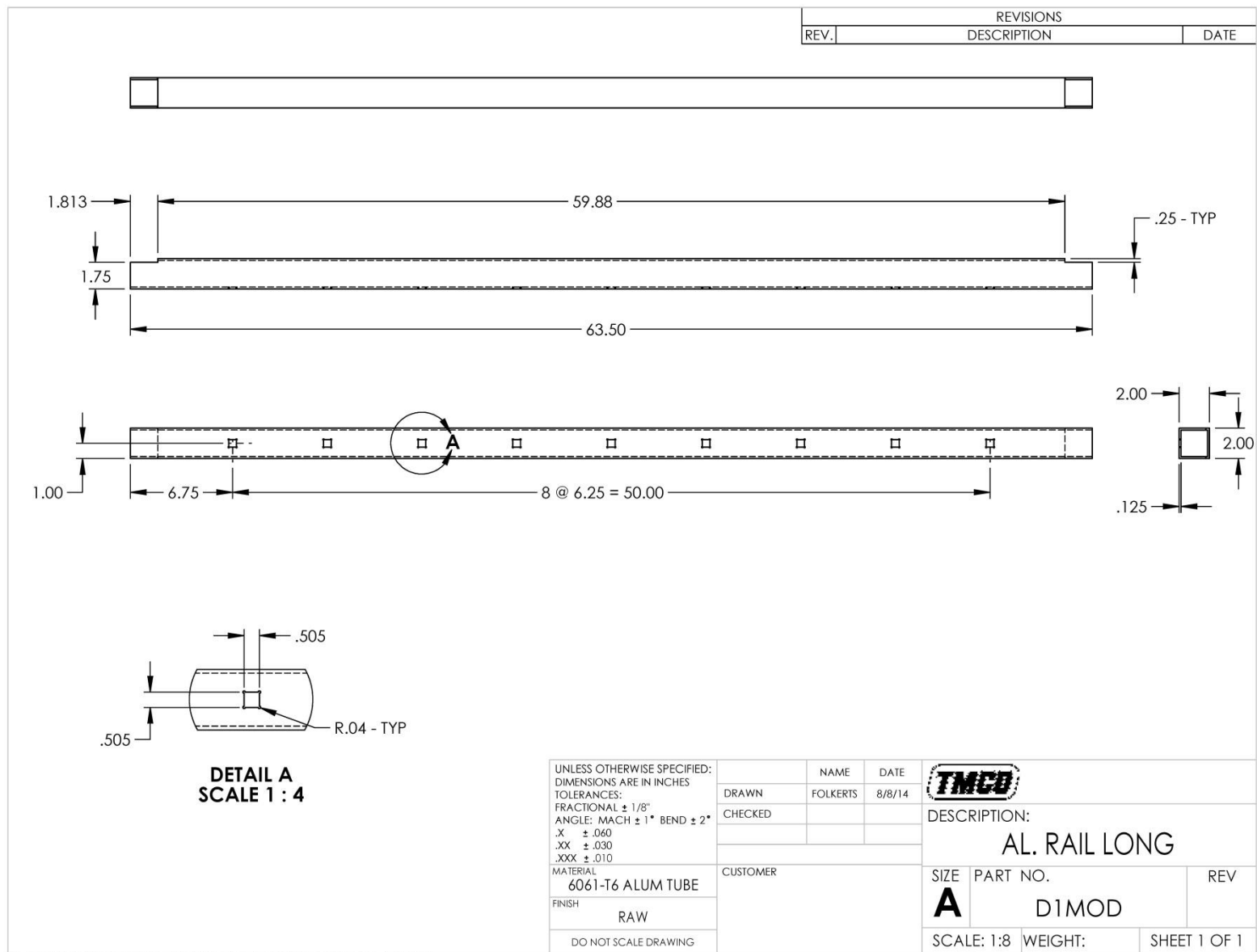


X:\MIDWEST ROADSIDE SAFETY\A3\A3
Figure F-5. Fabrication Drawings, Test Nos. APR-1 and APR-2



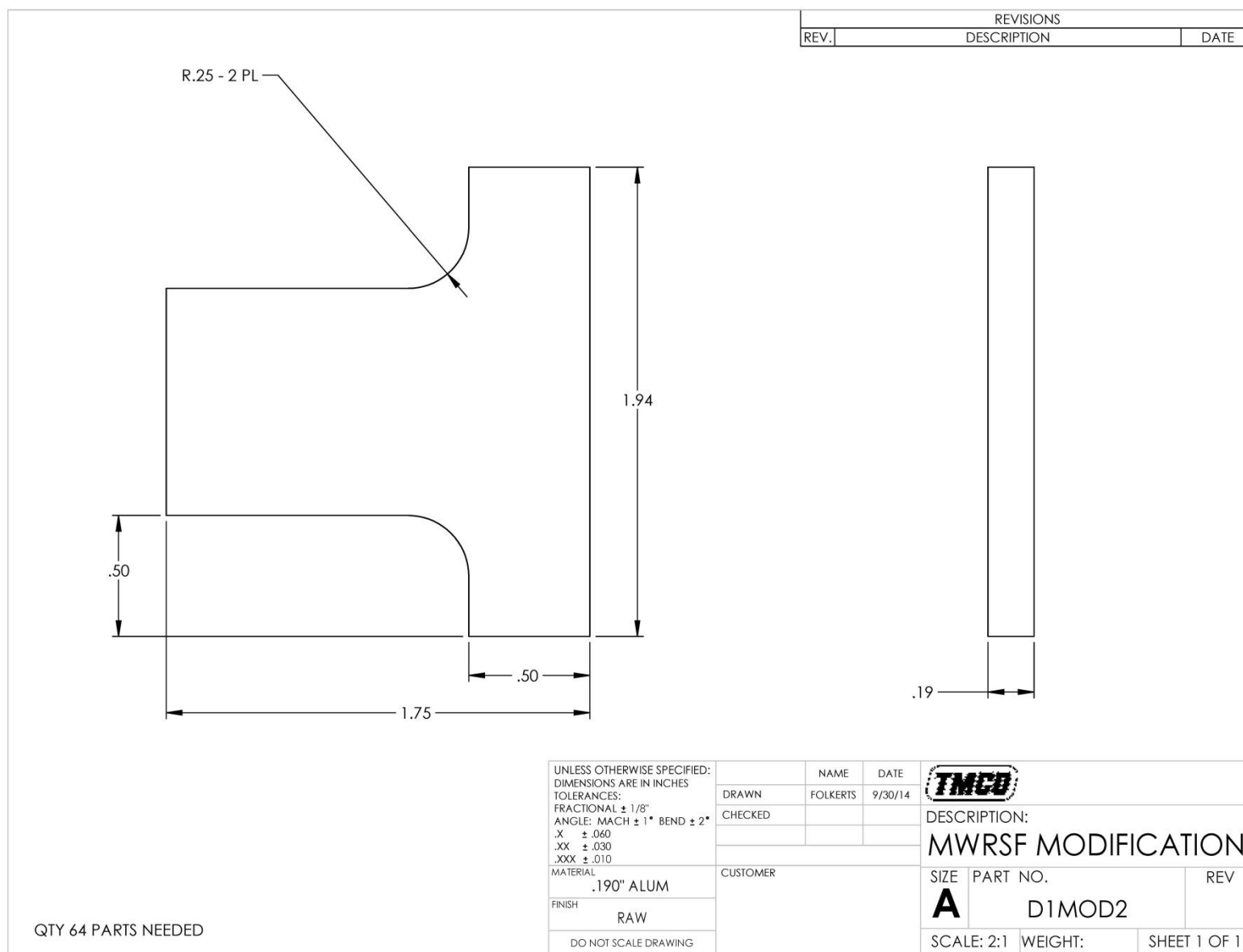
X:\MIDWEST ROADSIDE SAFETY\D1\D1

Figure F-6. Fabrication Drawings, Test Nos. APR-1 and APR-2



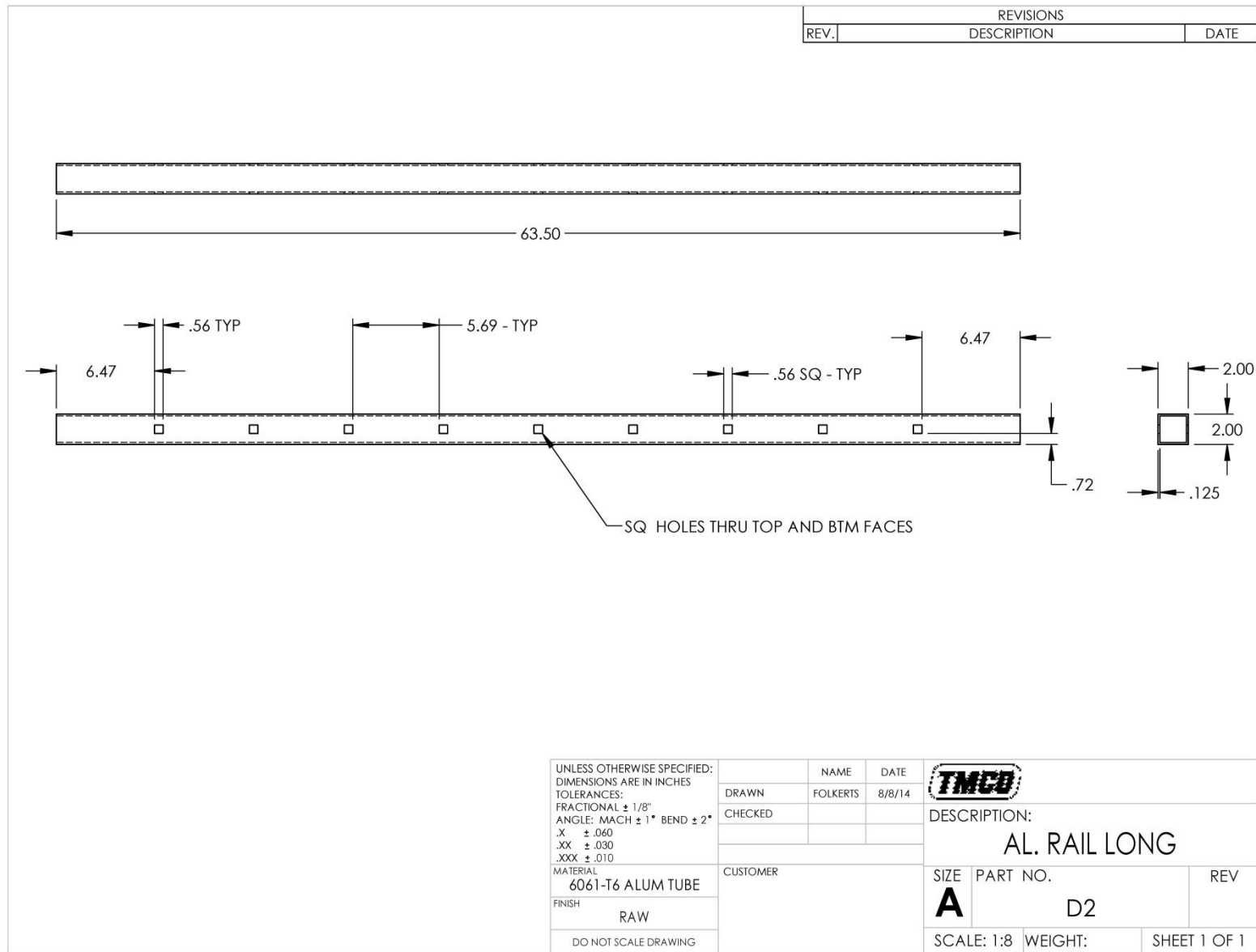
X:\MIDWEST ROADSIDE SAFETY\D1\D1MOD

Figure F-7. Fabrication Drawings, Test Nos. APR-1 and APR-2

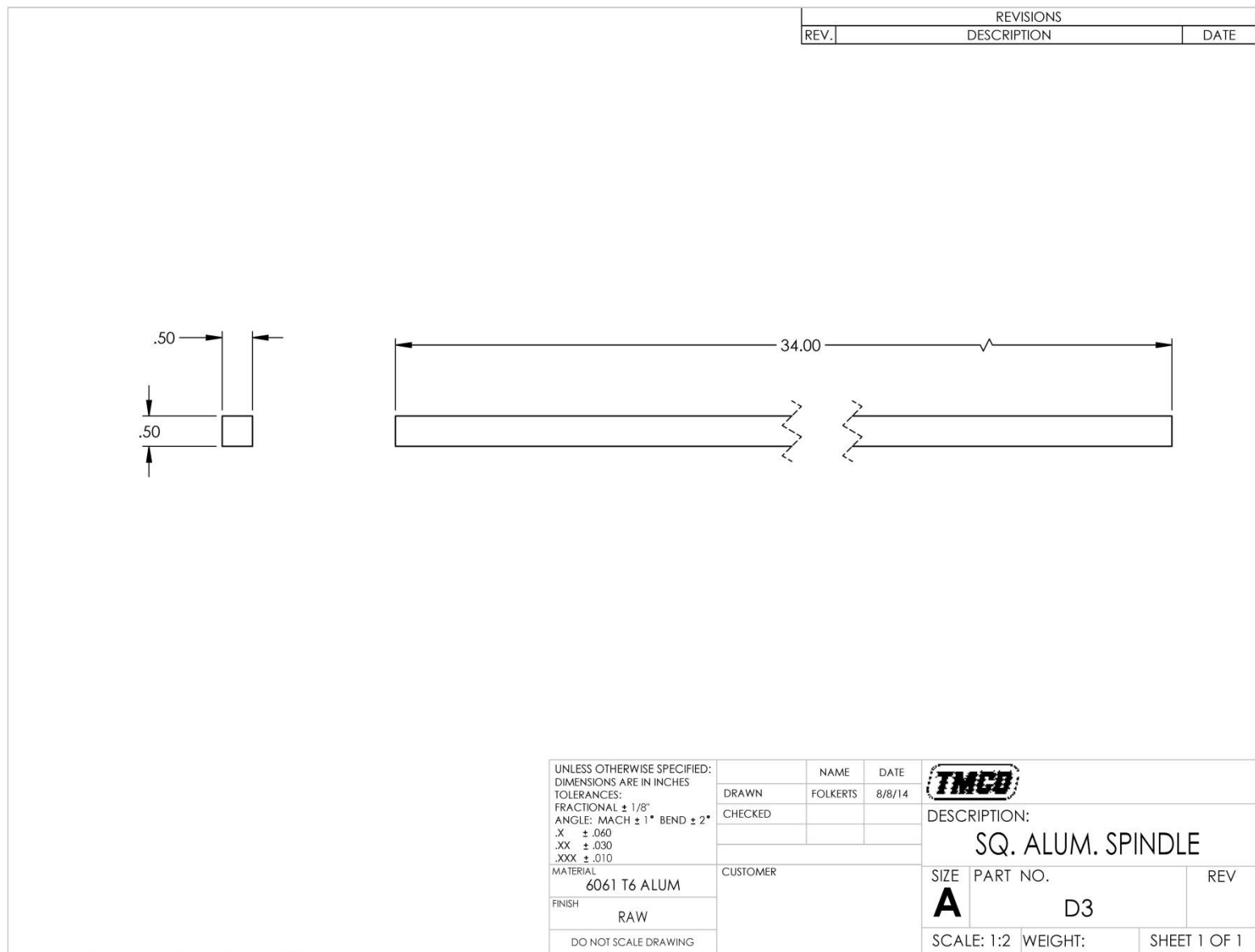


X:\MIDWEST ROADSIDE SAFETY\D1\D1MOD2

Figure F-8. Fabrication Drawings, Test Nos. APR-1 and APR-2



X:\MIDWEST ROADSIDE SAFETY\D2\D2
 Figure F-9. Fabrication Drawings, Test Nos. APR-1 and APR-2



X:\MIDWEST ROADSIDE SAFETY\D3\D3

Figure F-10. Fabrication Drawings, Test Nos. APR-1 and APR-2

Appendix G. Vehicle Deformation Record

VEHICLE PRE/POST CRUSH
FLOORPAN - SET 1

TEST: APR-1
VEHICLE: Rio

Note: If impact is on driver side need to
enter negative number for Y

POINT	X (in.)	Y (in.)	Z (in.)	X' (in.)	Y' (in.)	Z' (in.)	ΔX (in.)	ΔY (in.)	ΔZ (in.)
F1	28	-24 3/4	-1 3/4	28	-24 3/4	-1 3/4	0	0	0
2	30 1/4	-21 1/4	-4 1/4	30 1/4	-21 1/2	-4 1/2	0	- 1/4	- 1/4
3	30 3/4	-16	-5 1/2	30 3/4	-16 1/4	-5 3/4	0	- 1/4	- 1/4
4	30 1/2	-10	-5 3/4	30 1/2	-9 1/2	-5 3/4	0	1/2	0
5	22	-22 1/4	-9 3/4	22	-22 1/4	-9 3/4	0	0	0
6	22 1/4	-17	-9 1/2	22 1/2	-17 1/4	-9 1/2	1/4	- 1/4	0
7	22	-10	-9 1/2	22	-9 1/2	-9 3/4	0	1/2	- 1/4
8	16 3/4	-26 1/4	-9 3/4	16 3/4	-26	-9 3/4	0	1/4	0
9	16	-20	-9 1/2	16	-19 3/4	-9 1/2	0	1/4	0
10	16 1/2	-11 1/2	-10	16 3/4	-11	-10	1/4	1/2	0
11	11 1/4	-20 1/2	-9 1/4	11	-20 1/2	-9 1/4	- 1/4	0	0
12	12	-14 1/2	-9 1/4	12	-14	-9 1/4	0	1/2	0
13	1 3/4	-23	-5 1/4	1 3/4	-23	-5 1/2	0	0	- 1/4
14	1 3/4	-16 1/4	-5 1/4	1 3/4	-16 1/4	-5 1/2	0	0	- 1/4
15	1 3/4	-9 3/4	-5 1/4	1 3/4	-10	-5 1/2	0	- 1/4	- 1/4
16	30 1/4	8 3/4	-5 1/2	30 1/4	8 1/2	-5 1/2	0	- 1/4	0
17	30 3/4	13	-5	30 3/4	13 1/2	-5	0	1/2	0
18	27 1/4	18 1/2	-4 3/4	27	18 3/4	-5	- 1/4	1/4	- 1/4
19	24	3	-9	24	3	-9	0	0	0
20	24 1/4	10 1/2	-8 3/4	24 1/4	11	-9	0	1/2	- 1/4
21	24 1/4	15 1/2	-8 1/2	24 1/4	15 3/4	-8 3/4	0	1/4	- 1/4
22	19 1/4	3 3/4	-9 1/4	19 1/4	3 1/2	-9 1/2	0	- 1/4	- 1/4
23	19 1/2	10	-9 1/4	19 1/2	9 3/4	-9 1/2	0	- 1/4	- 1/4
24	20	19 1/4	-9	20	18 1/2	-9 1/4	0	- 3/4	- 1/4
25	10 3/4	5	-9 3/4	11	5 1/4	-10	1/4	1/4	- 1/4
26	10 1/4	12 1/2	-8 3/4	10 1/4	12 1/2	-9	0	0	- 1/4
27	10 1/4	20 1/4	-9 1/4	10 1/2	20 1/4	-9 1/2	1/4	0	- 1/4
28	1 1/4	3 3/4	-5 1/4	1 1/4	3 3/4	-5 1/2	0	-0	- 1/4
29	1	9 3/4	-5 1/4	3/4	9 3/4	-5 1/4	- 1/4	0	0
30	1 1/4	19 1/4	-4 3/4	1	19 1/4	-5	- 1/4	0	- 1/4
31							0	0	0

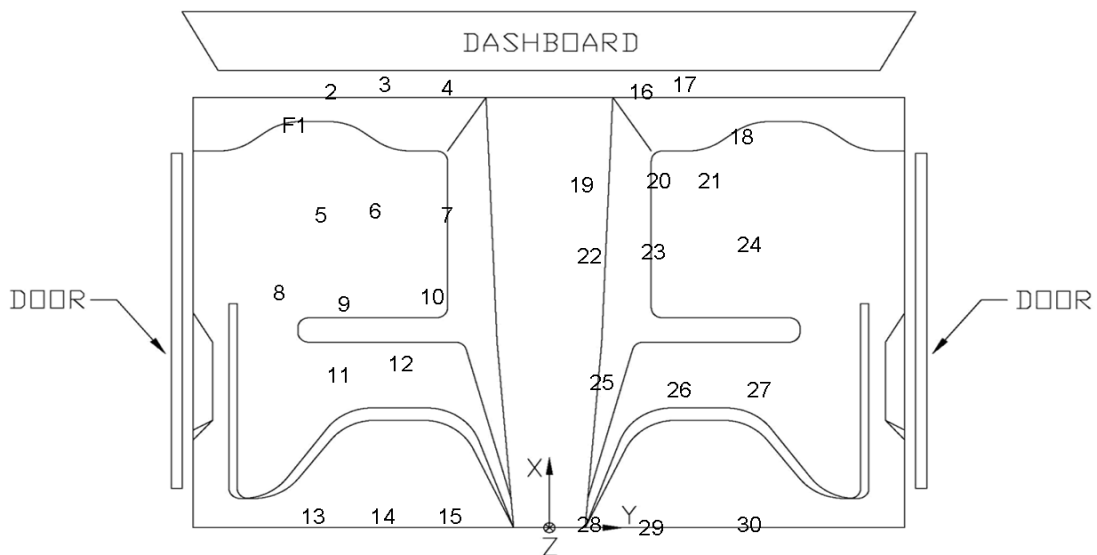


Figure G-1. Floorpan Deformation Data – Set 1, Test No. APR-1

VEHICLE PRE/POST CRUSH
FLOORPAN - SET 2

TEST: APR-1
VEHICLE: Rio

Note: If impact is on driver side need to
enter negative number for Y

POINT	X (in.)	Y (in.)	Z (in.)	X' (in.)	Y' (in.)	Z' (in.)	ΔX (in.)	ΔY (in.)	ΔZ (in.)
1	40	-19 1/2	-1 1/4	40	-19 3/4	-1	0	- 1/4	1/4
2	42 1/2	-15	-3 3/4	42 1/2	-15	-3 1/2	0	0	1/4
3	43	-9 3/4	-5 1/4	43	-9	-4 3/4	0	3/4	1/2
4	42 3/4	-4	-5 1/4	42 3/4	-4	-5	0	0	1/4
5	34 1/4	-16 3/4	-9	34 1/4	-16 1/4	-9	0	1/2	0
6	34 1/2	-11 1/4	-9	34 1/2	-11 3/4	-8 3/4	0	- 1/2	1/4
7	34 1/4	-3 3/4	-9	34 1/4	-4	-9	0	- 1/4	0
8	29 1/4	-20 1/2	-9 1/4	28 3/4	-20 1/2	-9	- 1/2	0	1/4
9	28 1/4	-14	-9	28 1/4	-14	-8 3/4	0	0	1/4
10	29	-4 3/4	-9 1/2	29	-5	-9 1/2	0	- 1/4	0
11	23 1/4	-14 3/4	-8 3/4	23 1/2	-15	-8 3/4	1/4	- 1/4	0
12	24 1/4	-8	-8 3/4	24 1/2	-8 1/4	-8 3/4	1/4	- 1/4	0
13	14	-17 1/2	-5	14	-17 1/2	-5	0	0	0
14	14	-10 1/2	-5	14	-10 3/4	-5	0	- 1/4	0
15	14	-4 1/4	-5	14	-4 1/4	-5	0	0	0
16	42 3/4	14 1/4	-4 3/4	42 3/4	14 3/4	-4 1/2	0	1/2	1/4
17	43 1/4	18 3/4	-4 1/4	43	19	-4	- 1/4	1/4	1/4
18	39 1/2	24	-4 1/4	39 1/2	24 1/2	-4	0	1/2	1/4
19	36 1/2	9	-8 1/2	36 1/2	9	-8 1/4	0	0	1/4
20	36 1/2	15 1/2	-8 1/4	36 3/4	16	-8 1/4	1/4	1/2	0
21	36 3/4	21	-8	36 3/4	21 1/2	-8	0	1/2	0
22	31 3/4	9 1/4	-8 1/4	31 3/4	9 1/4	-8 1/2	0	0	- 1/4
23	32	15 1/4	-8 3/4	32	15 1/2	-8 1/2	0	1/4	1/4
24	32 1/2	24 1/2	-8 1/4	32 1/2	24 3/4	-8 1/4	0	1/4	0
25	23 1/4	10 3/4	-9 1/4	23 1/4	10 3/4	-9	0	0	1/4
26	22 1/2	18 1/4	-8 1/4	22 3/4	18 1/4	-8 1/4	1/4	0	0
27	22 3/4	26 1/2	-8 3/4	23	26	-8 1/2	1/4	- 1/2	1/4
28	13 1/2	9 1/2	-5	13 1/2	9 1/4	-4 3/4	0	- 1/4	1/4
29	13 1/4	15 1/4	-4 1/2	13 1/4	15 1/4	-4 1/2	0	0	0
30	13 1/2	24 3/4	-4 1/4	13 1/2	24 3/4	-4 1/4	0	0	0
31							0	0	0

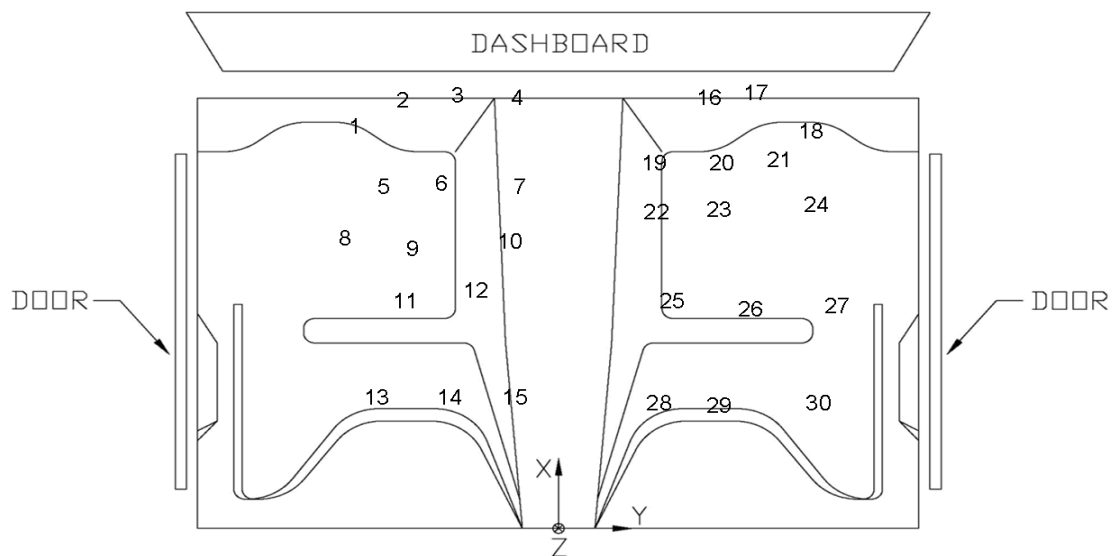


Figure G-2. Floorpan Deformation Data – Set 2, Test No. APR-1

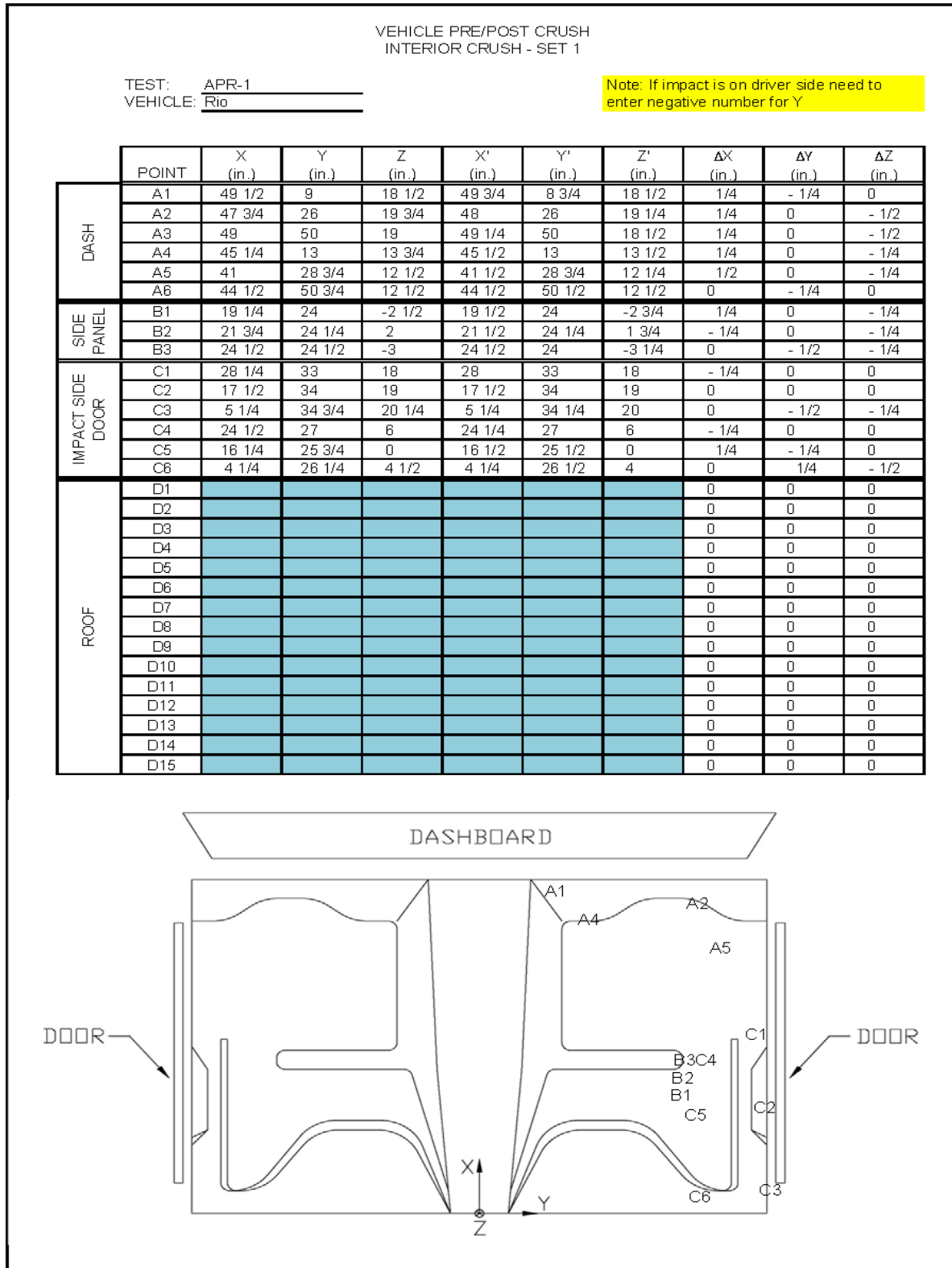


Figure G-3. Occupant Compartment Deformation Data – Set 1, Test No. APR-1

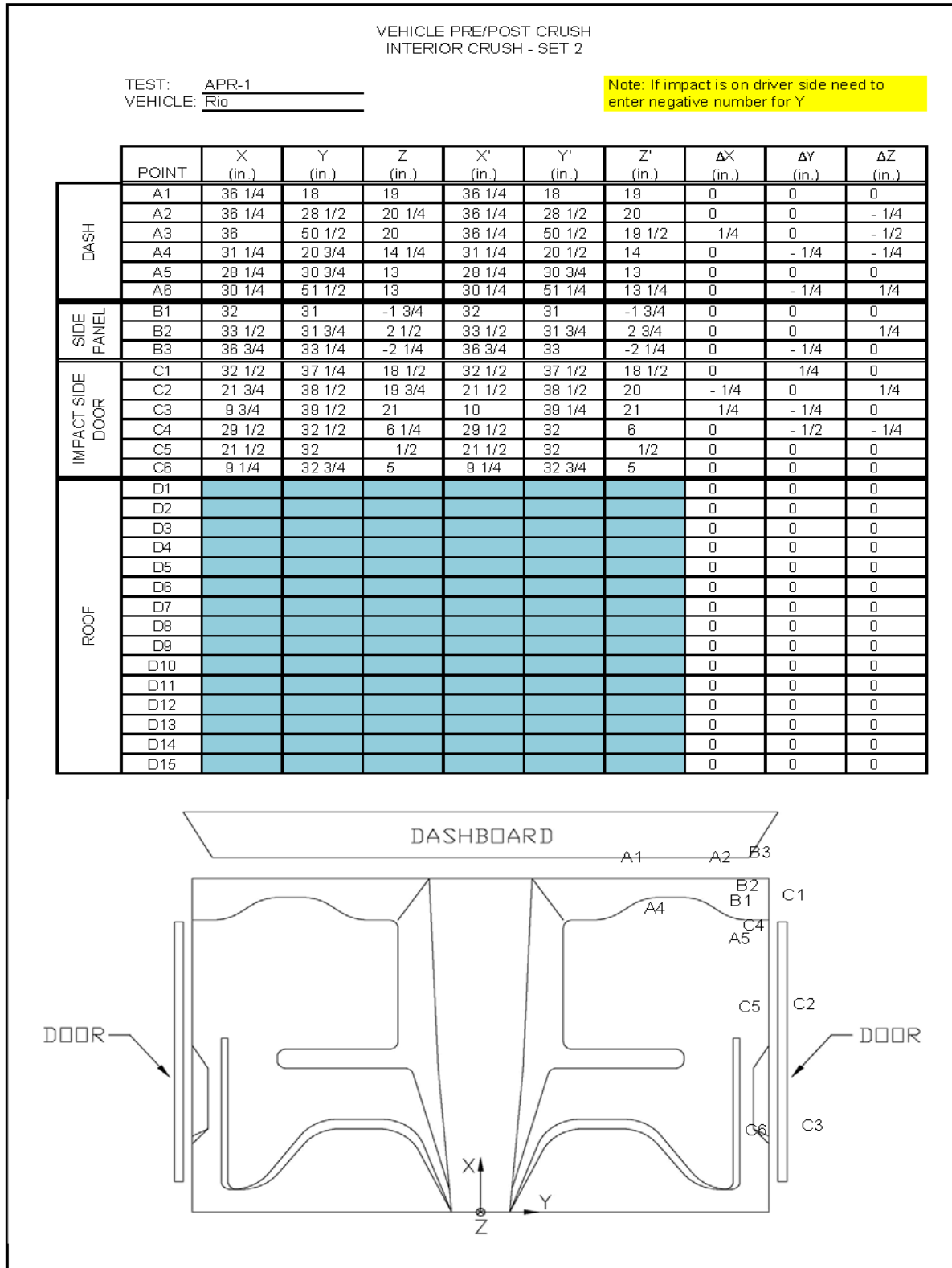
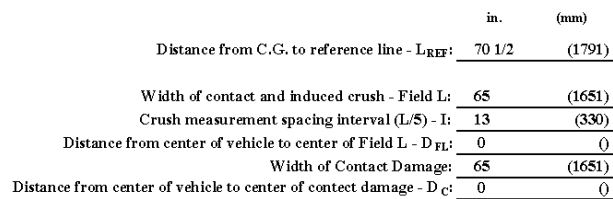


Figure G-4. Occupant Compartment Deformation Data – Set 2, Test No. APR-1



	Crush Measurement		Lateral Location		Original Profile Measurement		Dist. Between Ref. Lines		Actual	Crush
	in.	(mm)	in.	(mm)	in.	(mm)	in.	(mm)	in.	(mm)
C ₁	na	NA	-32 1/2	-(826)	24	(610)	-4 2/3	-(119)	NA	NA
C ₂	2 1/2	(64)	-19 1/2	-(495)	8 2/5	(214)			-1 2/9	-(31)
C ₃	8 1/2	(216)	-6 1/2	-(165)	6 1/6	(156)			7	(179)
C ₄	5 1/2	(140)	6 1/2	(165)	6 1/6	(156)			4	(102)
C ₅	3	(76)	19 1/2	(495)	8 2/5	(214)			- 5/7	-(18)
C ₆	na	NA	32 1/2	(826)	24	(610)			NA	NA
C _{MAX}	12	(305)	3 1/2	(89)	6	(152)			10 2/3	(272)

418

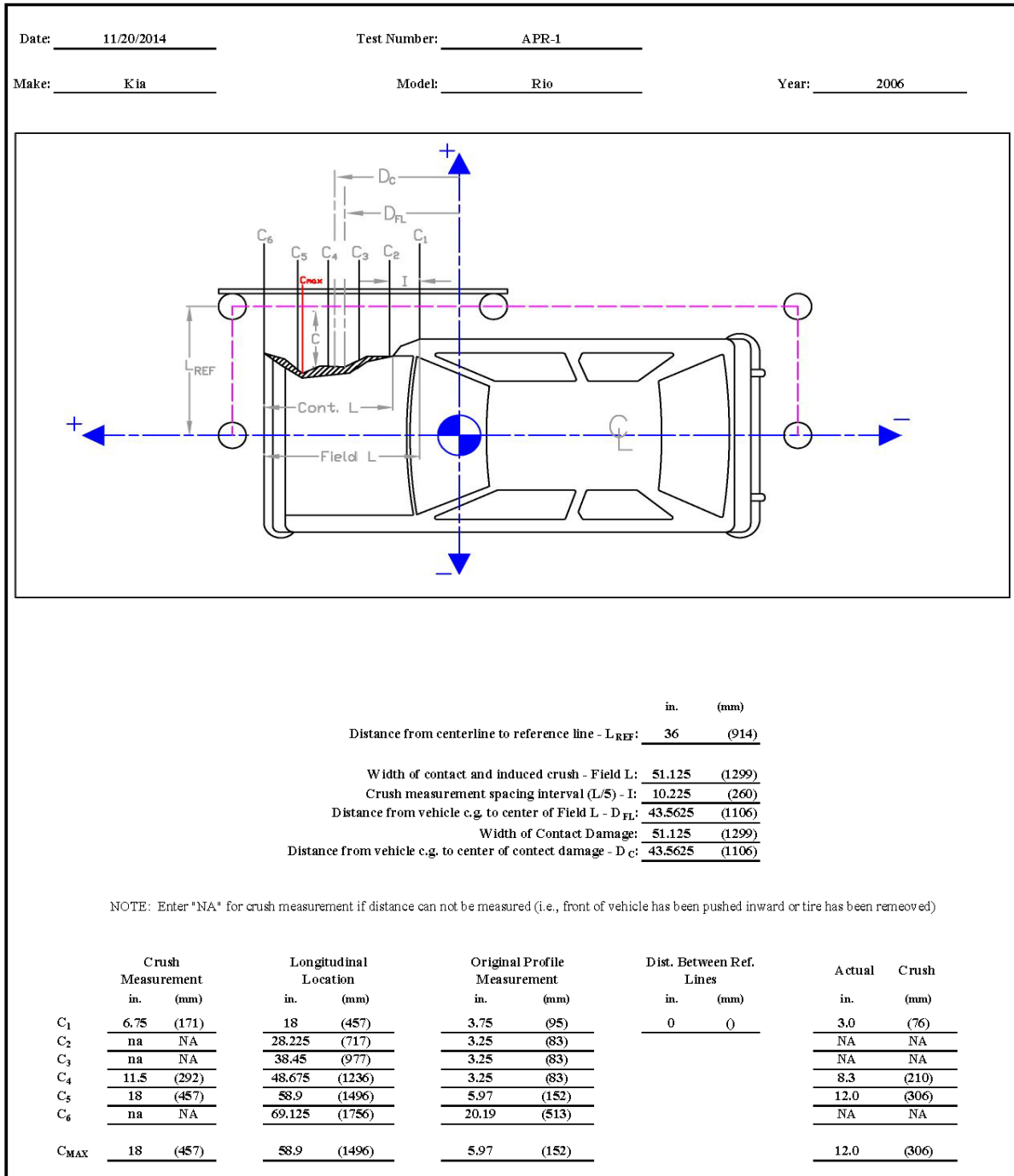


Figure G-6. Exterior Vehicle Crush (NASS) - Side, Test No. APR-1

VEHICLE PRE/POST CRUSH
FLOORPAN - SET 1

TEST: APR-2
VEHICLE: Rio

Note: If impact is on driver side need to
enter negative number for Y

POINT	X (in.)	Y (in.)	Z (in.)	X' (in.)	Y' (in.)	Z' (in.)	ΔX (in.)	ΔY (in.)	ΔZ (in.)
F1	28 3/4	-22	-1 3/4	28 3/4	-22 1/4	-1 1/2	0	- 1/4	1/4
2	30 1/2	-18 1/2	-3 3/4	30 1/2	-19	-3 3/4	0	- 1/2	0
3	31	-11	-4	31	-10 3/4	-4	0	1/4	0
4	25 1/2	-21 3/4	-7 1/4	25 1/4	-22	-7	- 1/4	- 1/4	1/4
5	25 1/2	-15 1/2	-7 1/4	25 1/2	-15 1/2	-7	0	0	1/4
6	26	-7 1/4	-6 3/4	25 3/4	-8	-7	- 1/4	- 3/4	- 1/4
7	20	-23	-8 1/4	20	-23	-8 1/4	0	0	0
8	20	-16 3/4	-8	20	-17	-8	0	- 1/4	0
9	20	-9	-8	20	-9 1/4	-8	0	- 1/4	0
10	12 3/4	-20 1/2	-8	12 3/4	-20 1/2	-8 1/4	0	0	- 1/4
11	12 1/4	-15 1/4	-8 1/4	12 1/2	-15 1/4	-8 1/4	1/4	0	0
12	12	-9	-8 3/4	12 1/4	-9	-9	1/4	0	- 1/4
13	1	-22 3/4	-4 1/2	1 1/4	-22 3/4	-4 1/4	1/4	0	1/4
14	1 1/4	-14 1/4	-4 1/2	1 1/4	-14 1/4	-4 1/2	0	0	0
15	1 1/4	-9 1/4	-4 1/2	1 1/4	-9 1/2	-4 1/2	0	- 1/4	0
16	30 3/4	6 1/4	-4	30 1/2	6	-4	- 1/4	- 1/4	0
17	31 1/4	10	-3 1/2	31 1/4	10 1/4	-3 1/2	0	1/4	0
18	30 3/4	11 1/4	-3 3/4	30 1/2	11 3/4	-3 1/2	- 1/4	1/2	1/4
19	28 3/4	17 1/2	-1 3/4	28 3/4	18 1/4	-1 3/4	0	3/4	0
20	20	4 3/4	-8 1/4	20	4 3/4	-8	0	0	1/4
21	20 1/2	19 3/4	-7 3/4	20 1/2	19 1/2	-7 3/4	0	- 1/4	0
22	16 1/2	6 1/2	-8 3/4	16 3/4	6 1/2	-8 3/4	1/4	0	0
23	16 3/4	12 3/4	-8	16 3/4	12 1/2	-8	0	- 1/4	0
24	16 1/2	17 3/4	-8 1/4	16 1/2	18	-8 1/4	0	1/4	0
25	11 3/4	5	-8 3/4	11 3/4	4 1/2	-8 3/4	0	- 1/2	0
26	11 1/4	10	-8	12 1/2	10	-8	1 1/4	0	0
27	12 3/4	16 1/4	-7 3/4	12 3/4	16	-8	0	- 1/4	- 1/4
28	1	5 1/2	-4 1/4	1	5 1/4	-4 1/2	0	- 1/4	- 1/4
29	1 1/4	12 1/2	-4 1/4	1	12 1/2	-4 1/4	- 1/4	0	0
30	1	19 1/4	-4 1/4	1 1/4	19 1/4	-4	1/4	0	1/4
31							0	0	0

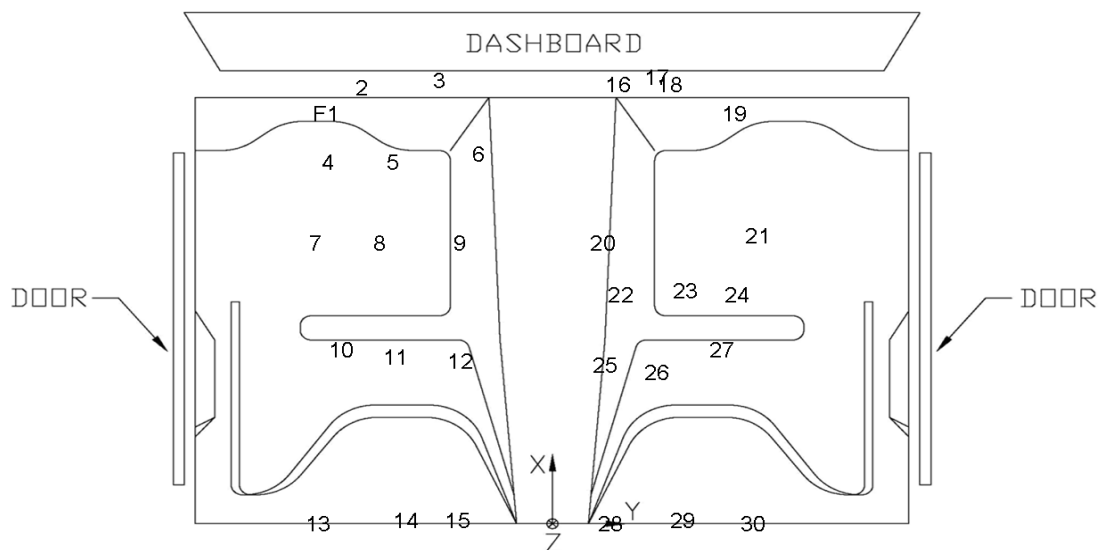


Figure G-7. Floorpan Deformation Data – Set 1, Test No. APR-2

VEHICLE PRE/POST CRUSH
FLOORPAN - SET 2

TEST: APR-2
VEHICLE: Rio

Note: If impact is on driver side need to
enter negative number for Y

POINT	X (in.)	Y (in.)	Z (in.)	X' (in.)	Y' (in.)	Z' (in.)	ΔX (in.)	ΔY (in.)	ΔZ (in.)
1	39	-16 1/2	-2 1/2	39	-17	-2 3/4	0	- 1/2	- 1/4
2	40 3/4	-13	-4 3/4	40 3/4	-13 1/2	-4 3/4	0	- 1/2	0
3	41 1/4	-5 3/4	-5	41	-6 1/4	-5	- 1/4	- 1/2	0
4	35 1/2	-16 1/4	-8	35 3/4	-16 1/2	-8	1/4	- 1/4	0
5	35 3/4	-10	-8	35 3/4	-10 1/2	-8	0	- 1/2	0
6	36 1/4	-2	-7 3/4	36	-2 1/2	-8	- 1/4	- 1/2	- 1/4
7	30 1/4	-17 1/2	-9	30 1/4	-17 3/4	-9	0	- 1/4	0
8	30 1/4	-11 1/4	-8 3/4	30 1/4	-11 1/4	-9	0	0	- 1/4
9	30 1/4	-3 1/2	-9	30 1/4	-3 1/2	-9	0	0	0
10	22 3/4	-15 1/4	-8 3/4	22 3/4	-15 1/4	-8 3/4	0	0	0
11	22 1/2	-10	-8 3/4	22 3/4	-10	-8 3/4	1/4	0	0
12	22	-3 3/4	-9 1/2	22 1/4	-3 1/2	-9 1/2	1/4	1/4	0
13	11 1/2	-17 1/2	-4 3/4	11 1/4	-17 1/4	-4 3/4	- 1/4	1/4	0
14	11 1/2	-9	-4 3/4	11 1/2	-9	-5	0	0	- 1/4
15	11 1/4	-4	-5	11 1/4	-4	-5	0	0	0
16	41	11 3/4	-5	41	12	-5	0	1/4	0
17	41 1/2	15 1/2	-4 3/4	41 1/2	15 3/4	-4 3/4	0	1/4	0
18	41	19 1/2	-5	40 3/4	19 1/2	-5	- 1/4	0	0
19	39	22 3/4	-3	39	22 1/2	-3	0	- 1/4	0
20	30 1/4	10	-9	30 1/4	10 1/4	-9	0	1/4	0
21	30 3/4	25 1/4	-9 1/4	30 3/4	24 3/4	-9	0	- 1/2	1/4
22	27	12	-9 3/4	27	11 3/4	-9 1/2	0	- 1/4	1/4
23	27	18 1/4	-9	27	18	-9	0	- 1/4	0
24	26 3/4	23 1/4	-9 1/2	27	23	-9 1/4	1/4	- 1/4	1/4
25	22	10 1/2	-9 3/4	22	10	-9 1/2	0	- 1/2	1/4
26	22 1/2	15 1/4	-9	22 1/2	15 1/2	-8 3/4	0	1/4	1/4
27	23	21 1/2	-8 3/4	23	21 1/4	-8 3/4	0	- 1/4	0
28	11 1/4	11	-5	11 1/4	10 3/4	-5	0	- 1/4	0
29	11 1/2	18	-5	11 1/4	17 3/4	-4 3/4	- 1/4	- 1/4	1/4
30	11 1/2	24 3/4	-4 3/4	11 1/4	24 3/4	-4 1/2	- 1/4	0	1/4
31							0	0	0

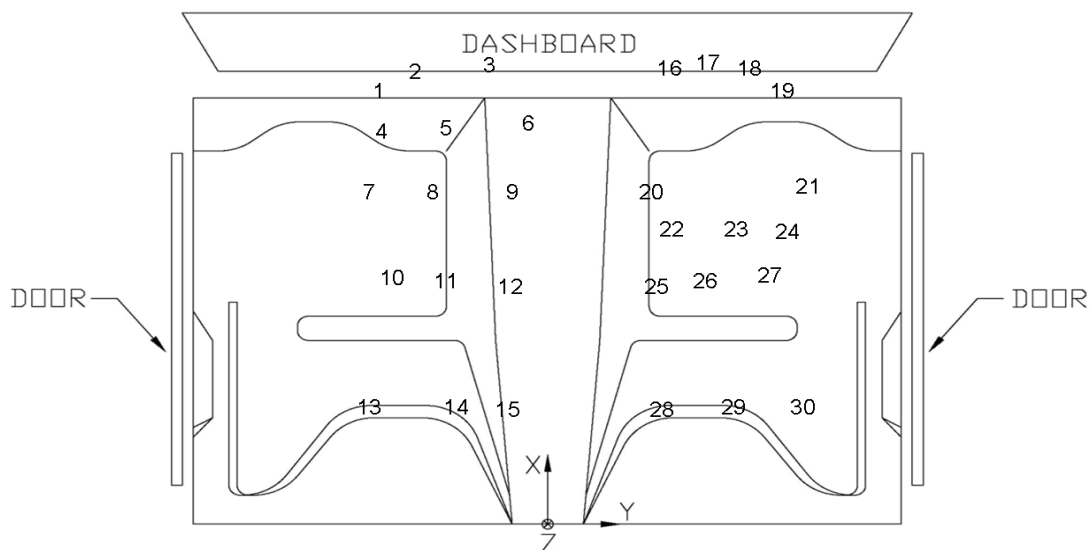


Figure G-8. Floorpan Deformation Data – Set 2, Test No. APR-2

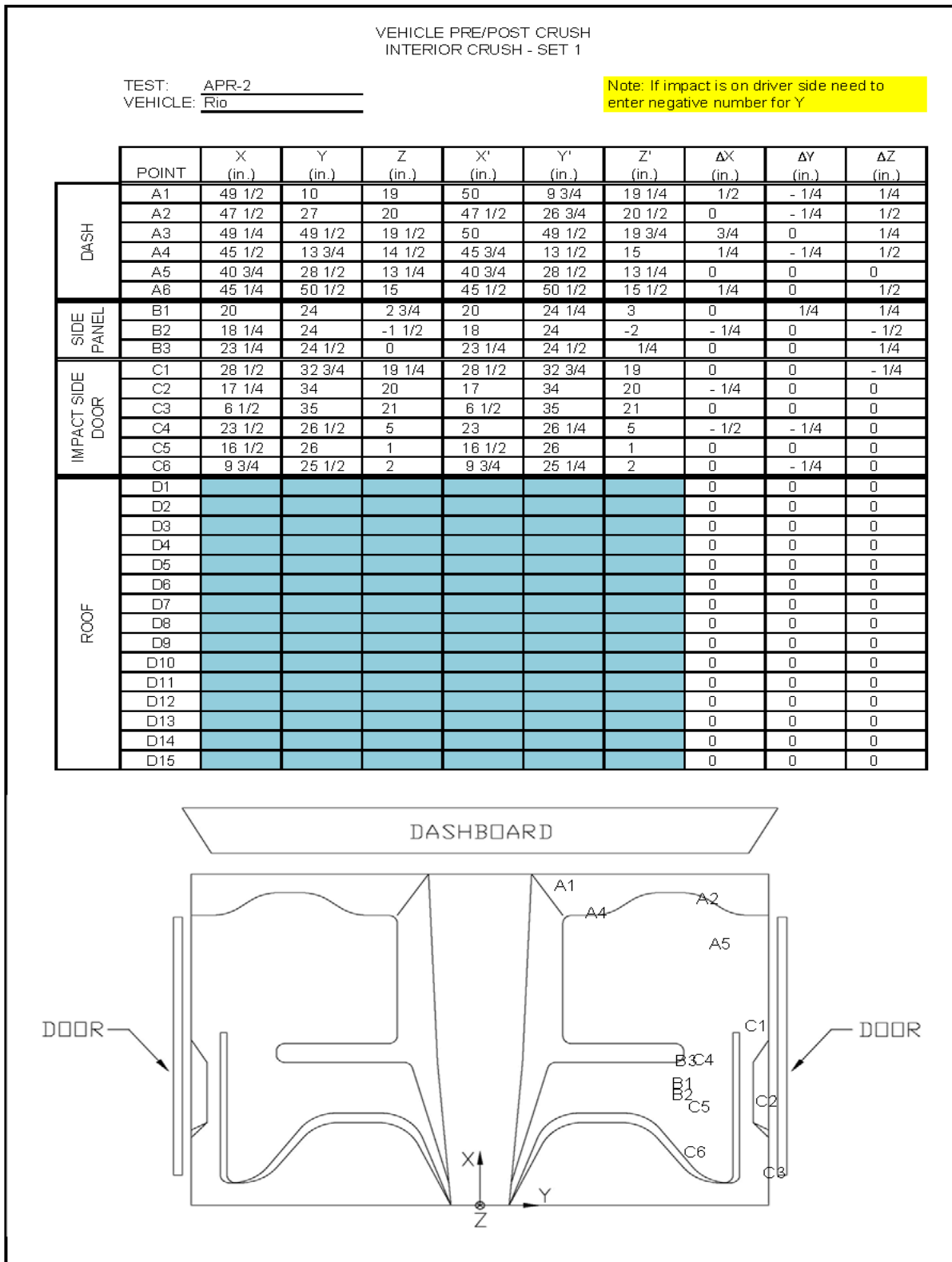


Figure G-9. Occupant Compartment Deformation Data – Set 1, Test No. APR-2

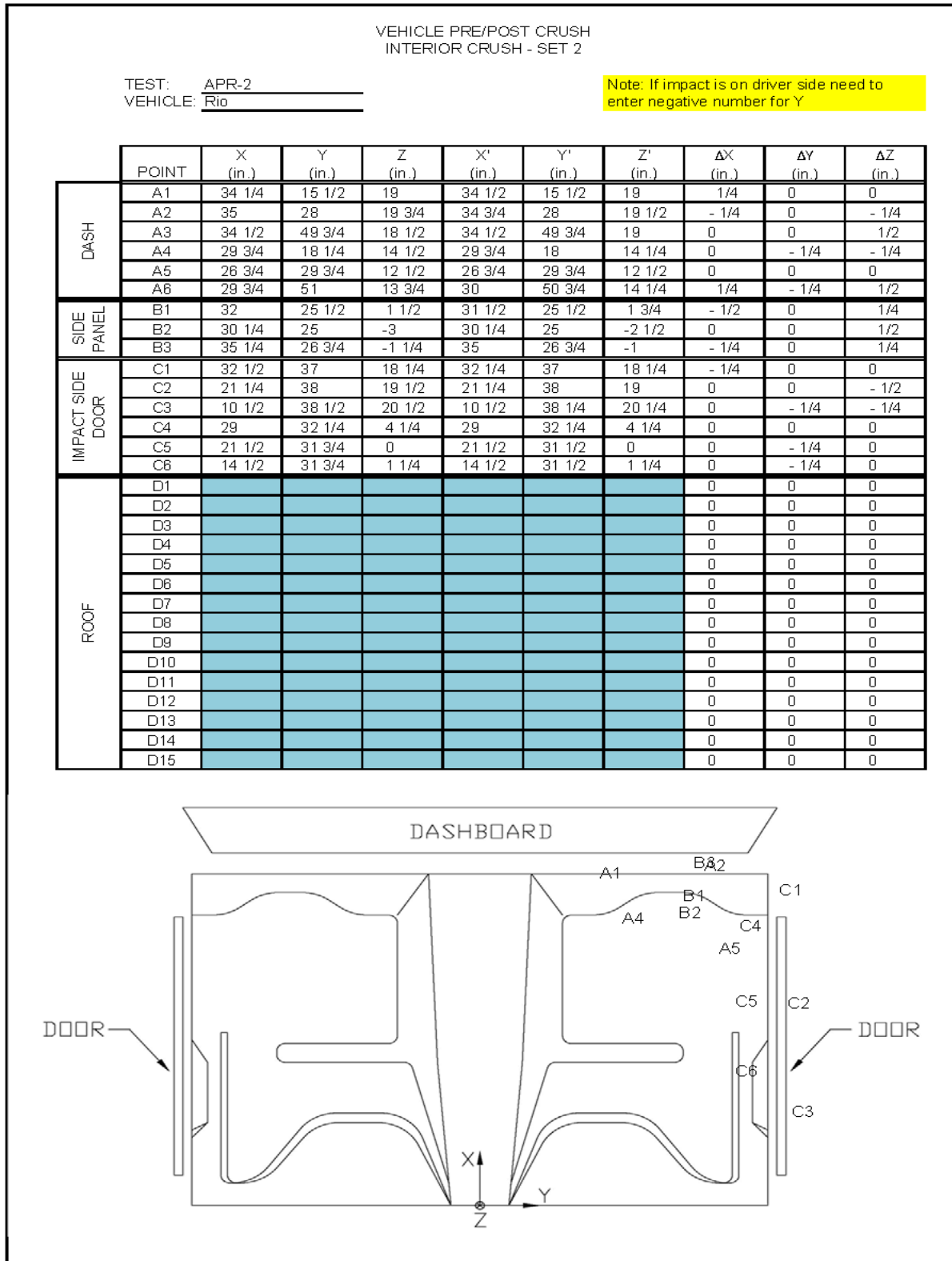


Figure G-10. Occupant Compartment Deformation Data – Set 2, Test No. APR-2

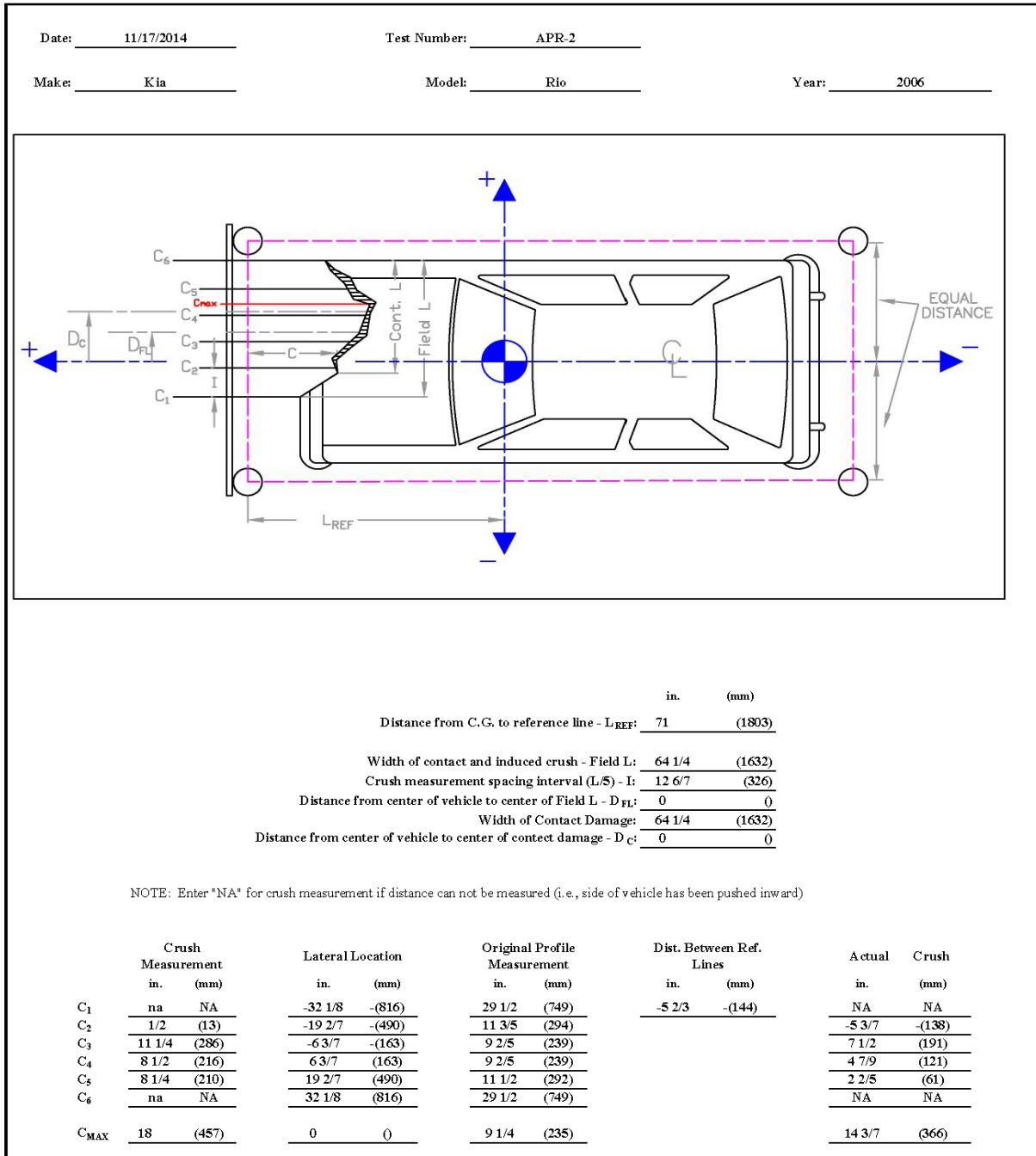


Figure G-11. Exterior Vehicle Crush (NASS) - Front, Test No. APR-2

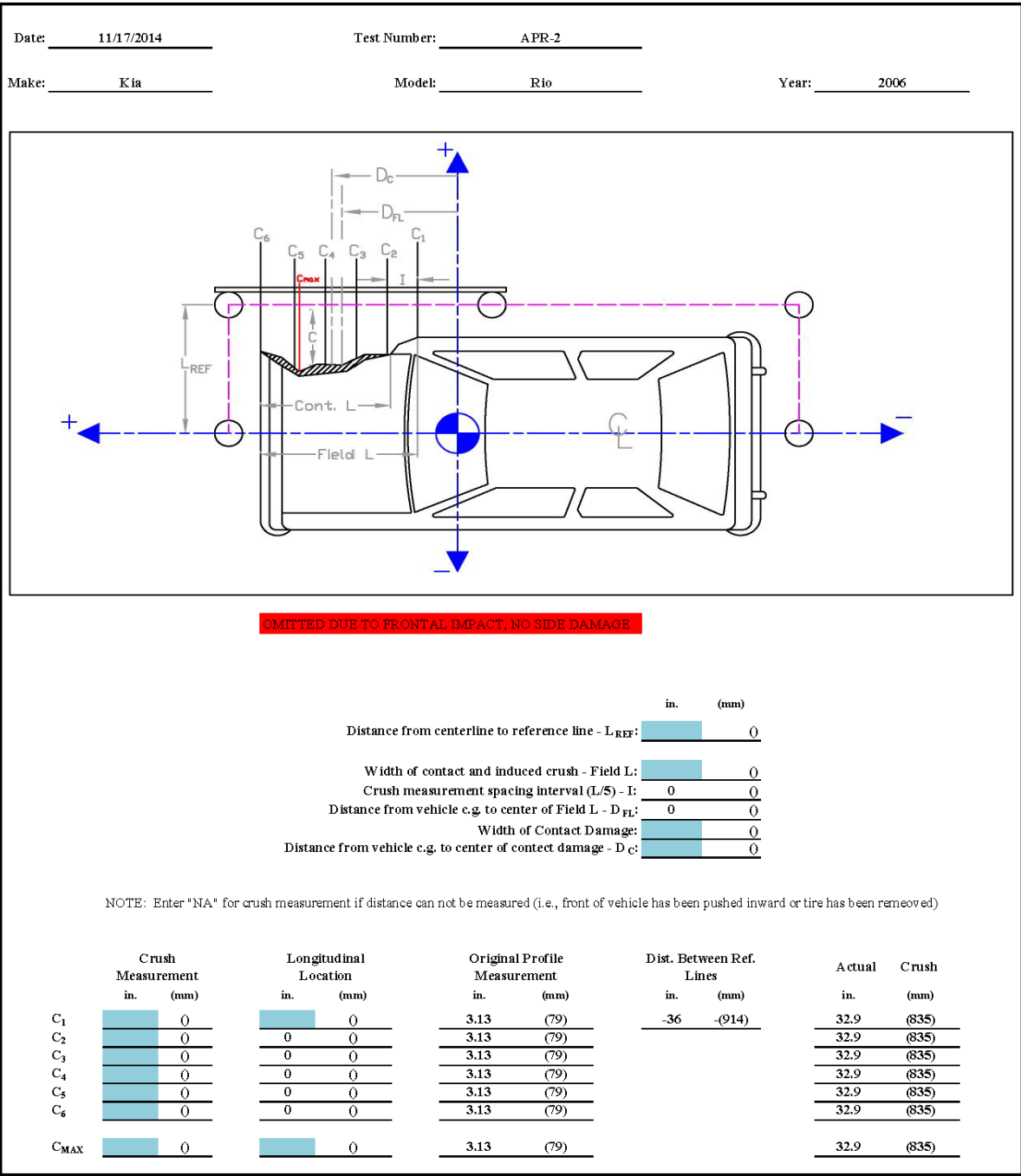


Figure G-12. Exterior Vehicle Crush (NASS) - Side, Test No. APR-2

Appendix H. Accelerometer and Rate Transducer Data Plots, Test No. APR-1

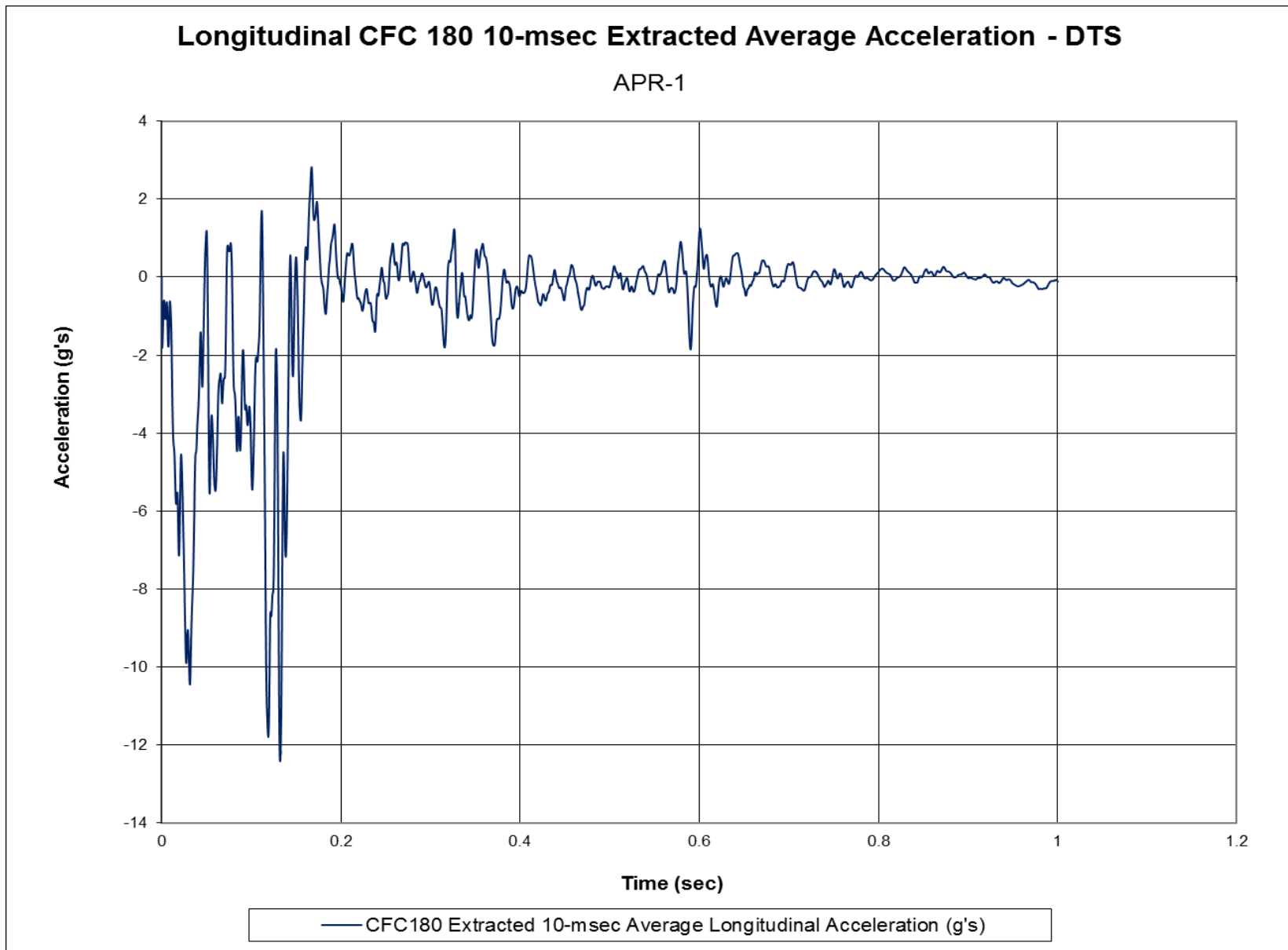


Figure H-1. 10-ms Average Longitudinal Deceleration (DTS), Test No. APR-1

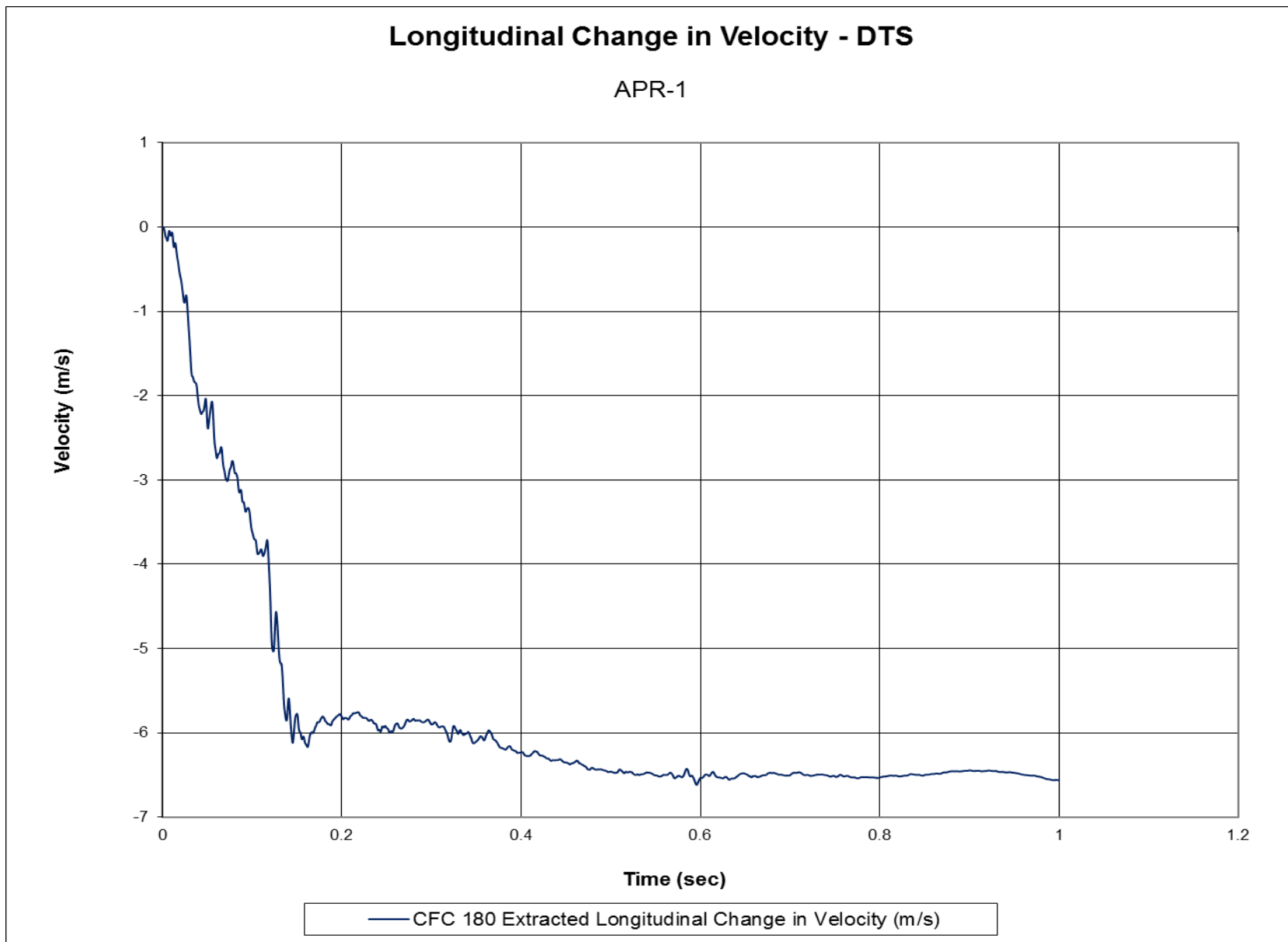


Figure H-2. Longitudinal Occupant Impact Velocity (DTS), Test No. APR-1

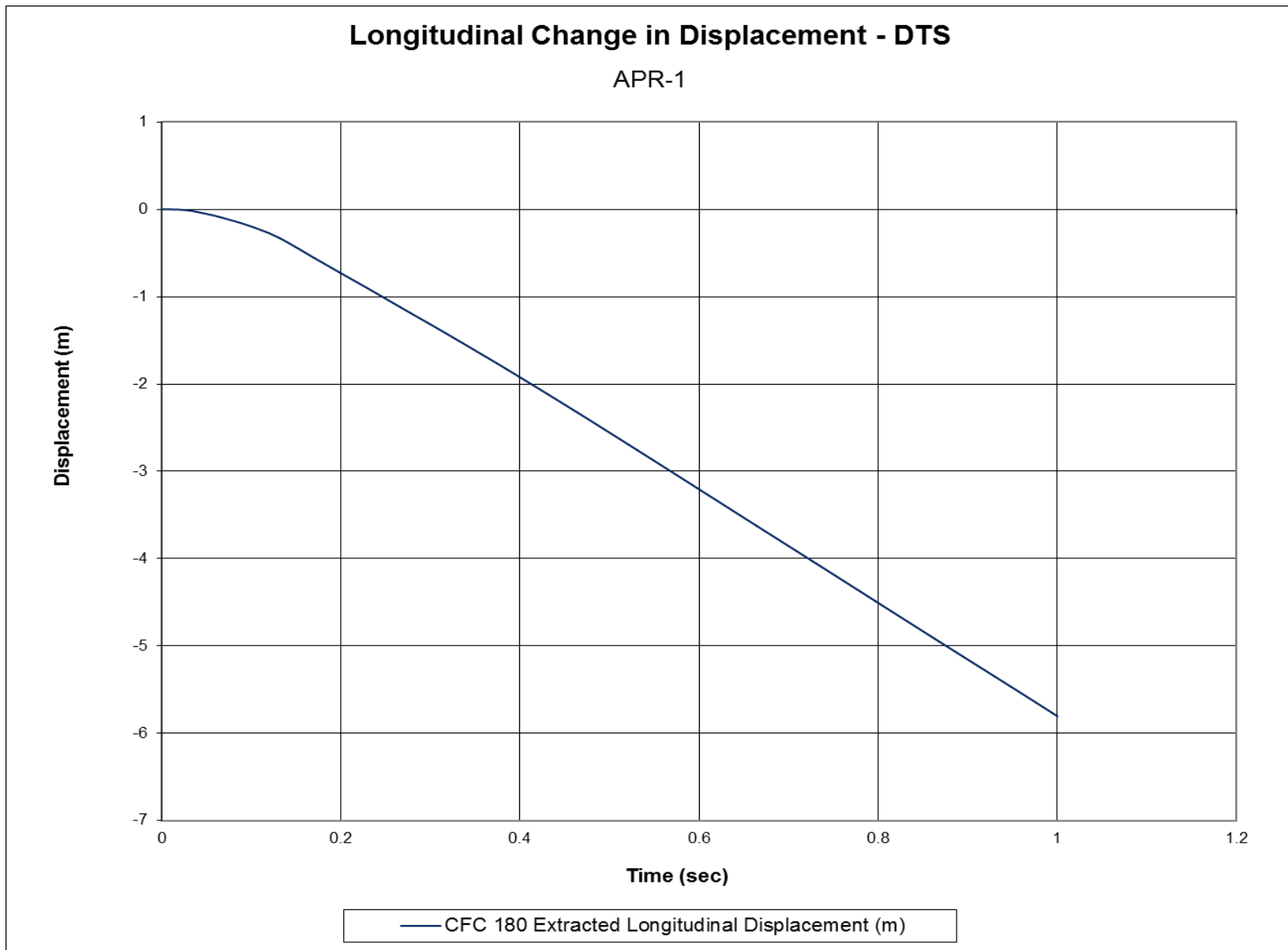


Figure H-3. Longitudinal Occupant Displacement (DTS), Test No. APR-1

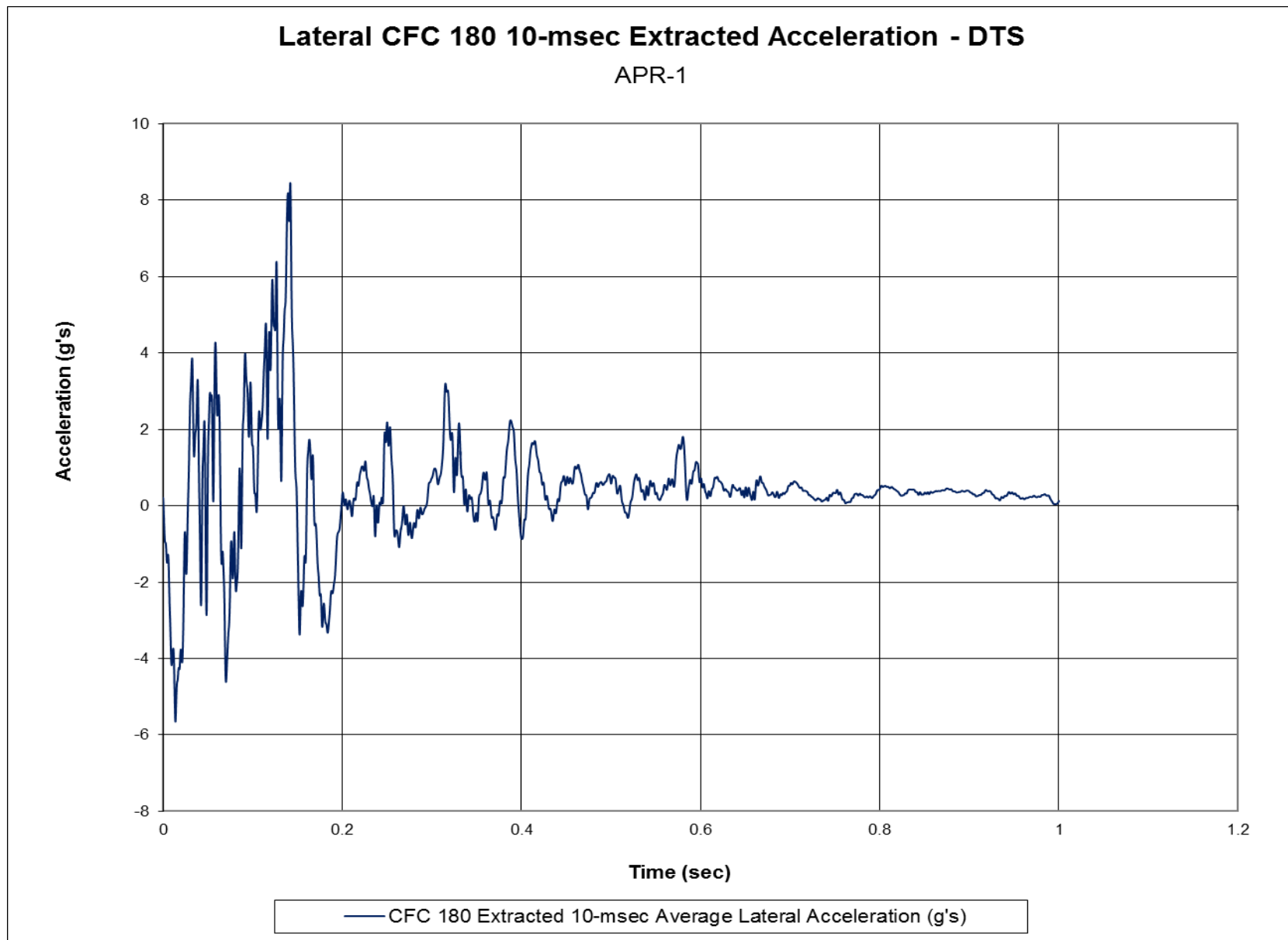


Figure H-4. 10-ms Average Lateral Deceleration (DTS), Test No. APR-1

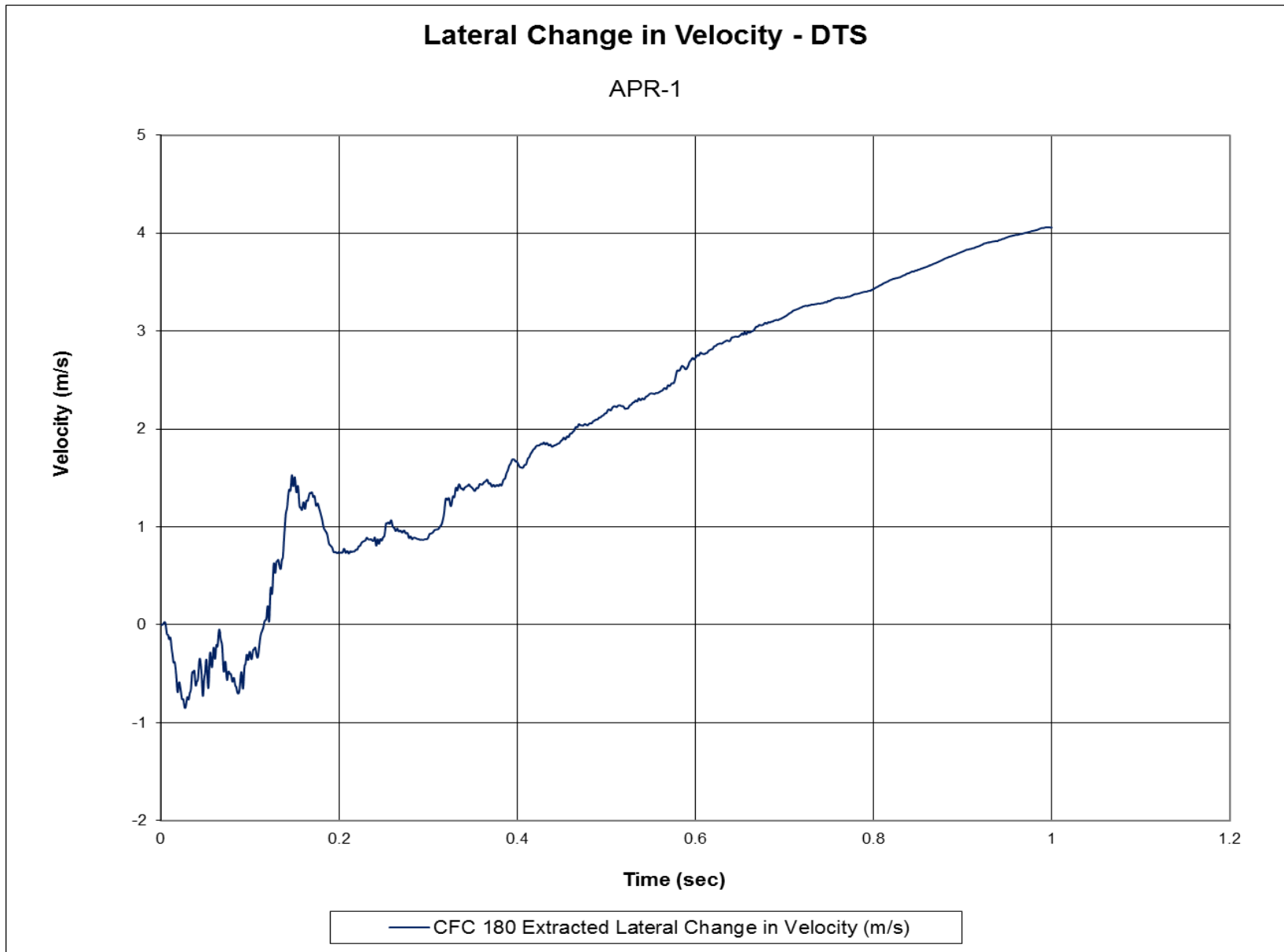


Figure H-5. Lateral Occupant Impact Velocity (DTS), Test No. APR-1

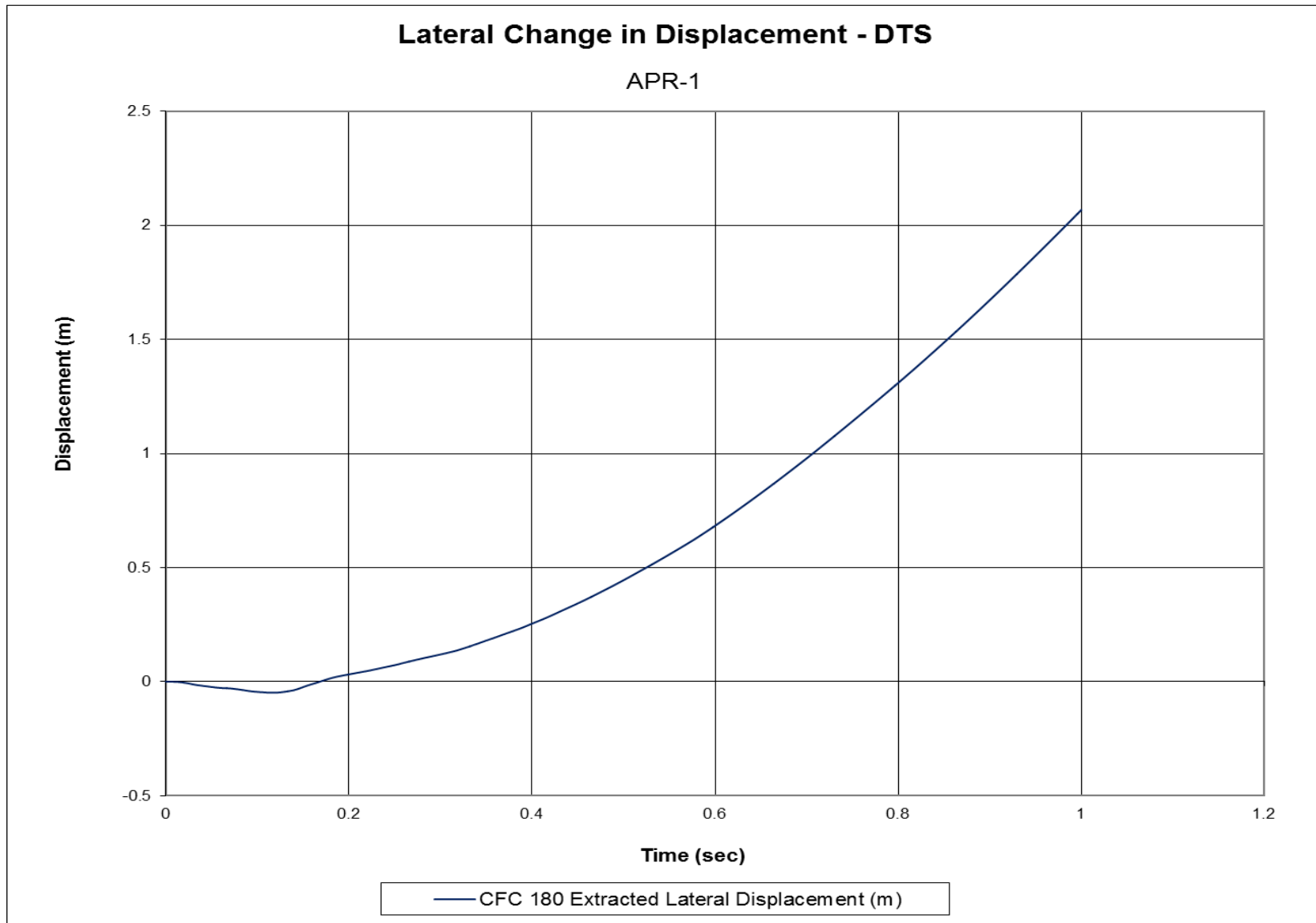


Figure H-6. Lateral Occupant Displacement (DTS), Test No. APR-1

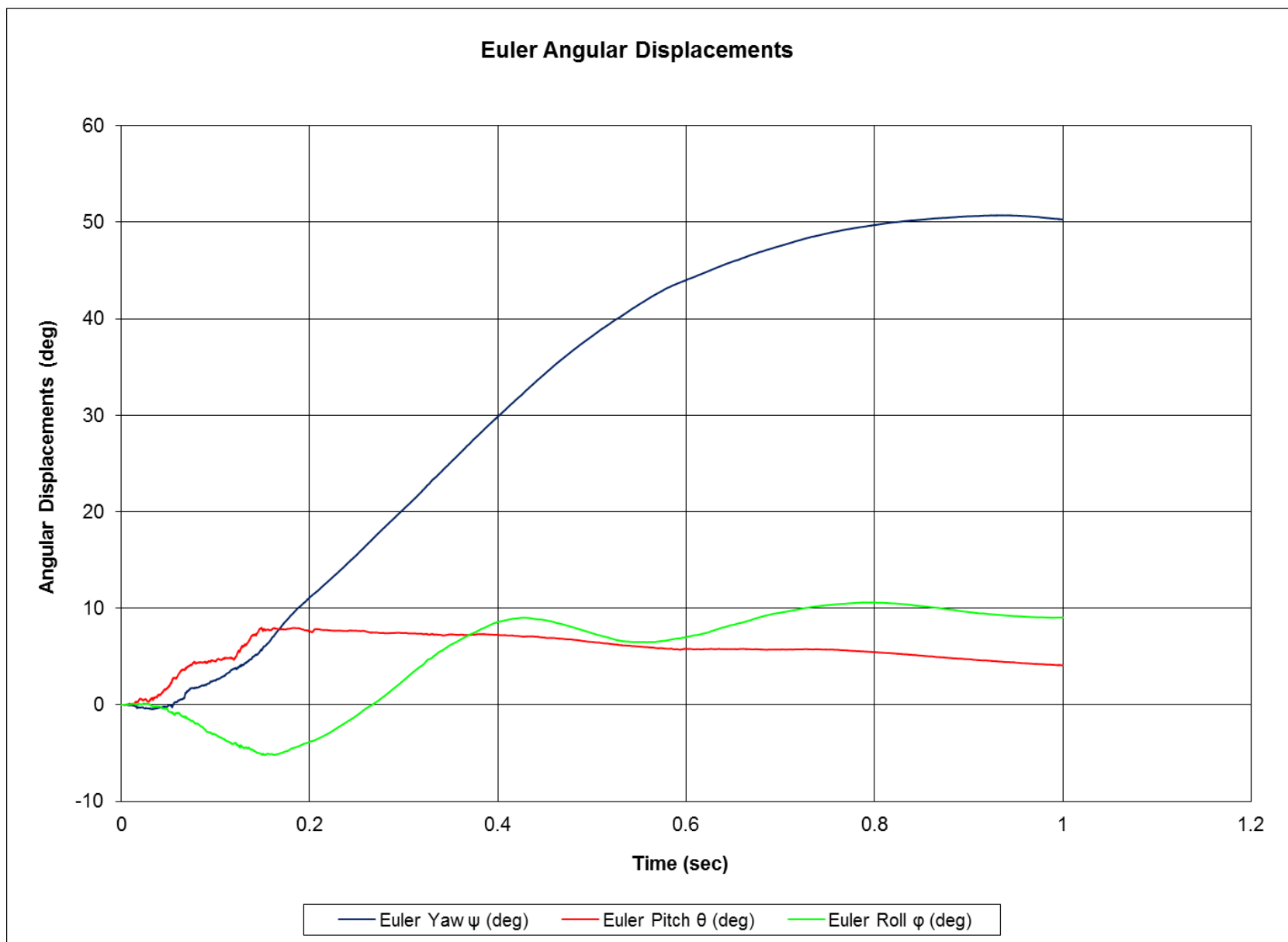


Figure H-7. Vehicle Angular Displacements (DTS), Test No. APR-1

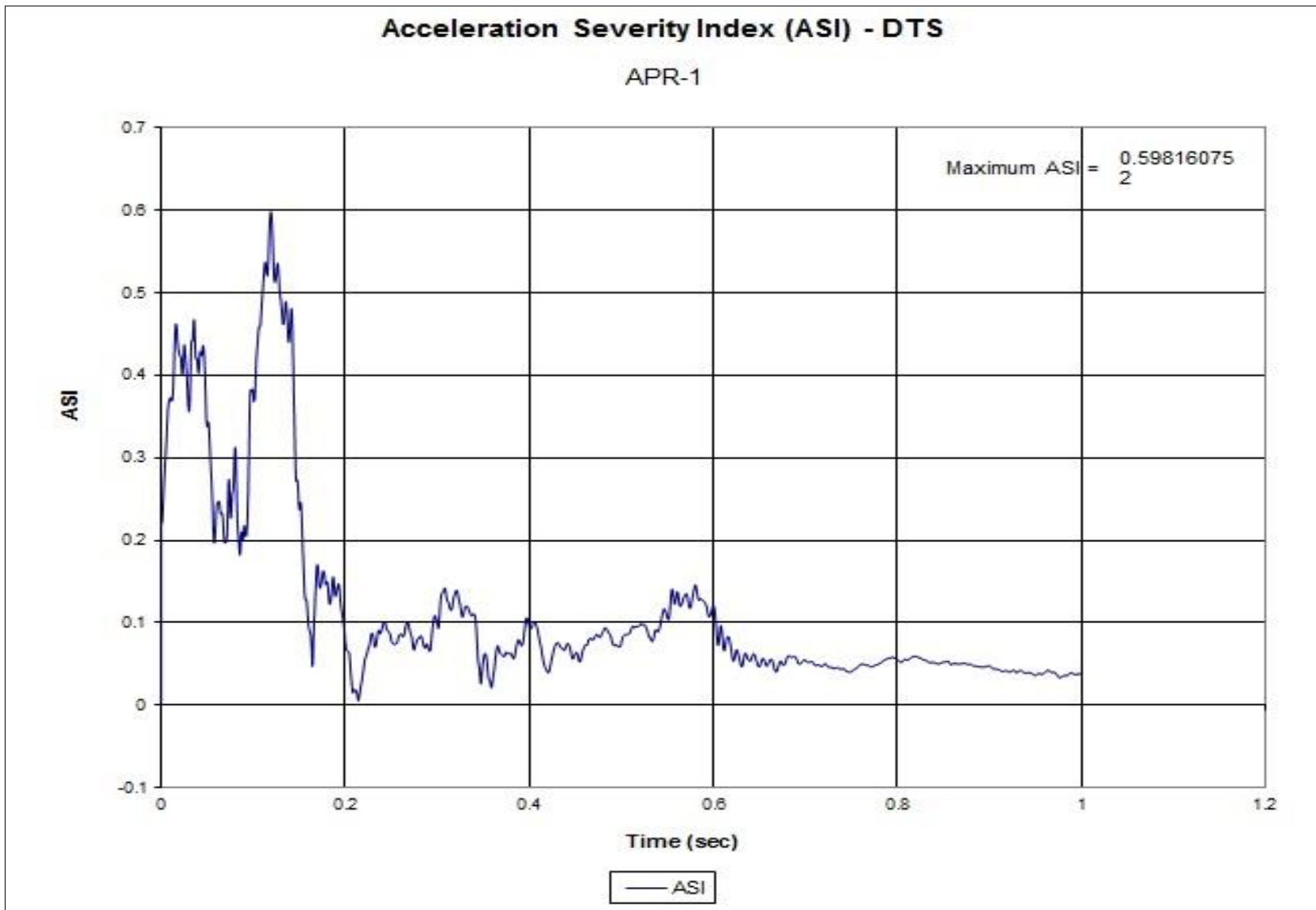
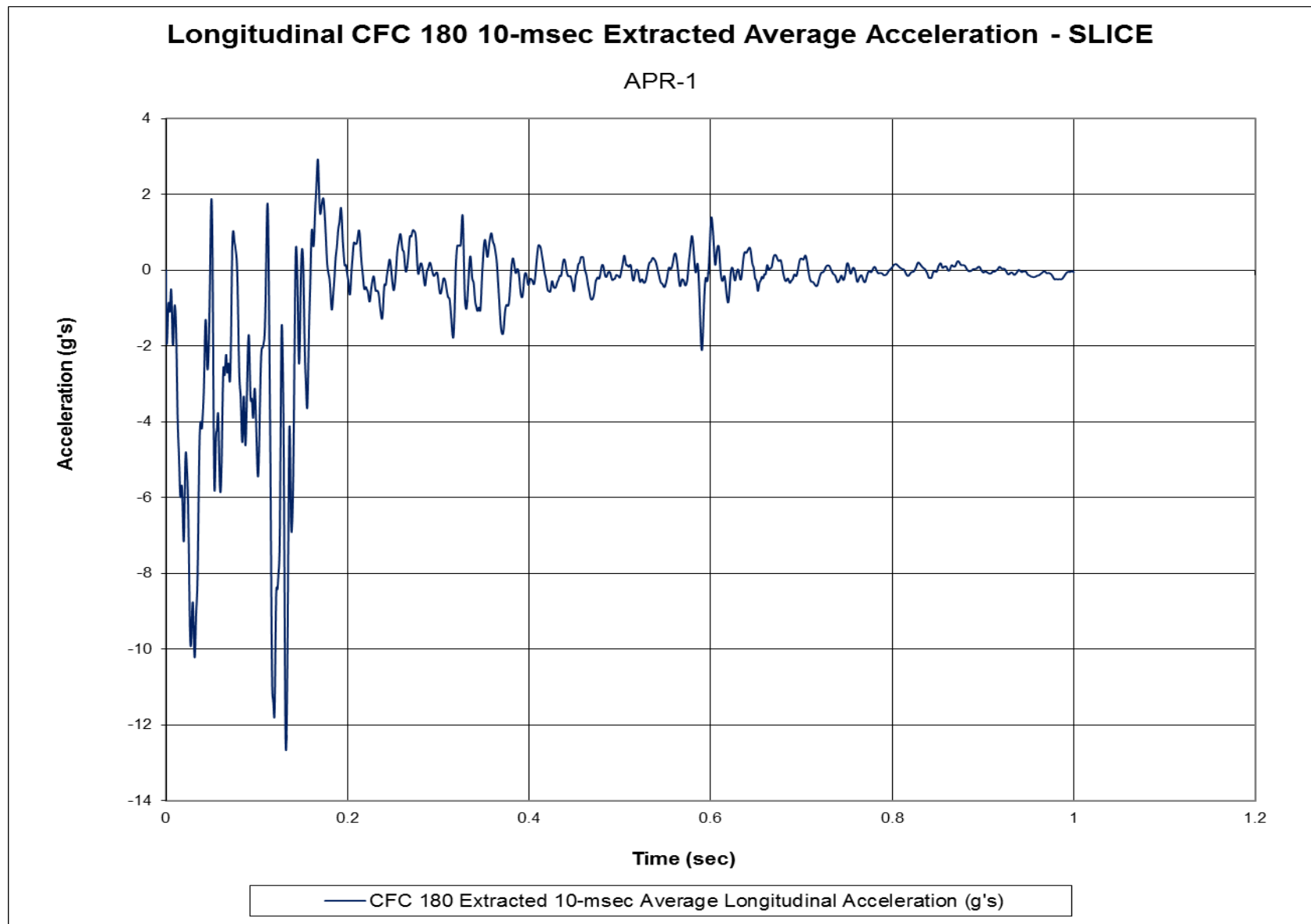


Figure H-8. Acceleration Severity Index (DTS), Test No. APR-1



10-ms Average Longitudinal Deceleration (SLICE-2), Test No. APR-1

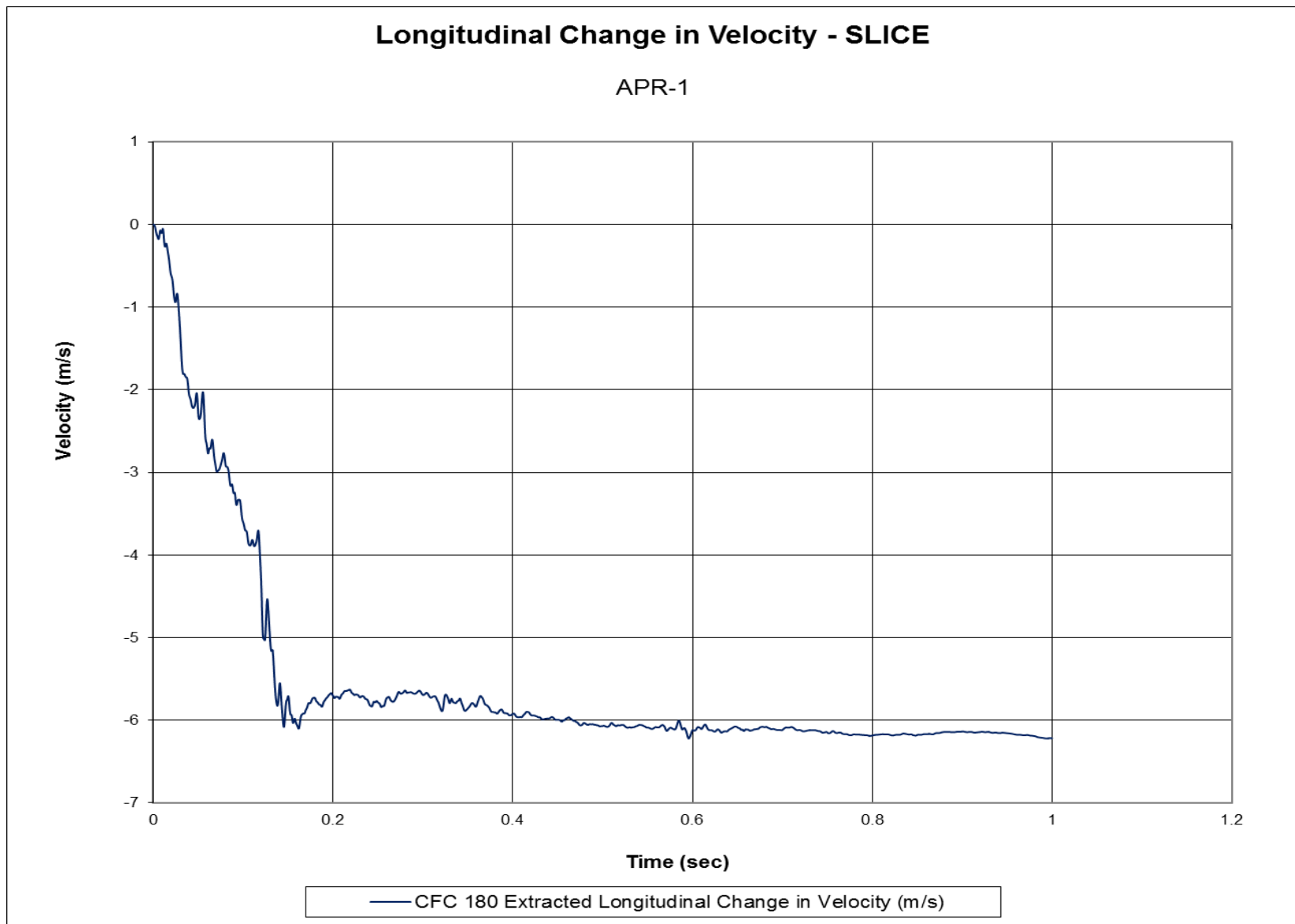


Figure H-9. Longitudinal Occupant Impact Velocity (SLICE-2), Test No. APR-1

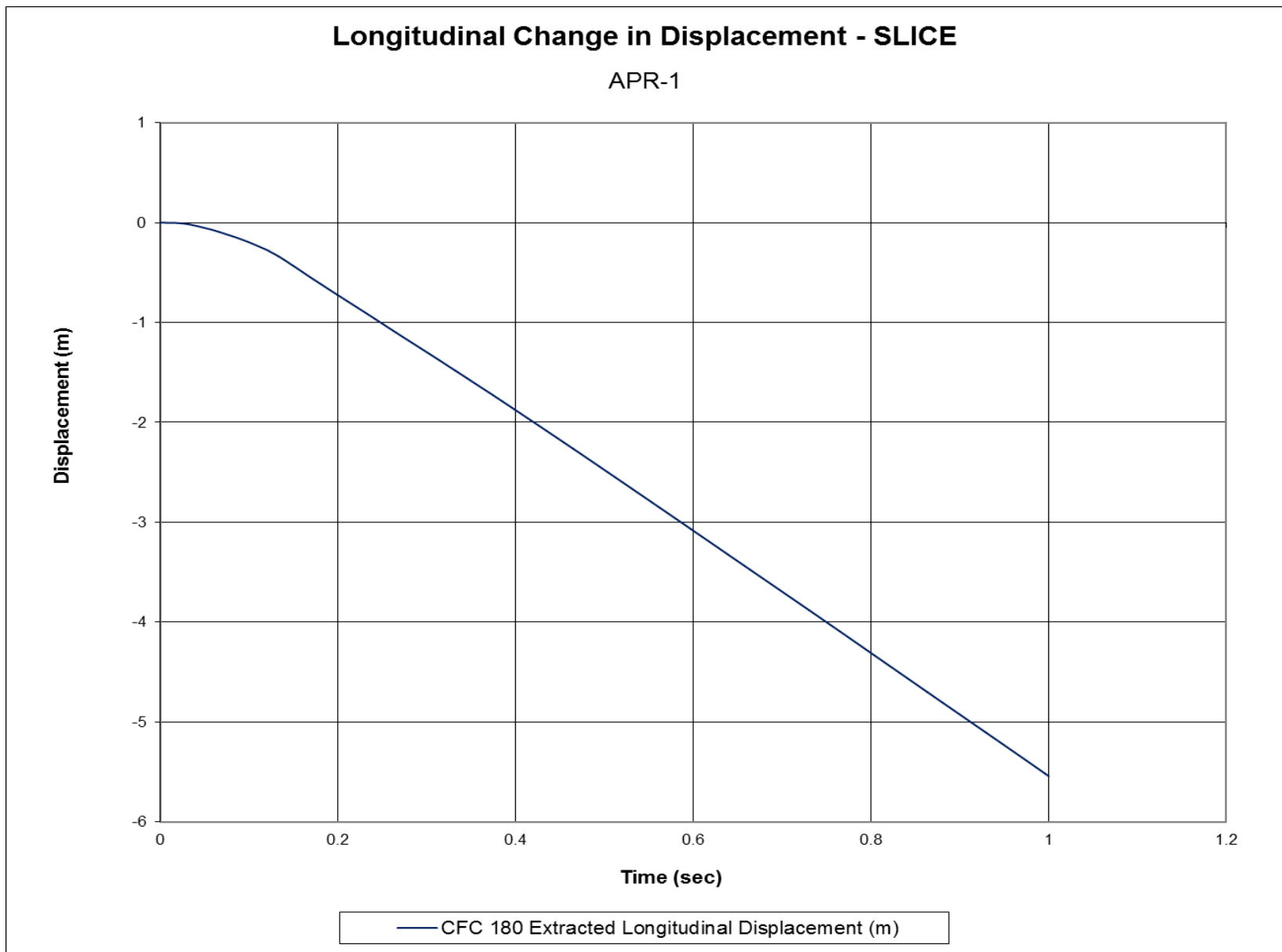


Figure H-10. Longitudinal Occupant Displacement (SLICE-2), Test No. APR-1

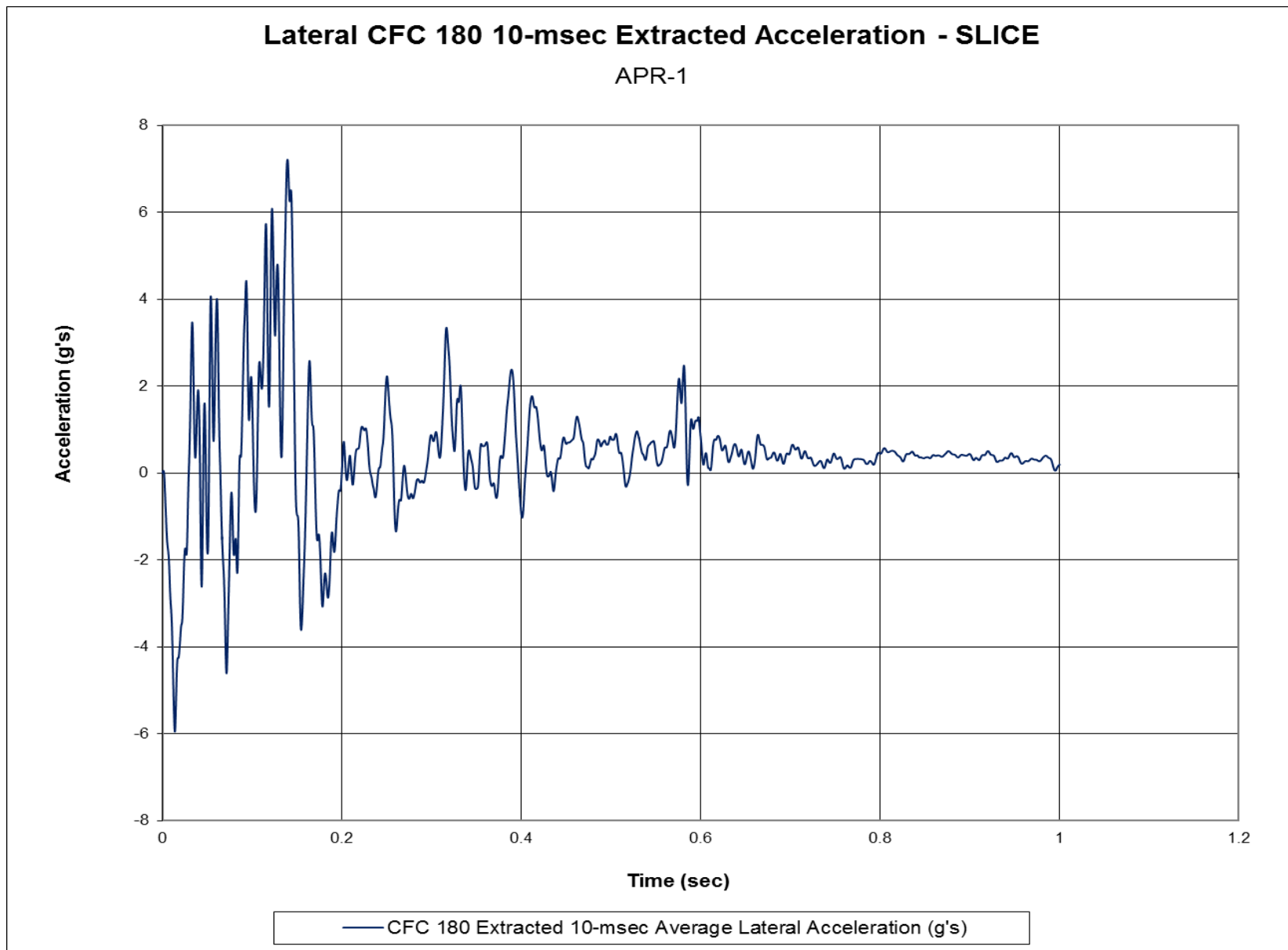


Figure H-11. 10-ms Average Lateral Deceleration (SLICE-2), Test No. APR-1

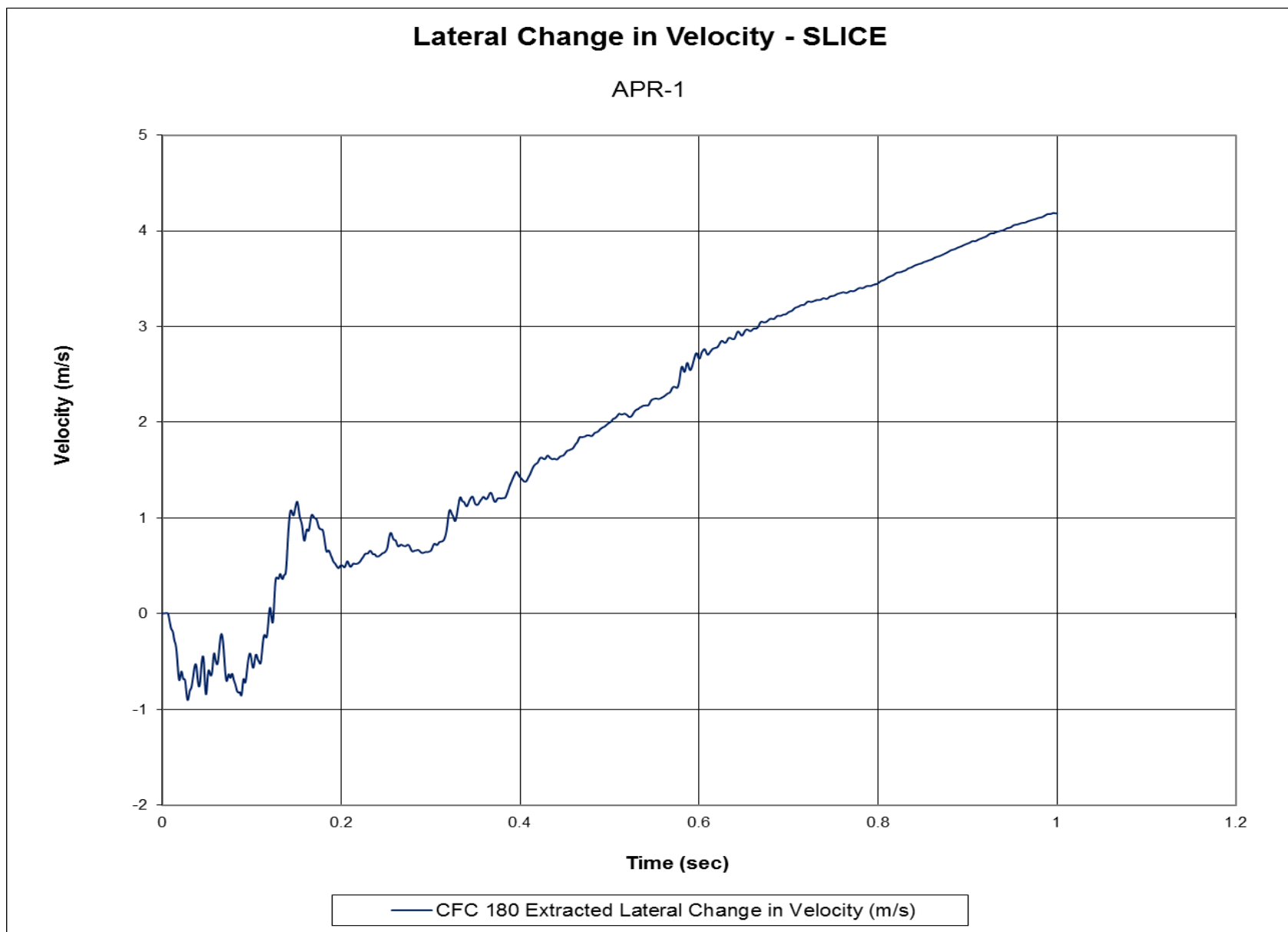


Figure H-12. Lateral Occupant Impact Velocity (SLICE-2), Test No. APR-1

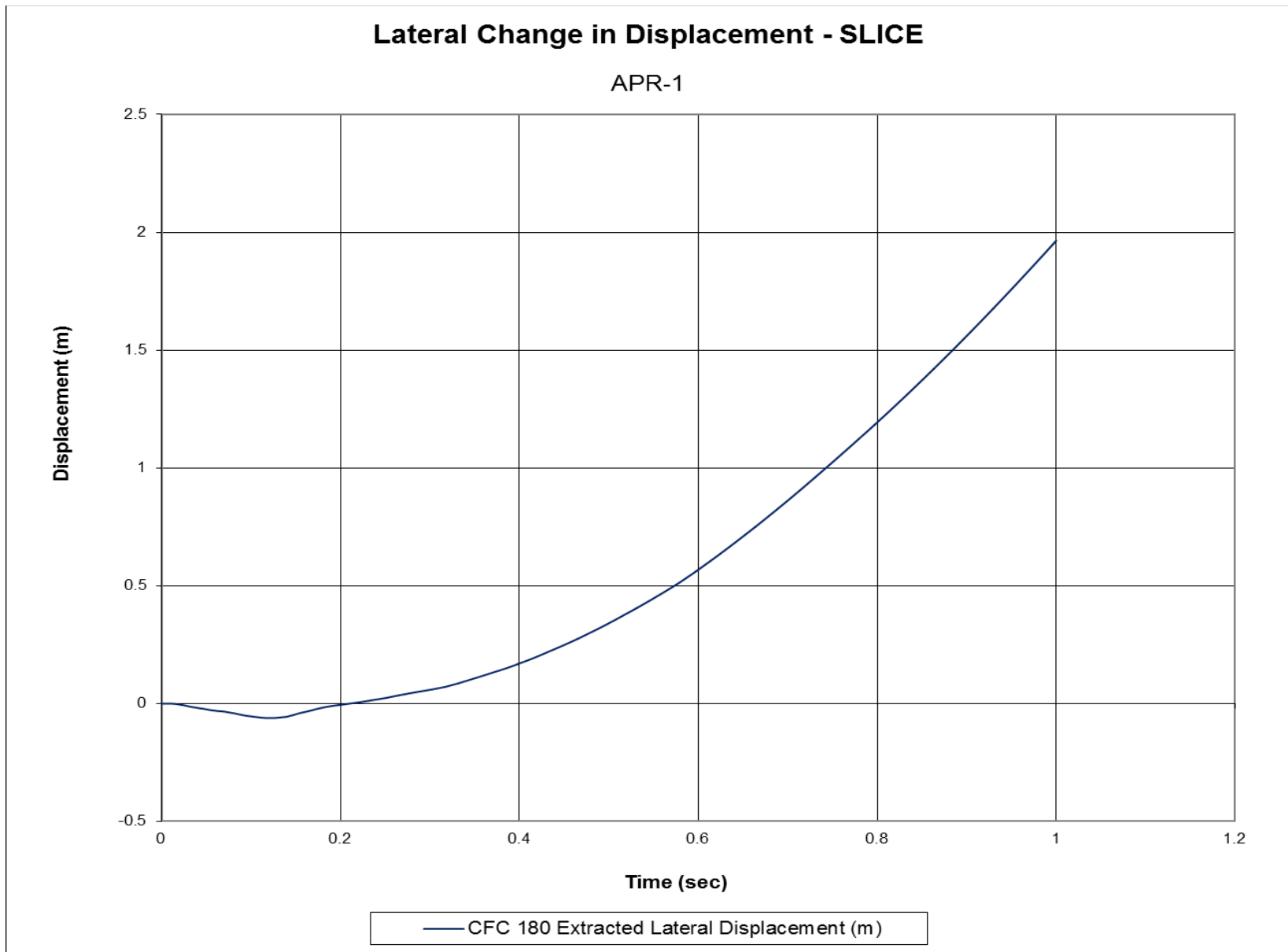


Figure H-13. Lateral Occupant Displacement (SLICE-2), Test No. APR-1

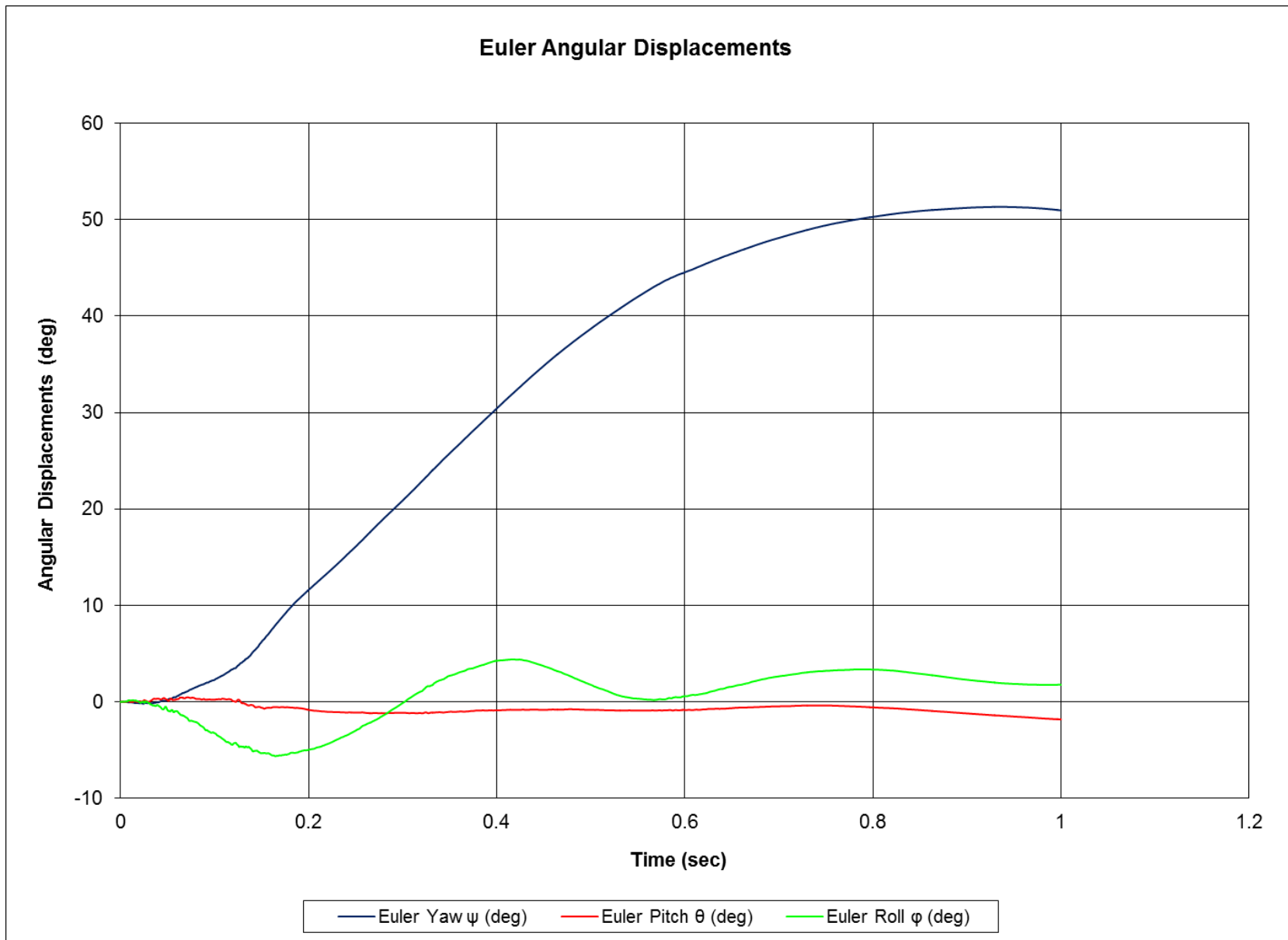


Figure H-14. Vehicle Angular Displacements (SLICE-2), Test No. APR-1

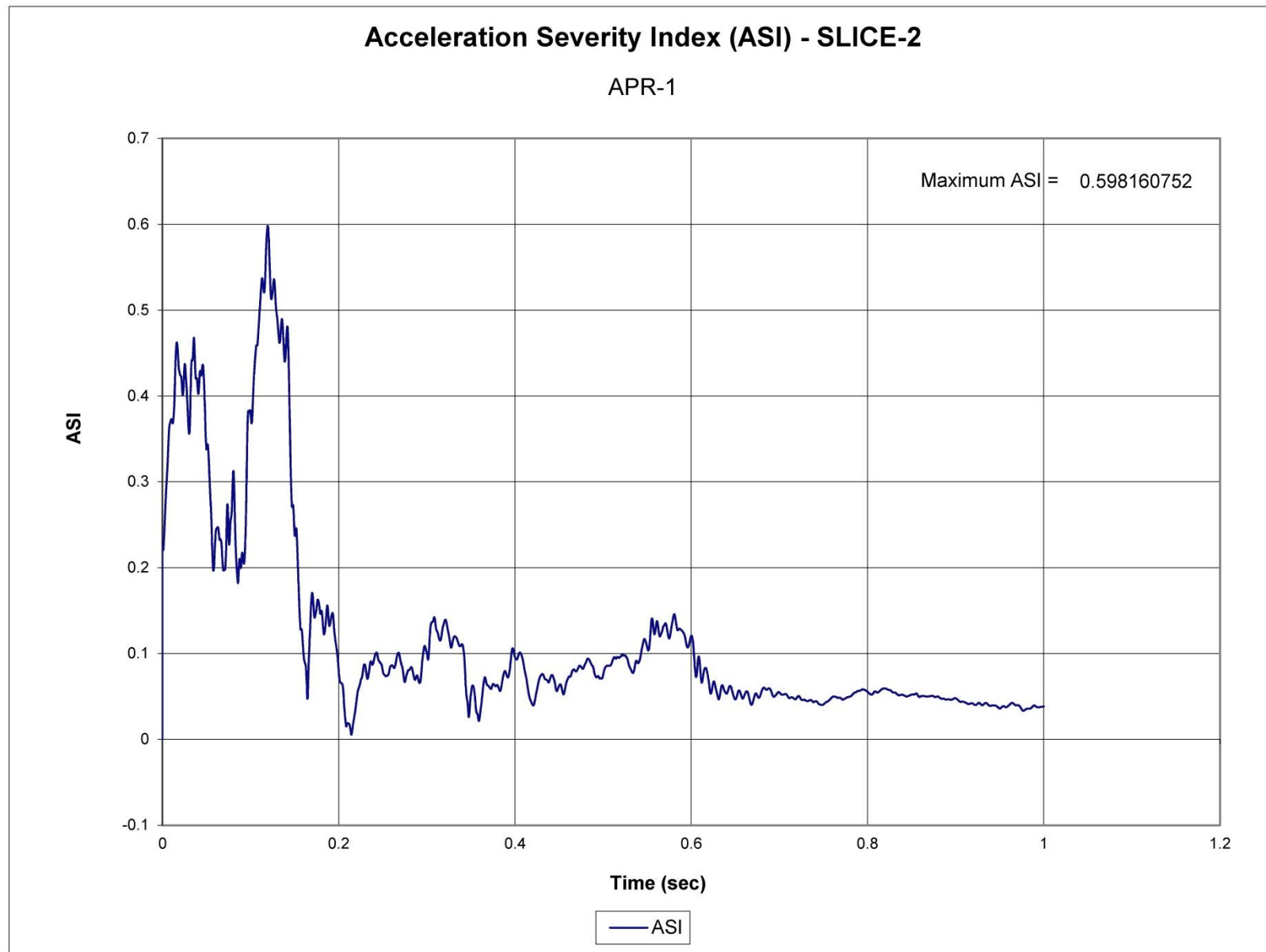


Figure H-15. Acceleration Severity Index (SLICE-2), Test No. APR-1

Appendix I. Accelerometer and Rate Transducer Data Plots, Test No. APR-2

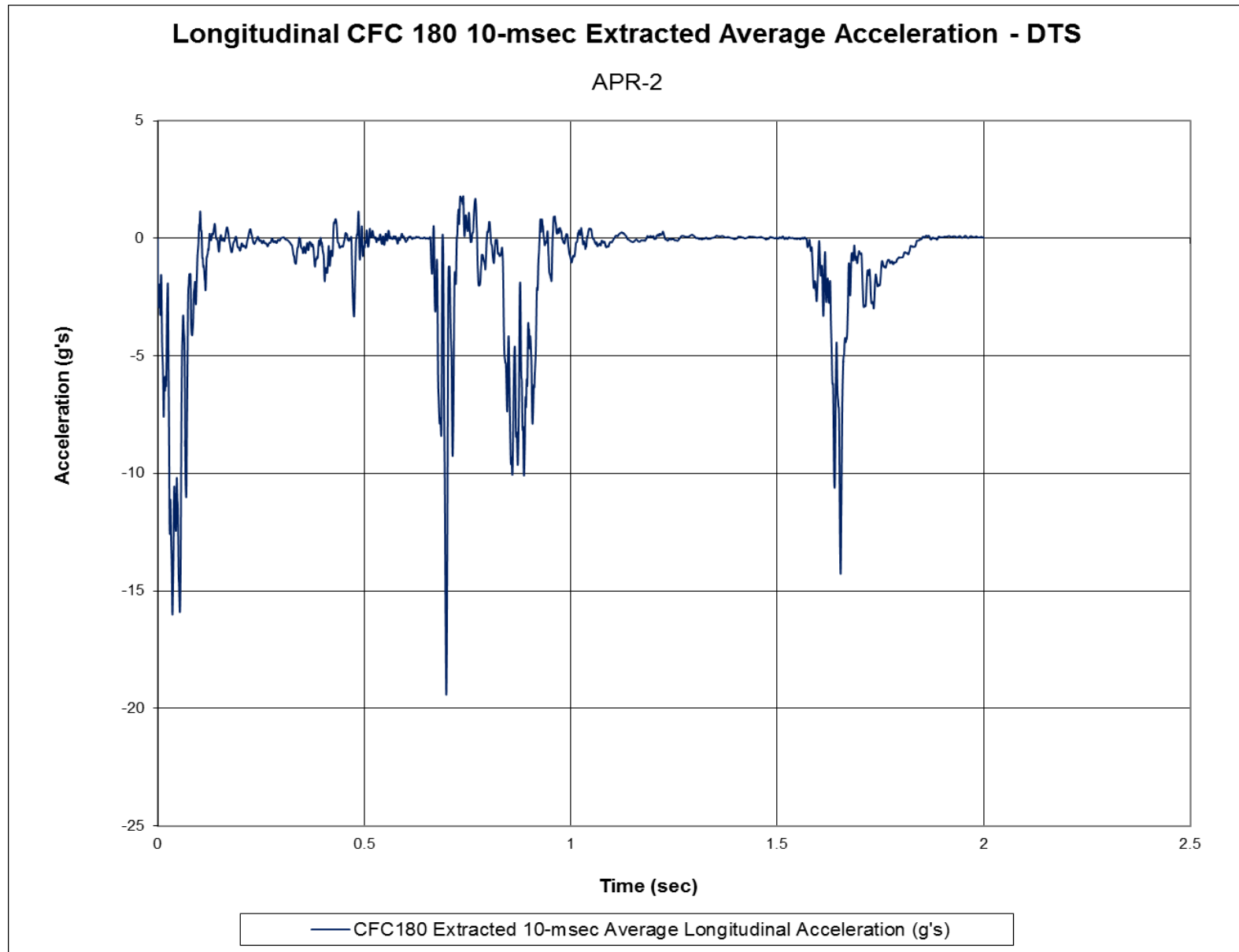


Figure I-1. 10-ms Average Longitudinal Deceleration (DTS), Test No. APR-2

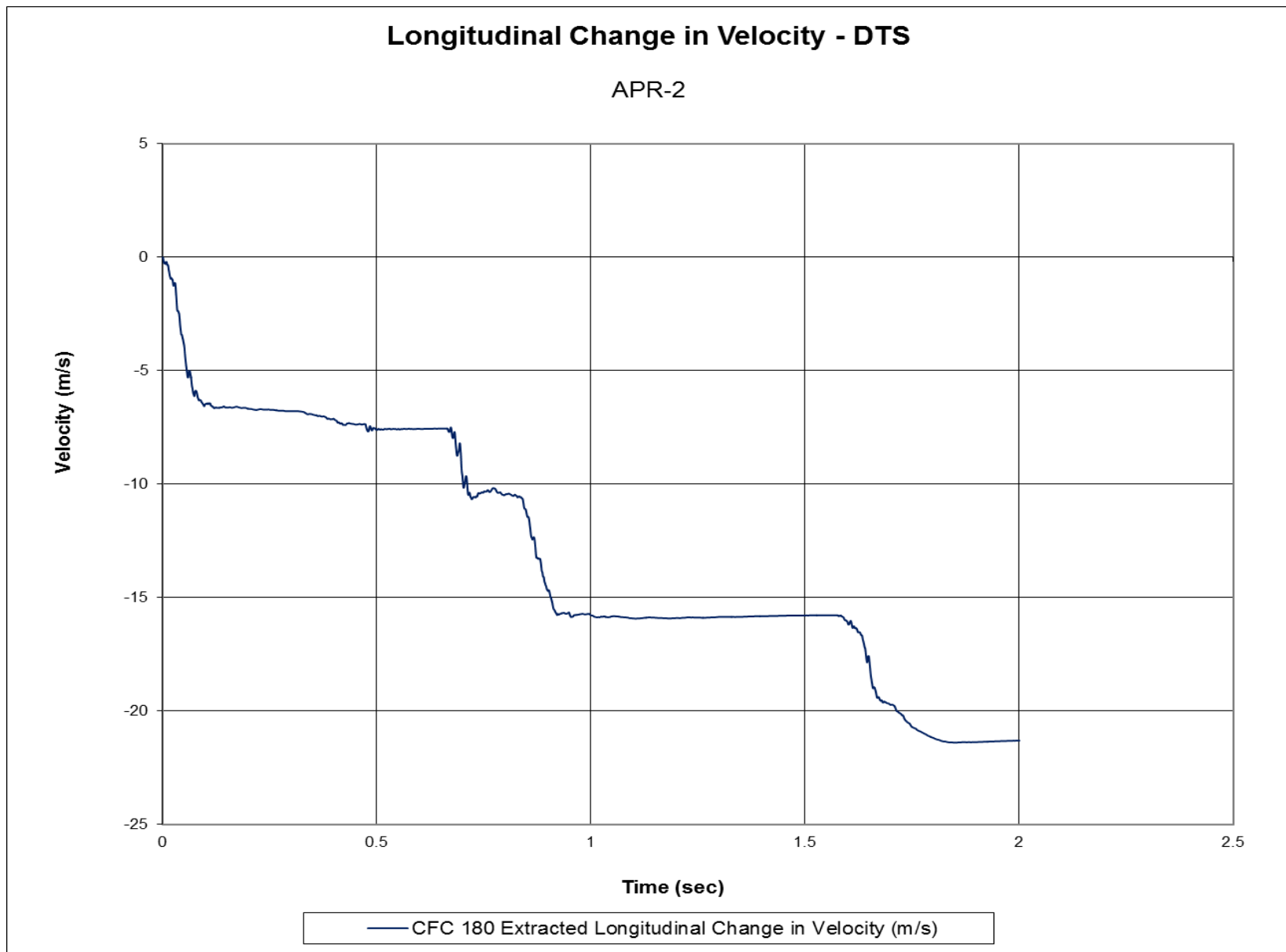


Figure I-2. Longitudinal Occupant Impact Velocity (DTS), Test No. APR-2

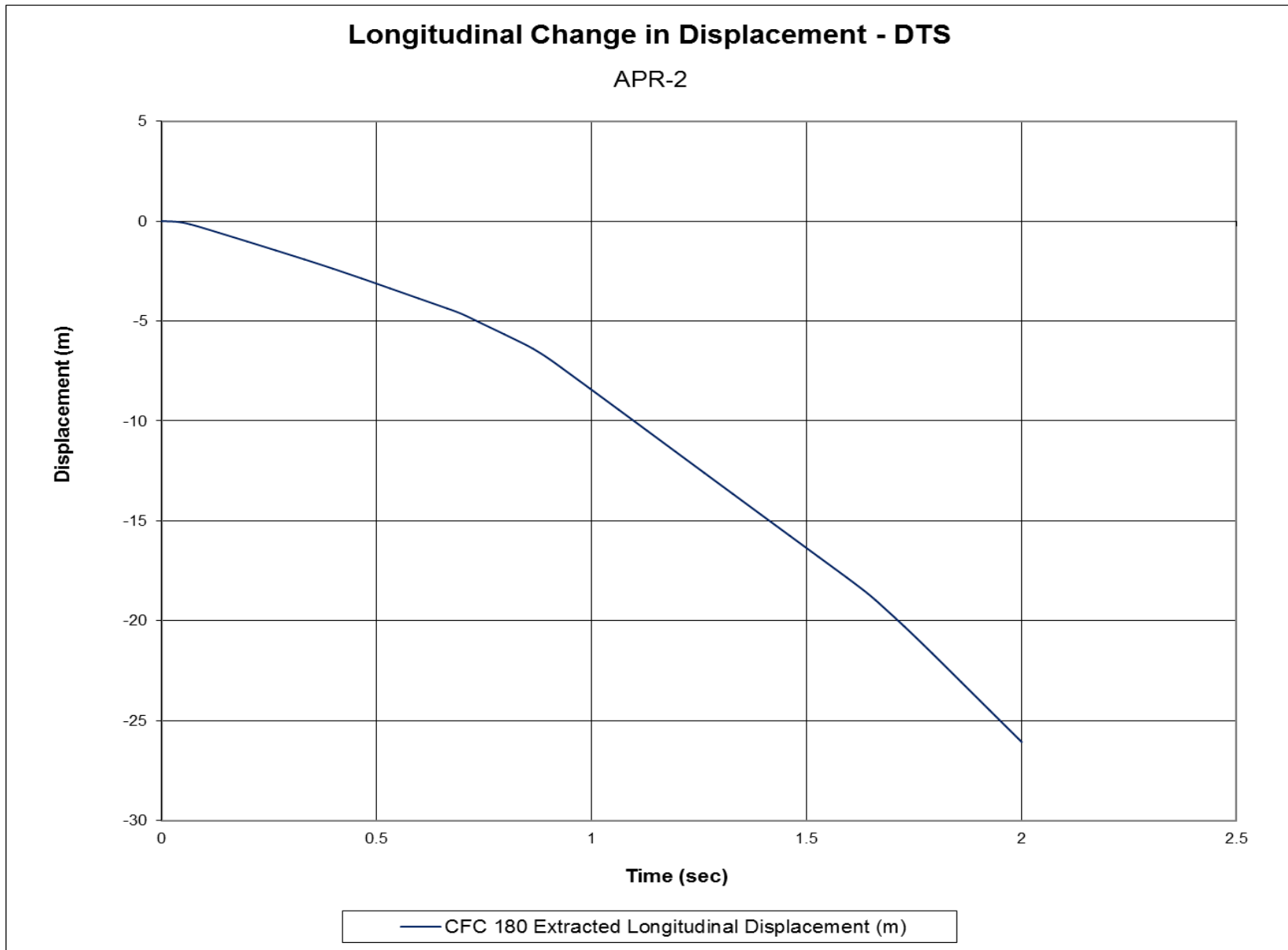


Figure I-3. Longitudinal Occupant Displacement (DTS), Test No. APR-2

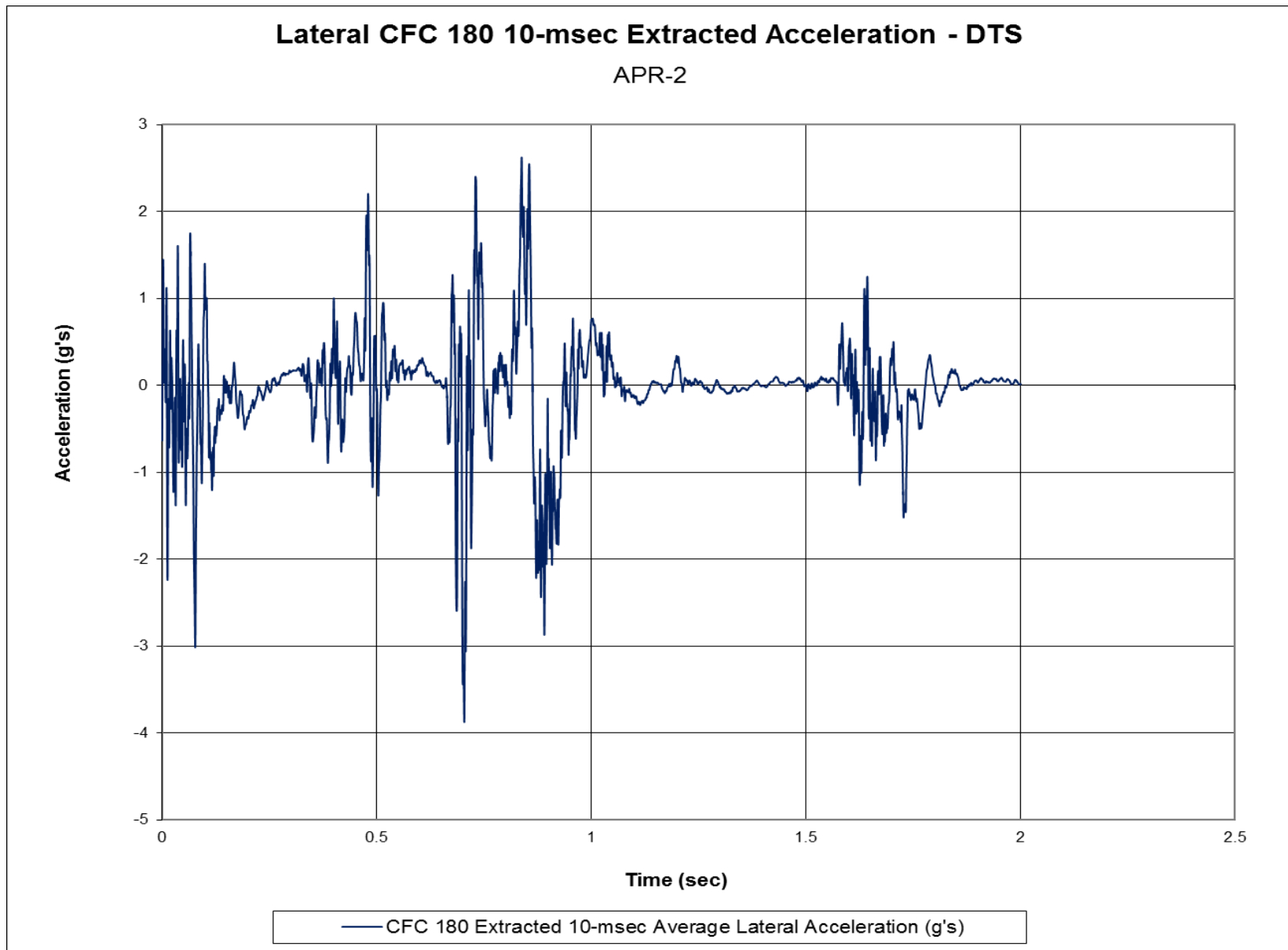


Figure I-4. 10-ms Average Lateral Deceleration (DTS), Test No. APR-2

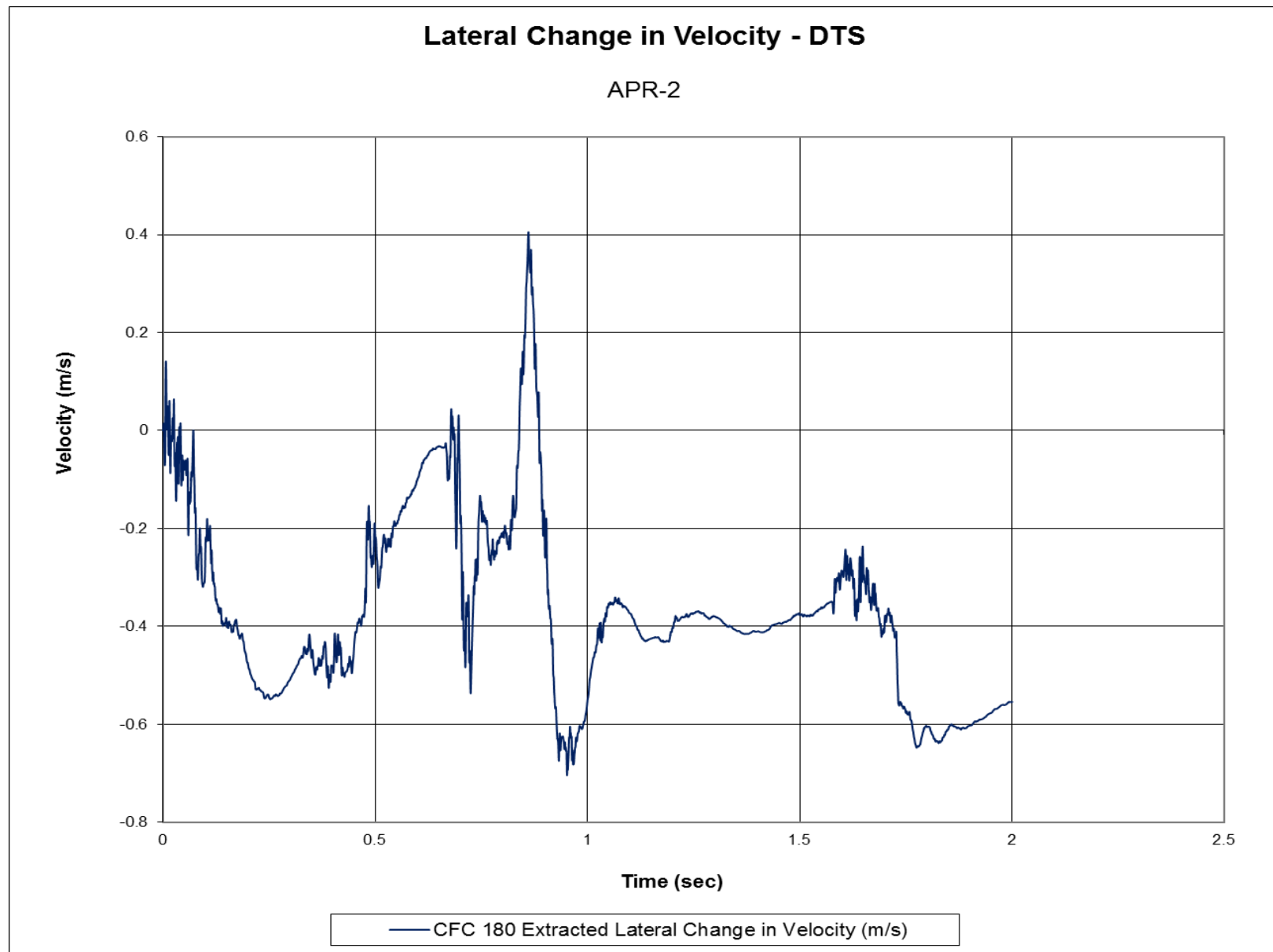


Figure I-5. Lateral Occupant Impact Velocity (DTS), Test No. APR-2

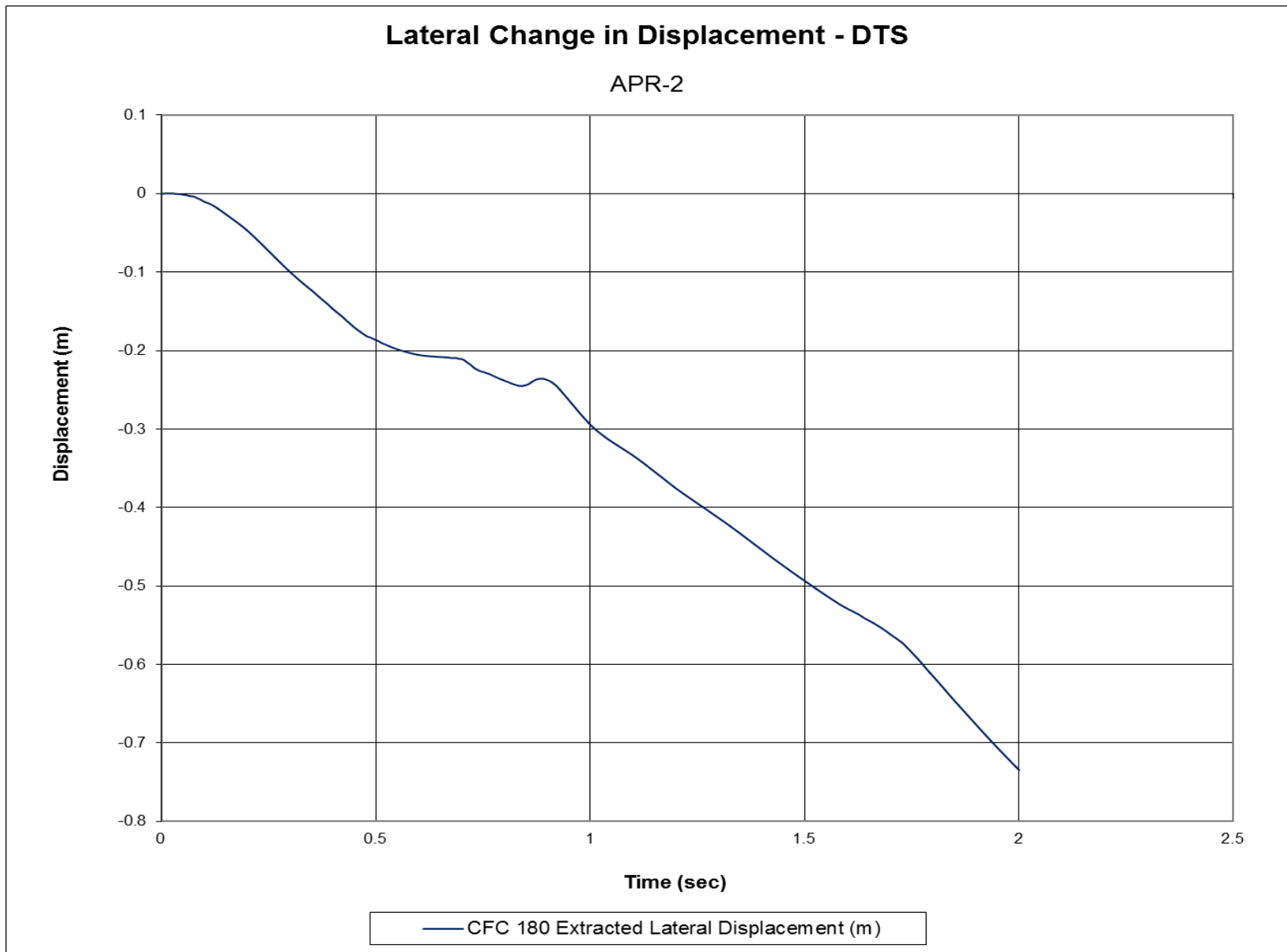


Figure I-6. Lateral Occupant Displacement (DTS), Test No. APR-2

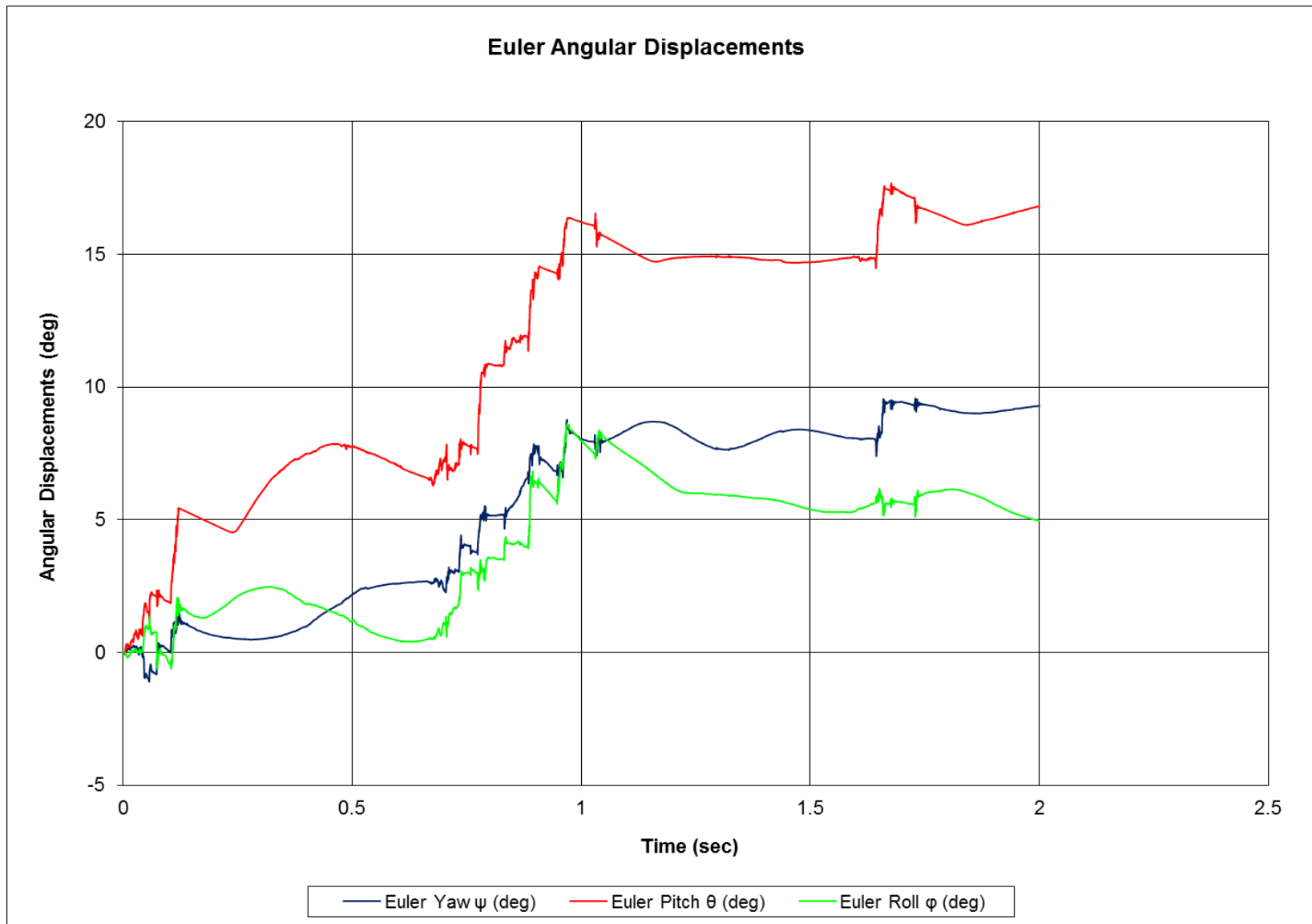


Figure I-7. Vehicle Angular Displacements (DTS), Test No. APR-2

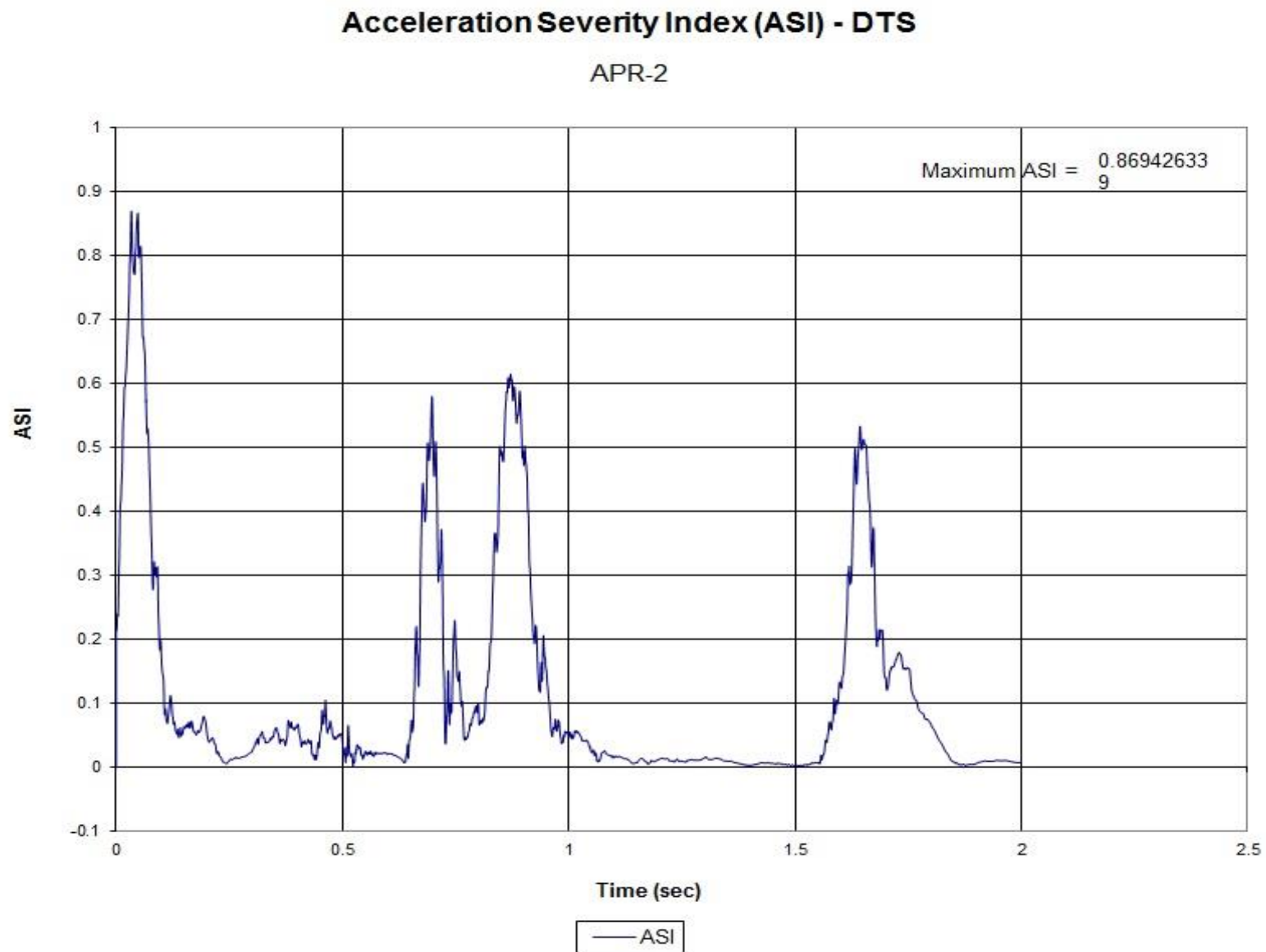


Figure I-8. Acceleration Severity Index (DTS), Test No. APR-2

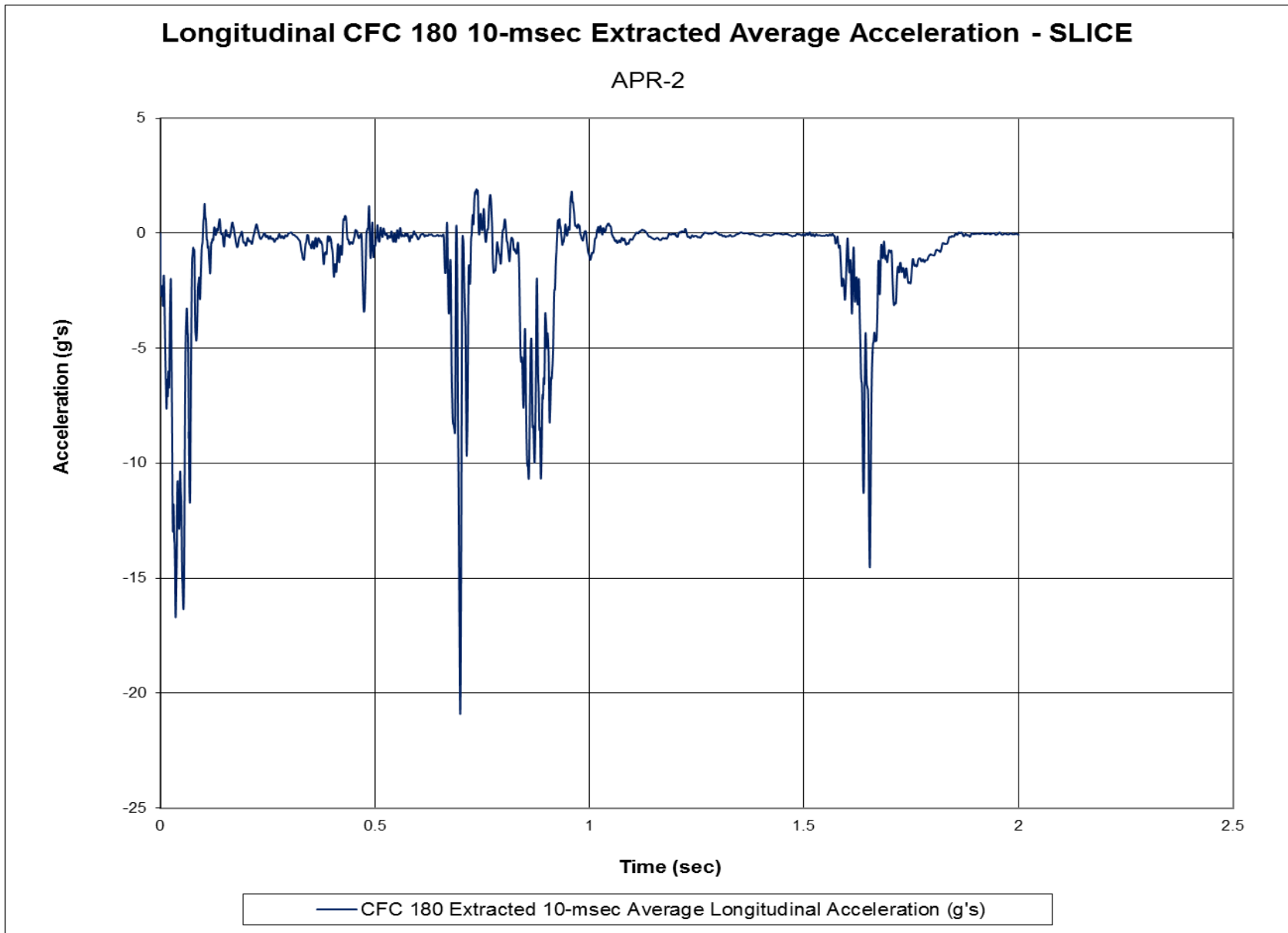


Figure I-9. 10-ms Average Longitudinal Deceleration (SLICE-2), Test No. APR-2

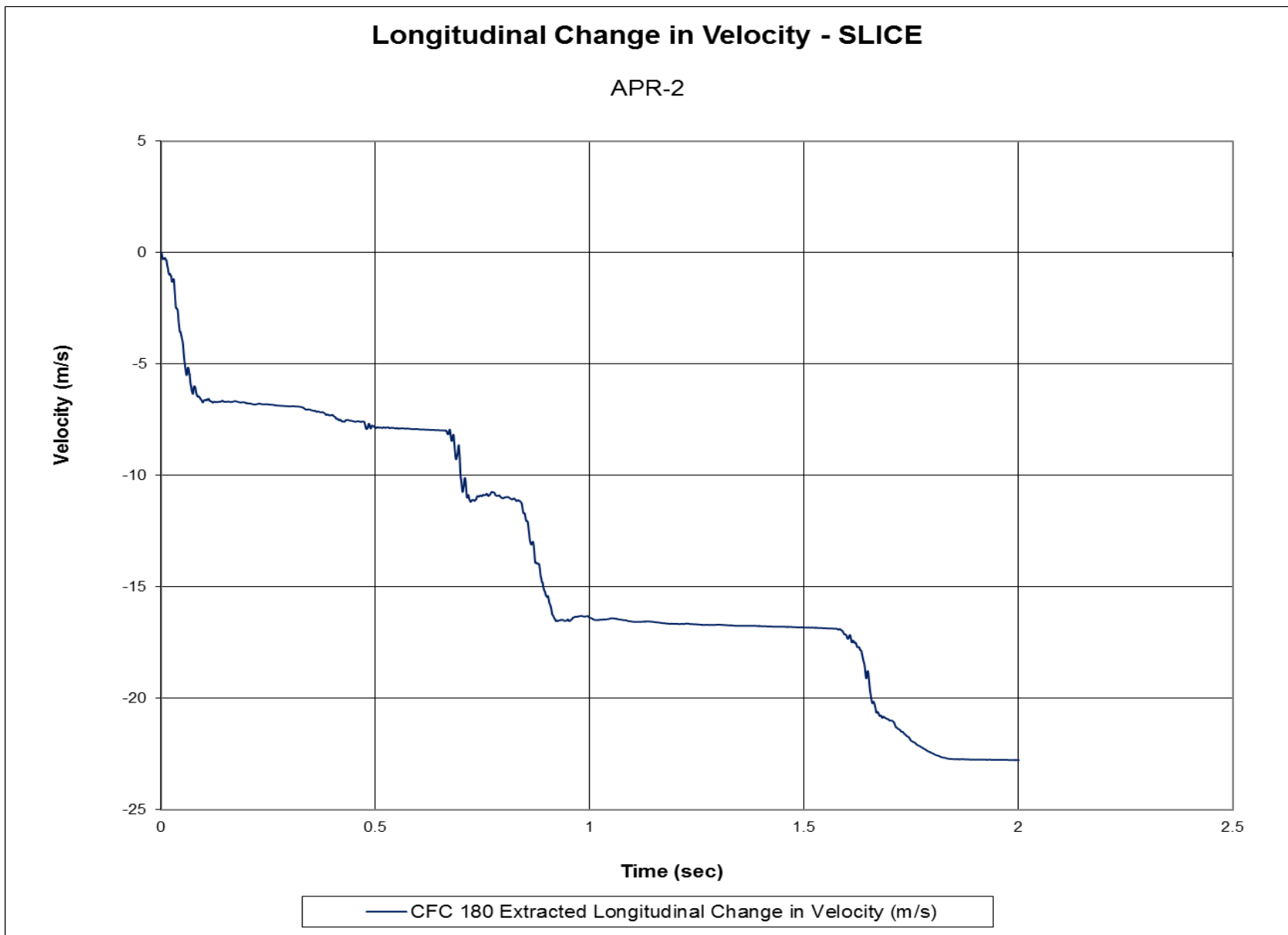


Figure I-10. Longitudinal Occupant Impact Velocity (SLICE-2), Test No. APR-2

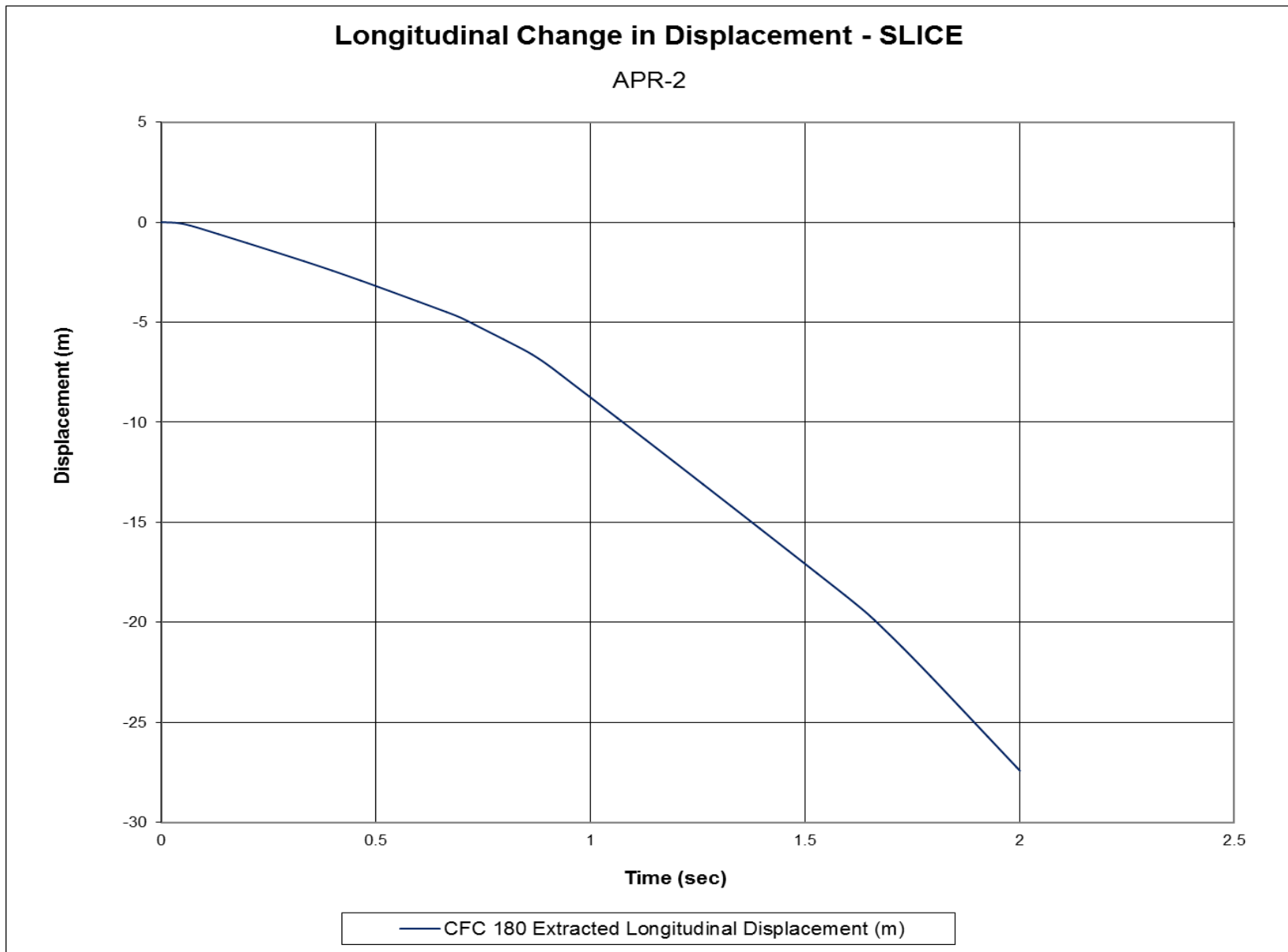


Figure I-11. Longitudinal Occupant Displacement (SLICE-2), Test No. APR-2

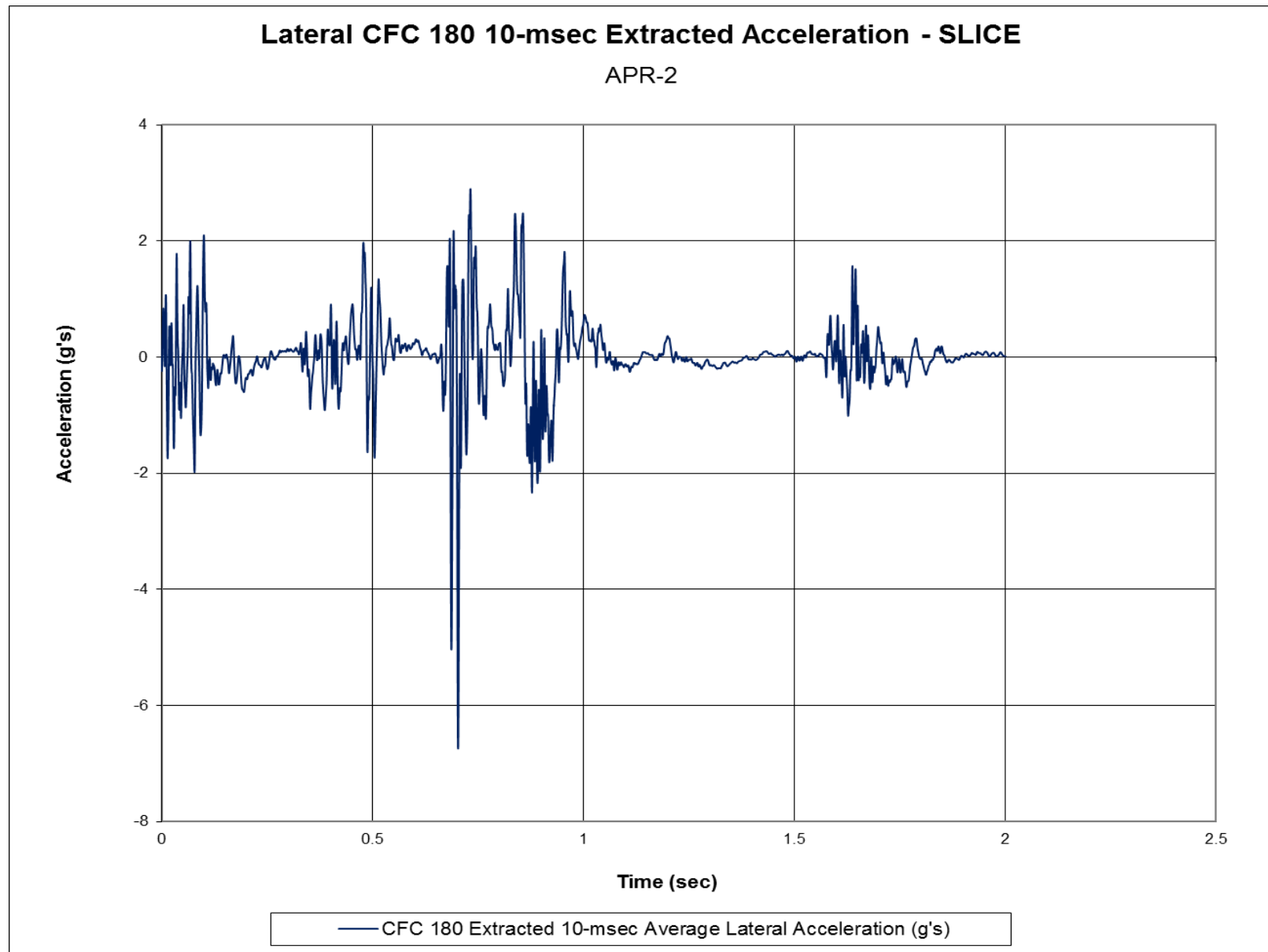


Figure I-12. 10-ms Average Lateral Deceleration (SLICE-2), Test No. APR-2

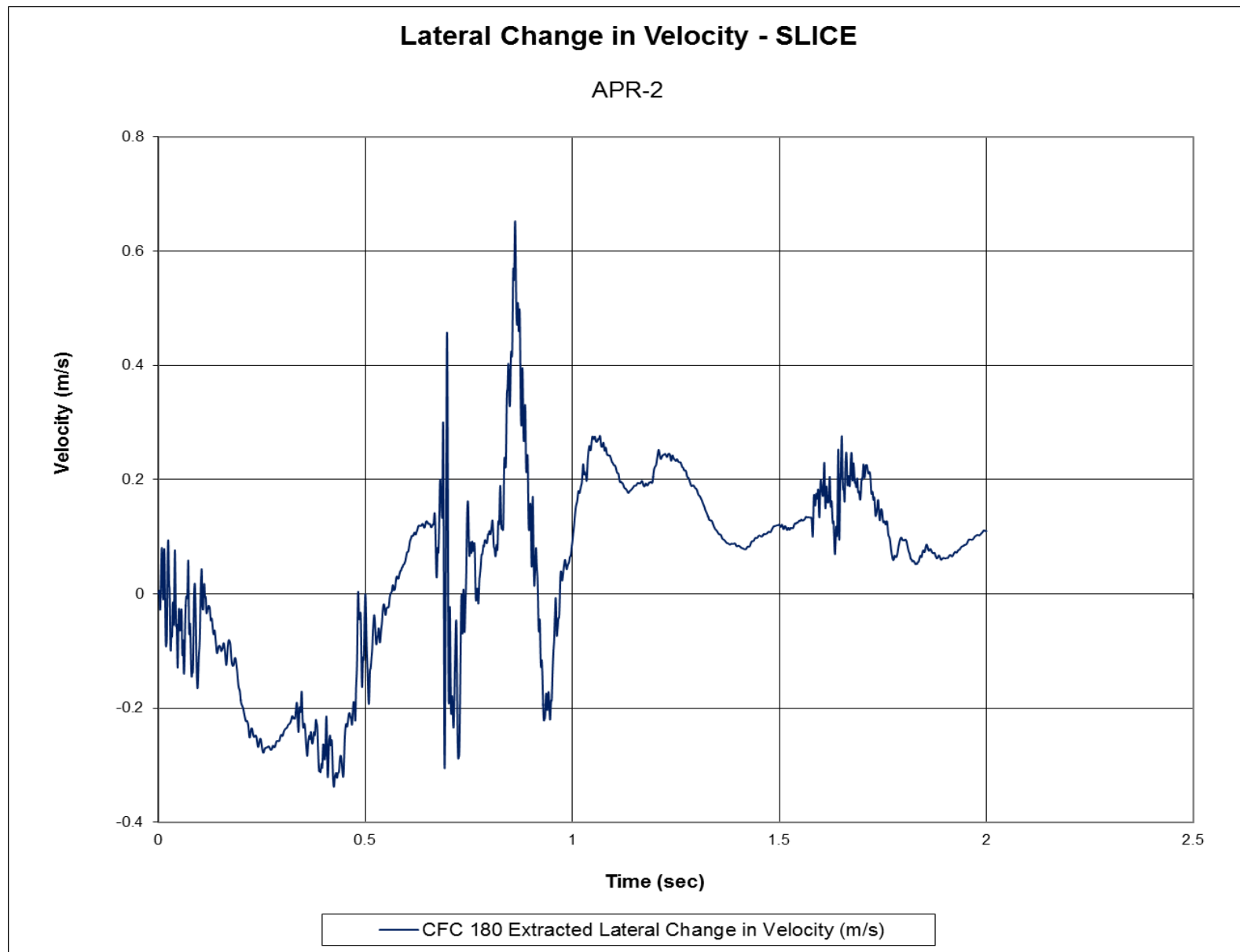


Figure I-13. Lateral Occupant Impact Velocity (SLICE-2), Test No. APR-2

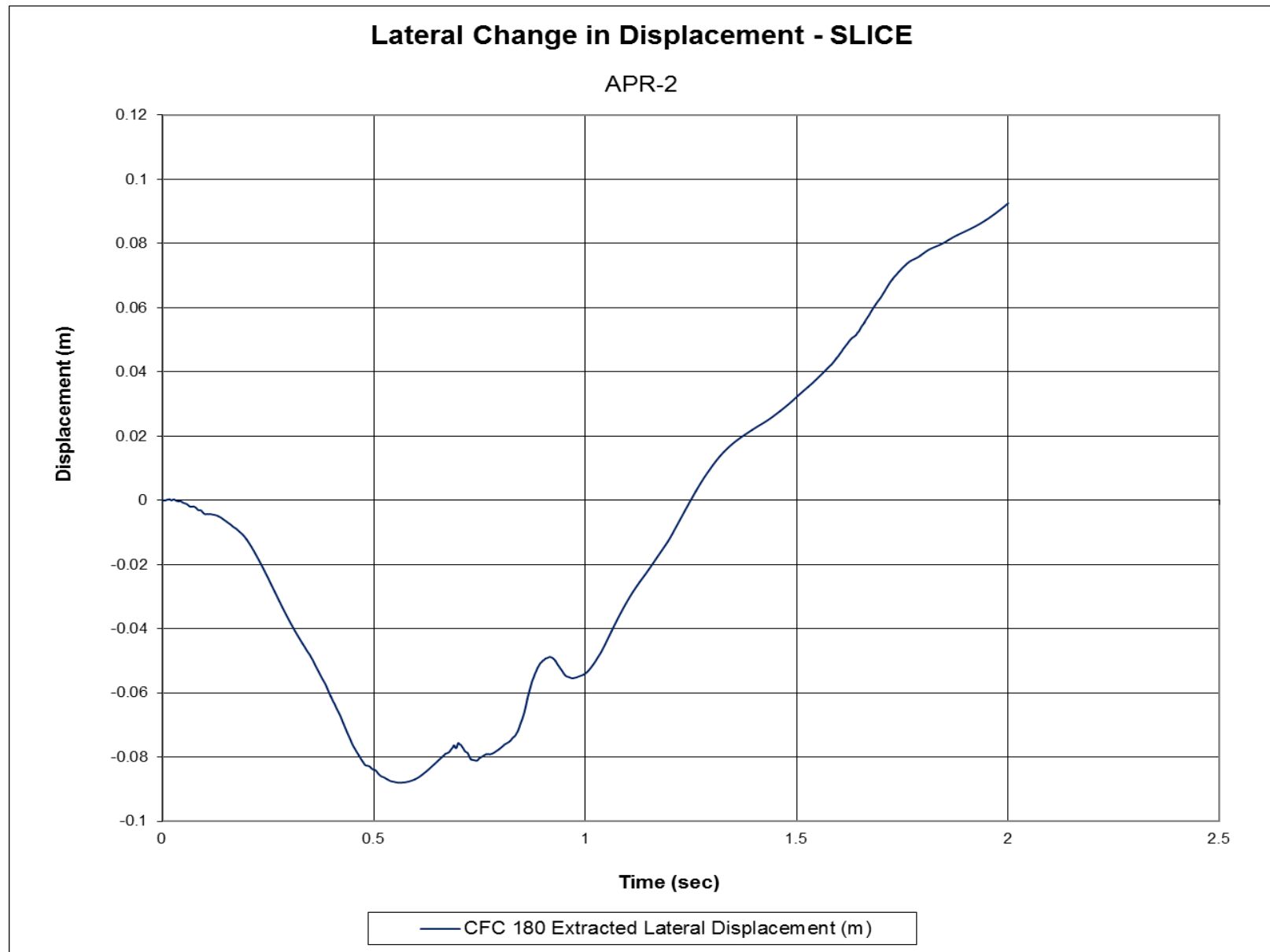


Figure I-14. Lateral Occupant Displacement (SLICE-2), Test No. APR-2

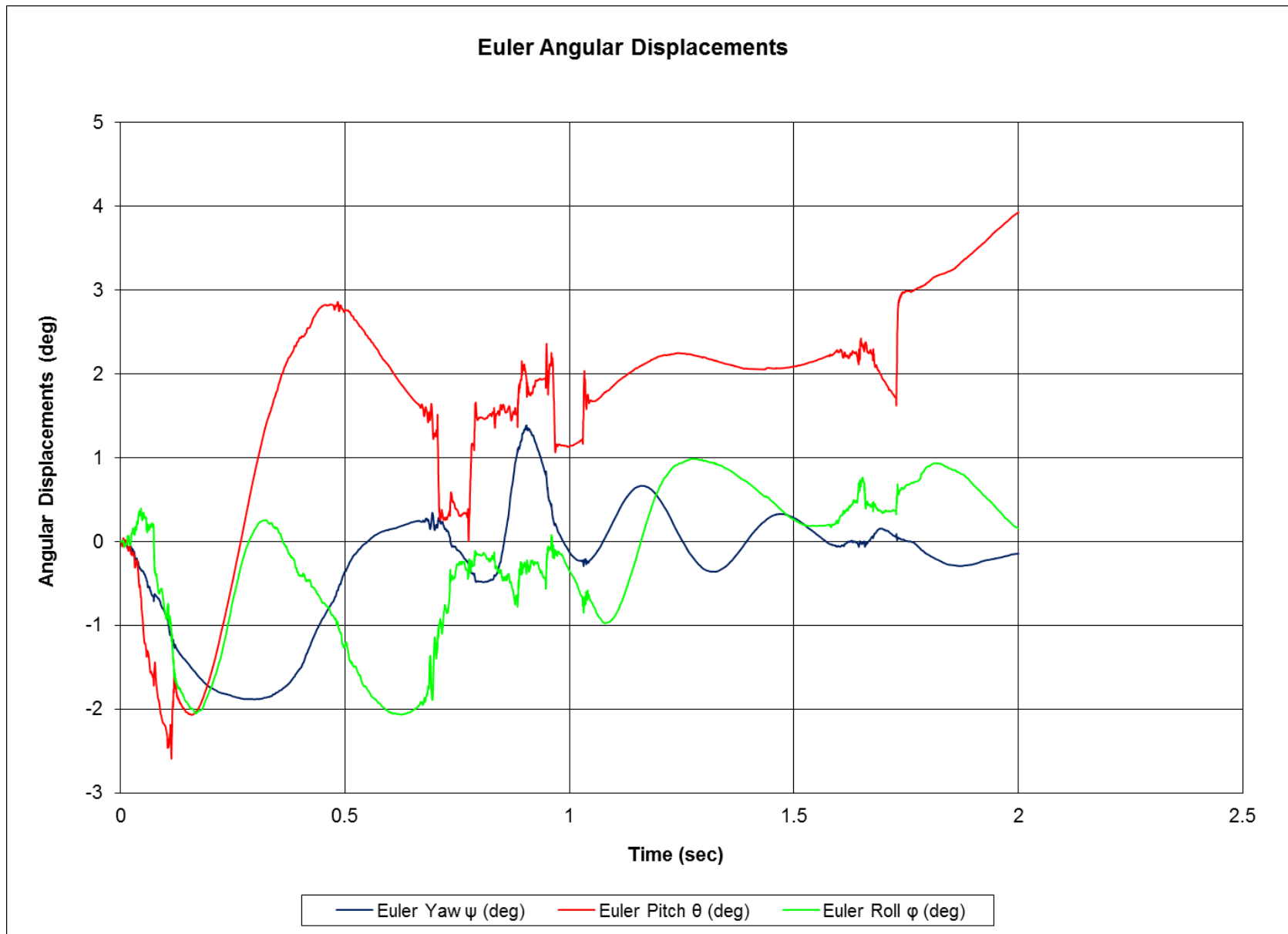


Figure I-15. Vehicle Angular Displacements (SLICE-2), Test No. APR-2

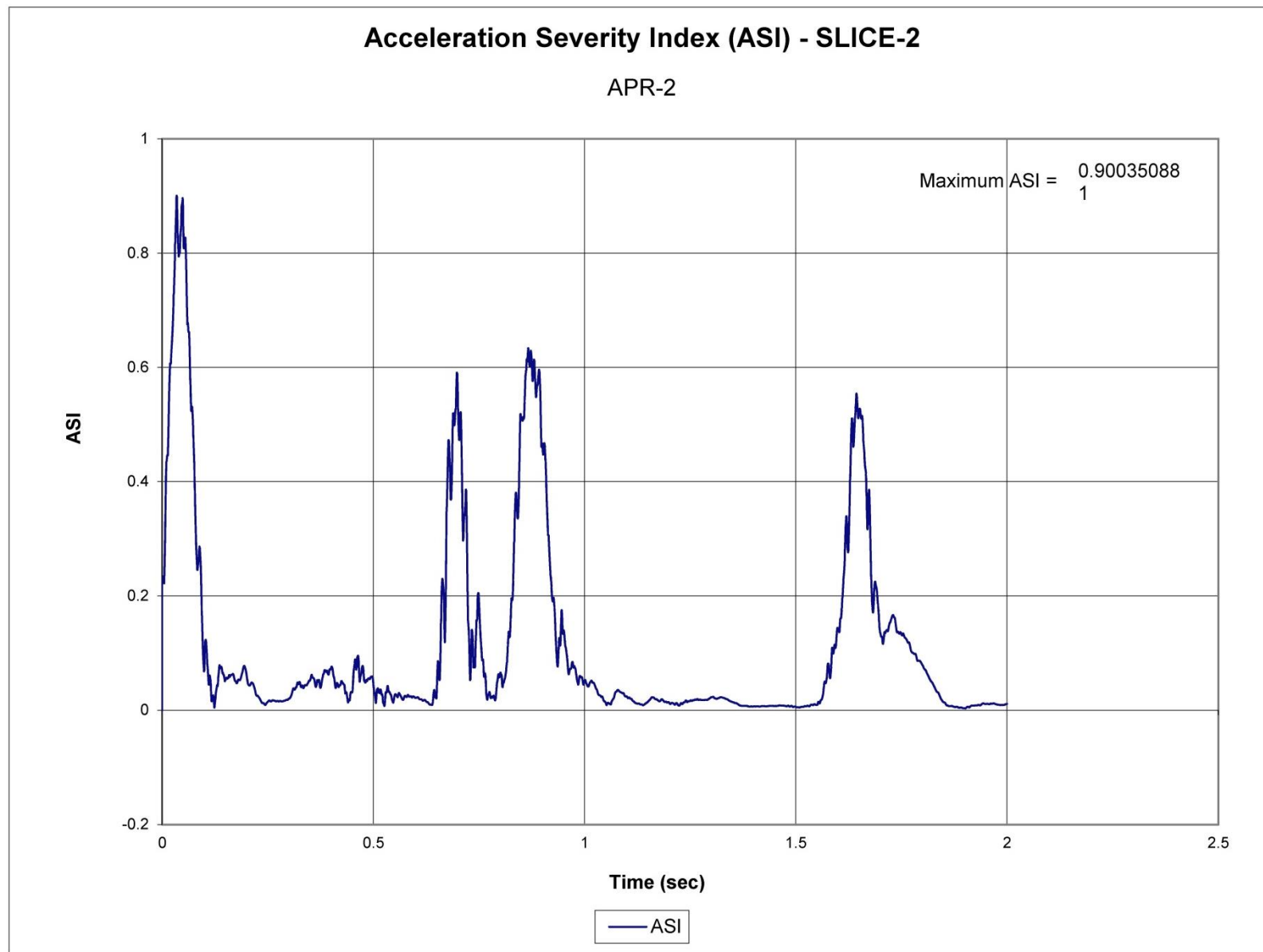


Figure I-16. Acceleration Severity Index (SLICE-2), Test No. APR-2

Appendix J. Test No. APR-2 Accelerometer Discussion

Email Correspondence with FHWA Regarding Test No. APR-2

From: will.longstreet@dot.gov [mailto:will.longstreet@dot.gov]
Sent: Thursday, February 12, 2015 9:44 AM
To: rbielenberg2@unl.edu
Cc: rfaller1@unl.edu; Nick.Artimovich@dot.gov
Subject: RE: Pedestrian Rail Test Results

Hi Bob:

Nick & I looked this one over & offer the following.

We've not seen this situation before (i.e., 2 conflicting accel readings). After review of video, we certainly agree w/your detailed assessment of test in regards to acceleration spike. As there is no existing policy for comparing accelerations from different transducer units on same test, we feel it best to recognize the implication of a higher value.

In addition as sponsoring state plans to further develop the design to improve its performance and lower the occupant risk values, was there any thoughts re. flying debris due to impact as well?

Please call me if you wish to further discuss & thanks for your patience.

Best,

Thursday, April 30, 2015 Task Force 13 Meeting Minutes

Subcommittee #7 Certification of Crash Test Facilities

Joined online by: John Jewell – CalTrans, Mike Dunlap – KARCO, Steven Matsusaka – KARCO

Sign in sheet sent around – make sure your name is on the list if you wanted to receive email correspondence in regards to ILCs. If not present at the meeting, email either Karla Lechtenberg (kpolivka2@unl.edu) or Lance Bullard (l-bullard@tamu.edu) if you want to receive ILC correspondence and have not been.

ILC discussion

- Accrediting body (A2LA) asking for a “plan” of at least 4 years of ILCs
- Each lab to email Karla Lechtenberg (kpolivka2@unl.edu) and idea for an ILC to be added to the “plan” by July 1, 2015.
- Need to add more “teeth” to the ILCs that are being conducted. Currently only sending out the results, but not discussion on who is correct and why the other labs are not. A report is needed that presents a description of the ILC, the results of the ILC, the differences between labs, the issues of why all are not matching/coming up with the same answer, and resolutions to the differences/issues.

Multiple accelerometer systems in a test vehicle discussion

- All labs use redundant accelerometer systems
- All labs do not analyze nor report all the accelerometer systems used in the tests
 - o MwRSF – analyzes and reports all data/systems
 - o Holmes Solution – only uses primary system, compares to other physical results. Only looks at and/or reports the secondary unit data if near the required limits for occupant risk
 - o TTI – only report primary
 - o TRC – only report primary
 - o CalTran – only look at primary unit, only analyze secondary unit if primary has issues. If within uncertainties, just use primary.
 - o TRC – analyzes and reports all data/units
- Most labs only mount the accelerometer systems at the x,y location of the c.g.
- Some labs stated that if primary fails or does not work then look at the secondary unit. If the occupant risk numbers are close to the threshold then the lab may have to rerun the test since it is unknown what effect not being mounted at the c.g. has on the occupant risk values.
- Consensus of laboratory representatives and FHWA present
 - o must report primary accelerometer unit (one at or within 2” of c.g.)
 - o may report all accelerometer units used, but must denote which is primary and secondary
 - o Placement of all accelerometer units must be noted within the reports.

¼-pt offset vs. centerline impact discussion (terminal/crash cushion)

- Currently impact is ¼-point offset which is critical for vehicle instability
- Not currently required, but centerline impact might be more critical for vehicle decelerations and occupant risk
- Staged devices – concerns for ORA vales

- Non-staged devices – OIV/ORA occurs before the vehicle yaws out
- Consensus of laboratory representatives present
- o Conduct the estimation procedure similar to the 1500A vehicle but with an 1100C vehicle could determine if that might be a critical impact.
- o Should be done for staged devices due to possible effects on ORA values

Debris “present undue hazard” discussion

- Began discussion
- MASH subjective on this topic. Not very clear.
- EN1317 uses 2 kg mas as the maximum debris
- Need to develop a consistency among the testing labs
- This topic needs more discussion.

END OF DOCUMENT